IEA Final Report

Mechanical Equipment & Control Strategies for a Chilled water and a Hot water system

A Report for the International Energy Agency's
SHC Task34 / ECBCS Annex 43 Subtask D
June 18, 2008

Written by

Clemens Felsmann
Institute of Thermodynamics and Building Systems Engineering
Technical University of Dresden

TECHNISCHE UNIVERSITÄT DRESDEN

SHC
SOLAR HEATING & COOLING PROGRAMME
INTERNATIONAL ENERGY AGENCY

International Energy Agency
Energy Conservation in Buildings and Community Systems Programme

Using Contributions from

Curtis Klaassen

IEC Energy Resource Station
Ankeny, Iowa, U.S.
curtk@energy.iastate.edu

Aad Wijsman

Vabi Software BV
Delft, The Netherlands
(Program VA114)
a.wijsman@vabi.nl

Vincent Lemort, Andres Rodríguez & Jean Lebrun

Thermodynamics Laboratory
Aerospace and Mechanical Engineering Department
University of Liège, Belgium
vincent.lemort@ulg.ac.be j.lebrun@ulg.ac.be

Heiko Werdin

ITG Dresden
Germany
werdin@itg-dresden.de

R. Henninger & M. Witte

GARD Analytics, Inc.,U.S.
rhenninger@gard.com mjwitte@gard.com

Special thanks also go to Dr. Greg Maxwell and Som Shrestha of Iowa State University, and Xiaohui Zhou of the Energy Resource Station for their efforts in developing and implementing the mechanical and control systems testing.

PREFACE

This report is a product of a joint effort between International Energy Agency Solar Heating and Cooling (IEA SHC) Task 34 and Energy Conservation in Buildings and Community Systems (ECBCS) Annex 43. Ron Judkoff of the National Renewable Energy Laboratory (NREL) was the Operating Agent for IEA 34/43 on behalf of the United States Department of Energy.

International Energy Agency

The International Energy Agency (IEA) was established in 1974 within the framework of the Organisation for Economic Co-operation and Development (OECD) to implement an international energy programme. A basic aim of the IEA is to foster co-operation among the twenty-four IEA participating countries and to increase energy security through energy conservation, development of alternative energy sources and energy research, development and demonstration (RD&D).

Solar Heating and Cooling Program

The Solar Heating and Cooling Program was one of the first IEA Implementing Agreements to be established. Since 1977, its members have been collaborating to advance active solar, passive solar and photovoltaic technologies and their application in buildings and other areas, such as agriculture and industry. Current members are:

Australia	Finland	Portugal
Austria	France	Spain
Belgium	Italy	Sweden
Canada	Mexico	Switzerland
Denmark	Netherlands	United States
European Commission	New Zealand	
Germany	Norway	

A total of 37 Tasks have been initiated, 26 of which have been completed. Each Task is managed by an Operating Agent from one of the participating countries. Overall control of the program rests with an Executive Committee comprised of one representative from each contracting party to the Implementing Agreement. In addition to the Task work, a number of special activities—Memorandum of Understanding with solar thermal trade organizations, statistics collection and analysis, conferences and workshops—have been undertaken.

The Tasks of the IEA Solar Heating and Cooling Programme, both underway and completed are as follows:

Current Tasks:

Task 27 *Performance of Solar Facade Components*

Task 29 *Solar Crop Drying*
Task 31 *Daylighting Buildings in the 21st Century*
Task 36 *Solar Resource Knowledge Management*
Task 37 *Advanced Housing Renovation with Solar & Conservation*
Task 38 *Solar Assisted Cooling Systems*
Task 39 *Polymeric Materials for Solar Thermal Applications*

Completed Tasks:

Task 1 *Investigation of the Performance of Solar Heating and Cooling Systems*
Task 2 *Coordination of Solar Heating and Cooling R&D*
Task 3 *Performance Testing of Solar Collectors*
Task 4 *Development of an Insulation Handbook and Instrument Package*
Task 5 *Use of Existing Meteorological Information for Solar Energy Application*
Task 6 *Performance of Solar Systems Using Evacuated Collectors*
Task 7 *Central Solar Heating Plants with Seasonal Storage*
Task 8 *Passive and Hybrid Solar Low Energy Buildings*
Task 9 *Solar Radiation and Pyranometry Studies*
Task 10 *Solar Materials R&D*
Task 11 *Passive and Hybrid Solar Commercial Buildings*
Task 12 *Building Energy Analysis and Design Tools for Solar Applications*
Task 13 *Advance Solar Low Energy Buildings*
Task 14 *Advance Active Solar Energy Systems*
Task 16 *Photovoltaic in Buildings*
Task 17 *Measuring and Modelling Spectral Radiation*
Task 18 *Advanced Glazing and Associated Materials for Solar and Building Application*
Task 19 *Solar Air Systems*
Task 20 *Solar Energy in Building Renovation*
Task 21 *Daylight in Buildings*
Task 22 *Building Energy Analysis Tools*
Task 23 *Optimization of Solar Energy Use in Large Buildings*
Task 24 *Solar Procurement*
Task 25 *Solar Assisted Air Conditioning of Building*
Task 26 *Solar Combisystems*
Task 28 *Solar Sustainable Housing*
Task 32 *Advanced Storage Concepts for Solar and Low Energy Buildings*
Task 33 *Solar Heat for Industrial Processes*
Task 34 *Testing and Validation of Building Energy Simulation Tools*
Task 35 *PV/Thermal Solar Systems*

Completed Working Groups:

CSHPSS, ISOLDE, Materials in Solar Thermal Collectors, and the Evaluation of Task 13 Houses

To find more IEA Solar Heating and Cooling Programme publications or learn about the Programme visit our Internet site at **www.iea-shc.org** or contact the SHC Executive Secretary, Pamela Murphy, e-mail: pmurphy@MorseAssociatesInc.com.

Energy Conservation in Buildings and Community Systems

The IEA sponsors research and development in a number of areas related to energy. The mission of one of those areas, the ECBCS - Energy Conservation for Building and Community Systems Programme, is to facilitate and accelerate the introduction of energy conservation, and environmentally sustainable technologies into healthy buildings and community systems, through innovation and research in decision-making, building assemblies and systems, and commercialisation. The objectives of collaborative work within the ECBCS R&D program are directly derived from the on-going energy and environmental challenges facing IEA countries in the area of construction, energy market and research. ECBCS addresses major challenges and takes advantage of opportunities in the following areas:

- exploitation of innovation and information technology;
- impact of energy measures on indoor health and usability;
- integration of building energy measures and tools to changes in lifestyles, work environment alternatives, and business environment.

The Executive Committee

Overall control of the program is maintained by an Executive Committee, which not only monitors existing projects but also identifies new areas where collaborative effort may be beneficial. To date the following projects have been initiated by the executive committee on Energy Conservation in Buildings and Community Systems (completed projects are identified by (*)):

Annex 1: Load Energy Determination of Buildings (*)
Annex 2: Ekistics and Advanced Community Energy Systems (*)
Annex 3: Energy Conservation in Residential Buildings (*)
Annex 4: Glasgow Commercial Building Monitoring (*)
Annex 5: Air Infiltration and Ventilation Centre
Annex 6: Energy Systems and Design of Communities (*)
Annex 7: Local Government Energy Planning (*)
Annex 8: Inhabitants Behaviour with Regard to Ventilation (*)
Annex 9: Minimum Ventilation Rates (*)
Annex 10: Building HVAC System Simulation (*)
Annex 11: Energy Auditing (*)
Annex 12: Windows and Fenestration (*)
Annex 13: Energy Management in Hospitals (*)
Annex 14: Condensation and Energy (*)
Annex 15: Energy Efficiency in Schools (*)
Annex 16: BEMS 1- User Interfaces and System Integration (*)
Annex 17: BEMS 2- Evaluation and Emulation Techniques (*)
Annex 18: Demand Controlled Ventilation Systems (*)
Annex 19: Low Slope Roof Systems (*)
Annex 20: Air Flow Patterns within Buildings (*)

Annex 21: Thermal Modelling (*)
Annex 22: Energy Efficient Communities (*)
Annex 23: Multi Zone Air Flow Modelling (COMIS) (*)
Annex 24: Heat, Air and Moisture Transfer in Envelopes (*)
Annex 25: Real time HEVAC Simulation (*)
Annex 26: Energy Efficient Ventilation of Large Enclosures (*)
Annex 27: Evaluation and Demonstration of Domestic Ventilation Systems (*)
Annex 28: Low Energy Cooling Systems (*)
Annex 29: Daylight in Buildings (*)
Annex 30: Bringing Simulation to Application (*)
Annex 31: Energy-Related Environmental Impact of Buildings (*)
Annex 32: Integral Building Envelope Performance Assessment (*)
Annex 33: Advanced Local Energy Planning (*)
Annex 34: Computer-Aided Evaluation of HVAC System Performance (*)
Annex 35: Design of Energy Efficient Hybrid Ventilation (HYBVENT) (*)
Annex 36: Retrofitting of Educational Buildings (*)
Annex 37: Low Exergy Systems for Heating and Cooling of Buildings (LowEx) (*)
Annex 38: Solar Sustainable Housing (*)
Annex 39: High Performance Insulation Systems (*)
Annex 40: Building Commissioning to Improve Energy Performance (*)
Annex 41: Whole Building Heat, Air and Moisture Response (MOIST-ENG)
Annex 42: The Simulation of Building-Integrated Fuel Cell and Other Cogeneration Systems (FC+COGEN-SIM)
Annex 43: Testing and Validation of Building Energy Simulation Tools
Annex 44: Integrating Environmentally Responsive Elements in Buildings
Annex 45: Energy Efficient Electric Lighting for Buildings
Annex 46: Holistic Assessment Tool-kit on Energy Efficient Retrofit Measures for Government Buildings (EnERGo)
Annex 47: Cost-Effective Commissioning for Existing and Low Energy Buildings
Annex 48: Heat Pumping and Reversible Air Conditioning
Annex 49: Low Exergy Systems for High Performance Built Environments and Communities
Annex 50: Prefabricated Systems for Low Energy / High Comfort Building Renewal

Working Group - Energy Efficiency in Educational Buildings (*)
Working Group - Indicators of Energy Efficiency in Cold Climate Buildings (*)
Working Group - Annex 36 Extension: The Energy Concept Adviser (*)
(*) – Completed

Participating countries in ECBCS:

Australia, Belgium, CEC, Canada, Czech Republic, Denmark, Finland, France, Germany, Greece, Israel, Italy, Japan, the Netherlands, New Zealand, Norway, Poland, Portugal, Sweden, Switzerland, Turkey, United Kingdom and the United States of America.

SHC Task 34 / ECBCS Annex 43: Testing and Validation of Building Energy Simulation Tools

Goal and Objectives

The goal of this Task/Annex is to undertake pre-normative research to develop a comprehensive and integrated suite of building energy analysis tool tests involving analytical, comparative, and empirical methods. These methods will provide for quality assurance of software, and some of the methods will be enacted by codes and standards bodies to certify software used for showing compliance to building energy standards. This goal will be pursued by accomplishing the following objectives:

Create and make widely available a comprehensive and integrated suite of IEA Building Energy Simulation Test (BESTEST) cases for evaluating, diagnosing, and correcting building energy simulation software. Tests will address modelling of the building thermal fabric and building mechanical equipment systems in the context of innovative low energy buildings.
Maintain and expand as appropriate analytical solutions for building energy analysis tool evaluation.
Create and make widely available high quality empirical validation data sets, including detailed and unambiguous documentation of the input data required for validating software, for a selected number of representative design conditions.

Scope

This Task/Annex investigates the availability and accuracy of building energy analysis tools and engineering models to evaluate the performance of innovative low-energy buildings. Innovative low-energy buildings attempt to be highly energy efficient through use of advanced energy-efficiency technologies or a combination of energy efficiency and solar energy technologies. To be useful in a practical sense such tools must also be capable of modelling conventional buildings. The scope of the Task is limited to building energy simulation tools, including emerging modular type tools, and to widely used innovative low-energy design concepts. Activities will include development of analytical, comparative and empirical methods for evaluating, diagnosing, and correcting errors in building energy simulation software.

The audience for the results of the Task/Annex is building energy simulation tool developers, and codes and standards (normes) organizations that need methods for certifying software. However, tool users, such as architects, engineers, energy consultants, product manufacturers, and building owners and managers, are the ultimate beneficiaries of the research, and will be informed through targeted reports and articles.

Means

The objectives are to be achieved by the Participants in the following Projects.

Comparative and Analytical Verification Tests:

Project A: Ground-Coupled Heat Transfer with respect to Floor Slab and Basement Constructions
Project B: Multi-Zone Buildings and Air Flow

Empirical Validation and Comparative Tests:
Project C: Shading/Daylighting/Load Interaction
Project D: Mechanical Equipment and Controls
Project E: Buildings with Double-Skin Facades

Other:
Project G: Web Site for Consolidation of Tool Evaluation Tests

Participants

The participants in the Task are Australia, Belgium, Canada, Czech Republic, Denmark, France, Germany, Japan, the Netherlands, Spain, Sweden, Switzerland, the United Kingdom, and the United States. The United States served as the Operating Agent for this Task, with Ron Judkoff of the National Renewable Energy Laboratory providing Operating Agent services on behalf of the U.S. Department of Energy.

This Report

This report documents work carried out under Project D: Mechanical Equipment and Control Strategies. It is divided into two parts: Part I is on a chilled water system and Part II is on a heating water system. Both systems are real installations found in a laboratory building. They are described in detail. Thus information provided in this report should allow to model and simulate the performance of certain components that are part of chilled and / or heating water system. A validation of simulation programs can be done using the exemple results and diagnosing methods also provided in this report but also using the very large data set that is provided on an additional CD. Some validation tests described in this report do need some further development. The work documented here may also help to improve such validation procedures in a future task.

The Subtask D was leaded by Clemens Felsmann, Technical University Dresden in co-operation with Jean Lebrun, University of Liege.
Participants of Project D are as follows:

Name of the Program	Location
VA114	VABI Software BV, Delft, The Netherlands
Matlab/Simulink	ITG Dresden , Germany
TRNSYS-TUD	Technical University Dresden, Germany
EES	Université de Liege, Belgium
EnergyPlus	GARD Analytics, Inc., U.S.

List of Figures

List of Tables

PART I.
Chilled Water system

Chapter 1 Introduction

This specification describes several comparative and empirical test cases for a chilled water system which are dedicated to validate HVAC simulation software. It was developed within the International Energy Agency (IEA) programs: Solar Heating and Cooling (SHC) Task 34 and Energy Conservation in Building and Community Systems (ECBCS) Annex 43.

The tests are designed for testing the capability of building energy simulation programs to predict the performance of the mechanical equipment of buildings including their control systems.

All input data for simulation are provided in separate files as part of this specification.

Chapter 2 Overall Test Description and Participants

2.1 General

The software validation tests are based on a chilled water system as shown at Figure 2-1.

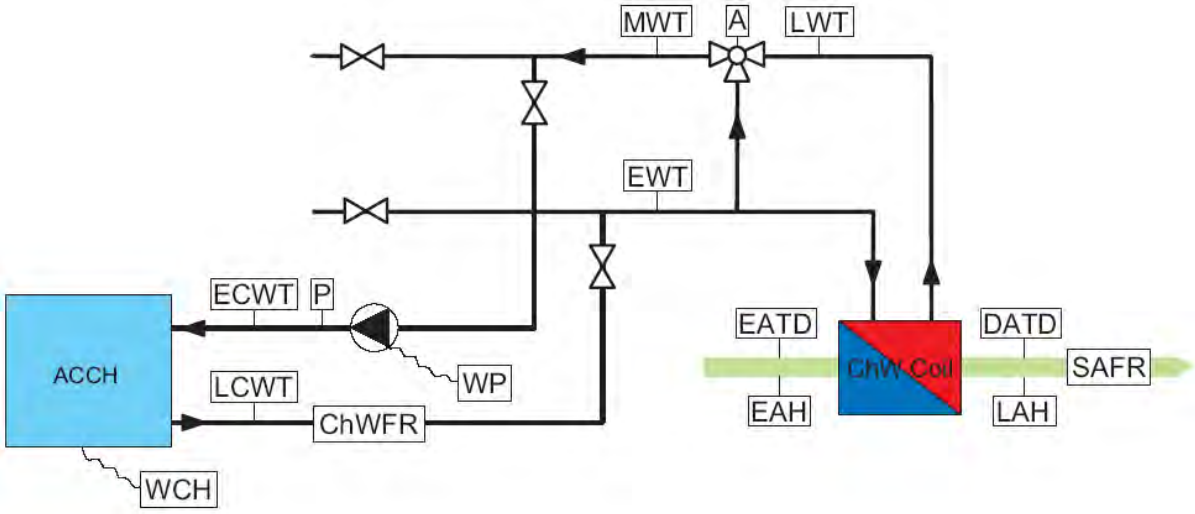

Figure 2-1 Scheme of the chilled water system with measuring points

The system consists of:

- An air-cooled scroll compressor chiller (ACCH)
- A Cooling coil located inside an air-handling unit (ChW Coil)
- Hydraulic network including a circulating pump and a mixing valve

and is used to serve cooling loads of an air conditioning system (Air Handling Unit – AHU) as depicted in Figure 2-2.

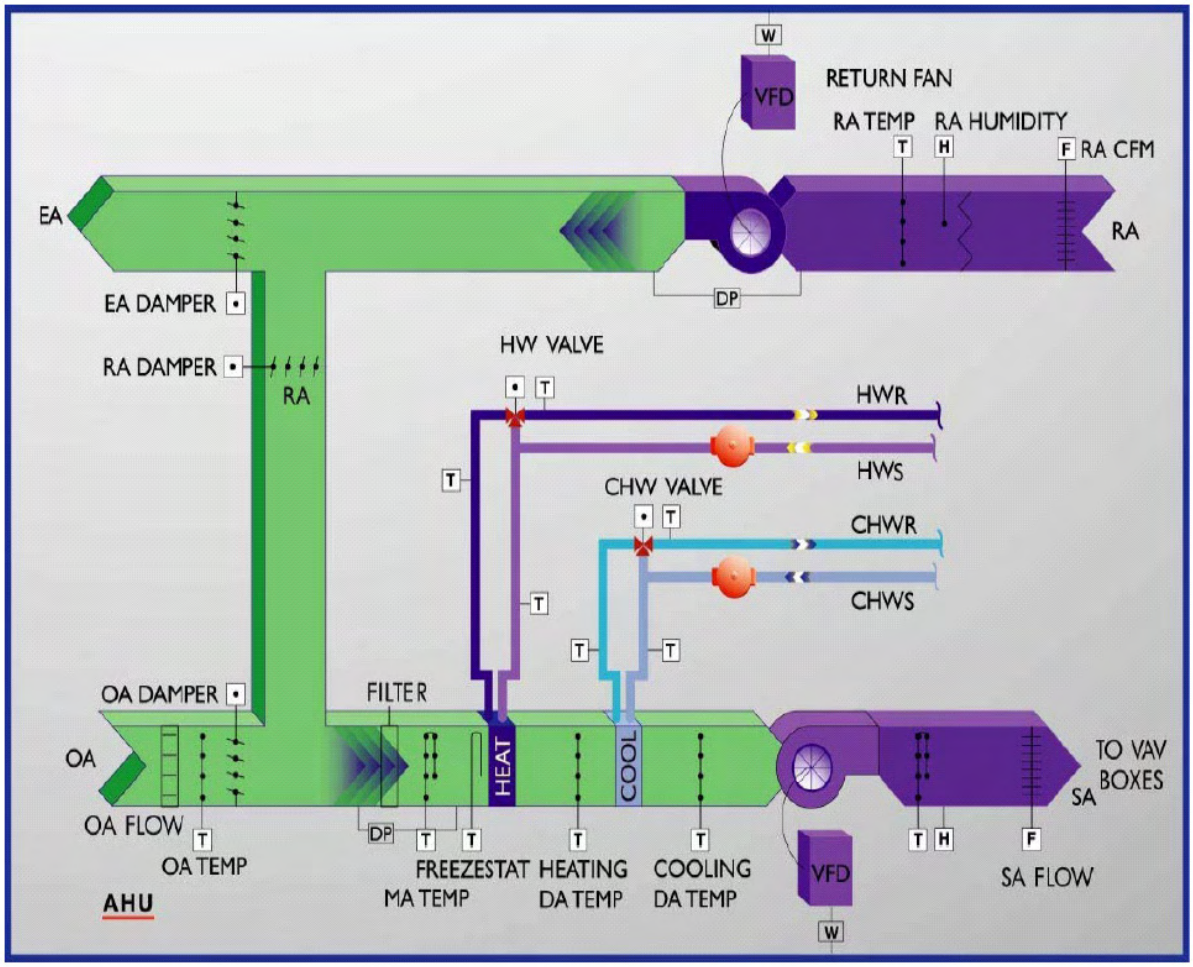

Figure 2-2 Schematic plot of AHU system with measuring points

This system is installed at the Energy Resource Station located at Ankeny, Iowa (USA). Further details about the test facility are available at http://www.energy.iastate.edu/ers/. A lot of physical data and detailed information about the mechanical system required to setup a simulation model is available via the Iowa Energy Center FTP site. This site is a limited access, password protected site. Nevertheless the ERS staff would be able to provide detailed information to interested parties in response to any requests.

The idea behind this chilled water system tests are as follows: for the validation of the simulation programs it should be possible to focus on the behaviour of the main components as well as have a look at the operation of the whole system. That is why the test specification consists of three separate exercises as summarized in Table 2-1.

Figure 2-3 Outside view of the AHU

Table 2-1 Chilled water system test case summary

# of exercise	Object of exercise	Comments
1	Chiller	- Two empirical tests Results of a comparative test that has been run in a very early stage of the project are provided.
2	Cooling coil	- A comparative test - Two empirical tests
3	Hydraulic network	No tests specifications provided but a description of the system

Some additional information about parameters and inputs required to run the simulations are given in the following chapters. There are also instructions on how to report the outputs of the simulation.

2.2 Physical properties of chilled water

For the purpose of validation two experiments have been performed at the ERS. Figure 2-4 shows time of running the experiments and the related glycol concentration of the chilled water system.

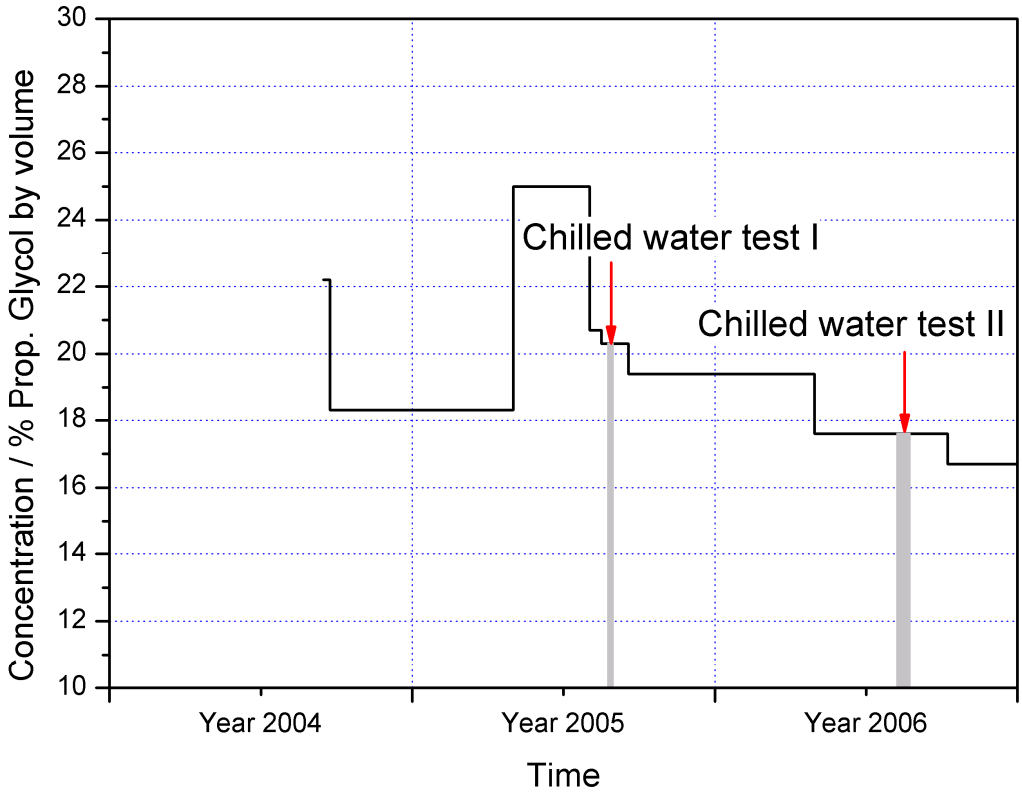

Figure 2-4: Historical to current ERS Chilled Water System Concentration

Table 2-2 and Table 2-3 contain the values for the physical properties of chilled water solutions of the heat transfer fluid DOWFROST that are 18 and 21 percent Propylene Glycol by volume, which are similar to the real concentrations.
For some comparative studies also an aqueous Ethylene Glycol solution with a 35% concentration by mass will be used. This is the mean value of the range given by the ARI-410 standard the coil performance data base on, look at chapter 4.2. Table 2-4 contains the known physical properties of this fluid.

Table 2-2 Physical properties of an aqueous solution of DOWFROST; 18 percent Propylene Glycol by volume

Physical properties		**Temperature**			
		-1.1°C (30°F)	**4.4°C (40°F)**	**10.0°C (50°F)**	**15.6°C (60°F)**
Thermal conductivity	W/(mK)	0.471	0.479	0.488	0.497
Specific heat	kJ/(kgK)	3.950	3.958	3.971	3.975
Viscosity	10^3 Pa s	3.94	3.18	2.61	2.18
Density	kg/m³	1023.8	1022.1	1020.5	1018.4

Table 2-3 Physical properties of an aqueous solution of DOWFROST; 21 percent Propylene Glycol by volume

Physical properties		**Temperature**			
		-3.9°C (25°F)	**1.7°C (35°F)**	**7.2°C (45°F)**	**12.8°C (55°F)**
Thermal conductivity	W/(mK)	0.454	0.462	0.471	0.478
Specific heat	kJ/(kgK)	3.908	3.916	3.929	3.941
Viscosity	10^3 Pa s	5.18	4.1	3.3	2.71
Density	kg/m³	1028	1026.4	1024.6	1022.7

Table 2-4 Physical properties of an aqueous Ethylene Glycol solution with 35 percent concentration by mass

Physical properties		Temperature			
		-3.9°C (25°F)	**1.7°C (35°F)**	**7.2°C (45°F)**	**12.8°C (55°F)**
Thermal conductivity	W/(mK)	0.414	0.421	0.428	0.435
Specific heat	kJ/(kgK)	3.521	3.539	3.556	3.573
Viscosity	10^3 Pa s	5.42	4.37	3.59	3.00
Density	kg/m³	1057.2	1055.7	1053.9	1052.1

2.3 Accuracy of data measurements

2.3.1 Chilled water temperature

Each of the chilled water temperature sensors receive a six point calibration across the specific range of operating temperature expected for that sensor. The temperature sensors are calibrated from the sensor to data output screen referencing a precision calibration bath with a secondary reference standard.

Based on calibration results for chiller entering (ACCH-EWT) and leaving water temperatures (ACCH-LWT), the following can be concluded for the absolute accuracy over the range of -5...20°C (23...68°F):

ACCH-EWT: Accuracy is: 0.036K (0.064°F) with maximum deviation of 0.01K (0.02°F) at 95% confidence interval.

ACCH-LWT: Accuracy is: 0.039K (0.070°F) with maximum deviation of 0.01K (0.02°F) at 95% confidence interval.

Since these temperature sensors are generally used to determine a temperature difference, these calibration results conclude a relative accuracy for the differential temperature of ACCH-EWT and ACCH-LWT that is 0.075K (0.134°F) with maximum deviation of 0.02K (0.029°F) at 95% confidence interval.

Based on this information the cooling load calculation at a chilled water flow of approximately 5.9m³/h (Propylene-Glycol mixture) has an error of

$$\begin{aligned}\Delta\dot{Q}_C &= 5.9\,\mathrm{m^3/h} \cdot 1/3600\,\mathrm{s/h} \cdot 1021\,\mathrm{kg/m^3} \cdot 3.97\,\mathrm{kJ/kgK} \cdot 0.074\,\mathrm{K} \\ &= 0.5\,\mathrm{kW}\end{aligned} \quad \textbf{(2.1)}$$

Take a look at the AHU Schematic in Figure 2-2 to determine the relative location of the temperature sensors.

2.3.2 Chilled water flow rate

The chilled water flow rate was measured using electromagnetic flowmeters. Their accuracy is depending on flow rate but higher than ±0.5%.

2.3.3 Relative air humidity and air temperature

The calibration of the sensors was conducted in December 2005. Information and accuracy statements for the sensors at that calibration are noted as follows:

The corresponding field calibration relative to these sensors was a sensor-to-data field calibration using a Thunder Scientific humidity generator, which has the accuracy of +/- 0.5% RH in the range of 10%RH – 95%RH. The sensor-to-data method eliminates all the intermediate uncertainties involved with the transducer, wiring, A/D conversion, etc. and can result in a greater accuracy for the measured value. The As Left results of that calibration were as follows:

CHWC-EAH:
The accuracy of the sensor is within +0.65%RH of the reference meter, thus the accuracy of the sensor is within +1.15%RH/-0.5%RH of the true relative humidity value (in the range of 10%RH – 95%RH).

CHWC-LAH:
The accuracy of the sensor is within +0.85%RH of the reference meter, thus the accuracy of the sensor is within +1.35%RH/-0.5%RH of the true relative humidity value (in the range of 10%RH – 95%RH).

CHWC-EAT and CHWC-LAT:
The final sensor-to-data accuracy indicates the sensor would be within +0.14°C/-0.17°C (+0.25°F/-0.31°F) of true value in the range of 10…25°C (50…77°F).

The CHWC-EAH sensor is a Vaisala HMP233 with the manufacturers stated accuracy of +/-1% RH over the range of 0% to 90% and +/-2% from 90% to 100% RH. The associated CHWC-EAT temperature sensor is rated at +/-0.10°C (+/-0.18°F) at 20°C (68°F).
The CHWC-LAH sensor is a Vaisala HMP243 with the manufacturers stated accuracy of +/- (0.5%RH plus 2.5% of reading). The associated CHWC-LAT temperature sensor is rated at +/-0.10°C (+/-0.18°F) at 20°C (68°F). An air intake distribution manifold was fabricated for continuous collection of air samples from across the face of the cooling coil to produce a better average of the cooling coil leaving air conditions. The single point temperature and humidity sensors are situated in the average air stream.

SA-TEMP:
The sensor is a platinum RTD 4-sensor array. The As-Left calibration result from a sensor-to-data calibration (performed March 2006) indicates the sensor would be within +0.11°C (+0.20°F) of true value in the range of 5…25°C (41…77°F). Note that the Supply Air Temperature sensor is located in the supply air ductwork downstream of the Supply Air Fan (see Figure 2-2).

SA-HUMD:
There is also a SA-HUMD sensor in the supply air duct downstream of the Supply Air Fan with a manufacturers stated accuracy of +/- 2% RH over the range of 10 to 90% RH at 20°C (68°F), however, the in place accuracy is uncertain since it is not on the calibration schedule.

The location of the temperature and RH sensors can be seen from the AHU Schematic in Figure 2-2. The CHWC-LAT and LAH sensors are located between the cooling coil and the supply air fan. The air from the leaving side of the cooling coil passes over the SA fan motor and into the inlet of the SA fan (a forward curved centrifugal fan) and continues out the fan discharge duct and about 7.6m (25 ft) down the duct passes over the SA-TEMP sensor and the SA-CFM airflow measuring station. As a result, the SA-TEMP includes the temperature rise across the SA fan/motor.

2.3.4 Air mass flow

The system mass flow rate should be calculated from density of the supply air as determined from the measurements of the SA-CFM volumetric flow sensor and SA-TEMP air temperature sensor. If any correction for air pressure is desired, the SA-SP duct static (gauge) pressure could be used (note that the SA-SP sensor is about 9…12 m (30…40 ft) downstream of the SA-TEMP and SA-CFM measuring station).

2.3.5 Measuring error compensation

Experimental data will be slightly corrected if necessary to get nearly equalized energy (energy at water side = energy at air side) and mass flow (moisture decrease in air = amount of condensation) balances. The corrections should be within the known error bands of sensors and will be documented for all input and output data used for validation of simulation models.

2.3.6 General

Modellers will be provided with both raw experimental data and corrected data that gives the opportunity to perform independent error compensation. Further information on sensors and equipment can be get from the before mentioned ERS ftp site.

Chapter 3 Chiller

This exercise focuses on the validation of a chiller model only. As to be seen from the schematic shown in Figure 3-1, neither the cooling coil, nor the hydraulic network is taken into consideration.

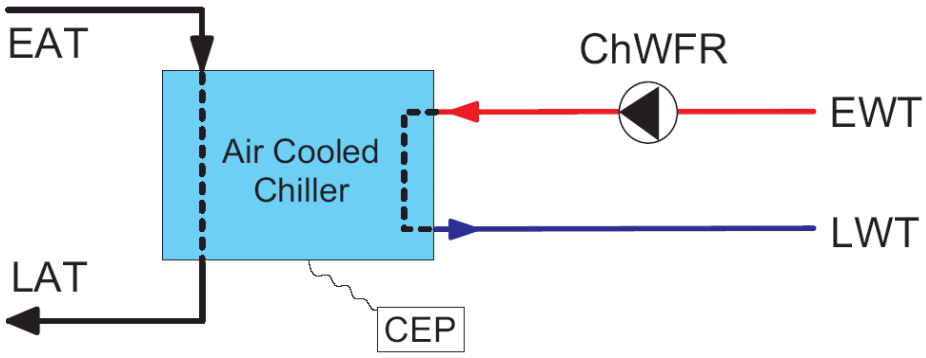

Figure 3-1 Chiller

The chiller that is examined here is an air-cooled liquid chiller manufactured by McQuay. Table 3-1 provides some general data. Most of the following descriptions are taken from the technical documentation of the chiller.

Table 3-1 Chiller general data

Chiller general data	
Manufacturer	McQuay International
Chiller Model	AGZ 010AS
Chiller type	Air Cooled Liquid Chiller
Nominal Unit @ ARI Conditions	35°C Entering Air Temperature
Capacity	34.3 kW (9.8 tons)
Flow Rate	1.51 l/s (24.0 gpm)
Leaving Water Temperature	6.7°C (44.0°F)
Full Load COP	2.84
Integrated Part Load COP	3.58
Refrigerant Type	HCFC -22
Refrigerant Circuits	1 Refrigerant Circuit
Heat Transfer Fluid	25% Propylene Glycol
Electrical Characteristics	460 Volt / 3 Phase / 60 Hz

The chiller by itself is a complete, self-contained automatic refrigerating unit that is completely assembled, factory wired, charged, and tested. It consists of air-cooled condensers, two Copeland Compliant Scroll hermetic compressors, one brazed plate-to-plate evaporator, and a complete refrigerant piping. Liquid line components include sightglass/moisture indicator, solenoid valve, and thermal expansion valve. The electrical control centre includes all equipment protection and operating controls necessary for automatic operation.
Dimensional data of the chiller can be taken from Figure 3-2.

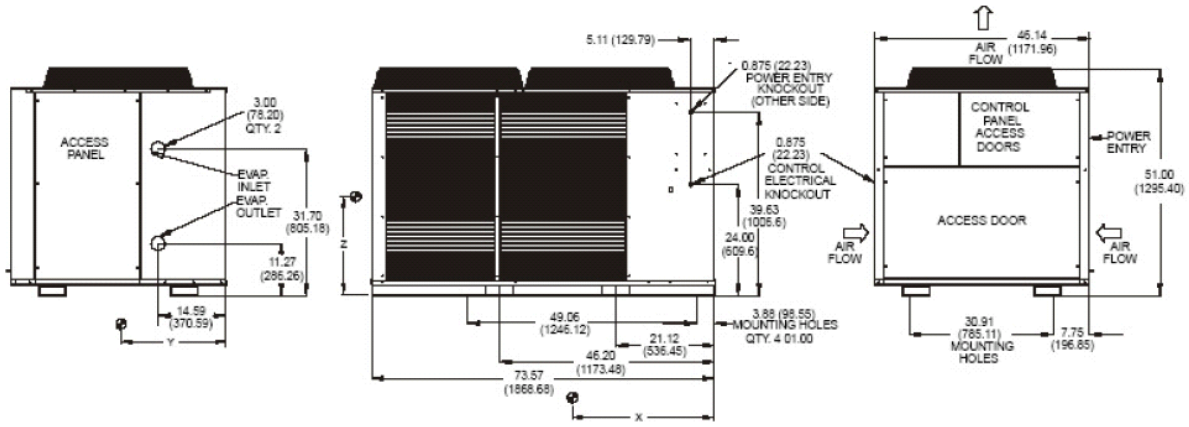

Figure 3-2 Chiller dimensional data

The chiller refrigeration circuit with all its components is shown in Figure 3-3. Figure 3-4 to Figure 3-6 offer exterior views on the chiller as well as a look into the compressor section. The Hot Gas Bypass is controlled by a solenoid valve. The solenoid valve is energized when hot gas bypass is required. The hot gas bypass valve is set to energize at 393 kPa (57 psig).

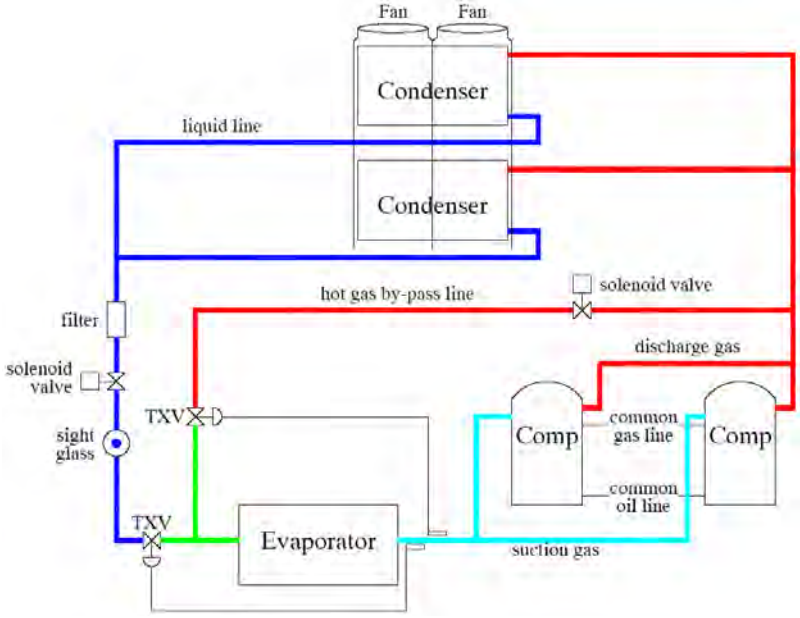

Figure 3-3 Air-cooled chiller refrigeration circuit

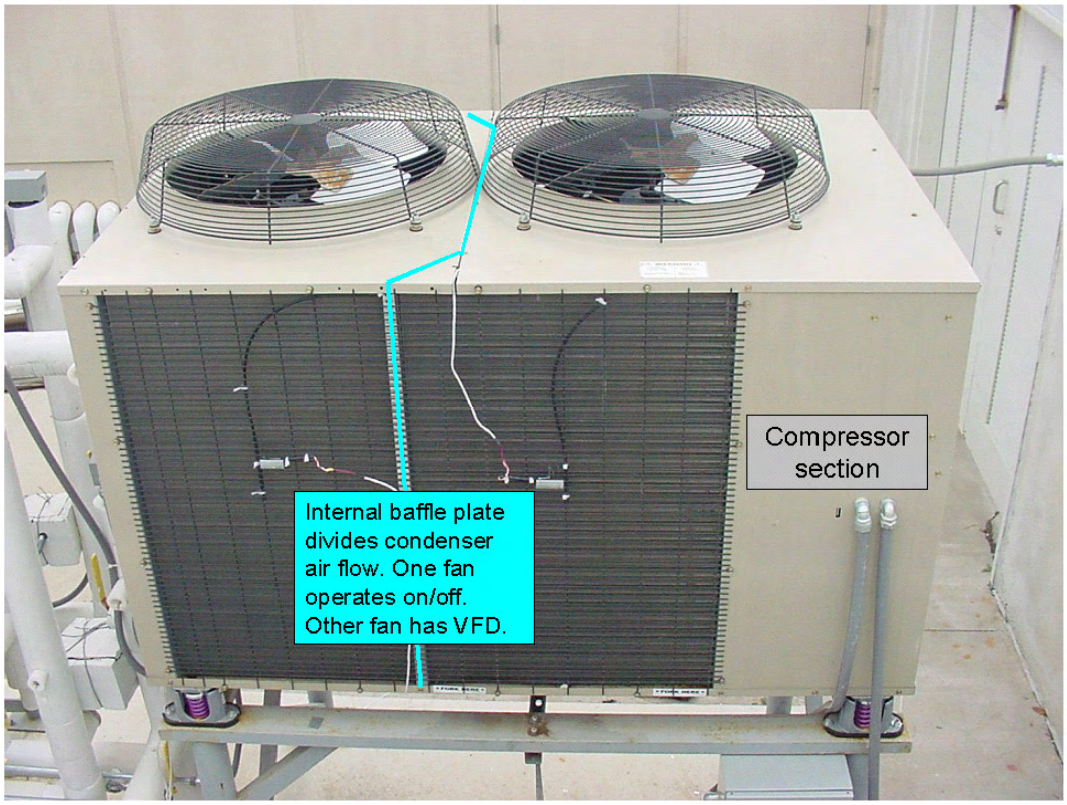

Figure 3-4 North facing side of the chiller

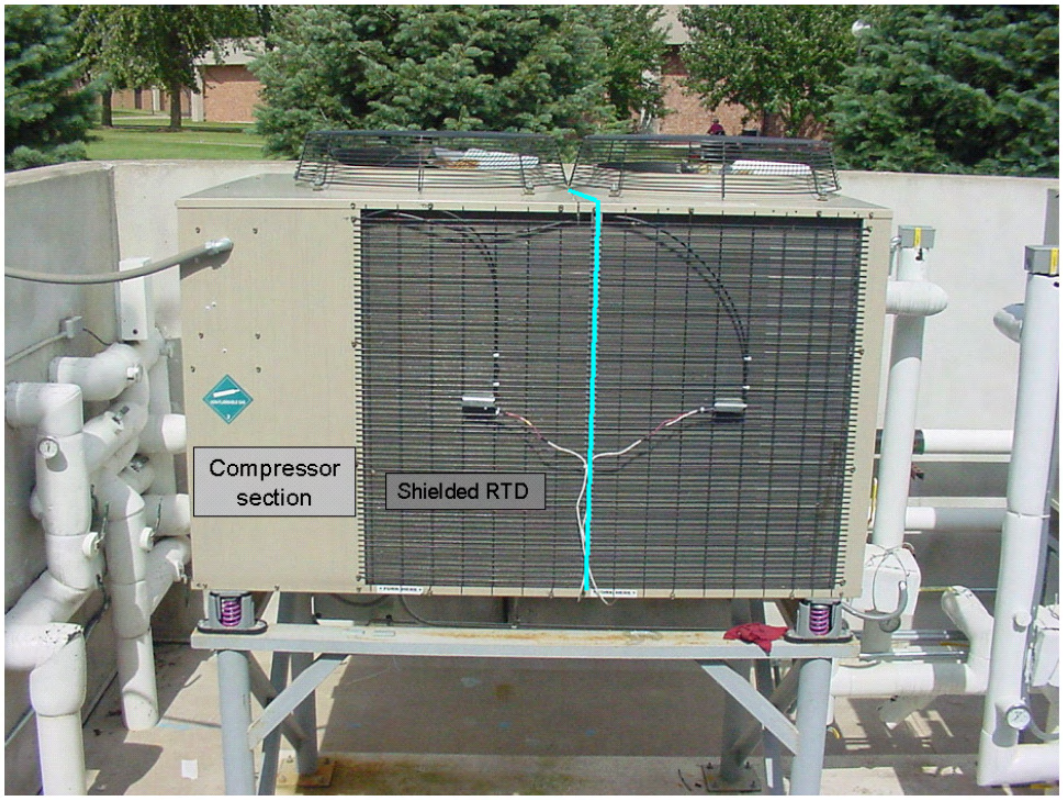

Figure 3-5 South facing side of the chiller

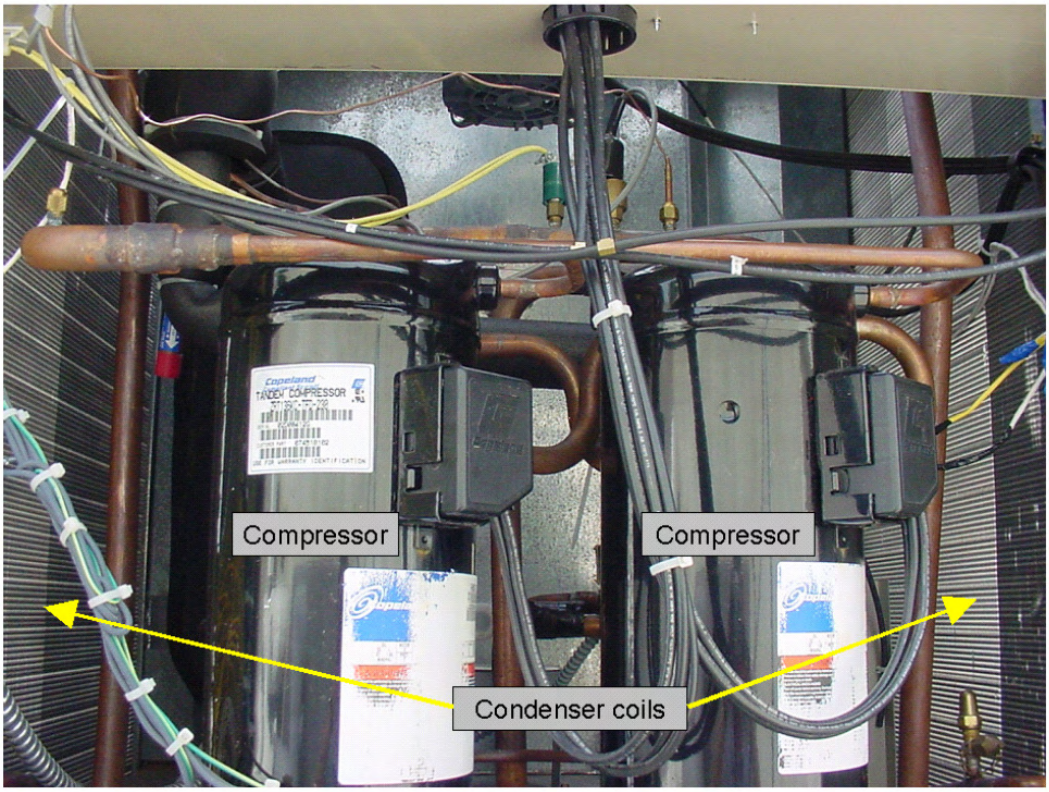

Figure 3-6 Interior of compressor section

3.1 Compressor

The chiller uses a Copeland's Compliant Scroll tandem compressor ZRT136KC-TFD that is made-up of two ZR68KC-TFD. These rugged hermetic compressors are constructed with an integral cast iron frame, cast iron scrolls, three Teflon impregnated bearings, and three oil filtration devices for each compressor.

The displacement of ZR68KC-TFD compressor is 93.013 cm^3 per revolution. This displacement corresponds to swept volume flow rate of 16.183 m^3/h at 50 Hz operation, and 19.533 m^3/h at 60 Hz operation.

The manufacturer of the equipment provides further descriptions:

"Using Copeland Compliant Scroll tandems provides two steps of modulation. One or both compressors can run, depending on the load of the system, resulting in part-load efficiency that is greater than full-load efficiency. The design also offers a large internal volume for liquid handling. In addition, the compressor is self-compensating for wear, handles liquid and debris….The compressor includes an internal power breakage for inherent thermal overload protection of the motor, four individual motor-winding sensors, a patented internal discharge temperature probe, and a patented shutdown feature that prevents reverse rotation. An internal discharge check valve helps prevent shutdown noise and comes standard with high- and low-pressure taps with Shrader valves, a sight glass, an oil level adjustment valve, and an off-cycle crankcase heater."

Table 3-2 contains most important compressor data.

Table 3-2 Compressor data

Compressor Data	
Number of Compressors	2 Compressors
Compressor Type	Hermetic Scroll ZRT136KC-TFD (made-up of two ZR68)
Compressor displacement	19.53 m³/h at 460 V / 60 Hz
Capacity Control	Compressor On / Off

The two scroll compressors are staged on and off as a function of leaving chilled water temperature, see Figure 3.8. Lead/lag is automatic and switched every ten starts (see chapter 3.9 for further details).

Performances of the compressor are presented in Table 3-3 and Table 3-4, giving the capacity and the power input of the compressor as a function of the evaporating and condensing temperatures. Rating conditions are:

- superheat at the compressor inlet: 20°F (11.11°C)
- subcooling at the condenser outlet: 15°F (8.33°C)
- ambient air temperature: 95 °F (35°C)
- 50Hz operation
- Refrigerant : HCFC R-22

Table 3-3 Capacity (W) of the compressor ZR68KC-TFD

	T_{ev} [C]									
T_{cd} [C]		-23.3	-17.8	-12.2	-6.7	-1.1	4.4	7.2	10.0	12.8
	26.7	5830	7880	10230	12980	16180	19840	21920	24120	26460
	32.2	5390	7380	9670	12310	15390	18930	20900	23040	25290
	37.8	4950	6920	9120	11660	14620	18050	19930	21980	24180
	43.3		6390	8530	11020	13860	17140	18960	20920	23040
	48.9			7880	10290	13040	16210	17960	19840	21860
	54.4				9470	12130	15180	16850	18670	20630
	60.0					11080	14010	15650	17410	19280
	65.6						12720	14300	15970	17790

The subcooling is defined as the difference between the compressor saturated discharge temperature (condensing temperature T_{cd}) and the actual liquid temperature at the expansion device. The suction superheat is the difference between the actual gas temperature at the compressor supply and the saturated suction temperature (evaporating temperature T_{ev}).

Table 3-4 Power input (W) of the compressor ZR68KC-TFD

T_{cd} [C]	T_{ev} [C]									
		-23.3	-17.8	-12.2	-6.7	-1.1	4.4	7.2	10.0	12.8
	26.7	2560	2570	2580	2620	2660	2710	2740	2780	2810
	32.2	2970	2960	2960	2970	3000	3030	3060	3090	3120
	37.8	3430	3400	3380	3380	3390	3420	3430	3460	3480
	43.3		3900	3870	3850	3850	3860	3870	3890	3910
	48.9			4420	4390	4370	4370	4380	4390	4410
	54.4				4990	4960	4950	4960	4860	4980
	60.0					5630	5610	5610	5610	5620
	65.6						6350	6340	6340	6350

The refrigerant mass flow rate swept by the compressor can be derived from the cooling capacity, the evaporating temperature, the compressor suction superheat and the condenser outlet subcooling. Table 3-5 contains refrigerant mass flow rates.

Table 3-5 Mass flow (g/s) of the compressor ZR68KC-TFD

T_{cd} [C]	T_{ev} [C]									
		-23.3	-17.8	-12.2	-6.7	-1.1	4.4	7.2	10.0	12.8
	26.7	32.3	43.0	55.0	69.0	84.9	102.9	113.0	123.7	135.0
	32.2	31.0	41.9	54.1	67.9	83.8	101.8	111.7	122.4	133.7
	37.8	29.7	40.8	53.0	66.9	82.8	100.9	110.7	121.4	132.7
	43.3		39.4	51.8	65.9	81.8	99.8	109.7	120.3	131.6
	48.9			50.1	64.3	80.4	98.5	108.5	119.0	130.3
	54.4				62.1	78.4	96.6	106.5	117.2	128.7
	60.0					75.3	93.7	103.9	114.8	126.3
	65.6						89.8	100.2	111.0	122.8

The cooling capacity is the enthalpy difference over the evaporator multiplied by the mass flow rate. The enthalpy at the evaporator inlet is equal to the one at the condenser outlet (including subcooling) and the enthalpy at the evaporator outlet is the one at the compressor suction.

3.2 Condenser Coils

The condenser coils consist of internally enhanced, seamless copper tubes arranged in a staggered row pattern. The coils are mechanically expanded into McQuay's lanced and rippled aluminum fins with full fin collars. Coil guards providing fin protection are standard equipment. Additional information is available in Table 3-6.

Table 3-6 Condenser heat exchanger data

Condenser Heat Exchanger	
Condenser Type	Copper Tube / Aluminum Plate Fin with Integral Subcooling
Number of Passes / Rows	2 Pass / Single Row Serpentine
Fin Spacing	630 Fins per meter (192 Fins per foot)
Finned Area	2134 mm wide by 1321 mm high (84 inches by 52 inches)
Coil Face Area	2.815 m² (30.3 ft²)
Tube Construction	Copper Tube
Tube outside diameter	0.95mm (3/8 inch) OD diameter
Tube Wall Thickness	0.51mm (0.020 inch) wall thickness

The chiller entering air temperature is measured at the inlet grille of the chiller condenser coils and the chillers are located in the outside mechanical area at the ERS with concrete walls near two sides of the chiller. See Figure 3-5. During periods of strong solar irradiation, this area is heated by the sun which makes the surrounding air temperature greater than the official outside air temperature that is recorded from a sensor on the weather station and is located about 25 feet above grade. The temperature differences are less during the night time hours or on cloudy days. See Figure 3-7. It is also possible that a portion of the heat discharge upwards from the top mounted condenser fans is drawn down and back into the condenser coil inlet, thereby increasing the temperature at that point.

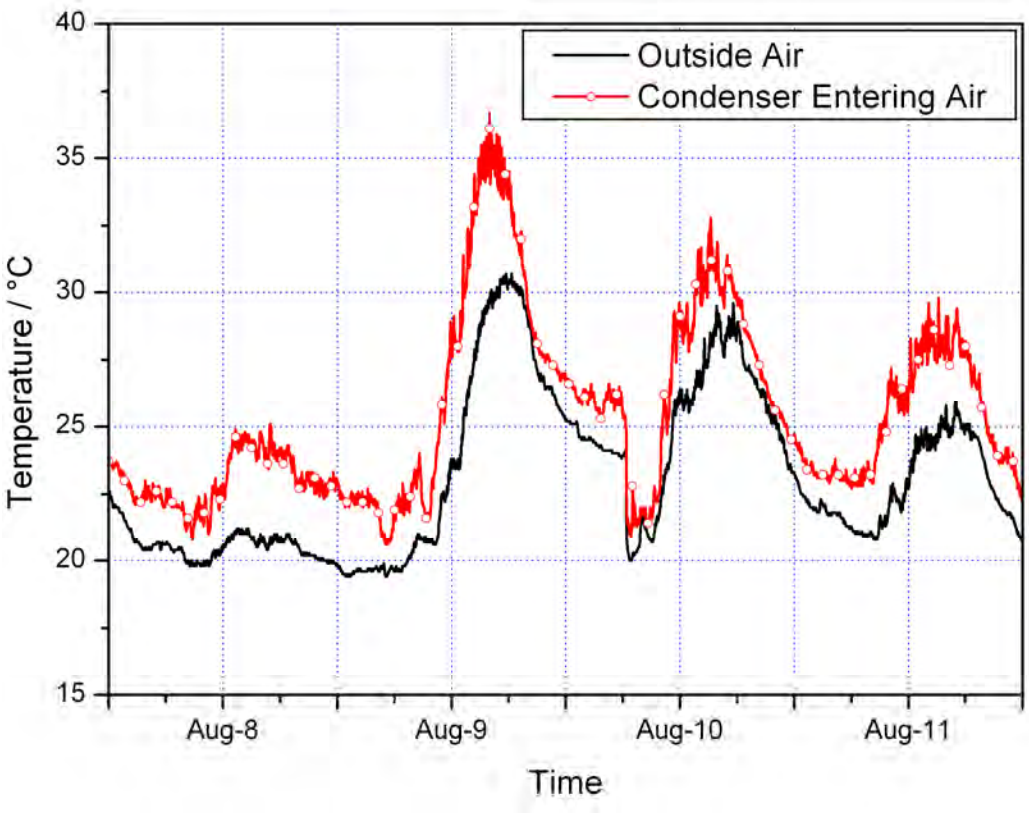

Figure 3-7 Chiller entering air temperature and outside air temperature profiles from August 8 to August 11, 2006

3.3 Condenser Fans and Motors

The direct-drive propeller fans operate in formed bell-shaped orifices at low tip speeds for maximum efficiency and minimum noise and vibration. A heavy-gauge close mesh fan guard protects each fan. Each condenser fan has a heavy-duty, three-phase TEAO motor with permanently lubricated ball bearings and inherent overload protection. Condenser fan motors are three-phase (except single-phase on No. 1 fan with SpeedTrol option) and started by their own contactors and have inherent overload protection. The condenser fans will not operate with ductwork on the fan outlet. Condenser fan data are summarized in Table 3-7.

3.4 Evaporator

The evaporator is a compact, high efficiency, single circuit, brazed plate-to-plate type heat exchanger consisting of parallel stainless steel plates. The evaporator is protected with an electric resistance heater and insulated with 19 mm (3/4“) thick closed-cell polyurethane insulation. This combination provides freeze protection down to –29°C (–20°F) ambient air temperature. The water side working pressure is 2413 kPa (350 psig). Evaporators are designed and constructed according to, and listed by, Underwriters Laboratories (UL). Evaporator data are listed in Table 3-8.

Table 3-7 Condenser fan data

Condenser Fans	
Condenser Fan Type	Direct Drive Propeller Fan
Number and Size of Fans	2 Fans at 26 inches Diameter each
Number and Type of Motors	2 Motors (1 variable & 1 fixed speed)
Fan Motor Power	0.746 kW each Fan Motor
Fan Rated Speed	1140 1/min
Condenser Rated Airflow	23700 m³/h total
Fan Sequencing	Variable Speed Fan: first on / last off Fixed Speed Fan: last on / first off

Table 3-8 Evaporator heat exchanger data

Evaporator Heat Exchanger	
Evaporator Type	Refrigerant to Liquid Flat Plate HX
Liquid Solution	25% Propylene Glycol
Liquid Flow rate	1.48 l/s (Water) 1.54 l/s (25% Propylene Glycol)
Liquid Pressure Drop	16.74 kPa (Water) 18.54 kPa (25% Propylene Glycol)
Liquid Side Volume	3.56 l
Fouling Factor	0.0001 Factor

Evaporator flow rate must fall between the minimum and maximum values shown in Table 5.6. Flow rates outside of these limits result in a chilled water Delta-T outside the operating range of the controller. Figure 5.8 shows the full evaporator pressure drop curve.

3.5 Performance

The performance data of the chiller in dependence from both leaving water temperature (LWT) as well as ambient air temperature can be derived from Table 3-9 and Table 3-10. The notes have to be considered.

Notes: 1. Ratings in accordance with ARI Standard 550/590-98.
2. Ratings based on HCFC-22, evaporator fouling factor of 0.0001, evaporator water flow of 43 l/kJ (2.4 gpm/ton) and sea level altitude.
3. kW input is for compressor only. COP (EER) is for the entire unit,

including compressors, fan motors and control power.

4. Interpolation is allowed; extrapolation is not permitted.
   Consult McQuay for performance outside the cataloged ratings.
5. For LWT below 4.4°C please refer to Application Considerations.

Table 3-9 Chiller performance data SI units

LWT (°C)	Ambient Air Temperature (°C)														
	25			30			35			40			45		
	Unit kW	PWR kW	Unit COP	Unit kW	PWR kW	Unit COP	Unit kW	PWR kW	Unit COP	Unit kW	PWR kW	Unit COP	Unit kW	PWR kW	Unit COP
5	35.0	8.0	3.4	33.7	8.8	3.0	32.3	9.7	2.7	30.9	10.7	2.4	29.4	11.8	2.1
6	36.2	8.1	3.5	34.9	8.9	3.1	33.5	9.8	2.8	32.1	10.8	2.5	30.5	11.9	2.2
7	37.5	8.2	3.6	36.2	9.0	3.2	34.8	9.9	2.9	33.3	10.9	2.5	31.7	12.0	2.2
8	38.9	8.3	3.7	37.5	9.1	3.3	36.0	9.9	2.9	34.5	10.9	2.6	32.8	12.1	2.3
9	40.2	8.4	3.8	38.8	9.1	3.4	37.3	10.0	3.0	35.7	11.0	2.7	34.0	12.2	2.4
10	41.6	8.4	3.9	40.1	9.2	3.5	38.6	10.1	3.1	36.9	11.1	2.8	35.2	12.3	2.4

Table 3-10 Chiller performance IP units

LWT (°F)	Ambient Air Temperature (°F)														
	75			85			95			105			115		
	Unit Tons	PWR kWi	Unit EER	Unit Tons	PWR kWi	Unit EER	Unit Tons	PWR kWi	Unit EER	Unit Tons	PWR kWi	Unit EER	Unit Tons	PWR kWi	Unit EER
40	9.8	7.8	11.7	9.4	8.7	10.3	9.0	9.6	9.1	8.6	10.8	7.9	8.1	12.0	6.8
42	10.2	7.9	12.0	9.8	8.8	10.7	9.4	9.7	9.4	8.9	10.8	8.2	8.4	12.1	7.0
44	10.6	8.0	12.4	10.2	8.8	11.0	9.8	9.8	9.7	9.3	10.9	8.4	8.8	12.2	7.3
46	11.1	8.1	12.8	10.6	8.9	11.3	10.2	10.2	10.0	9.7	11.0	8.7	9.2	12.3	7.5
48	11.5	8.2	13.2	11.0	9.0	11.7	10.6	10.6	10.3	10.1	11.1	9.0	9.5	12.4	7.8
50	11.9	8.3	13.5	11.4	9.1	12.0	11.0	11.0	10.6	10.5	11.2	9.3	9.9	12.5	8.0

The part load performance of the chiller is described with the data from Table 3-11.

Table 3-11 Chiller part load data certified according to ARI Standard 550/590-98 (water application)

Chiller Performance (Water Application)				
Percent of Rated Capacity	100 %	75 %	50 %	25 %
Capacity kW	34.5	25.7	17.2	8.4
Unit kW Input	12.1	7.4	4.6	2.4
COP	2.84	3.49	3.69	3.52
Entering Liquid Temp °C	12.22	10.83	9.44	8.06
Leaving Liquid Temp. °C	6.67			
Liquid Flow l/s	1.48			
Entering Air Temp. °C	35	26.7	18.3	12.8

The chiller can operate with a leaving chilled fluid temperature range of −6°C (20°F) to 16°C (60°F). A glycol solution is required when leaving chilled fluid temperature is below 4°C (40°F). The use of glycol will reduce the performance of the unit depending on concentration; see Table 3-12 and Table 3-13.

Table 3-12 Chiller performance (25 % Propylene Glycol Application)

Chiller Performance (25% Propylene Glycol Application)	
Percent of Rated Capacity	100%
Cooling Output (kW / Tons)	33.8 / 9.6
Unit kW Input	12.0
COP	2.81
Entering Liquid Temp. °C	12.22
Leaving Liquid Temp. °C	6.67
Liquid Flow l/s	1.51
Entering Air Temp. °C	35

Table 3-13 Adjustment factors for use of propylene glycol anti-freeze fluids

% P.G.	Freeze Point					
	°F	°C	Cap.	Power	Flow	PD
10	26	-3	0.987	0.992	1.01	1.068
20	19	-7	0.975	0.985	1.028	1.147
30	9	-13	0.962	0.978	1.05	1.248
40	-5	-21	0.946	0.971	1.078	1.366
50	-27	-33	0.929	0.965	1.116	1.481

3.6 Evaporator Temperature Drop Factors

Performance tables are based on a 5°C (10°F) temperature drop through the evaporator. Adjustment factors for applications having temperature drops from 3°C to 9°C (6°F to 16°F) are in 3.11. Temperature drops outside this range can affect the control system's capability to maintain acceptable control and are not recommended. The maximum water temperature that can be circulated through the evaporator in a non-operating mode is 38°C (100°F).

3.7 Altitude Correction Factors

Performance tables are based at sea level. Elevations other than sea level affect the performance of the unit. The decreased air density will reduce condenser capacity and

reduce the unit's performance. For performance at elevations other than sea level refer to 3.11. ERS is located at an altitude of 286m (938 ft).

3.8 Fouling Factor

Performance tables are based on water with a fouling factor of 0.0001 ft2h_F/Btu (0.0176 m²K/kW) per ARI 550/590-98. As fouling is increased, performance decreases.

For performance at other than 0.0001 (0.0176) fouling factor, refer to Table 3-14. Foreign matter in the chilled water system will change the heat transfer capability of the evaporator, and could increase the pressure drop and reduce the water flow. A water strainer must be installed in the return line at the entrance of the evaporator. For optimum unit operation, maintain proper water treatment.

Table 3-14 Capacity and Power dates

Altitude	Chilled Water Temperature Range		Fouling Factor							
			0.0001 (0.0176)		0.00025 (0.044)		0.00075 (0.132)		0.00175 (0.308)	
	°C	°F	Cap.	Power	Cap.	Power	Cap.	Power	Cap.	Power
Sea Level	3.3	6	0.995	0.999	0.990	0.997	0.973	0.992	0.939	0.982
	4.4	8	0.997	0.999	0.992	0.998	0.974	0.992	0.941	0.982
	5.6	10	1.000	1.000	0.995	0.998	0.977	0.993	0.944	0.983
	6.7	12	1.004	1.001	0.998	1.000	0.981	0.994	0.947	0.984
	6.8	14	1.008	1.002	1.003	1.001	0.985	0.996	0.951	0.986
	8.9	16	1.012	1.003	1.006	1.002	0.988	0.997	0.955	0.987
609.6 m 2000 ft	3.3	6	0.993	1.005	0.988	1.004	0.971	0.998	0.938	0.988
	4.4	8	0.995	1.006	0.990	1.004	0.972	0.999	0.939	0.989
	5.6	10	0.998	1.007	0.993	1.005	0.975	1.000	0.942	0.990
	6.7	12	1.002	1.008	0.997	1.006	0.979	1.001	0.946	0.991
	6.8	14	1.006	1.009	1.000	1.007	0.983	1.002	0.949	0.992
	8.9	16	1.010	1.010	1.004	1.009	0.987	1.003	0.953	0.993

3.9 Control

3.9.1 Compressors

The chiller is controlled depending on leaving water temperature. According to the control scheme Figure 3-8 the compressor stages are switched on and off.

The dead band is automatically set of 60% of the user defined temperature difference between chiller entering water temperature and the leaving water temperature set point.

$$T_{DB} = 0.6 \times \Delta T_{Evap}$$

$$\Delta T_{Evap} = T_{EWT} - T_{LWT,set}$$

Compressor start and stop is determined by the dead band and ΔT_{Start} settings. ΔT_{Start} is the number of degrees above the temperature setting that determines when the lead compressor starts.

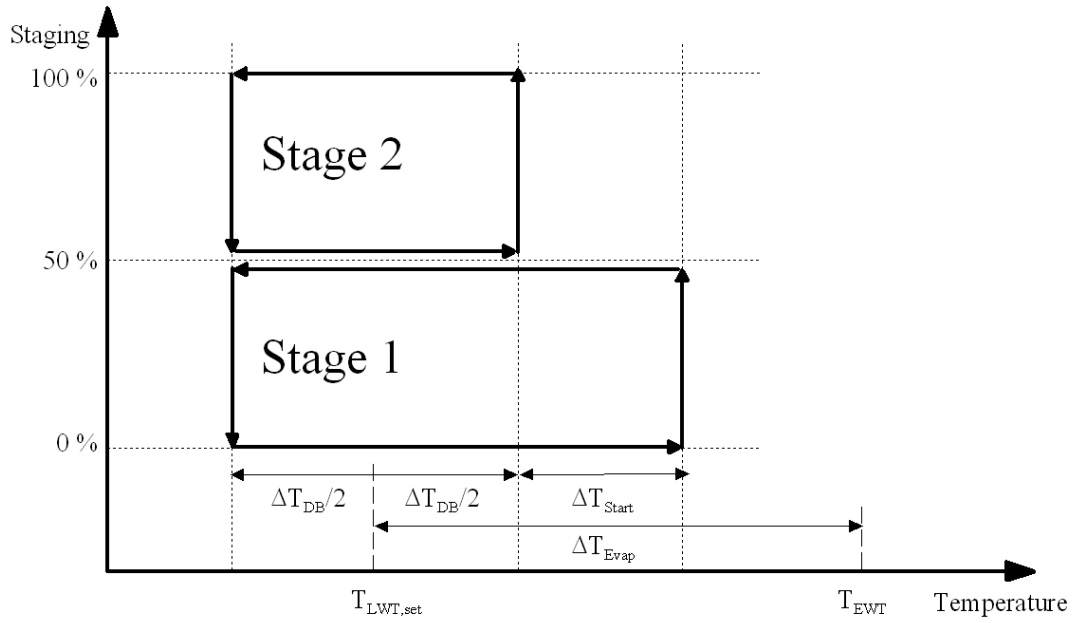

Figure 3-8 Chiller control scheme

For a warm start-up the lead compressor will start at any temperature above $\Delta T_{LWT,set} + 0.5T_{DB} + \Delta T_{Start}$. The lag will start after the start interval Δt_{up} has timed out. The chilled water temperature will begin to be pulled down. At $\Delta T_{LWT,set} - 0.5T_{DB}$ the lag compressor will shut off. If the temperature climbs above $\Delta T_{LWT,set} - 0.5T_{DB}$ within a limited time range Δt_{down}, the lead compressor will remain on. This would be normal operation. If for some reason the temperature does not rise, the lead compressor will also shut off. The lead compressor will start again when the chilled water temperature reaches $\Delta T_{LWT,set} + 0.5T_{DB} + \Delta T_{Start}$. The compressor designated as the lead will be the first to start and the last to shut off. Lead/lag designation is switched based on the number of starts. After 10 starts on Compressor #1 as lead, Compressor #2 starts as Lead for 10 starts, and then the cycle is repeated. Table 3-15 summarizes the rules for staging the compressors.
The time delays Δt_{up} and Δt_{down} are fixed as follows:

$\Delta t_{uo} = 240\,s$
$\Delta t_{down} = 30\,s$

Table 3-15 Compressor staging rules

Description	Occurs When:	Action Taken	
		Lead Compressor	Lag Compressor
Stage #1 ON	$LWT > T_{LWT,set} + (\Delta T_{DB}/2) + \Delta T_{Start}$	ON	OFF
Stage #2 ON	$\Delta t > \Delta t_{up}$ $LWT > T_{LWT,set} + (\Delta T_{DB}/2)$	ON	ON
Stage #2 OFF	$\Delta t > \Delta t_{down}$ $LWT < T_{LWT,set} - (\Delta T_{DB}/2)$	ON	OFF
Stage #1 OFF	$\Delta t > \Delta t_{down}$ $LWT < T_{LWT,set} - (\Delta T_{DB}/2)$	OFF	OFF

3.9.2 Condenser Fans

Condenser fan motors are automatically cycled in response to condenser pressure by a standard method of head pressure control called FanTrol. This function is controlled by the microprocessor, maintains head pressure and allows the unit to run at low ambient air temperatures down to 1.7°C (35°F). Fans are normally staged as follows:

Stage 1: On 1034 kPa (150 psig)
Off with unit
Stage 2: On 2000 kPa (290 psig)
Off 1172 kPa (170 psig)

Fan #1 is on with first compressor above 24°C (75°F).
The SpeedTrol method of head pressure control operates in conjunction with FanTrol by modulating the motor speed on system #1 fan in response to condenser pressure. By reducing the speed of the last fan as the condensing pressure falls, the unit can operate down to -18°C (0°F) ambient air temperature. Beside this electric power for fan operation is reduced, see Figure 3.10.

3.10 Chiller Electricity Power

The chiller has several components that consume power in the standby mode. They include one crankcase heater for each of the two compressors that is continuously on when the compressor is off. Each crankcase heater is rated at 70 W. The controller and BACNet control module for the chiller consume between 40 and 50 W and consume power any time the chiller is energized and enabled (essentially continuously). The other item is one control box heater that is cycled with a thermostat to maintain the temperature in the chiller control box and is rated at 100 W. Due to the high ambient temperature during the tests, this control box heater would not be expected to be on. At all a power of 198.8 W for the standby mode of the chiller was observed during the tests.

Figure 3-9 shows total electric power when the chiller is running. Total power input to the chiller includes both compressors, both condensers, both crankcase heaters, controller power, and control box heaters mentioned previously. Curves were extracted from experimental data. There are two curves for total electric power consumption depending on the control stages. Figure 3-10 shows a similar curve but for condenser fan power only. Condenser fan #2 was always off during the tests due to low condenser pressure. That is why there is no data available for the second fan.

I should be taken into account that pressures used in diagram are no absolute but gauge pressures.

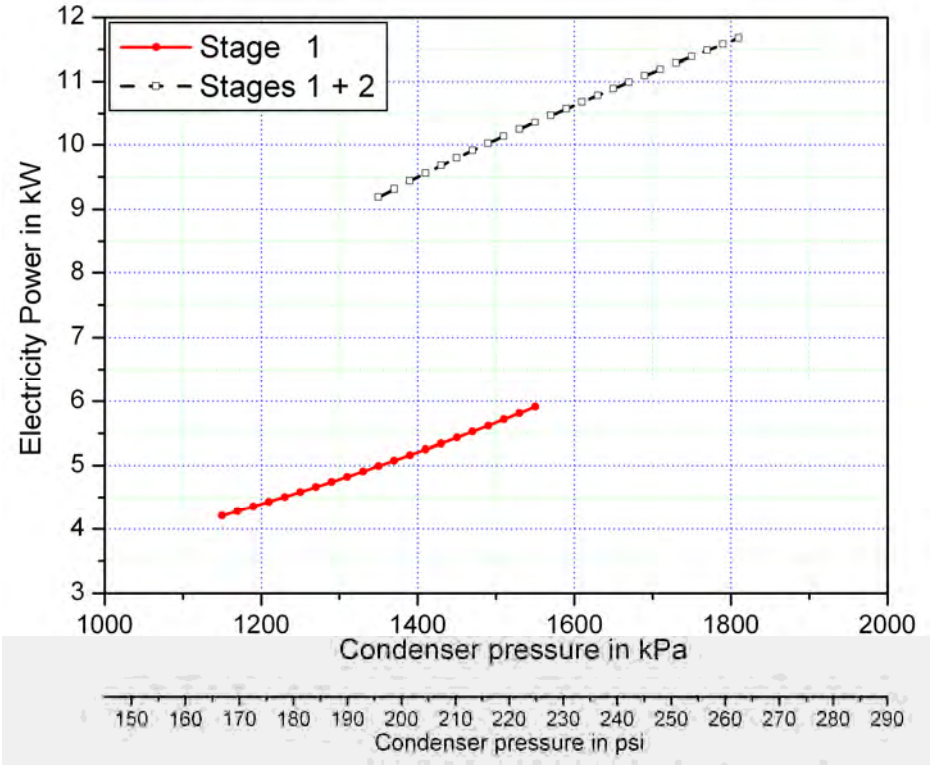

Figure 3-9 Total power of the chiller as function of condenser pressure

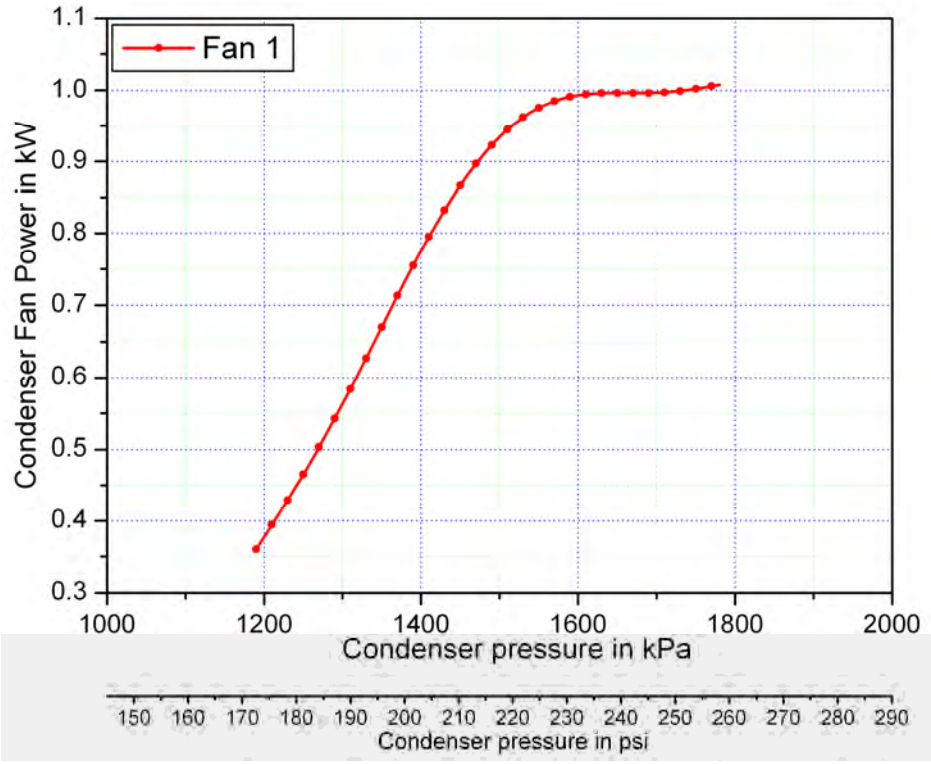

Figure 3-10 Condenser fan power as function of condenser pressure

3.11 Chiller Empirical Test I

3.11.1 Test configuration and overall goal

The goal of this empirical test is to predict chiller capacity, electric power consumption as well as conditions of chilled water leaving the chiller. Input data come from an experiment which was conducted at the ERS from August 24-30, 2005. Simulation results will be compared to the empirical data from measurements.

The chilled water temperature was set at 6°C (42°F) and the chilled water pump rpm was kept constant. Chilled water flow rate was observed as 5.5m³/h (24.3gpm). Chiller entering air temperature (EAT) is the average temperature of four RTD sensors installed at suction side of condenser and chiller leaving air temperature (LAT) is the average of two RTD sensors installed discharge side of condenser.

3.11.2 Input data

The following input data in a minute-by-minute time step for the period August 24 to August 30 are given in a separate file CHEmpInput1.txt:

Row	Shortcut	Description
1	Time	Month
2	Time	Day
3	Time	Hour
4	Time	Minute
5	EWT	Chilled water entering temperature in °C
6	ChWFR	Total chilled water flow rate through the chiller in l/s
7	EAT	Chiller entering air temperature, dry bulb in °C
8	BARP	Barometric pressure of outside air in kPa

For this test an aqueous solution of propylene glycol (DOWFROST) was used as a secondary refrigerant and the concentration of the solution was 20.3% by volume. Table 2.3 contains values for the physical properties of the fluid.

3.11.3 Outputs

The following outputs also in minute-by-minute time steps are requested and should be submitted in a single file.

Row	Shortcut	Description
1	Time	
2	EWT	Chilled water entering temperature in °C
3	LWT	Chilled water leaving temperature in °C
4	ChWFR	Total chilled water flow rate through the chiller in l/s
5	EAT	Chiller entering air temperature, dry bulb in °C
6	LAT	Chiller leaving air temperature, dry bulb in °C
7	CLT	Chiller cooling capacity in kW

8	CEP	Electric power in kW

3.12 Chiller Empirical Test II

3.12.1 Test configuration and overall goal

The goal of this empirical test is to predict chiller capacity, electric power consumption as well as conditions of chilled water leaving the chiller. Input data come from an experiment which was conducted at the ERS from August 8-23, 2006. Simulation results will be compared to the empirical data from measurements.

The chiller was operated according to the manufacturer's specification. The chilled water temperature was set at 4°C (40°F) and the chilled water pump rpm was kept constant. Average chilled water flow rate was observed as 5.9m³/h (26 gpm). Chiller entering air temperature (EAT) is the average temperature of four RTD sensors installed at suction side of condenser and Chiller leaving air temperature (LAT) is the average of two RTD sensors installed at discharge side of condenser.

3.12.2 Input data

The following input data in a minute-by-minute time step for the period August 8 to August 23 are given in a separate file CHEmpInput2.txt:

Row	Shortcut	Description
1	Time	Month
2	Time	Day
3	Time	Hour
4	Time	Minute
5	EWT	Chilled water entering temperature in °C
6	ChWFR	Total chilled water flow rate through the chiller in l/s
7	EAT	Chiller entering air temperature, dry bulb in °C
8	BARP	Barometric pressure of outside air in kPa

For this test an aqueous solution of the heat transfer fluid DOWFROST with a concentration of 17.6% Propylene-Glycol by volume was used. Table 2.2 contains the values for the physical properties of the fluid.

3.12.3 Outputs

The following outputs also in minute-by-minute time steps are requested and should be submitted in a single file.

Row	Shortcut	Description
1	Time	
2	EWT	Chilled water entering temperature in °C
3	LWT	Chilled water leaving temperature in °C
4	ChWFR	Total chilled water flow rate through the chiller in l/s
5	EAT	Chiller entering air temperature, dry bulb in °C
6	LAT	Chiller leaving air temperature, dry bulb in °C

7	CLT	Chiller cooling capacity in kW
8	CEP	Electric power in kW

Chapter 4 Cooling Coil

4.1 Geometry

The high performance fin tube coil is an integral part of a central station air handling unit manufactured by Trane. It can be used for general purposes. The horizontal coil section operates as a full coil. It consists of a chilled water single serpentine with 6 rows. Figure 4-1 shows an exterior view of the coil as well as directions of water and air flows.

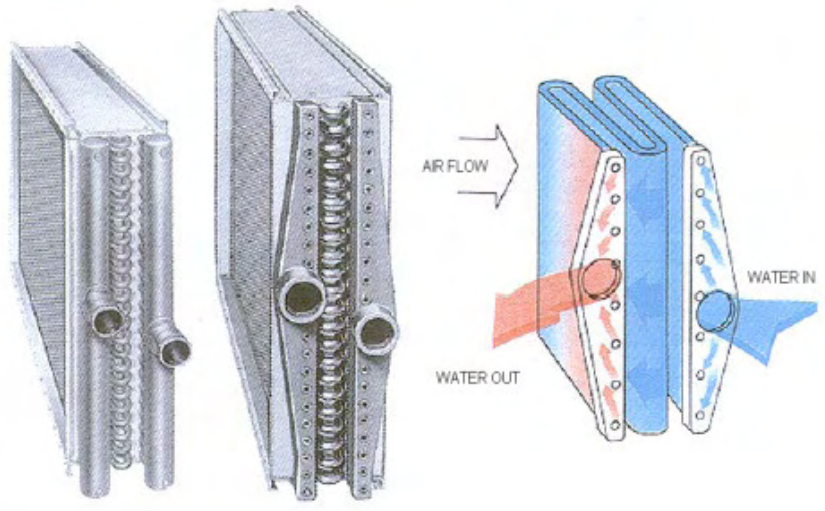

Figure 4-1 Standard water cooling coil

Some general data about the coil can be taken from Table 4-1. The given face area is the actual area. This may differ slightly from the nominal size due to rounding. The cast iron headers are brazed copper headers, extruded at tube-to-header joint for strength and low-resistance water flow.

Dimensions and sizes of the coil are given in Figure 4-2 with values C = 64.8 cm (25 1/2“), D = 28.6 cm (11 1/4“), and H = 31.8 cm (12 1/2“). All dimensions are approximately.

Figure 4-3 and Figure 4-4 allow a look at inlet and outlet sides of the cooling coil. Turbulators inside the tubes are used to reduce heat transfer resistance and to improve performance of the cooling coil. Figure 4-5 shows such a typical turbulator.

Table 4-1 Cooling Coil general data

Cooling Coil	
Manufacturer	Trane
Air Handling Unit Model	CLCH Size 06
Cooling Coil Number	Trane Type "UW" coil
Cooling Coil Type	Copper Tube / Aluminum Plate Fin
Cooling Coil Header	Drainable Copper Header
Number of Passes / Rows	6 Rows / Standard Single Serpentine
Fin Spacing	377 Fins per meter (115 Fins per foot)
Finned Area	914 mm wide by 610 mm high (36 inches by 24 inches)
Coil Face Area	0.544 m² (30.3 ft²)
Tube Construction	Copper Tube – 1/2 " O.D.
Tube outside diameter	15.9 mm
Turbulators	Water side turbulators

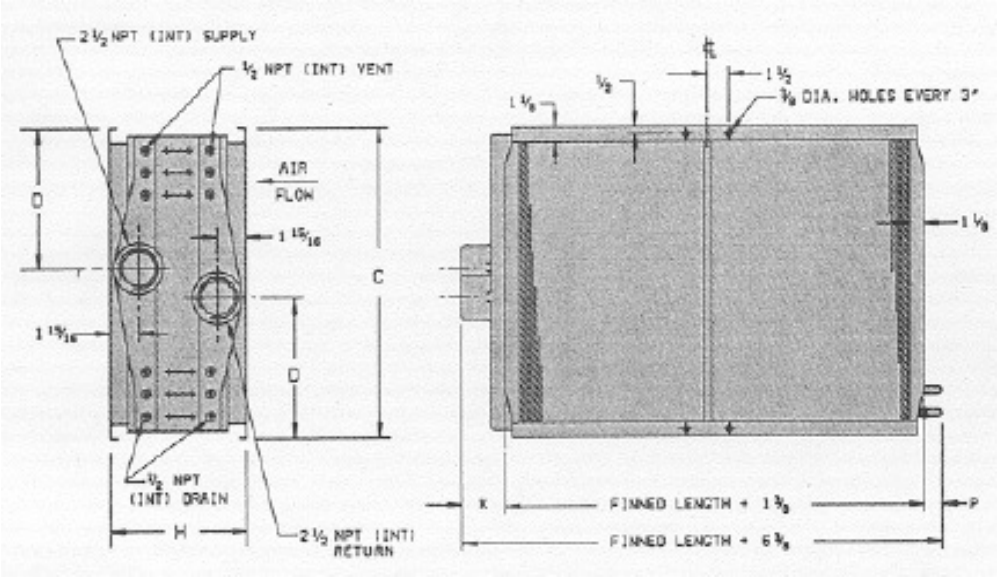

Figure 4-2 Cooling coil dimension data

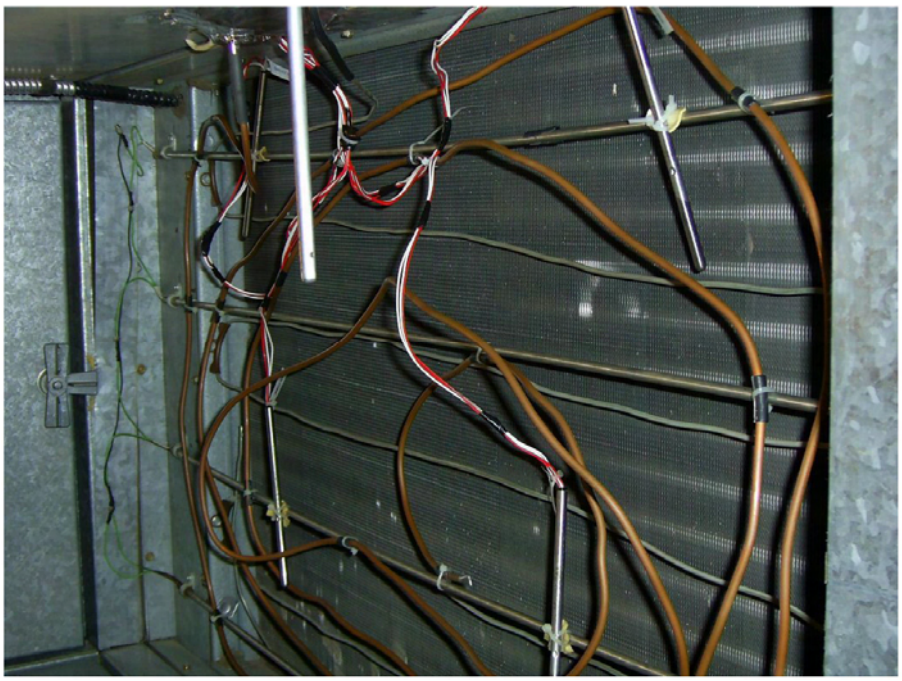

Figure 4-3 Cooling coil viewed from the entering air side of the coil

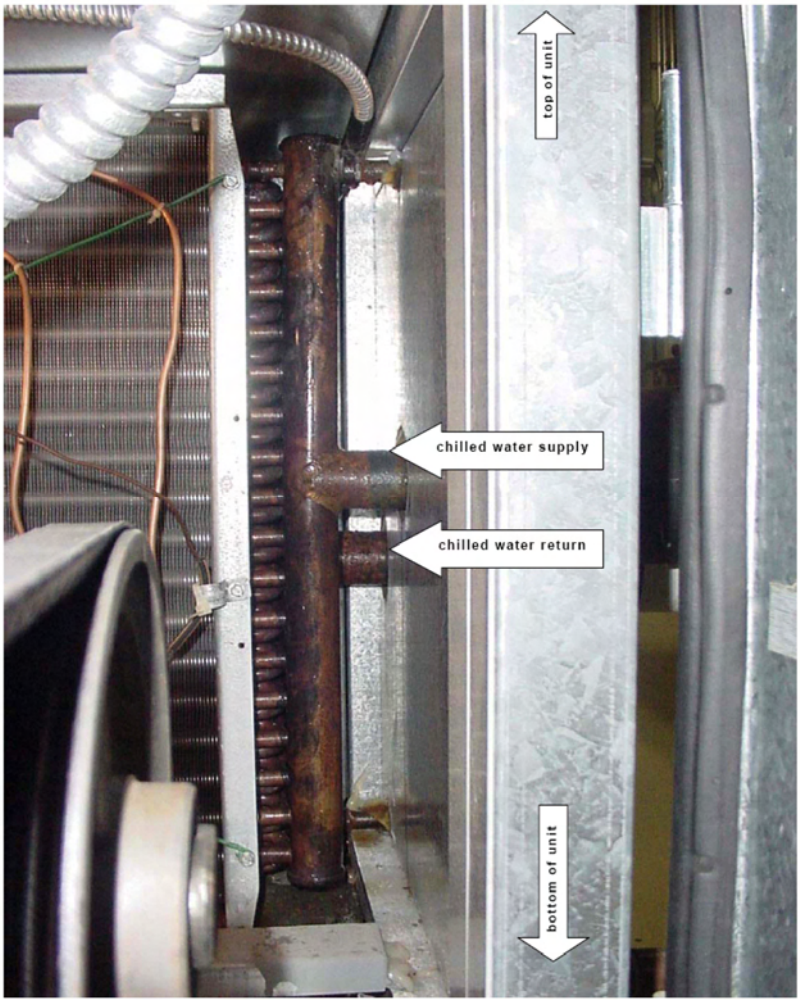

Figure 4-4 Chilled water coil header viewed from the leaving air side of the coil

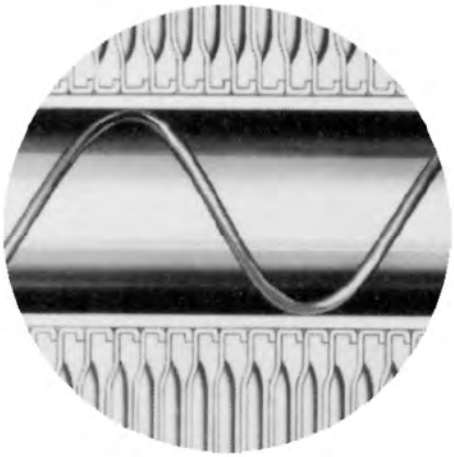

Figure 4-5 Typical turbulator [TRANE]

4.2 Performance

Information about the performance of the cooling coil can be taken from the equipment submittal. However the submittal available for this cooling coil only describes one operating state rated with ARI Standard 410[1]. From this single state again only limited knowledge about the full range of coil performance can be extracted.

All data from the equipment submittal are listed in Table 4-2.

The given coil rating is based on conditions as described in ARI-410. Values of entering temperatures as well as flow rates are within the ranges defined by the standard. It is assumed that the coil was provided with an aqueous Ethylene Glycol solution. Then the concentration by mass of this chilled water should have been 35% which is the mean value of the range given by the ARI standard. Physical properties of the Ethylene Glycol solution can be seen from Table 2-4. Performance data from Table 4-2 can thus be recalculated as follows:

$$\begin{aligned}\dot{Q} &= \dot{m} c_p \Delta\vartheta \\ &= \dot{V} \rho c_p \Delta\vartheta \\ &= 1.77 \frac{\mathrm{l}}{\mathrm{s}} \cdot 1057 \frac{\mathrm{kg}}{\mathrm{m}^3} \cdot 3.55 \frac{\mathrm{kJ}}{\mathrm{kgK}} \cdot \left(12.06^\circ C - 6.67^\circ C\right) \\ &= 35.8\,\mathrm{kW}\end{aligned} \qquad \textbf{(4.1)}$$

[1] ARI Standard 410 for forced-circulation air-cooling and air-heating coils

Table 4-2 Cooling coil performance data (Data marked with *) were calculated and are not part of the equipment submittal)

Cooling Coil Performance		
Barometric pressure*)	kPa	101.3
Entering Air Temperature	°C Dry bulb °C Wet bulb	27.8 19.2
Entering Air Relative Humidity*)	%	44.4
Entering Air Moisture*)	kg/kg	0.0104
Leaving Air Temperature	°C Dry bulb °C Wet bulb	12.5 12.2
Leaving Air Relative Humidity*)	%	96.9
Leaving Air Moisture*)	kg/kg	0.0087
Leaving Air Density	kg/m³	1.23
Air Flow Rate at leaving air conditions *)	m³/h	5430
Air Pressure Drop	kPa	0.194
Entering Liquid Temp.	°C	6.7
Leaving Liquid Temp.	°C	12.1
Liquid Flow	l/s	1.8
Liquid Pressure Drop	kPa	22.4
Total Cooling Capacity	kW	35.8
Latent Cooling Capacity*)	kW	7.3

The air flow rate, which was originally not known from the manufacture's submittal, can be estimated from given temperatures and coil capacity. For that purpose the air enthalpies at both sides of the coil were calculated as

$$h_{out} = 34.4\,\mathrm{kJ/kgK} \qquad \textbf{(4.2)}$$

The air flow rate is then

$$\begin{aligned} SAFR &= \frac{\dot{Q}_{tot}}{\rho(h_{in} - h_{out})} \\ &= \frac{35.8\,kW}{1.23\,kg/m^3 \cdot (53.7\,kJ/kgK - 34.4\,kJ/kgK)} \\ &= 5432\,m^3/h \end{aligned} \quad \textbf{(4.3)}$$

The latent cooling capacity was defined by the following equation.

$$\begin{aligned} \dot{Q}_{lat} &= SAFR \cdot \rho_{air} \cdot (x_{in} - x_{out}) \cdot \Delta h_V \\ &= 5432\,m^3/h \cdot 1.23\,kg/m^3 \cdot (10.4\,g/kg - 8.7\,g/kg) \cdot 2.45\,kJ/kg \\ &= 7.3\,kW \end{aligned} \quad \textbf{(4.4)}$$

In addition to the nominal performance data of Table 4-2 which are given by the manufacturer the performance data for different quasi-steady state part load conditions were extracted from experimental data. See Tables 4.4 and 4.6 for further details.

4.3 Cooling Coil test logic

The validation of a cooling coil model in the context of this IEA task should be done according to the overall test logic that is shortly described in this chapter.

There have been three tests created for cooling coil validation purposes:

- Comparative test (chapter 4.4),
- Empirical test I (chapter 4.5),
- Empirical test II (chapter 4.6).

The tests should be run step-by-step beginning with the comparative test. The idea behind this consecutive process is to start with a simulation model that has been calibrated based on some general information about coil performance that was available from the manufacturer submittal and to end with a model calibrated based on detailed experimental data collected from coil operation in a real plant. From the manufacturer submittal only one single point of coil performance was known (see Table 4-2) that roughly represents a full load coil performance. No more information about part load performance is available for running the comparative tests. Thus the modeller has to run the comparative tests with their own standard model part load approach that can considerably differ between models. The additional calibration points provided to the modeller when running the empirical tests should allow calibrating the model with respect to both part load performance as well as real installation and operating conditions (i.e. physical properties of the chilled water) that differ from the performance conditions found in the manufacturer submittal.

The overall cooling coil test logic is illustrated in Figure 4-6. It also refers to some diagnostic checks that can help to find the probable cause of errors, i.e. when the model predictions do not agree with results neither from other models nor from experimental data. Those diagnostic checks are described in Chapter 6.2.5.

Since there is no truth standard (as for instance an analytical solution would be) it is up to the modeller to decide whether their results are in agreement for a specific test case, or whether there is disagreement that requires further examination of their program or inputs.

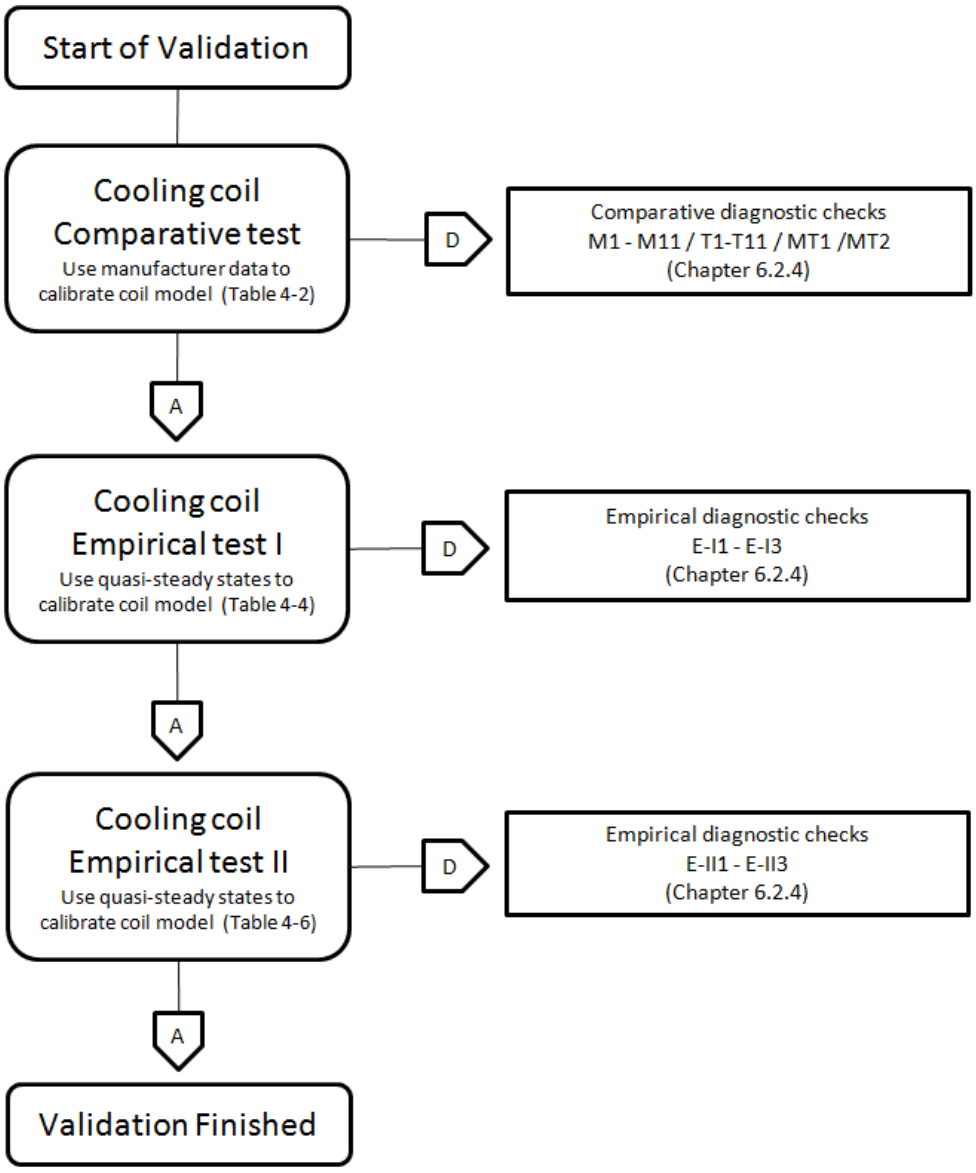

Abbreviations: A=Agree; D=Disagree

Figure 4-6 Cooling coil overall test logic

4.4 Cooling Coil comparative test

4.4.1 Test configuration and overall goal

The goal of this comparative test is to predict both cooling loads as well as operational conditions of water entering the coil required to maintain a given set point of discharge air temperature. The prediction horizon is limited to the months May - September. Outside air conditions are taken from a TMY2 data set.

There are in general two different configurations that can be used to control the performance of the coil:

1. Variable water flow rate with a constant water inlet temperature (m_{var})
   The performance of the cooling coil is controlled by changing the flow rate through the coil. A schematic of the hydraulic circuit is depicted in Figure 4-7. The total chilled water flow rate ChWFRSystem is the flow rate through the cooling coil ChWFRCoil plus the flow rate in the by-pass line.

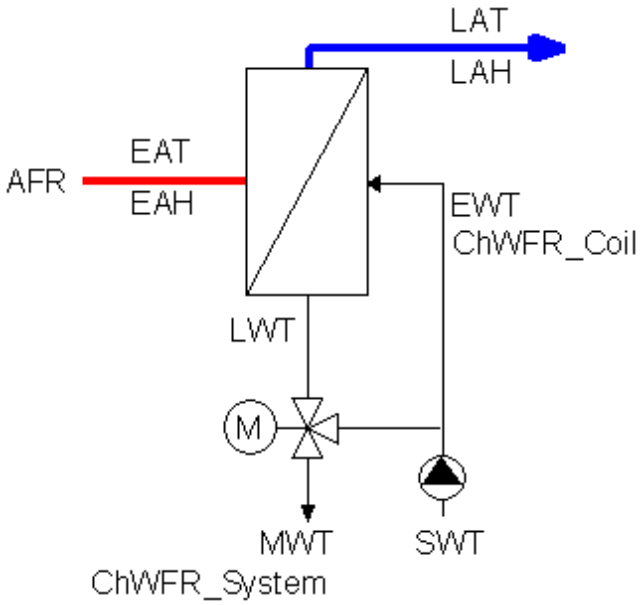

Figure 4-7 Cooling coil with variable water flow rate

   The maximum water flow rate entering the coil is 1.77 l/s, which represents the nominal value given in Table 4-2. The entering water temperature and supply water temperature are identical but mixing water temperature is different from leaving water temperature depending on the flow rate in the by-pass.
   This configuration describes the built-in situation of the cooling coil at the ERS. For this reason it also could be used for the empirical validation of the cooling coil model (see Chapter 4.5 and Chapter 4.6).

2. Constant water flow rate with a variable water inlet temperature (T_{var})
   The performance of the cooling coil is controlled by changing the coil entering water temperature. A schematic of the hydraulic circuit is depicted in Figure 4-8.

The total chilled water flow rate ChWFRSystem is the flow rate through the cooling coil ChWFRCoil minus the flow rate in the by-pass line.

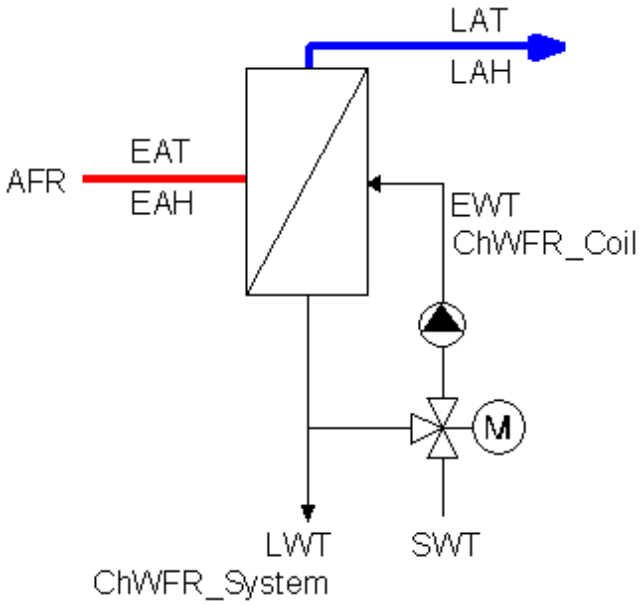

Figure 4-8 Cooling coil with constant water flow rate

The constant water flow rate entering the coil is fixed at 1.77 l/s, which represents the nominal value given in Table 4-2. The coil entering water temperature results from the mixture of supply water temperature and coil leaving water temperature.

This comparative test does not take into consideration the action of the control valve and focuses on the operation of the cooling coil only. If there is no cooling load the chilled water pump has to switch off.
For further information on input data air side and water side please refer to Chapter 4.4.2.

4.4.2 Input data

The outside air input conditions are taken from the Des Moines, Iowa TMY2 data set that is distributed as a part of this specification. The TMY2 weather is used for the comparative test only. It is average weather data for Des Moines, Iowa and does not represent any actual specific on-site weather data for the ERS.
It is assumed that there is 100% outside air with no re-circulated air through the coil. Furthermore two different systems have to be taken into consideration regarding the air flow rate:

1. Constant air volume (CAV)
   The air flow rate is constant all the time at 3000m³/h.
2. Quasi-Variable air volume (VAV)
   The air flow rate switches between 2000m³/h (6 p.m. to 7 a.m.) and 5000m³/h (7 a.m. to 6 p.m.); see Figure 4-9.

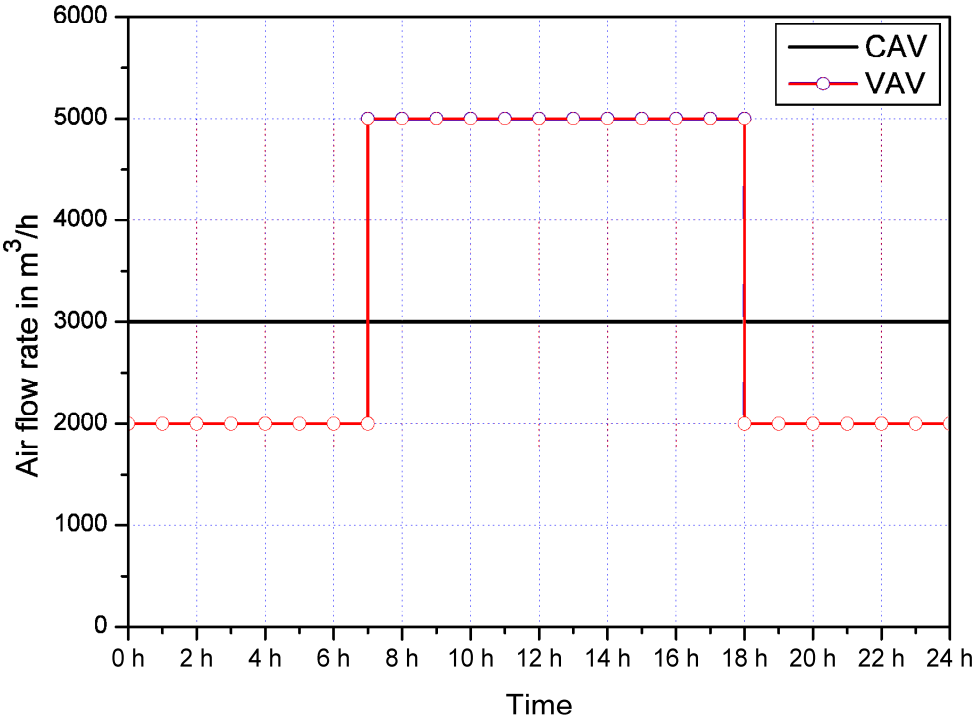

Figure 4-9 Air flow rate daily profile

The time schedule given refers to time of the day. A daylight saving effects was not taken into account. Air flow rate is defined at supply air conditions. As the impact of the supply fan on air side conditions is neglected supply air conditions (temperature, humidity) are identical to coil leaving air conditions.

The discharge air set point temperature is fixed at also two different levels:

1. Low set point temperature
   The discharge air temperature is set to 13°C (55.4°F), which should lead to a cooling coil that certainly operates in a wet regime.
2. High set point temperature
   The discharge air temperature is set to 18°C (64.4°F), which should lead to a operation in a predominant dry regime.

Both set points do not vary and are thus to be held as a constant for the entire simulation period. The chilled water supply temperature (SWT) is constant at 6°C (42.8°F). Chilled water supply temperature and entering water temperature are identical if the coil operates with a variable water flow rate.

The atmospheric pressure inside the coil is set to 98 kPa. Physical properties of chilled water can be seen from Chapter 2.2.

Table 4-3 gives an overview of comparative test cases that should be implemented.

4.4.3 Outputs

The following outputs also in minute-by-minute time steps are requested and should be submitted in a single file.

Row	Shortcut	Description
1	Time	
2	EAT	Entering air temperature, dry bulb in °C
3	EArH	Entering air relative humidity in %
4	EAH	Entering air humidity in kg/kg
5	LAT	Discharge/Leaving air temperature, dry bulb in °C
6	LArH	Discharge/Leaving air relative humidity in %
7	LAH	Discharge/Leaving air humidity in kg/kg
8	AFR	Air flow rate in m³/h
9	EWT	Chilled water coil entering temperature in °C
10	LWT	Chilled water coil leaving temperature in °C
11	$ChWFR_{Coil}$	Chilled water flow rate through the coil in l/s
12	UA	Overall UA-Value of the coil in kW/K
13	CLT	Total cooling load in kW
14	CLS	Sensible cooling load in kW
15	CLL	Latent cooling load in kW

The overall UA-Value of the coil has to be calculated from sensible cooling load and mean logarithmic temperature difference ΔT_m using Eq.(4.5).

$$UA = \frac{CLS}{\Delta T_m} \tag{4.5}$$

Mean logarithmic temperature difference ΔT_m is defined by Eq.(4.6)

$$\Delta T_m = \frac{(LWT - EAT) - (EWT - LAT)}{ln\frac{LWT - EAT}{EWT - LAT}} \tag{4.6}$$

It should me mentioned that UA-value calculated with Equation 4.5 is not equal to the dry UA-value. The so calculated UA-value is lower than the dry UA-value; only in the case that there is no condensation both UA-values are identical.

Table 4-3 Cooling coil comparative test case matrix

Test Case	Configuration	Air Flow	Fluid	DCA-ST
CC100	m_{var}	CAV	35% Ethylene Glycol	13
CC120				18
CC140			18% Propylene Glycol	13
CC160				18
CC200		VAV	35% Ethylene Glycol	13
CC220				18
CC240			18% Propylene Glycol	13
CC260				18
CC300	T_{var}	CAV	35% Ethylene Glycol	13
CC320				18
CC340			18% Propylene Glycol	13
CC360				18
CC400		VAV	35% Ethylene Glycol	13
CC420				18
CC440			18% Propylene Glycol	13
CC460				18

4.5 Cooling Coil Empirical Test I

4.5.1 Test configuration and overall goal

The goal of this empirical test is to predict cooling loads as well as conditions of both air and water leaving the coil. Input data come from an experiment which was conducted at the ERS from August 24-30, 2005. Simulation results will be compared to the empirical data from measurements.

The test configuration corresponds to a coil with variable water flow as described in Figure 4-7. The three-way chilled water control valve was modulated to produce a constant supply air temperature. An exception to this condition occurred when the system load exceeded the chiller capacity.

In addition to the nominal performance data of Table 4-2 which are from the manufacturer submittal four quasi-steady state points extracted from the experimental data are given in Table 4-4 and can be used to calibrate the cooling coil model.

Table 4-4 Quasi-steady state points based on experimental data for test I (Data marked with *) have been calculated and are not part of the recorded experimental data)

Cooling Coil Performance I		#1	#2	#3	#4
Barometric pressure*)	kPa	97.8	98.1	98.4	98.4
Entering Air Temp.	°C	22.2	22.5	22.9	23.4
Entering Air Relative Humidity*)	%	51.2	50.3	68.5	65.0
Entering Air Moisture*)	kg/kg	0.0088	0.0088	0.0120	0.0121
Leaving Air Temp.	°C	11.8	11.7	12.6	11.7
Leaving Air Relative Humidity*)	%	96.3	96.3	100	100
Leaving Air Moisture*)	kg/kg	0.0086	0.0085	0.0093	0.0088
Air Flow Rate at coil leaving air conditions*)	m³/h	2910	3786	2834	3200
Entering Liquid Temp.	°C	4.60	6.27	7.15	4.74
Leaving Liquid Temp.	°C	12.14	10.95	11.05	9.10
Mixing Liquid Temp.	°C	6.34	8.72	9.81	8.44
Liquid Flow*)	l/s	0.36	0.79	1.04	1.28
Total Cooling Capacity*)	kW	10.91	15.02	16.32	22.24
Latent Cooling Capacity*)	kW	0.55	0.92	6.61	9.25

4.5.2 Data compensation

For the cooling coil empirical test I mainly experimental data of relative air humidity had to be compensated whereas air and water temperatures underlay small changes only. Compensation rules were found manually with regard to

- Air and water side energy balance at the coil.
  This balance is shown for the whole test period in Figure 6-46.
- Amount of condensation that was re-calculated from experimental data and compared to the measurements.
- Accuracy of sensors.

Figure 4-10 and Figure 4-11 show temperature and humidity compensations of experimental data. The air and water side energy balance of the coil show good agreement due to data compensation. See Figure 6-48 for further details.
Performance data given in Table 4-4 represent compensated experimental data not raw data from the measurements.
The file CCEmpInput1_raw.txt contains uncompensated raw experimental data where also leaving water temperature, mixed water temperature and chilled water system flow rate are given instead of chilled water flow rate through the coil.

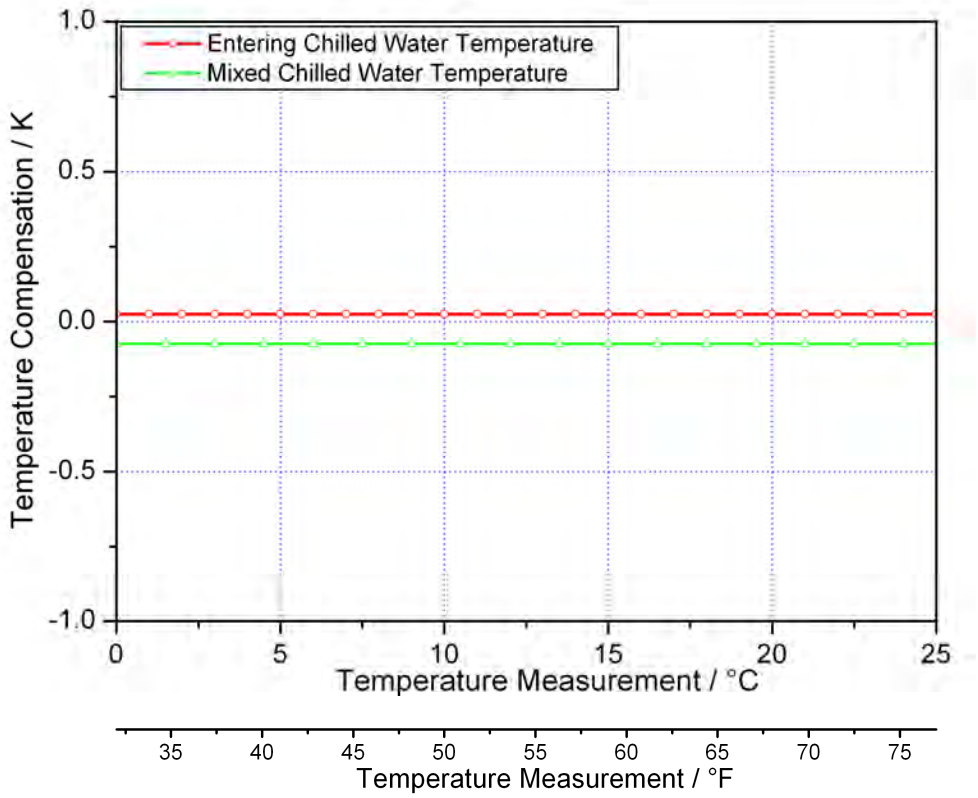

Figure 4-10 Cooling coil empirical test I - Compensation of water temperature measurements

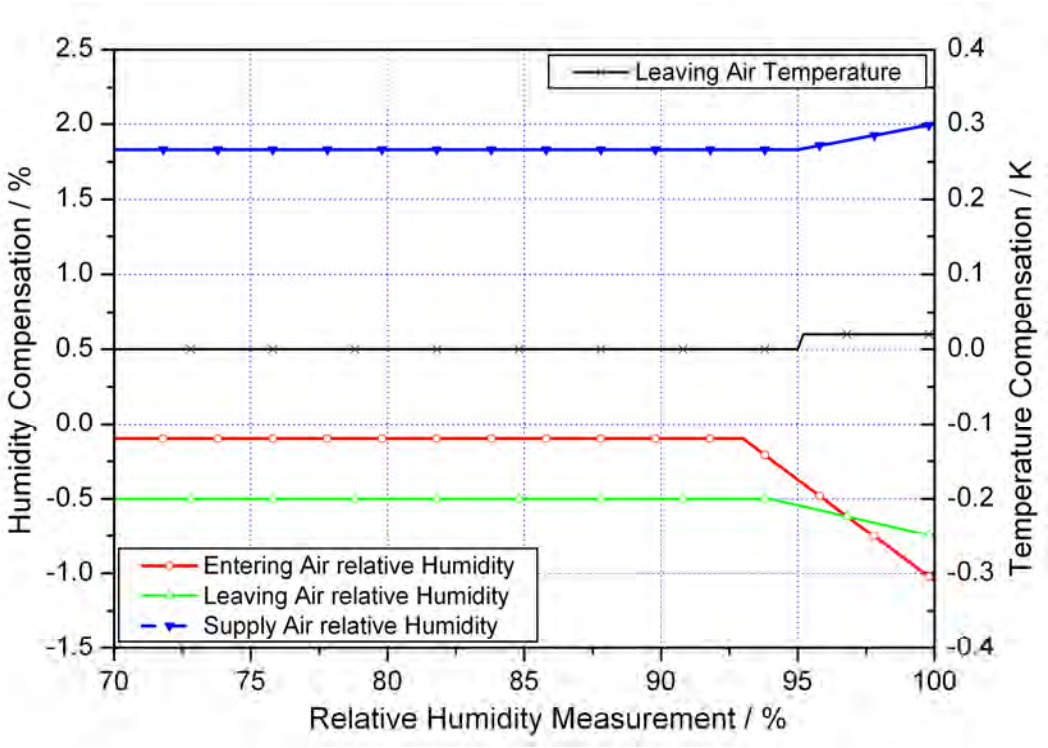

Figure 4-11 Cooling coil empirical test I- Compensation of air humidity and air temperature measurements

4.5.3 Input data

The following input data in a minute-by-minute time step for the period August 24 to August 30 are given in a separate file CCEmpInput1.txt:

Row	Shortcut	Description
1	Time	Month
2	Time	Day
3	Time	Hour
4	Time	Minute
5	EAT	Entering air temperature, dry bulb in °C
6	EArH	Entering air relative humidity in %
7	AFR	Air flow rate in m³/h
8	AFR_T	Temperature of given air flow rate AFR
9	AFR_rH	Relative Humidity of given air flow rate AFR
10	EWT	Chilled water entering temperature in °C
11	$ChWFR_{Coil}$	Chilled water flow rate through the coil in l/s
12	BARP	Barometric pressure of outside air in kPa

The water entering temperature is not really constant and varies from 4 to 9°C as to be seen from Figure 4-12 due to the operation of the chiller plant.

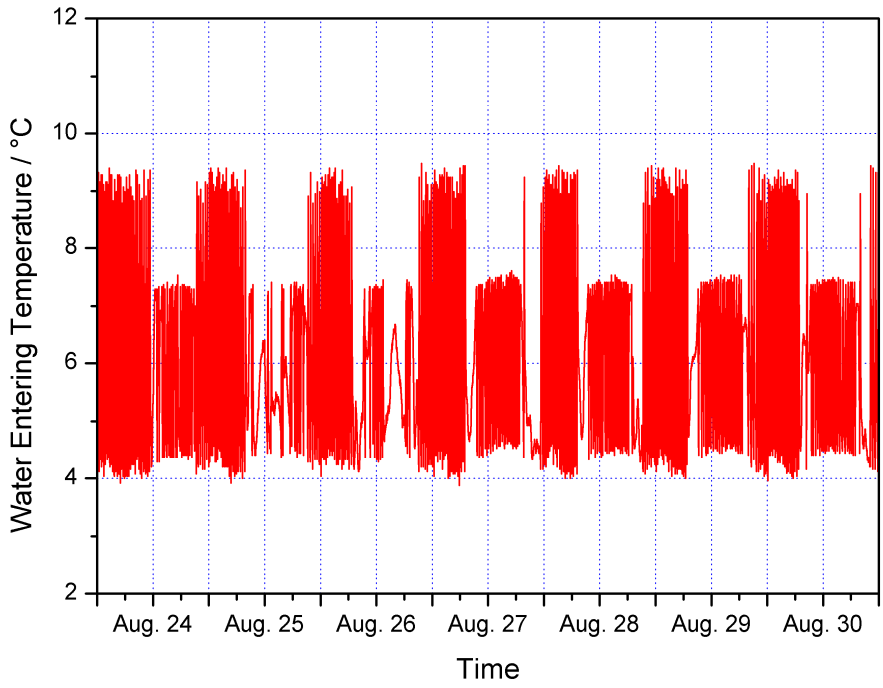

Figure 4-12 Water temperature entering the cooling coil

Chilled water flow rate through the coil has not been measured but was calculated based on the total flow rate from mass and energy balances at the three-way valve (see Figure 4-7) by Eq.(4.7).

$$\mathrm{ChWFR_{Coil}} = \mathrm{ChWFR_{System}} \frac{\mathrm{MWT} - \mathrm{EWT}}{\mathrm{LWT} - \mathrm{EWT}} \qquad \textbf{(4.7)}$$

For this test an aqueous solution of propylene glycol (DOWFROST) was used as a secondary refrigerant and the concentration of the solution was 20.3% by volume. Table 2.3 contains values for the physical properties of the fluid.

4.5.4 Outputs

The following outputs also in minute-by-minute time steps are requested and should be submitted in a single file.

Row	Shortcut	Description
1	Time	
2	EAT	Entering air temperature, dry bulb in °C
3	EArH	Entering air relative humidity in %
4	EAH	Entering air humidity in kg/kg
5	LAT	Discharge/Leaving air temperature, dry bulb in °C
6	LArH	Discharge/Leaving air relative humidity in %

7	LAH	Discharge/Leaving air humidity in kg/kg
8	AFR	Air flow rate in m³/h
9	EWT	Chilled water coil entering temperature in °C
10	LWT	Chilled water coil leaving temperature in °C
11	$ChWFR_{Coil}$	Chilled water flow rate through the coil in l/s
12	UA	Overall UA-Value of the coil in kW/K
13	CLT	Total cooling load in kW
14	CLS	Sensible cooling load in kW
15	CLL	Latent cooling load in kW

The overall UA-Value of the coil has to be calculated based on the mean logarithmic temperature difference ΔT_m which is defined by Eq.(4.6).

4.6 Cooling Coil Empirical Test II

4.6.1 Test configuration and overall goal

The goal of this empirical test is to predict cooling loads as well as conditions of both air and water leaving the coil. Input data come from an experiment which was conducted at the ERS from August 8 to August 23, 2006 and tested cold dry, cold humid, hot dry and hot humid conditions before the cooling coil. Simulation results will be compared to the empirical data from measurements.

Hot climate conditions of air entering the cooling coil have been artificially generated using the heating coil. Also steam from a humidifier was injected in the return duct for the cold humid and hot humid tests. Hot humid test was conducted twice, one with the humidifier but without outside air and another with 100% outside air without the humidifier.

Table 4-5 Climatic conditions for cooling coil empirical test II

Climatic conditions	
Cold dry	August 8 - 11
Hot dry	August 12 - 14
Hot humid (100% Outside Air)	August 15 – 16
Hot humid	August 18 - 20
Cold humid	August 21 - 23

The three-way chilled water control valve was modulated on the cooling coil to produce a constant supply air temperature. The chilled water plant used was a McQuay air-cooled chiller. The chilled water set point temperature was set to a fixed value. The chilled water temperature varied about the set point when the chiller cycled under part-load conditions.

In addition to the nominal performance data of Table 4-2 which are from the manufacturer submittal ten quasi-steady state points extracted from the experimental data are given in Table 4-6 and can be used to calibrate the cooling coil model.

4.6.2 Data compensation

For the cooling coil empirical test II mainly experimental data of relative air humidity had to be compensated whereas air and water temperatures underlay small changes only. Compensation rules were found manually with regard to

- Air and water side energy balances at the coil.
  These balances are shown for the different climates of the whole test period in Figure 6-52, Figure 6-58, Figure 6-64, Figure 6-70, and Figure 6-76 respectively.
- Amount of condensation that was re-calculated from experimental data and compared to the measurements.
- Accuracy of sensors.

Figure 4-13 and Figure 4-14 show temperature and humidity compensations of experimental data. Supply air flow rate was compensated according to Figure 4-15. Experimental data of total chilled water flow rate $ChWFR_{Coil}$ was reduced by 2.5%. Nevertheless there some differences between air and water side energy balance of the coil. See Figure 6-54, Figure 6-60, Figure 6-66, Figure 6-72, Figure 6-78 for further details.

Performance data given in Table 4-6 represent compensated experimental data not raw data from the measurements. The file CCEmpInput2_raw.txt contains uncompensated raw experimental data where also leaving water temperature, mixed water temperature and chilled water system flow rate are given instead of chilled water flow rate through the coil.

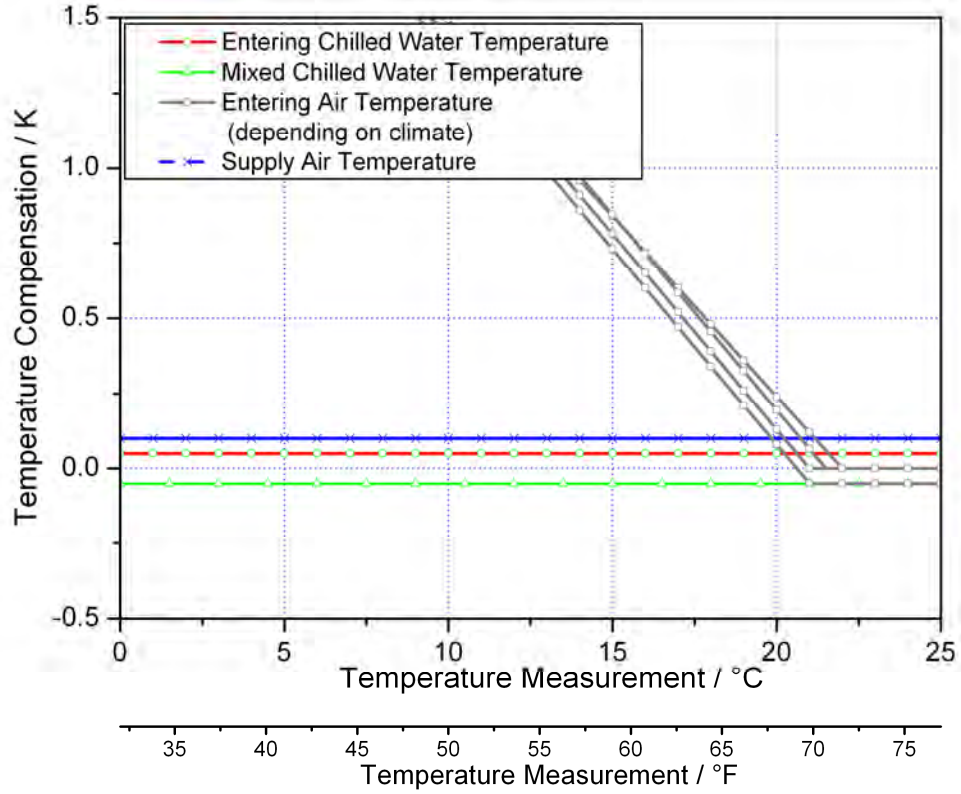

Figure 4-13 Cooling coil empirical test II - Compensation of water temperature measurements

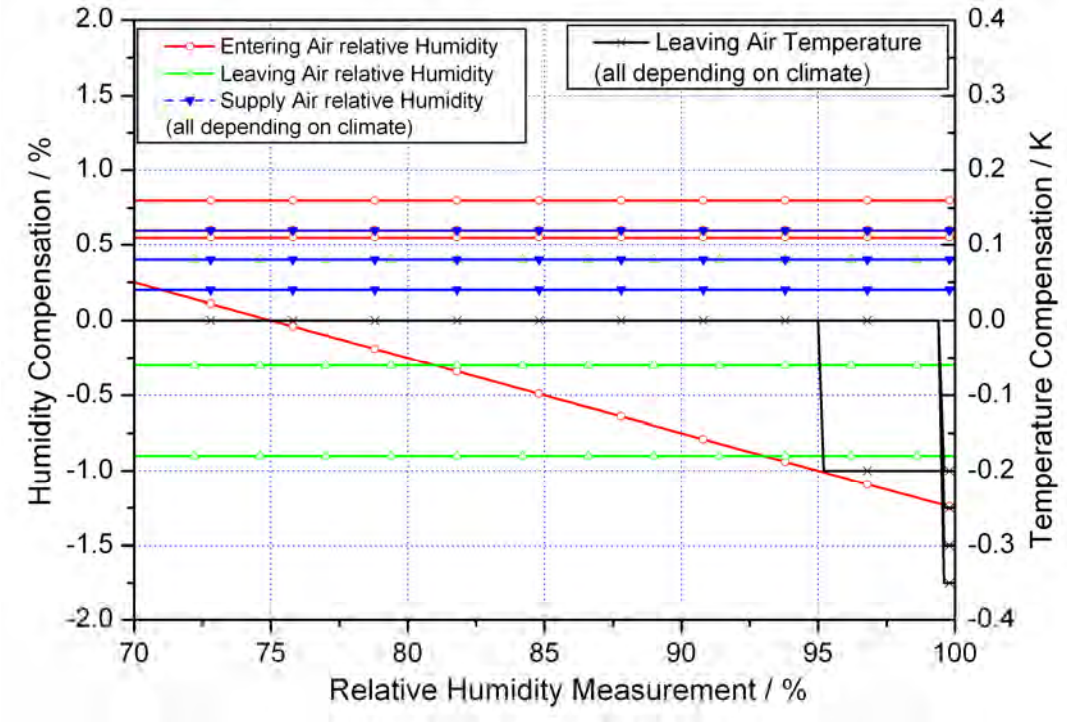

Figure 4-14 Cooling coil empirical test II - Compensation of air humidity and air temperature measurements

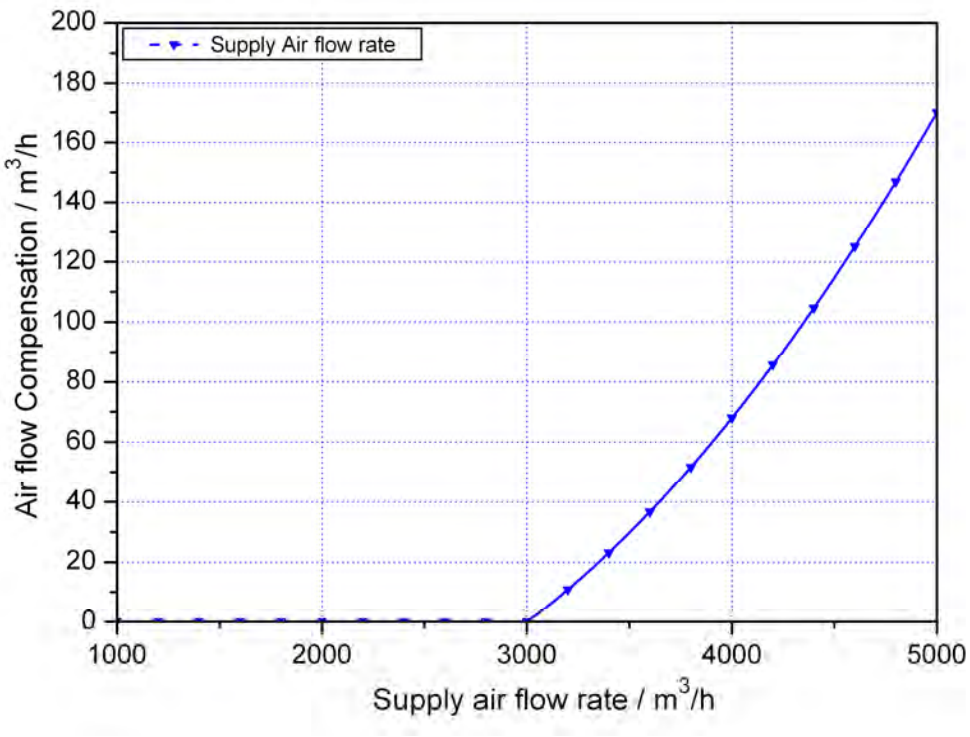

Figure 4-15 Cooling coil empirical test II - Compensation of supply air flow measurements

4.6.3 Input Data

The following input data in a minute-by-minute time step for the five time periods with different climatic inlet conditions from August 8 to August 23 are given in a separate file CCEmpInput2.txt:

Row	Shortcut	Description
1	Time	Month
2	Time	Day
3	Time	Hour
4	Time	Minute
5	EAT	Entering air temperature, dry bulb in °C
6	EArH	Entering air relative humidity in %
7	AFR	Air flow rate in m3/h
8	AFR_T	Temperature of given air flow rate AFR
9	AFR_rH	Relative Humidity of given air flow rate AFR
10	EWT	Chilled water entering temperature in °C
11	$ChWFR_{Coil}$	Chilled water flow rate through the coil in l/s
12	BARP	Barometric pressure of outside air in kPa

Chilled water flow rate through the coil has not been measured but was calculated based on the total flow rate from mass and energy balances at the three-way valve by Eq.(4.7).

For this test an aqueous solution of the heat transfer fluid DOWFROST with a concentration of 17.6% Propylene-Glycol by volume was used. Table 2.2 contains the values for the physical properties of the fluid.

4.6.4 Outputs

The following outputs also in minute-by-minute time steps are requested and should be submitted in a single file.

Row	Shortcut	Description
1	Time	
2	EAT	Entering air temperature, dry bulb in °C
3	EArH	Entering air relative humidity in %
4	EAH	Entering air humidity in kg/kg
5	LAT	Discharge/Leaving air temperature, dry bulb in °C
6	LArH	Discharge/Leaving air relative humidity in %
7	LAH	Discharge/Leaving air humidity in kg/kg
8	AFR	Air flow rate in m3/h
9	EWT	Chilled water coil entering temperature in °C
10	LWT	Chilled water coil leaving temperature in °C
11	$ChWFR_{Coil}$	Chilled water flow rate through the coil in l/s
12	UA	Overall UA-Value of the coil in kW/K
13	CLT	Total cooling load in kW
14	CLS	Sensible cooling load in kW
15	CLL	Latent cooling load in kW

The overall UA-Value of the coil has to be calculated based on the mean logarithmic temperature difference ΔT_m which is defined by Eq.(4.6).

Table 4-6 Quasi-steady state points based on experimental data for test II (Data marked with *) have been calculated and are not part of the recorded experimental data)

Cooling Coil Performance II		#1	#2	#3	#4	#5	#6	#7	#8	#9	#10
Barometric pressure*)	kPa	98.5	98.5	98.5	98.7	98.9	98.9	98.4	98.8	98.9	98.8
Entering Air Temp.	°C	22.9	22.9	26.4	27.5	23.2	19.0	27.9	28.0	23.6	23.5
Entering Air Relative Humidity*)	%	46.9	46.8	39.9	35.8	56.1	80.3	49.6	48.8	51.3	56.0
Entering Air Moisture*)	kg/kg	0.0084	0.0084	0.0088	0.0084	0.0102	0.0113	0.0120	0.0118	0.0095	0.0104
Leaving Air Temp.	°C	11.6	11.8	11.1	11.7	11.9	11.8	11.8	11.5	11.3	11.8
Leaving Air Relative Humidity*)	%	95.1	95.0	97.1	95	99.6	99.7	99.1	99.1	99.1	99.1
Leaving Air Moisture*)	kg/kg	0.0083	0.0084	0.0082	0.0084	0.0088	0.0088	0.0087	0.0086	0.0084	0.0087
Air Flow Rate at coil leaving air conditions*)	m³/h	3997	3882	1513	1689	3211	3008	1709	1790	4725	3136
Entering Liquid Temp.	°C	5.40	5.07	3.46	5.04	4.96	2.69	4.41	4.89	3.09	4.98
Leaving Liquid Temp.	°C	11.64	12.10	13.85	15.11	11.24	11.09	12.86	12.43	9.21	11.38
Mixing Liquid Temp.	°C	7.80	7.35	4.74	6.41	7.51	4.83	6.56	7.14	6.86	7.58
Liquid Flow*)	l/s	0.61	0.52	0.20	0.23	0.64	0.41	0.41	0.48	0.97	0.65
Total Cooling Capacity*)	kW	15.4	14.6	8.4	9.0	16.2	13.7	14.1	14.8	24.0	16.9
Latent Cooling Capacity*)	kW	0.3	0.1	0.7	0.0	3.9	6.4	4.7	4.8	4.3	4.4

Chapter 5 Hydraulic network, water circuit

In fact the hydraulic network investigated is only a small part of a more complex chilled water system (see chapter 2. The view to only this network keeps the exercise manageable.
Figure 5-1 shows the chilled water flow diagram of the hydraulic network. Beside this a detailed 3D-drawing of the chilled water system is provided with the file 3d_piping_AHU_A_CHWS.dwg.

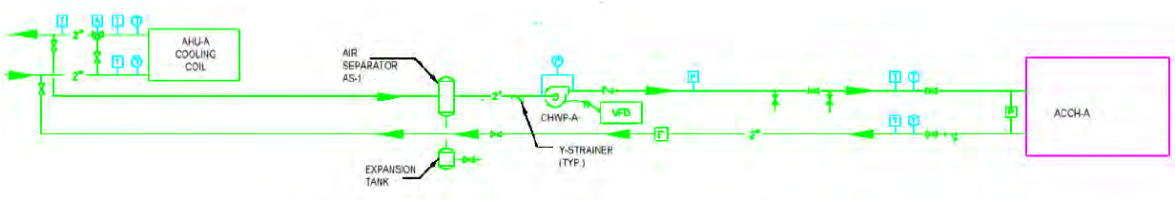

Figure 5-1 Chilled water flow diagram

The modelling of the hydraulic system can either be done in a detailed way based on the information taken from the 3D-drawing or in a simplified way based on the scheme depicted in Figure 5-2.

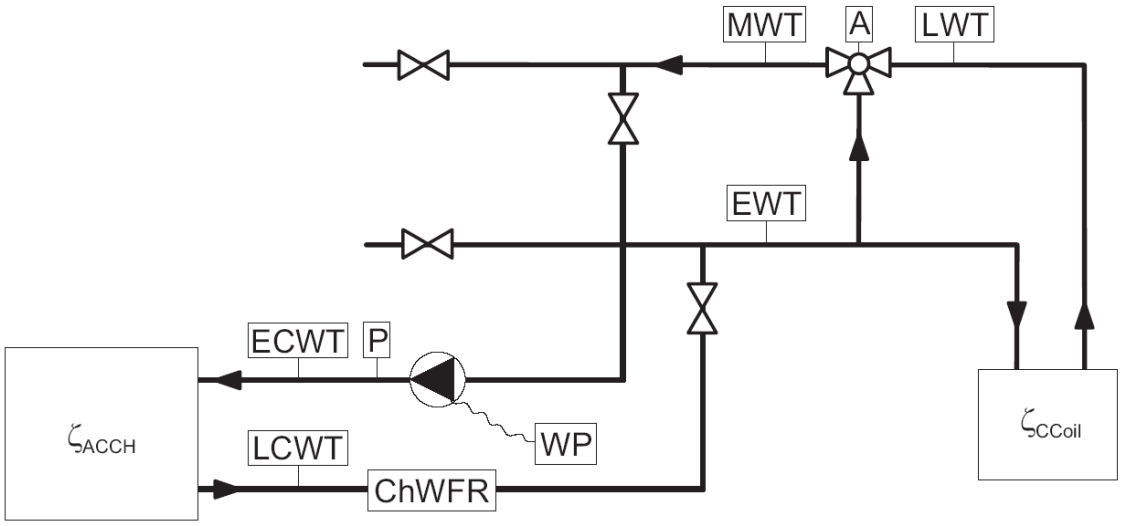

Figure 5-2 Simplified scheme of the chilled water hydraulic network system

The hydraulic network it is subdivided into several sections 1 . . . 8 to easily describe the subsections. Table 5-1 gives information about size, length and flow resistances for each of these sections. Table 5-2 contains some general data about dimensions and physical characteristics of the pipes. All pipes are assumed to be well-insulated. The environmental temperature is set to be 20°C.
Flow resistances are described in more detail in Chapter 5.1 to Chapter 5.5.

Table 5-1 Description of the hydraulic network sections

Section	Begin	End	Size	Length in m	Flow resistances
1	ACCH	T-piece	2" 1"	25.6 0.5	4 ball valves 1 reducer 1 widening 1 flow meter 3 three-way tees 14 bends
2	T-piece	T-piece bypass	2"	3.7	1 strainer 1 ball valve 2 bends
3	T-piece bypass	Cooling coil	2"	2.4	1 balancing valve 2 bends
4	Cooling coil	Valve	2"	2.3	2 bends
5	T-piece bypass	Valve	1.5"	1.1	3 bends 1 balancing valve
6	Valve	T-piece	2"	4.6	1 ball valve 2 bends
7	T-piece	Pump	2"	15.3	3 ball valves 1 three-way tee 1 four-way tee for air separator, expansion tank and fill station 1 reducer 5 bends
8	Pump	ACCH	2"	12.4	2 ball valves 1 check valve 1 strainer 1 widening 9 bends

Table 5-2 Dimensions and physical characteristics of pipes

Pipe characteristics			
Material	Copper type L		
Smoothness	C=140 (Hazen-Williams roughness constant) ε =1.5 μm (wall roughness)		
Nominal size	1"	1.5"	2"
Inside diameter / mm	26.04	38.23	50.42
Outside diameter / mm	28.58	41.28	53.98
Wall thickness / mm	1.27	1.52	1.78

5.1 Valve

The control valve is VG7842Nt+ three-way mixing valve manufactured by Johnson Controls. The kV -value is 10m³/h with regard to a pressure drop of 100 kPa (the CV -value is 11.6 gpm with regard to a pressure drop of 1 psi). Further technical information about the valve can be taken from Table 5-3. Figure 5-3 shows valve body and flow directions.

Table 5-3 Valve general data

Valve general data	
Product family	Cast Bronze
Body type	Three-Way Mixing
Flow characteristics	Linear
Nominal Size	DN25 (1in)
Kv (Cv)	10.0 m³/h (11.6 gpm)
Valve Stroke	13 mm (1/2 in)
Close off	1.255/1.469 MPa (182/213 psi)
Max. Operating Diff. Pressure	0.241 MPa (35 psig)
Leakage	0.01 % of Maximum Flow

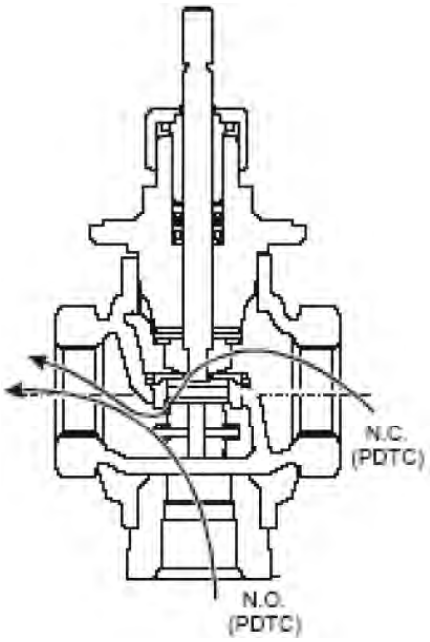

Figure 5-3 Valve body and flow directions

5.2 Air separator

In chilled water systems circulators are usually found in the return line to the chiller, between the air handler/heat exchangers and the chiller. The optimum place for the air separator is in this part of the line before the intake of the circulator. Here, the highest available temperature and lowest system pressure is found. Spirovent®JuniorMicrobubble™Separator used here is an air eliminator for fast and effective removal of all forms of air, including tiny micro bubbles. Exterior views as well as some dimensional data are given in Figure 5-4.

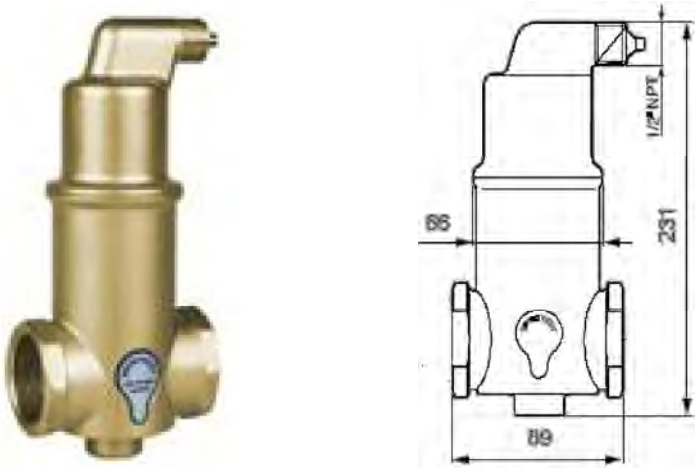

Figure 5-4 Spirovent air separator

Table 5-4 Air separator general data

Air separator	
Body	Brass
Nominal size	1 ½"
Kv (Cv)	47.6 m³/h (55 gpm)

5.3 Pump

It is a Bell & Gossett 1 1/2 AA Series 60® maintenance-free in-line pump. Figure 5-5 shows an exterior view of the pump.

The performance of the pump can be either seen from the original equipment submittal in Figure 5-6 or from the extracted lines of total head and pump efficiency in Figure 5-7.

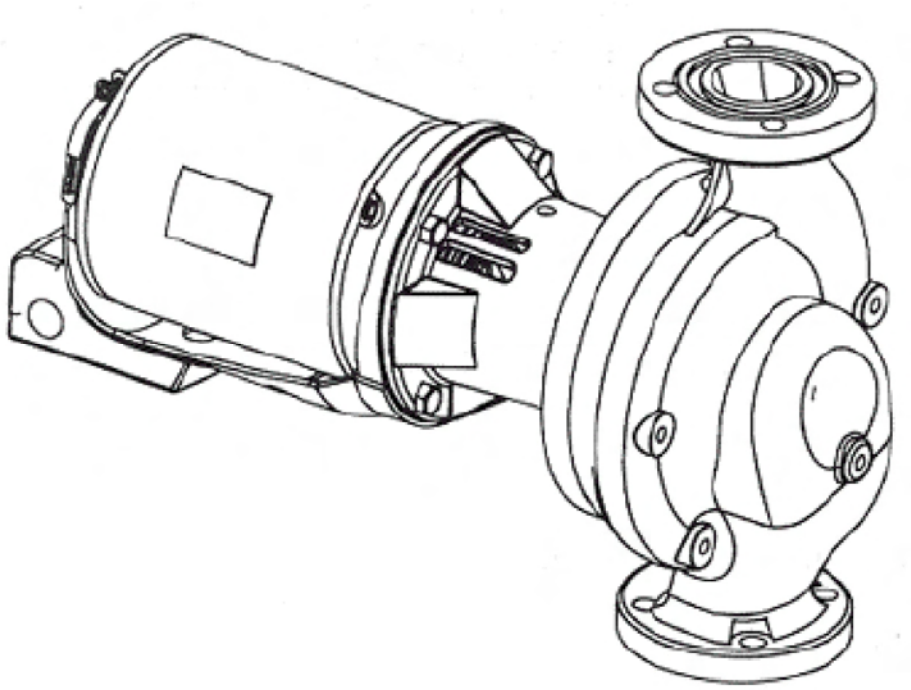

Figure 5-5 Chilled water pump

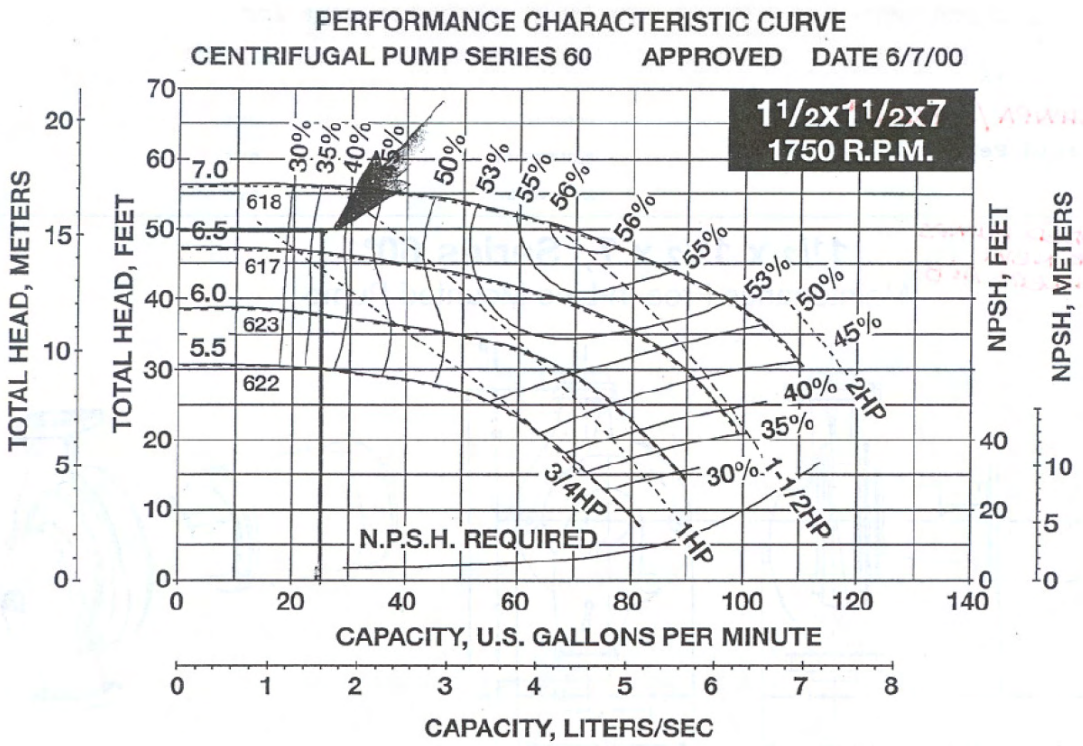

Figure 5-6 Pump performance curve

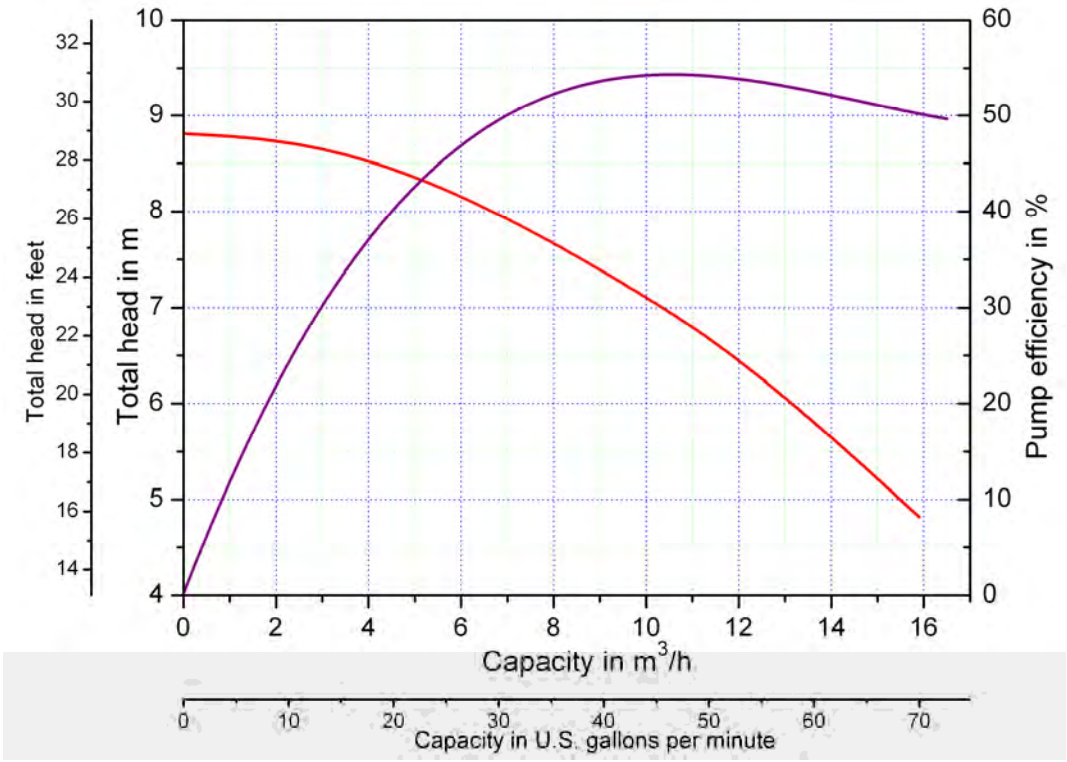

Figure 5-7 Chilled water pump performance curve extract

5.4 Cooling Coil

The high performance fin tube coil is part of a central station air handling unit manufactured by Trane. It can be used for general purposes. The horizontal coil section operates as a full coil. It consists of a chilled water single serpentine with 6 rows. Figure 4-1 shows an exterior view of a standard coil as well as directions of water and air flows.

Hydraulic performance data of the coil can be taken from Table 5-5. These data are valid only for an Ethylene-glycol fluid with a concentration of 35% by mass.

Table 5-5 Hydraulic performance data of the coil

Cooling Coil Performance	
Fluid	Ethylene Glycol
Concentration	35 % by mass
Flow Rate	1.77 l/s
Entering Fluid Temp.	6.67 °C
Leaving Fluid Temp.	12.06 °C
Pressure Drop	22.4 kPa

Figure 4-3 and Figure 4-3 allow a look at inlet and outlet sides of the cooling coil.

5.5 Chiller

Evaporator flow rate must fall between the minimum and maximum values shown in Table 5-6. Flow rates outside of these limits result in a chilled water Delta-T outside the operating range of the controller. Figure 5-8 shows the full evaporator pressure drop curve.

Table 5-6 Evaporator water pressure drop

Evaporator Water Pressure Drop				
	Flow Rate		Pressure Drop	
	l/s	gpm	kPa	ft
Minimum Flow	0.9	15	7.1	2.4
Nominal Flow	1.5	24	17.3	5.8
Maximum Flow	2.5	40	45.5	15.2

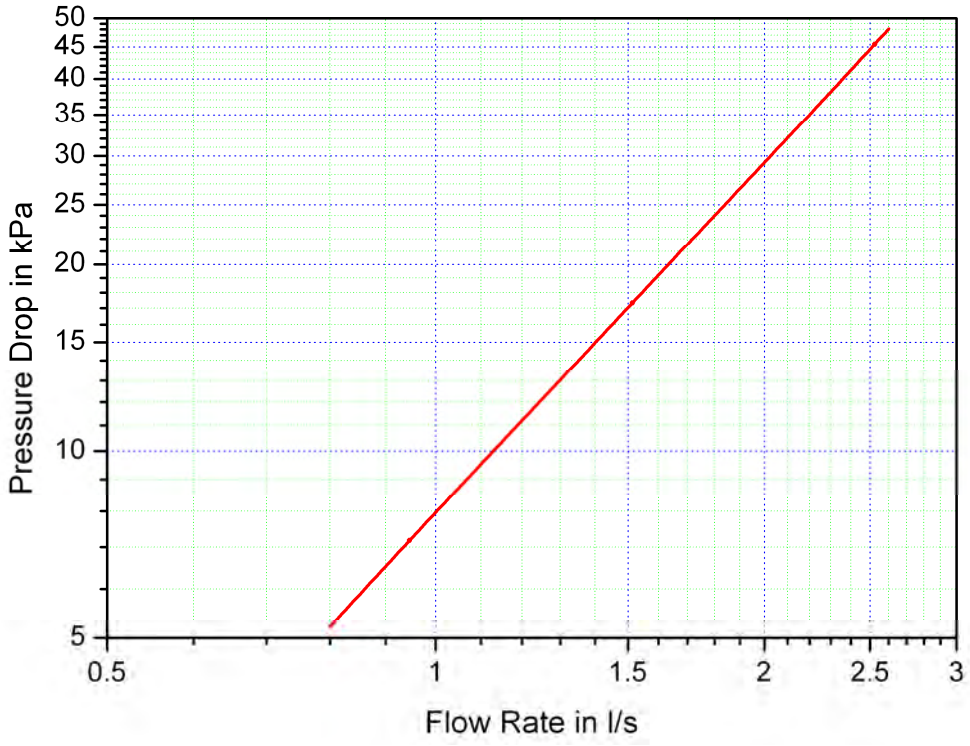

Figure 5-8 Evaporator water pressure drop

5.6 Hydraulic System Empirical Test I

5.6.1 Test configuration and overall goal

The goal of this empirical test is to predict the performance of chilled water pump. Input data come from an experiment which was conducted at the ERS from August 24-30, 2005.
Simulation results will be compared to the empirical data from measurements.
The chilled water temperature was set to 5.56°C (42°F) and the chilled water pump rpm was kept constant.

5.6.2 Input data

The following input data in a minute-by-minute time step for the period August 24 to August 30 are given in a separate file CHydrEmpInput1.txt:

Row	Shortcut	Description
1	Time	Month
2	Time	Day
3	Time	Hour
4	Time	Minute
5	CHWT	Chilled water temperature leaving the chiller in °C
6	CHWCFDBK	Three-Way-Valve position in % opened

For this test an aqueous solution of propylene glycol (DOWFROST) was used as a secondary refrigerant and the concentration of the solution was 20.3% by volume. Table 2.3 contains values for the physical properties of the fluid.

5.6.3 Outputs

The following outputs also in minute-by-minute time steps are requested and should be submitted in a single file.

Row	Shortcut	Description
1	Time	
2	CHWT	Chilled water temperature leaving the chiller in °C
3	CHWT	Chilled water temperature entering the chiller in °C
4	ChWFR	Total chilled water flow rate through the system in l/s
5	ChWFRCoil	Chilled water flow rate through the coil in l/s

5.7 Hydraulic System Empirical Test II

5.7.1 Test configuration and overall goal

The goal of this empirical test is to predict the performance of chilled water pump. Input data come from an experiment which was conducted at the ERS from August 8-23, 2006.
Simulation results will be compared to the empirical data from measurements.
The chilled water temperature was set at 4.44°C (40°F) and the chilled water pump rpm was kept constant.

5.7.2 Input data

The following input data in a minute-by-minute time step for the period August 8 to August 23 are given in a separate file CHydrEmpInput2.txt:

Row	Shortcut	Description
1	Time	Month
2	Time	Day
3	Time	Hour
4	Time	Minute
5	CHWT	Chilled water temperature leaving the chiller in °C
6	CHWCFDBK	Three-Way-Valve position in % opened

For this test an aqueous solution of the heat transfer fluid DOWFROST with a concentration of 17.6% Propylene-Glycol by volume was used. Table 2.2 contains the values for the physical properties of the fluid.

5.7.3 Outputs

The following outputs also in minute-by-minute time steps are requested and should be submitted in a single file.

Row	Shortcut	Description
1	Time	
2	CHWT	Chilled water temperature leaving the chiller in °C
3	CHWT	Chilled water temperature entering the chiller in °C
4	ChWFR	Total chilled water flow rate through the system in l/s
5	ChWFRCoil	Chilled water flow rate through the coil in l/s

Chapter 6 Results

6.1 Chiller

6.1.1 Comparative Test

Two simulation programs participated in field trials of the comparative chiller test:

Table 6-1 List of participants of the comparative chiller test

Name of the program	Modeler
TRNSYS-TUD	Technical University Dresden, Germany
EES	Université de Liège, Belgium

This test was performed at a very early stage of this task and no detailed analyses have been done. Nevertheless results available from two programs should be presented here that gives a better idea on test conditions and how this comparative test could work.

Figure 6-1 shows chilled water temperatures whereat both return temperature and leaving water temperature were given to the modeller and leaving water temperature had to be predicted by the models. There have been two levels of leaving water temperature set point defined. During chiller full load operation – characterized by high return temperatures - both models calculate leaving water temperatures that are slightly higher than the set point. In addition to that the TRNSYS-TUD chiller model also switches off when cooling load is too small, i.e. at low return temperatures. See Figure 6-2 for the related cooling load profile. The load profile was cross check with a calorific estimation of cooling load based on given temperature conditions.
Figure 6-3 and Figure 6-4 show chiller electric energy consumption and COP of the chiller, respectively.

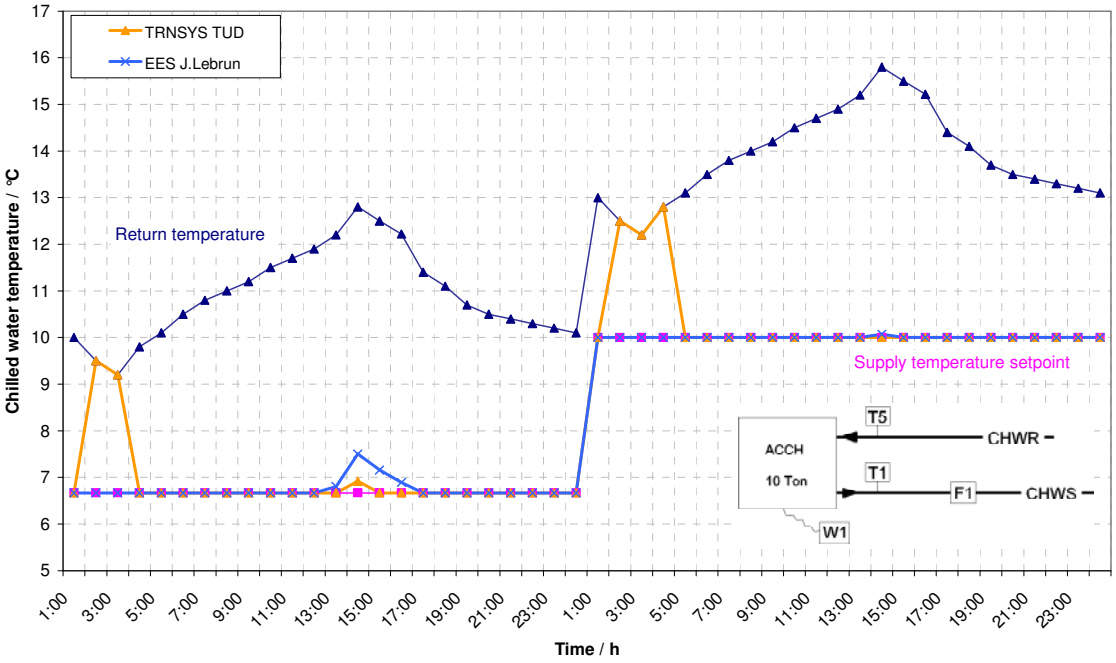

Figure 6-1 Chiller Comparative Test – Chilled water temperatures

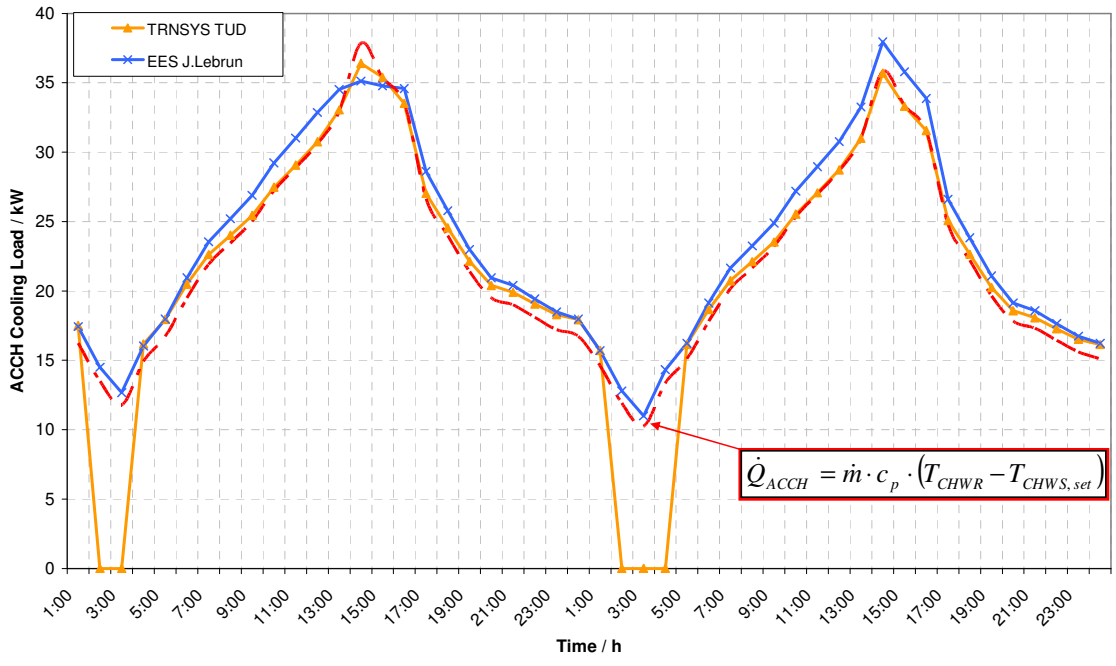

Figure 6-2 Chiller Comparative Test – Cooling load

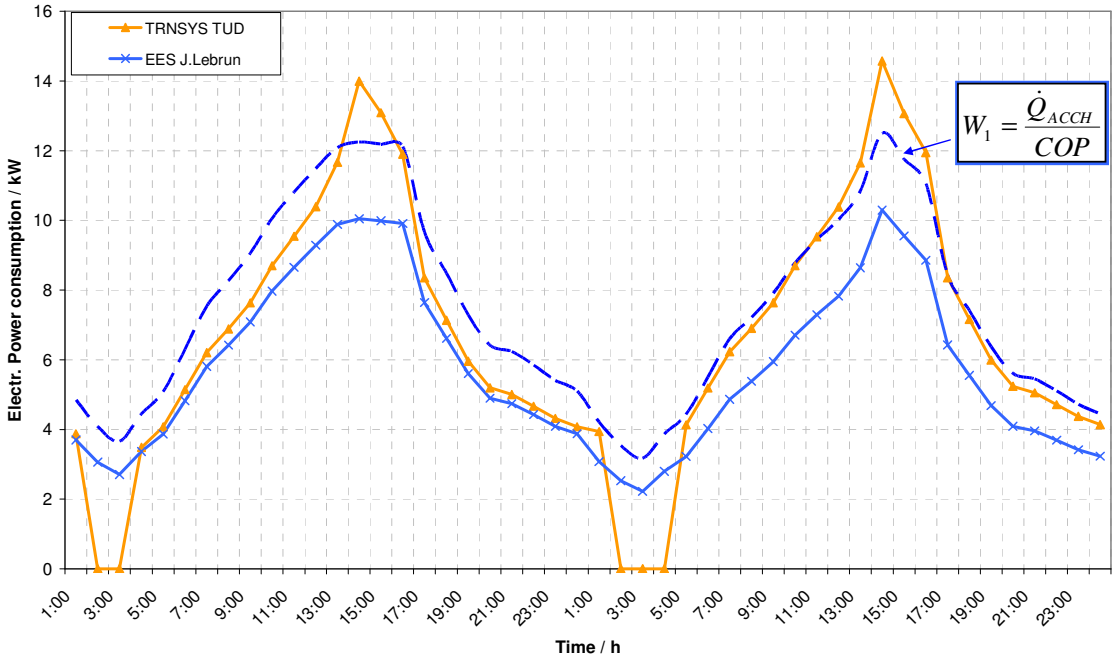

Figure 6-3 Chiller Comparative Test – Electric power consumption

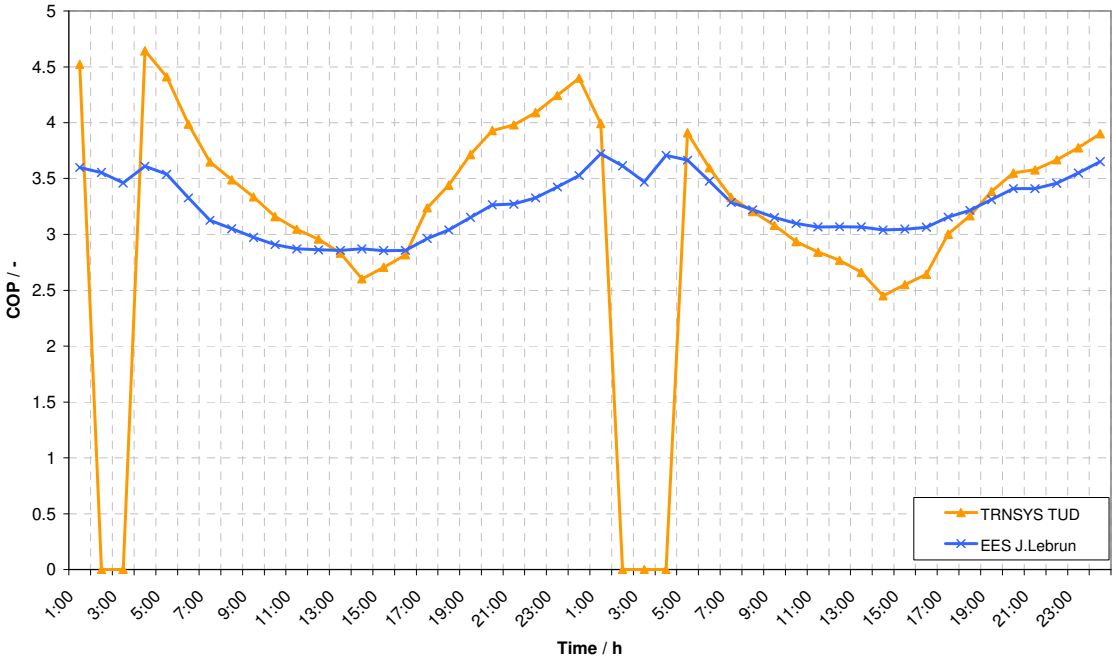

Figure 6-4 Chiller Comparative Test – Chiller COP

6.1.2 Empirical Test I (August 24 – August 30, 2005)

The empirical chiller test I has been run by only one program as specified in Table 6-2.

Table 6-2 List of participants of the empirical chiller test I

Name of the program	Modeler
EES	Université de Liège, Belgium

The EES model uses an ideal temperature control that maintains leaving water temperature at the given temperature set point without any deviation due to chiller control. From Figure 6-5 it can be seen that leaving water temperature recorded during the experiment normally fluctuates by ±1K around the set point. Leaving air temperature predicted by the simulation model considerably differs from the measurement. Temperature profile displayed in Figure 6-6 shows a quite constant offset between model prediction and experimental data that is about 3K. This offset may be also affected by the location of the condenser entering air temperature sensor. See Figure 3-7 for more details. Averaged daily cooling load profile as well as electric load of the chiller are shown in Figure 6-7 and Figure 6-8, respectively. Chiller cooling load predictions in general agree with experimental data but have some minor deviation during early morning. This corresponds to the leaving water temperature deviations and may be caused by a very part load operation of the chiller. Chiller electric load predictions do also not correctly cover high chiller operation at higher loads.

Table 6-3 (cooling load), Table 6-4 (electric load), and Table 6-5 (leaving water temperature) summarize some statistical information about validation. Leaving air temperature is not statistical analyzed since temperature measurement seems to be not clearly identified as condensing air temperature as used in the simulation program.

A detailed analysis of this test is presented in a companion report (Lemort et al., 2008).

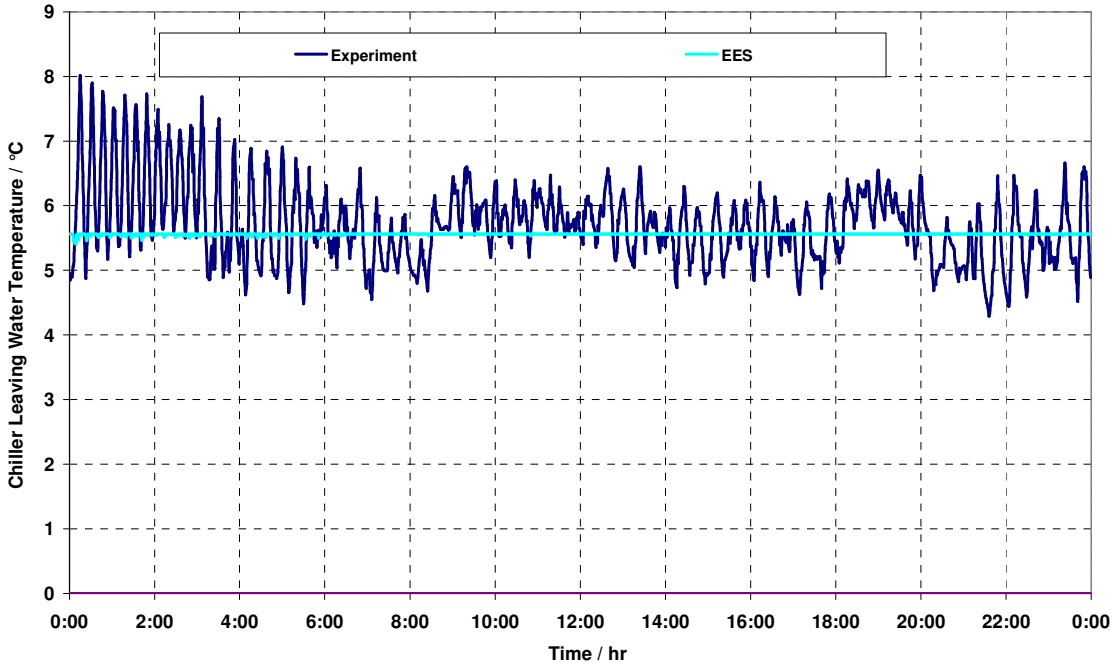

Figure 6-5 Chiller Empirical Test I – Averaged Daily Leaving Water Temperature

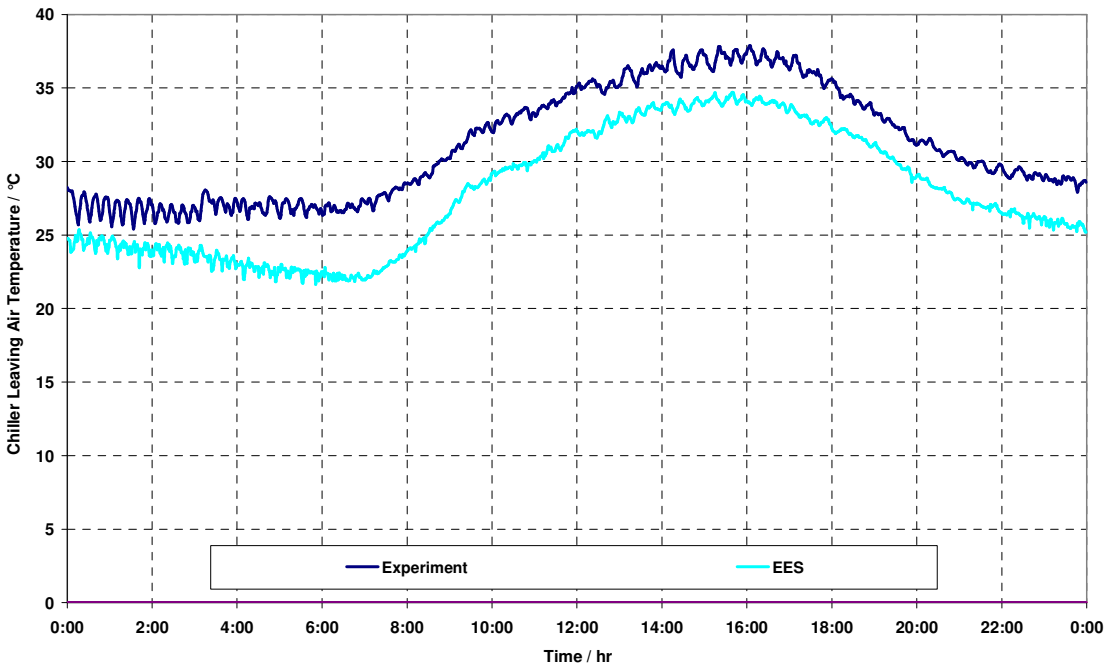

Figure 6-6 Chiller Empirical Test I – Averaged Daily Leaving Air Temperature (Condenser side)

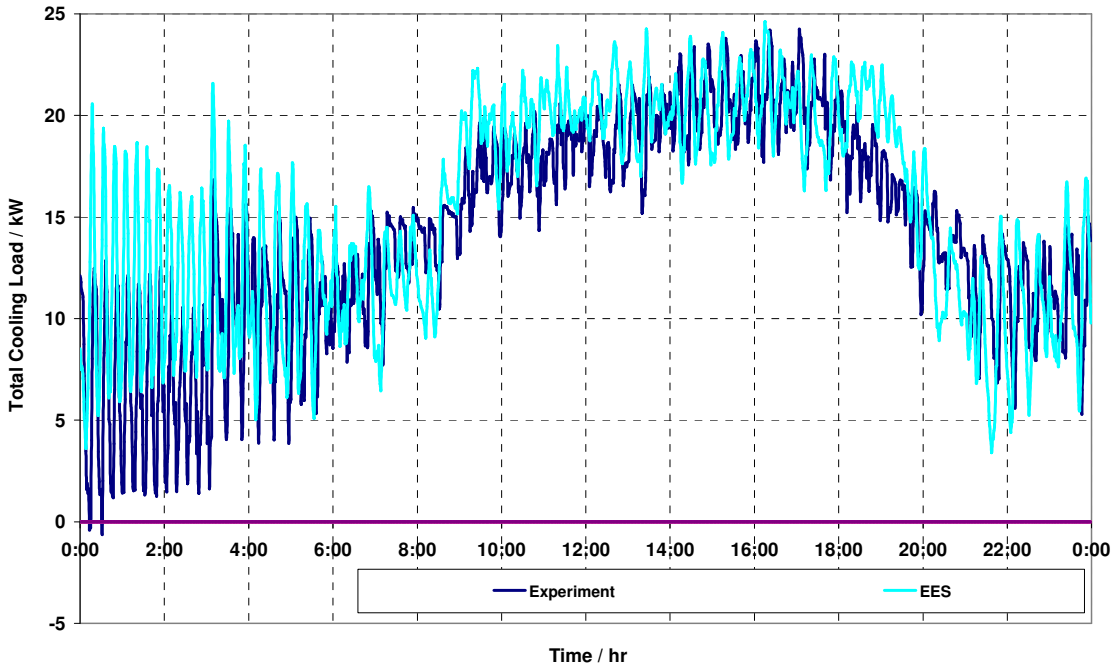

Figure 6-7 Chiller Empirical Test I – Averaged Daily Chiller Cooling Load

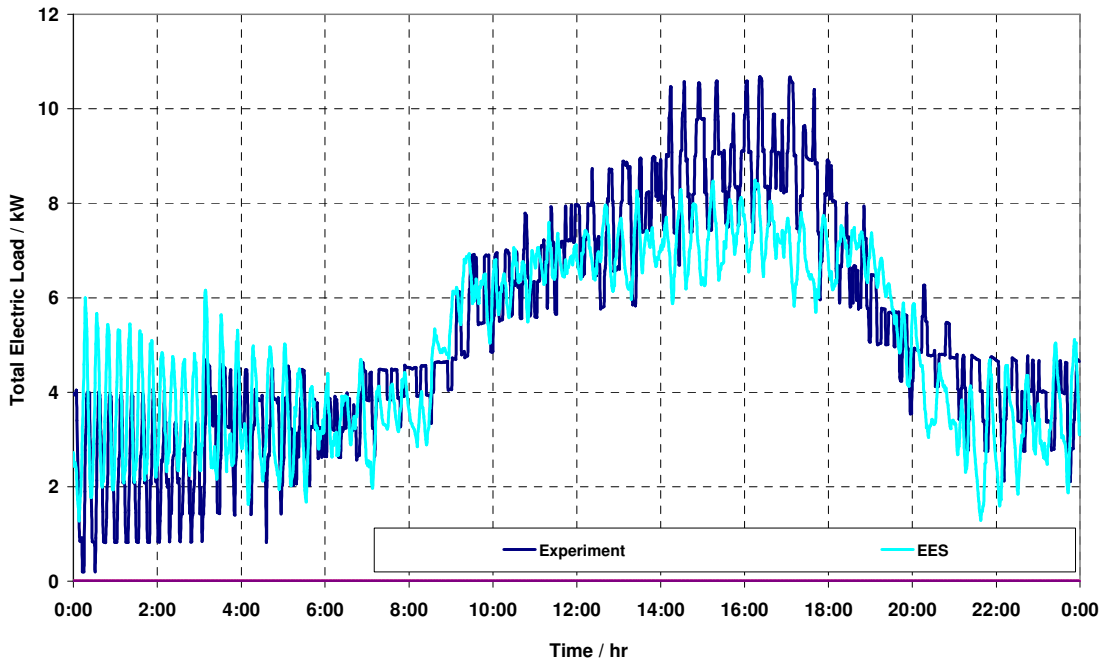

Figure 6-8 Chiller Empirical Test I – Averaged Daily Chiller Electric Load

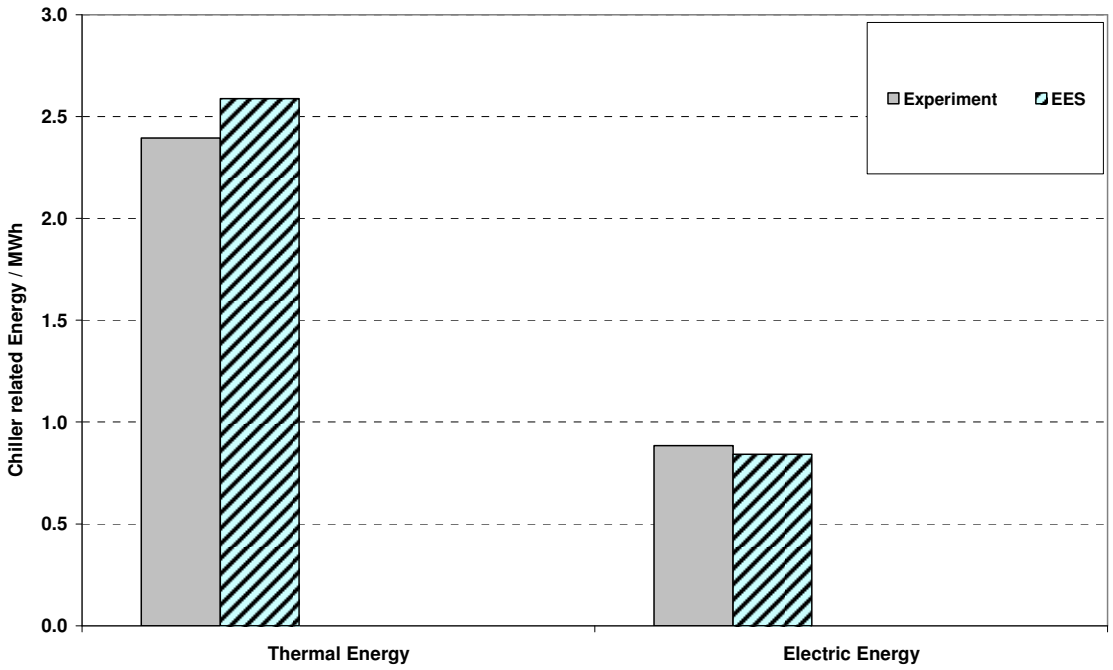

Figure 6-9 Chiller Empirical Test I – Chiller Total Thermal and Electric Energy

Table 6-3 Chiller empirical Test I – Total Cooling Load Statistics

CLT	Exp.				EES
$\overline{x}$	14.26				15.40
S	7.20				7.93
x_{min}	-1.94				0.00
x_{max}	27.40				32.07
$\overline{D}$					1.14
$\overline{\lvert D \rvert}$					6.39
$\lvert D \rvert_{max}$					23.93
$\lvert D \rvert_{min}$					0.00
D_{rms}					7.76
$D_{95\%}$					15.61

Table 6-4 Chiller empirical Test I –Total Electric Statistics

CEP	Exp.				EES
$\overline{x}$	5.26				5.01
S	3.08				2.55
x_{min}	0.18				0.20
x_{max}	11.58				10.57
$\overline{D}$					-0.25
$\overline{\lvert D \rvert}$					2.49
$\lvert D \rvert_{max}$					7.01
$\lvert D \rvert_{min}$					0.00
D_{rms}					2.89
$D_{95\%}$					8.81

Table 6-5 Chiller empirical Test I – Leaving Water Temperature Statistics

LWT	Exp.				EES
$\overline{x}$	5.72				5.56
S	1.23				0.02
x_{min}	3.47				4.90
x_{max}	9.31				5.56
$\overline{D}$					-0.16
$\overline{\lvert D \rvert}$					1.03
$\lvert D \rvert_{max}$					3.75
$\lvert D \rvert_{min}$					0.02
D_{rms}					1.24
$D_{95\%}$					1.44

6.1.3 Empirical Test II (August 8 – August 23, 2006)

The empirical chiller test II has been run by only one program specified in Table 6-6.

Table 6-6 List of participants of the empirical chiller test II

Name of the program	Modeler
EES	Université de Liège, Belgium

Results of the chiller empirical test II will be presented here according to the different time periods defined in Table 4-5. Although the subdivision of the 15-day-test period into five sub-periods originally was done to easily distinguish different cooling coil operating conditions it may be useful to also analyze results of chiller empirical test II according to different operating conditions caused by the cooling load profile served by the cooling coil.

Cold Dry Climate (August 8 – August 11, 2006)

The results presented in the following Figures do in principle confirm the evaluation made for the chiller empirical test I, i.e. leaving water temperature control does not account for realistic operation but assumes an ideal temperature. This again has an affect on chiller cooling load since small deviation in temperature lead to quite big deviation in chiller cooling load. Chiller electric load is connected to the cooling load and therefore also shows big differences compared to the experiment. Chiller leaving air temperature is a little bit closer to the measurement than it was in the empirical I test. From Figure 6-13Figure 6-12 and Figure 6-13 it can be seen that the chiller always operates at stage 1 but switches to stage 2 during the afternoon.

Again Table 6-7, Table 6-8 (electric load), and Table 6-9 (leaving water temperature) provide some statistical information about chiller operation.

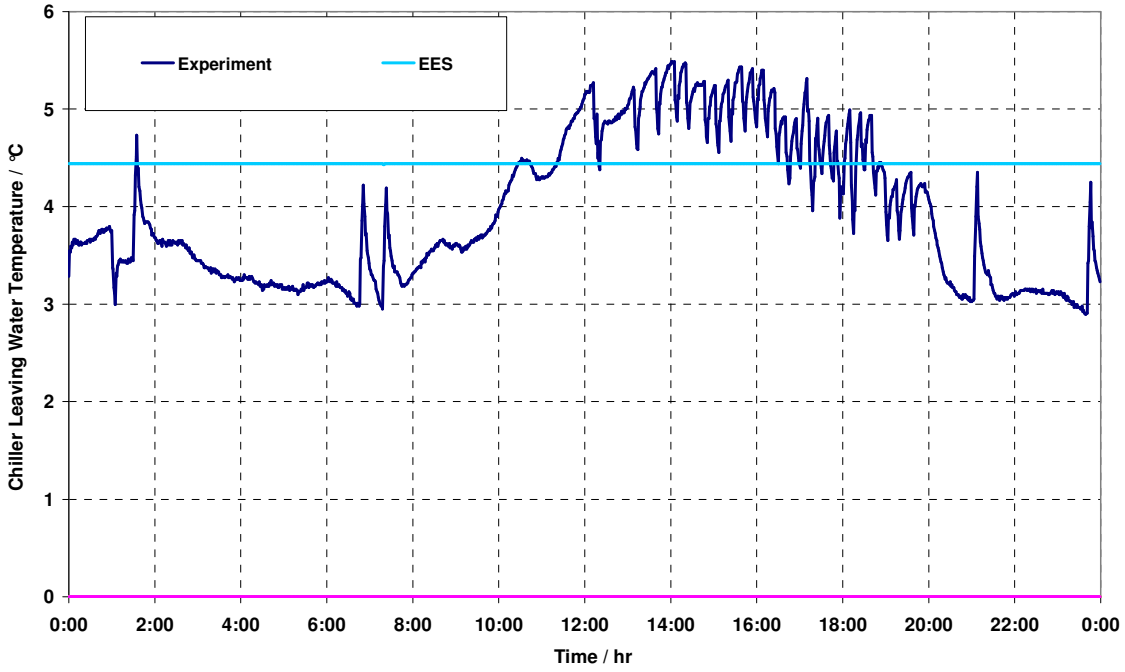

Figure 6-10 Chiller Empirical Test II (Cold Dry climate) – Averaged Daily Leaving Water Temperature

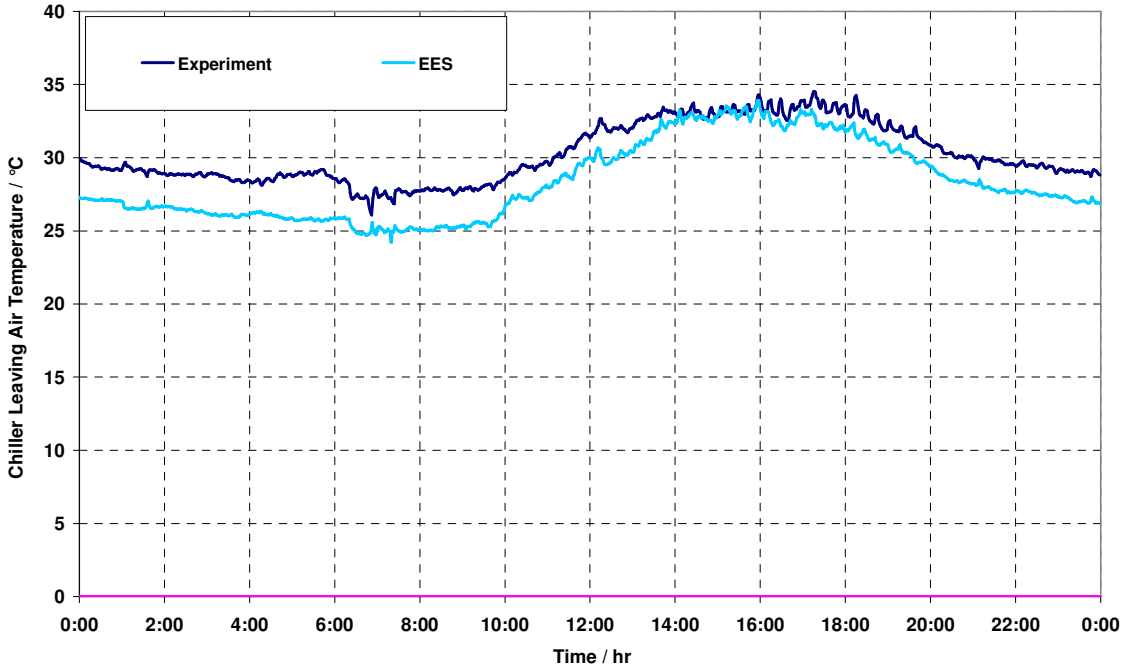

Figure 6-11 Chiller Empirical Test II (Cold Dry climate) – Averaged Daily Leaving Air Temperature (Condenser side)

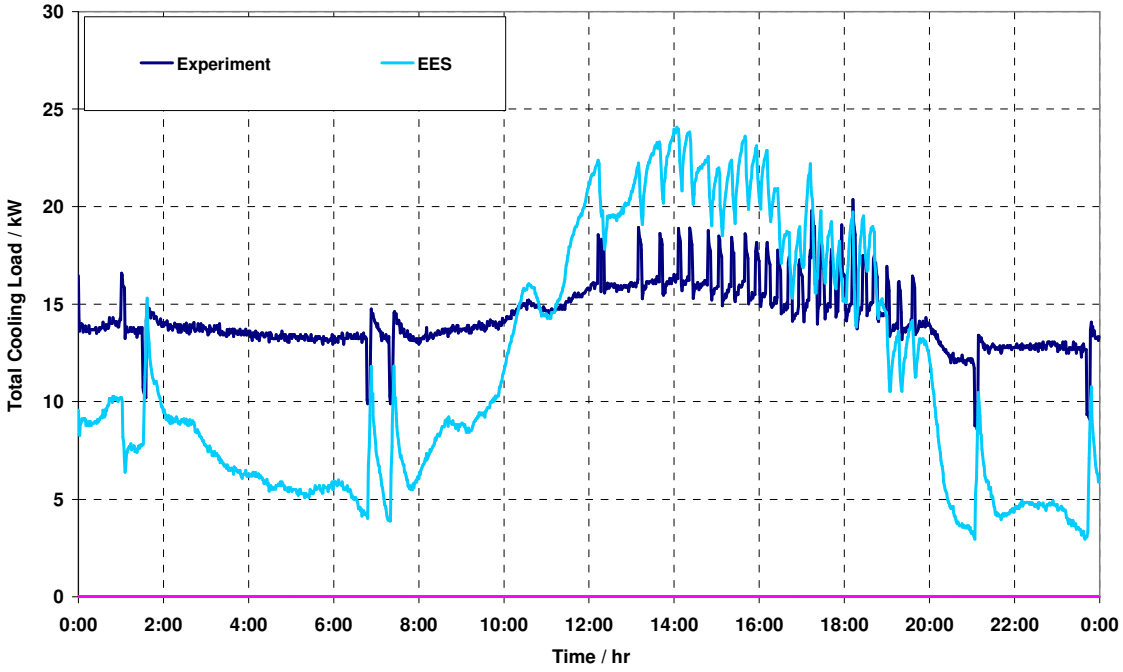

Figure 6-12 Chiller Empirical Test II (Cold Dry climate) – Averaged Daily Chiller Cooling Load

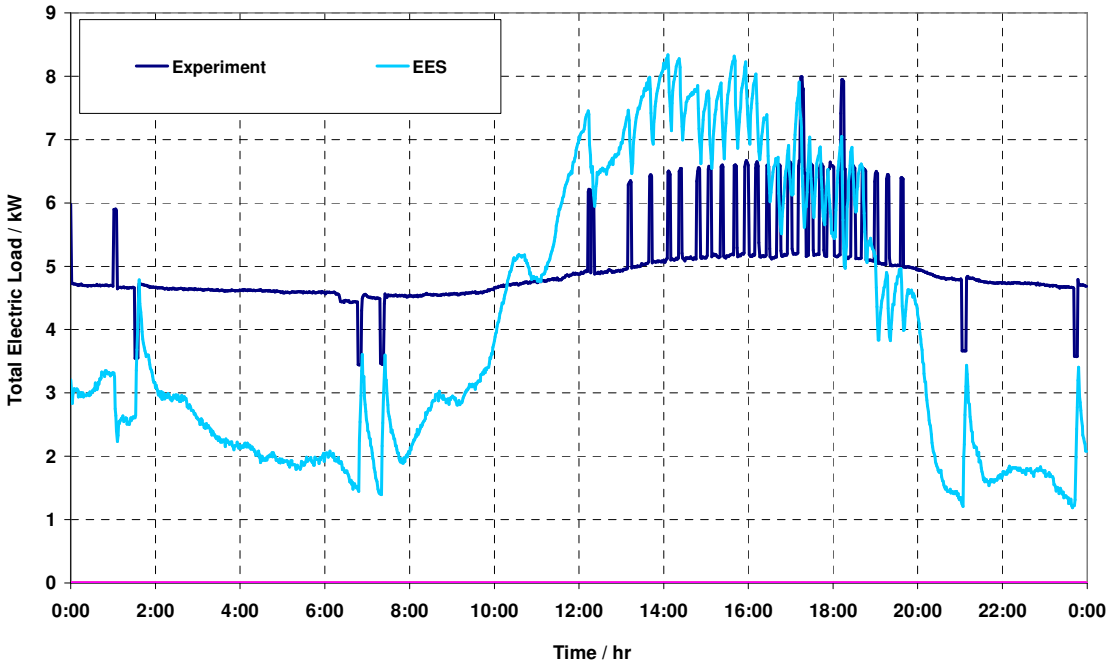

Figure 6-13 Chiller Empirical Test II (Cold Dry climate) – Averaged Daily Chiller Electric Load

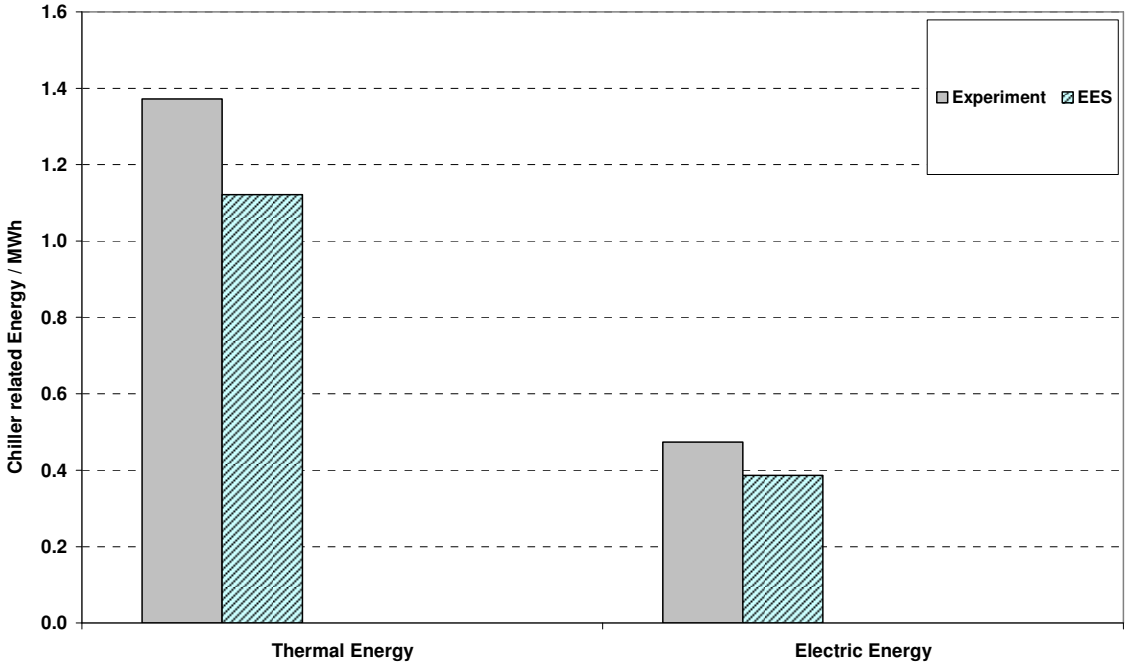

Figure 6-14 Chiller Empirical Test II (Cold Dry climate) – Chiller Total Thermal and Electric Energy

Table 6-7 Chiller empirical Test II (Cold Dry climate) – Total Cooling Load Statistics

CLT	Exp.				EES
$\overline{x}$	14.30				11.68
S	2.58				8.02
x_{min}	-1.66				0.00
x_{max}	27.33				31.39
$\overline{D}$					-2.62
$\overline{\lvert D \rvert}$					6.27
$\lvert D \rvert_{max}$					23.70
$\lvert D \rvert_{min}$					0.00
D_{rms}					7.04
$D_{95\%}$					10.60

Table 6-8 Chiller empirical Test II (Cold Dry climate) –Total Electric Statistics

CEP	Exp.				EES
$\overline{x}$	4.93				4.02
S	1.08				2.67
x_{min}	0.19				0.20
x_{max}	11.53				10.60
$\overline{D}$					-1.87
$\overline{\lvert D \rvert}$					2.02
$\lvert D \rvert_{max}$					6.09
$\lvert D \rvert_{min}$					0.00
D_{rms}					2.27
$D_{95\%}$					3.69

Table 6-9 Chiller empirical Test II (Cold Dry climate) – Leaving Water Temperature Statistics

LWT	Exp.				EES
$\overline{x}$	3.95				4.44
S	0.98				0.00
x_{min}	2.47				4.41
x_{max}	7.90				4.44
$\overline{D}$					0.49
$\overline{\lvert D \rvert}$					0.97
$\lvert D \rvert_{max}$					3.46
$\lvert D \rvert_{min}$					0.01
D_{rms}					1.09
$D_{95\%}$					1.68

Hot Dry Climate (August 12 – August 14, 2006)

The results presented in the following Figures do in principle confirm the evaluation made for the previous time period: leaving water temperature is idealized fixed to a certain value and measured leaving air temperature was underestimated. The very low cooling load – Figure 6-17 shows load s that are between 5…10kW only - causes quite high frequent control cycles: the chiller operates in on-off-mode. Only during the afternoon the chiller operates at stage 1. Both thermal and electrical amount of energy is overestimated.

Table 6-10 (cooling load), Table 6-11 (electric load), and Table 6-12 (leaving water temperature) provide some statistical information about chiller operation.

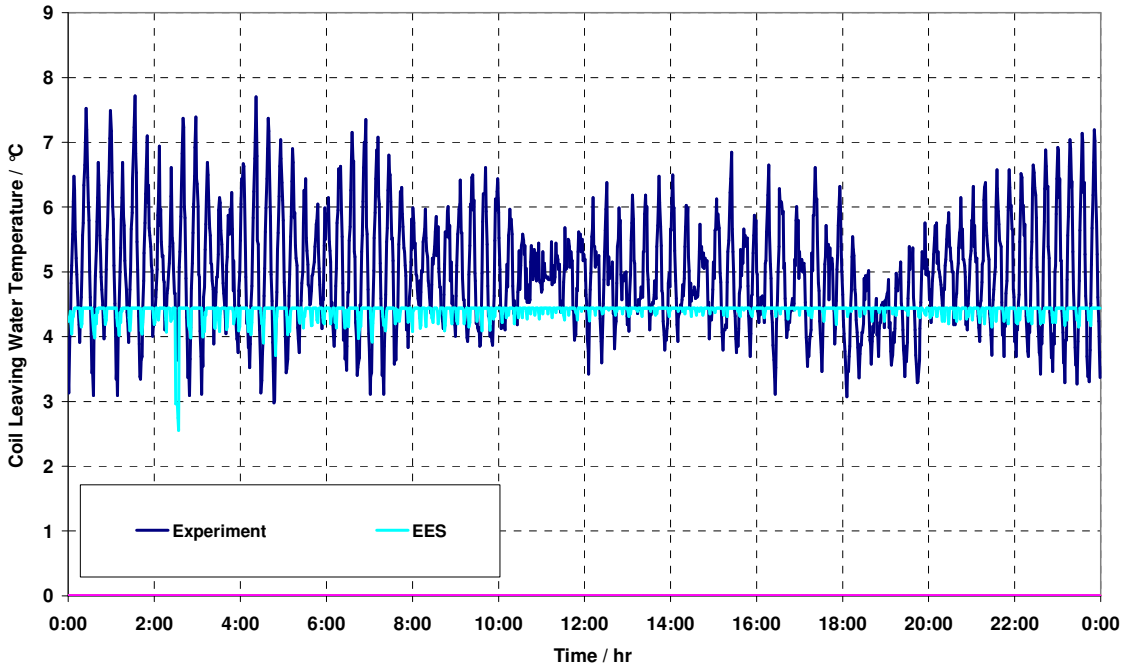

Figure 6-15 Chiller Empirical Test II (Hot Dry climate) – Averaged Daily Leaving Water Temperature

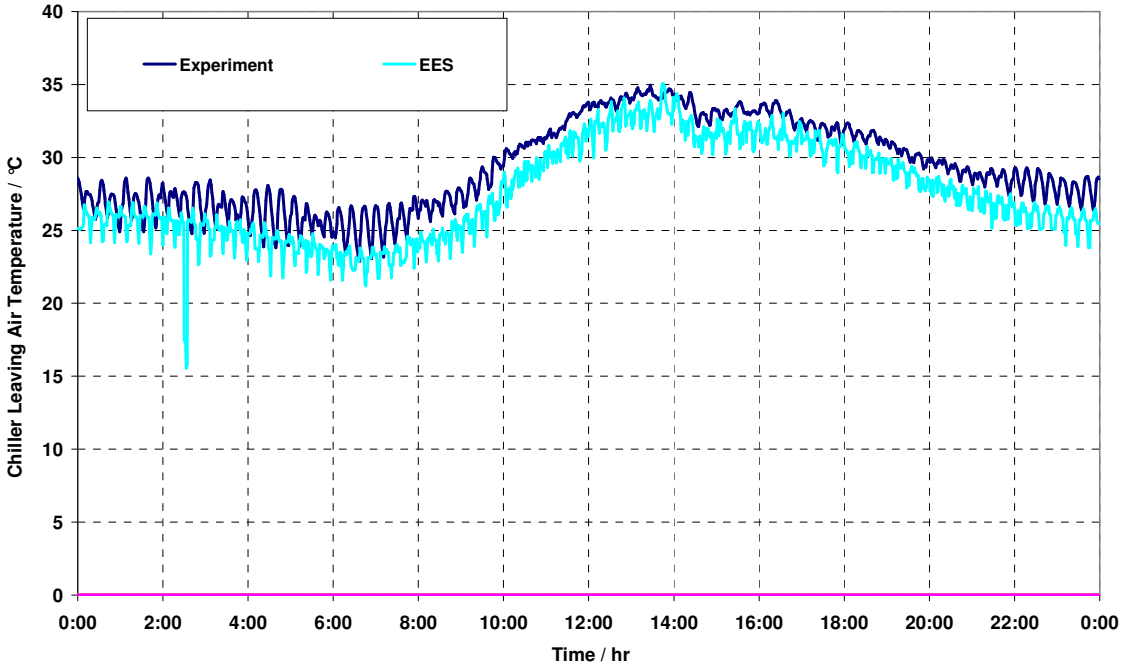

Figure 6-16 Chiller Empirical Test II (Hot Dry climate) – Averaged Daily Leaving Air Temperature (Condenser side)

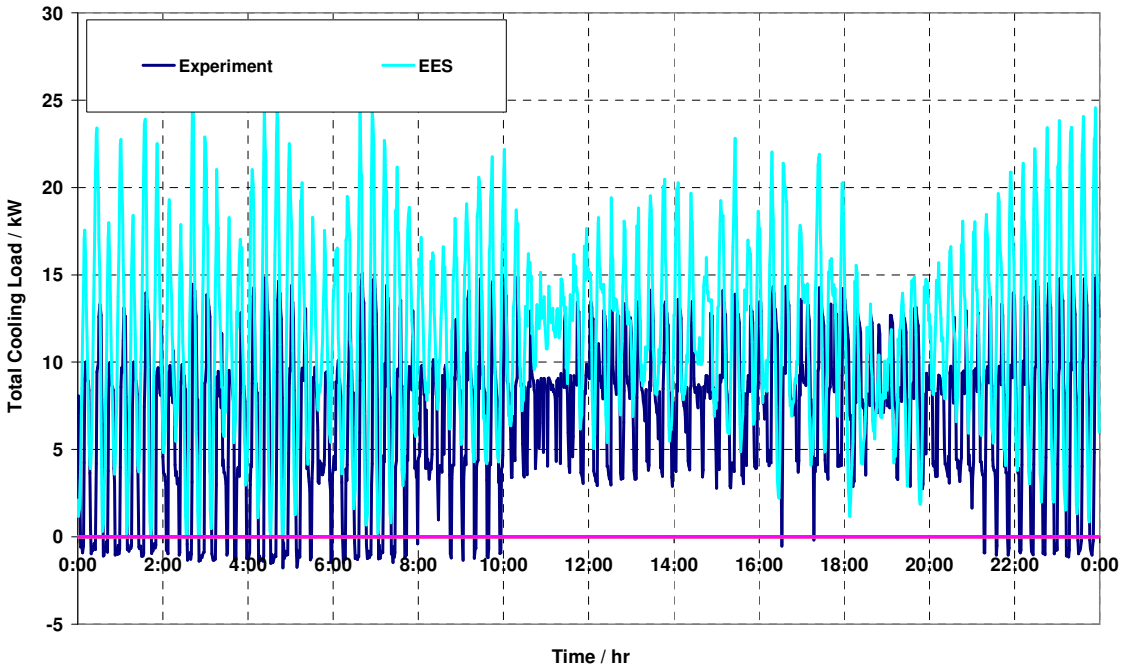

Figure 6-17 Chiller Empirical Test II (Hot Dry climate) – Averaged Daily Chiller Cooling Load

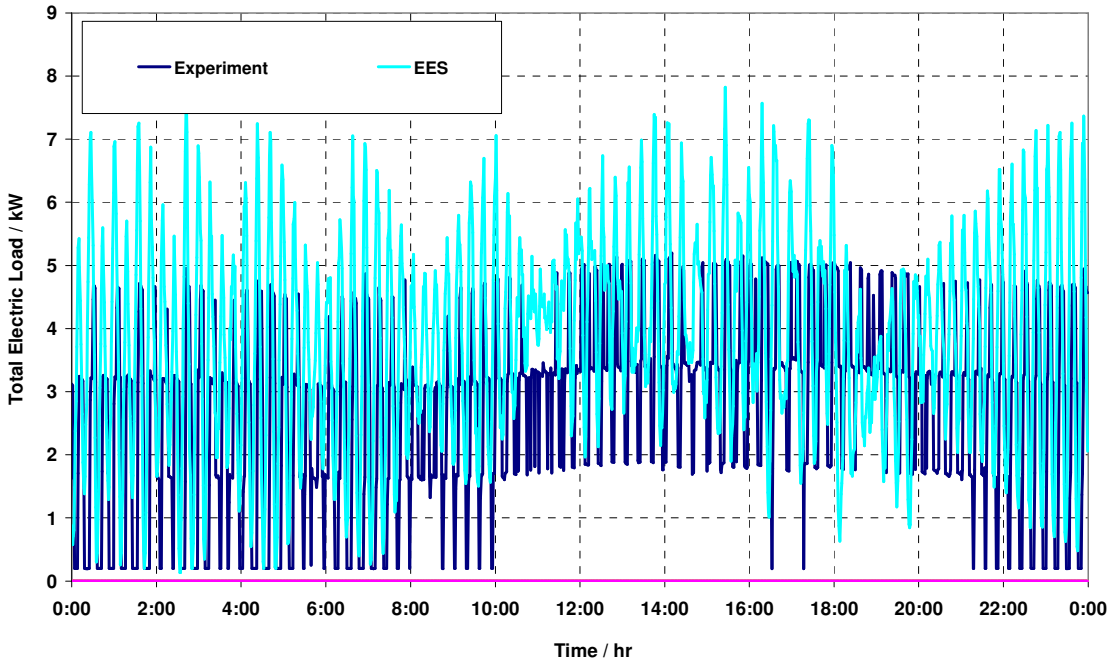

Figure 6-18 Chiller Empirical Test II (Hot Dry climate) – Averaged Daily Chiller Electric Load

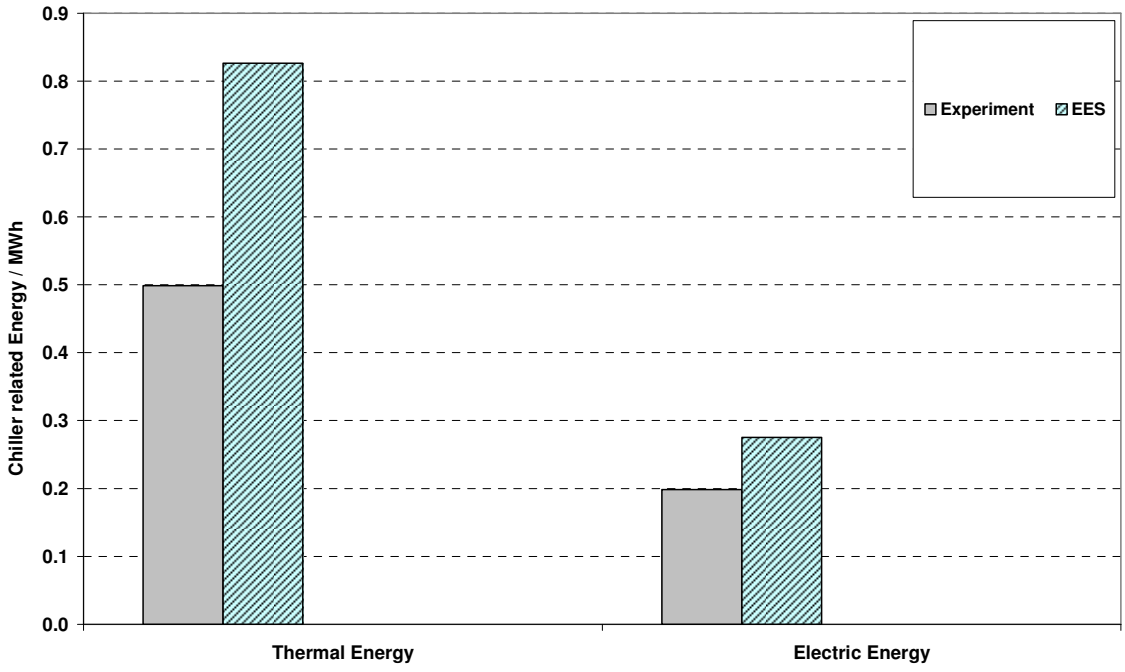

Figure 6-19 Chiller Empirical Test II (Hot Dry climate) – Chiller Total Thermal and Electric Energy

Table 6-10 Chiller empirical Test II (Hot Dry climate) – Total Cooling Load Statistics

CLT	Exp.				EES
$\overline{x}$	6.92				11.49
S	7.14				8.68
x_{min}	-2.57				0.00
x_{max}	18.06				32.39
$\overline{D}$					4.56
$\overline{\lvert D \rvert}$					8.35
$\lvert D \rvert_{max}$					25.28
$\lvert D \rvert_{min}$					0.00
D_{rms}					10.39
$D_{95\%}$					21.03

Table 6-11 Chiller empirical Test II (Hot Dry climate) –Total Electric Statistics

CEP	Exp.				EES
$\overline{x}$	2.75				3.83
S	2.29				2.69
x_{min}	0.19				0.20
x_{max}	5.55				10.95
$\overline{D}$					1.07
$\overline{\lvert D \rvert}$					2.59
$\lvert D \rvert_{max}$					8.29
$\lvert D \rvert_{min}$					0.00
D_{rms}					3.21
$D_{95\%}$					6.02

Table 6-12 Chiller empirical Test II (Hot Dry climate) – Leaving Water Temperature Statistics

LWT	Exp.				EES
$\overline{x}$	5.00				4.40
S	1.42				0.15
x_{min}	2.24				3.06
x_{max}	8.13				4.44
$\overline{D}$					-0.60
$\overline{\lvert D \rvert}$					1.22
$\lvert D \rvert_{max}$					3.69
$\lvert D \rvert_{min}$					0.01
D_{rms}					1.52
$D_{95\%}$					3.05

100% Outside Air (August 15 – August 16, 2006)

The chiller operates in all three modes available: on/off, stage 1, and stage 2 respectively. Significant deviations between experimental data and model predictions occur during early morning when the chiller continuously operates at stage 1. Cooling energy as well as electric energy is slightly underestimates as shown in Figure 6-24. The leaving air temperature predictions again have an offset of about 7K against the measurements.

Table 6-13 (cooling load), Table 6-14 (electric load), and Table 6-15 (leaving water temperature) provide some statistical information about chiller operation.

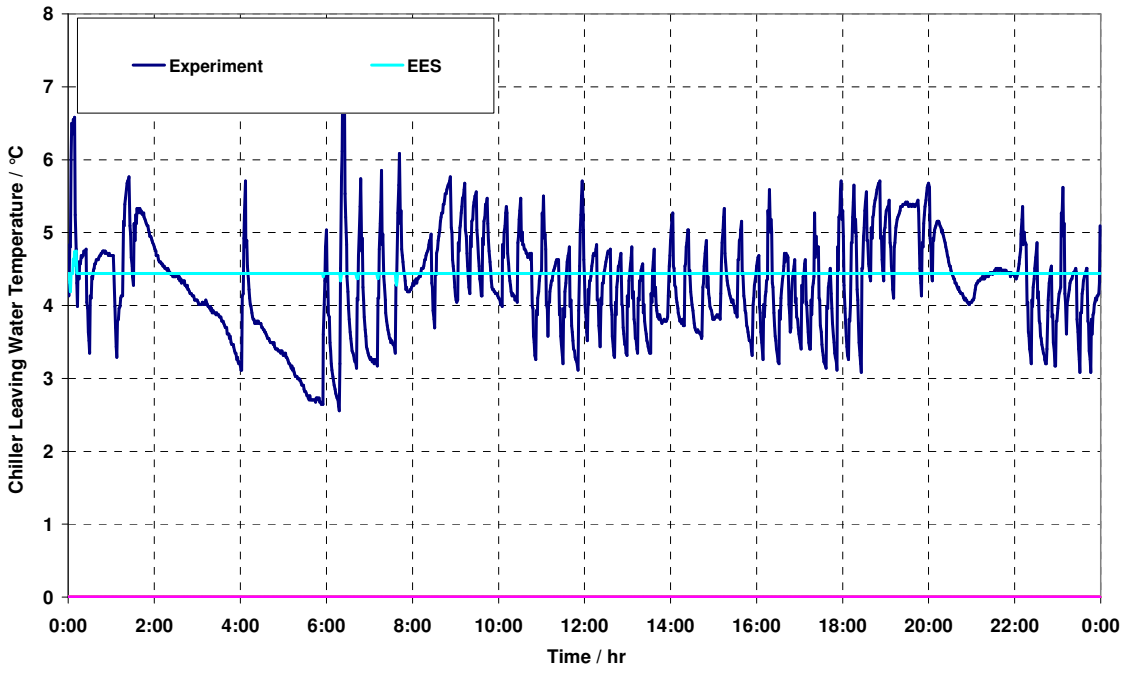

Figure 6-20 Chiller Empirical Test II (100% Outside air) – Averaged Daily Leaving Water Temperature

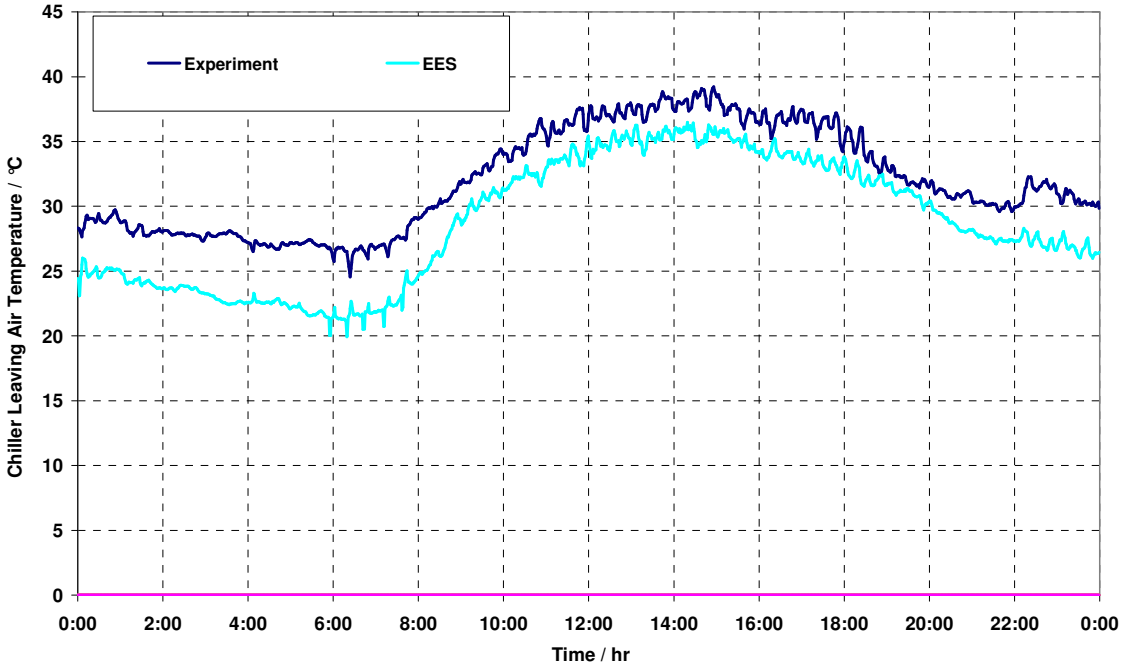

Figure 6-21 Chiller Empirical Test II (100% Outside air) – Averaged Daily Leaving Air Temperature (Condenser side)

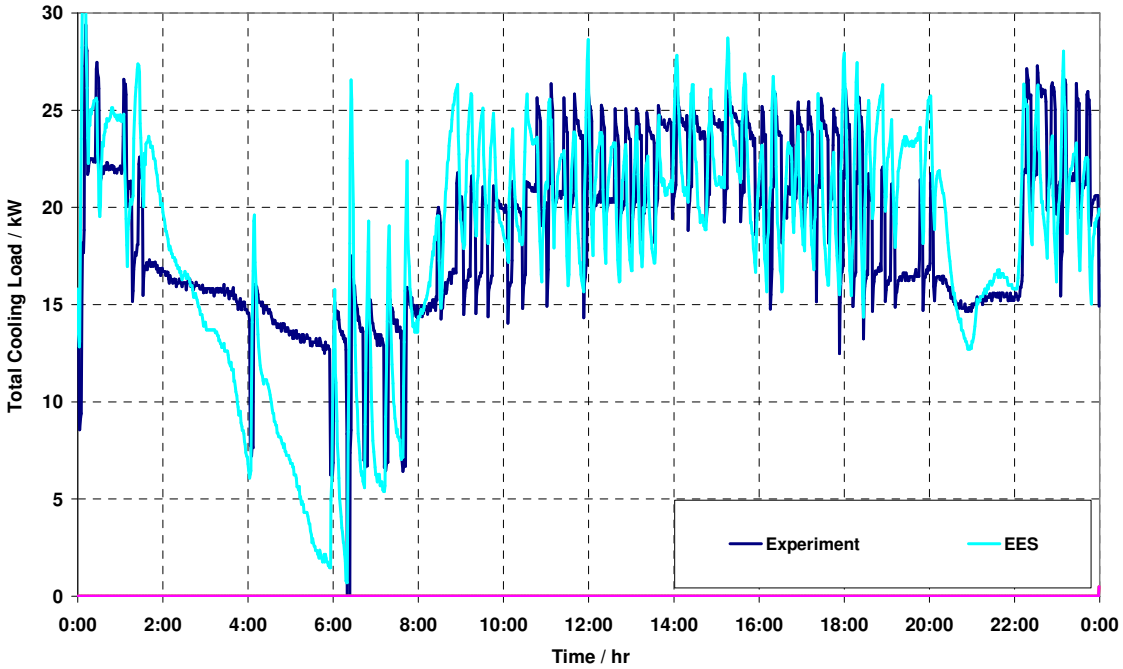

Figure 6-22 Chiller Empirical Test II (100% Outside air) – Averaged Daily Chiller Cooling Load

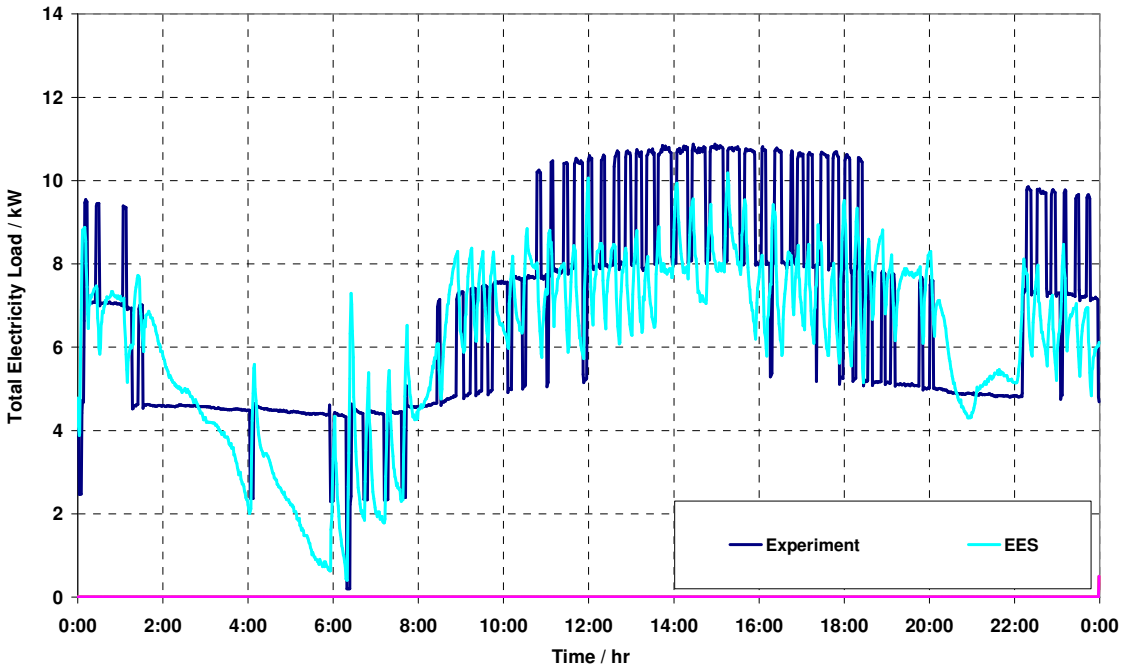

Figure 6-23 Chiller Empirical Test II (100% Outside air) – Averaged Daily Chiller Electric Load

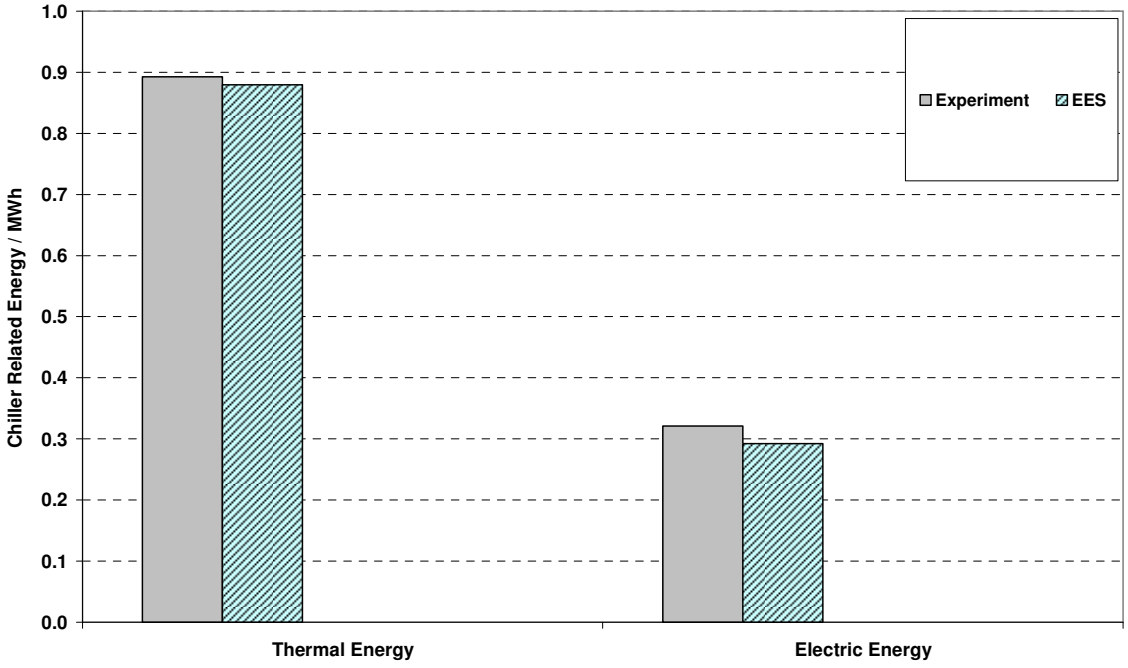

Figure 6-24 Chiller Empirical Test II (100% Outside air) – Chiller Total Thermal and Electric Energy

Table 6-13 Chiller empirical Test II (100% Outside air) – Total Cooling Load Statistics

CLT	Exp.				EES
$\overline{x}$	18.60				18.32
S	5.18				6.88
x_{min}	-1.37				0.00
x_{max}	31.11				35.67
$\overline{D}$					-0.27
$\overline{\lvert D \rvert}$					5.25
$\lvert D \rvert_{max}$					23.56
$\lvert D \rvert_{min}$					0.00
D_{rms}					6.13
$D_{95\%}$					10.52

Table 6-14 Chiller empirical Test II (100% Outside air) –Total Electric Statistics

CEP	Exp.				EES
$\overline{x}$	6.68				6.09
S	2.81				2.30
x_{min}	0.19				0.20
x_{max}	11.03				10.69
$\overline{D}$					-0.59
$\overline{\lvert D \rvert}$					2.36
$\lvert D \rvert_{max}$					6.21
$\lvert D \rvert_{min}$					0.00
D_{rms}					2.70
$D_{95\%}$					4.41

Table 6-15 Chiller empirical Test II (100% Outside air) – Leaving Water Temperature Statistics

LWT	Exp.				EES
$\overline{x}$	4.28				4.44
S	0.94				0.03
x_{min}	2.35				3.94
x_{max}	7.90				5.07
$\overline{D}$					0.16
$\overline{\lvert D \rvert}$					0.82
$\lvert D \rvert_{max}$					3.46
$\lvert D \rvert_{min}$					0.01
D_{rms}					0.95
$D_{95\%}$					1.65

Hot Humid Climate (August 18 – August 20, 2006)

Averaged daily chiller load is predicted well since the chiller mostly operates at stage 1 without much stage switching. Leaving air temperature measurement oscillate with ±1K at the given temperature set point. The amount of chiller cooling energy as well as electric energy is slightly overestimated.

Table 6-16 (cooling load), Table 6-17 (electric load), and Table 6-18 (leaving water temperature) provide some statistical information about chiller operation.

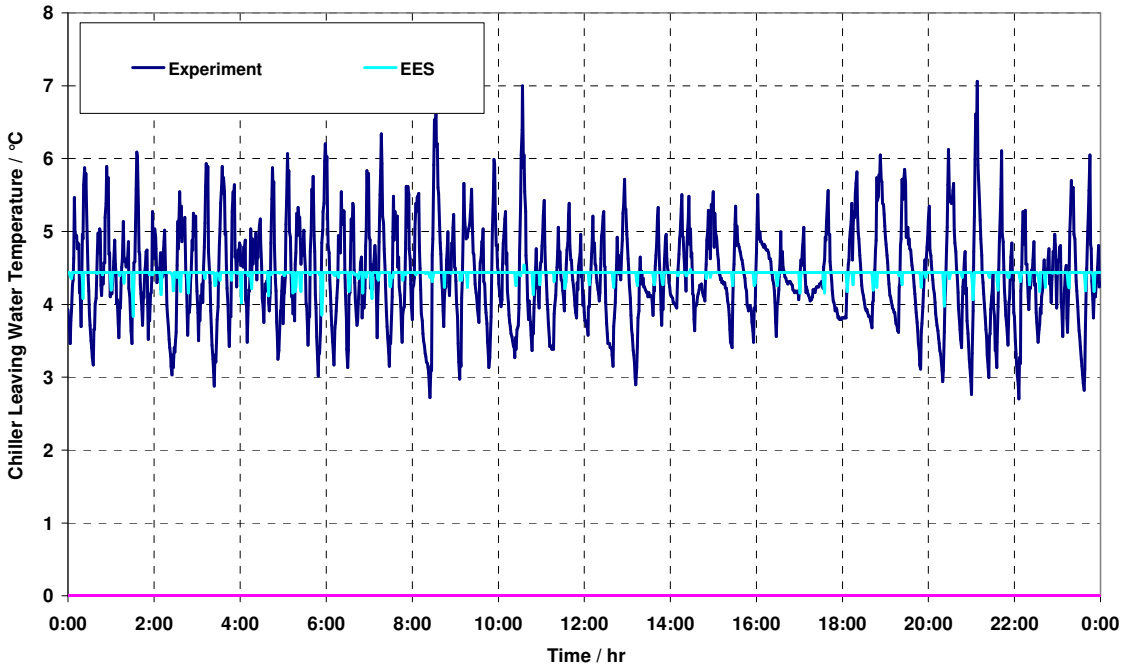

Figure 6-25 Chiller Empirical Test II (Hot Humid climate) – Averaged Daily Leaving Water Temperature

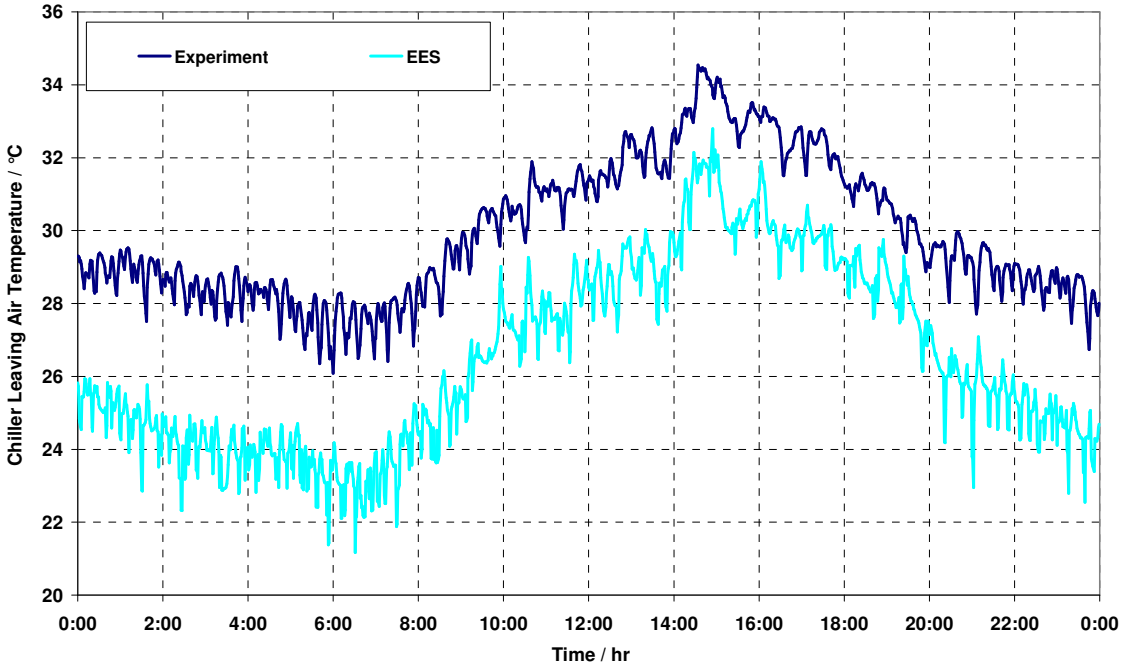

Figure 6-26 Empirical Test II (Hot Humid climate) – Averaged Daily Leaving Air Temperature (Condenser side)

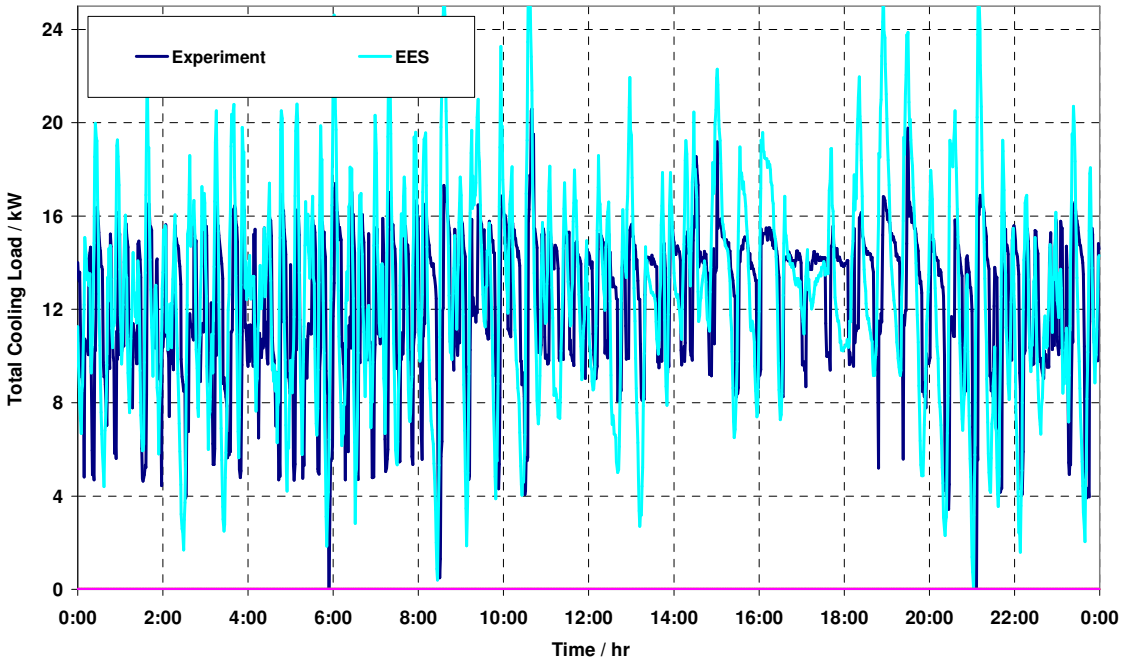

Figure 6-27 Chiller Empirical Test II (Hot Humid climate) – Averaged Daily Chiller Cooling Load

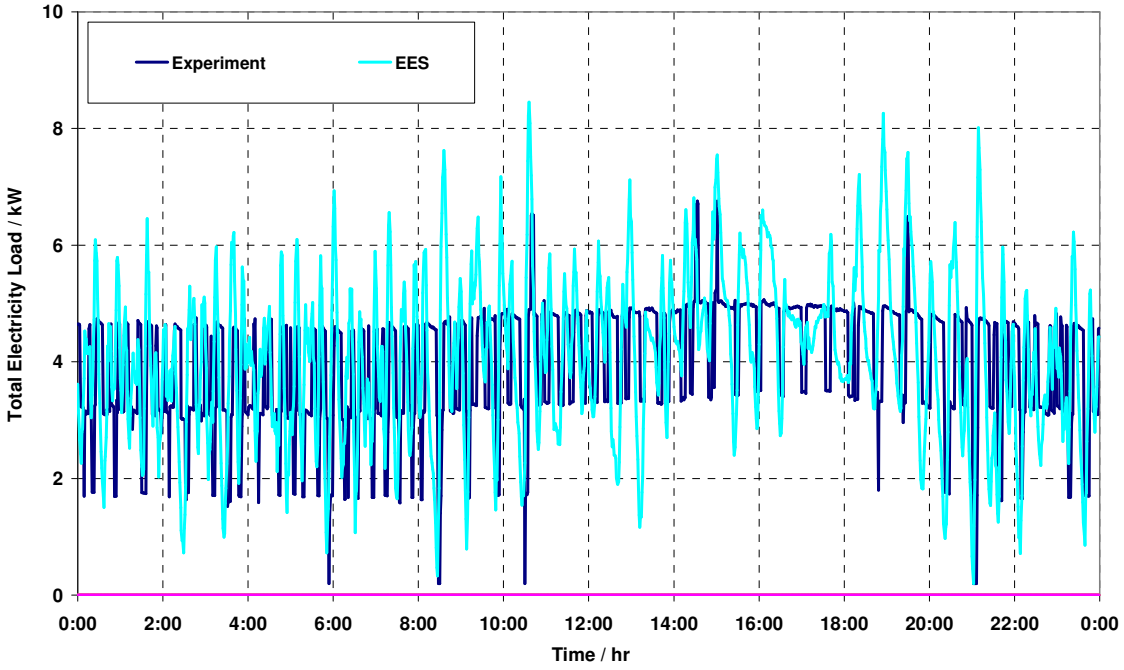

Figure 6-28 Chiller Empirical Test II (Hot Humid climate) – Averaged Daily Electric Load

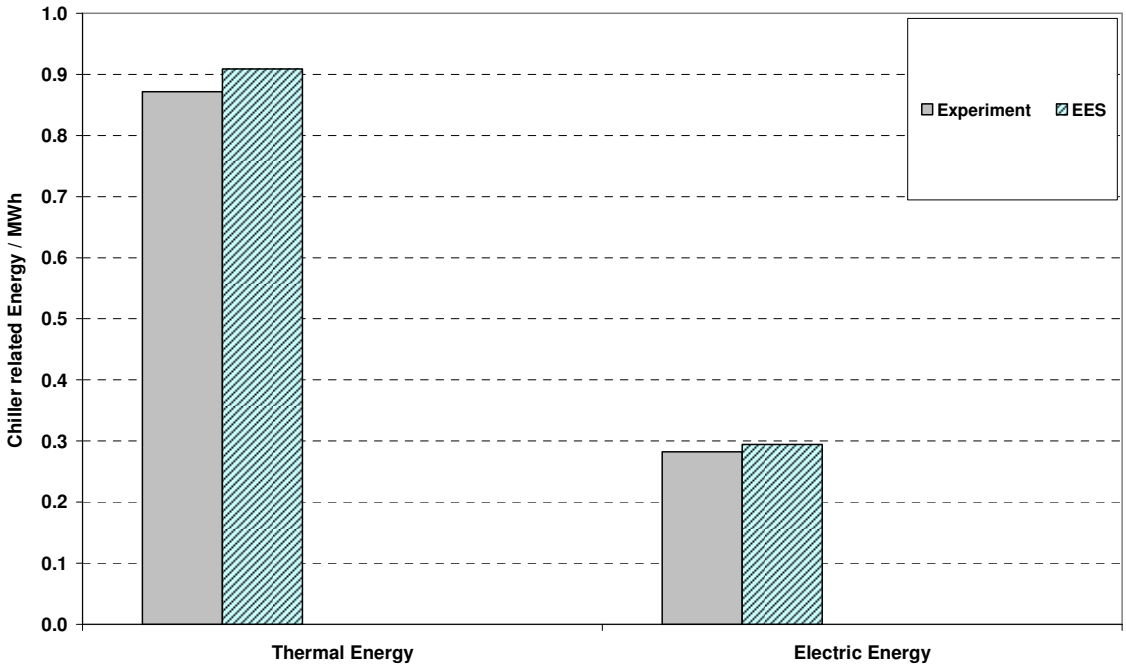

Figure 6-29 Chiller Empirical Test II (Hot Humid climate) – Chiller Total Thermal and Electric Energy

Table 6-16 Chiller empirical Test II (Hot Humid climate) – Total Cooling Load Statistics

CLT	Exp.				EES
$\overline{x}$	12.11				12.63
S	6.09				8.44
x_{min}	-2.13				0.00
x_{max}	28.85				33.75
$\overline{D}$					0.52
$\overline{\lvert D \rvert}$					6.66
$\lvert D \rvert_{max}$					24.70
$\lvert D \rvert_{min}$					0.00
D_{rms}					8.38
$D_{95\%}$					16.55
OU					

Table 6-17 Chiller empirical Test II (Hot Humid climate) –Total Electric Statistics

CEP	Exp.				EES
$\overline{x}$	3.92				4.09
S	1.83				2.51
x_{min}	0.19				0.20
x_{max}	10.37				11.00
$\overline{D}$					-0.33
$\overline{\lvert D \rvert}$					2.06
$\lvert D \rvert_{max}$					6.06
$\lvert D \rvert_{min}$					0.00
D_{rms}					2.58
$D_{95\%}$					4.31
OU					

Table 6-18 Chiller empirical Test II (Hot Humid climate) – Leaving Water Temperature Statistics

LWT	Exp.				EES
$\overline{x}$	4.40				4.42
S	1.25				0.10
x_{min}	2.18				3.18
x_{max}	8.01				4.76
$\overline{D}$					0.00
$\overline{\lvert D \rvert}$					0.00
$\lvert D \rvert_{max}$					0.01
$\lvert D \rvert_{min}$					0.00
D_{rms}					0.00
$D_{95\%}$					0.00

Cold Humid Climate (August 21 – August 23, 2006)

The chiller normally operates in stage 1 but switches to stage 2 during the afternoon. The EES model does not correctly predicts the right operating mode during late night. When during the experiment the chiller already switches to stage 1 the EES model still assumes a stage 2 operation chiller. For that reason the EES model overestimates chiller cooling load as well as chiller electricity load.

Table 6-19 (cooling load), Table 6-20 (electric load), and Table 6-21 (leaving water temperature) provide some statistical information about chiller operation.

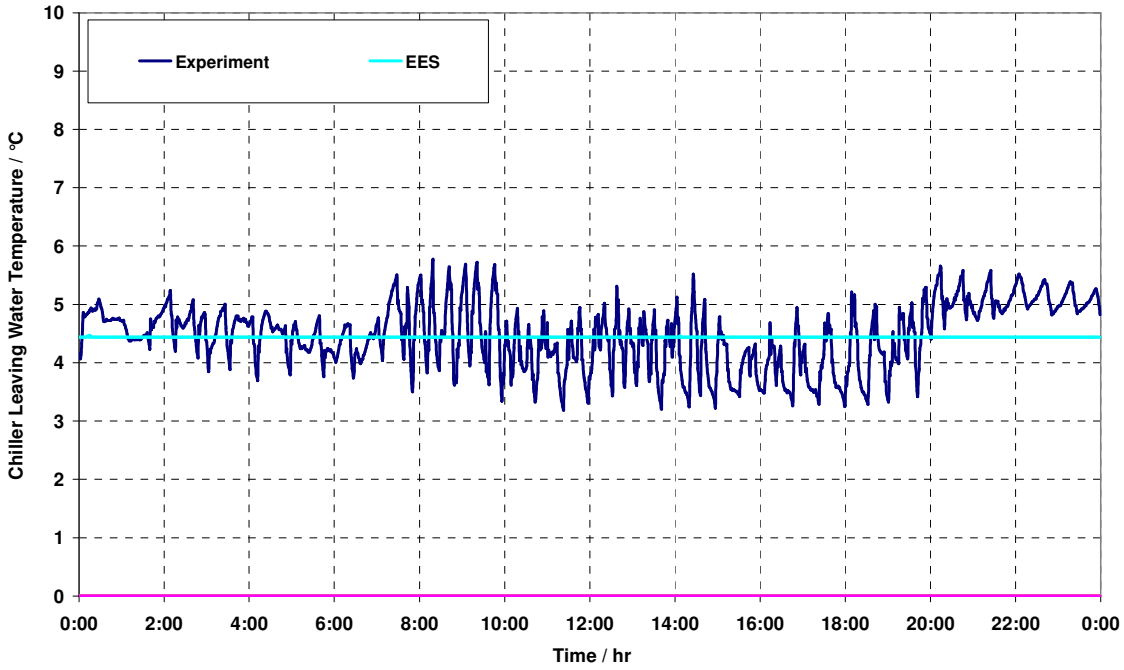

Figure 6-30 Chiller Empirical Test II (Cold Humid climate) – Averaged Daily Leaving Water Temperature

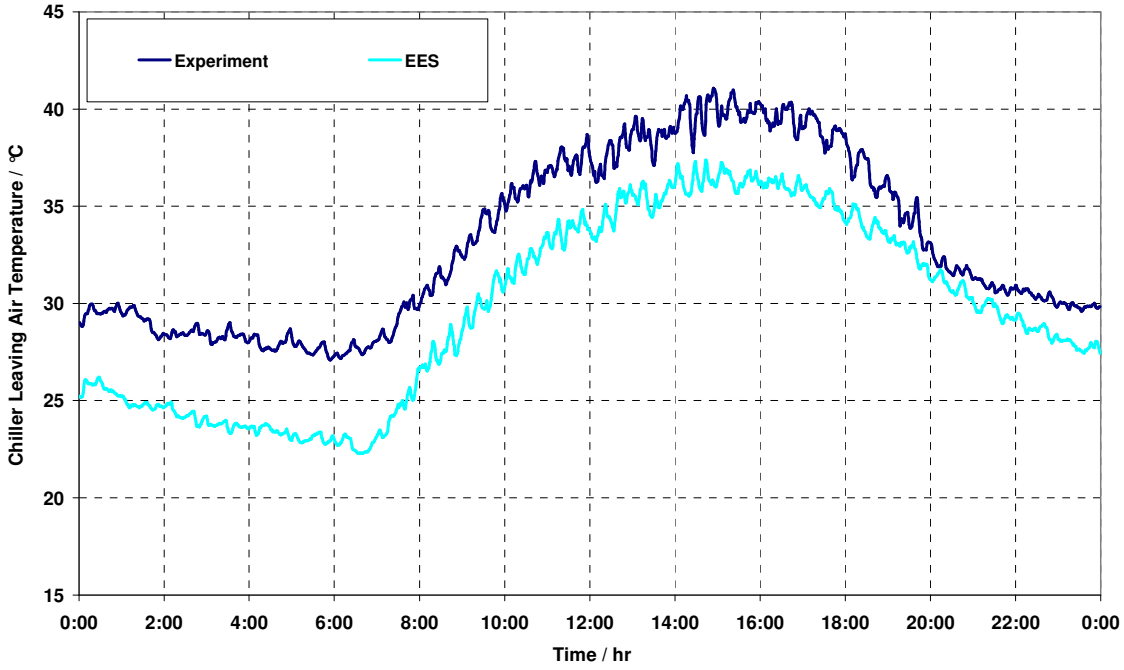

Figure 6-31 Empirical Test II (Cold Humid climate) – Averaged Daily Leaving Air Temperature (Condenser side)

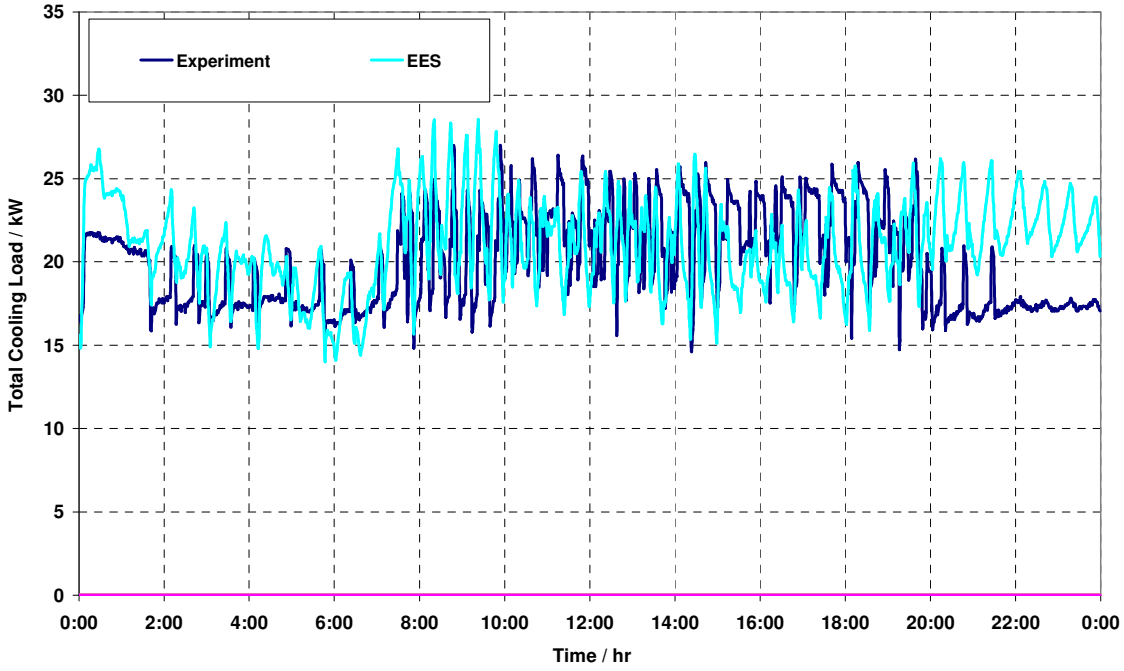

Figure 6-32 Chiller Empirical Test II (Cold Humid climate) – Averaged Daily Chiller Cooling Load

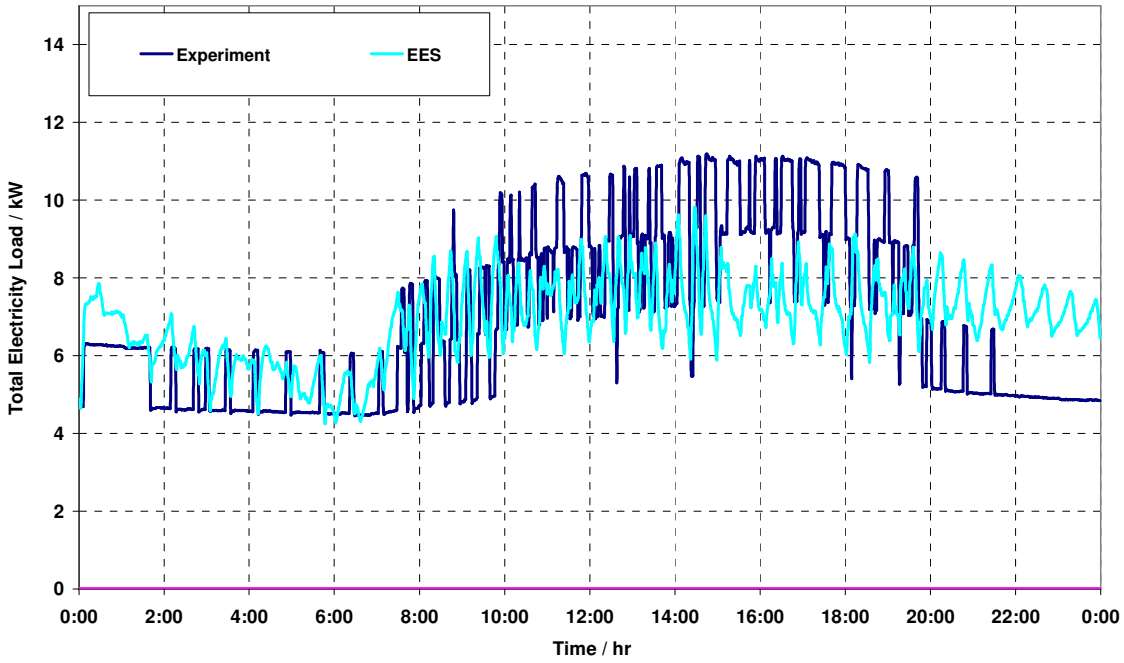

Figure 6-33 Chiller Empirical Test II (Cold Humid climate) – Averaged Daily Electric Load

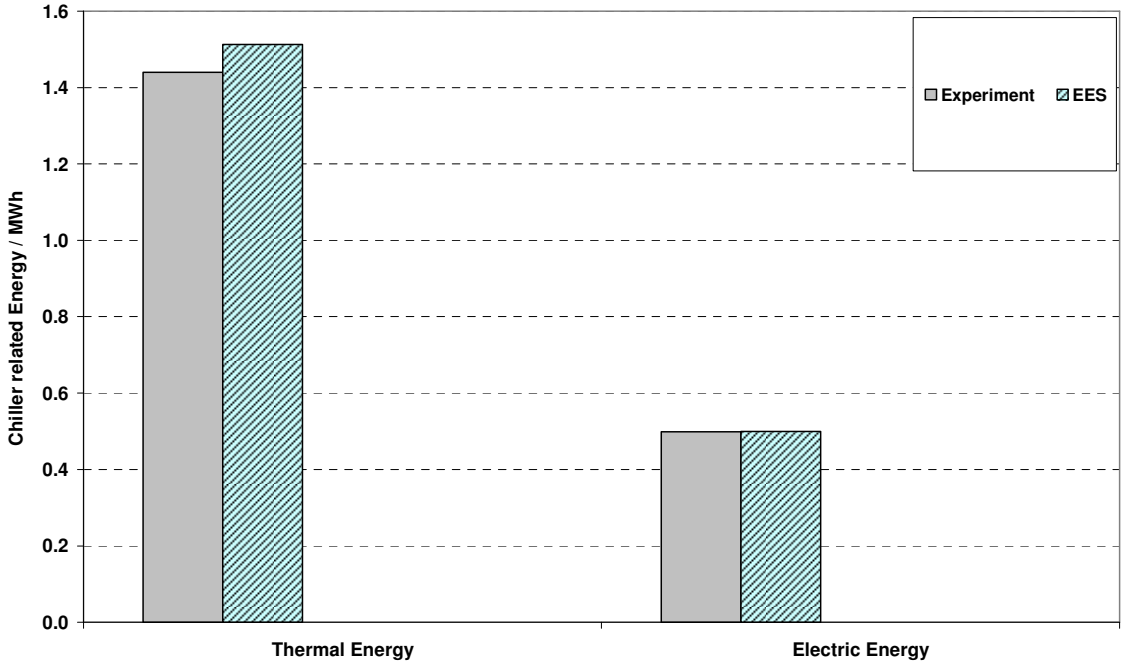

Figure 6-34Chiller Empirical Test II (Cold Humid climate) – Chiller Total Thermal and Electric Energy

Table 6-19 Chiller empirical Test II (Cold Humid climate) – Total Cooling Load Statistics

CLT	Exp.				EES
$\overline{x}$	19.99				21.01
S	4.17				4.35
x_{min}	12.13				6.15
x_{max}	30.73				35.12
$\overline{D}$					1.02
$\overline{\lvert D \rvert}$					4.65
$\lvert D \rvert_{max}$					12.47
$\lvert D \rvert_{min}$					0.00
D_{rms}					5.37
$D_{95\%}$					9.25

Table 6-20 Chiller empirical Test II (Cold Humid climate) –Total Electric Statistics

CEP	Exp.				EES
$\overline{x}$	6.93				6.94
S	2.77				1.44
x_{min}	4.28				2.07
x_{max}	11.64				11.65
$\overline{D}$					0.01
$\overline{\lvert D \rvert}$					2.36
$\lvert D \rvert_{max}$					5.43
$\lvert D \rvert_{min}$					0.00
D_{rms}					2.74
$D_{95\%}$					4.54

Table 6-21 Chiller empirical Test II (Cold Humid climate) – Leaving Water Temperature Statistics

LWT	Exp.				EES
$\overline{x}$	4.47				4.44
S	0.81				0.00
x_{min}	2.82				4.44
x_{max}	6.20				4.55
$\overline{D}$					-0.03
$\overline{\lvert D \rvert}$					0.70
$\lvert D \rvert_{max}$					1.76
$\lvert D \rvert_{min}$					0.01
D_{rms}					0.81
$D_{95\%}$					1.36

6.2 Cooling Coil

6.2.1 A Short Description of Cooling Coil Models

The modellers have been asked to give some detailed information on how their models work and on which general calculation approaches it is based on. Table 6-22 summarizes the answers submitted by the participants of this task. Two main findings can be described:

1. Most models get their characteristics from the performance data (Manufacturer point and/or additional points derived from measurements).The only one model that is based on geometry and material directly is the Matlab/Simulink model.
2. The EnergyPlus model is the only model that does not account for variable heat transfer coefficients UA dependent from air/water flow rates.

Table 6-22 Summary of information about cooling coil models submitted by the modelers

1. Program name and version number	**EES V7.888-3D**	**VA114 - version 2.25**	**EnergyPlus 2.2.0.023**	**TRNSYS-TUD**	**Matlab 6.5/Simulink**
2. Name of organization performed the simulations	ULG	Vabi Software bv	GARD Analytics, Inc	TU-Dresden	iTG-Dresden
3. Name of person performed simulations and contact information	Vincent Lemort Laboratoire de Thermodynamique Campus Sart Tilman B49 B-4000 Liège Belgium Vincent.lemort@ulg.ac.be	A.Wijsman a.wijsman@vabi.nl	Michael Witte mjwitte@gard.com Bob Henninger rhenninger@gard.com	Clemens Felsmann Technical University of Dresden 01062 Dresden Germany felsmann@itg-dresden.de	ITG Dresden Germany werdin@itg-dresden.de
4. Program status	Commercial	Commercial	U.S. Department of Energy Office of Building Technologies Washington DC	Research	Commercial
5. Time convention for weather data: first interval in the weather input lasts 00:00-01:00, climate is assumed constant over the sampling interval	Yes	Yes	Yes, if TimeStep is set = 1 hour No, if TimeStep is set <1 hour the climate data is interpolated to determine the value at each time step	Yes, but it depends on the user how to handle weather data. It is possible to keep climate constant or to interpolate between to points at each time step.	No, climate is interpolated, weather data are assumed to be instantaneous values
6. The heat transfer between air and cooling fluid is described by	three heat transfer coefficients: air to coil, coil metal, coil to cooling fluid	three heat transfer coefficients: air to coil, coil metal, coil to cooling fluid	three heat transfer coefficients: one between air-coil, one for the coil metal and one between coil-cooling fluid	two heat transfer coefficients: air to coil and coil to cooling fluid	three heat transfer coefficients: air to coil, coil metal, coil to cooling fluid

	EES V7.888-3D	VA114 - version 2.25	EnergyPlus 2.2.0.023	TRNSYS-TUD	Matlab 6.5/Simulink
7. The heat transfer dependency on flow rate is taken into account	at the air side and the water side of the coil	at the air side and the water side of the coil	is not taken into account (so the UA is fixed)	at the air side and the water side of the coil	at the air side and the water side of the coil
8. Dependency on air flow rate is taken into account (laminar and turbulent region)	$\left(\frac{\text{Flow}_{air}}{\text{Flow}_{air0}}\right)^{0.6}$	$\left(\frac{\text{Flow}_{air}}{\text{Flow}_{air0}}\right)^{0.56}$	-	$\left(\frac{\text{Flow}_{air}}{\text{Flow}_{air0}}\right)^{0.33}$	U=f(NU,Re,Pr)
9. Dependency on cooling fluid flow rate is taken into account (laminar and turbulent region)	$\left(\frac{\text{Flow}_{water}}{\text{Flow}_{water0}}\right)^{0.8}$	$\left(\frac{\text{Flow}_{water}}{\text{Flow}_{water0}}\right)^{0.8}$	-	$\left(\frac{\text{Flow}_{water}}{\text{Flow}_{water0}}\right)^{0.67}$	U=f(NU,Re,Pr)
10. Condensation and Evaporation in the cooling coil model	Only condensation	Only condensation	Only condensation	Only condensation	Both condensation and evaporation
11. Characteristics of cooling coil model	derived from more measuring points	derived from the Manufacturer point only	derived from the Manufacturer point only	derived from more measuring points (but not at the same time)	Mainly derived from the user given dimensions of cooling coil and fine tuned based on manufacturer or measuring points
12. Dynamics of cooling coil model	steady state model	steady state model	steady state model	steady state model	transient model

6.2.2 Comparative Test

The comparative cooling coil tests have been run by five different programs specified in Table 6-23.

Table 6-23 List of participants of the comparative cooling coil test

Name of the program	Modeler
VA114	VABI Software BV, Delft, The Netherlands
Matlab/Simulink	ITG Dresden , Germany
TRNSYS-TUD	Technical University Dresden, Germany
EES	Université de Liege, Belgium
EnergyPlus	GARD Analytics, Inc., U.S.

The EnergyPlus model was not able to provide simulation results for the temperature controlled coil or for the coil operating with a Propylen-Glycol fluid.

Figure 6-35 shows total cooling energy that was predicted by the different programs. Total cooling energy is that amount of energy that is needed from May to September to maintain leaving air temperature at a given set point. As to be seen there are two classes of cooling energy: 20…25 MWh and 45…60 MWh that mainly depends on leaving air temperature set point. Deviations between programs are normally less than 10%. Biggest differences between programs occur when leaving air temperature set point is low (13°C instead of 18°C) and air flow rate is variable (VAV instead of CAV).

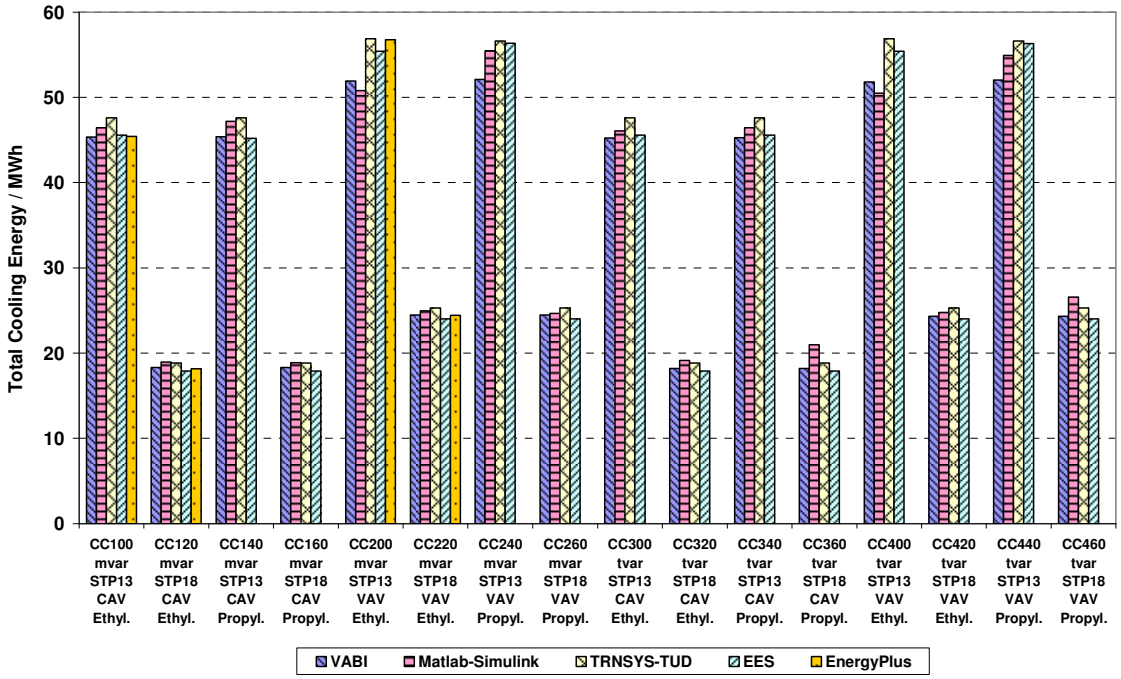

Figure 6-35 Cooling Coil Comparative Test - Total Cooling Energy

Figure 6-36 and Figure 6-37 show two different cooling load profiles: a hot dry day for CC100 and a hot humid day for CC200. It is obvious that all models agree very well in predicting a cooling load that is less than the nominal load known from the manufacturer submittal. Latent portion of total cooling load is about 20…30% at August 13. In opposite to that the total cooling load predicted by the programs for July 31 differs by 30 kW which is quite a lot compared to a total load that is between 50…80 kW. Such big differences only occur when air flow rate is increased and for that reason coil performance is outside of the nominal performance given by the manufacturer. That also means that leaving air temperature set point cannot be met. Latent portion of total cooling load is about 50% at July 31.

In addition to the total cooling energy prediction also the half year amount of both sensible as well as latent cooling energy can be used to qualify a model to be in accordance with the comparative cooling coil test. In Figure 6-38 and Figure 6-39 model prediction for both parts of cooling energy are depicted. It must be realized that deviations in long term cooling energy predictions between programs are in general too small to be used as a safety indicator for probable errors or model inaccuracies. That is also due to the fact that for given coil entering air conditions and given leaving air temperature set point cooling energy is nearly known.

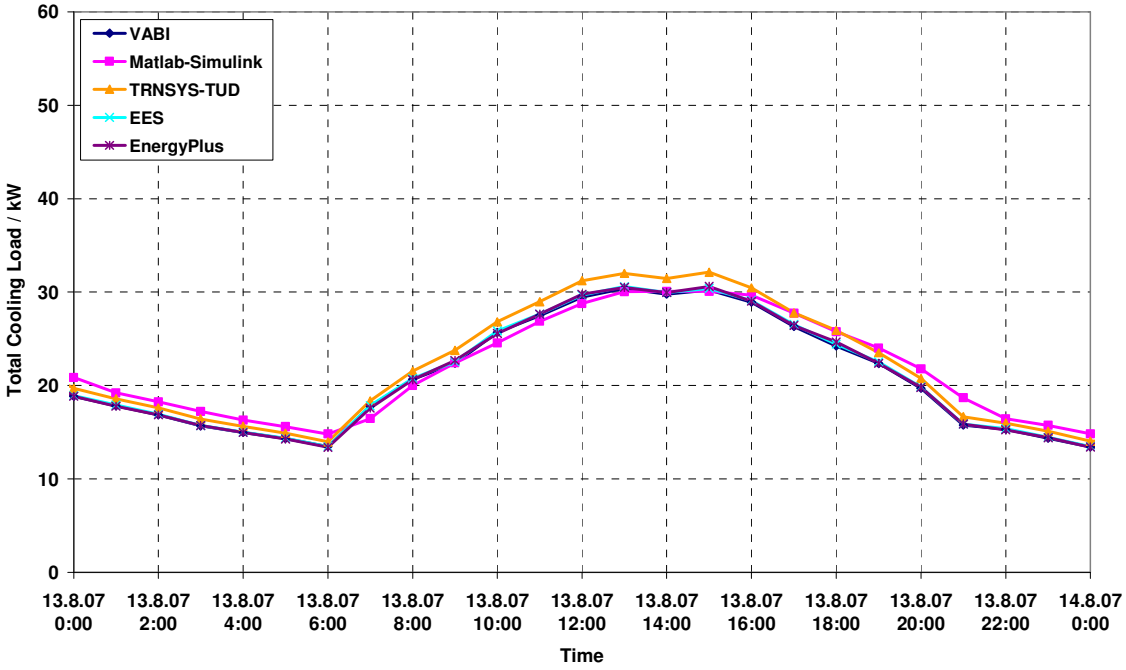

Figure 6-36 Cooling Coil Comparative Test Case CC100 - Total Cooling Load on August 13 (hot dry)

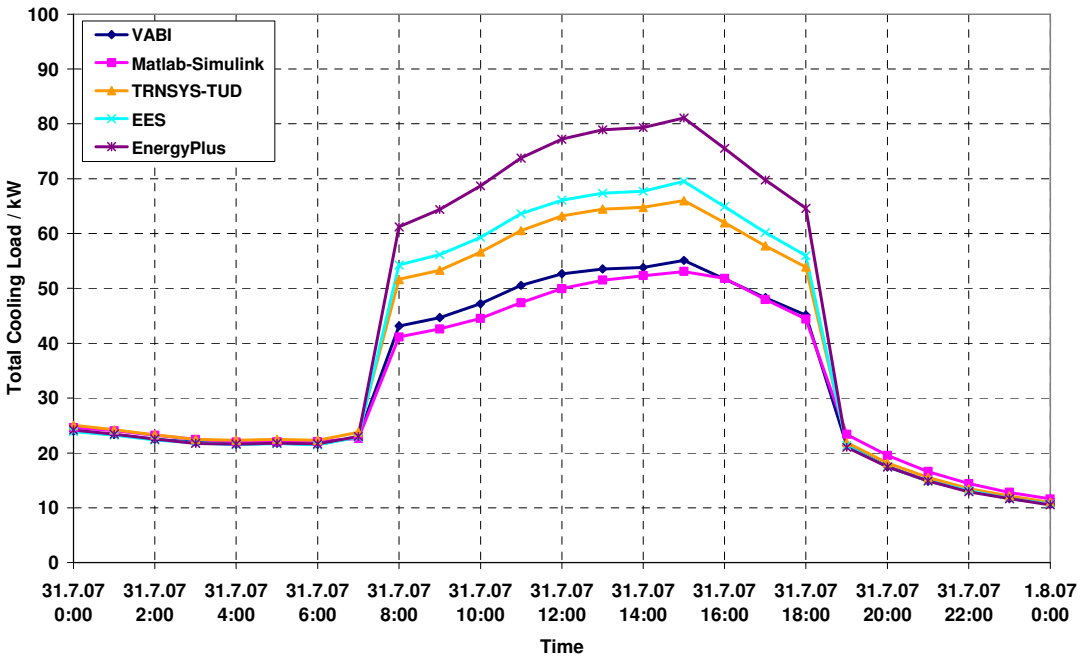

Figure 6-37 Cooling Coil Comparative Test Case CC200 - Total Cooling Load on July 31 (hot humid)

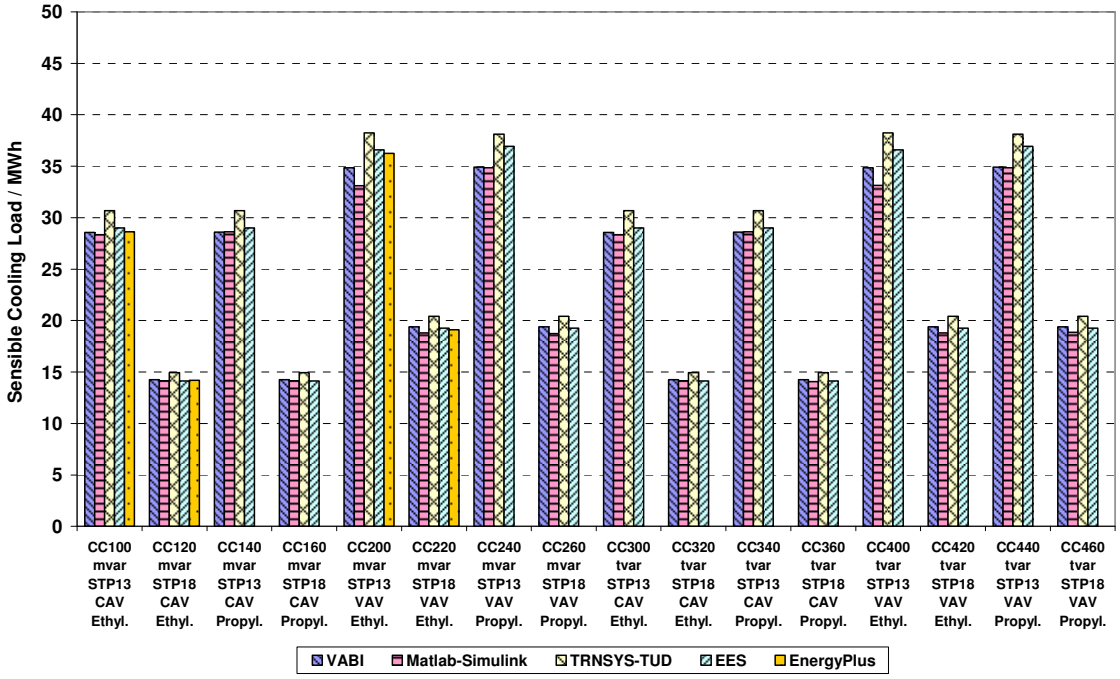

Figure 6-38 Cooling Coil Comparative Test - Sensible Cooling Energy

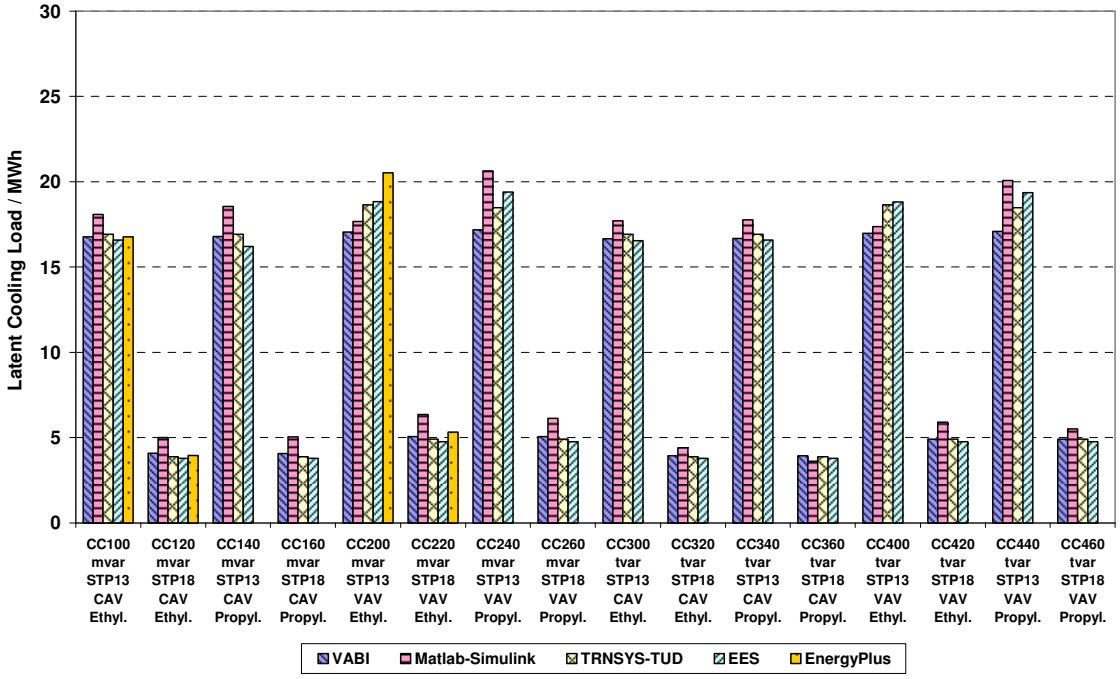

Figure 6-39 Cooling Coil Comparative Test - Latent Cooling Energy

For that reason some other variables seems to be more suitable to be used as an qualification indicator as for instance amount of condensation, total chilled water volume that has been circulated or leaving water temperature. These outputs are summarized in Figure 6-40, Figure 6-41, and Figure 6-45, respectively. Especially chilled water flow rate (for the mass flow controlled coil only; when the coil is temperature controlled water flow rate is assumed to be constant) and leaving water temperature give some more insight into cooling coil performance.

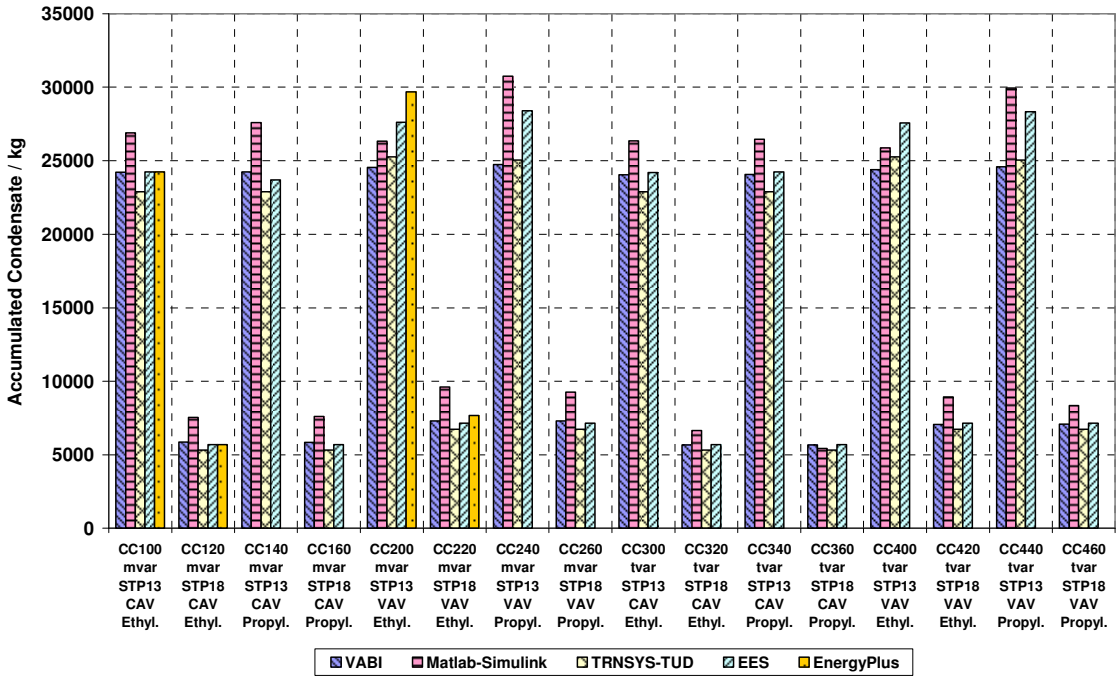

Figure 6-40 Cooling Coil Comparative Test - Condensation accumulated

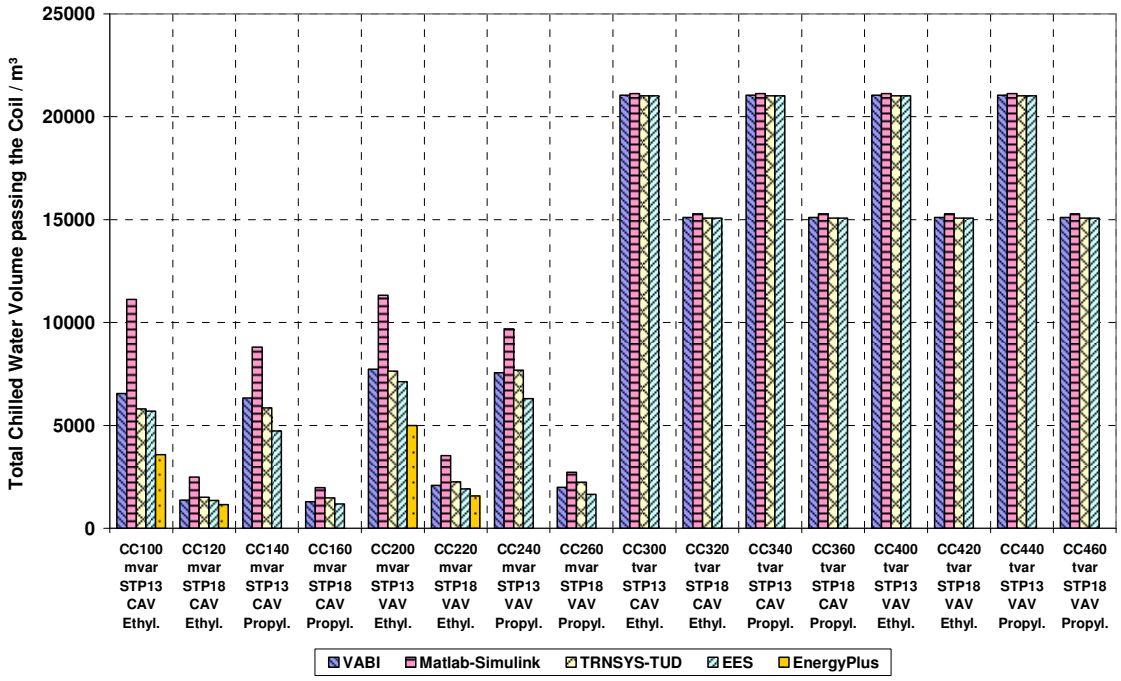

Figure 6-41 Cooling Coil Comparative Test - Chilled Water Volume circulated

Flow rate profiles depicted in Figure 6-42, Figure 6-43, and Figure 6-44 show big differences between programs. Chilled water flow rate (and so the Leaving Water Temperature) is very sensitive for taking into account the flow dependency of the specific capacity. Having cooling load profiles in mind it can be easily found that either different flow rates are needed to transfer a certain load from water to air side or different loads can be transferred for a given (constant or maximum) flow rate.

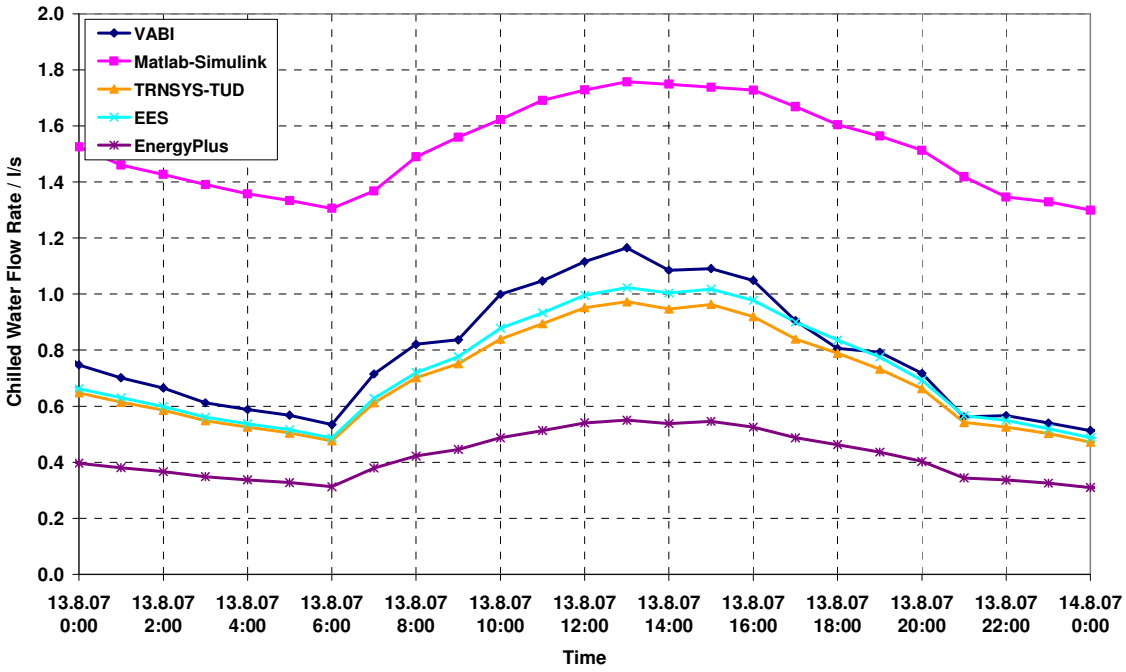

Figure 6-42 Cooling Coil Comparative Test CC100 - Chilled Water Flow Rate on August 13 (hot dry)

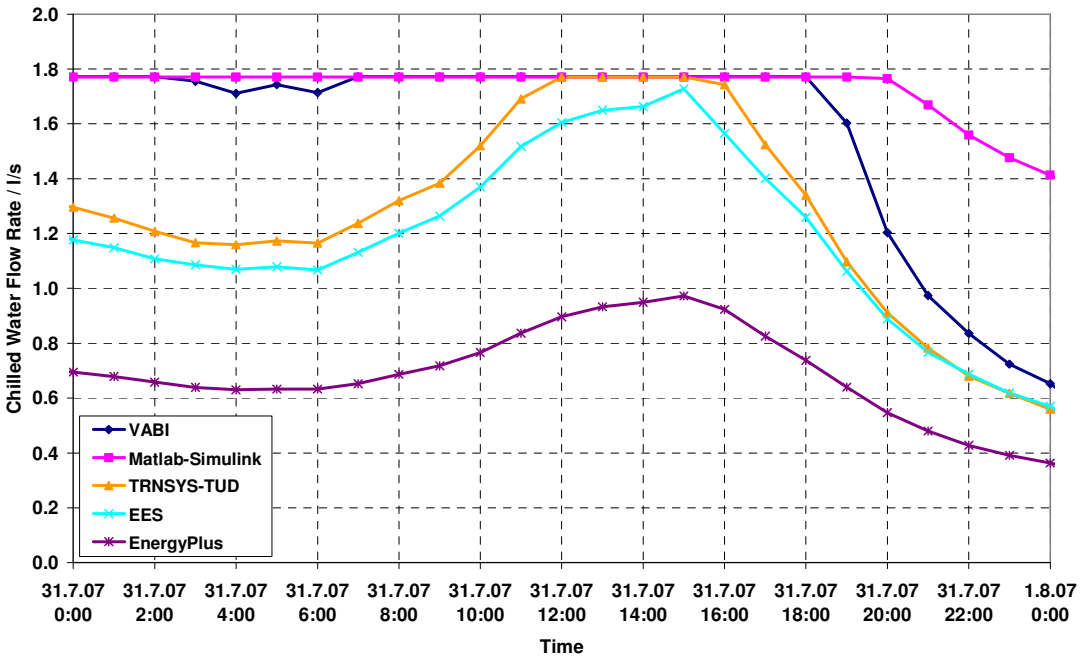

Figure 6-43 Cooling Coil Comparative Test CC100 - Chilled Water Flow Rate on July 31 (hot humid)

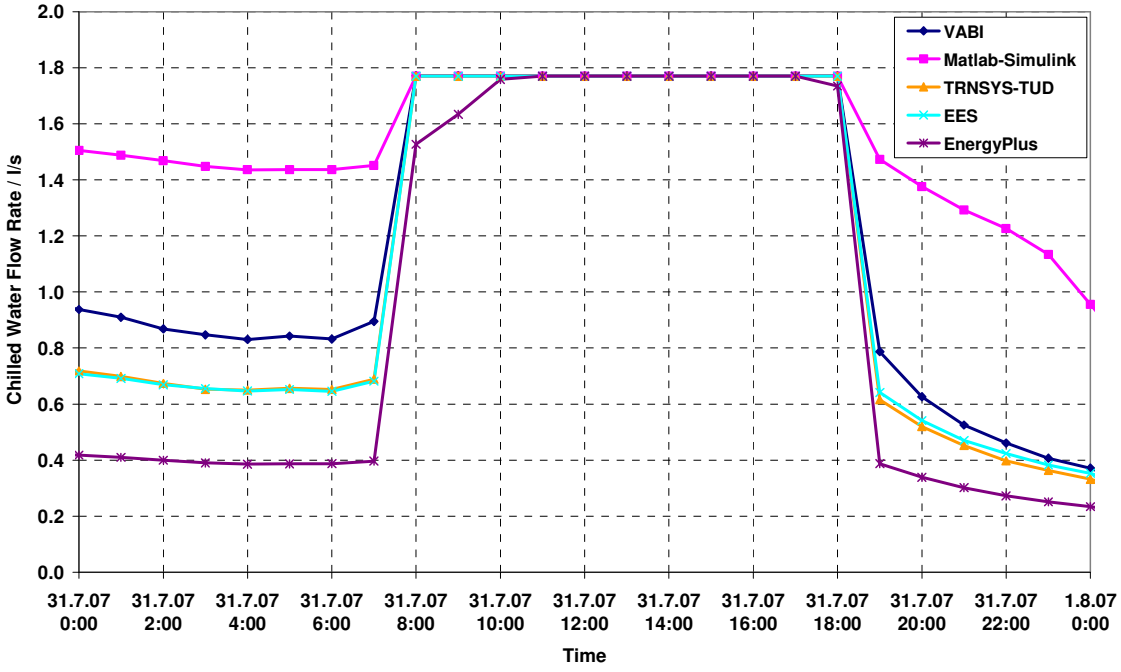

Figure 6-44 Cooling Coil Comparative Test CC200 - Chilled Water Flow Rate on July 31 (hot humid)

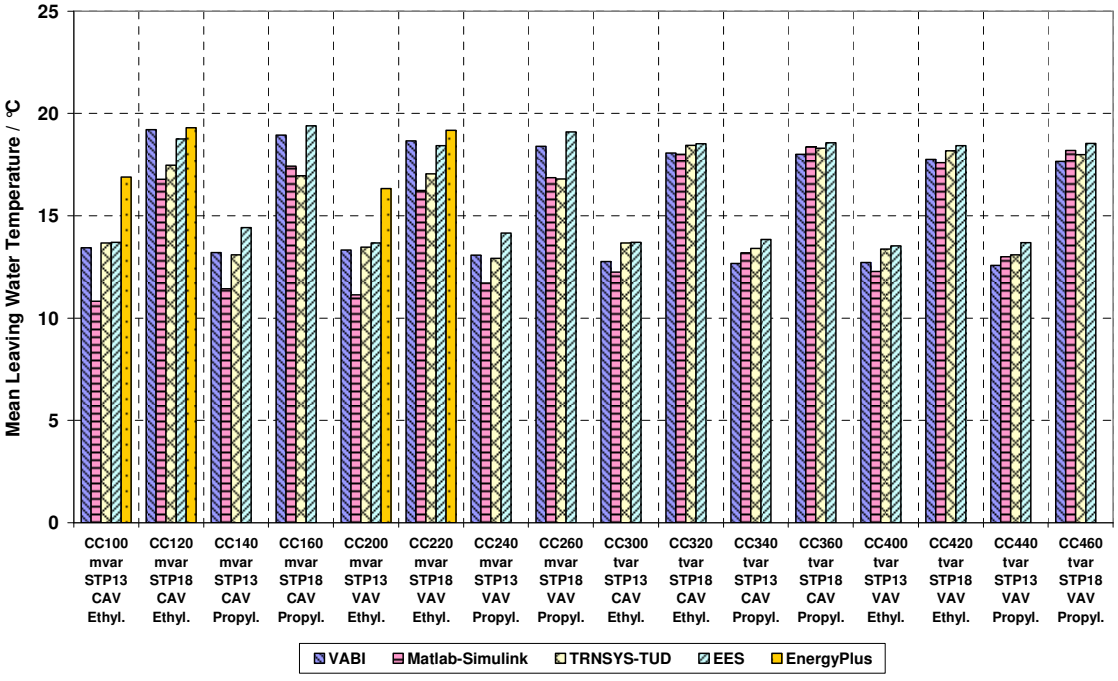

Figure 6-45 Cooling Coil Comparative Test - Mean Leaving Water Temperatur

6.2.3 Empirical Test I (August 24 – August 30, 2005)

The empirical cooling coil test I has been run by four different programs as specified in Table 6-24.

Table 6-24 List of participants of the empirical cooling coil test I

Name of the program	Modeler
VA114	VABI Software BV, Delft, The Netherlands
Matlab/Simulink	ITG Dresden, Germany
TRNSYS-TUD	Technical University Dresden, Germany
EES	Université de Liège, Belgium

Figure 6-46 shows the averaged daily energy balance of the cooling coil (air and water side) as well as cooling load of the chiller. The energy balance check gives some information about the basic reliability of experimental data.

The most important issue for model validation is to find an agreement between cooling energy balanced at both air and water side of the coil. For that reason inaccuracies originally found in the experimental data set have been compensated as described in chapter Data compensation4.5.2.

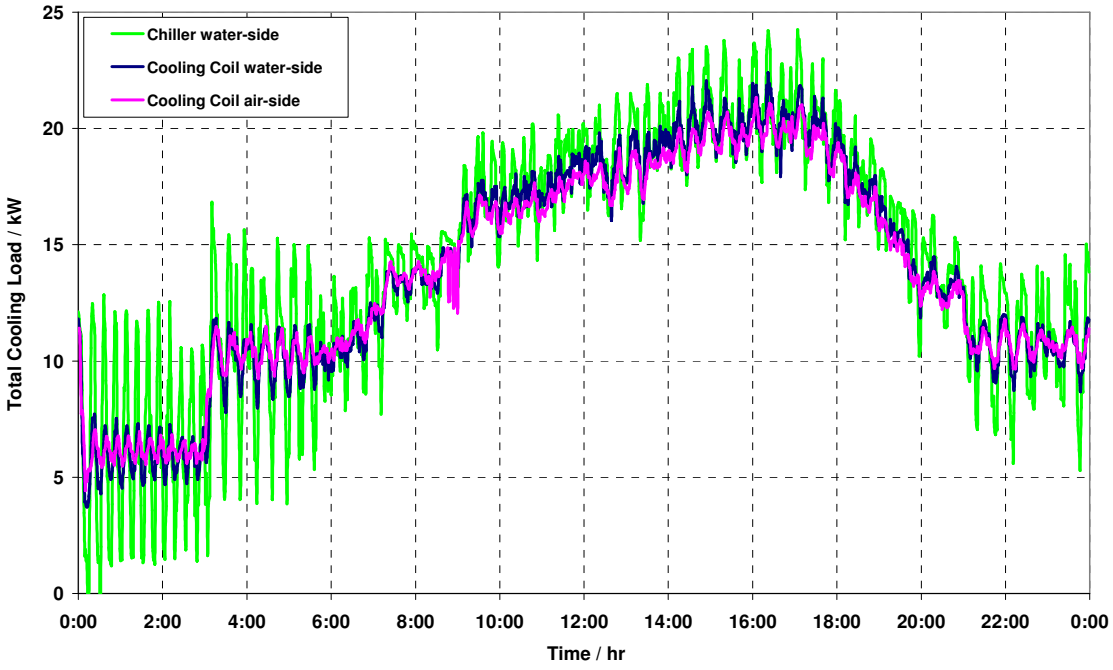

Figure 6-46 Cooling Coil Empirical Test I - Averaged Daily Energy Balance (Experiment)

Water side cooling load will be used for validation of cooling coil models. Although in this case air and water side cooling loads do agree very well it seems to be more suitable to validate models using water side loads rather than air side cooling loads. Main reason for doing is this way is the uncertainty in calculating latent cooling load from air side conditions.

Figure 6-47 shows a comparison between averaged daily cooling loads that were calculated based on the cooling loads predicted by the models and the experimental data. Agreement is quite good. Figure 6-48 represents total, sensible and latent cooling energy for the 7-day-period. From that graph a maximum difference of 7% between model predictions and measurements can be derived. Air side and water side energy balance of the coil do agree very well.

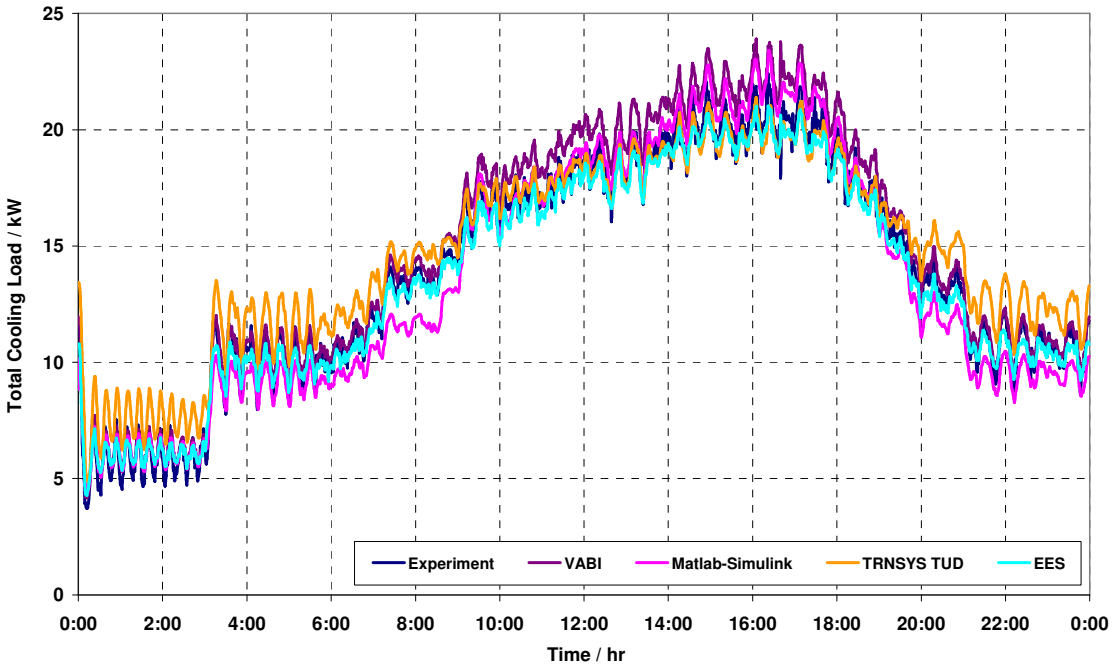

Figure 6-47 Cooling Coil Empirical Test I - Averaged Daily Cooling Load

Coil leaving air temperature (see Figure 6-49) and coil leaving water temperature (see Figure 6-50) show a very good agreement between models and measurements during daytime but some minor differences during night time. This might be caused by different air flow rates: during night air flow is about 1500m³/h whereas during daytime the air flow rate is three times higher.

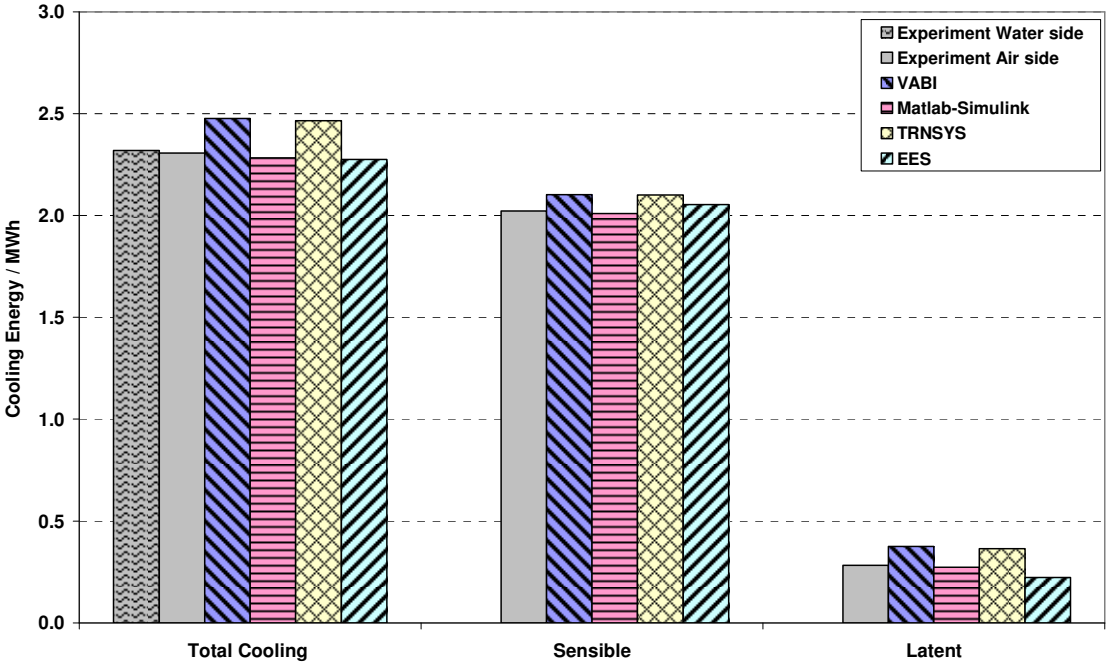

Figure 6-48 Cooling Coil Empirical Test I - Cooling Energy

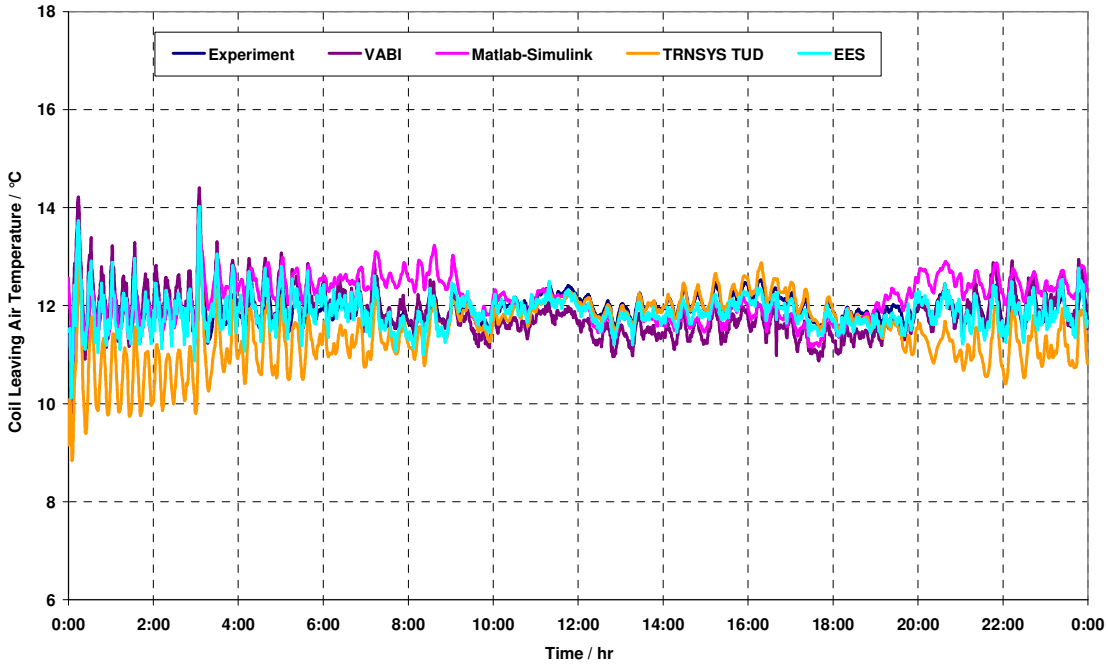

Figure 6-49 Cooling Coil Empirical Test I - Averaged Daily Coil Leaving Air Temperature

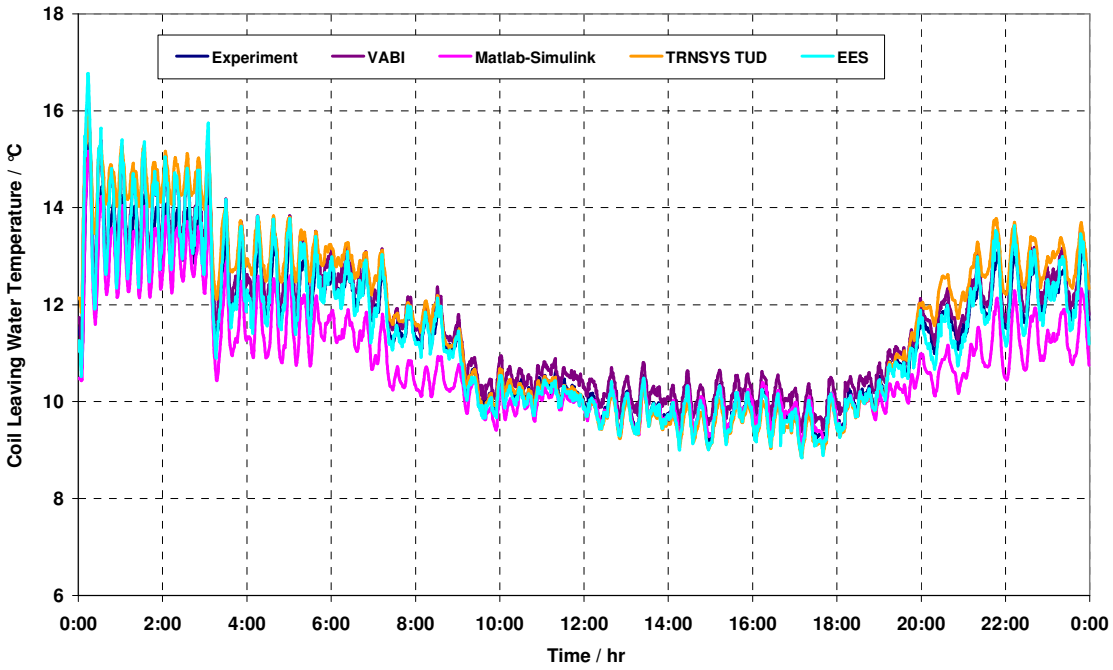

Figure 6-50 Cooling Coil Empirical Test I - Averaged Daily Coil Leaving Water Temperature

Biggest model uncertainties are related to the amount of condensation. The condensation mass flow was not asked for to be reported by the programs but it was calculated afterwards based on entering and leaving air conditions temperature and humidity. Figure 6-51 represents the condensation mass that was accumulated during the 7-day-validation period. The difference between programs and experiment is more than 110 kg which is an error of more than 25%.

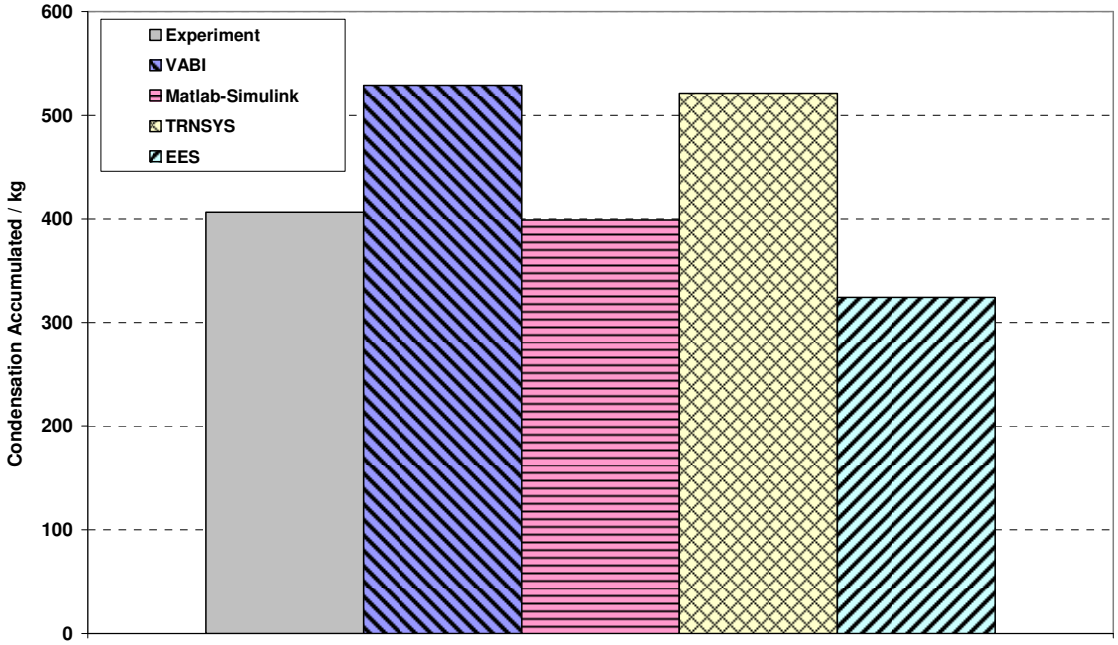

Figure 6-51 Cooling Coil empirical Test I - Condensate Accumulated

Some statistics can be found in Table 6-25 (total cooling load), Table 6-26 (leaving air temperature), and Table 6-27 (leaving water temperature), respectively.

Table 6-25 Cooling Coil empirical Test I – Total Cooling Load Statistics

CLT	Exp.	VABI	Simulink	TRNSYS-TUD	EES
$\overline{x}$	13.81	14.74	13.59	14.68	13.55
S	5.29	5.82	5.88	4.53	4.96
x_{min}	-0.15	3.07	0.00	3.56	3.25
x_{max}	24.86	30.01	28.67	24.18	25.06
$\overline{D}$		0.94	-0.22	0.87	-0.26
$\overline{\lvert D \rvert}$		1.10	1.30	1.37	0.79
$\lvert D \rvert_{max}$		30.16	15.34	17.82	25.21
$\lvert D \rvert_{min}$		0.00	0.00	0.00	0.00
D_{rms}		1.40	1.61	1.74	1.07
$D_{95\%}$		2.49	3.04	3.29	1.74

Table 6-26 Cooling Coil empirical Test I – Leaving Air Temperature Statistics

LAT	Exp.	VABI	Simulink	TRNSYS-TUD	EES
$\overline{x}$	11.93	11.82	12.12	11.47	11.86
S	0.59	0.90	0.72	1.04	0.79
x_{min}	9.21	6.72	9.27	0.00	7.40
x_{max}	14.41	17.75	15.13	15.50	17.42
$\overline{D}$		-0.12	0.19	-0.46	-0.07
$\overline{\lvert D \rvert}$		0.51	0.46	0.60	0.41
$\lvert D \rvert_{max}$		5.97	3.53	11.23	5.45
$\lvert D \rvert_{min}$		0.00	0.00	0.00	0.00
D_{rms}		0.68	0.54	0.80	0.56
$D_{95\%}$		1.38	0.94	1.59	1.37

Table 6-27 Cooling Coil empirical Test I – Leaving Water Temperature Statistics

LWT	Exp.	VABI	Simulink	TRNSYS-TUD	EES
$\overline{x}$	11.31	11.64	10.82	11.65	11.32
S	1.62	1.71	1.45	1.99	1.92
x_{min}	7.69	4.93	8.10	7.88	6.27
x_{max}	17.31	18.85	16.94	16.32	19.60
$\overline{D}$		0.33	-0.49	0.34	0.01
$\overline{\lvert D \rvert}$		0.44	0.58	0.51	0.43
$\lvert D \rvert_{max}$		6.28	1.73	3.84	6.98
$\lvert D \rvert_{min}$		0.00	0.00	0.00	0.00
D_{rms}		0.60	0.71	0.71	0.67
$D_{95\%}$		1.29	1.19	1.47	1.38

6.2.4 Empirical Test II (August 8 – August 23, 2006)

The empirical cooling coil test II has been run by four different programs as specified in Table 6-28.

Table 6-28 List of participants of the empirical cooling coil test II

Name of the program	Modeler
VA114	VABI Software BV, Delft, The Netherlands
Matlab/Simulink	ITG Dresden, Germany
TRNSYS-TUD	Technical University Dresden, Germany
EES	Université de Liège, Belgium

As described in Chapter 3.12 this empirical test consists of five separate sub-tests which will be analyzed separately as well.

Cold Dry Climate (August 8 – August 11, 2006)

The averaged daily cooling profiles of the water side of the chiller, the water sides of the cooling coil as well as the air side of the cooling coil - each calculated based on the measured data – are shown in Figure 6-52. These load profiles are used to check energy balances at the coil. The load profiles for this test period offer some significant deviations that indicate a non-balanced energy transfer. It is remarkable that neither both water sides - chiller and cooling coil - nor both sides of the cooling coil – air and water side – completely agree over the whole test period. This kind of disagreement does not satisfy the requirements for a high-quality validation test set.

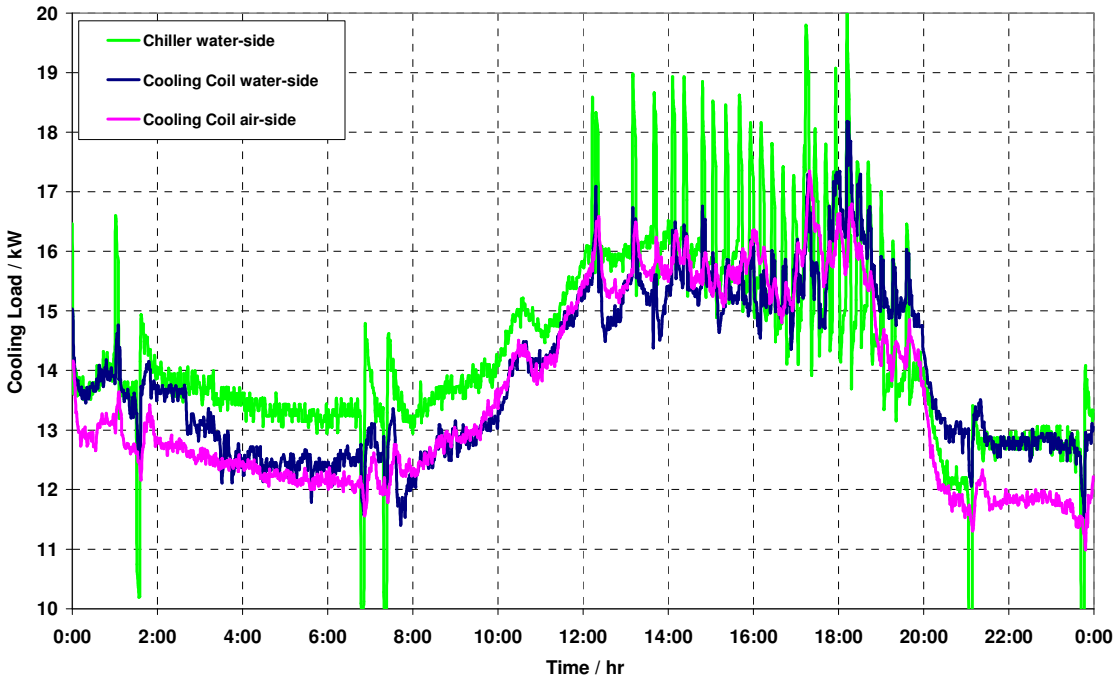

Figure 6-52 Cooling Coil Empirical Test II (Cold Dry climate) - Cooling Averaged Daily Energy Balance (Experiment)

For validation purposes the cooling load at the water side of the cooling coil will be used. Two programs (VA114 and EES) predict this total cooling load pretty well and do agree with the experimental data quite well. The other programs (Matlab/Simulink and TRNSYS-TUD) underestimate or overestimate total cooling load, see Figure 6-53. A similar trend can be seen from the cooling energy summary depicted in Figure 6-54. The air flow rate during this test varies between 3000…4000 m³/h. Air and water leaving temperatures predicted by the programs are within a range of 3 K. Leaving air temperature predictions do not agree as good as leaving water temperature predictions, see Figure 6-55 and Figure 6-56 for further details. Statistical data for this test are summarized in Table 6-29 (total cooling load), Table 6-30 (leaving air temperature), and Table 6-31 (leaving water temperature), respectively.

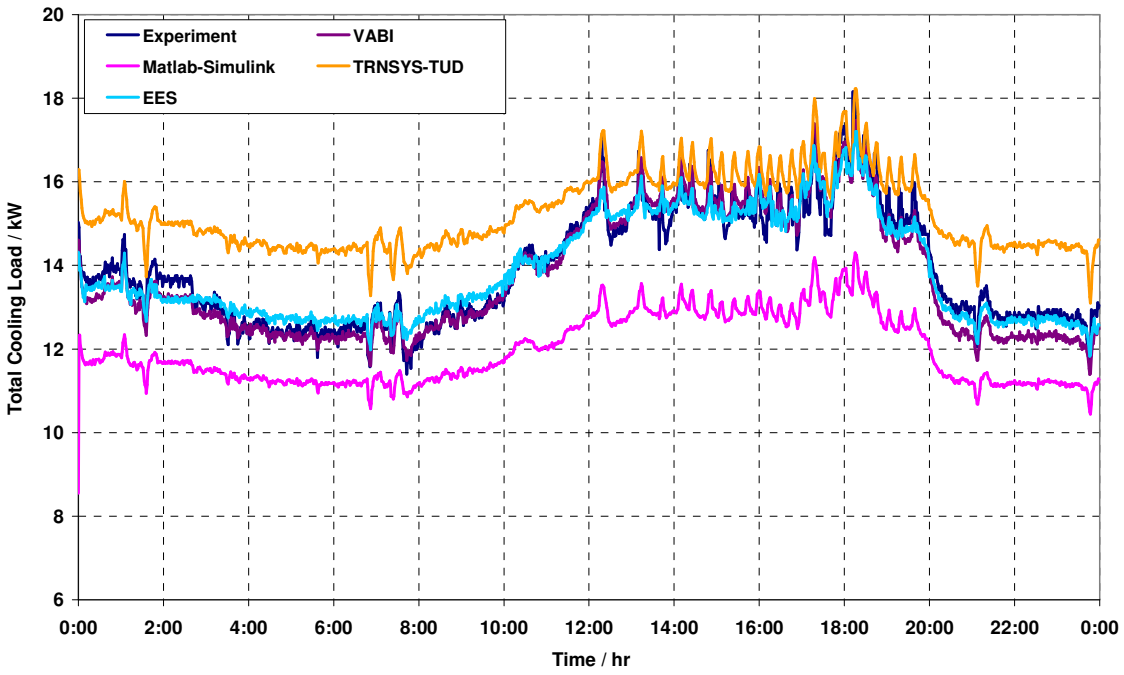

Figure 6-53 Cooling Coil Empirical Test II (Cold Dry climate) - Averaged Daily Cooling Load

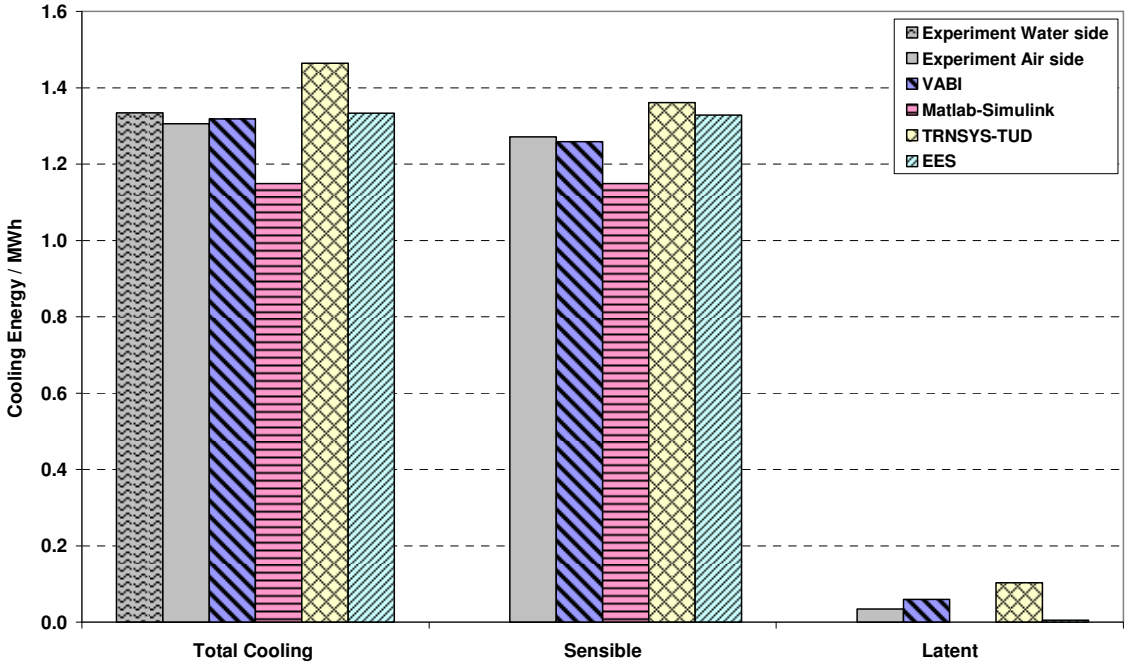

Figure 6-54 Cooling Coil Empirical Test II (Cold Dry climate) - Cooling Energy

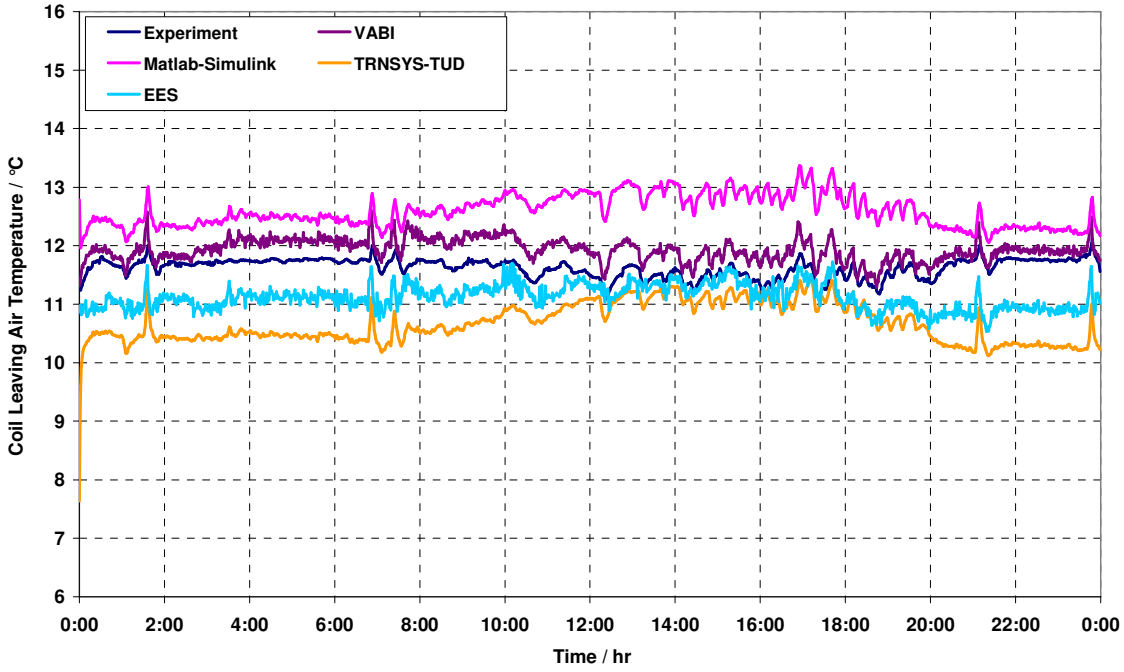

Figure 6-55 Cooling Coil Empirical Test II (Cold Dry climate) - Averaged Daily Coil Leaving Air Temperature

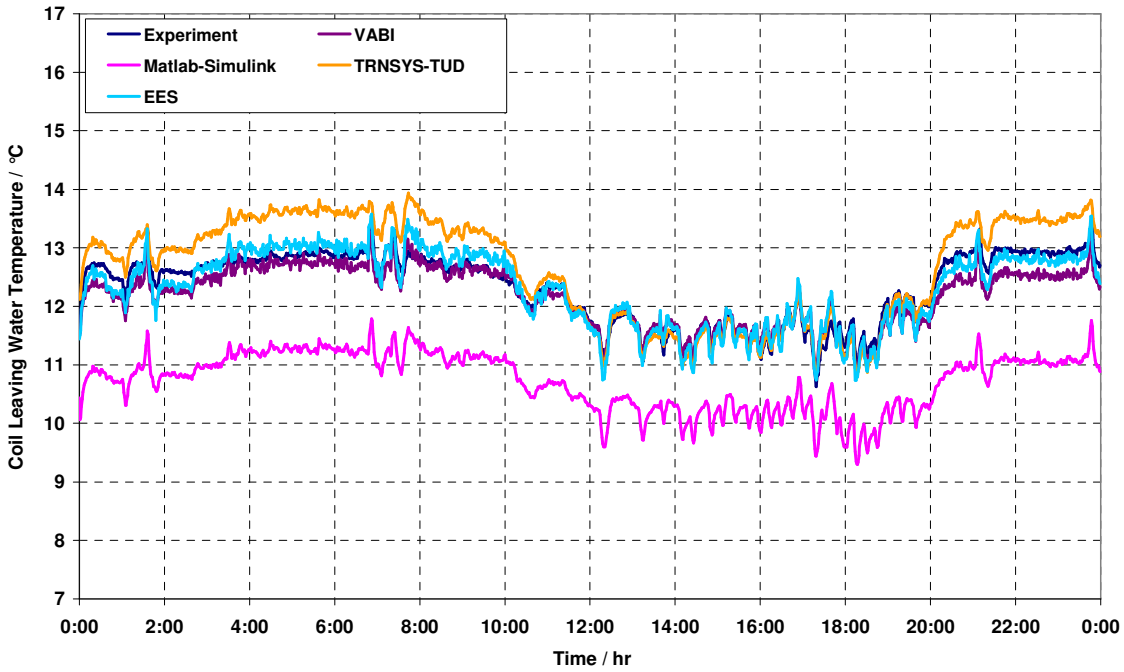

Figure 6-56 Cooling Coil Empirical Test II (Cold Dry climate) - Averaged Daily Coil Leaving Water Temperature

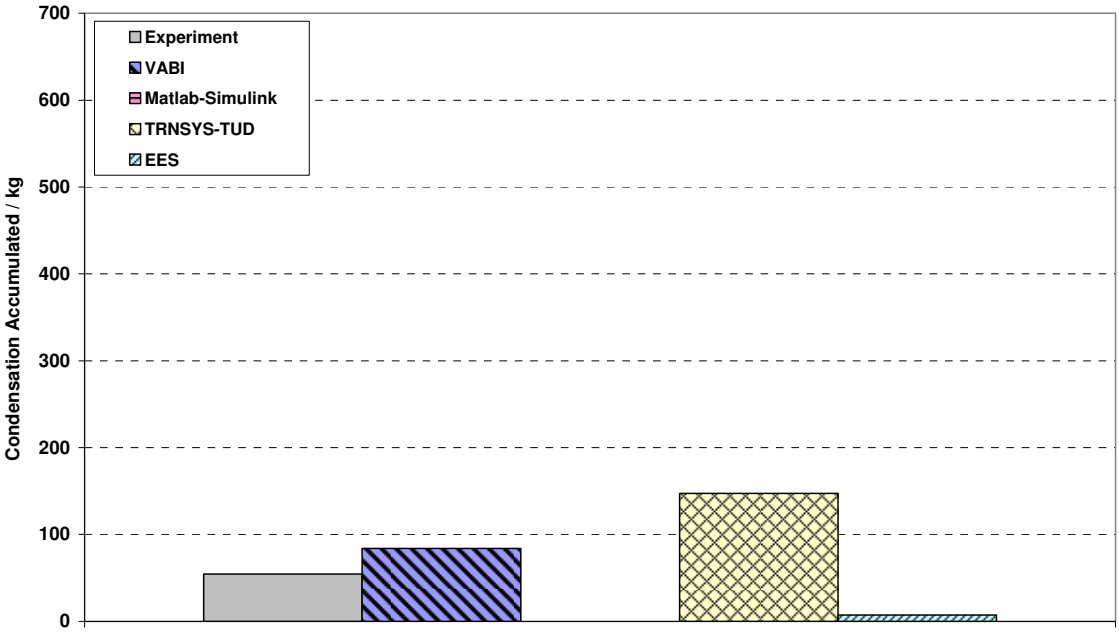

Figure 6-57 Cooling Coil empirical Test II (Cold Dry climate) - Condensate Accumulated

Table 6-29 Cooling Coil empirical Test II (Cold Dry climate) – Total Cooling Load Statistics

CLT	Exp.	VABI	Simulink	TRNSYS-TUD	EES
$\overline{x}$	13.60	13.73	11.97	15.25	13.88
S	2.10	1.98	1.16	1.39	1.65
x_{min}	9.09	1.00	0.00	1.00	1.00
x_{max}	19.92	20.73	16.13	20.93	19.70
$\overline{D}$		0.13	-1.63	1.65	0.29
$\overline{\lvert D \rvert}$		0.48	1.64	1.69	0.70
$\lvert D \rvert_{max}$		3.11	19.16	3.78	2.59
$\lvert D \rvert_{min}$		0.00	0.00	0.00	0.00
D_{rms}		0.62	1.98	1.97	0.82
$D_{95\%}$		1.22	3.34	3.22	1.45

Table 6-30 Cooling Coil empirical Test II (Cold Dry climate) – Leaving Air Temperature Statistics

LAT	Exp.	VABI	Simulink	TRNSYS-TUD	EES
$\overline{x}$	11.62	11.93	12.59	10.67	11.12
S	0.25	0.34	0.41	0.47	0.39
x_{min}	10.54	10.34	11.51	0.00	9.99
x_{max}	12.93	14.61	14.77	13.42	13.90
$\overline{D}$		0.31	0.97	-0.96	-0.50
$\overline{\lvert D \rvert}$		0.35	0.97	0.96	0.59
$\lvert D \rvert_{max}$		2.22	3.99	10.77	1.72
$\lvert D \rvert_{min}$		0.00	0.04	0.00	0.00
D_{rms}		0.42	1.08	1.11	0.67
$D_{95\%}$		0.79	1.66	1.74	1.19

Table 6-31 Cooling Coil empirical Test II (Cold Dry climate) – Leaving Water Temperature Statistics

LWT	Exp.	VABI	Simulink	TRNSYS-TUD	EES
$\overline{x}$	12.33	12.19	10.72	12.66	12.31
S	0.77	0.68	0.69	1.11	0.89
x_{min}	9.27	9.41	7.92	9.26	9.05
x_{max}	15.06	15.46	13.95	14.76	15.98
$\overline{D}$		-0.14	-1.61	0.33	-0.02
$\overline{\lvert D \rvert}$		0.29	1.61	0.46	0.25
$\lvert D \rvert_{max}$		1.99	2.45	2.08	2.51
$\lvert D \rvert_{min}$		0.00	0.01	0.00	0.00
D_{rms}		0.38	1.64	0.55	0.38
$D_{95\%}$		0.75	2.24	0.94	0.80

Hot Dry Climate (August 12 – August 14, 2006)

Figure 6-58 contains a graph that shows energy balances at water and air side of the cooling coil based on error compensated experimental data In general air and water side cooling do agree quite well but have some small deviations during night. Chiller cooling load that serves the coil shows big fluctuations that are cause by the chiller control.

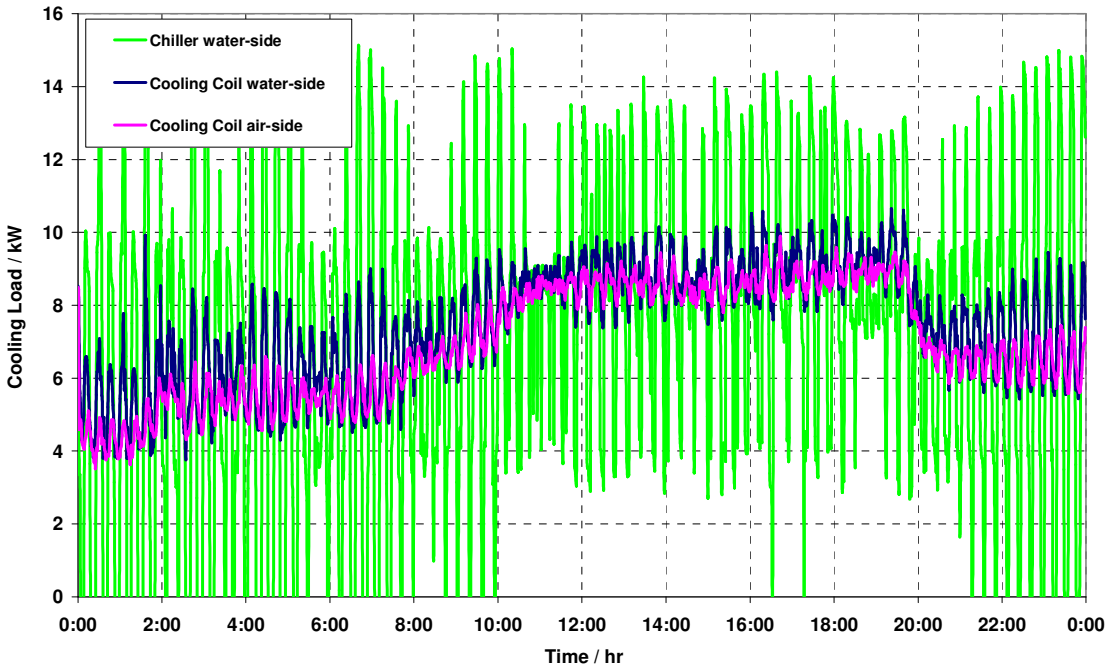

Figure 6-58 Cooling Coil Empirical Test II (Hot Dry climate) - Cooling Averaged Daily Energy Balance (Experiment)

Cooling load predicted by the programs matches the experimental based cooling load very well but TRNSYS-TUD model overestimates cooling load, see Figure 6-59. Figure 6-60 helps to clarify that deviation of the TRNSYS-TUD results are caused by both sensible and latent parts of the cooling load. The air flow is within a range of 500…2000m³/h which is quite low. Both coil leaving air temperatures and coil leaving water temperatures predicted by the models deviate from the measured data by less than 1K. TRNSYS-TUD underestimates coil leaving air temperature by 2K.

Statistics for this test case are summarized in Table 6-32 (total cooling load), Table 6-33 (leaving air temperature), and Table 6-34 (leaving water temperature), respectively.

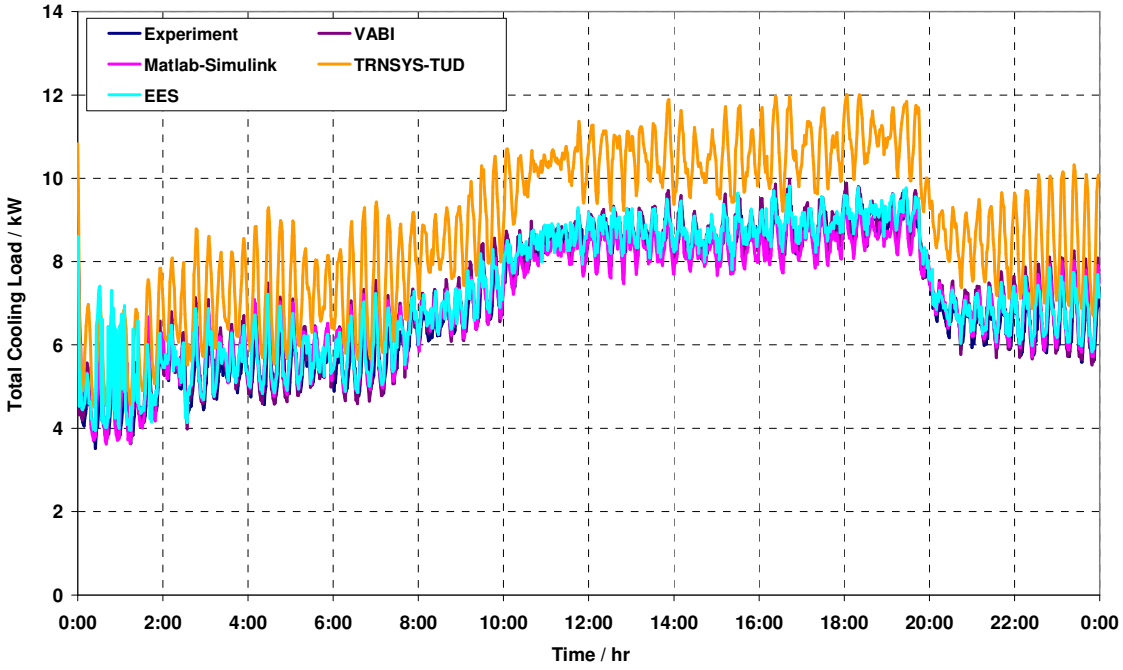

Figure 6-59 Cooling Coil Empirical Test II (Hot Dry climate) - Averaged Daily Cooling Load

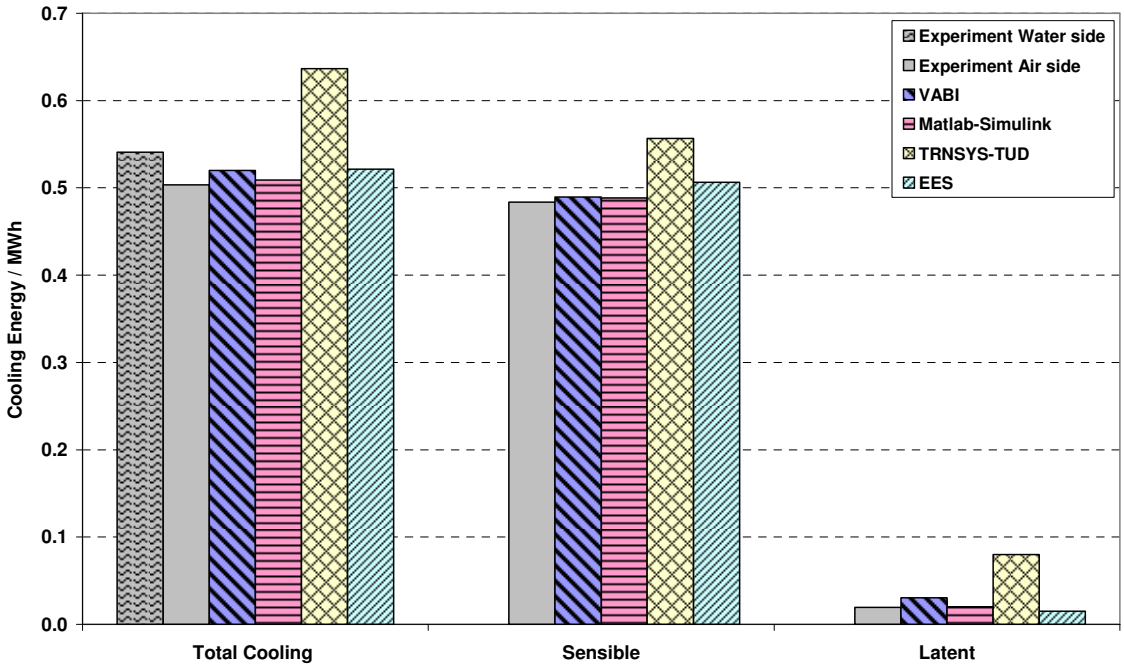

Figure 6-60 Cooling Coil Empirical Test II (Hot Dry climate) - Cooling Energy

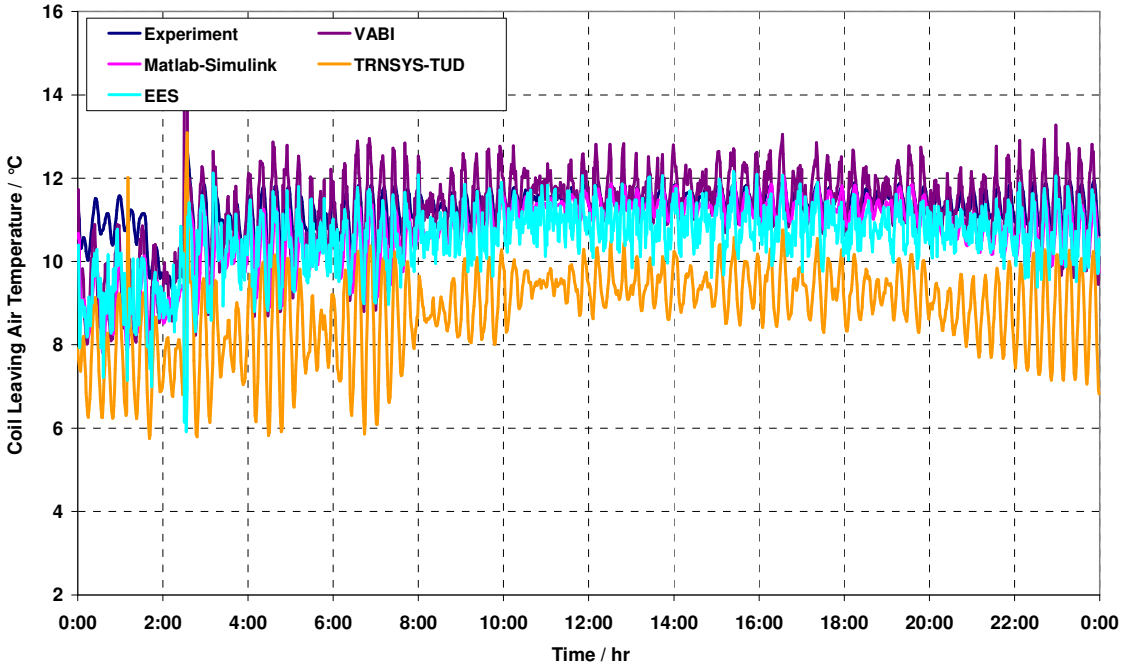

Figure 6-61 Cooling Coil Empirical Test II (Hot Dry climate) - Averaged Daily Coil Leaving Air Temperature

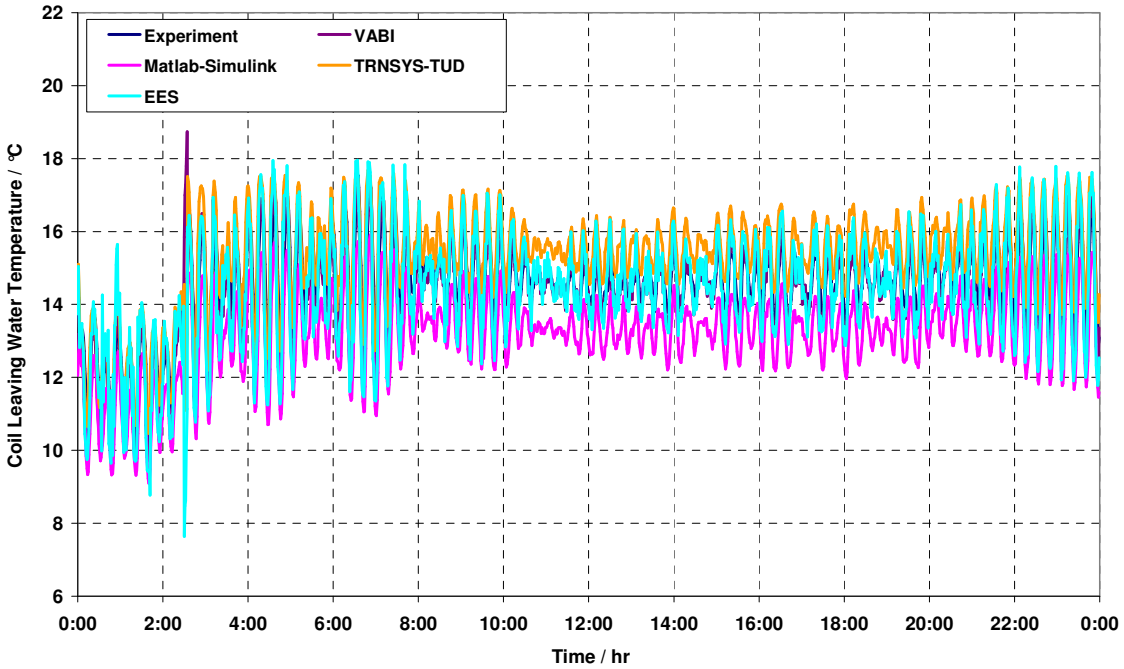

Figure 6-62 Cooling Coil Empirical Test II (Hot Dry climate) - Averaged Daily Coil Leaving Water Temperature

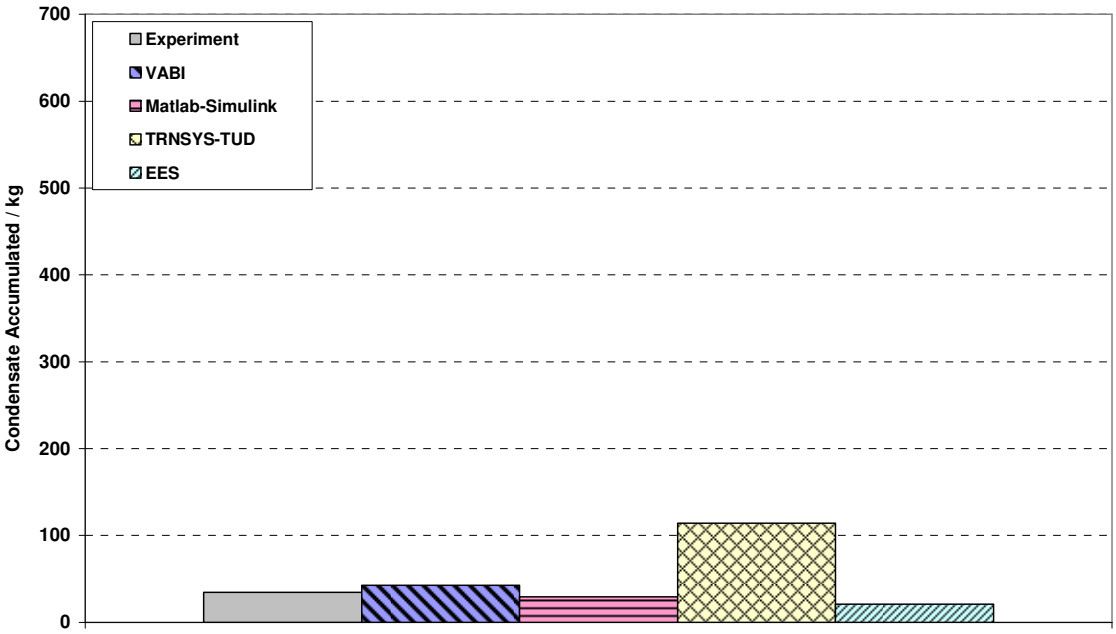

Figure 6-63 Cooling Coil empirical Test II (Hot Dry climate) - Condensate Accumulated

Table 6-32 Cooling Coil empirical Test II (Hot Dry climate) – Total Cooling Load Statistics

CLT	Exp.	VABI	Simulink	TRNSYS-TUD	EES
$\overline{x}$	6.99	7.22	7.07	8.84	7.26
S	2.11	2.17	1.95	2.60	2.05
x_{min}	0.18	0.08	-0.49	0.00	0.24
x_{max}	12.54	12.46	11.56	14.57	12.82
$\overline{D}$		0.23	0.07	1.85	0.25
$\overline{\lvert D \rvert}$		0.50	0.49	1.85	0.44
$\lvert D \rvert_{max}$		2.21	9.42	4.67	6.54
$\lvert D \rvert_{min}$		0.00	0.00	0.00	0.00
D_{rms}		0.64	0.66	2.04	0.69
$D_{95\%}$		1.24	1.25	3.04	1.04

Table 6-33 Cooling Coil empirical Test II (Hot Dry climate) – Leaving Air Temperature Statistics

LAT	Exp.	VABI	Simulink	TRNSYS-TUD	EES
$\overline{x}$	11.26	11.20	10.70	8.83	10.57
S	0.84	1.75	1.33	1.61	1.36
x_{min}	4.69	2.65	3.07	2.98	2.60
x_{max}	15.48	23.68	13.66	23.60	13.41
$\overline{D}$		-0.06	-0.56	-2.44	-0.69
$\overline{\lvert D \rvert}$		0.93	0.60	2.46	0.88
$\lvert D \rvert_{max}$		12.44	6.84	8.19	7.63
$\lvert D \rvert_{min}$		0.00	0.00	0.04	0.00
D_{rms}		1.26	0.92	2.63	1.18
$D_{95\%}$		1.95	1.28	3.95	2.07

Table 6-34 Cooling Coil empirical Test II (Hot Dry climate) – Leaving Water Temperature Statistics

LWT	Exp.	VABI	Simulink	TRNSYS-TUD	EES
$\overline{x}$	14.52	14.36	13.17	15.28	14.42
S	2.09	2.34	2.01	2.38	2.59
x_{min}	2.89	3.03	3.08	3.04	3.08
x_{max}	17.73	23.96	16.34	17.94	19.21
$\overline{D}$		-0.16	-1.35	0.76	-0.11
$\overline{\lvert D \rvert}$		0.70	1.36	0.93	1.00
$\lvert D \rvert_{max}$		10.65	2.60	8.28	7.46
$\lvert D \rvert_{min}$		0.00	0.02	0.00	0.00
D_{rms}		0.97	1.40	1.17	1.24
$D_{95\%}$		1.81	1.85	2.07	2.33

100% Outside Air (August 15 – August 16, 2006)

The energy balance of water side of the chiller, water side of the coil, and air side of the coil is perfectly fulfilled as to be seen from the graph in Figure 6-64. Also cooling load predicted by the models do agree very well with the measured data but has some bigger deviations for the Matlab/Simulink model, see Figure 6-65. Figure 6-67 and Figure 6-68 include graphs that show air and water temperatures leaving the coil. The Matlab/Simulink model has an error of about 2 K in predicting temperatures whereas the TRNSYS-TUD model underestimates the coil leaving air temperature by 1K but shows good agreement for the coil leaving water temperature. The air flow is quite constant and varies in a range of 2000…3500m³/h.

Statistics for this sub-test can be found in Table 6-35 (total cooling load), Table 6-36 (leaving air temperature), and Table 6-37 (water leaving air temperature), respectively.

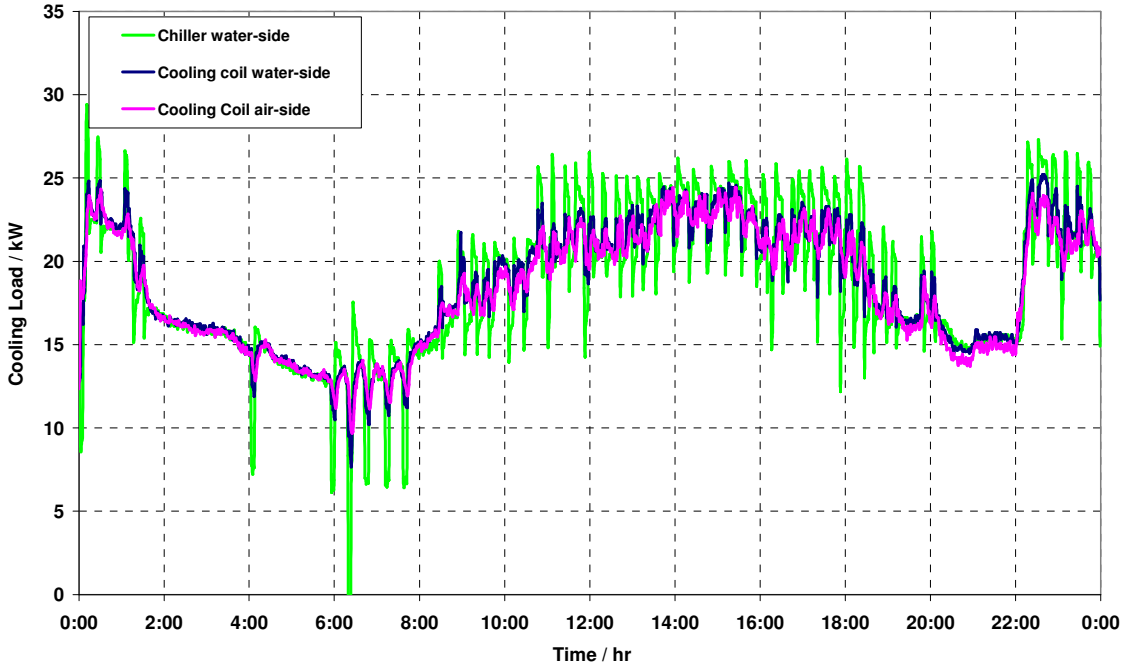

Figure 6-64 Cooling Coil Empirical Test II (100% OA) - Cooling Averaged Daily Energy Balance (Experiment)

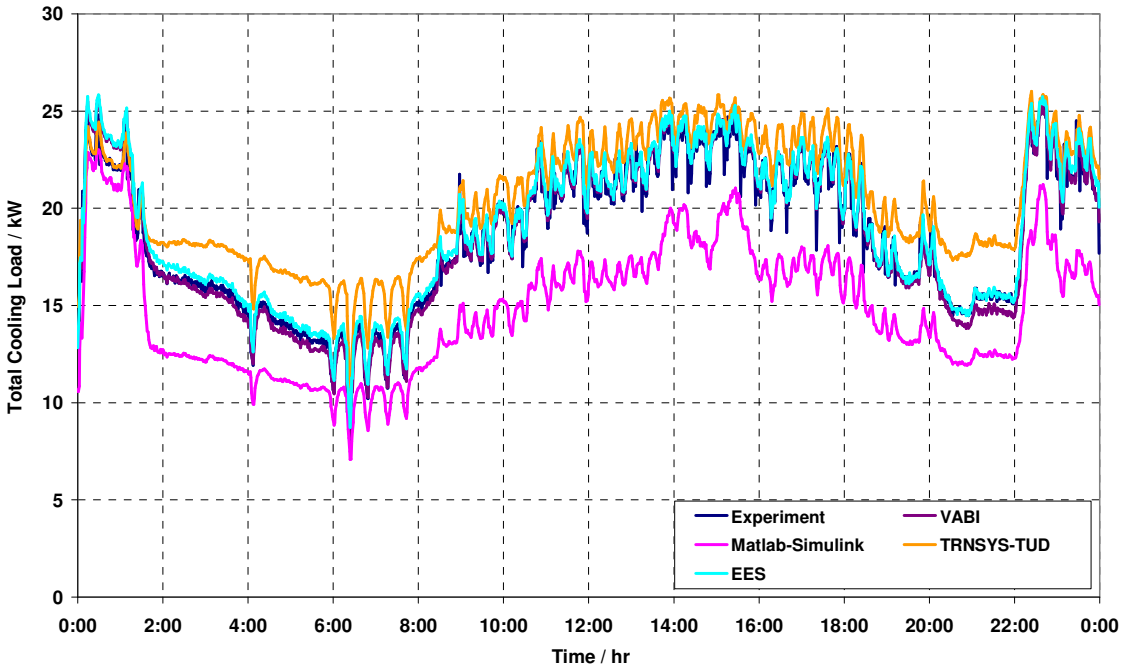

Figure 6-65 Cooling Coil Empirical Test II (100% OA) - Averaged Daily Cooling Load

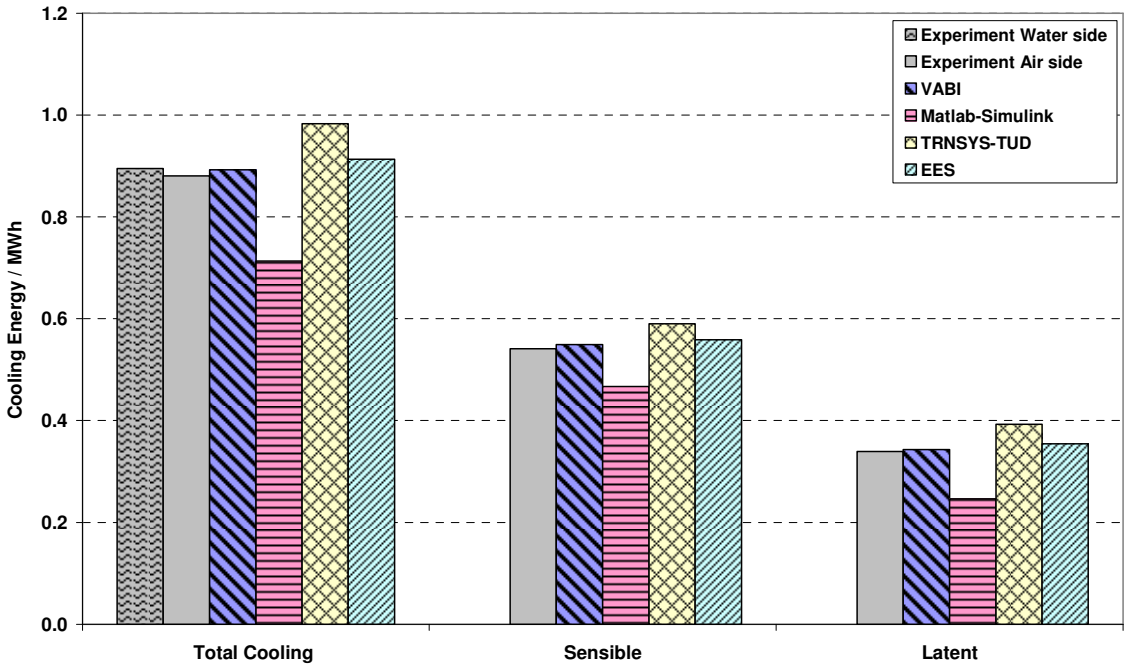

Figure 6-66 Cooling Coil Empirical Test II (100% OA) - Cooling Energy

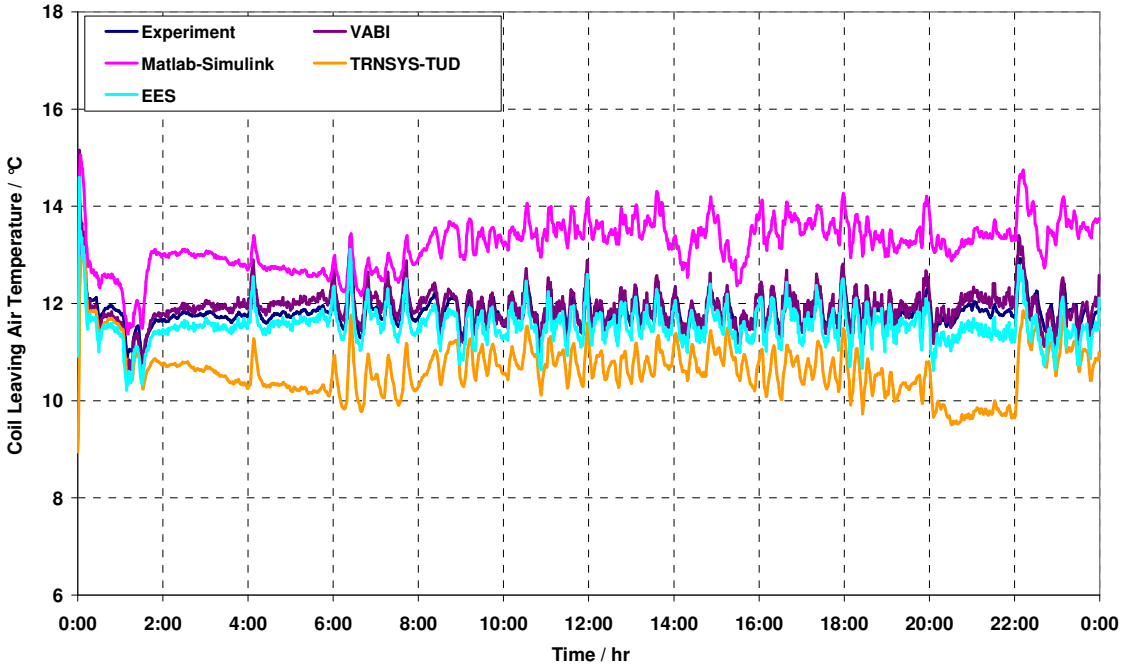

Figure 6-67 Cooling Coil Empirical Test II (100% OA) - Averaged Daily Coil Leaving Air Temperature

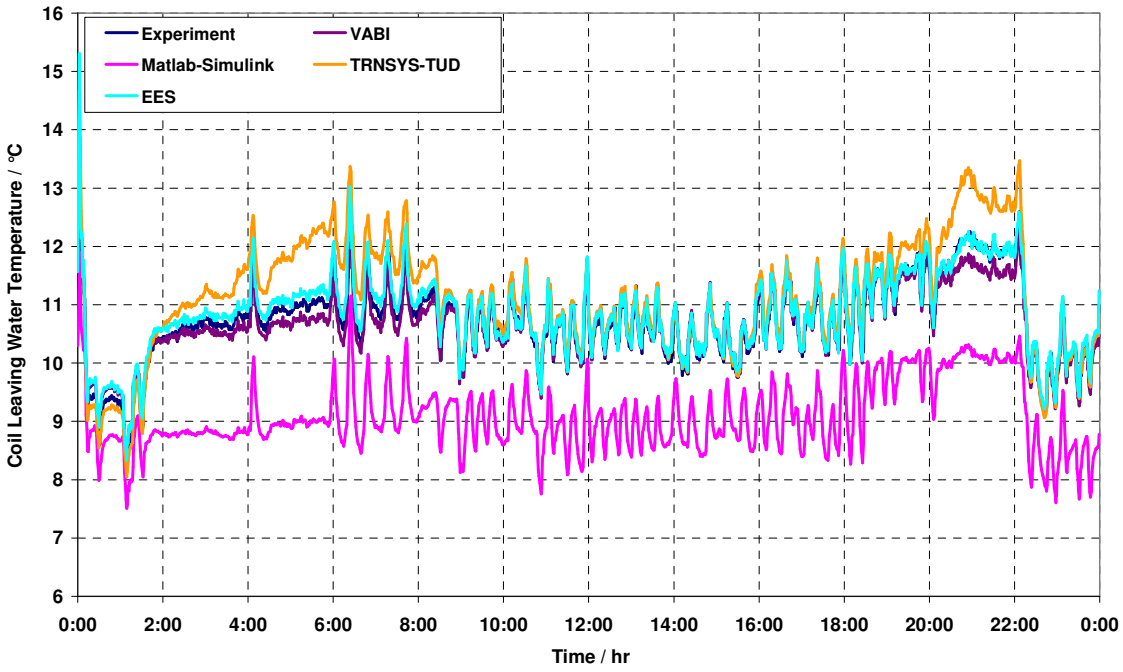

Figure 6-68 Cooling Coil Empirical Test II (100% OA) - Averaged Daily Coil Leaving Water Temperature

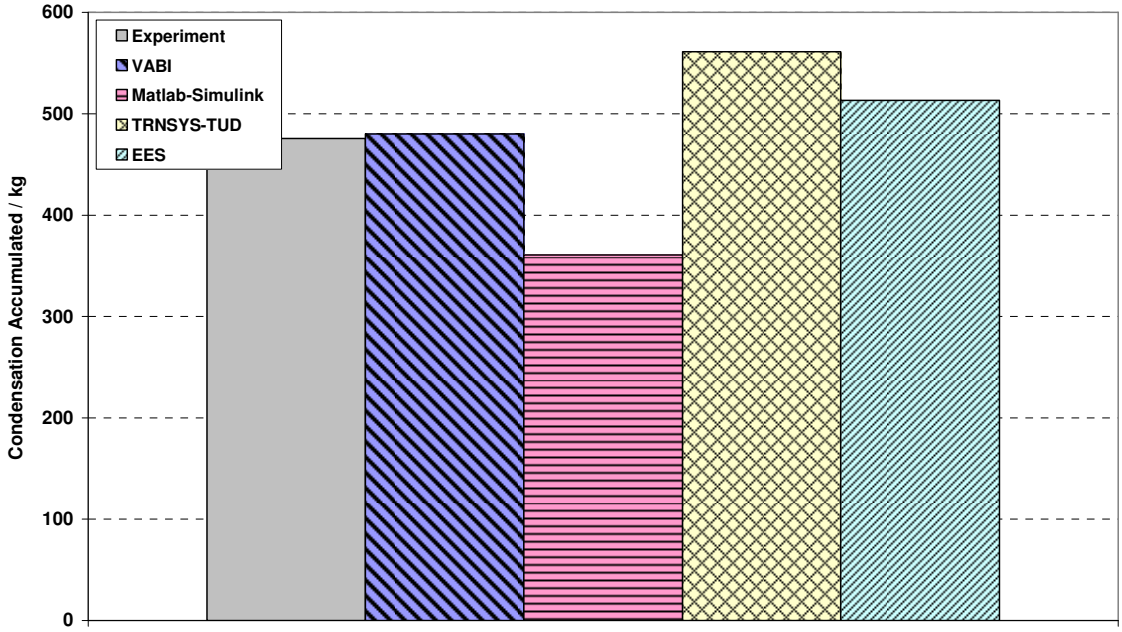

Figure 6-69 Cooling Coil empirical Test II (100% OA) - Condensate Accumulated

Table 6-35 Cooling Coil empirical Test II (100% OA) – Total Cooling Load Statistics

CLT	Exp.	VABI	Simulink	TRNSYS-TUD	EES
$\overline{x}$	18.65	18.59	14.86	20.47	19.03
S	4.08	4.35	3.78	3.52	4.16
x_{min}	6.62	7.09	6.09	9.03	7.08
x_{max}	27.47	29.85	30.03	26.69	29.66
$\overline{D}$		-0.05	-3.78	1.83	0.39
$\overline{\lvert D \rvert}$		0.10	3.91	1.94	-0.26
$\lvert D \rvert_{max}$		3.87	8.71	6.40	4.45
$\lvert D \rvert_{min}$		0.00	0.00	0.00	0.00
D_{rms}		0.73	4.13	2.12	0.74
$D_{95\%}$		1.57	6.02	3.18	1.57

Table 6-36 Cooling Coil empirical Test II (100% OA) – Leaving Air Temperature Statistics

LAT	Exp.	VABI	Simulink	TRNSYS-TUD	EES
$\overline{x}$	11.81	11.91	13.21	10.64	11.55
S	0.39	0.51	0.69	0.61	0.50
x_{min}	9.77	9.33	9.60	6.77	9.17
x_{max}	14.65	18.24	16.20	14.47	17.51
$\overline{D}$		0.10	1.41	-1.17	-0.26
$\overline{\lvert D \rvert}$		0.22	1.43	1.18	0.31
$\lvert D \rvert_{max}$		5.41	2.39	3.85	4.68
$\lvert D \rvert_{min}$		0.00	0.01	0.01	0.00
D_{rms}		0.30	1.51	1.26	0.38
$D_{95\%}$		0.55	2.11	1.98	0.69

Table 6-37 Cooling Coil empirical Test II (100% OA) – Leaving Water Temperature Statistics

LWT	Exp.	VABI	Simulink	TRNSYS-TUD	EES
$\overline{x}$	10.74	10.68	9.08	11.10	10.84
S	0.86	0.78	0.73	1.13	0.85
x_{min}	7.01	7.27	6.98	6.76	7.21
x_{max}	16.92	18.65	14.55	18.49	19.73
$\overline{D}$		-0.06	-1.65	0.36	0.10
$\overline{\lvert D \rvert}$		0.18	1.66	0.40	0.16
$\lvert D \rvert_{max}$		3.47	2.53	3.31	4.55
$\lvert D \rvert_{min}$		0.00	0.01	0.00	0.00
D_{rms}		0.25	1.71	0.54	0.24
$D_{95\%}$		0.45	2.06	1.17	0.40

Hot Humid Climate (August 18 – August 20, 2006)

Figure 6-70 shows the cooling averaged daily energy balance for both sides of the coil (air and water) and also for the water side of the chiller. Energy fluxes are well-balanced. VABI and EES models are able to match the experimental based cooling load profile whereas Matlab/Simulink and TRNSYS-TUD show some bigger deviations compared to the measurement, see Figure 6-71. Deviations that can be observed in the load profiles also lead to deviations related to the amount of cooling energy – total, sensible, and latent – that can be illustrated in Figure 6-72. The TRNSYS-TUD model underestimates leaving air temperature by at least 3 K but overestimates leaving water temperature by 2K. The results from VABI and EES models do match the measurements. The air flow during this period is quite low and varies between 1000…2000m³/h.

Some statistical data are summarized in Table 6-38 (total cooling load), Table 6-39 (leaving air temperature), and Table 6-40 (leaving water temperature).

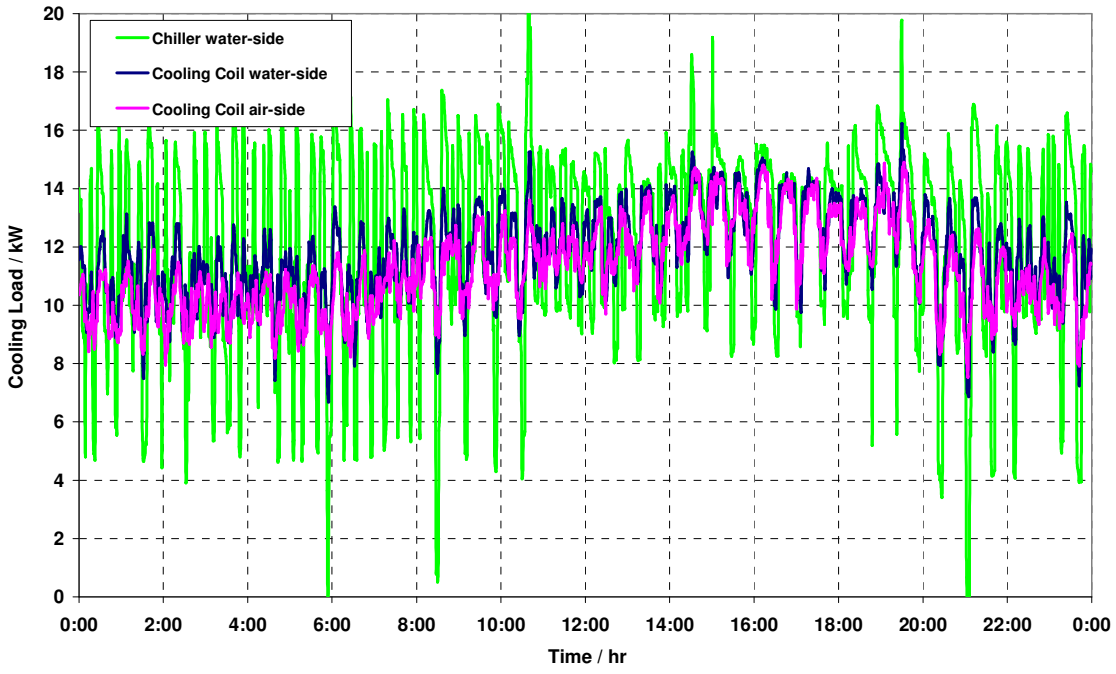

Figure 6-70 Cooling Coil Empirical Test II (Hot Humid climate) - Cooling Averaged Daily Energy Balance (Experiment)

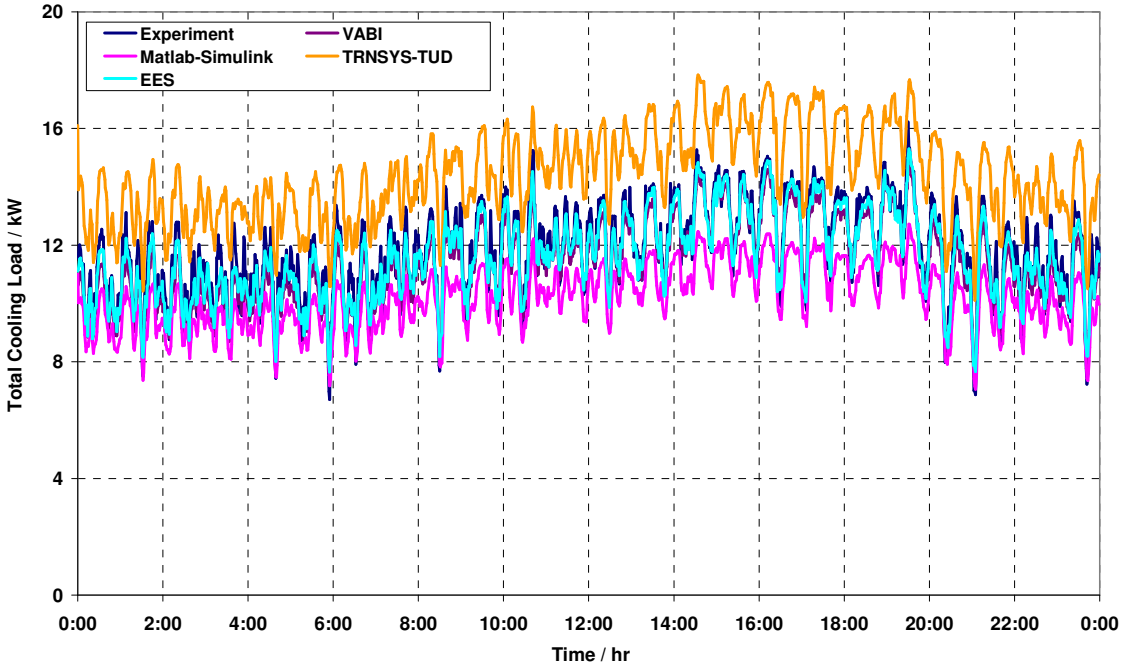

Figure 6-71 Cooling Coil Empirical Test II (Hot Humid climate) - Averaged Daily Cooling Load

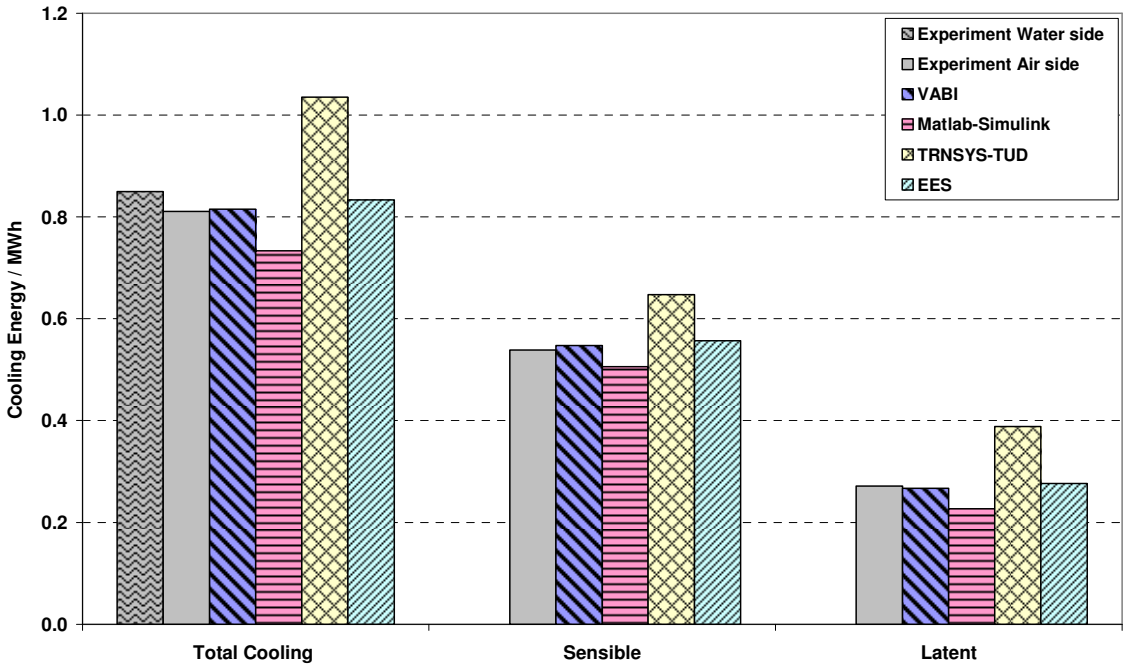

Figure 6-72 Cooling Coil Empirical Test II (Hot Humid climate) - Cooling Energy

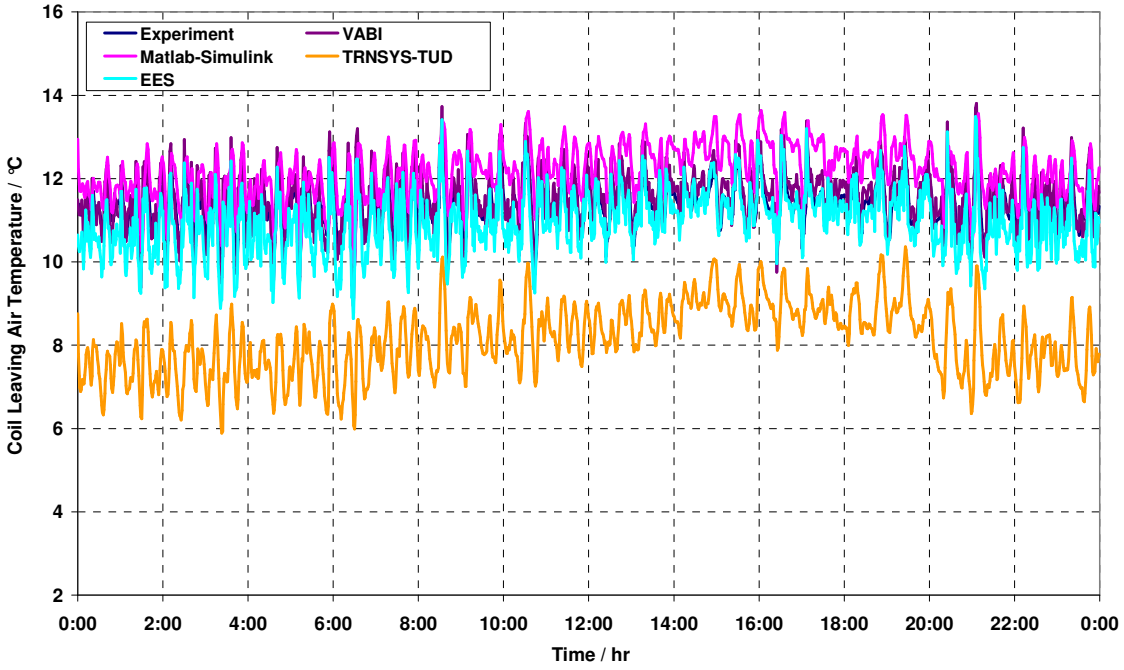

Figure 6-73 Cooling Coil Empirical Test II (Hot Humid climate) - Averaged Daily Coil Leaving Air Temperature

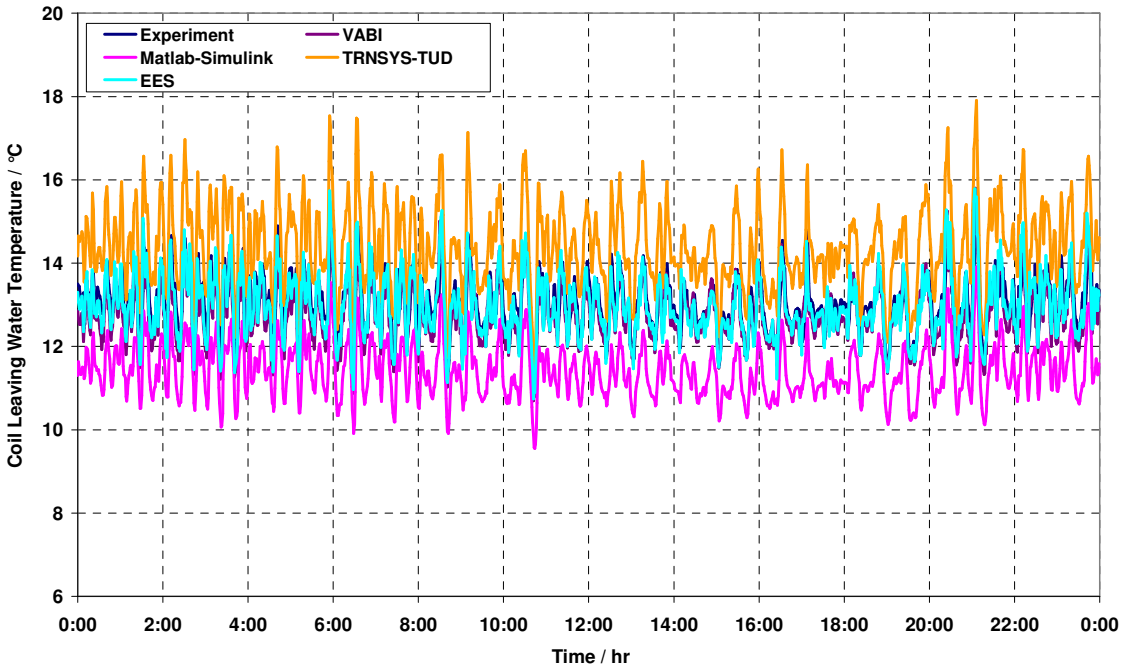

Figure 6-74 Cooling Coil Empirical Test II (Hot Humid climate) - Averaged Daily Coil Leaving Water Temperature

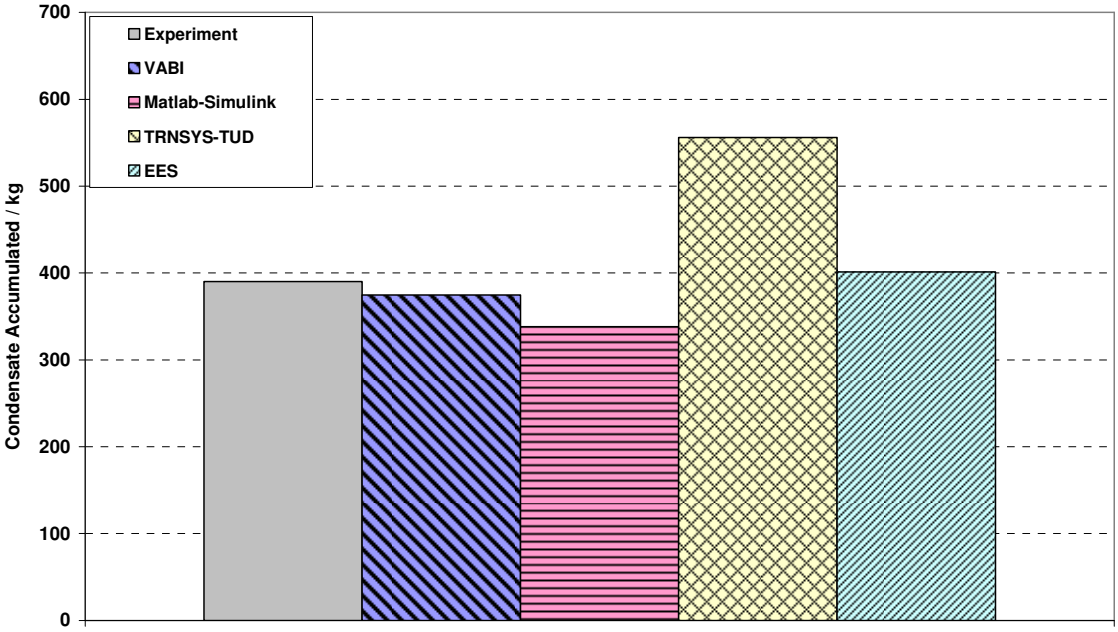

Figure 6-75 Cooling Coil empirical Test II (Hot Humid climate) - Condensate Accumulated

Table 6-38 Cooling Coil empirical Test II (Hot Humid climate) – Total Cooling Load Statistics

CLT	Exp.	VABI	Simulink	TRNSYS-TUD	EES
$\overline{x}$	11.80	11.32	10.19	14.38	11.58
S	2.60	2.23	1.70	2.41	2.33
x_{min}	3.69	5.42	5.08	7.32	5.18
x_{max}	19.48	17.86	14.61	20.30	18.28
$\overline{D}$		-0.48	-1.62	2.58	-0.22
$\overline{\lvert D \rvert}$		0.09	1.77	2.59	-0.44
$\lvert D \rvert_{max}$		3.91	6.17	9.90	4.03
$\lvert D \rvert_{min}$		0.00	0.00	0.00	0.00
D_{rms}		0.98	1.99	2.81	0.81
$D_{95\%}$		1.87	3.11	4.23	1.71

OU

Table 6-39 Cooling Coil empirical Test II (Hot Humid climate) – Leaving Air Temperature Statistics

LAT	Exp.	VABI	Simulink	TRNSYS-TUD	EES
$\overline{x}$	11.39	11.48	12.14	8.13	10.96
S	0.92	1.27	1.05	1.31	1.27
x_{min}	8.55	7.19	8.54	5.02	7.15
x_{max}	13.75	15.60	14.64	11.82	15.55
$\overline{D}$		0.09	0.75	-3.26	-0.44
$\overline{\lvert D \rvert}$		0.53	0.87	3.26	0.69
$\lvert D \rvert_{max}$		3.71	3.09	5.86	4.00
$\lvert D \rvert_{min}$		0.00	0.00	0.33	0.00
D_{rms}		0.74	0.99	3.37	0.89
$D_{95\%}$		1.61	1.63	4.67	1.74

Table 6-40 Cooling Coil empirical Test II (Hot Humid climate) – Leaving Water Temperature Statistics

LWT	Exp.	VABI	Simulink	TRNSYS-TUD	EES
$\overline{x}$	13.07	12.82	11.41	14.39	12.96
S	1.16	1.31	1.14	1.77	1.35
x_{min}	9.73	9.28	8.49	9.73	9.22
x_{max}	16.92	17.84	15.19	20.49	17.59
$\overline{D}$		-0.25	-1.65	1.32	-0.10
$\overline{\lvert D \rvert}$		0.65	1.65	1.32	0.51
$\lvert D \rvert_{max}$		4.92	3.18	5.83	4.62
$\lvert D \rvert_{min}$		0.00	0.07	0.00	0.00
D_{rms}		0.85	1.70	1.59	0.76
$D_{95\%}$		1.74	2.16	3.02	1.66

Cold Humid Climate (August 21 – August 23, 2006)

The averaged daily cooling load profiles for the experimental data depicted in Figure 6-76 display a well-balanced cooling coil. Models can predict cooling load profile quite well but Matlab/Simulink model considerably underestimates cooling load, see Figure 6-77. These predicting errors also can be found when looking at coil leaving air temperatures displayed in Figure 6-79 (air side) and Figure 6-80 (water side). The air flow varies within a range of 3000…4500m³/h. Also condensation accumulated during the test period shows big deviations between programs, see Figure 6-81.

Table 6-41 (total cooling load), Table 6-42 (leaving air temperature), and Table 6-43 (leaving water temperature).

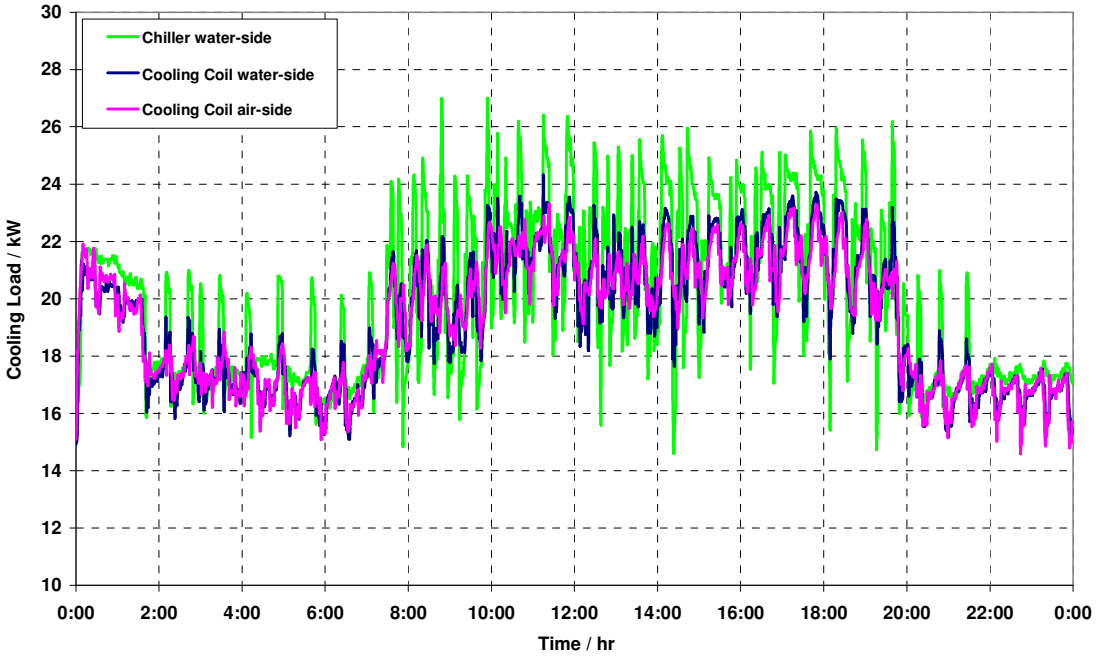

Figure 6-76 Cooling Coil Empirical Test II (Cold Humid climate) - Cooling Averaged Daily Energy Balance (Experiment)

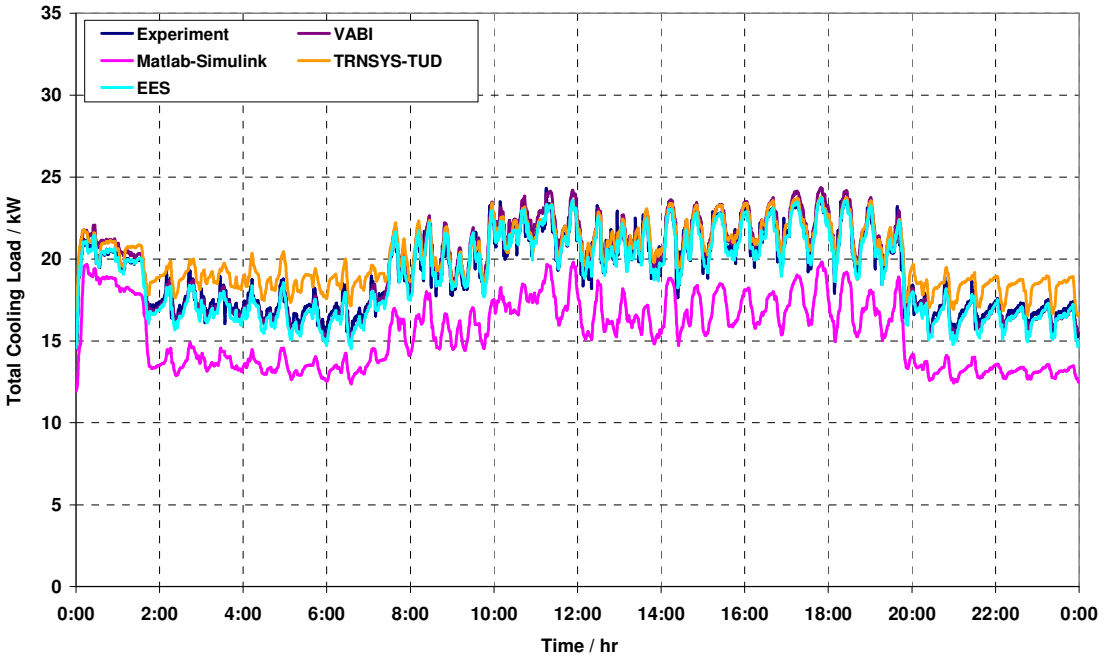

Figure 6-77 Cooling Coil Empirical Test II (Cold Humid climate) - Averaged Daily Cooling Load

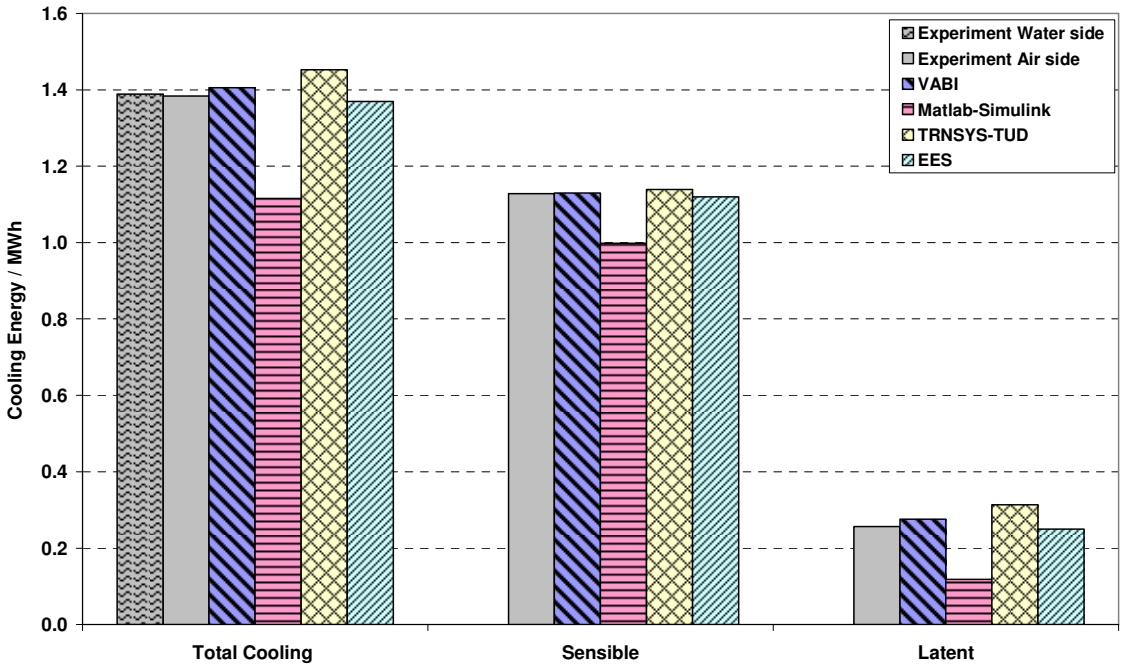

Figure 6-78 Cooling Coil Empirical Test II (Cold Humid climate) - Cooling Energy

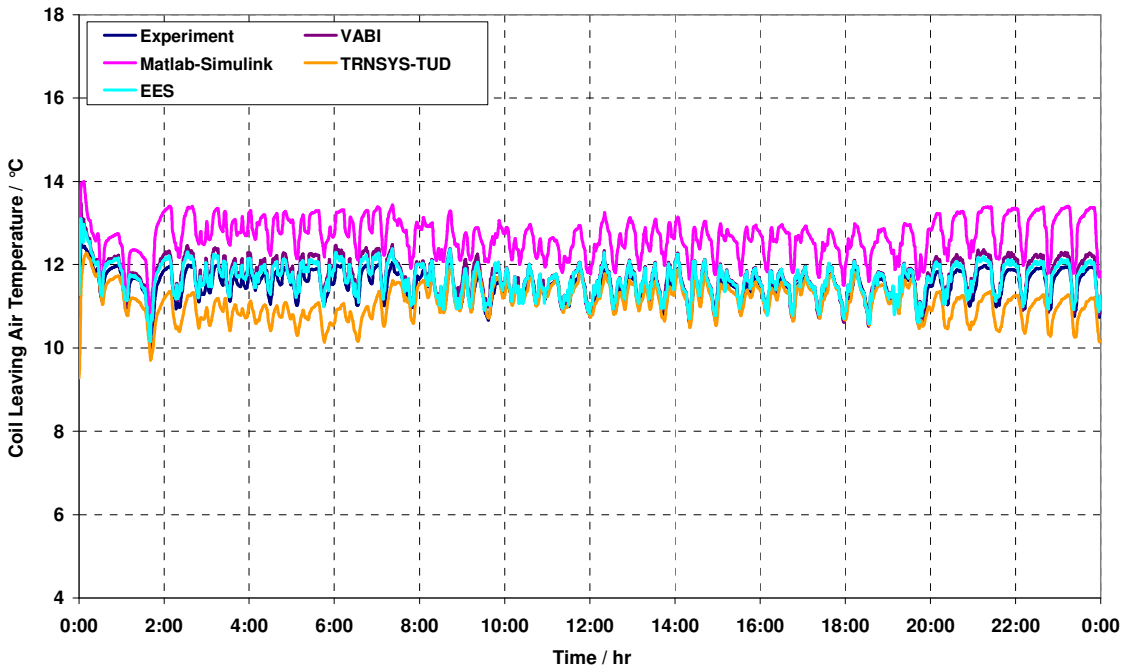

Figure 6-79 Cooling Coil Empirical Test II (Cold Humid climate) - Averaged Daily Coil Leaving Air Temperature

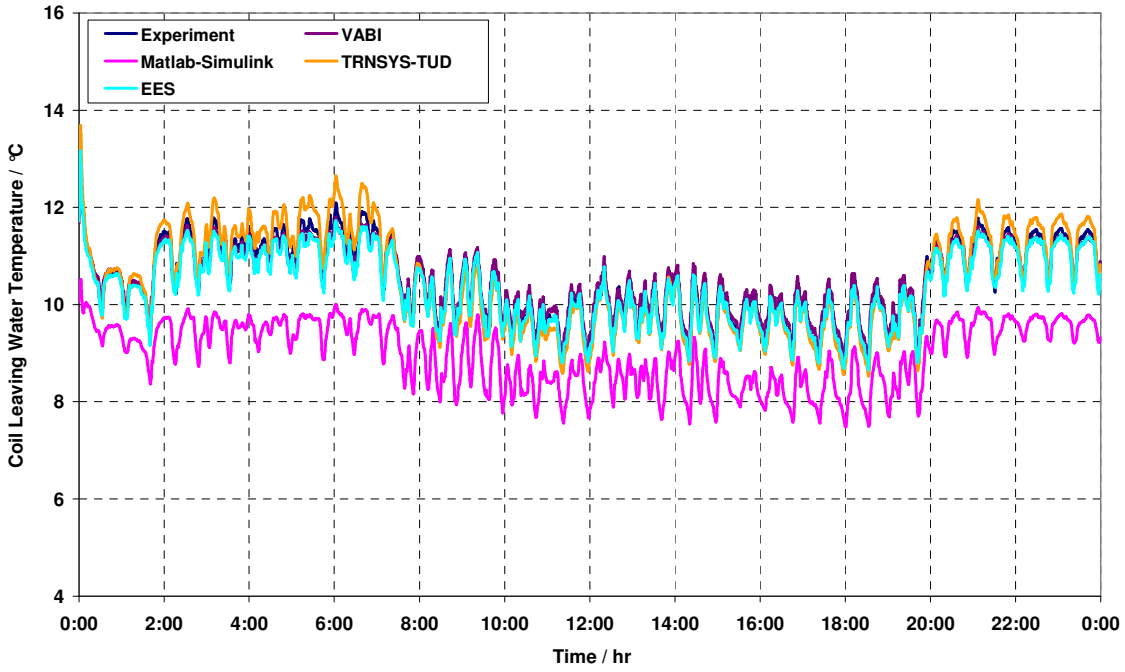

Figure 6-80 Cooling Coil Empirical Test II (Cold Humid climate) - Averaged Daily Coil Leaving Water Temperature

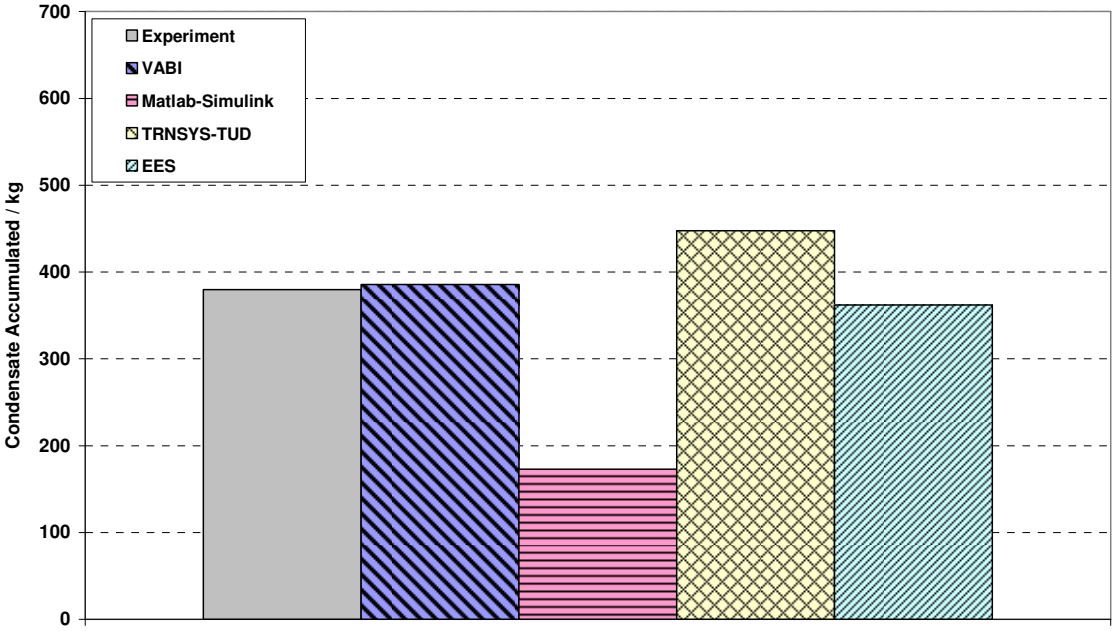

Figure 6-81 Cooling Coil empirical Test II (Cold Humid climate) - Condensate Accumulated

Table 6-41 Cooling Coil empirical Test II (Cold Humid climate) – Total Cooling Load Statistics

CLT	Exp.	VABI	Simulink	TRNSYS-TUD	EES
$\overline{x}$	19.28	19.52	15.49	20.18	19.02
S	3.03	3.40	3.07	2.33	3.14
x_{min}	11.68	11.35	10.41	15.35	11.98
x_{max}	30.84	32.49	32.53	28.00	30.23
$\overline{D}$		0.24	-3.79	0.89	-0.26
$\overline{\lvert D \rvert}$		0.22	3.89	1.17	0.16
$\lvert D \rvert_{max}$		4.93	8.67	5.59	4.21
$\lvert D \rvert_{min}$		0.00	0.10	0.00	0.00
D_{rms}		0.84	4.04	1.45	0.67
$D_{95\%}$		1.79	5.69	2.49	1.20

Table 6-42 Cooling Coil empirical Test II (Cold Humid climate) – Leaving Air Temperature Statistics

LAT	Exp.	VABI	Simulink	TRNSYS-TUD	EES
$\overline{x}$	11.49	11.70	12.68	11.11	11.64
S	0.52	0.66	0.72	0.59	0.60
x_{min}	8.55	8.16	8.23	7.04	8.47
x_{max}	14.25	16.07	15.55	14.60	15.24
$\overline{D}$		0.22	1.19	-0.37	0.16
$\overline{\lvert D \rvert}$		0.30	1.22	0.44	0.24
$\lvert D \rvert_{max}$		2.99	1.94	3.77	1.93
$\lvert D \rvert_{min}$		0.00	0.02	0.00	0.00
D_{rms}		0.37	1.25	0.58	0.31
$D_{95\%}$		0.66	1.51	1.11	0.62

Table 6-43 Cooling Coil empirical Test II (Cold Humid climate) – Leaving Water Temperature Statistics

LWT	Exp.	VABI	Simulink	TRNSYS-TUD	EES
$\overline{x}$	10.47	10.50	8.97	10.48	10.35
S	1.04	0.90	0.84	1.26	0.98
x_{min}	6.83	7.05	6.61	6.53	6.79
x_{max}	15.24	16.20	12.11	17.40	16.79
$\overline{D}$		0.04	-1.50	0.02	-0.12
$\overline{\lvert D \rvert}$		0.17	1.51	0.24	0.17
$\lvert D \rvert_{max}$		2.06	3.13	3.26	2.65
$\lvert D \rvert_{min}$		0.00	0.01	0.00	0.00
D_{rms}		0.23	1.55	0.30	0.23
$D_{95\%}$		0.45	1.99	0.59	0.41

6.2.5 Diagnosing Results

Comparative Test

Figure 6-84 and Figure 6-92 show two different diagnostic flow diagrams that can be used to locate probable causes of disagreement between results predicted by the model that has to be validated and results from a set of other programs that have already passed the comparative test. In principle there are always two paths for either a mass flow (M1-M11; CC100-C200 series) or a temperature (T1-T11; CC300-C400 series) controlled coil that can be followed. Differences between both control configurations can again be seen from Figure 4-7 and Figure 4-8.

The first one of the diagnostic logic flow diagrams shown in Figure 6-84 always references discrete results of certain hours instead of outputs that cover a span of time. It starts with a definition of a so called "Basic Performance Model" which represents conditions that are similar to those defined by the manufacturer submittal. Although agreement is not perfect it is the best point that can be found from comparative test conditions. Main differences are related to air flow rate and humidity of entering air. The chilled water flow rate is either an outcome of the models (CC200) or a fixed input value (CC400). See Figure 6-82 and Figure 6-83 for further details.

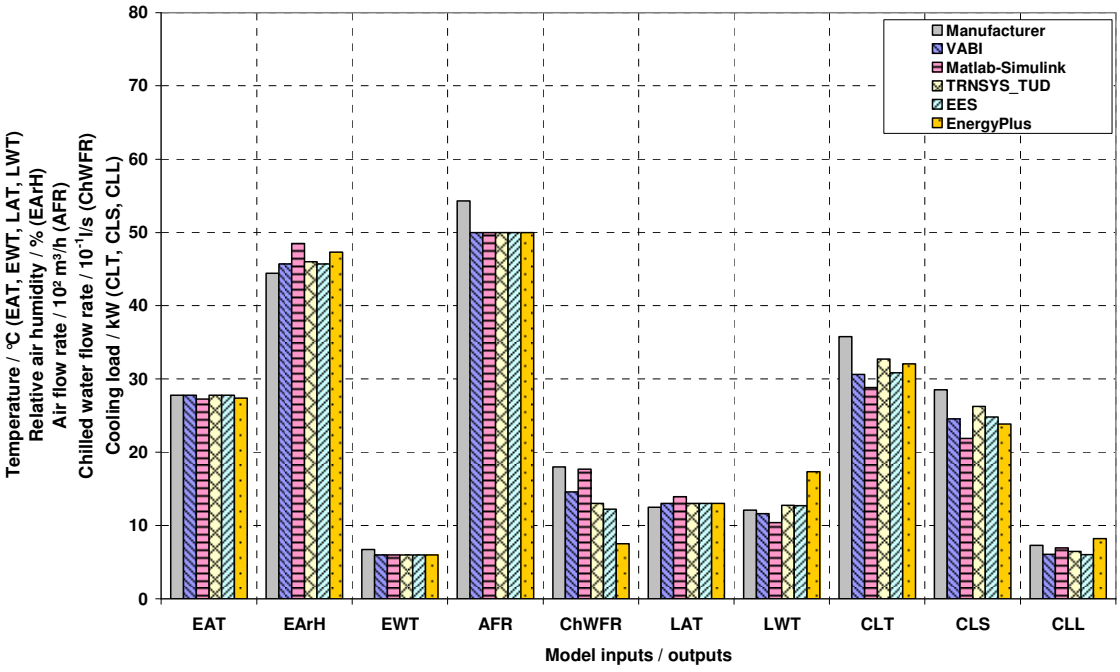

Figure 6-82 Results of the M1 check: "Basic Performance Model"; CC200 May31, 11:00

Based on the so defined "Basic Performance Model" at least one other discrete hour from the half year test period can be found that shows quite similar conditions for all input parameters but has a significant difference related to only one of the inputs. This fact allows the definition

of a set of sensitivity checks M1-M8 and T1- T8 as described in the diagnostic logic flow diagram Figure 6-84.

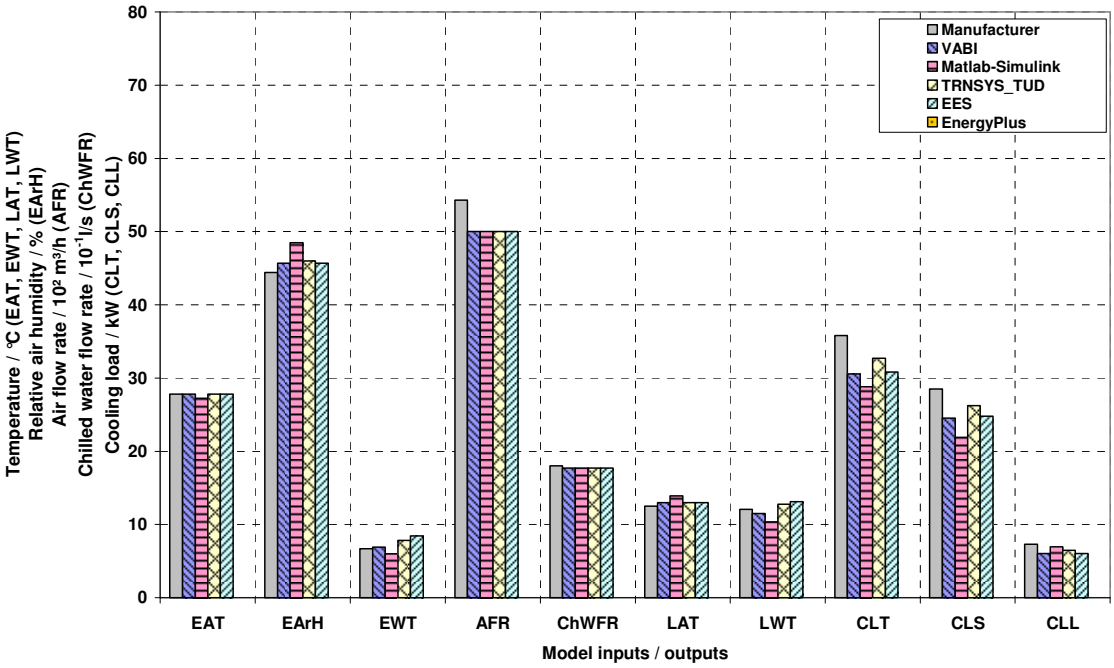

Figure 6-83 Results of the T1 check: "Basic Performance Model"; CC400 May31, 11:00

Several examples on how to use the diagnostic checks are given here: Figure 6-85 to Figure 6-91 show the results of the M2…M8 checks. The M2 check analyzes the sensitivity against a lower entering air temperature. From Figure 6-85 it can be derived that the entering air temperature at May 3, 15:00, is 10 K lower than for the "Basic Performance Model". It should be taken into account that also entering air relative humidity changes by approximately 1% which will have a slightly impact on the results but should be insignificant compared to a 10K change of entering air temperature. Whereas total cooling load differ by about 3 kW (which is approximately 14%) chilled water flow rate predicted by the models differs by factor 2 (which is 100%). That indicates different UA-values which also have an impact on leaving water temperature. Figure 6-86 shows the M3 check. This check is similar to M2 but accounts for an increasing entering air temperature.

The M4 check counts for the sensitivity of coil performance against a lower entering air relative humidity. The underlying hour of May 30 17:00 is characterized by an air relative humidity that is 6% lower than under basic condition which again reduces latent cooling load by about 50%. From Figure 6-87 it can be seen that impact of a lower entering air relative humidity on predicted coil performance is quite different for all the models. Figure 6-88 shows the M5 check. This check is similar to M4 but accounts for an increasing entering air relative humidity.

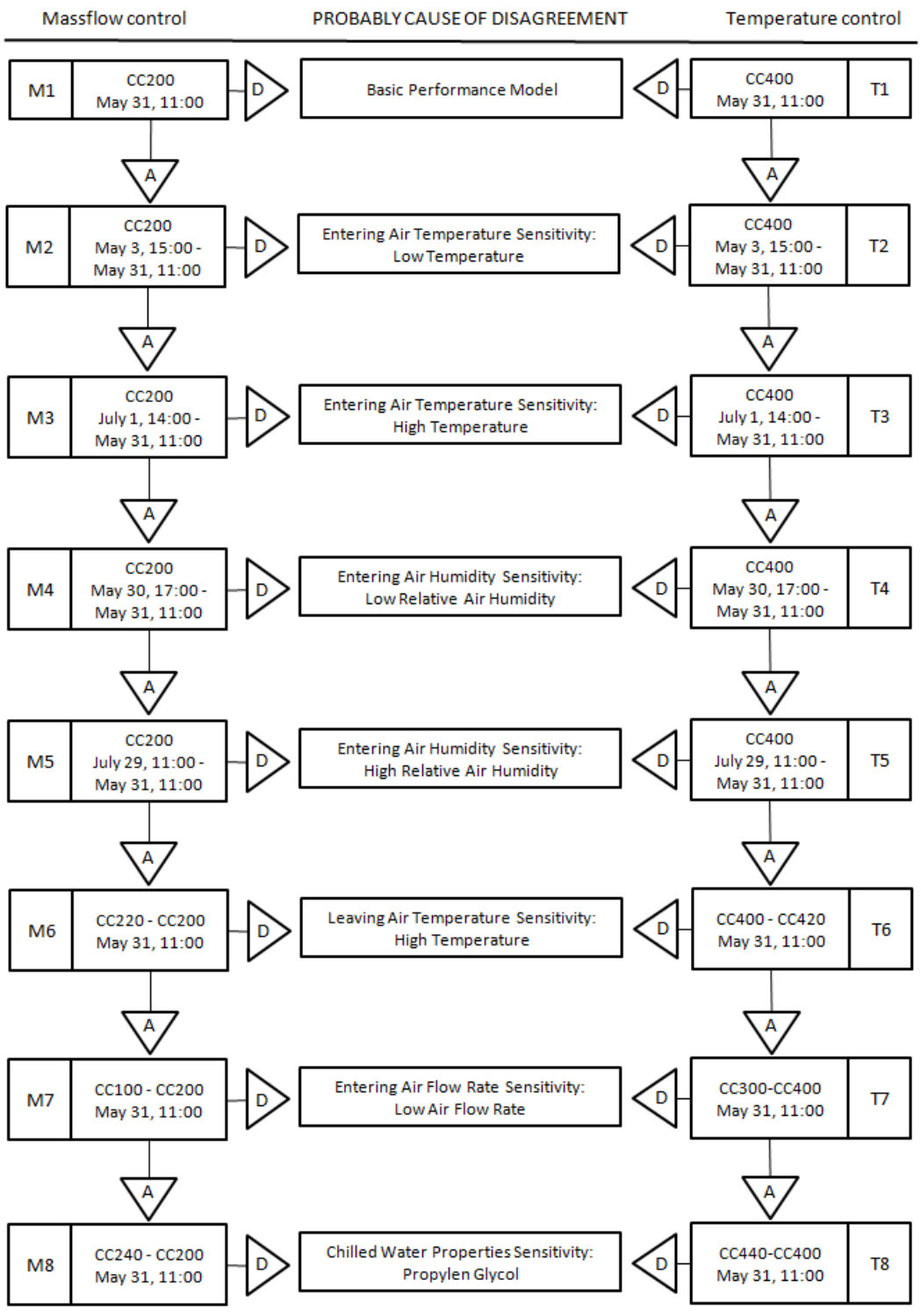

Abbreviations: A=Agree; D=Disagree

Figure 6-84 Cooling coil comparative test cases diagnostic logic flow diagram M1-M8 /T1-T8

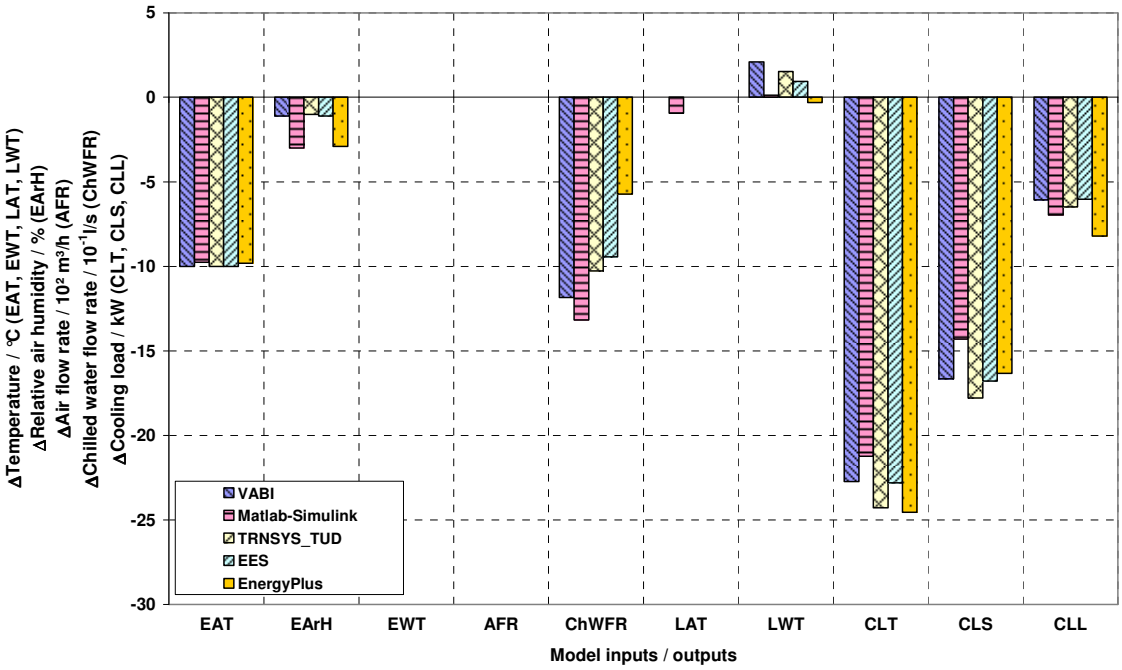

Figure 6-85 Results of the M2 check: Entering Air Temperature Decrease Sensitivity

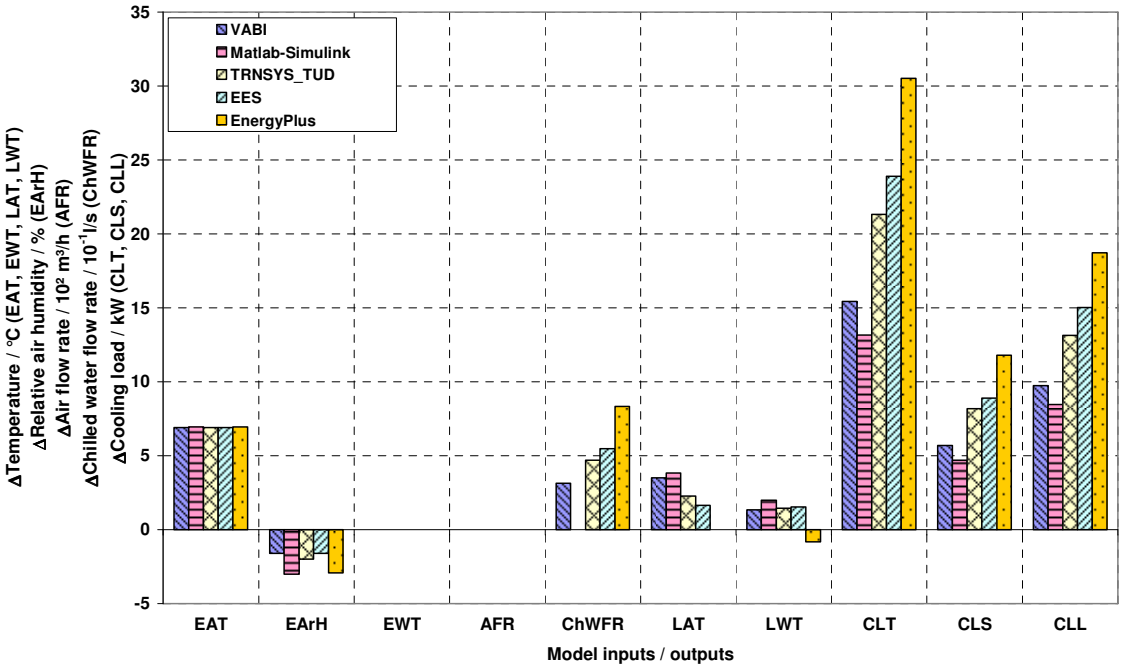

Figure 6-86 Results of the M3 check: Entering Air Temperature Increase Sensitivity

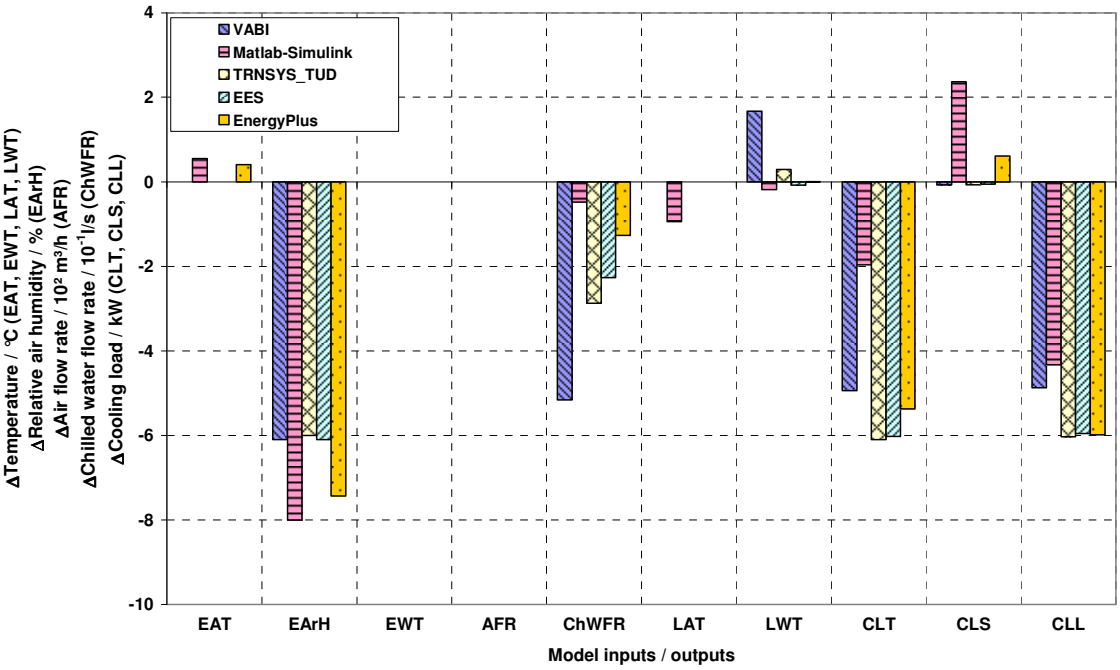

Figure 6-87 Results of the M4 check: Entering Air Humidity Decrease Sensitivity

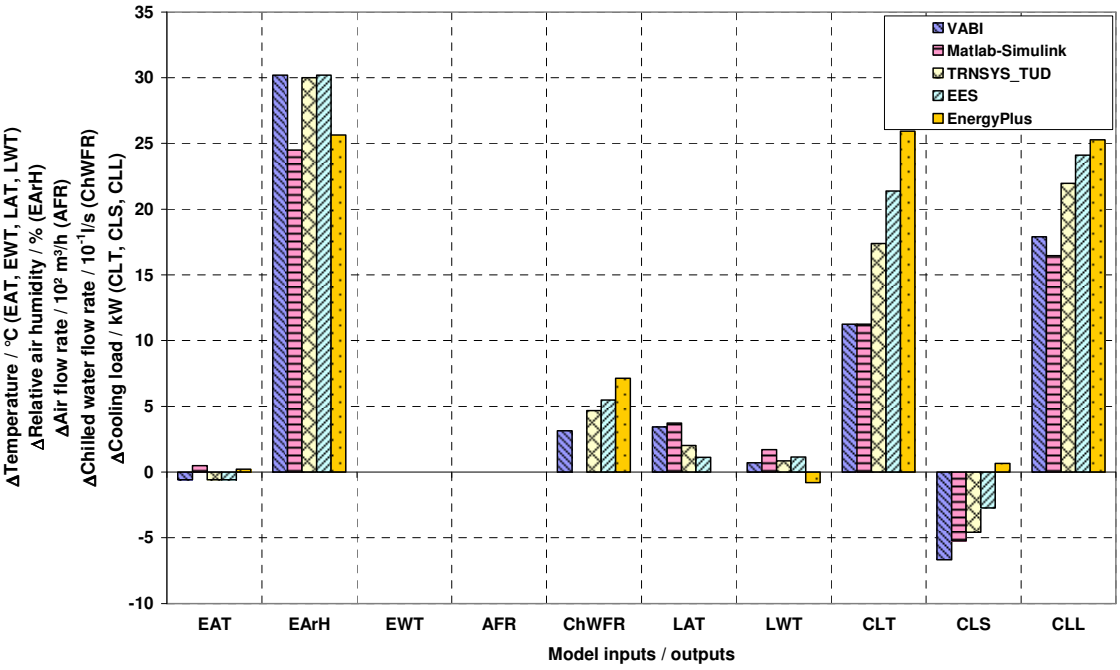

Figure 6-88 Results of the M5 check: Entering Air Humidity Increase Sensitivity

Diagnostic checks M6, M7, and M8, respectively account for the impact of increased air temperature set point, decreased air flow rate, and physical properties of chilled water fluid on the coil performance.

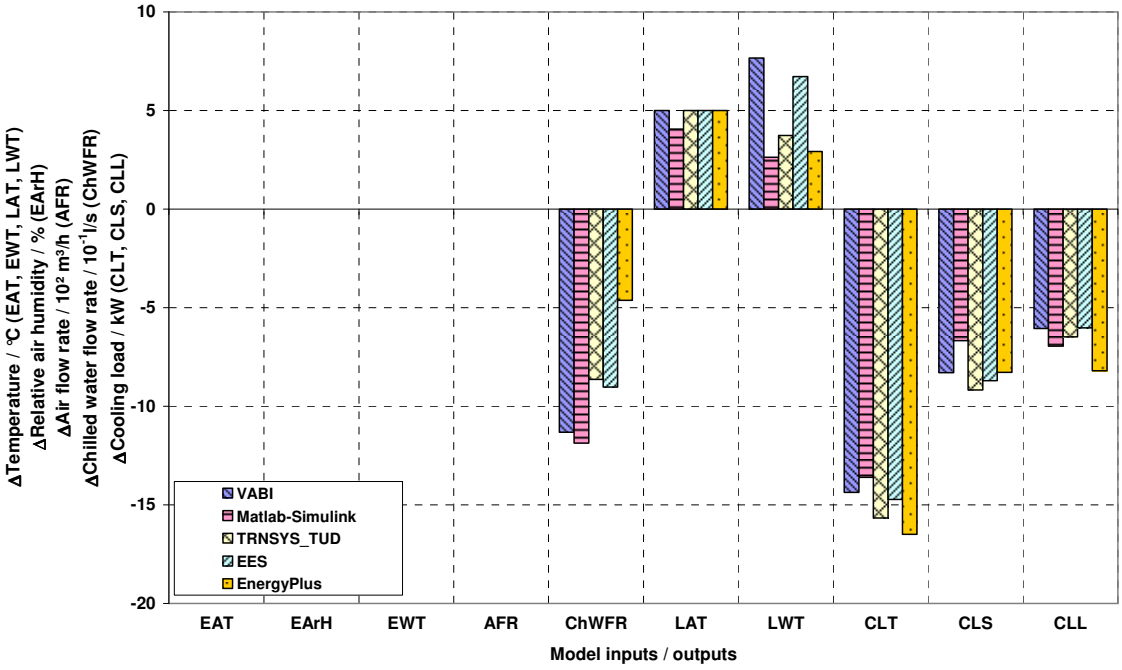

Figure 6-89 Results of the M6 check: Leaving Air Temperature Increase Sensitivity

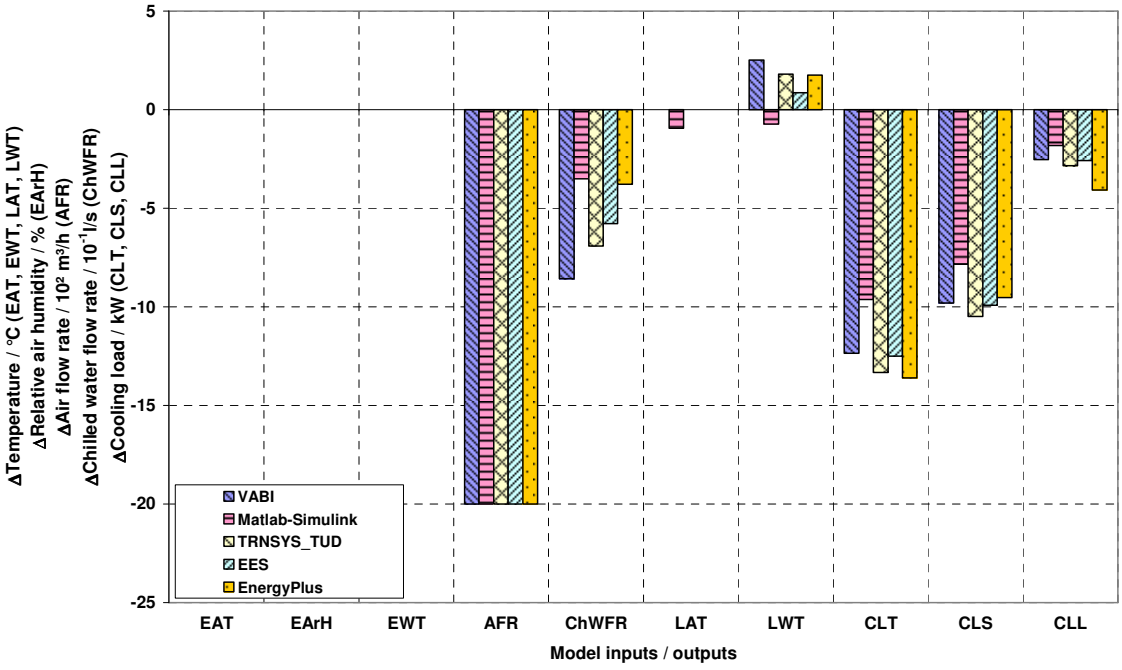

Figure 6-90 Results of the M7 check: Air Flow Rate Decrease Sensitivity

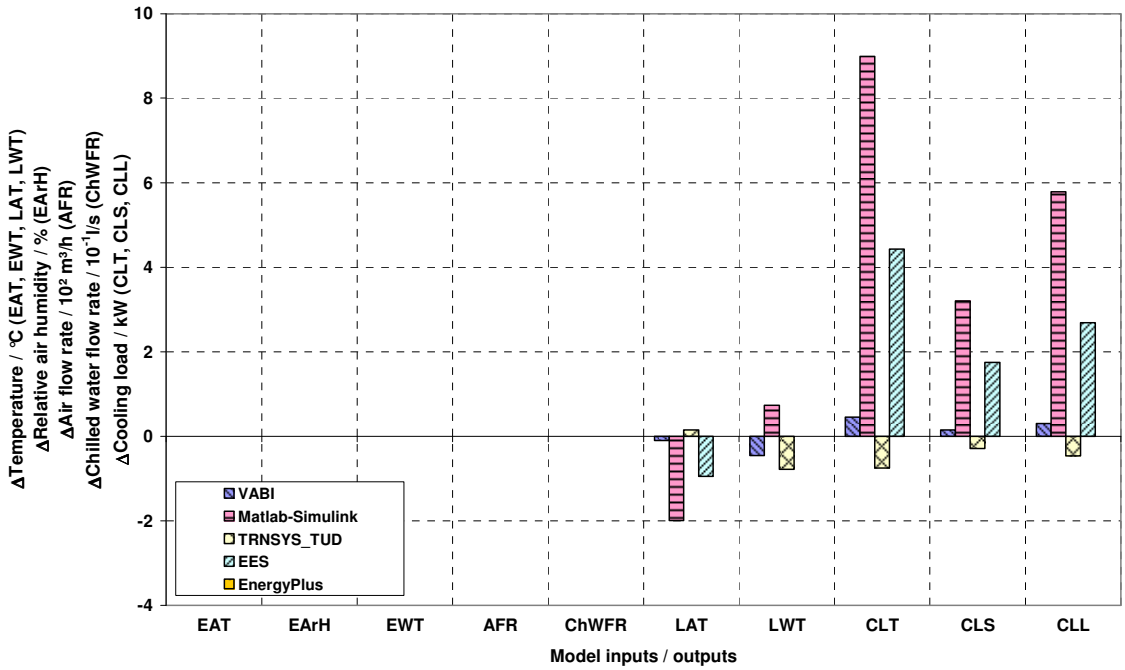

Figure 6-91 Results of the M8 check: Chilled Water Properties Sensitivity

In addition to the discrete hour based diagnostic flow diagram of Figure 6-84 another diagnostic method could be helpful to find probable causes of model disagreement. This method uses the logic flow shown in Figure 6-92 based on cross checks and test case comparisons. Thus the sensitive of the model against certain input and/or output parameters can be analyzed. At all four different parameters can be tested by using this diagnosing method. The modeler has to calculate the differences between two test cases according to the flow diagram. If the delta results do agree with or are in a similar range than those deltas available from other models the sensitivity seems to be all right. These diagnosing studies can be done either based on the overall results that refer to the whole validation period of May-September or to any daily or hourly prediction horizon. It is up to the modeler to find a time span that best meets the demands.

Due to different configurations defined in the test matrix Table 4-3 each of the sensitivity studies can be done under four different boundary conditions. These conditions depend on the test cases that are compared to each other. As an example: When calculating the difference CC100-CC120 it is for chilled water fluid of 35% Ethylene-Glycol fluid but the difference CC140-CC160 is for 18% Propylene-Glycol. Nevertheless both studies account for leaving air temperature sensitivity. Figure 6-93 and Figure 6-94 exemplary show the delta results for the #9 and #11 checks.

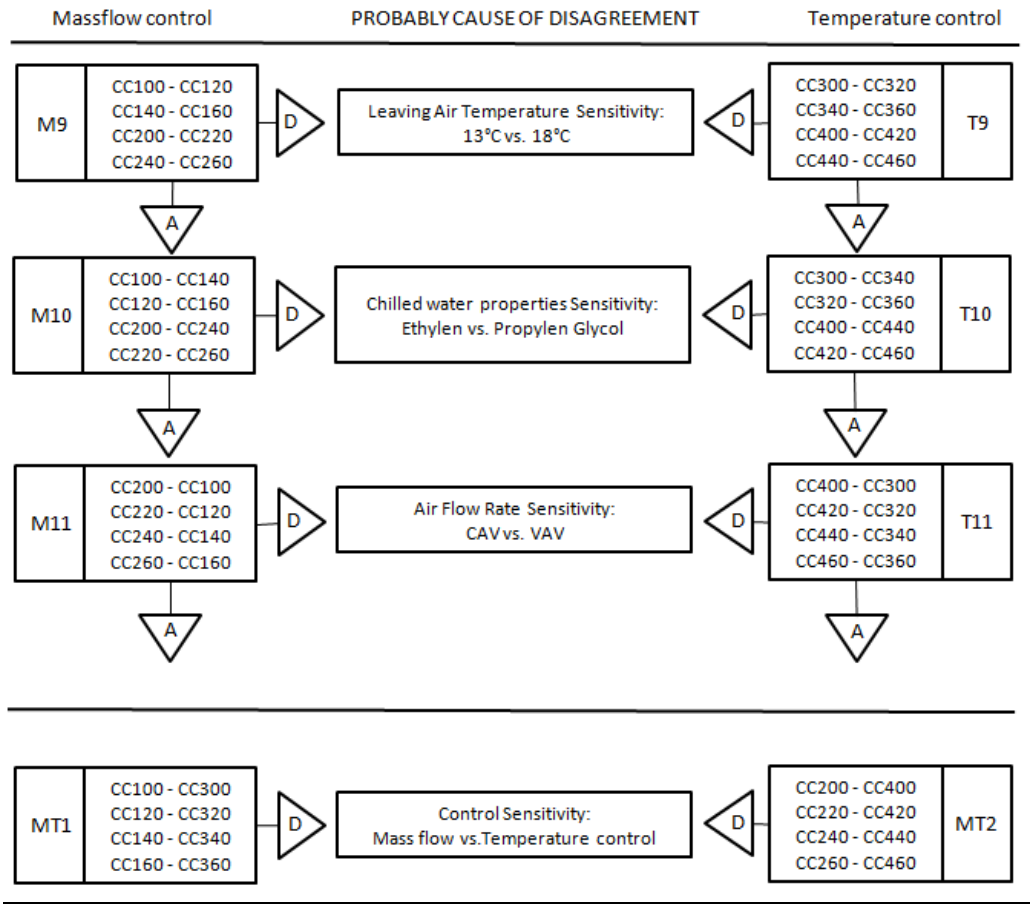

Abbreviations: A=Agree; D=Disagree

Figure 6-92 Cooling coil comparative test cases diagnostic logic flow diagram M9-M11 /T9-T11 / MT1 / MT2

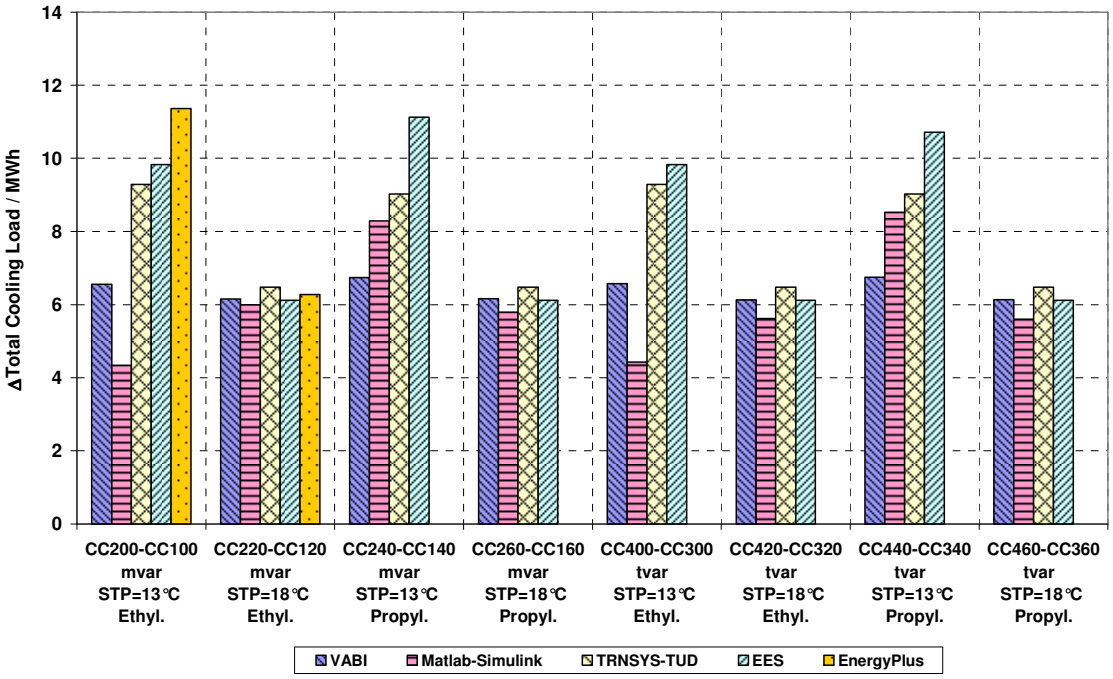

Figure 6-93 Results of the AFR sensitivity checks M11 & T11: Total Cooling load

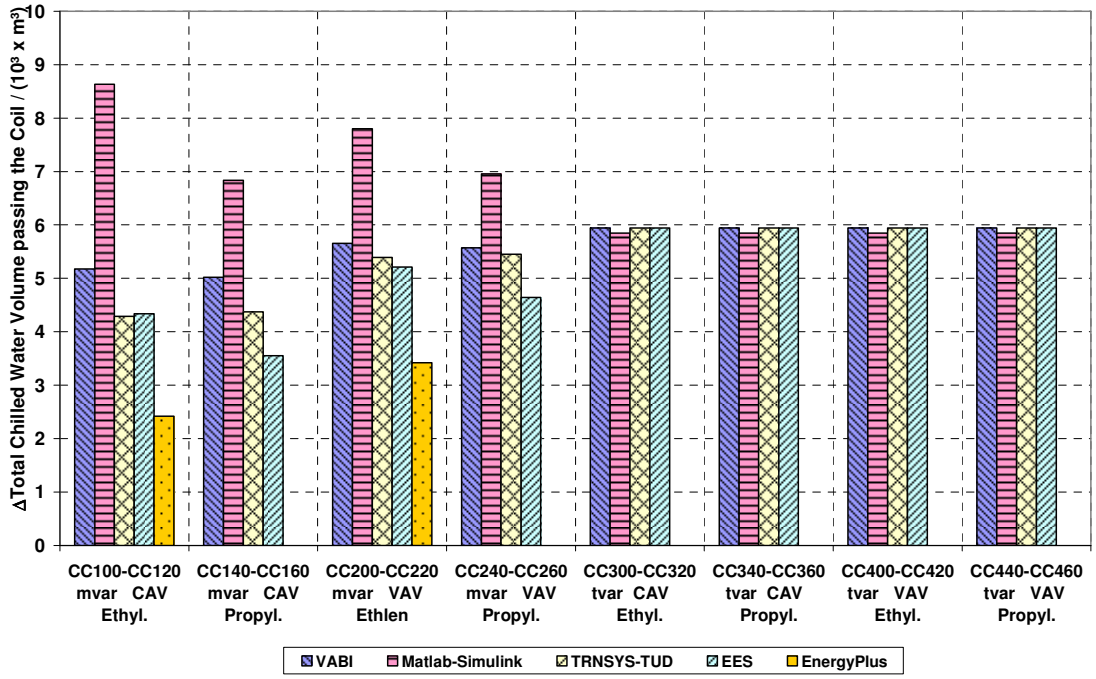

Figure 6-94 Results of the LAT sensitivity checks M9 & T9: Total Chilled water volume

A more basic sensitivity study on cooling coil performance is related to the UA value of the coil that mainly determines heat transfer from the air to the water side. UA value depends on several parameters as air and water flow rates, physical properties of chilled water, and coil temperatures, respectively. Based on at least one rating point for coil performance that already accounts for the fluid physics different load performances can be easily estimated using an UA function that depends on air and water flow rates. In the modeler reports of Chapter 7 more detailed information is provided from the modelers that give some insight into such UA approaches. Exemplarily Figure 6-95 shows the UA value of the cooling coil against chilled water flow rate. The UA value depicted here is calculated according to Eq.(4-5) of the specification taking into account sensible cooling load and temperature condition at the coil. Due to condensing effects the UA-value also varies independently from the water flow rate. Air flow rate is constant in CC100 that is why air flow rate dependency is eliminated from this graphic.

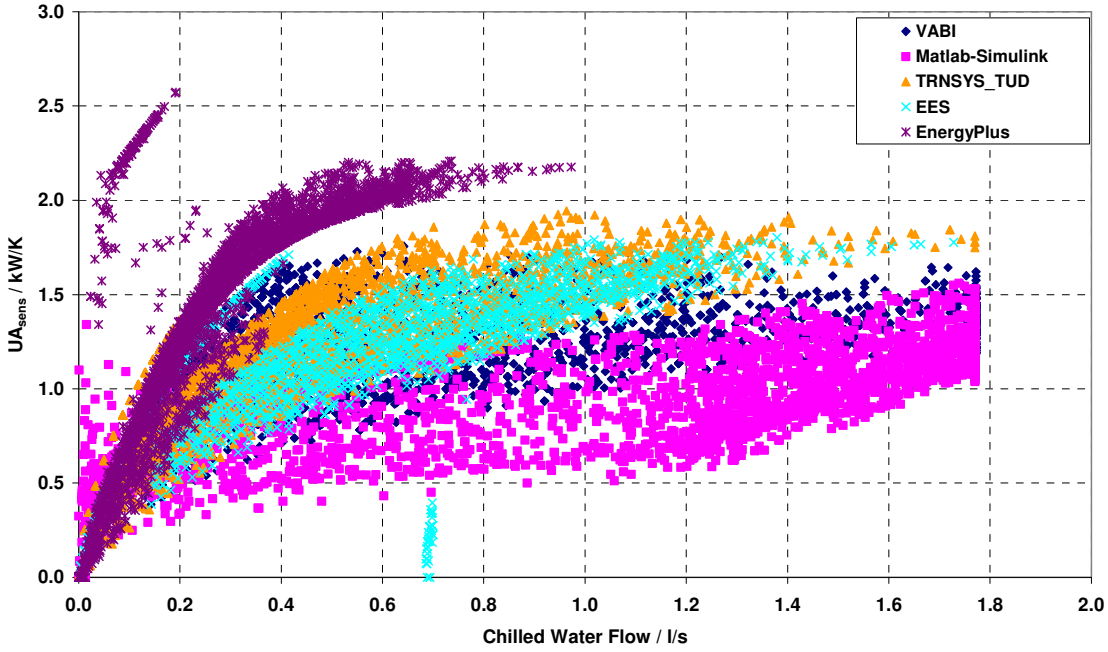

Figure 6-95 Sensitivity of UA_{sens} against chilled water mass flow rate; CC100

From the above Figure it is obvious that different UA approaches of the models result in quite different UA sensitivities. Especially UA values calculated from the EnergyPlus and the Matlab/Simulink models deviate from the average. Whereas Matlab/Simulink is at any rate in the range of other programs for high water flow rates EnergyPlus overestimates UA value. This again also has an impact on water flow rate that therefore in CC100 is much lower than for other programs. In addition to that UA_{sens} analyses Figure 6-96 contain a graph that shows the UA_{tot} value dependency on water flow rate instead of t he UA_{sens}. UA_{tot} is calculated in the

same way as UA_{sens} but referring to total cooling load instead of sensible cooling load. The Figure much more clarifies differences between modeling approaches of the programs. So we can propose for the test to take the sensitivity on UAtot rather than on UAsens. Again EnergyPlus and Matlab/Simulink significantly differ from other programs. EES and TRNSYS-TUD model do agree in their performance.

As heat transfer directly depends on UA values also coil temperatures and therefore condensation depends on chilled water mass flow rate. Figure 6-97 exemplarily shows the condensation mass flow rate against chilled water flow.

Both UA and condensation sensitivity may help to detect plausible causes of disagreement between models.

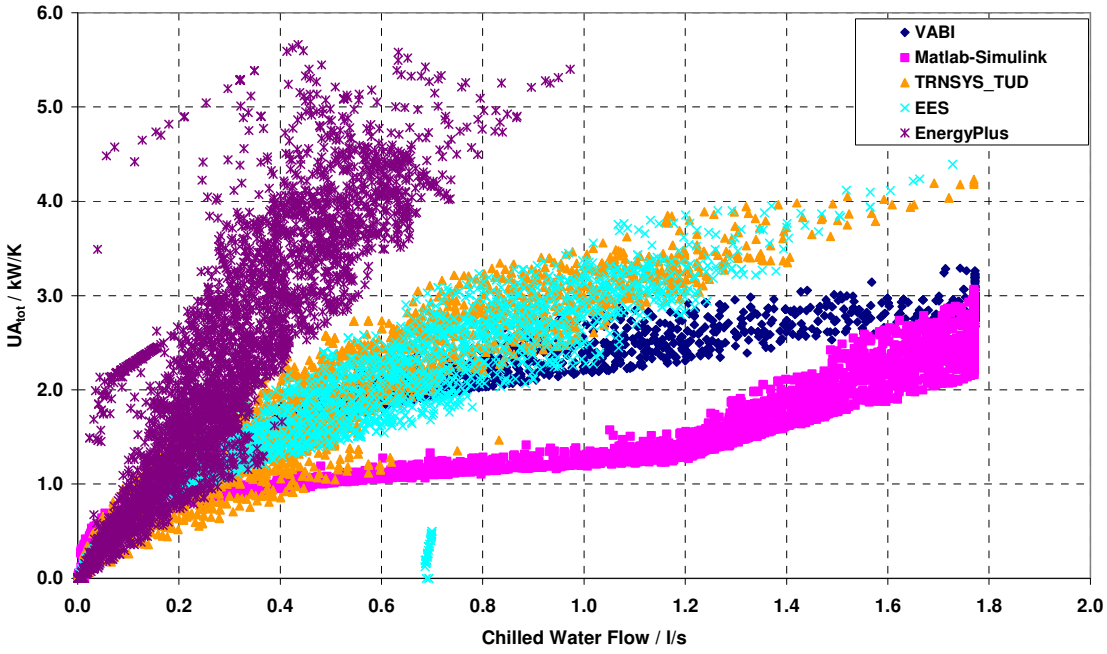

Figure 6-96 Sensitivity of UA_{tot} against chilled water mass flow rate; CC100

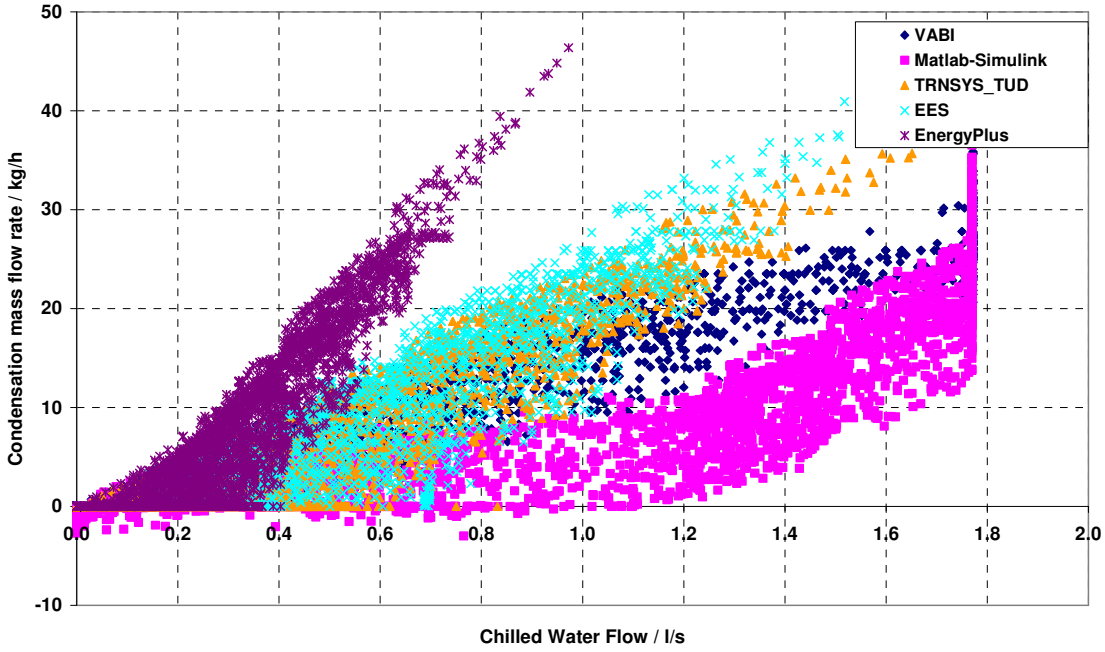

Figure 6-97 Condensation mass flow against chilled water mass flow rate; CC100

6.3 Chilled Water Hydraulics

There are some simulation results available provided from University of Liege (using program EES) and from Technical University of Dresden (using TRNSYS-TUD) during a very early stage of this validation project. These simulation results have been calculated based on input data derived from experimental data that have been collected at October 2, 2004. Since this data has neither been used for further empirical tests nor for any analyses in this final report such simulation results will not be represented here.

Chapter 7 Modellers Reports

7.1 Chiller

7.1.1 ULG – EES

The modeller report from University of Liege is provided in a separate file. It is titled "Simulation of HVAC Components with the Help of an Equation Solver" written by Vincent Lemort, Andres Rodríguez and Jean Lebrun.

.

7.1.2 TUD – TRNSYS-TUD

At Technical University of Dresden only comparative chiller tests have been performed during a very early stage of Task34/43. That means that the specification has not completely been finished yet when running the tests. Nevertheless it was tried to calculate chiller performance based on that information that were available at this time.
The chiller model was found in a free software library offered by the Solar Energy Laboratory at the University of Wisconsin which is the official distributor of the TRNSYS program. The model is called type68 and the equation, which is used in this Type68, is:

$$P_{tot} = P_{des}\left(\frac{T_{EEW}}{T_{EEW,des}}\right)^{a}\left[b + c\left(\frac{\dot{Q}_{load}}{\dot{Q}_{des}}\right) + d\left(\frac{\dot{Q}_{load}}{\dot{Q}_{des}}\right)^{2}\right]\left[1 + e\left(T_{ECA} - T_{ECA,des}\right) - f\left(T_{LEW} - T_{LEW,des}\right)\right]$$

where "P_{tot}" and "P_{des}" are the actual and design power requirements, "Q_{load}" and "Q_{des}" are the actual and design loads, "T_{ECA}" and " $T_{ECA,des}$" are the actual and design entering condenser air temperatures, and "T_{LEW}" and "$T_{LEW,des}$" are the actual and design leaving evaporator water temperatures.

The design parameters are fixed as follows: $T_{LEW,des}$= 6.7°C (44.0°F)
$T_{ECA,des}$= 35.0°C (95.0°F)
and the coefficients have been defined in the source code as:

a = 2.095829474 b = 0.117227656 c = 0.523137746
d = 0.359637843 e = 0.011598241 f =-0.015

It was originally planned to use this simple model as a basis for a further development of the chiller model but due to limited time and financial budget there was capacity to do so. Hopefully both the existing test description as well as experimental data collected during the experiments can be used later for validation and improvement of the chiller model.

7.2 Cooling Coil

7.2.1 ULG – EES

The modeller report from University of Liege is provided in a separate file. It is titled "Simulation of HVAC Components with the Help of an Equation Solver" written by Vincent Lemort, Andres Rodríguez and Jean Lebrun.

7.2.2 VABI – VA114

IEA SHC Task 34 / ECBCS Annex 43
Subtask D: Mechanical Equipment and Control Strategies

Cooling Coil - Modeler Report

VA114

VABI Software BV
P.O. Box 29
2600 AA Delft
The Netherlands
October 03, 2007 (fifth draft)
Report by A. Wijsman

Remark:
This report is a fifth draft. The cooling coil model was further improved. Problem is still the determination of the cooling coil characteristics (specific heat exchange capacity, split into external(A11), metal(C11) and internal (B11) part) from the available data (Manufacturer data (1 point), extra data from empirical tests). Tests were done again and reported in this draft of the report..

Cooling Coil – Modeler Report – VABI Software bv

Report by A. Wijsman and Szymon Szufa

1. Introduction

The Building simulation program VA114 is developed and distributed by VABI Software bv. The current version is 2.25.

The program calculates the Demand, the Supply, the Distribution and the Generation of heat and cold for a building with its energy supply system. Moreover the internal comfort temperature and overheating are calculated.

VA114 is a multi-zone program.

The time step applied in VA114 is 1 hour.

The heat and cold supply can happen by supply of conditioned air and by local devices.

The conditioning of the supply air can be in two steps:
- Pre-conditioning by a mixing valve, by heat recovery or by other
- Post-conditioning by heating coil, cooling coil, humidifier, de-humidifier

The cooling coil is fed by a cold water network. Air that passes this cooling coil is cooled down and de-humidification can occur.

The current program VA114 models a cooling coil. In chapter 2 a description of the applied model is given.

In July 2005 the cooling coil model was subjected to the IEA 34/43 – Cooling Coil – tests [1]. See second draft of this report for the results [2]. In January 2006 the tests were re-defined [3] and run. In the third draft of this report the results for the re-defined test cases are given:
- results of cooling coil comparative tests
- results of cooling coil empirical tests.

During the Iowa-meeting (April 2006) results for the Cooling Coil Tests showed reasonable discrepancies between the participating programs. The following questions raised:
- should flow dependency be taken into account?
- is one given data point (Manufacturer data) sufficient for characterization of the Cooling Coil model?

At VABI Software bv attention was paid to these questions. At first for the heating coil:

- a literature study was done on the flow dependency of the heat transfer at the external (air) side and the one at the internal (water) side
- a method was developed to split the specific capacity of the coil in an external part and an internal part
- for this method an extra given data point of the coil is required.

The Heating Coil model was adapted and tested. The results were reported [4]. The results were promising.

In August 2006 the same was done for the Cooling Coil model. The method to determine factor 'A11' (to split the specific capacity of the coil in an external and an internal part) is different from the method applied for the Heating Coil model. Because of the extra condensation process. Three methods were studied (see appendix C). All methods require an extra given data point of the coil.

In the fourth draft of this report information is given. Tests were done again and reported.

Now, August 2007, the cooling coil model was further improved. Distinguished are the external (air) side, the intermediate (metal) part and the internal (water) side. The method to determine these 3 individual parts has been adjusted.

Based on experiences with the heating coil tests the air volume flow rate to be used for the tests was better defined: to a volume flow rate belong air conditions (temperature and humidity).

Beside the Manufacturer data point extra points from empirical tests came available to determine the coil characteristics. Problem is still the determination of the cooling coil characteristics (specific heat exchange capacity, split into external(A11), metal(C11) and internal (B11) part) from the available data (Manufacturer data (1 point), extra data from empirical tests). The points are too less specific!! Probably only by fitting techniques the required parameters can be determined.

Re-runs for both comparative and empirical tests were done.

Background information and results of re-runs can be found in this fifth draft of the report.

2. Model description

In figure 1 a cooling coil is shown schematically.

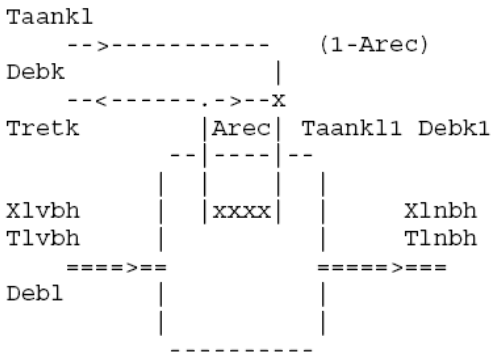

Figure 1: Cooling Coil schematically

Explanation:

Water

Debk	= water mass flow in the cold water network
Taankl	= water supply temperature of the cold water network
Tretk	= water return temperature of the cold water network
Debk1	= water mass flow over the cooling coil
Taankl1	= water temperature at entrance to the cooling coil
Arec	= recirculation fraction
	= (Taankl-Taankl1)/(Taankl-Tretk)

Air

Debl	= air mass flow through cooling coil
Tlvbh	= air temperature at entrance of cooling coil
Xlvbh	= air humidity at entrance of cooling coil
Tlnbh	= air humidity at exit of cooling coil
Xlnbh	= air humidity at exit of cooling coil

Control of the unit happens by valve ‘x’:

- Arec = 0 ‘Maximum’ cooling capacity
- Arec = 1 ‘Zero’ cooling capacity

The water mass flow over the coil is constant, the supply temperature at the entrance of the coil is controlled by valve ‘x’.

Characteristics of cooling coil

The model asks product information as input data: cooling power at given water supply temperature, water return temperature, air temperature and relative humidity at the entrance, air temperature and relative humidity at the exit. In table 1 this information is shown.

From this input data follow the water mass flow and the air mass flow. With this information the specific capacity of the coil (W/K) is derived (see appendix B).

With this specific capacity the performance of the cooling coil under any actual condition (water flow and supply temperature, air flow and supply temperature / humidity) can be determined.

Table 1: Input data for the cooling coil (example)

```
-> 2. Koelbatterij
Vermogen (in W)- waterA/Rtemp.      - LuchtAtemp./RV  -  LuchtRtemp./RV  -  deb.fract.
   QCEKLMX      TWBAT2A    TWBAT2R    TLBAT2A  RVLBAT2A  TLBAT2R  RVLBAT2R  DBFRW2
  16000.0           5.0       11.0      27.4     45.0       8.5     98.0    1.00
```

The model of the cooling coil

Subroutine 'Wwdrgnat' decribes the model of the cooling coil.

The heat exchange in this model happens both sensible and latent (condensation). Therefore the cooling coil has two parts: a dry part and a completely wet part (see figure 2).

The subroutine structure of 'Wwdrgnat' is given in figure 3

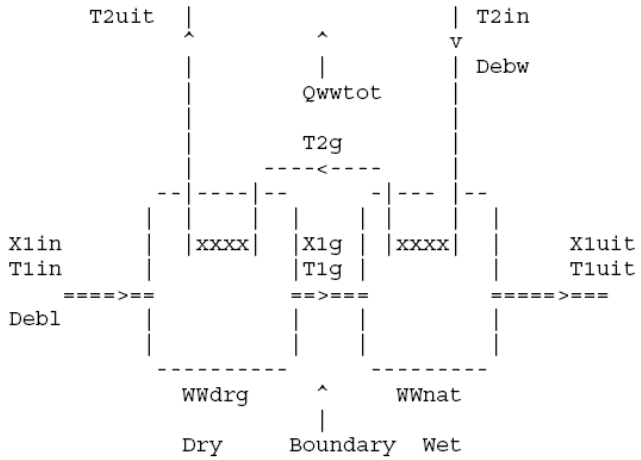

Figure 2: Division of cooling coil in a dry and a wet part

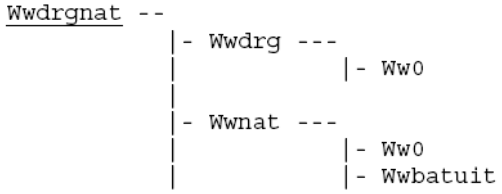

Figure 3: Subroutine structure of subroutine 'Wwdrgnat'

The dry part is described by subroutine 'Wwdrg' and the wet part by subroutine 'Wwnat'. Iteratively in subroutine 'Wwdrgnat' it is determined what part is wet (Fnat) and what part is dry (1-Fnat). For Fnat = 0,0 the entire cooling coil is dry, for Fnat = 1,0 the entire cooling coil is wet.

Subroutine 'Wwdrg' calls subroutine 'Ww0', that describes the pure sensible heat exchange between water and air flow.

Subroutine 'Wwnat' calls both subroutine 'Ww0' (enthalpy exchange) and subroutine 'Wwbatuit': condition (T en X) of the air at the outlet of the wet part of the cooling coil.

The specific capacity AFWW

In reality the specific capacity is built up out of 3 parts:

- the heat transfer between air flow and the cooling coil external surface; the air flow rate influences this coefficient
- the heat transfer inside the cooling coil
- the heat transfer between the cooling coil internal surface and the cooling fluid; the cooling fluid flow rate influences this coefficient

However the VABI cooling coil model assumes the specific capacity AFWW (in W/K) is constant, so independent of air flow rate and cooling fluid flow rate.

Moreover the model assumes the specific capacity is split into only two parts:

- an external AFWWEXT
- an internal AFWWINT

The external AFWWEXT is between air flow and cooling coil (including part of internal resistance); the internal AFWWINT is between cooling coil (including part of internal resistance) and cooling fluid.

In August 2006 the flow dependency was built in. The flow dependency was given by a correction factor 'f' for the two individual parts

Now, August 2007, the model has again been modified. It is assumed the specific capacity AFWW is split into three parts:

- an external AFWWEXT
- an intermediate AFMET
- an internal AFWWINT

The external AFWWEXT is between air flow and cooling coil (including part of internal resistance); the internal AFWWINT is between cooling coil (including part of internal resistance) and cooling fluid.

The flow dependency is given by a correction factor 'f' for the two individual parts:

- at the external (air) side: $f_{air} = (flow_{air}/flow_{air,0})^{0.56}$
- at the internal (water) side: $f_{water} = (flow_{water}/flow_{water,0})^{0.80}$

Remark: it is assumed both flows are in the turbulent region and stay in that region

So

- AFWWEXT = f_{air} * AFWWEXT0
- AFWWINT = f_{water} * AFWWINT0

And

AFWW = 1 / (1/AFWWEXT + 1/AFWWMET + 1/AFWWINT)

Remark: the AFWW has a lower limit, which is put on 10% of the AFWW0. That 10% is still an arbitrary value.

Important is to know the individual AFWWEXT0, AFWWMET and the AFWWINT0 for the given data point (Manufacturer data).

Definition:

- external AFWWEXT0 = 3,0 * A11*AFWW0
- internal AFWWINT0 = 3,0 * B11*AFWW0
- intermediate AFWWMET = 3,0 * C11*AFWW0

In series these three parts give the overall specific capacity AFWW0. This leads to the following relationship between A11, B11 and C11:

1,0/A11 + 1,0/B11 + 1/C11 = 3,0

Important question: How to obtain the specific capacity AFWW0 and these 3 parameters from available experimental data??

From that one data point (Manufacturer data) nothing can be said about the individual parts (see appendix D). All 3 parts equally sized for that data point can be an assumption (so A11 = B11 = C11 = 1,0)

However in case two or more extra data points are available this is in specific cases possible (see appendix E): A11, B11 and C11 can be determined. Preferably the extra points must be far away from the first point (for instance at 25% of the air flow rate and/or at 25% of the water flow rate).

By these model improvements for the Cooling Coil model three steps (levels of detail) for the specific capacity AFWW can be distinguished:

- step 1: AFWW is independent of the flows. A11, B11 and C11 are assumed to be 1,0
- step 2: AFWW is dependent on the flows. A11, B11 and C11 are assumed to be 1,0
- step 3: AFWW is dependent on the flows. A11, B11 and C11 are derived from 2 or more extra data points

The tests are carried out for those 3 modelling steps.

Remark: because a specific second data point was not yet available factor ‘a’ was kept the same as in the old model (=0,25)

3. Modeling Assumptions

In general

- Comparative tests.
The cooling coil model is tested insitu of the VA114 simulation program. Actual weather data from the Des Moines, Iowa TMY2-file is used to obtain the conditions of the air at the air inlet.

- Empirical tests.
The cooling coil model is tested outside the VA114 simulation program. Air flow rate, water flow rate, entering air temperature and entering water temperature are available from file CCEmpInput1.txt (Empirical test I) and CCEmpInput2.txt (Empirical test II)

For both tests:

Important are the cooling fluid and atmospheric pressure:

- for what cooling fluid and atmospheric pressure the manufacturer's data is given
- what cooling fluid is used during the tests and what atmospheric pressure occurs.

The cooling fluid for which the manufacturer's data is given, is an aqueous Ethylene Glycol solution (35% concentration by mass).

The atmospheric pressure for which the manufacturer's data is given, is the atmospheric pressure at sea level (101,300 kPa).

The comparative tests were done for both the Ethylene Glycol solution (35% concentration by mass) and for an aqueous Propylene Glycol solution (18% concentration by mass).

The empirical tests were only done for the aqueous Propylene Glycol solution (18% concentration by mass).

The atmospheric pressure during the tests is the atmospheric pressure at Des Moines (97,825 kPa – 294 m above sea level).

More specific

The specific capacity AFWW is derived from table 4.2. and according to appendix B (assumption in VA114 factor 'a' = 0,25):

Specific capacity AFWW = 3163 W/K
Air mass flow rate $Flow_{air}$ = 1,851 kg/s *)
Fluid mass flow rate = 1,871 kg/s

*) Belonging air volume flow rate = 5530 m^3/h (at 20 ^oC and 101,3 kPa)

The cooling fluid applied at table 4.2 was an aqueous Ethylene Glycol solution (35%):

- specific mass SMW = 1056 kg/m^3
- specific heat SWW = 3550 J/kg.K

The specific capacity AFWW (in W/K) can be either constant or flow dependent. Depending on the type of model (step 1, 2 or 3)

The specific capacity is assumed to be split into three parts:

- an external AFWWEXT = 3,0 * A11*AFWW
- an internal AFWWINT = 3,0 * B11*AFWW
- an intermediate AFWWMET = 3.0 * C11*AFWW

Factor A11, B11 and C11 are depending on the type of model (step 1, 2 or 3).

In short:
For the Cooling Coil model three steps (levels of detail) for the specific capacity AFWW are distinguished:

- step 1: AFWW is independent of the flows. A11, B11 and C11 are assumed to be 1,0
- step 2: AFWW is dependent on the flows. A11, B11 and C11 are assumed to be 1,0
- step 3: AFWW is dependent on the flows. A11, B11 and C11 are derived from 2 or more extra data points

4. Modeling Options

The tests involved:

- heating coil comparative tests
- heating coil empirical tests

Cooling coil comparative tests

The tests involved the influence of:

- air volume over the cooling coil
- type of cooling fluid
- type of control at the "water" side
- air outlet temperature

Air volume over the cooling coil
Two options: Constant air volume (CAV – constant all the time at 3000 m^3/h) and Quasi-Variable air volume (VAV – 2000 m^3/h from 6 p.m. to 7 a.m. and 5000 m^3/h for the other hours)

Type of cooling fluid
Two options: the tests were conducted for the Ethylene Glycol solution (35%) as the cooling fluid (IEA43ME= +1 or -1), but also for a Propylene Glycol solution (18%) (IEA43ME= +2 or -2):

Ethylene Glycol solution:

- specific mass SMW = 1056 kg/m^3
- specific heat SWW = 3550 J/kgK

Propylene Glycol solution:

- specific mass SMW = 1020 kg/m^3
- specific heat SWW = 3974 J/kgK

Type of control at the "water" side
Two options: the water flow over the cooling coil is constant (cooling power is controlled by varying the water inlet temperature T_{var} (IEA43ME = positive value = +1 or +2) or the water inlet temperature is constant m_{var} (IEA43ME = negative value= -1 or -2).

Air outlet temperature
Two options: the air outlet temperature has as set point 13 ^oC and 18 ^oC.

The conducted tests are numbered (CC100 etc.) and given in table 1.

Further information
Simulation period: 153 days – from May 1 till September 30.
Weather file: 14933.tm2 (Des Moines - Iowa)

Table1: Conducted tests

Testcase	Configuratie	Airflow	Fluid	DCA-ST	IEA43ME
				Degree C	
CC100	m_{var}	CAV	Ethylen-glycol	13	1
CC120			Ethylen-glycol	18	1
CC140			Propylen-glycol	13	2
CC160			Propylen-glycol	18	2
CC200	m_{var}	VAV	Ethylen-glycol	13	1
CC220			Ethylen-glycol	18	1
CC240			Propylen-glycol	13	2
CC260			Propylen-glycol	18	2
CC300	T_{var}	CAV	Ethylen-glycol	13	-1
CC320			Ethylen-glycol	18	-1
CC340			Propylen-glycol	13	-2
CC360			Propylen-glycol	18	-2
CC400	T_{var}	VAV	Ethylen-glycol	13	-1
CC420			Ethylen-glycol	18	-1
CC440			Propylen-glycol	13	-2
CC460			Propylen-glycol	18	-2

Cooling coil empirical tests

The cooling coil model is tested outside the VA114 simulation program. Air flow rate, water flow rate, entering air temperature, entering water temperature and atmospheric pressure are available from file:

- Empirical test I: file CCEmpInput1.txt (period August 24 - 30, 2005)
- Empirical test II: file CCEmpInput2.txt (period August 08 – 23, 2006)

Special subroutine was developed to read the data and to write the results to the results file.

5. Modeling Difficulties

Cooling coil comparative tests

Air inlet temperature lower than the required set point
Cooling of the air is only required in case the air inlet temperature is higher than the set point. In case the air inlet temperature is lower than the set point the air is not conditioned and leaves the cooling coil with the same temperature. Also at the water side the water outlet temperature is the same as the water inlet temperature (6 ^{o}C)

Type of control at the "water" side
Standard the cooling coil in VA114 has a constant water flow over the coil; cooling power is controlled by varying the water inlet temperature (T_{var}).
For these tests the cooling coil model was extended with the option "constant water inlet temperature"; cooling power is controlled by varying the water flow over the coil (m_{var})

Required output simulation results
The required output is not standard coming from VA114. An adaptation of the program was made to get the required output.

There are no other modeling difficulties.

Cooling coil empirical tests

There are no other modeling difficulties.

General remark
We think in this IEA-group special attention should be paid to uniform nomenclature for the input and output parameters. This for future users of the tests.
At the moment the nomenclature is not uniform. This remark is valid for both the heating coil and the cooling coil tests.

6. Software errors discovered and/or Comparison between different versions of the same software.

No software errors were discovered until now, but it was observed the iteration process (to determine the part of the coil that is wet) in the Cooling Coil model has some difficulty to converge at very low air flow rates (lower than 5 % of the design flow rate). This difficulty was only observed for step 1 (AFWW is independent of the flows) for the Empirical test II (after 5700-5800 minutes the air flow is very low)

7. Results

7.1 Results concerning given specifications cooling coil

- From the Manufacturer data point:

The specific capacity AFWW is derived from table 4.2. of the spec's [3] and according to appendix B (assumption in VA114: factor 'a' = 0,25):

Specific capacity AFWW = 3163 W/K
Air mass flow rate $Flow_{air}$ = 1,851 kg/s *)
Fluid mass flow rate = 1,871 kg/s **)

*) Belonging air volume flow rate = 5530 m^3/h (at 20 ^oC and 101,3 kPa)
**) Belonging fluid volume flow rate = 1,77 l/s (Ethylene Glycol – 35 %)

No information about the factors A11, B11 and C11 came available to determine the individual parts.

- From the 10 data points of empirical test II

In table 4.6 the 10 data points available from empirical test II are given. From point #1 follow the specific capacity

Specific capacity AFWW = 1804 W/K
Air mass flow rate $Flow_{air}$ = 1,350 kg/s *)
Fluid mass flow rate = 0,622 kg/s **)

*) Belonging air volume flow rate = 4030 m^3/h (at 20 ^oC and 101,3 kPa)
**) Belonging fluid volume flow rate = 0,61 l/s (Propylene Glycol – 18 %)

From fitting with the other 9 points the factors A11, B11 and C11 are estimated:

A11 = 0,90
C11 = 3,00
B11 = 0,64.

More information about the fitting can be found in appendix F.

Remark: the specific capacity here differs from the one determined from the Manufacturer data because it is given at deviating flow rates.

Remark: during the comparative tests it should be checked the right fluid flow rate in the system is present. Reason: in VA114 the system fluid flow rate is initially the same as the design flow rate of the coil and ….. those design fluid flows are very different (see above: 1,77 l/s and 0,61 l/s); VA114 has in second stage the possibility to adjust that system flow rate

7.2 Results of the several tests

For the Cooling Coil model three steps (levels of detail) for the specific capacity AFWW are distinguished:

- step 1: AFWW is independent of the flows (fixed); A11 = B11 = C11 = 1,0
- step 2: AFWW is dependent on the flows;A11 = B11 = C11 = 1,0
- step 3: AFWW is dependent on the flows; AFWW, and factors A11, B11/C11 are derived from extra data points

The tests are carried out for those 3 modelling steps.

Results of the Cooling coil comparative tests

Results are available hourly and as total over the simulation period (May 1 till September 30).

The hourly results are available for the cases 200 and 400 in file "Results cc-cases 200 and 400-hourly-20070813.xls"; the totals for the entire simulation period are given in table 2 a,b and c (see also files "Results cc-cases-totals-i-20070813.xls" with i=1,2,3=step). In this table the peak power is given too.

Comments to the totals – step 1 (see table 2a):

- The VAV-cases show a higher cooling load than the CAV-cases. Two reasons: the higher '24-hour' average air flow rate (3375 m3/h in stead of 3000 m3/h) and the higher flow rate at day-time (at day-time the air inlet temperature is higher and the moisture content is higher than at night time)
- Control at the "water" side by controlling the fluid flow (water inlet temperature is constant) shows a higher cooling load because of a higher de-humidification that occurs
- The influence of the type of cooling fluid is zero, except for the cases were peak cooling is equal to the maximum capacity of the coil (this happens at day-time for VAV-cases); cooling coil with Propylene Glycol has a somewhat higher maximum power than the cooling coil with Ethylene Glycol. Remark: maximum power occurs at July 31 at hour 15 (ambient temperature = 34,4 oC and Relative Humidity = 64,3 %) and is 55,4 kW for Ethylene Glycol and 56,1 kW for Propylene Glycol.

Comments to the totals – step 2 (see table 2b):

Step 1 has a flow independent AFWW, step 2 has a flow dependent AFWW. For both steps A11 = B11 = C11 = 1,00. Values in table 2b differ from table 2c (both higher and lower); in some cases the difference is bigger than in other cases

Comments to the totals – step 3 (see table 2c):

Step 2 and step 3 have both a flow dependent AFWW. Both the AFWW, mass flow rates (other point as reference) and the factors A11, B11 and C11 differ (see 7.1)

This means the wall temperature of the cooling coil for step 3 will be somewhat different from step 2 and so more condensation will occur. All values (both Cooling load and Peak Cooling) in table 2c are somewhat higher than in table 2c; in some cases the difference is bigger than in other cases.

Table 2a: Total cooling results for the several tests - – step 1
(AFWW is independent of flow, A11= B11 = C11 = 1,00)

Testcase	Configuratie	Airflow	Fluid	DCA-ST	IEA43ME	Cooling	Peak Cooling
				Degree C		kWh	kW
CC100	m_{var}	CAV	Ethylen-glycol	13	1	45486	46904
CC120			Ethylen-glycol	18	1	18457	40414
CC140			Propylen-glycol	13	2	45504	47309
CC160			Propylen-glycol	18	2	18461	40414
CC200	m_{var}	VAV	Ethylen-glycol	13	1	52134	55436
CC220			Ethylen-glycol	18	1	24707	55436
CC240			Propylen-glycol	13	2	52339	56129
CC260			Propylen-glycol	18	2	24715	56129
CC300	T_{var}	CAV	Ethylen-glycol	13	-1	45272	46904
CC320			Ethylen-glycol	18	-1	18155	40414
CC340			Propylen-glycol	13	-2	45289	47309
CC360			Propylen-glycol	18	-2	18155	40415
CC400	T_{var}	VAV	Ethylen-glycol	13	-1	51928	55436
CC420			Ethylen-glycol	18	-1	24285	55436
CC440			Propylen-glycol	13	-2	52131	56129
CC460			Propylen-glycol	18	-2	24291	56129

Table 2b: Total cooling results for the several tests – step 2
(AFWW is flow dependent, A11= B11 = C11 = 1,00

Testcase	Configuratie	Airflow	Fluid	DCA-ST	IEA43ME	Cooling	Peak Cooling
				Degree C		kWh	kW
CC100	m_{var}	CAV	Ethylen-glycol	13	1	45346	45603
CC120			Ethylen-glycol	18	1	18318	40429
CC140			Propylen-glycol	13	2	45371	45993
CC160			Propylen-glycol	18	2	18310	40429
CC200	m_{var}	VAV	Ethylen-glycol	13	1	51900	55077
CC220			Ethylen-glycol	18	1	24469	55077
CC240			Propylen-glycol	13	2	52105	55765
CC260			Propylen-glycol	18	2	24474	55765
CC300	T_{var}	CAV	Ethylen-glycol	13	-1	45231	45603
CC320			Ethylen-glycol	18	-1	18183	40430
CC340			Propylen-glycol	13	-2	45258	45993
CC360			Propylen-glycol	18	-2	18182	40430
CC400	T_{var}	VAV	Ethylen-glycol	13	-1	51802	55077
CC420			Ethylen-glycol	18	-1	24311	55077
CC440			Propylen-glycol	13	-2	52009	55765
CC460			Propylen-glycol	18	-2	24318	55765

Table 2c: Total cooling results for the several tests – step 3
(AFWW is flow dependent, A11=0,90; C11 = 3,00 and B11 = 0,64)

Testcase	Configuratie	Airflow	Fluid	DCA-ST	IEA43ME	Cooling	Peak Cooling
				Degree C		kWh	kW
CC100	m_{var}	CAV	Ethylen-glycol	13	1	45751	46052
CC120			Ethylen-glycol	18	1	18611	40606
CC140			Propylen-glycol	13	2	45751	46052
CC160			Propylen-glycol	18	2	18611	40606
CC200	m_{var}	VAV	Ethylen-glycol	13	1	52613	56938
CC220			Ethylen-glycol	18	1	25040	56938
CC240			Propylen-glycol	13	2	52613	56938
CC260			Propylen-glycol	18	2	25040	56938
CC300	T_{var}	CAV	Ethylen-glycol	13	-1	45569	46052
CC320			Ethylen-glycol	18	-1	18374	40606
CC340			Propylen-glycol	13	-2	45569	46052
CC360			Propylen-glycol	18	-2	18374	40606
CC400	T_{var}	VAV	Ethylen-glycol	13	-1	52474	56938
CC420			Ethylen-glycol	18	-1	24780	56938
CC440			Propylen-glycol	13	-2	52474	56938
CC460			Propylen-glycol	18	-2	24780	56938

Cooling coil empirical tests I

Results of the test are presented in the output file 'Results exercise 2-emp1-per minute-20071002.xls' for the 3 earlier mentioned steps

In figure 4a-f the input data is given: air volume rate, fluid flow rate, entering air temperature, entering air relative humidity, entering air humidity and entering water temperature

Entering air temperature and entering air humidity are almost constant during the test.

In figure 5a-f the output data for the 3 steps is given: the cooling load, the specific capacity AFWW, the leaving air temperature and leaving water temperature during a small period with low fluid flow rate and during a small period with high fluid flow rate.

The influence of the 3 steps is good to see:
- From step 1 to step 2 the influence is rather big
- From step 2 to step 3 the influence is not so big

Measured data was distributed for the first day (1440 minutes). In figure 5g-j a comparison between measured data and modelling results is made:
- step 2 and 3 come close to the measurements
- at low flow rates the measured data shows lower peaks and is somewhat delayed with respect to the modelling results (mass effect of cooling coil?)

To conclude: modelling step 1 is too rough to model the cooling coil, modelling step 2 and step 3 come much closer.

Figure 4a: Empirical test I input data: Air Volume flow rate

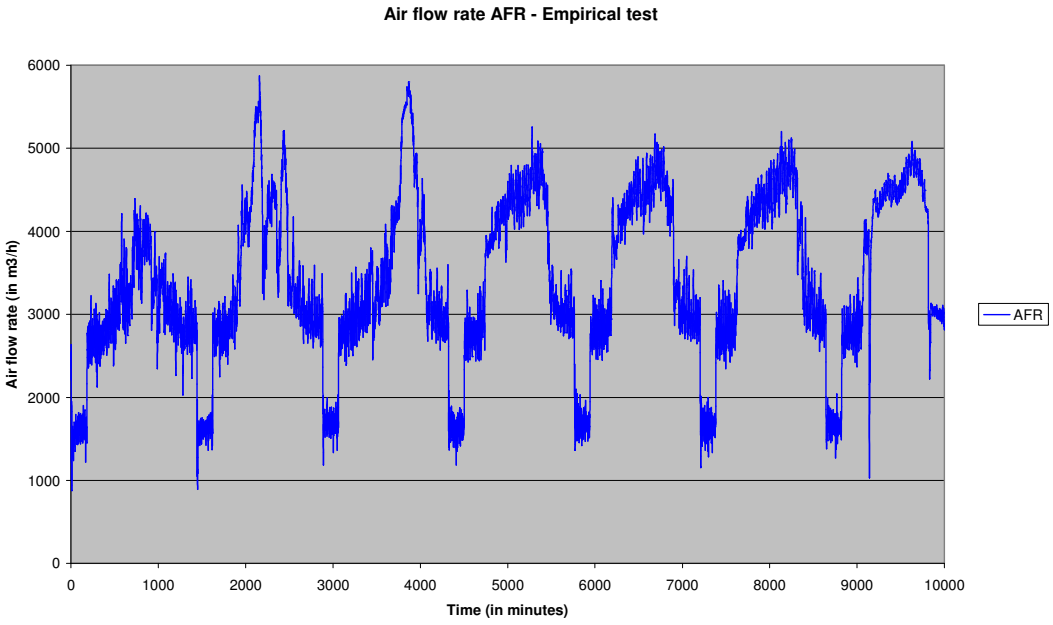

Figure 4b: Empirical test I input data: Fluid Volume flow rate

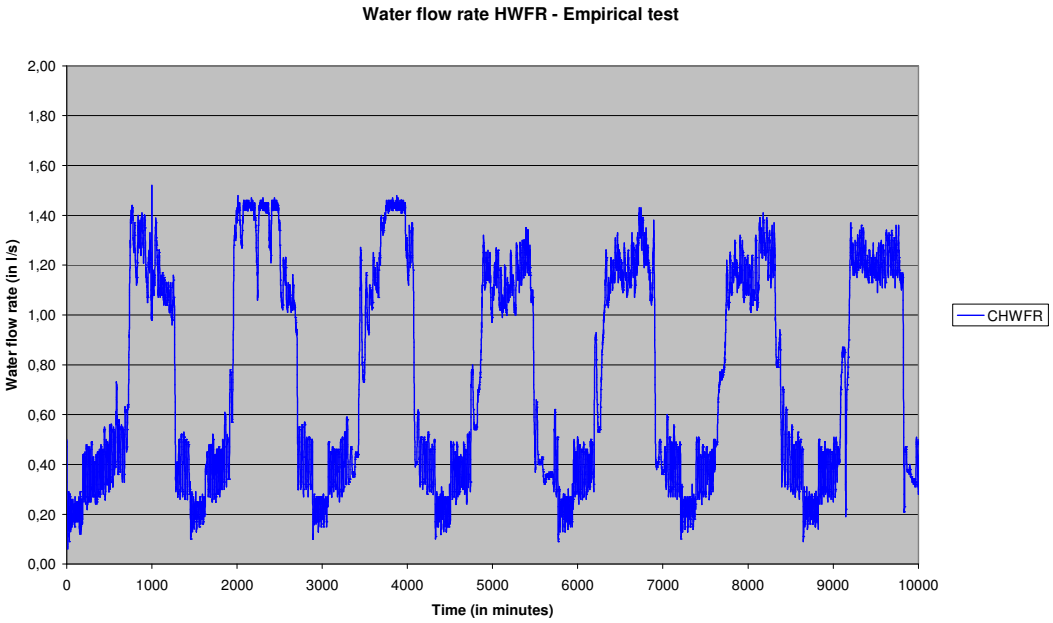

Figure 4c: Empirical test I input data: Entering air temperature

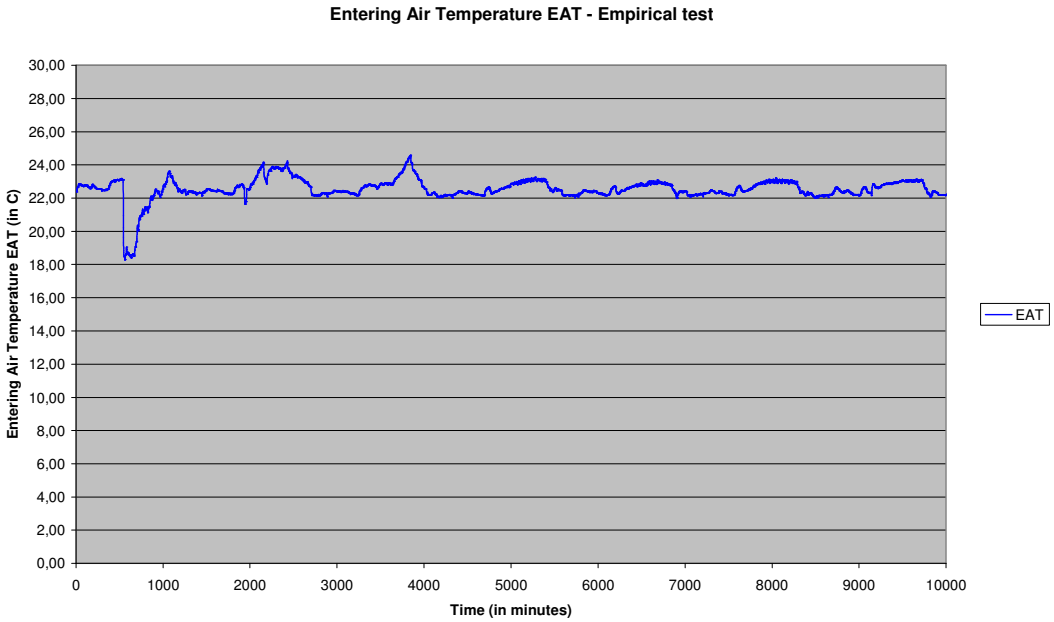

Figure 4d: Empirical test I input data: Entering air relative humidity

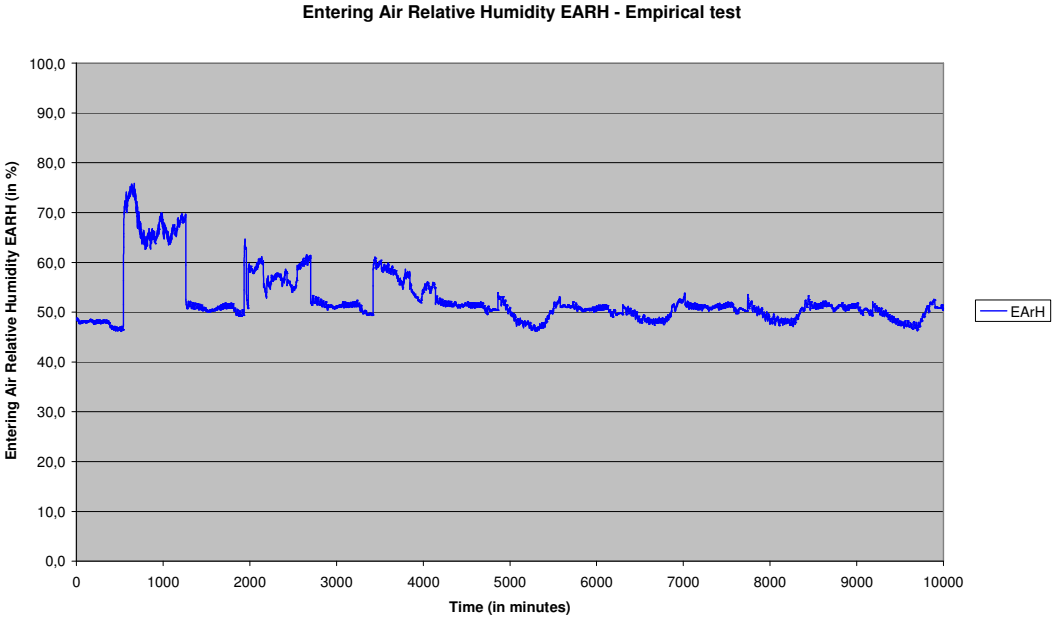

Figure 4e: Empirical test I input data: Entering air humidity

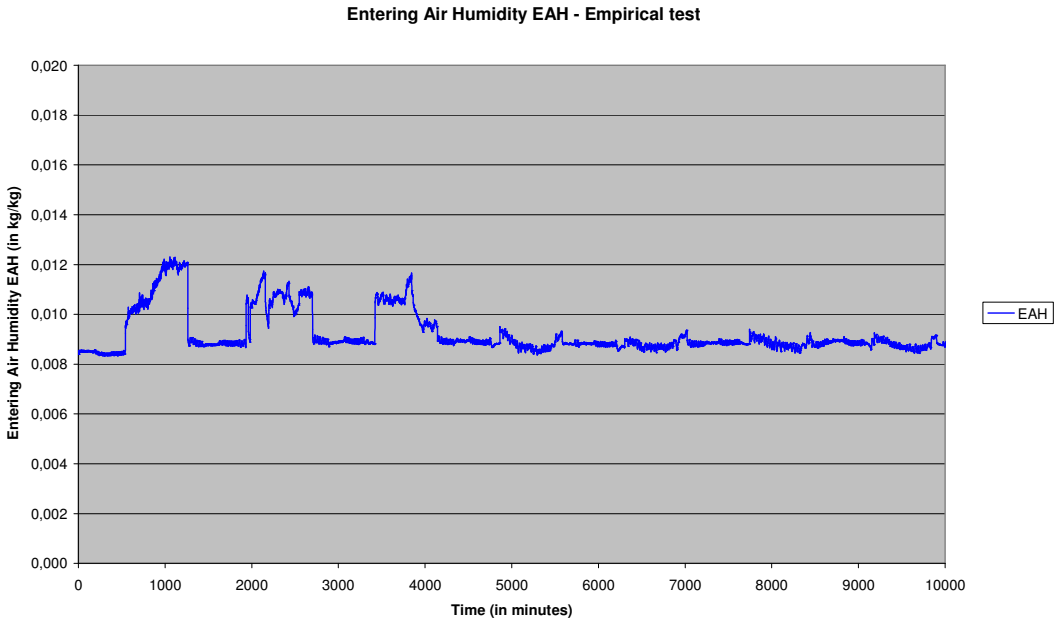

Figure 4f: Empirical test I input data: Entering water temperature

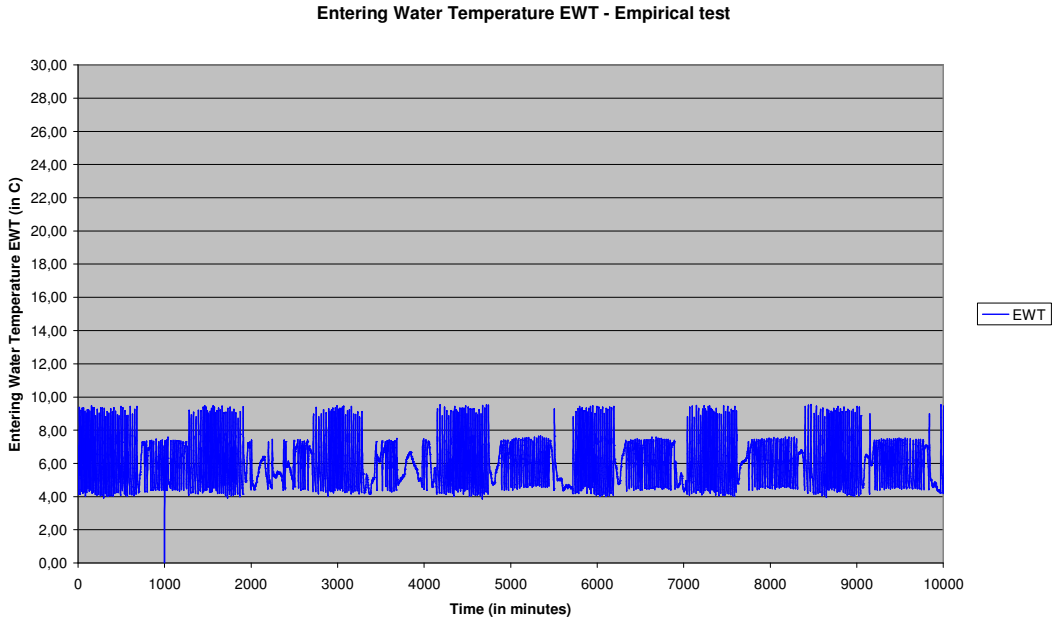

Figure 5a: Empirical test I output data: Cooling load

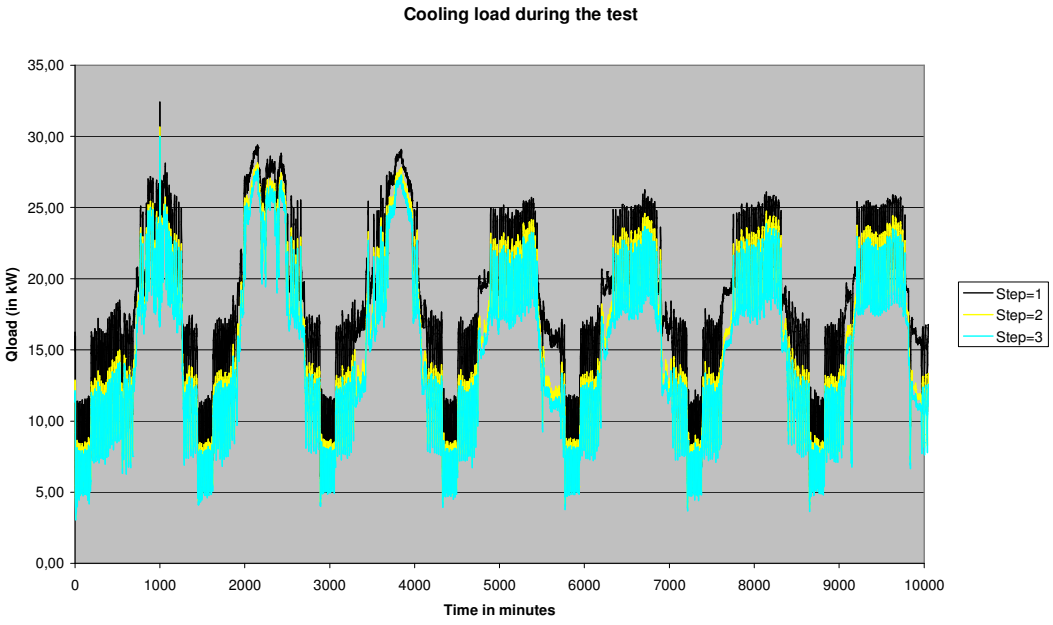

Figure 5b: Empirical test I output data: Specific cooling capacity

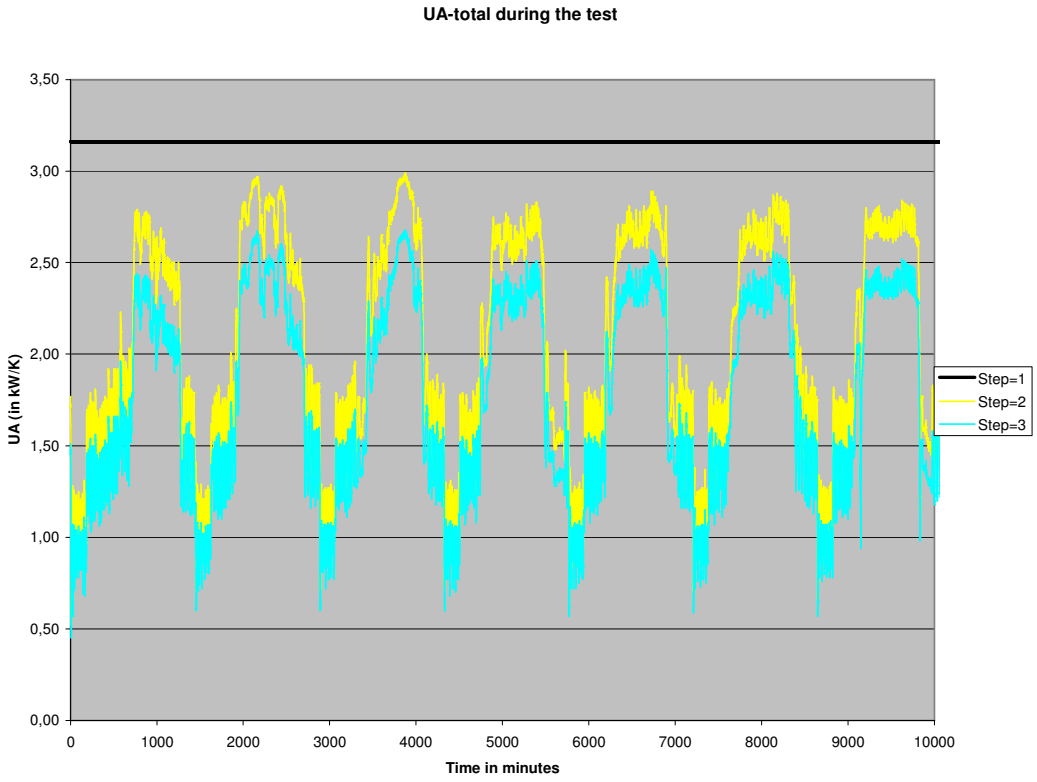

Figure 5c: Empirical test I output data: Leaving air temperature (low air flow rate and low fluid flow rate)

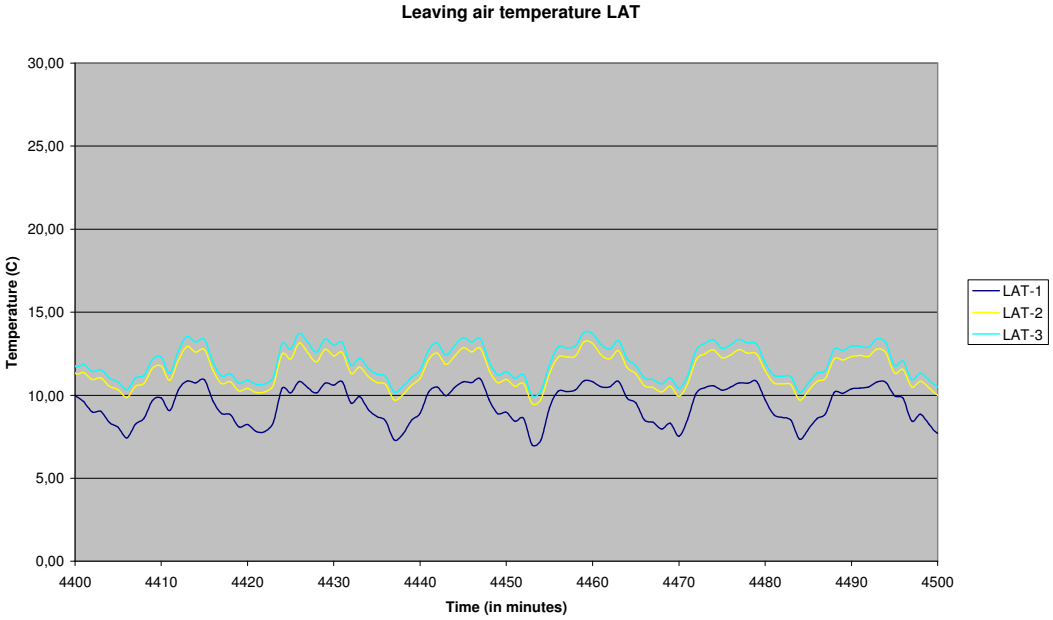

Figure 5d: Empirical test I output data: Leaving water temperature (low air flow rate and low fluid flow rate)

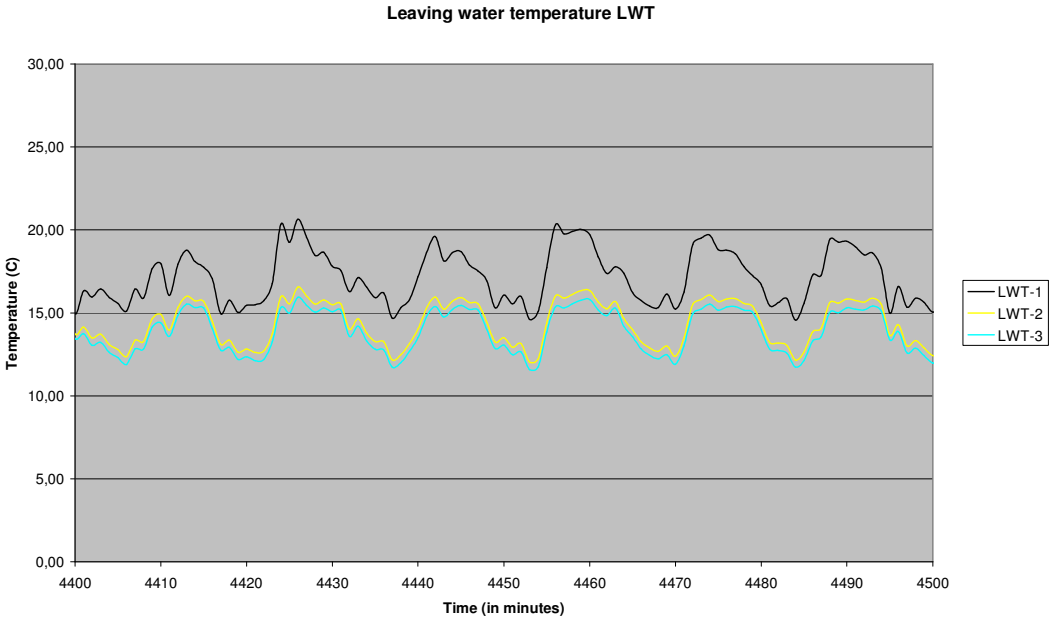

Figure 5e: Empirical test I output data: Leaving air temperature (high air flow rate and high fluid flow rate)

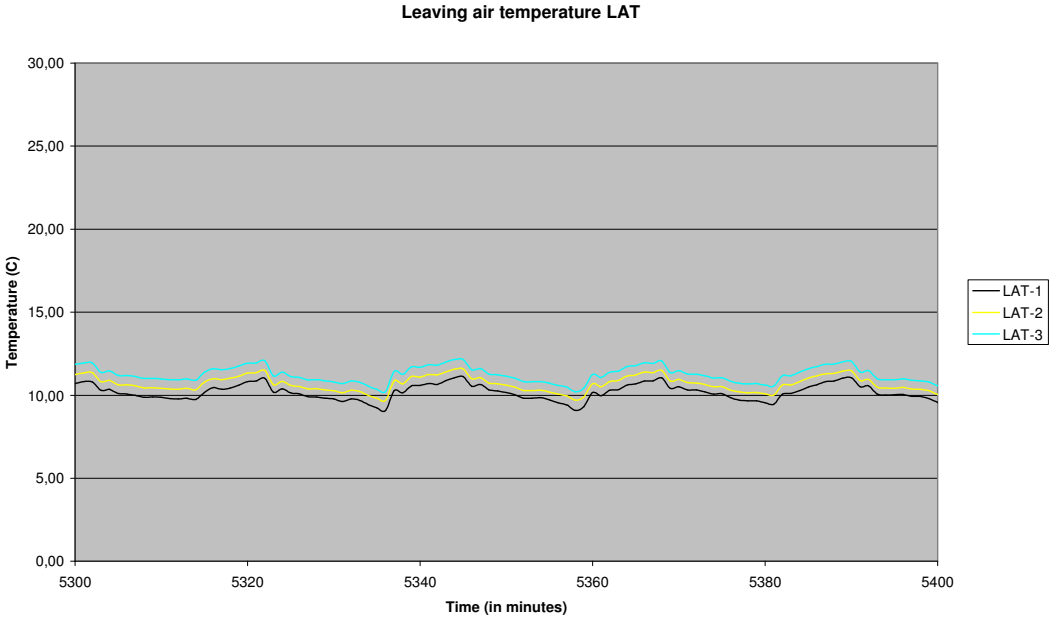

Figure 5f: Empirical test I output data: Leaving water temperature (high air flow rate and high fluid flow rate)

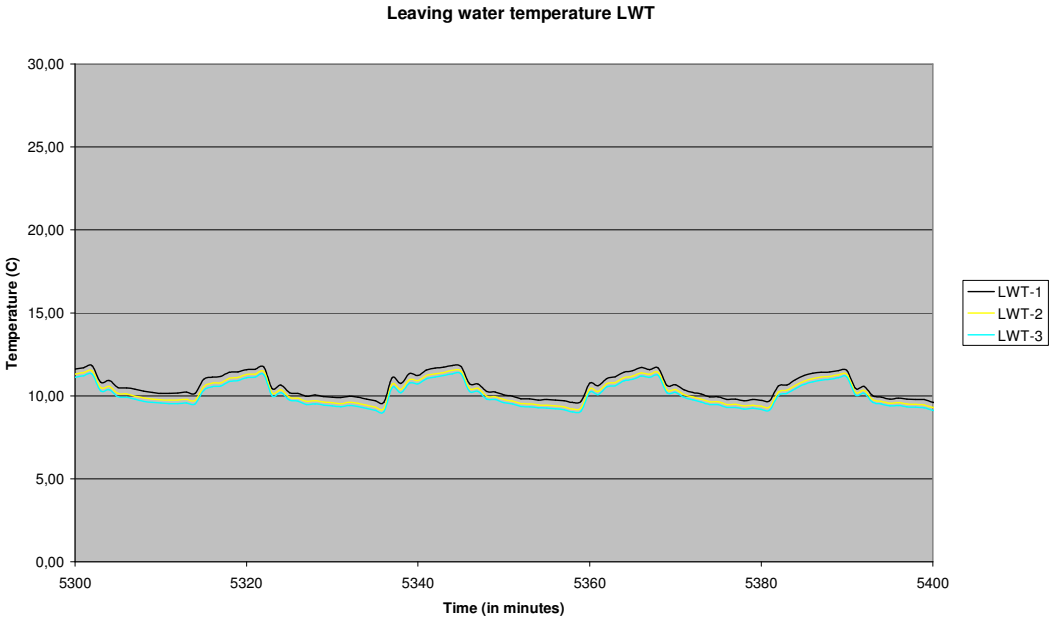

Figure 5g: Empirical test I – Measured data against modelling results: Leaving air temperature (low air flow rate and low fluid flow rate)

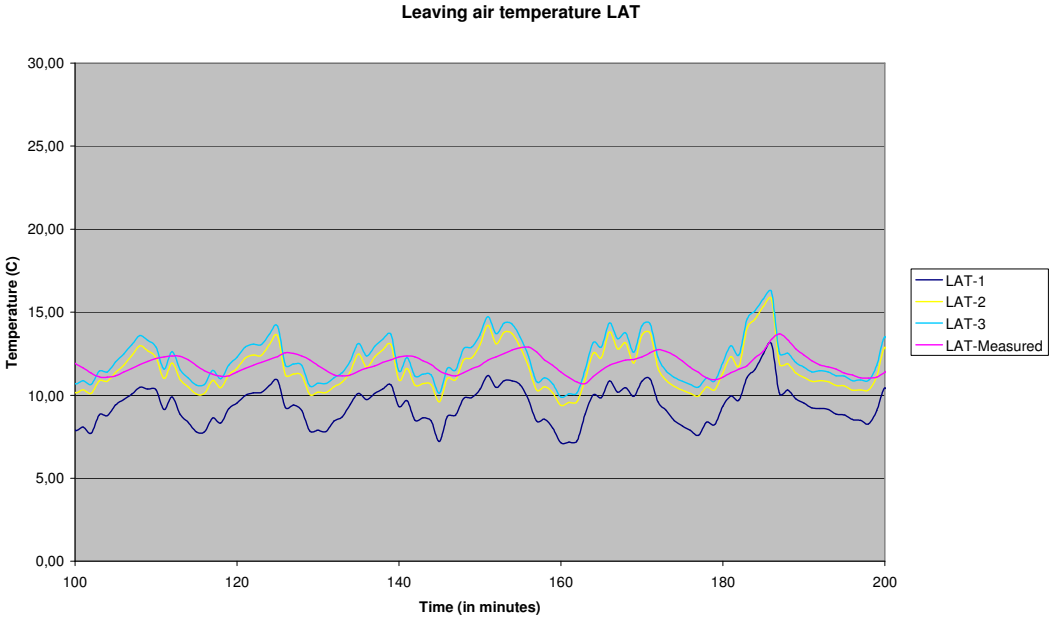

Figure 5h: Empirical test I – Measured data against modelling results: Leaving water temperature (low air flow rate and low fluid flow rate)

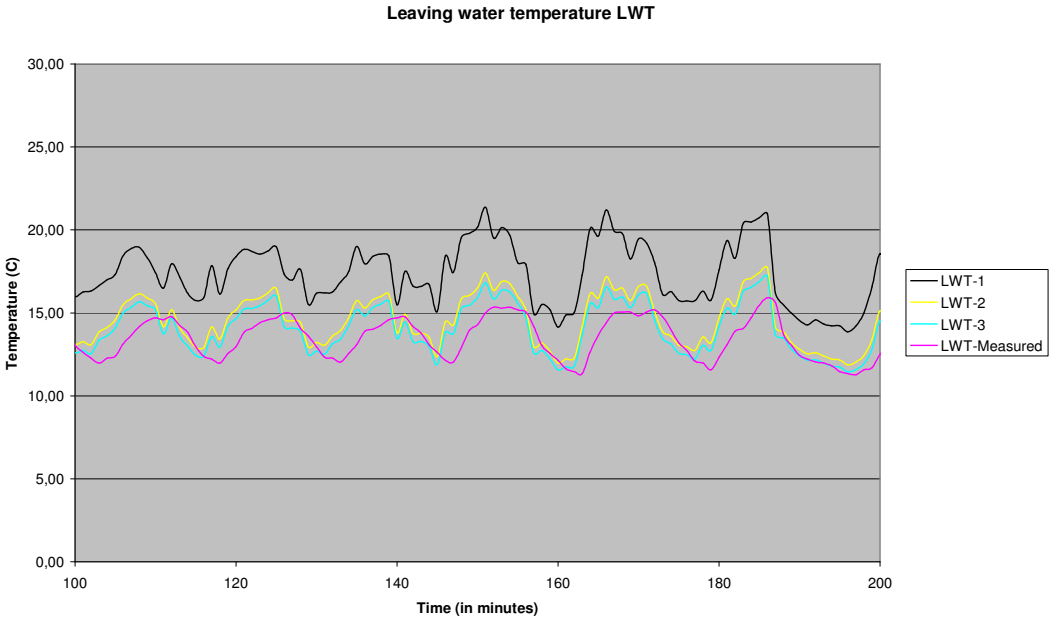

Figure 5i: Empirical test I – Measured data against modelling results: Leaving air temperature (high air flow rate and high fluid flow rate)

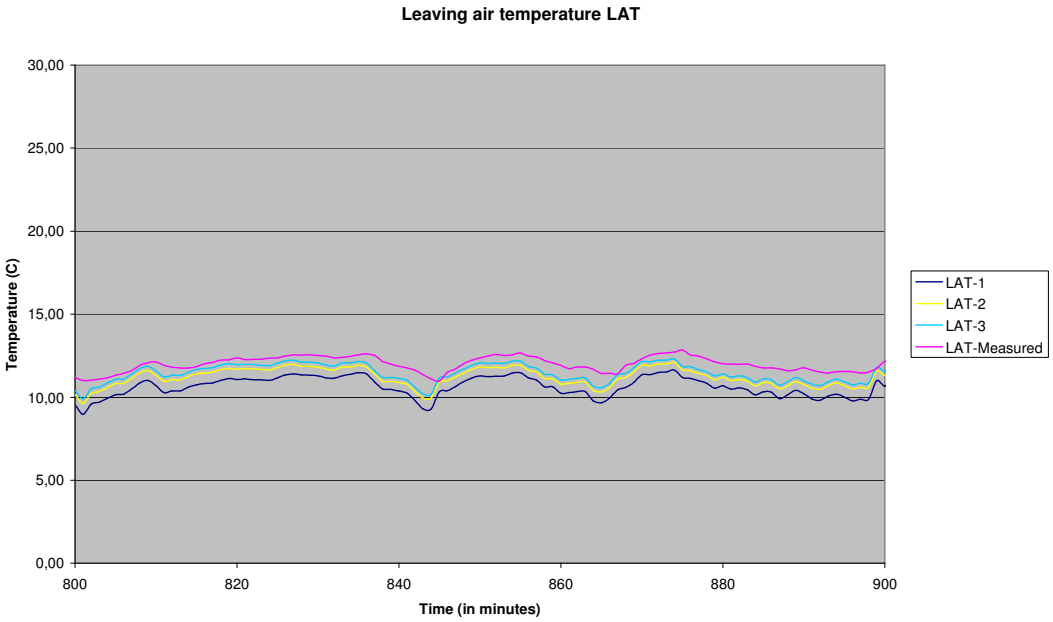

Figure 5j: Empirical test I – Measured data against modelling results: Leaving water temperature (high air flow rate and high fluid flow rate)

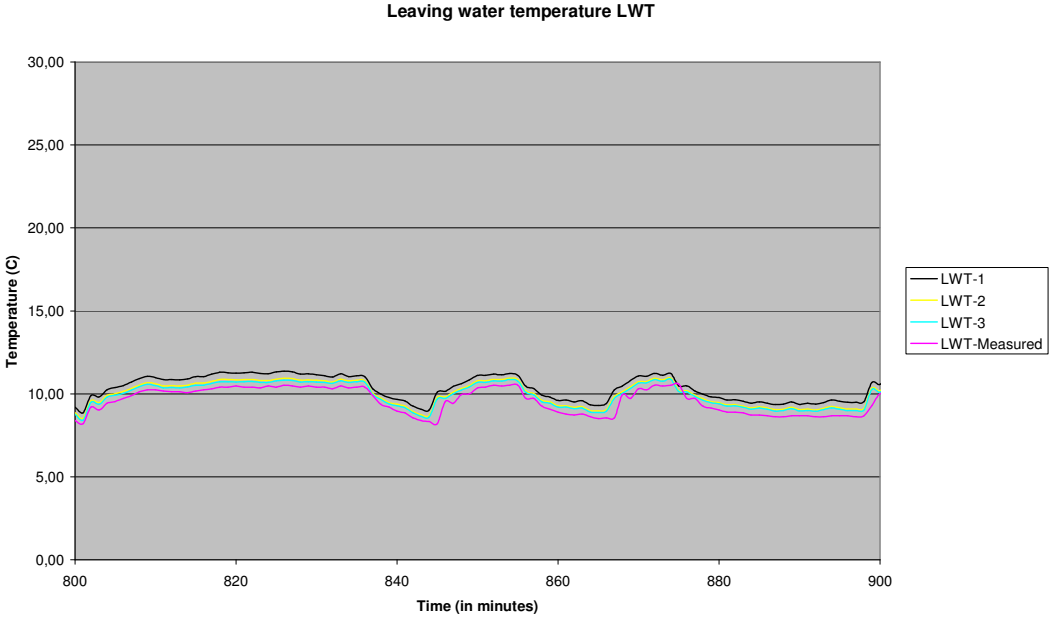

Results of Cooling coil empirical test II

Results of the test are presented in the output file 'Results exercise 2-emp2-per minute-20071002.xls' for the 3 earlier mentioned steps

In figure 6a-f the input data is given: air volume rate, fluid flow rate, entering air temperature, entering air relative humidity, entering air humidity and entering water temperature

None of the input parameters is almost constant during the test.

In figure 7a-f the output data for the 3 steps is given: the cooling load, the specific capacity AFWW, the leaving air temperature and leaving water temperature during a small period with low air flow rate and low fluid flow rate and during a small period with high air flow rate and high fluid flow rate.

The influence of the 3 steps is good to see:

- From step 1 to step 2 the influence is rather big
- From step 2 to step 3 the influence is not so big

No measured data was distributed, so no comparison between measured data and modelling results can be made

To conclude: modelling step 1 seems to be too rough to model the cooling coil, modelling step 2 and step 3 come much closer.

Figure 6a: Empirical test II input data: Air Volume flow rate

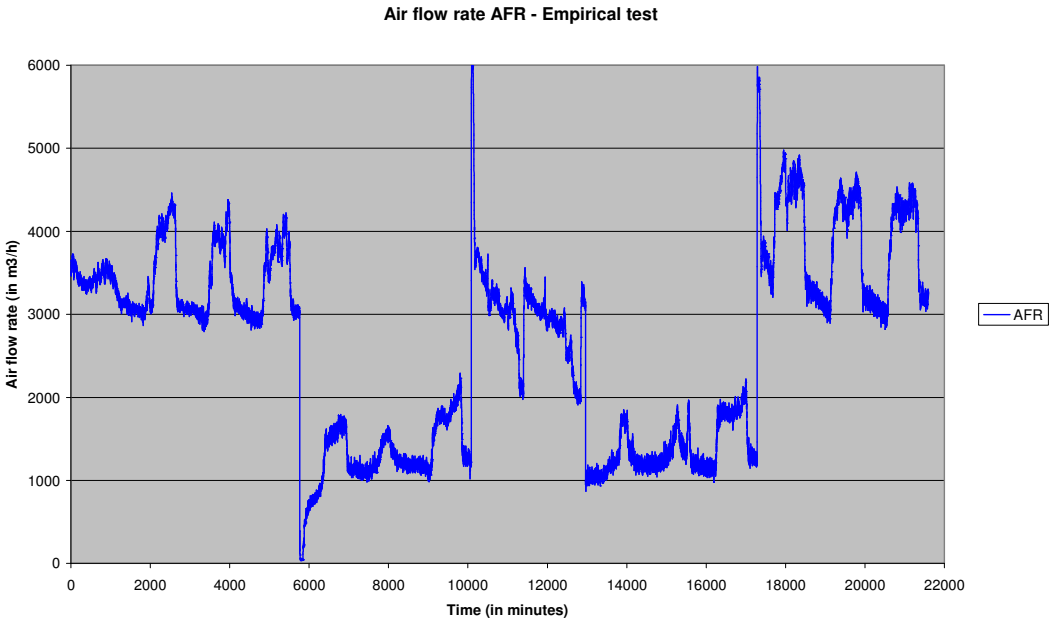

Figure 6b: Empirical test II input data: Fluid Volume flow rate

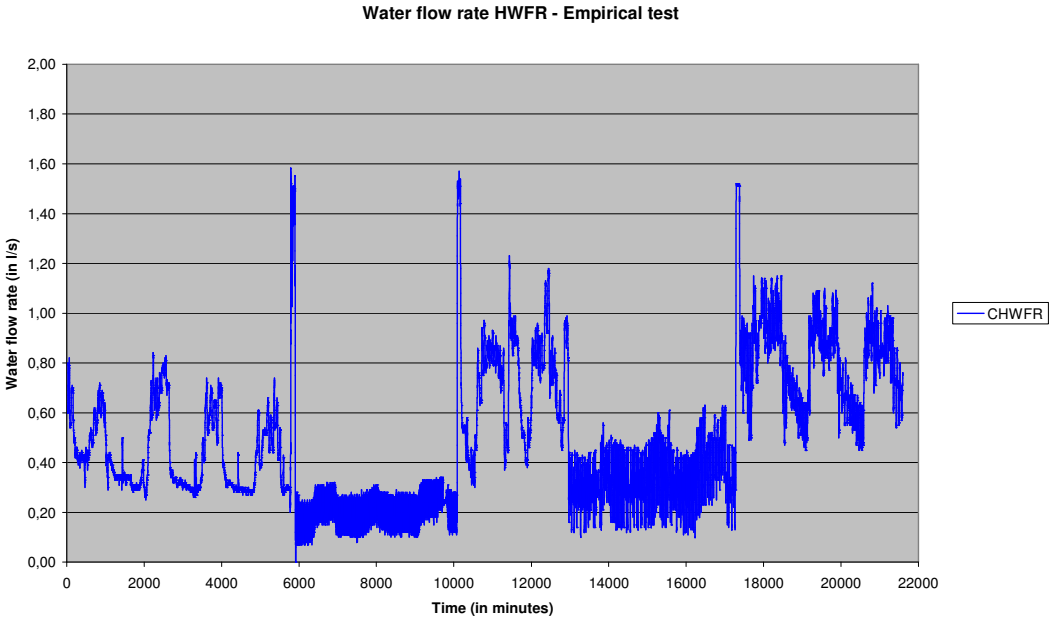

Figure 6c: Empirical test II input data: Entering air temperature

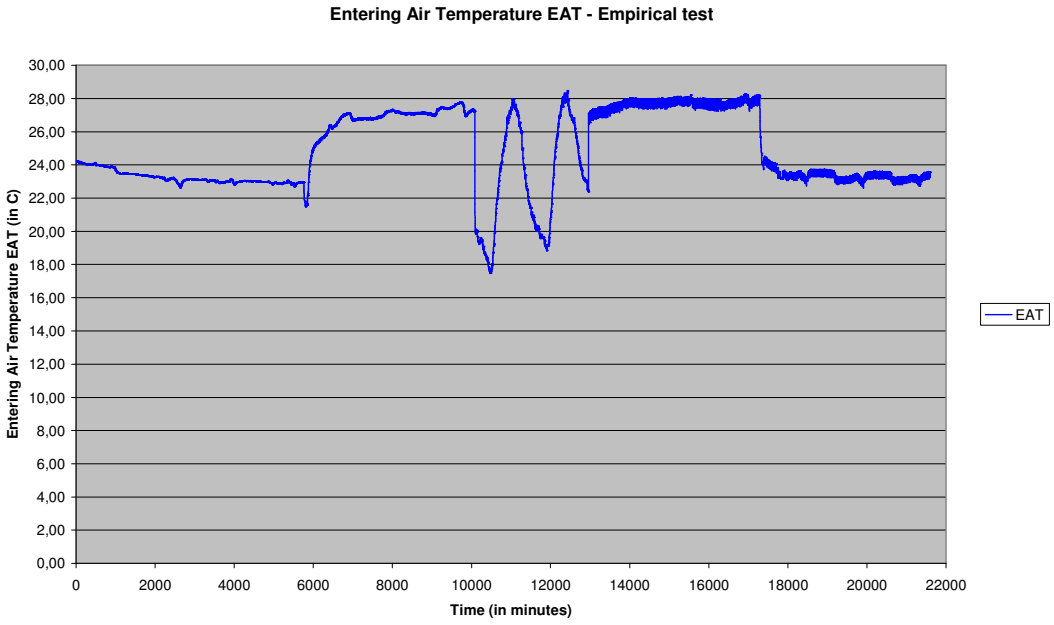

Figure 6d: Empirical test II input data: Entering air relative humidity

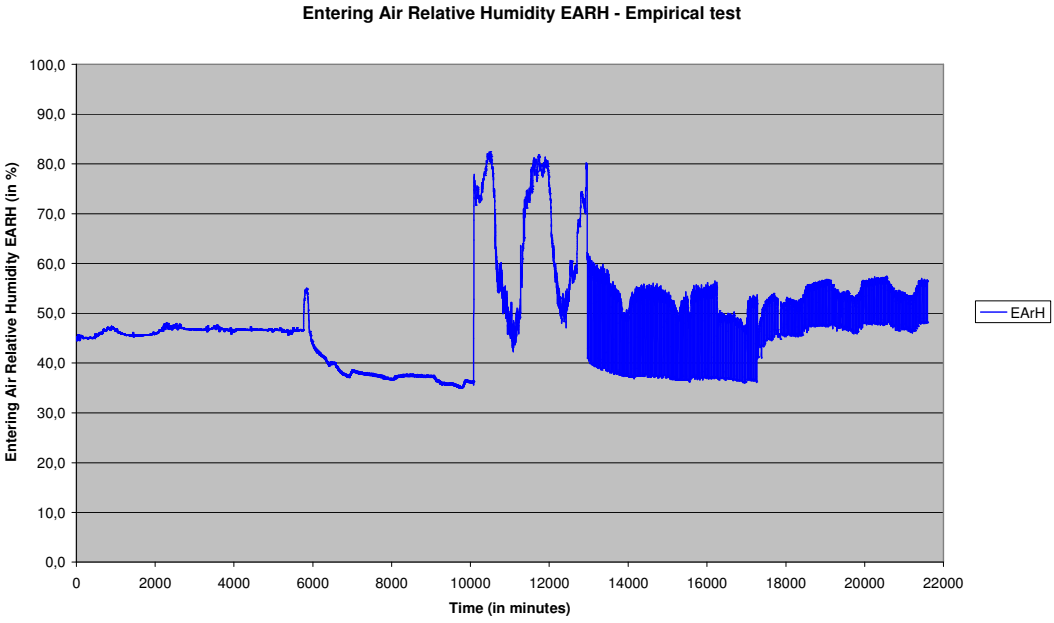

Figure 6e: Empirical test II input data: Entering air humidity

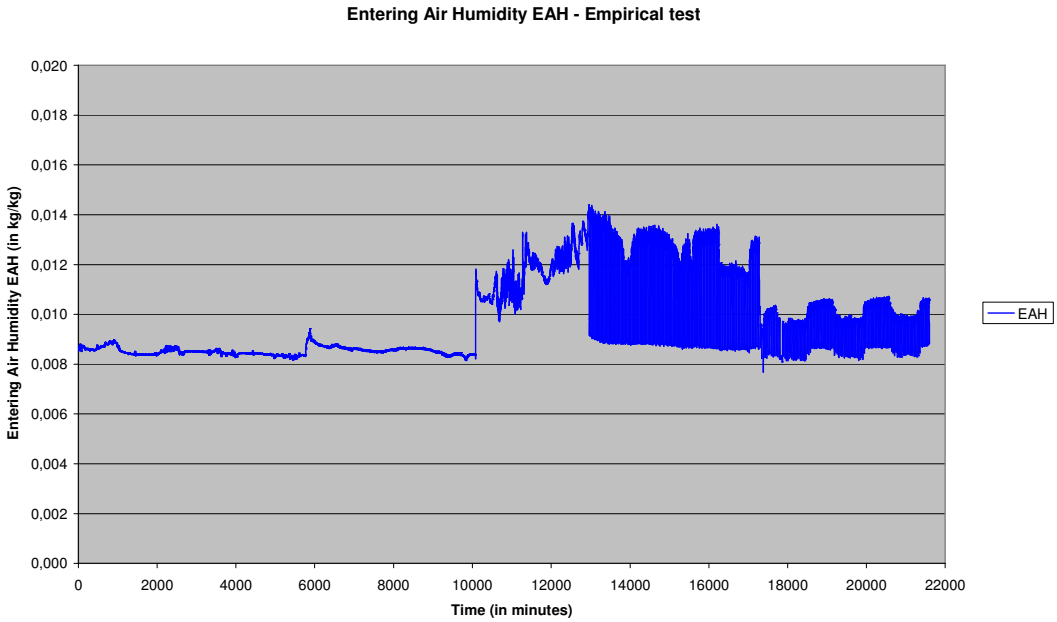

Figure 6f: Empirical test II input data: Entering water temperature

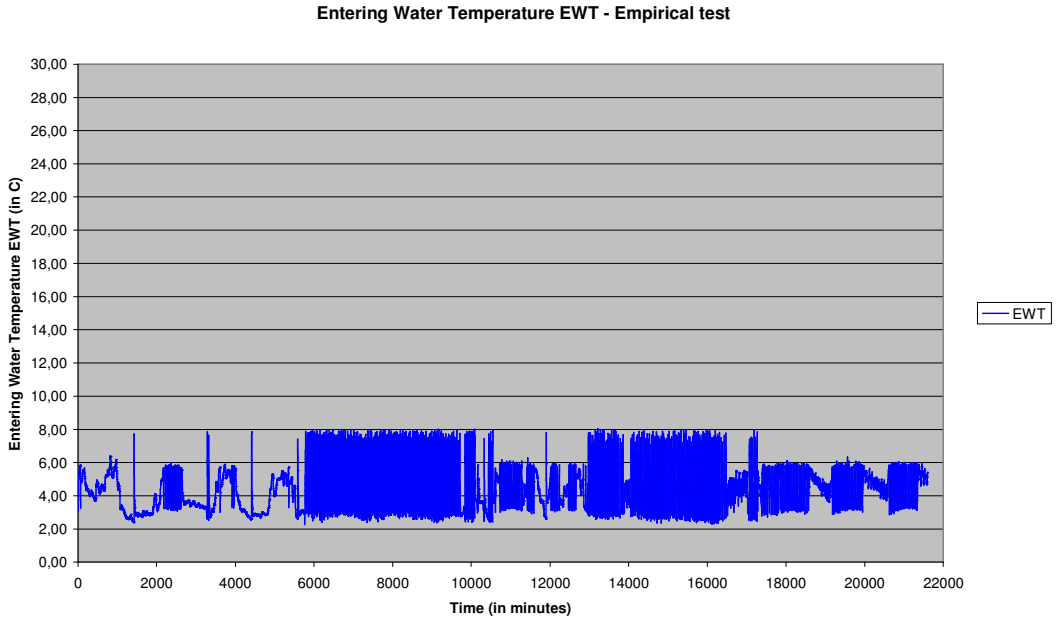

Figure 7a: Empirical test II output data: Cooling load

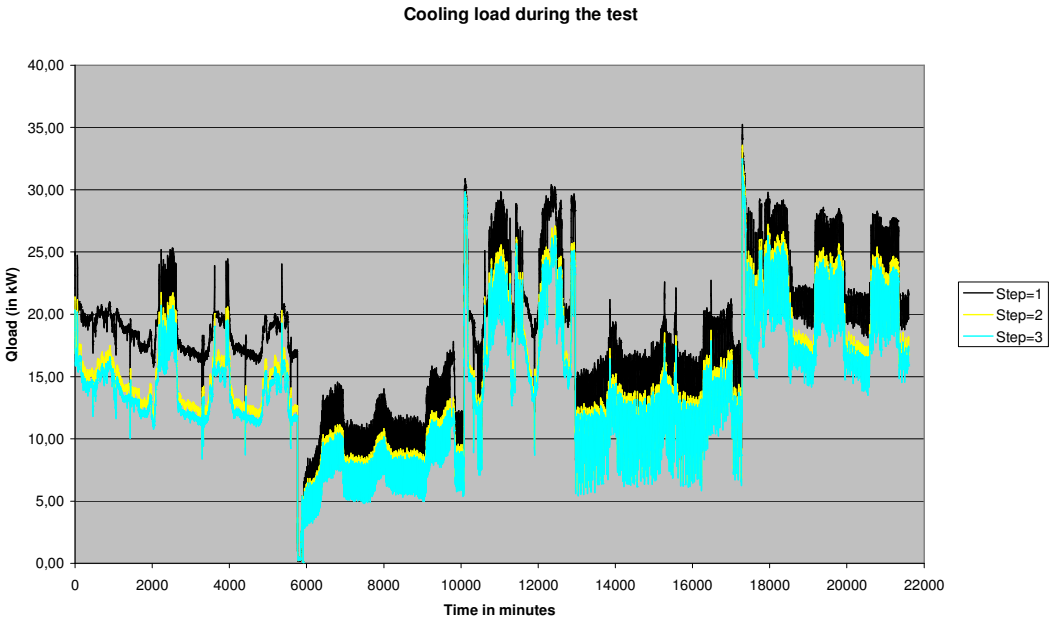

Figure 7b: Empirical test II output data: Specific cooling capacity

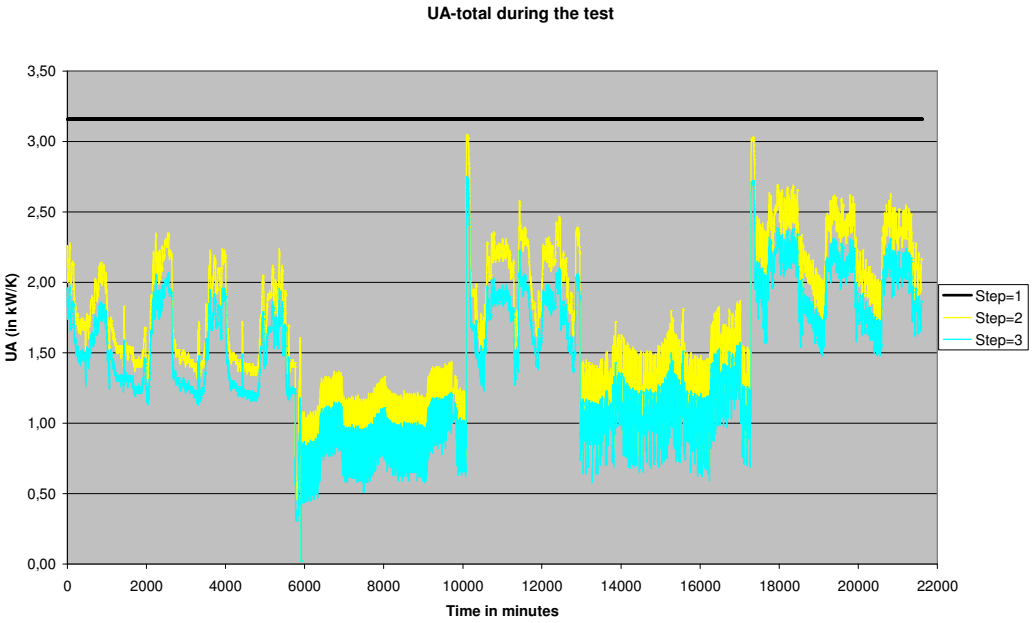

Figure 7c: Empirical test II output data: Leaving air temperature (low air flow rate and low fluid flow rate)

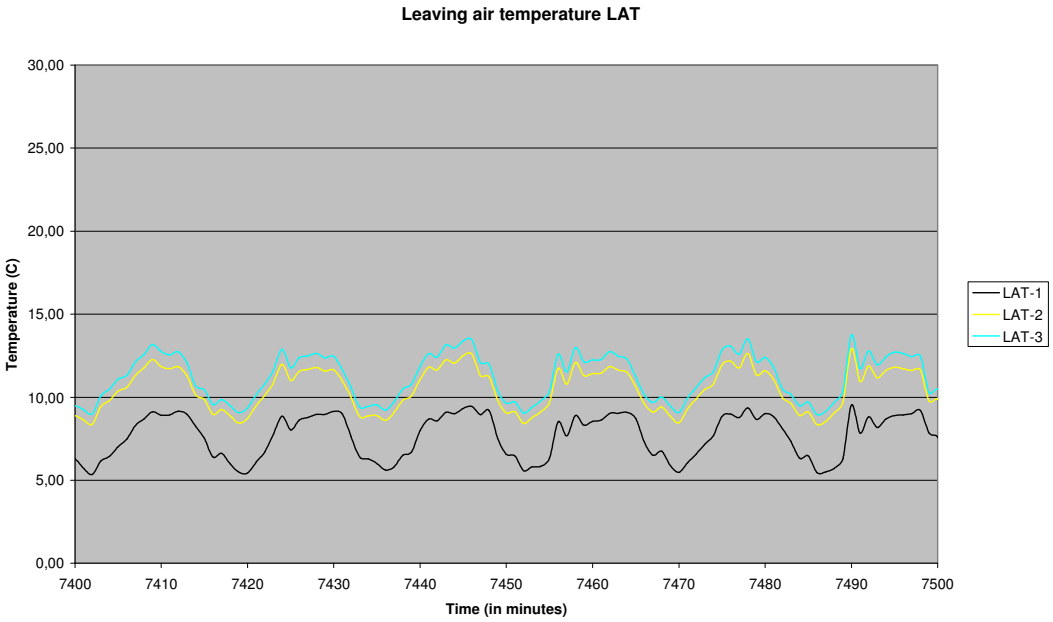

Figure 7d: Empirical test II output data: Leaving water temperature (low air flow rate and low fluid flow rate)

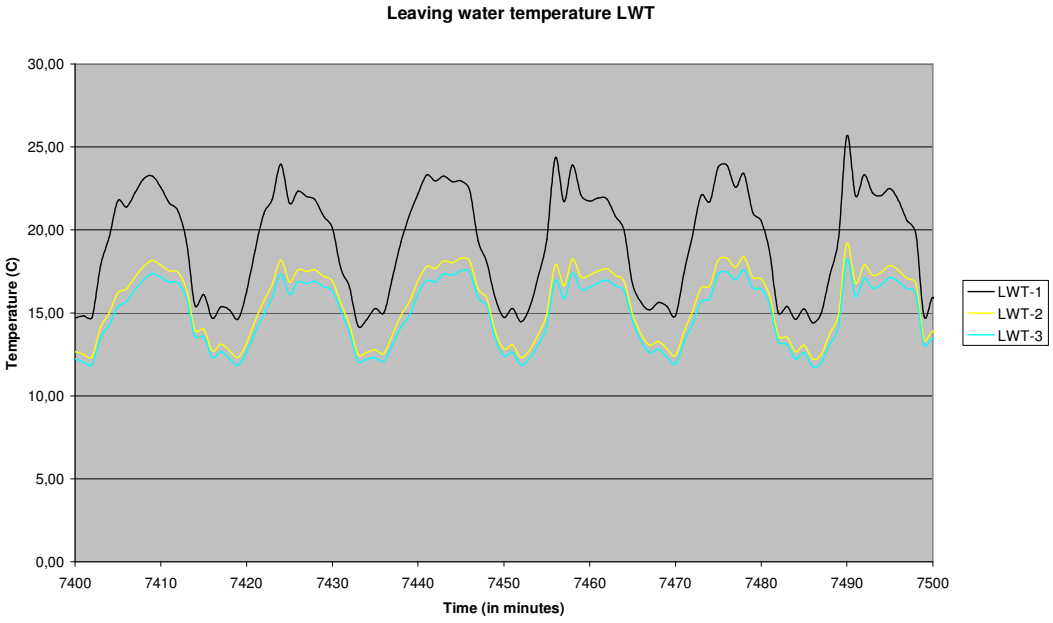

Figure 7e: Empirical test II output data: Leaving air temperature (high air flow rate and high fluid flow rate)

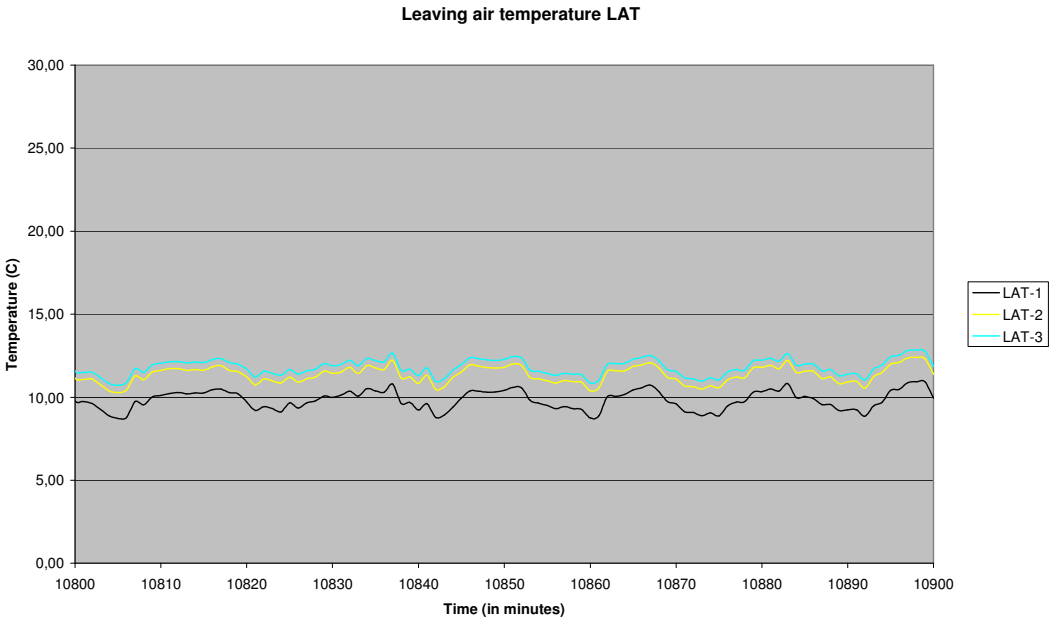

Figure 7f: Empirical test II output data: Leaving water temperature (high air flow rate and high fluid flow rate)

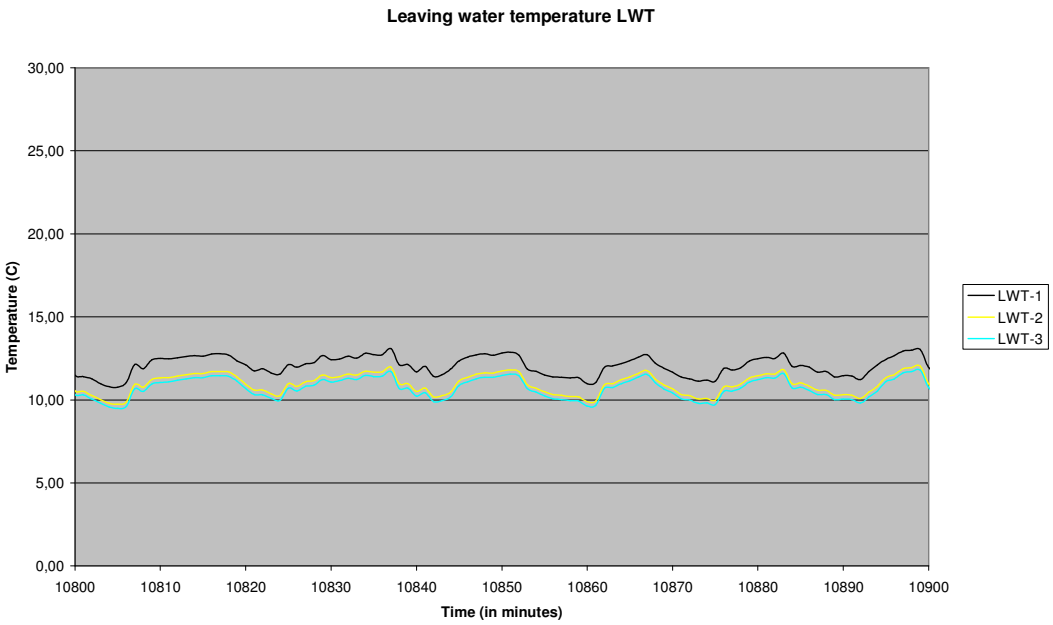

8. Other (optional)

No other tests were done

9. Conclusions and Recommendations

Test data and results of other participating cooling coil models are available. A first comparison between models was made, which led to fine tuning of the test specs. Now a new comparison can be made, which will result in some smaller differences between the models.

Remark:
To determine the coil characteristics 11 data points (1 x Manufacturer and 10 x Empirical) were available. These points were not optimal:

- Is the Manufacturer point trusty?
- Many input conditions were changed at the same time

Required are better data points: do only a few measurements but at defined flow rates (air – water is resp. 100%-100%, 20%-100%, 100%-20%, 20%-20%) and at defined entering conditions (fixed entering temperatures; only entering air humity is changing) instead of many measurements for continuous changing circumstances during a longer test period.

To determine the characteristics of the cooling coil several methods were discussed in this report, the required specific measuring data points were not available

Modelling step 1 (specific cooling capacity AFWW is independent of the flows) seems to be too rough. Modelling step 2 (specific cooling capacity AFWW is dependent on the flows; AFWW at design conditions split into 3 equal parts – A11=B11=C11=1,00), gives much better results. Modelling step 3 (specific cooling capacity AFWW is dependent on the flows; A11, B11, C11 are determined from extra data points) is different from step 2, but not so much (for this case only?!)

10. References

[1] Felsmann, C.
"Chilled water system – a set of comparative test cases: exercise 2 – Cooling Coil (chapter 4)", IEA: SHC Task 34 / ECBCS Annex 43, June 27, 2005.

[2] Wijsman, A.
"Cooling Coil – Modeler Report VA114 – draft 2", IEA: SHC Task 34 / ECBCS Annex 43, July 12, 2005.

[3] Felsmann, C.
"Chilled water system – a set of comparative test cases: exercise 2 – Cooling Coil (chapter 4)", IEA: SHC Task 34 / ECBCS Annex 43, January 2, 2006.

[4] Wijsman, A. and S. Szufa
"Heating Coil – Modeler Report VA114 – draft 2", IEA: SHC Task 34 / ECBCS Annex 43, July 27, 2006.

[5] Wijsman, A.
"Cooling Coil – Modeler Report VA114 – draft 3", IEA: SHC Task 34 / ECBCS Annex 43, February 24, 2006.

[6] Wijsman, A. and S. Szufa
"Cooling Coil – Modeler Report VA114 – draft 4", IEA: SHC Task 34 / ECBCS Annex 43, August 31, 2006.

Appendix A: The cooling coil model – factor 'A11' and factor 'a'

In figure A.1 a cooling coil is given schematically.

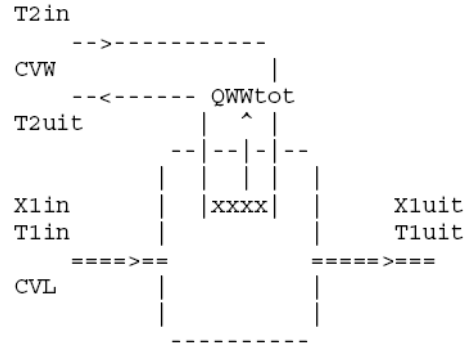

Figure A.1: Definition of the several parameters

Definition of the several parameters:

- at the air side: the air flow rate, the temperature and humidity at the entrance, the temperature and humidity at the exit.
- at the water side: the water flow rate, the temperature at the entrance and the temperature at the exit.

The cooling coil has a specific capacity AFWW: the heat exchange per degree temperature difference (W/K) for the situation without condensation.

In general the heat exchange as function of the air humidity X1in (kg/kg) at the entrance is as given in figure A.2: for low X's there is no condensation, for high X's there is.

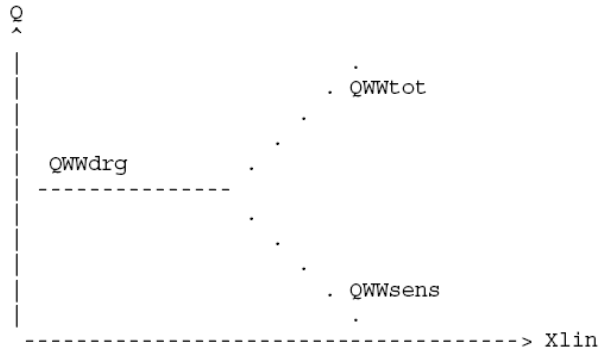

Figure A.2 Heat exchange as function of the air humidity X1in at the entrance.

In the dry regime the exchanged heat is QWWdrg, in the wet regime QWWtot (sensible part is QWWsens).

The specific capacity AFWW

In reality the specific capacity is built up out of 3 parts:

- the heat transfer between air flow and the cooling coil external surface; the air flow rate influences this coefficient
- the heat transfer inside the cooling coil
- the heat transfer between the cooling coil internal surface and the cooling fluid; the cooling fluid flow rate influences this coefficient

The VABI cooling coil model assumes the specific capacity AFWW (in W/K) is split into those three parts:

- an external AFWWEXT
- an intermediate AFWWMET
- an internal AFWWINT

The external AFWWEXT is between air flow and cooling coil; the intermediate AFWWMET is within the material of the heating coil; the internal AFWWINT is between cooling coil and cooling fluid.

Important for the condensation process is the ratio between AFWWEXT and AFWWMET // AFWWINT. Therefore factor 'A11', 'C11' and 'B11' are introduced.

Definition:

- external AFWWEXT0 = 3,0 * A11*AFWW0
- internal AFWWINT0 = 3,0 * B11*AFWW0
- intermediate AFWWMET = 3,0 * C11*AFWW0

In series these three parts give the overall specific capacity AFWW0. This leads to the following relationship between A11, B11 and C11:

1,0/B11 = 3,0 – 1,0/A11 – 1,0/C11

with

1,0/3,0 \< A11 < infinitive

1,0/(3,0-1,0/A11) \< C11 < infinitive

For instance: A11 = 1,0 and C11 = 1,0 B11 = 1,0; all parts are equal.

Remark: if A11 is taken smaller the temperature of the cooling coil surface is closer to the temperature of the cooling fluid more condensation will occur.

Influence of factor 'A11'

With the cooling coil model the influence of A11 is calculated. The total specific capacity AFWW, the air and water flow rates, the condition at the air and water entrance are kept the same. A11 has influence on the shape of the line in figure A.2.

In figure A.3 the results are given.

The higher A11 the lower is the QWWtot (less condensation occurs).

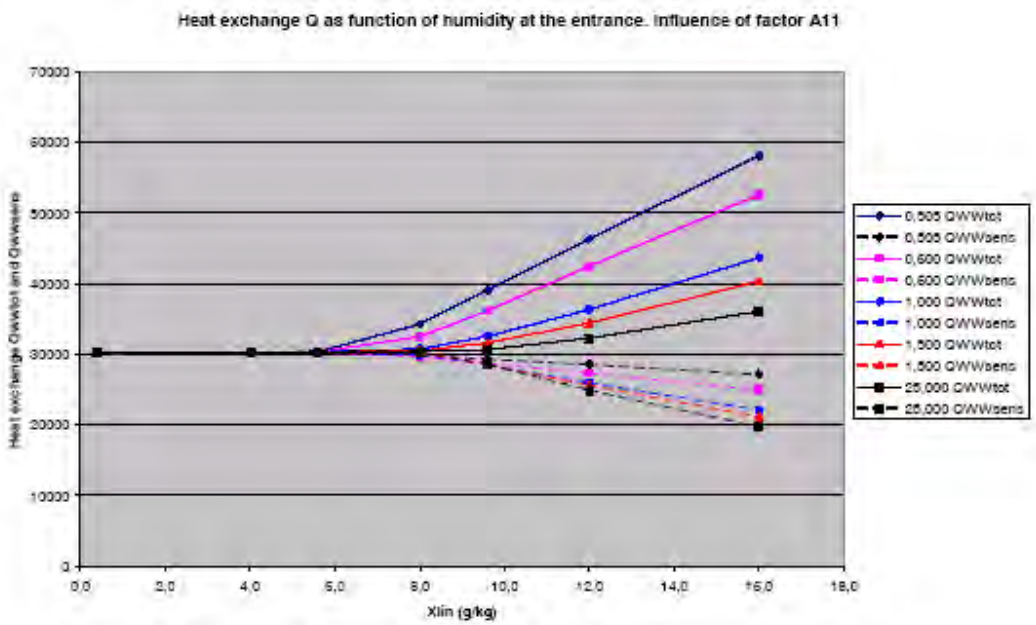

Figure A.3 Heat exchange as function of the air humidity X1in at the entrance. Influence of factor 'A11'.

Definition of factor 'a'

In general for QWWdrg (heat exchange without condensation) the following equation applies (see figure A.4):

$$QWWdrg = a * QWWtot1 + (1-a) * QWWsens1$$

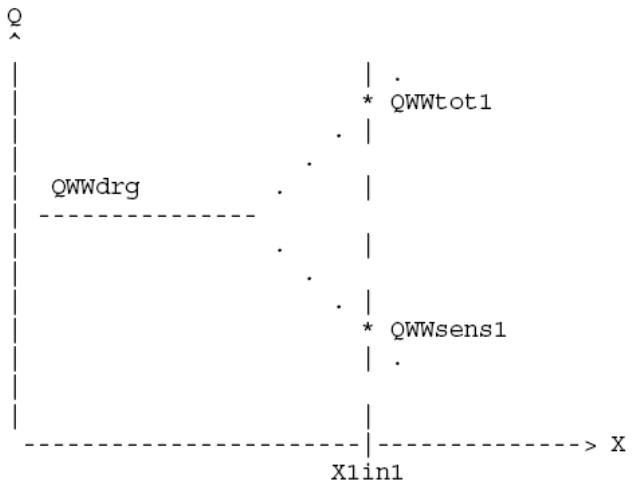

Figure A.4 Heat exchange as function of the air humidity X1in at the entrance.

In case factor ‘a’ is known QWWdrg can be determined from QWWtot1 and QWWsens1. In case QWWdrg, QWWtot1 and QWWsens1 are known factor ‘a’ can be calculated.

Relation between factor ‘a’ and factor ‘A11’

In figure A.3 the influence of factor ‘A11’ is given. For data points QWWdrg, QWWtot1 and QWWsens1 are known, so factor ‘a’ can be calculated:

a = (QWWdrg – QWWsens1)/(QWWtot1 – QWWsens1)

In figure A.5 this is plotted for Xlin = 9,6 g/kg, 12,0 g/kg and 16,0 g/kg.

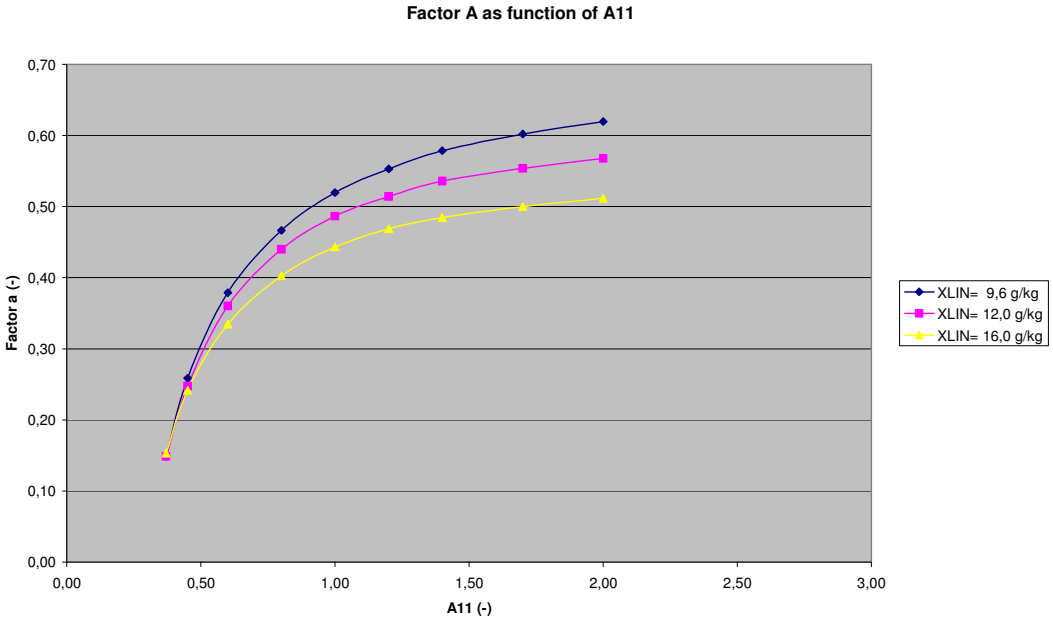

Figure A.5: Factor ‘a’ as function of factor ‘A11’

For small values of ‘A11’ (0,35 < A11 < 1,50) the relation is about one line. This is a practical range. So in case factor ‘a’ is known the factor ‘A11’ can be found from this curve. Use the line for 12,0 g/kg. So for factor ‘a’ = 0,45 the factor ‘A11’ = 0,80

Appendix B: Determination of the specific capacity of the cooling coil

The specific capacity of the cooling coil AFWW is the heat exchange per degree temperature difference (W/K) for the situation without condensation.

In figure B.1 the several parameters are defined.

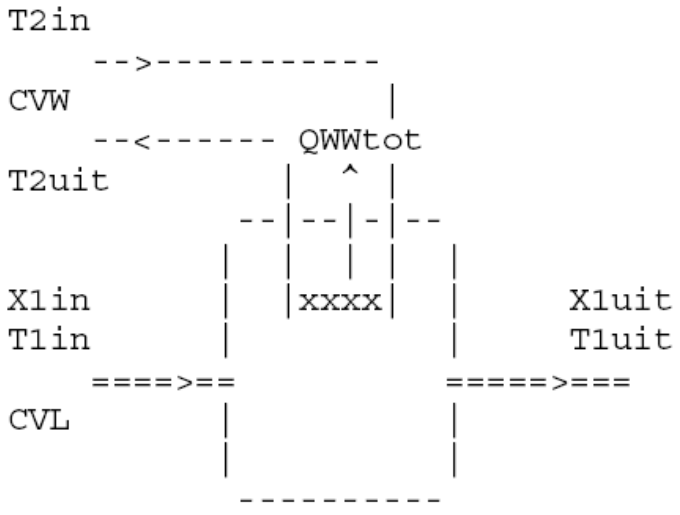

Figure B.1: Definition of the several parameters

In general the heat exchange as function of the air humidity X1in (kg/kg) at the entrance is as given in Figure B.2: for low X's there is no condensation, for high X's there is.

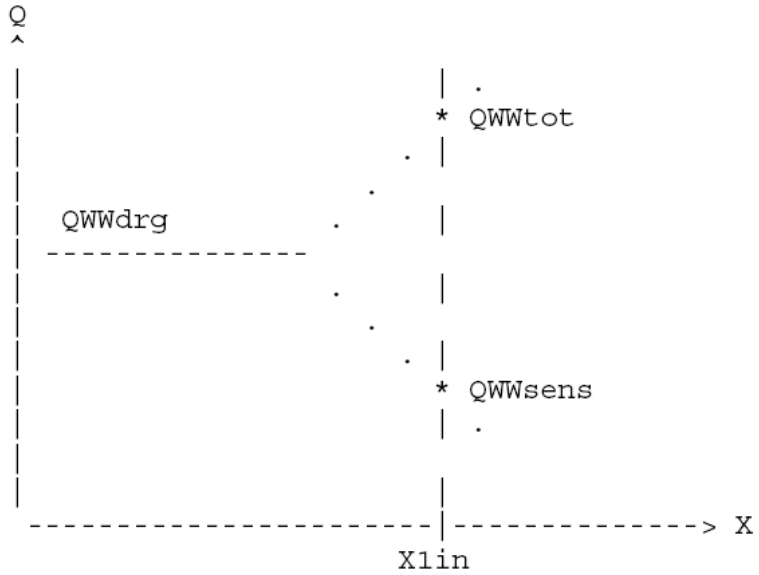

Figure B.2 Heat exchange as function of the air humidity X1in at the entrance.

From the input data are known:

- QWWtot
- T1in and X1in
- T1uit and X1uit

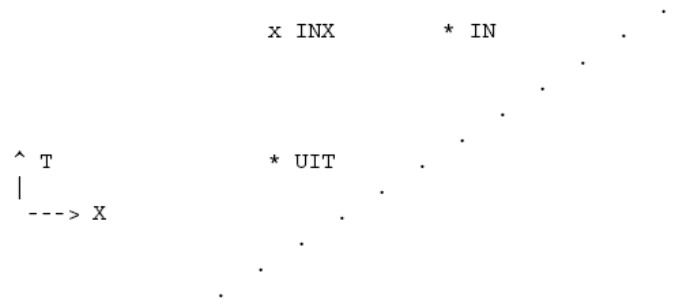

Figure B.3: Situation in the Mollier-diagram

With this information and with the help of the Mollier-diagram (see figure A.3) the sensible part QWWsens can be derived:

```
QWWsens = (H1inx-H1uit)/(H1in-H1uit) * QWWtot
```

With

H1in = enthalpy of the air at the entrance (T1in,X1in)
H1uit = enthalpy of the air at the outlet (T1uit,X1uit)
H1inx = enthalpy of the air with condition (T1in,X1uit)

In general for QWWdrg (heat exchange without condensation) the following function applies (see figure B.2):

```
QWWdrg = a * QWWtot + (1-a) * QWWsens
```

This factor 'a' should be known (see also appendix C).

Remark: In VA114's cooling coil model the factor 'a' is set to 0,25 (for two cooling coils this factor was derived from the product information and with the help of the simulation model to determine Figure B.2; for factor 'a' the values 0,21 and 0,28 were found – so by empirical determination)*).

*) In case two points (Q at two conditions) are given the factor 'a' can easily be derived

Remark:

There is also a maximum to QWWdrg:
the air outlet temperature is always higher than the water inlet temperature. So QWWdrgmx0 is found: value with air outlet temperature is equal to the water inlet temperature. It is assumed QWWdrgmx is 0,98 of that value.

Finally:

```
QWWdrg = MIN (QWWdrg,QWWdrgmx)
```

From this information the specific capacity AFWW can be derived.

Appendix C: Methods to determine factor 'A11' and factor 'a' from data

The model of the cooling coil requires the specific capacity AFWW and the factor 'A11' as 'input'.

In practice only the Manufacturer data of the cooling coil is available. This data consists of one point only (see table C.1).

Table C.1: Manufacturer data of a cooling coil

-> 2. Koelbatterij							
Vermogen (in W)	- waterA/Rtemp.		- LuchtAtemp./RV	-	LuchtRtemp./RV	-	deb.fract.
QCBKLMX	TWBAT2A	TWBAT2R	TLBAT2A	RVLBAT2A	TLBAT2R	RVLBAT2R	DBFRW2
35800.0	6.67	12.06	27.78	44.4	12.50	96.9	1.00

To determine the AFWW from this 'one point'-data factor 'a' is required (see appendix B).

There is a relation between factor 'A11' and factor 'a' (see appendix A). So if one of these two factors can be determined then both factors are known.

Remark: until now a good guess for factor 'a' was made: a = 0,25. This guess was based on Manufacturer data (product information) of two cooling coils; with the help of the simulation model Figure A.1 was constructed; for factor 'a' the values 0,21 and 0,28 were found.

Three methods to determine factor 'a'/factor 'A11' are discussed now (all methods require at least 2 points):

- Method 1: Factor 'a' is determined from two data points (point 1 and 2) in the wet regime (see figure C.1). Point 1 is the Manufacturer data and point 2 is a point that only differs from point 1 because the air humidity at the entrance of the cooling coil is higher (so with the same air and water flow rate, the same air and water temperatures at the entrances as point 1). With the relation between factor 'a' and factor 'A11' the latest can be derived.
- Method 2: Factor 'A11' is determined from two data points (point 3 and 4) in the dry regime (see figure C.2). Point 3 only differs from point 1 (Manufacturer data) because the air humidity at the entrance of the cooling coil is so low, that condensation does not occur (so with the same air and water flow rate, the same air and water temperatures at the entrances as point 1). Point 4 has the same air humidity at the entrance as point 3, but has a rather low air flow rate and water flow rate (say 20-30%). With these two point factor 'A11' can be derived; in the same way as for the heating coil. With the relation between factor 'a' and factor 'A11' the former can be derived.
- Method 3: Factor 'a' is determined from two data points (point 1 and 5) in the wet regime (see figure C.3). Point 1 is the Manufacturer data and point 5 is a point that differs from point 1 because the air flow rate and water flow rate are rather low (say 20-30%); the air humidity at the entrance of the cooling coil may differ from point 1. Remark: the air and water temperatures at the entrances are the same as point 1. With the relation between factor 'a' and factor 'A11' the latest can be derived.

Most promising seems to be method 1.

In more detail:

- Method 1

Factor ‘a’ is determined from two data points (point 1 and 2) in the wet regime (see figure C.1).

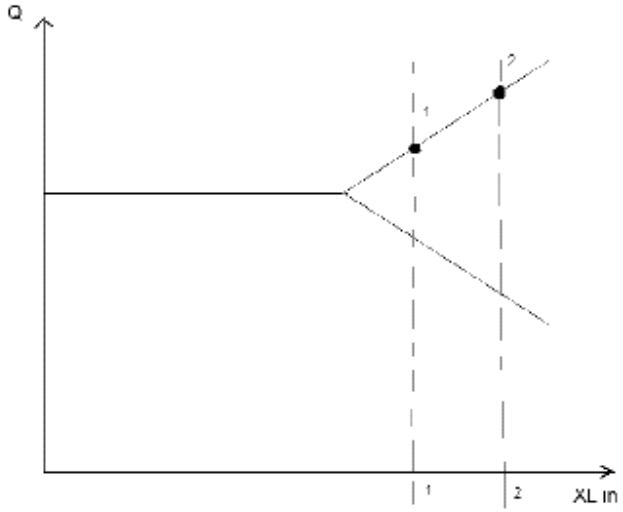

Figure C.1: Points used by method 1

Point 1 is the Manufacturer data and point 2 is a point that only differs from point 1 because the air humidity at the entrance of the cooling coil is higher (so with the same air and water flow rate, the same air and water temperatures at the entrances as point 1).

For point 1:

```
QWWdrg = a * QWWtot1 + (1-a) * QWWsens1 (1)
```

For point 2:

```
QWWdrg = a * QWWtot2 + (1-a) * QWWsens2 (2)
```

From these two equations follow for factor ‘a’:

```
a       = 1 / (1 - p) (3)
```

With

```
p = (QWWtot2 -QWWtot1) / (QWWsens2 - QWWsens1) (4)
```

So factor ‘a’ is known and with the relation between factor ‘a’ and factor ‘A11’ the latest can be derived.

- Method 2

Factor ‘A11’ is determined from two extra data points (point 3 and 4) in the dry regime (see figure C.2).

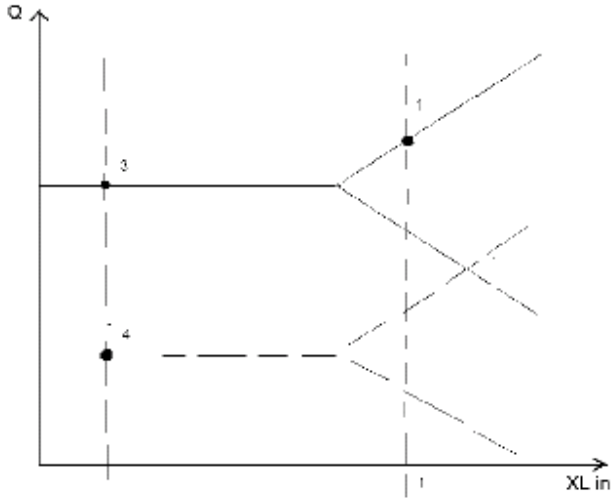

Figure C.2: Points used by method 2

Point 3 only differs from point 1 (Manufacturer data) because the air humidity at the entrance of the cooling coil is so low, that condensation does not occur (so with the same air and water flow rate, the same air and water temperatures at the entrances as point 1). Point 4 has the same air humidity at the entrance as point 3, but has a rather low air flow rate and water flow rate (say 20-30%).

With these two point factor ‘A11’ can be derived; in the same way as for the heating coil. See appendix B of heating coil report [4].

With the relation between factor ‘a’ and factor ‘A11’ the former can be derived.

- Method 3

Factor ‘a’ is determined from two data points (point 1 and 5) in the wet regime (see figure C.3).

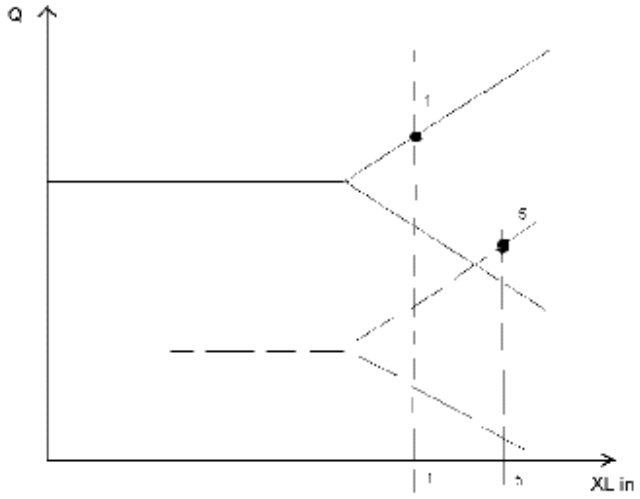

Figure C.3: Points used by method 3

Point 1 is the Manufacturer data and point 5 is a point that differs from point 1 because the air flow rate and water flow rate are rather low (say 20-30%); the air humidity at the entrance of the cooling coil may differ from point 1.

Remark: the air and water temperatures at the entrances are the same as point 1.

With the relation between factor ‘a’ and factor ‘A11’ the latest can be derived.

Remark: the method is still under development. At one side it is promising, because two arbitrary data points can be taken, but at the other side it is very complex.

The method is based on translation of the points 1 and 5 to ‘help’ points 3 and 4.

Appendix D: Number of data points required to characterize a cooling coil

A cooling coil is characterized by:

- The overall heat capacity AFWW0 at design flow rates (air and water)
- The split of this heat capacity in 3 parts (Air side, water side, metal), described by the parameters A11, B11 and C11
- The flow dependency at the air side and at the water side

For more details see *)

For a given cooling coil with given flow rates and given inlet temperatures the cooling power will be a function of humidity of the inlet air. In figure D.1 this function is given: at low air humidity there will not occur any condensation, at a high air humidity there will. In the plot this can be seen from the split in cooling power in a sensible part and a latent part.

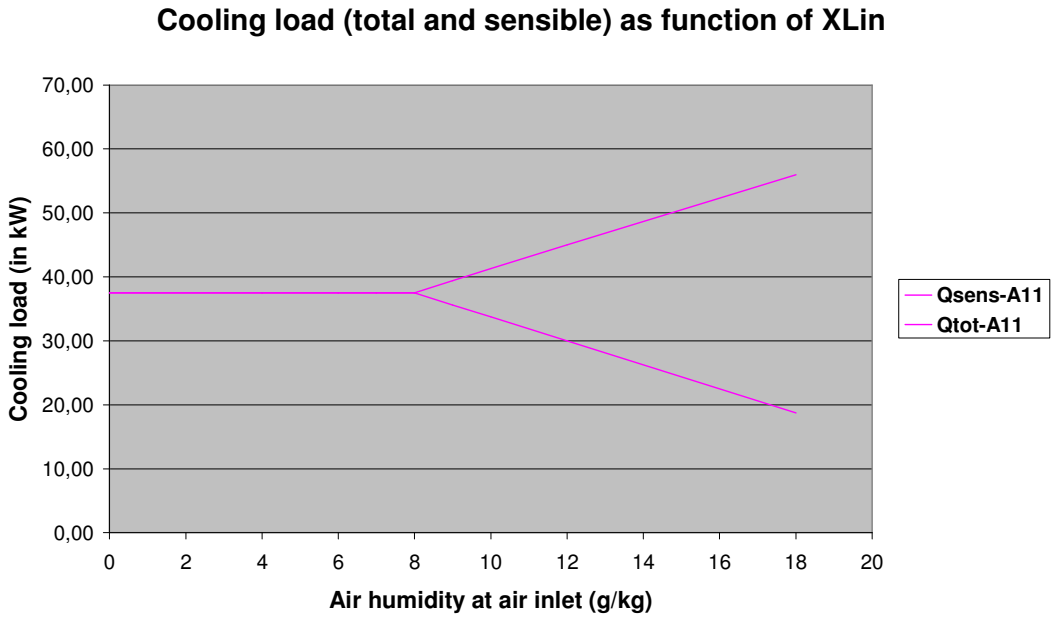

Figure D.1: Cooling power as function of humidity of inlet air

Determination of the cooling coil characteristics from measuring data

To model the cooling coil the characteristics of the cooling coil should be available (AFWW0, A11, B11 and C11). In practice mainly manufacturer data is available, consisting of the cooling power at defined inlet and outlet conditions (see figure D.2). This is not sufficient to determine the just mentioned characteristics. Below this is discussed.

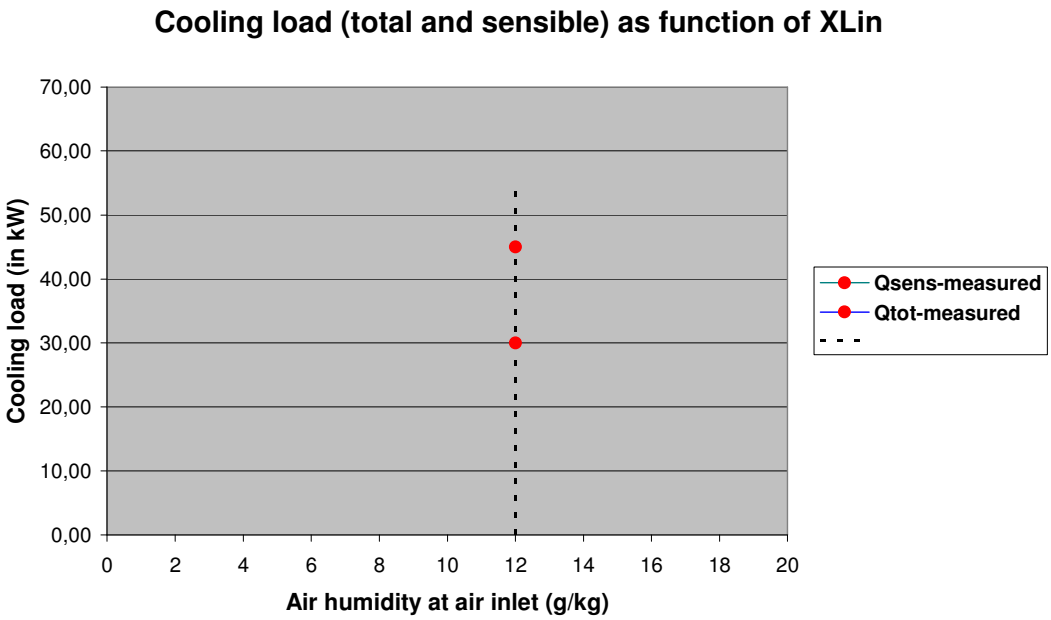

Figure D.2: Cooling power (sensible and latent = total) for Manufacturer data

Number of points required:

- Only 1 point in the wet regime (see figure D.2) is not sufficient to characterize a cooling coil: about nothing can be said about AFWW0 and about A11, B11, C11; the points can be part of many function lines (see figure D.3). Manufacturer data is such a data point

- Only 1 point in the dry regime (see figure D.4) is not sufficient to characterize a cooling coil: the AFWW0 can be determined, but nothing can be said about A11, B11, C11.

- 2 Specific points (1 in the dry regime and 1 in the wet regime (see figure D.5) or 2 in the wet regime (see figure D.6) can give the AFWW0 and A11, but not B11/C11. So not sufficient to fully characterize the cooling coil. 'Specific' means: points at same flow rates, same inlet temperatures at both air side and water side

- 2 points in the dry regime can give the AFWW0 and A11, but not B11/C11. So not sufficient to fully characterize the cooling coil. The points should have really different flow rates (say 100-50% at both air side and water side); inlet temperatures are preferably the same (at both air side and water side)

- 3 points in the dry regime can give the AFWW0 and A11, B11, C11 (see figure D.7). So sufficient to fully characterize the cooling coil. The points should have really different flow rates (say 100-50-25 % at both air side and water side); inlet temperatures are preferably the same (at both air side and water side).

Remark:
For the characterization of a heating coil 3 points are required too. The same method (3 points in the dry regime) can be applied.

Remark:
Available are about 10 data points, but these points are not specific (see figure D.8): different flow rates, different inlet temperatures, different air humidity. Probably only with fitting techniques the required parameters can be determined. The 3 points most on the left are almost in the dry regime, may be to be used for the method called before (3 points in the dry regime).

*) Characterization in more detail:

Definition:

- external AFWWEXT0= 3,0 * A11 * AFWW0
- internal AFWWINT0 = 3,0 * B11 * AFWW0
- metal AFWWMET = 3,0 * C11 * AFWW0

and

AFWW0 = 1 / (1/AFWWEXT0 + 1/AFWWMET + 1/AFWWINT0)

Flow dependency at the air side and at the water side is given by theoretical functions (correction factors f):

- at the air side: fair = (flowair/flowair,0) 0.56
- at the water side: fwater = (flowwater/flowwater,0) 0.80

So

- AFWWEXT = fair * AFWWEXT0
- AFWWINT = f water * AFWWINT0

And
AFWW = 1 / (1/AFWWEXT + 1/AFWWMET + 1/AFWWINT)

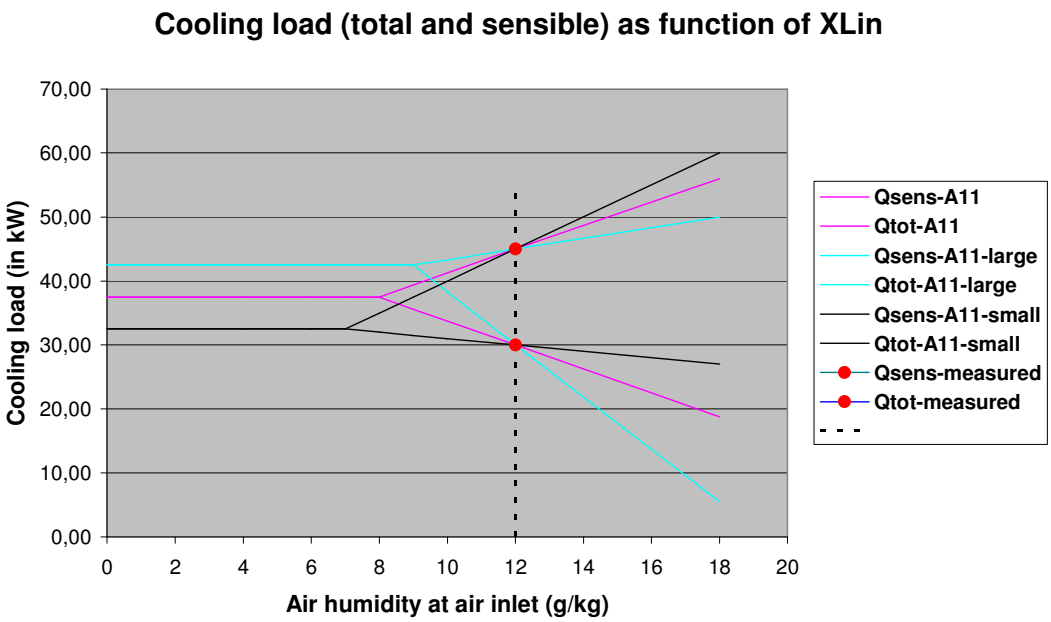

Figure D.3: Cooling power (sensible and latent = total) for 1 point in wet regime

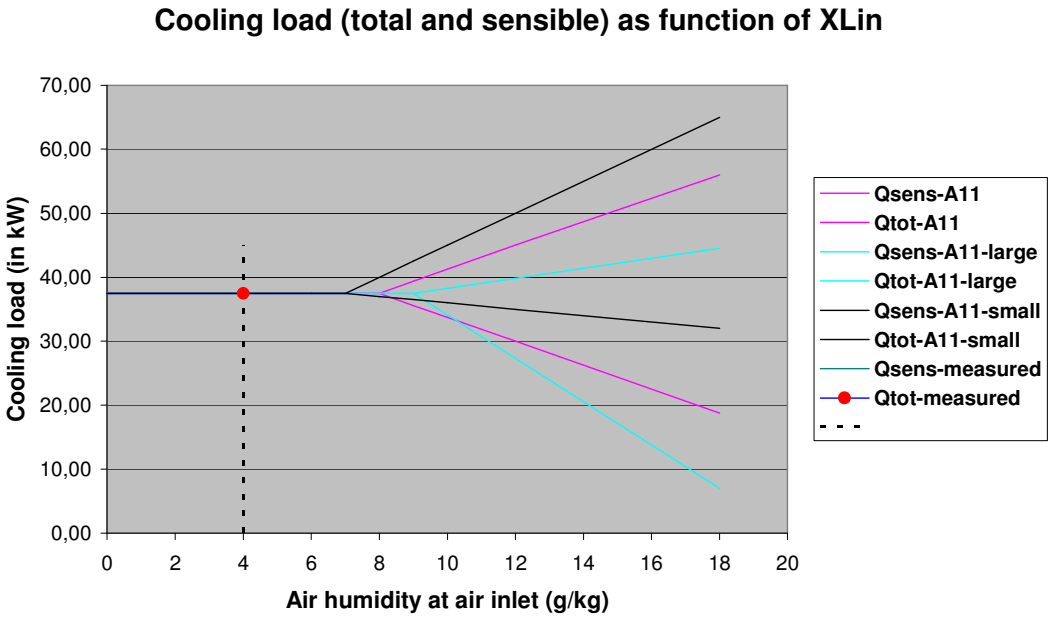

Figure D.4: Cooling power (sensible and latent = total) for 1 point in dry regime

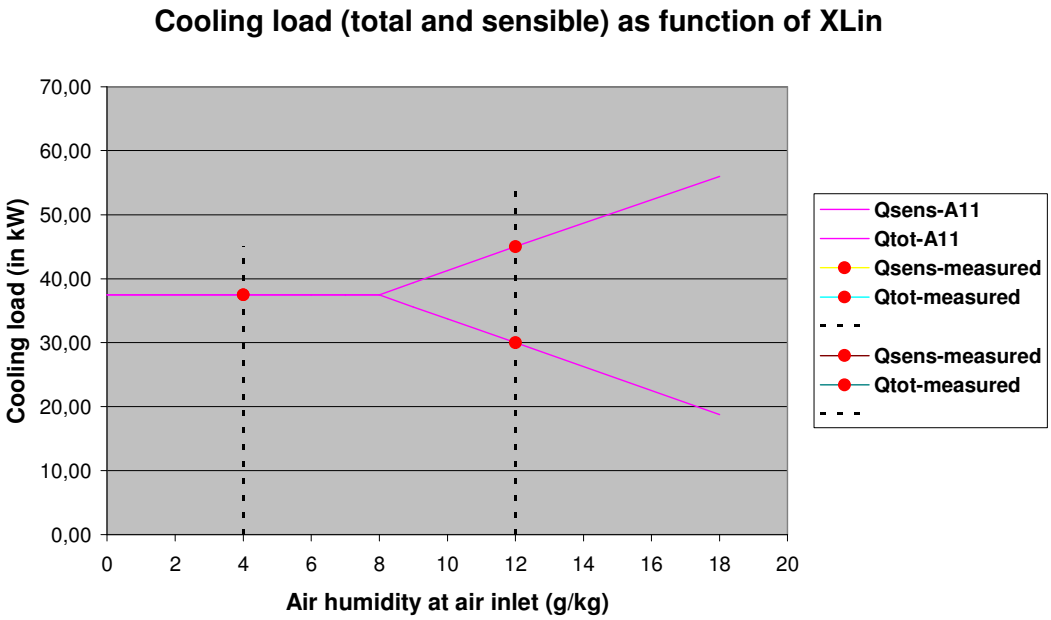

Figure D.5: Cooling power (sensible and latent = total) for 2 points (1 in dry regime and 1 point in wet regime)

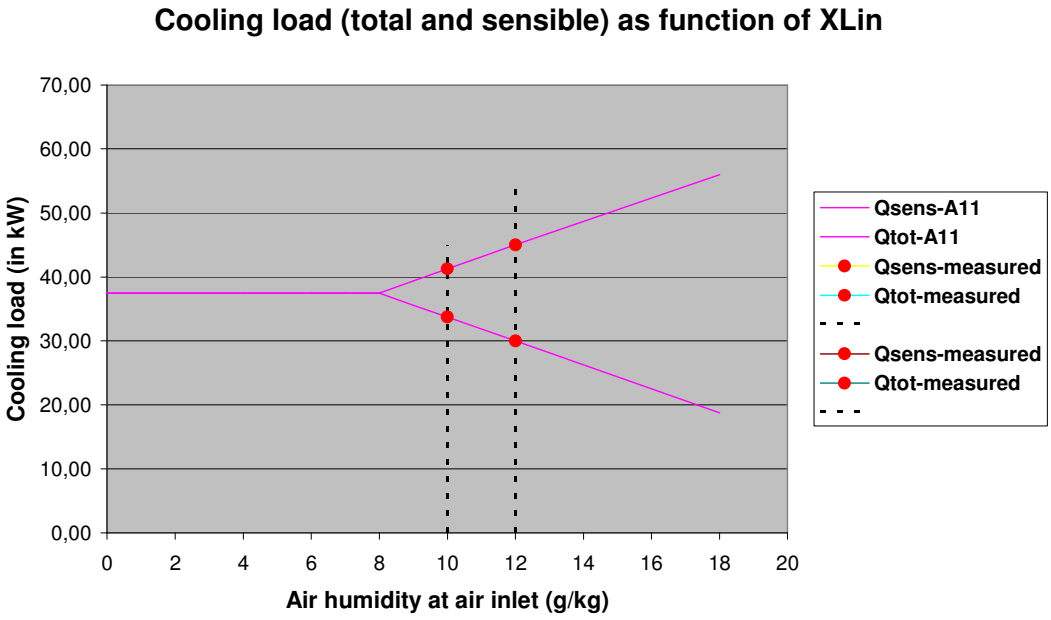

Figure D.6: Cooling power (sensible and latent = total) for 2 points (both points in wet regime)

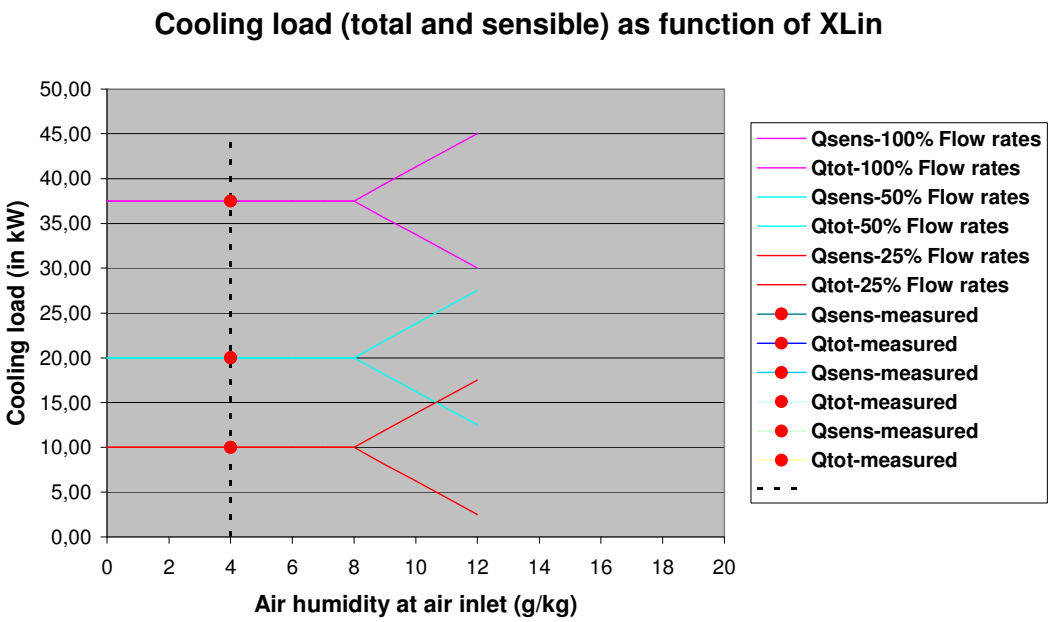

Figure D.7: Cooling power (sensible and latent = total) for 3 points in dry regime

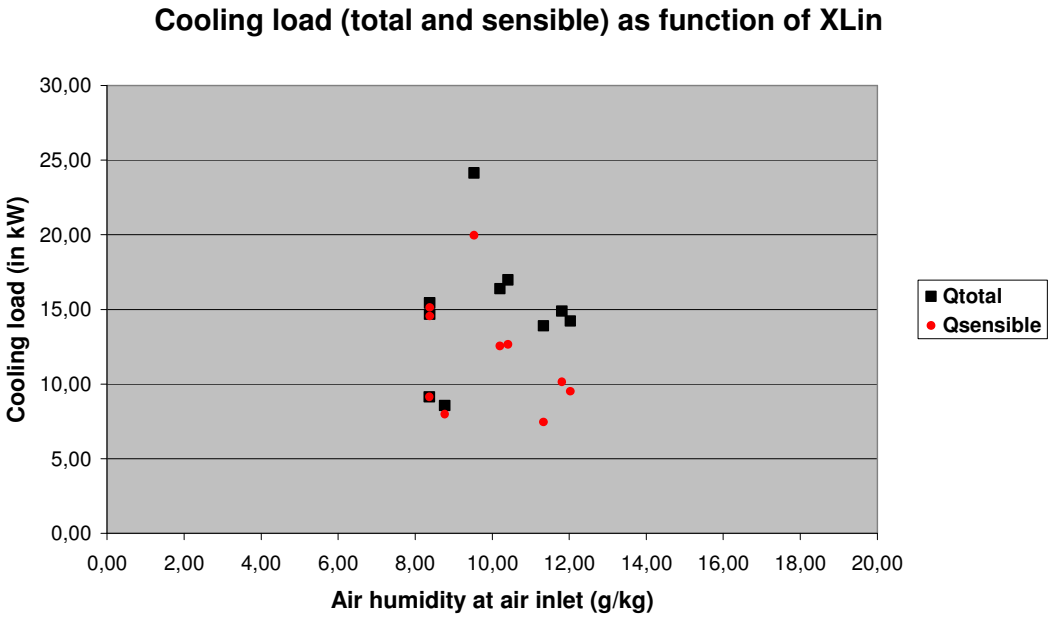

Figure D.8: Cooling power (sensible and latent = total) for 10 random measuring points (both in dry and wet regime)

Appendix E: Determination of A11, B11 and C11 from extra data points in dry regime

At present time Manufacturer data is given for 1 point:

- Load Q
- Air inlet and air outlet temperature
- Water inlet and water out temperature

From this data follow air flow (FLOWair0) and water flow (FLOWwater0); also the overall UA-value of the coil can be derived (see appendix A).

At other air / water flow rates the overall UA-value will be different and that is dependent on the individual UA,air and UA,water:

$$UA = \frac{1}{1/UA,air + 1/UA,metal + 1/UA,water} \qquad (1)$$

UA,air and UA,water are both flow dependent:

$$UA,air = fair * UA,air0 \qquad (2a)$$

$$UA,water = fwater * UA,water0 \qquad (2b)$$

Factors fair and f water are correction factors for the flow dependency. Index '0' means at manufacturer flows.

Definition:

$$UA,air0 = 3.0 * A11 * UA0 \qquad (3a)$$

$$UA,water0 = 3.0 * B11 * UA0 \qquad (3b)$$

$$UA,metal = 3.0 * C11 * UA0 \qquad (3c)$$

So

$$1/B11 = 3.0 - 1/A11 - 1/C11 \qquad (3d)$$

Statement:
If data for a second and third point is available the ratio A11 and C11 (and B11) can be derived.

Determination of A11 and B11 from 3 data points

Second data point:

For a second point the UA2, FLOWair2 and FLOWwater2 can be derived.

With equation (1)

$$UA2 = \frac{1}{1/UA,air2 + 1/UA,metal + 1/UA,water2} \quad (4)$$

With equations (2) in equation (4)

$$UA2 = \frac{1}{1/(fair2*UA,air0)+1/UA,metal+1/(fwater2*UA,water0)} \quad (5)$$

And equations (3) in equation (5)

$$UA2 = UA0 * \frac{3}{1/(fair2*A11) + 1/C11 + 1/(fwater2*B11)} \quad (6)$$

Define

$$frac2 = UA2/UA0 \quad (7)$$

From (6) and (7)

$$3/frac2 = 1/(fair2*A11) + 1/(fwater2*B11) + 1/C11 \quad (8)$$

Use equation (3d)

$$3/frac2 = (1/A11)/fair2+(3-1/A11-1/C11)/fwater2+1/C11 \quad (9)$$

or

$$3/frac2-3/fwater2 = 1/A11*(1/fair2-1/fwater2)+1/C11*(1-1/fwater2) \quad (10)$$

or

$$K2 = 1/A11*L2 + 1/C11*M2 \quad (11)$$

Two unknowns: A11 and C11

Third data point:

The same as for data point 2:

$$3/frac3-3/fwater3 = 1/A11*(1/fair3-1/fwater3)+1/C11*(1-1/fwater3) \quad (12)$$

or

$$K3 = 1/A11*L3 + 1/C11*M3 \quad (13)$$

Two equations and two unknowns

So there are two equations (11 and 13) and two unknowns (A11 and C11); so A11 and C11 can be derived.

```
A11 = (M3L2 - M2L3)/(M3K2-M2K3)                                    (14a)
```

and

```
C11 = (M2L3 - M3L2)/(L3K2-L2K3)                                    (14b)
```

And the individual UA,air0 and UA,water0 and UA,metal are known.

Information about fair and fwater

From literature study it was found

```
fair        = (FLOWair/FLOWair0)0.56                               (15a)

fwater      = (FLOWwater/FLOWwater0)0.80                           (15b)
```

Both for turbulent flow. It was found in almost all cases the flow is turbulent.

Test of this method:

Take as second point Part,air = 20 % and Part,water = 20 % and the belonging load Q and the inlet and outlet temperature at both the water and the air side.

Determine UA2 and so frac2 (according to (7)). Determine fair2 and fwater2.

Take as third point Part,air = 50 % and Part,water = 50 % and the belonging load Q and the inlet and outlet temperature at both the water and the air side.

Determine UA3 and so frac3 (according to (7)). Determine fair3 and fwater3.

And so A11 and C11 become available.

Experience with this method:

With the 3 data points (#0 – Manufacturer data and #1, #2 - Empirical data) this method to determine A11, B11 and C11 was tested. The results were not so good. Probably caused by the fact the Manufacturer data is not so trusty. May be also the small range of the air flow rates causes this.

Below a simpler method, derived from this method, is given. That method supposes C11 is given.

Determination of A11 and B11 from 2 data points (C11 is given)

The method is the same for the first two data points. It results in equation (11):

$$K2 = 1/A11*L2 + 1/C11*M2 \qquad (11)$$

Two equations with two unknowns.

It is now assumed the UA,metal is given, so C11 is known.

$$C11 = UA,metal/(3.0 * UA0) \qquad (16)$$

One unknown: A11

$$A11 = L2*C11/(K2*C11 - M2) \qquad (17)$$

And the individual UA,air0 and UA,water0 and UA,metal are known.

Test of this simpler method:

Take as second point Part,air = 20 % and Part,water = 20 % and the belonging load Q and the inlet and outlet temperature at both the water and the air side.

Determine UA2 and so frac2 (according to (7)). Determine fair2 and fwater2.

And so A11 become available.

Experience with this method:

With the 2 data points (#1, #2 - Empirical data) this method to determine A11, B11 and C11 was tested. The results were reasonably good. For this simpler method the influence of C11 (from large to small) on the result (A11 and B11) was determined. For C11 > 10 the A11 = 0,60 and B11= 0,77; for smaller C11 it was found B11 is about independent (for this case?!) of C11 (B11 = 0,77). For some C11's (and belonging A11's) the tests were done. The influence was not so big. Therefore it was decided to take C11 = 1,0 and so A11 became 1,43

Remark: this method was tested too with data points #0 (Manufacturer data) and #2 (empirical data). The experience was the same, the resulting A11 (0,82) and B11 (1,28) were reasonably different!! Is it the Manufacturer datapoint??!!

Appendix F: Determination of A11, B11 and C11 from extra data points

From Empirical test II 10 extra data points were derived. In table F.1 these data points are given (see table 4.6 of final report of this subtask).

Table F.1: Quasi-steady state points based on Empirical test II

Imin	EAT	EArH	EAH	LAT	LArH	LAH	AFR	EWT	LWT	ChWFR	UA	CLT	CLS	CLL
-	oC	%	kg/kg	oC	%	kg/kg	m3/h	oC	oC	l/s	kW/K	kW	kW	kW
1	22,88	46,9	0,00838	11,63	95,1	0,00833	4016	5,40	11,64	0,614	1,800	15,43	15,13	0,30
2	22,92	46,8	0,00838	11,76	95,0	0,00839	3899	5,07	12,10	0,519	1,750	14,68	14,56	0,12
3	26,35	39,9	0,00877	11,10	97,1	0,00822	1520	3,46	13,85	0,203	1,150	8,57	7,99	0,58
4	27,45	35,8	0,00837	11,71	95,0	0,00835	1697	5,04	15,11	0,228	1,220	9,14	9,14	0,00
5	23,19	56,1	0,01020	11,86	99,6	0,00883	3324	4,96	11,24	0,647	1,690	16,39	12,55	3,84
6	19,03	80,3	0,01133	11,85	99,7	0,00883	3019	2,69	11,09	0,411	1,580	13,90	7,46	6,44
7	27,90	49,6	0,01203	11,78	99,1	0,00878	1717	4,41	12,86	0,414	1,300	14,22	9,52	4,70
8	27,97	48,8	0,01181	11,57	99,1	0,00863	1798	4,89	12,43	0,483	1,340	14,89	10,14	4,75
9	23,58	51,3	0,00953	11,37	99,1	0,00849	4752	3,09	11,37	0,972	1,960	24,14	19,96	4,18
10	23,53	56,0	0,01041	11,84	99,1	0,00878	3150	4,98	11,84	0,653	1,660	16,98	12,66	4,32

Data point #1 was taken as the starting point:

Specific capacity AFWW = 1804 W/K
Air mass flow rate Flowair = 1,350 kg/s *)
Fluid mass flow rate = 0,622 kg/s **)

*) Belonging air volume flow rate = 4030 m3/h (at 20 oC and 101,3 kPa)
**) Belonging fluid volume flow rate = 0,61 l/s (Propylene Glycol – 18 %)

A11 and C11 were varied (B11 follows from A11 and C11) and modelling results for the several parameters were compared with the measurements.

From this fitting with the other 9 points the factors A11, B11 and C11 are estimated:

A11 = 0,90
C11 = 3,00
B11 = 0,64.

In the figures F.1a-f the results are given for those values of A11, B11 and C11.

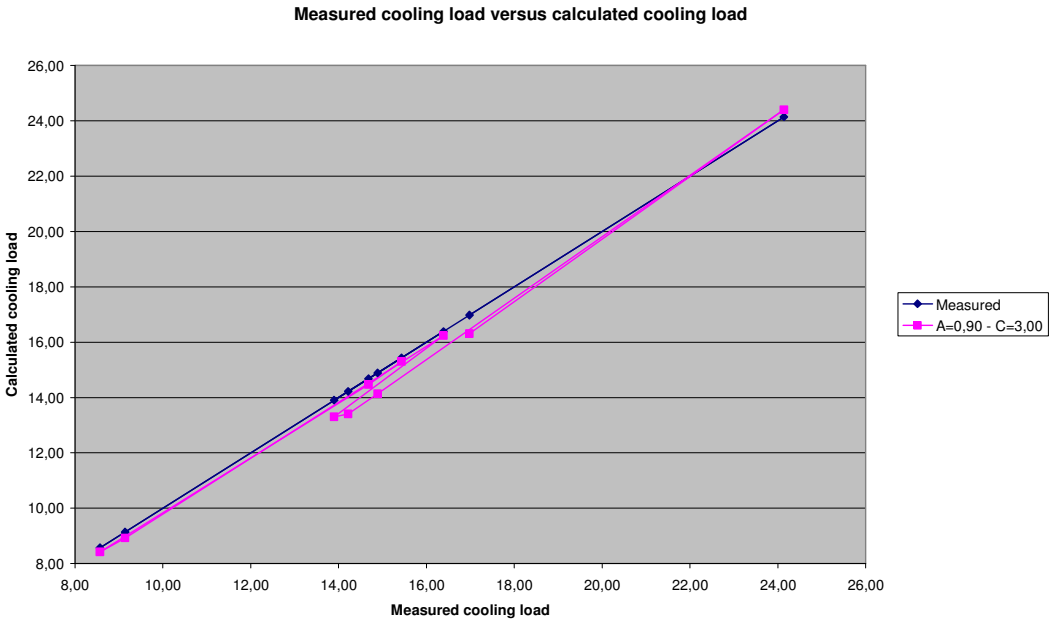

Figure F.1.a: Measured cooling load versus calculated cooling load

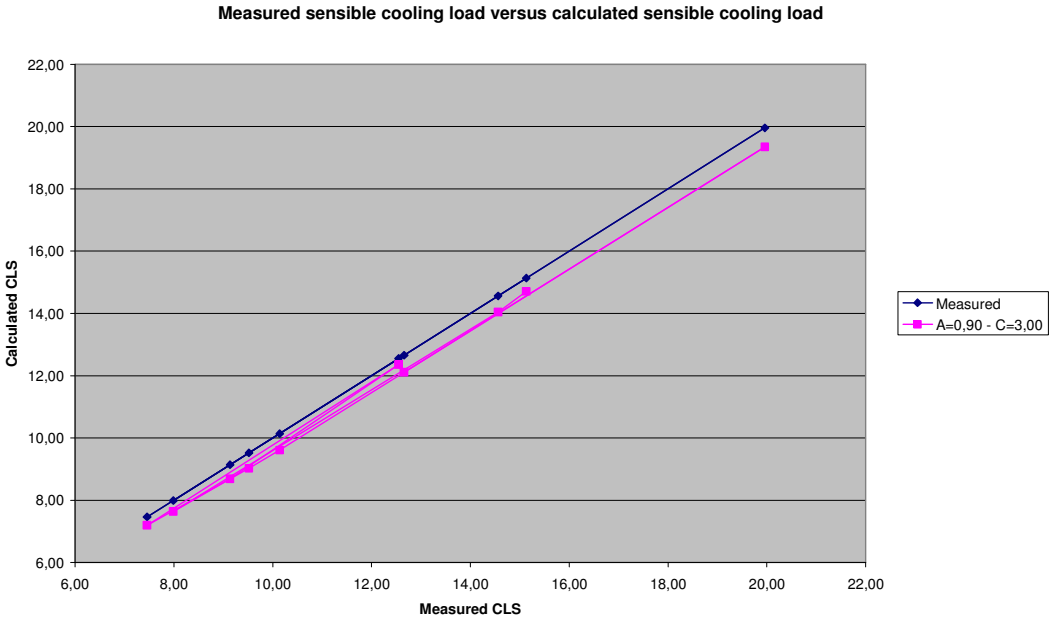

Figure F.1.b: Measured sensible cooling load versus calculated sensible cooling load

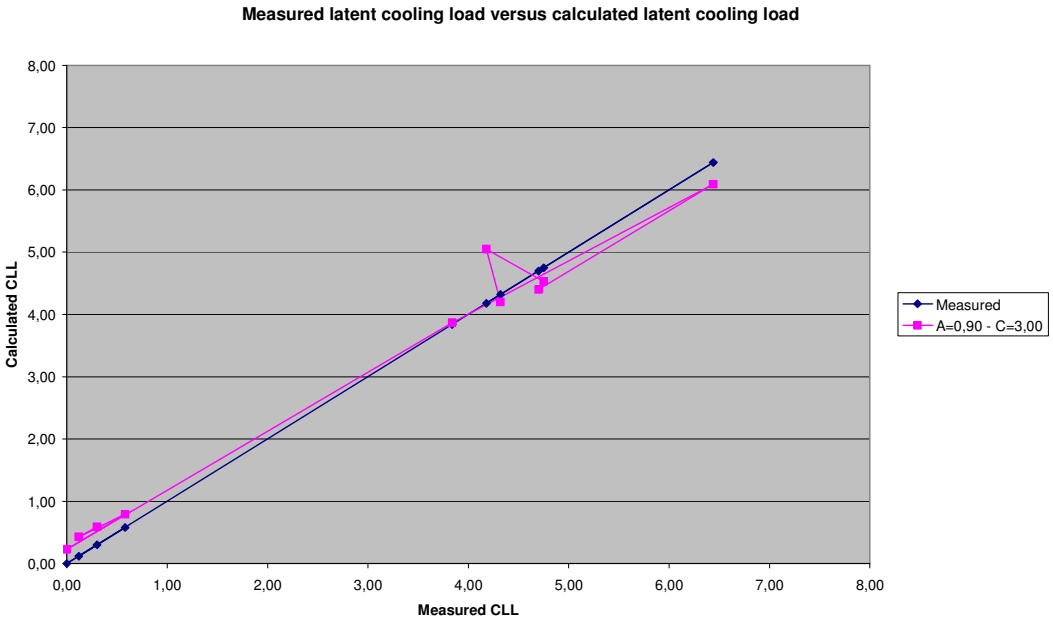

Figure F.1.c: Measured latent cooling load versus calculated latent cooling load

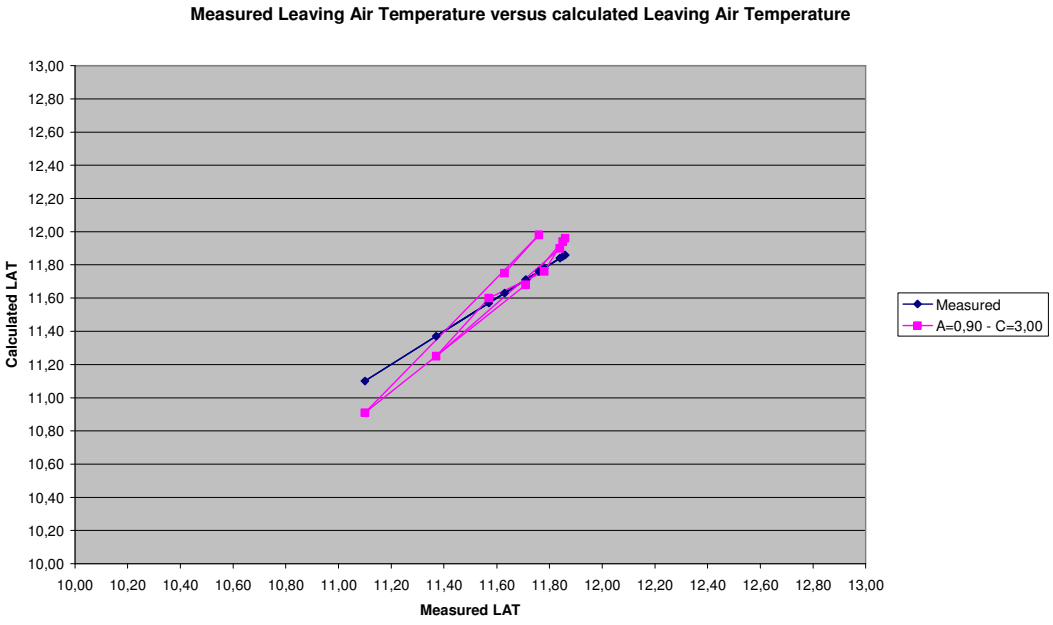

Figure F.1.d: Measured Leaving Air Temperature versus calculated Leaving Air Temperature

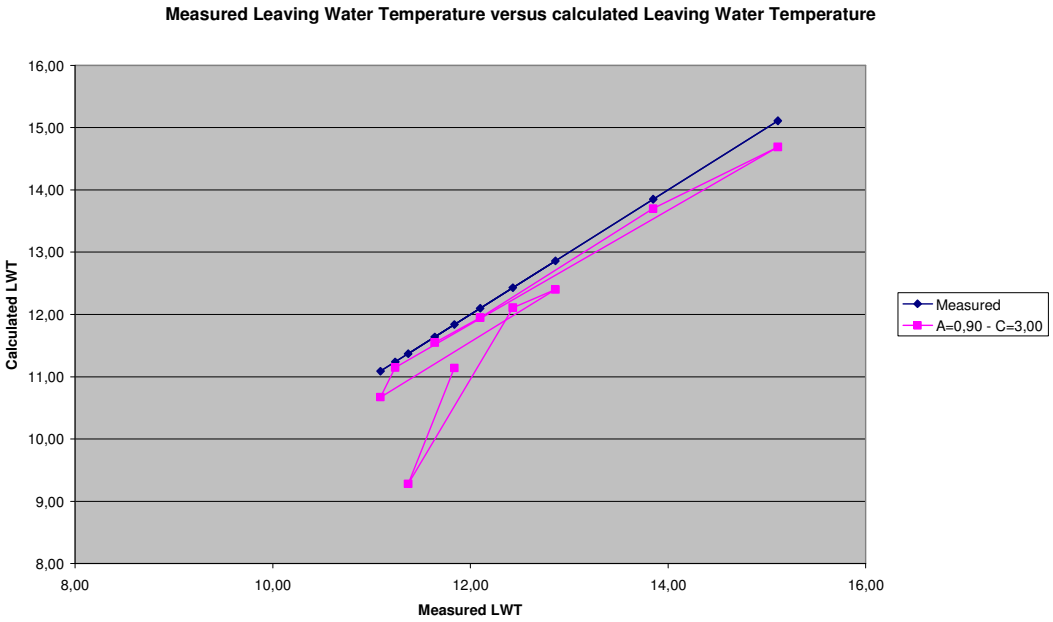

Figure F.1.e: Measured Leaving Water Temperature versus calculated Leaving Water Temperature

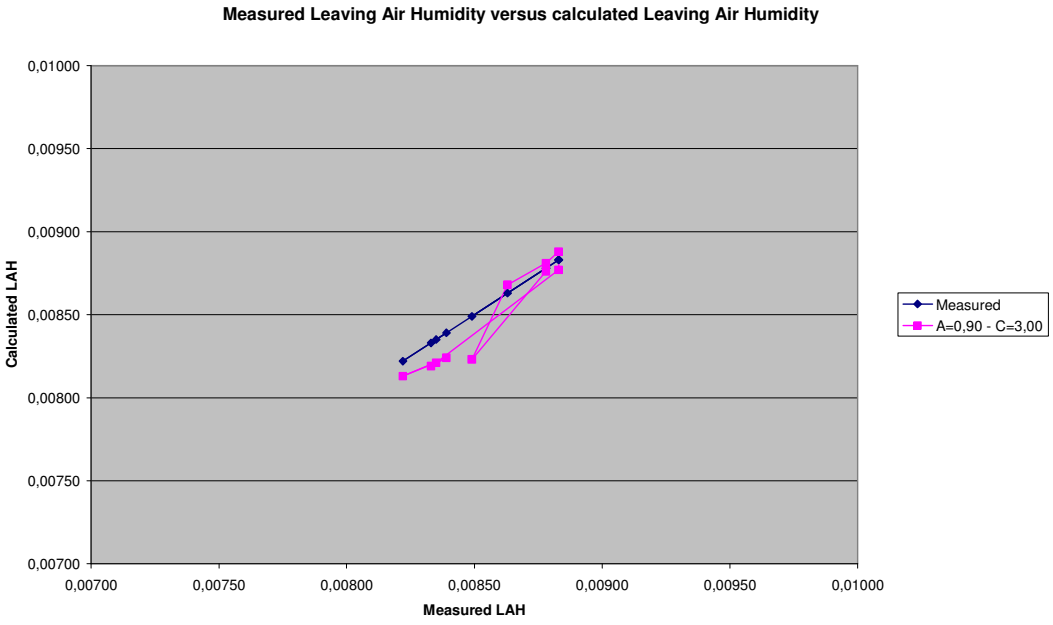

Figure F.1.f: Measured Leaving Air Humidity versus calculated Leaving Air Humidity

7.2.3 Gard – EnergyPlus

IEA MECHANICAL EQUIPMENT COMPARATIVE COOLING COIL TESTREPORT CASES CC100, CC120, CC200, CC220 ENERGYPLUS VERSION 2.2.0.023

Prepared by
R. Henninger & M. Witte, GARD Analytics, Inc.

April 2008

---

1. Introduction

Software:	EnergyPlus Version 2.2.0.023
Authoring Organization:	U.S. Department of Energy Energy Efficiency and Renewable Energy Office of Building Technologies
Authoring Country:	USA

This report describes the modeling methodology and results for Round 2 of testing done for the IEA Chilled Water System, Cooling Coil Comparative Tests, Cases: CC100, CC120, CC200 and CC220 which were simulated using the EnergyPlus software. The specifications for the test suite are described in *Chilled Water System – A Set of Comparative and Empirical Test Cases, IEA: SHC Task 34 / ECBCS Annex 43, Subtask D: Mechanical Equipment and Control Strategies* dated January 12, 2007 (referred to as the Chilled Water System specification in this report). The other 12 cases that are part of the Cooling Coil Comparative Test (Section 4.3 of the specification) and the Cooling Coil Empirical Tests (Section 4.4 and 4.5) could not be modeled by the EnergyPlus software due to the following limitations:

a) Only water can currently be modeled as the chilled water fluid. The ability to model glycol solutions has not yet been added to chillers and chilled water coils EnergyPlus.
b) Varying water supply temperatures to cooling coils with constant water flow rates cannot currently be modeled by EnergyPlus.

2. Modeling Assumptions

The following comments are provided in regards to user inputs that were used with EnergyPlus to model Cases CC100, CC120, CC200 and CC220 in the Chilled Water System specification. Except where discussed below, all other requirements of the specification for these cases were met.

a) In order to generate the required cooling coil load each hour of the simulation period as required by the Chilled Water System specification, the EnergyPlus user must model the whole building including the building envelope, a thermal zone, HVAC system including cooling coil, and plant equipment including chilled water cooling equipment. For this test situation, a one zone building was modeled with an adiabatic building shell, no windows and no internal loads.

b) Since Table 4.5 of the specification indicates that the air flow network is VAV for some cases, the HVAC system was modeled as a variable volume system using the SINGLE DUCT:VAV:NOREHEAT object in EnergyPlus with input parameters set as shown below:

```
SINGLE DUCT:VAV:NOREHEAT,
      ZONE ONE VAV Reheat,              !- Name of System
      COMPACT HVAC-ALWAYS 1,            !- System Availability schedule
      ZONE ONE Supply Inlet,            !- UNIT Air Outlet Node
      ZONE ONE Zone Equip Inlet,        !- UNIT Air Inlet Node
      0.8333,                           !- Maximum air flow rate {m3/s}
      1.;                               !- Zone Minimum Air Flow Fraction
```

The VAV system as described in the specification is not a typical fully variable volume air flow system but is referred to in Section 4.3.2 of the specification as "Quasi-Variable Air Volume" since the air flow rate was either 2000 m3/h or 5000 m3/h depending on the time of day. The VAV system modeled in EnergyPlus was therefore forced to operate as a constant volume system by setting the zone minimum air flow fraction to 1.0. For Cases CC100 and CC120 the maximum air flow rate was set to 3000 m3/h (0.8333 m3/s). For Cases CC200 and CC220 where supply air flow changed from 2000 m3/h (0.5555 m3/s) to 5000 m3/h (1.3889 m3/s) depending on time of day, two separate simulations were performed, one at the high flow rate and one at the low flow rate for the entire simulation period, and then the appropriate results were linked into the results spreadsheet. The supply fan heat added to the air stream was forced to be 0.0 by setting the fan delta pressure to 0.0. The VAV system supply air flow was set to 100% outdoor air as follows with the min and max flow rates set accordingly for each test case:

```
CONTROLLER:OUTSIDE AIR,
      SYSTEM-1 OA Controller,           !- Name
      NO ECONOMIZER,                    !- EconomizerChoice
      NO RETURN AIR TEMP LIMIT,         !- ReturnAirTempLimit
      NO RETURN AIR ENTHALPY LIMIT,     !- ReturnAirEnthalpyLimit
      NO LOCKOUT,                       !- Lockout
      PROPORTIONAL MINIMUM,             !- MinimumLimit
      SYSTEM-1 Mixed Air Outlet,        !- Control Node
      SYSTEM-1 Outside Air Inlet,       !- Actuated Node
      0.8333,                           !- minimum outside air flow rate {m3/s}
      0.8333,                           !- maximum outside air flow rate {m3/s}
      ,                                 !- temperature limit {C}
      ,                                 !- temperature lower limit {C}
```

```
,                                          !- enthalpy limit {J/kg}
SYSTEM-1 Relief Air Outlet,                !- Relief Air Outlet Node
SYSTEM-1 Air Loop Inlet,                   !- Return Air Node
COMPACT SYSTEM-1 Outside Air Sched,  !- Min.Outside Air Schedule Name
;                                          !- Name of VENTILATION:
                                             MECHANICAL object
```

c) The cooling coil was modeled using the COIL:WATER:COOLING object in EnergyPlus with input parameters set as shown below:

```
COIL:WATER:Cooling,
    SYSTEM-1 Cooling Coil,                 !- Coil Name
    COMPACT HVAC-ALWAYS 1,                 !- Available Schedule
    0.001505,                              !- Design Water Flow Rate of Coil
    1.54778,                               !- Design Air Volume Flow Rate
    6.67,                                  !- Design Inlet Water Temperature
    27.78,                                 !- Design Inlet Air Temperature
    12.50,                                 !- Design Outlet Air Temperature
    0.0104,                                !- Design Inlet Air Humidity Ratio
    0.0087,                                !- Design Outlet Air Humidity Ratio
    SYSTEM-1 Cooling Coil ChW Inlet,       !- Coil Water Inlet Node
    SYSTEM-1 Cooling Coil ChW Outlet,      !- Coil Water Outlet Node
    SYSTEM-1 Supply Fan Outlet,            !- Coil Air Inlet Node
    SYSTEM-1 Cooling Coil Outlet,          !- Coil Air Outlet Node
    DETAILEDANALYSIS,                      !- Type of Analysis
    CROSSFLOW,                             !- Heat Exchanger Configuration
    ;                                      !- Name of Water Storage Tank for
                                             Condensate Collection
```

The coil design parameters were taken from Table 4.2 in the Chilled Water System specification.

d) Number of timesteps per hour was set to 4 although results were reported on an hourly basis.

e) The 14933.tm2 weather file provided with the test suite was converted to EnergyPlus format (14933TM2.epw) using the EnergyPlus weather conversion program. As instructed in separate correspondence with Dr. Clemens Felsmann, author of the BESTEST Multi-Zone with Airflow specification, daylight savings time was ignored during the simulation.

3. Modeling Options

EnergyPlus has two models available for simulating a water cooling coil:

a) COIL:WATER:Cooling
This coil model has the ability to give detailed output with simplified inputs. Inputting

of complicated coil geometry is not required by the user. Instead, the coil requires thermodynamic inputs such as temperatures, mass flow rates and humidity ratios. This model uses the NTU-effectiveness approach to model heat transfer and has two types of flow arrangements, cross-flow and counter-flow. For this test series the CROSSFLOW arrangement was used. This EnergyPlus cooling coil model allows the user to choose between a Simple Analysis method or Detailed Analysis method. The difference between the two methods being, the Simple Analysis assumes that the coil is either all dry or all wet while the Detailed Analysis method checks for part wet and part dry operation and reports the surface area wet fraction of the coil. The Detailed Analysis option was chosen for this test series.

b) COIL:WATER:DetailedFlatCooling
This model requires the user to input the detailed coil geometry in terms of tube outside and inside surface area, coil depth, fin diameter and thickness, tube inside and outside diameter, tube and fin thermal conductivity, fin spacing, tube depth spacing, and number of tube rows. Since none of these details were available for the cooling coil from the specification, this cooling coil was not used.

4. Modeling Difficulties

Only four of the Cooling Coil Comparative Test cases (CC100, CC120, CC200 and CC220) described in Section 4.3 of the specification were able to be modeled by EnergyPlus, and these were modeled with WATER as the cooling fluid instead of the glycol solutions called for by the specification. EnergyPlus does not yet have the capability to model glycol solutions as part of the chilled water or hot water loops. The other cooling coil comparative cases and the Cooling Coil Empirical Test could not be modeled by EnergyPlus due to one of the following reasons:

a) They required the use of glycol solutions

b) They required the use a varying water supply temperature to the cooling coils with the water flow rate remaining constant. EnergyPlus will allow different water supply temperatures but currently cannot control the supply temperature of the water entering the coil to meet the load.

Regarding comment (a) above, the use of a 35% Ethylene Glycol solution was approximated in the simulations by adjusting the design water flow rate of the cooling coil based on the ratio of specific heats and densities of water and the glycol solution using the data provided in Table 4.3 of the specification. This was arrived at as follows:

0.00177 m3/s * (3.5543 kJ/(kgK) * 1054.08 kg/m3) / (4.180 kJ/(kgK) * 998.2 kg/m3)
= 0.001589 m3/s

Cases CC200 and CC220 both required that the supply air flow rate be fixed at two different values depending on the time of day: 2000 m3/h from 6 p.m. to 7 a.m. and 5000 m3/h from 7 a.m. to 6 p.m. This was modeled in EnergyPlus by two separate simulations, one at 2000 m3/h for the full simulation period and one at 5000 m3/h for the full simulation period. The results summarized in the spreadsheet then linked to the proper hourly results from the two separate EnergyPlus runs. This does not introduce errors at the transitions because the cooling coil input air stream was always 100% outdoor air and not affected by the zone conditions.

5. Results

As requested in Section 4.4.3 of the specification, the following hourly outputs over the five month (May through September) simulation period are provide in two attached Excel spreadsheets named

IEA Cooling Coil Results-EnergyPlus-4-22-08-Ver220-023-SimpleSolution-Unlinked.xls
IEA Cooling Coil Results-EnergyPlus-4-22-08-Ver220-023-DetailedSolution-Unlinked.xls.

1	Time	
2	EAT	Entering air temperature, dry bulb, C
3	EArH	Entering air relative humidity, %
4	EAH	Entering air humidity, kg/kg
5	LAT	Discharge/Leaving air temperature, dry bulb, C
6	LArH	Discharge/Leaving air relative humidity, %
7	LAH	Discharge/Leaving air humidity, kg/kg
8	AFR	Air flow rate, m3/h
9	EWT	Chilled water coil entering temperature, C
10	LWT	Chilled water coil leaving temperature, C
11	ChWFR	Chilled water flow rate through the coil, l/s
12	UA	Overall UA-Value of the coil, kW/K
13	CLT	Total cooling load, kW
14	CLS	Sensible cooling load, kW
15	CLL	Latent cooling load, kW

Charts displaying some of the results from each of the four test cases are shown on the following pages. It should be noted that the target leaving air temperature for each case was able to be met except for Case CC200 where there were several hours of high outdoor air temperature and humidity where the coil could not maintain the required 13 C leaving air temperature. A brief description of the controlling parameters for each test case is presented below.

Case CC100
Constant air flow = 3000 m3/h = 0.8333 m3/s
100% outside air with conditions taken from 14933.tm2 weather file
Constant air discharge temperature from coil = 13C
Constant chilled water supply temperature to cooling coil = 6C
Variable chilled water supply flow to cooling coil
Maximum chilled water supply flow rate = 1.77 l/s = 0.00177 m3/s

Case CC120
Constant air flow = 3000 m3/h = 0.8333 m3/s
100% outside air with conditions taken from 14933.tm2 weather file
Constant air discharge temperature from coil = 18C
Constant chilled water supply temperature to cooling coil = 6C

Variable chilled water supply flow to cooling coil
Maximum chilled water supply flow rate = 1.77 l/s = 0.00177 m3/s

Case CC200
Constant air flow = 2000 m3/h = 0.5555 m3/s from 6PM to 7AM
Constant air flow = 5000 m3/h = 1.3889 m3/s from 7AM to 6PM
100% outside air with conditions taken from 14933.tm2 weather file
Constant air discharge temperature from coil = 13C
Constant chilled water supply temperature to cooling coil = 6C
Variable chilled water supply flow to cooling coil
Maximum chilled water supply flow rate = 1.77 l/s = 0.00177 m3/s

Case CC220
Constant air flow = 2000 m3/h = 0.5555 m3/s from 6PM to 7AM
Constant air flow = 5000 m3/h = 1.3889 m3/s from 7AM to 6PM
100% outside air with conditions taken from 14933.tm2 weather file
Constant air discharge temperature from coil = 18C
Constant chilled water supply temperature to cooling coil = 6C
Variable chilled water supply flow to cooling coil
Maximum chilled water supply flow rate = 1.77 l/s = 0.00177 m3/s

As was explained in Section 3(a), the EnergyPlus COIL:WATER:COOLING has two methods of analysis – SIMPLE ANALYSIS and DETAILED ANALYSIS. The results reported on the charts on the following pages and in the attached Excel spreadsheet are for the SIMPLE ANALYSIS option. A second set of EnergyPlus simulations were performed but this time using the DETAILED ANALYSIS option. The comparison between both sets of EnergyPlus results is shown in the table below. In some cases there are significant differences and the reason for such large differences is of concern and is being investigated. The results for the SIMPLE ANALYSIS appear to be closer to the results of the other programs participating in the IEA project.

6. Issues

The results reported above are not to be considered final for this first round of testing due to several issues that still need to be resolved:

- Glycol solutions cannot be modeled directly for chilled water coils.

- The EnergyPlus cooling coil object used in these tests (COIL:WATER:COOLING) has two modeling options. Differences in results between the SIMPLE analysis and the DETAILED analysis methods will be looked into further by the EnergyPlus Development Team.

- No further testing can be done on the other parts of the IEA Chilled Water System test suite, i.e. chiller and hydronic network, until the IEA specification is completed and finalized.

IEA Mechanical

Cooling Coil Comparative Tests

EnergyPlus 2.2.0.023

	Simple Solution			Detailed Soultion			Difference (Detailed - Simple)			% Difference		
	QS	QL	QT	QS	QL	QT	QS	QL	QT	QS	QL	QT
	(kW)	(kW)	(kW)	(kW)	(kW)	(kW)	(kW)	(kW)	(kW)			
CC100	28634.4	16767.6	45402.0	28634.4	18076.4	46710.7	-0.08	1308.78	1308.70	0.00%	7.24%	2.80%
CC120	14206.9	3944.9	18202.2	14206.8	6333.4	20540.2	-0.09	2388.49	2338.01	0.00%	37.71%	11.38%
CC200	36239.7	20529.0	56768.7	36239.6	21847.8	58623.3	-0.06	1318.73	1854.59	0.00%	6.04%	3.16%
CC220	19109.1	5319.7	24428.8	19109.0	8128.4	27237.4	-0.08	2808.67	2808.59	0.00%	34.55%	10.31%

CC100 and CC200 have constant discharge air temp = 13C

CC120 and CC220 have constant discharge air temp = 18C

CC100 and CC120 have constant air flow rate of 0.8333 m3/s

CC200 and CC220 have air flow rate of 0.5555 m3/s for 6 pm to 7 am and 1.3889 m3/s for 7 am to 6 pm

Results are taken from an EnergyPlus cvs file where hourly output values are in (J).

Case CC100

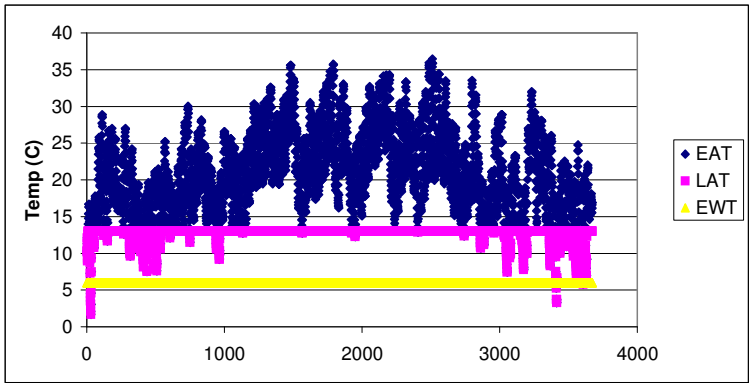
Temp (C)
40
35
30
25
20
15
10
5
0
0
1000
2000
3000
4000
EAT
LAT
EWT

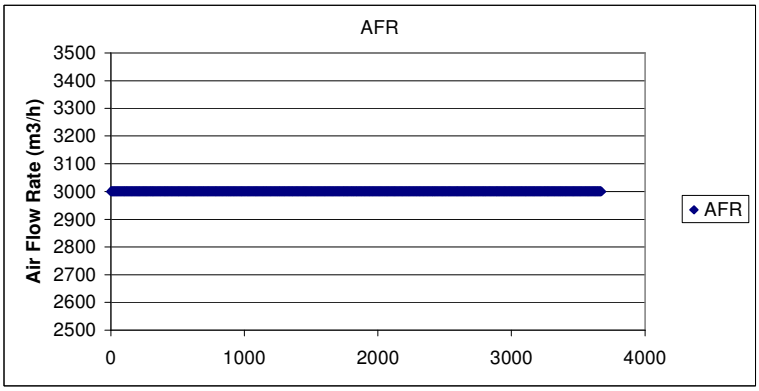
AFR
Air Flow Rate (m3/h)
3500
3400
3300
3200
3100
3000
2900
2800
2700
2600
2500
0
1000
2000
3000
4000
AFR

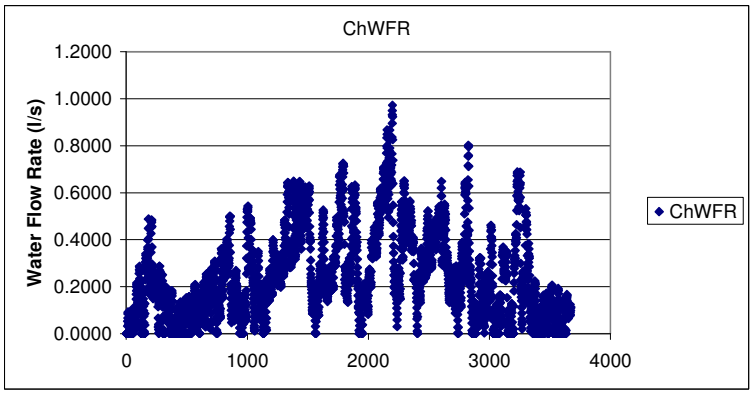
ChWFR
Water Flow Rate (l/s)
1.2000
1.0000
0.8000
0.6000
0.4000
0.2000
0.0000
0
1000
2000
3000
4000
ChWFR

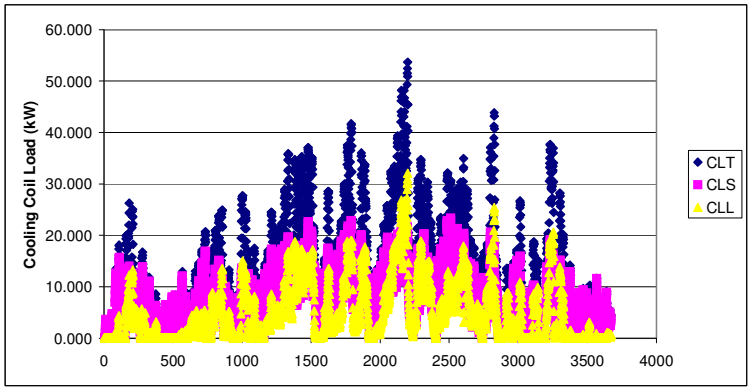
Cooling Coil Load (kW)
60.000
50.000
40.000
30.000
20.000
10.000
0.000
0
500
1000
1500
2000
2500
3000
3500
4000
CLT
CLS
CLL

Case CC120

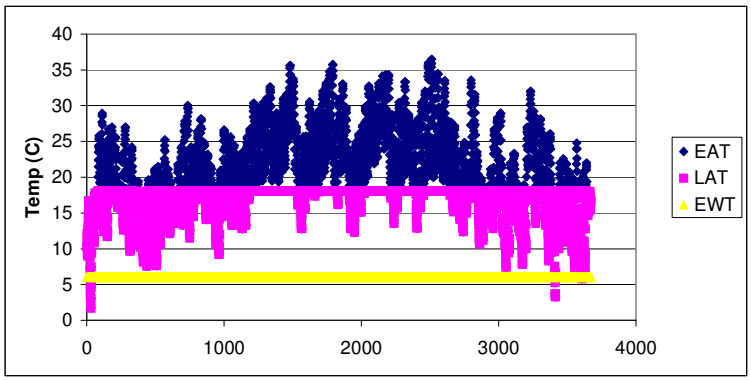
Temp (C)
40
35
30
25
20
15
10
5
0
0
1000
2000
3000
4000
EAT
LAT
EWT

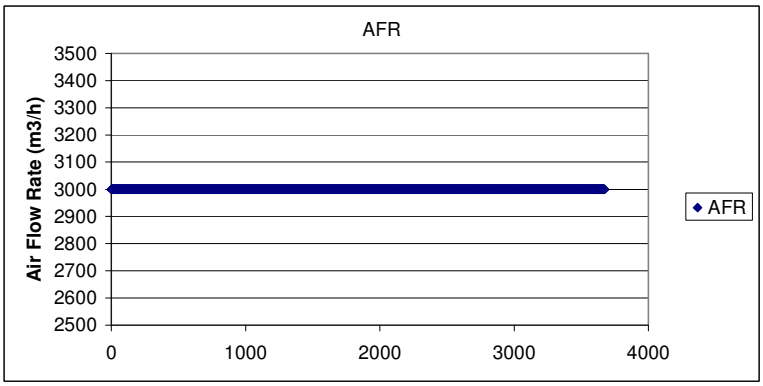
AFR
Air Flow Rate (m3/h)
3500
3400
3300
3200
3100
3000
2900
2800
2700
2600
2500
0
1000
2000
3000
4000
AFR

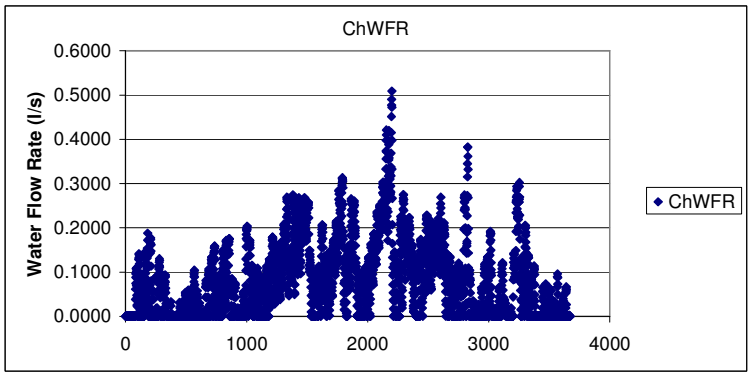
ChWFR
Water Flow Rate (l/s)
0.6000
0.5000
0.4000
0.3000
0.2000
0.1000
0.0000
0
1000
2000
3000
4000
ChWFR

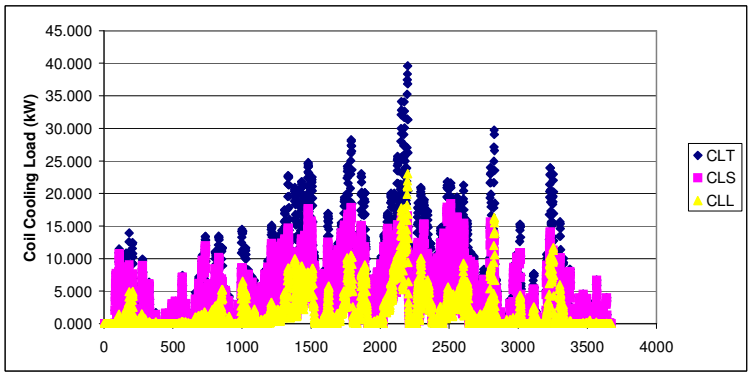
Coil Cooling Load (kW)
45.000
40.000
35.000
30.000
25.000
20.000
15.000
10.000
5.000
0.000
0
500
1000
1500
2000
2500
3000
3500
4000
CLT
CLS
CLL

Case CC200

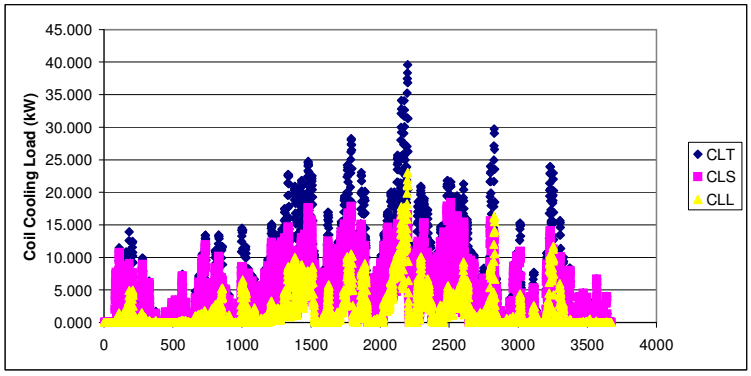
Coil Cooling Load (kW)
45.000
40.000
35.000
30.000
25.000
20.000
15.000
10.000
5.000
0.000
0
500
1000
1500
2000
2500
3000
3500
4000
CLT
CLS
CLL

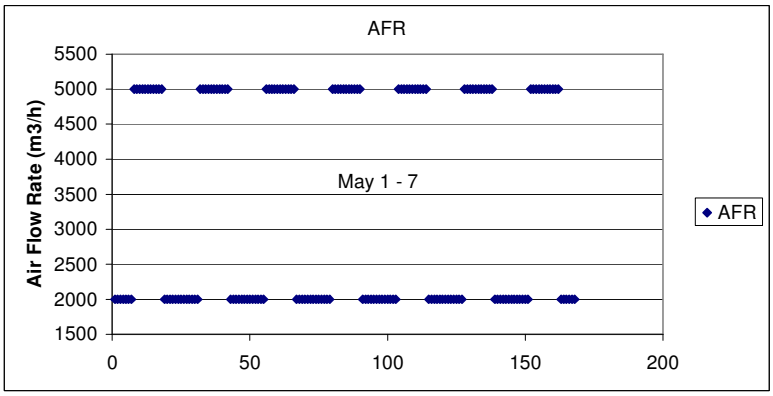
AFR
Air Flow Rate (m3/h)
5500
5000
4500
4000
3500
3000
2500
2000
1500
May 1 - 7
0
50
100
150
200
AFR

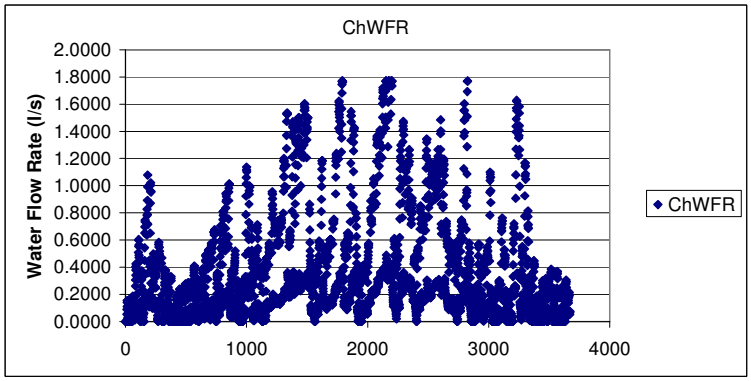
ChWFR
Water Flow Rate (l/s)
2.0000
1.8000
1.6000
1.4000
1.2000
1.0000
0.8000
0.6000
0.4000
0.2000
0.0000
0
1000
2000
3000
4000
ChWFR

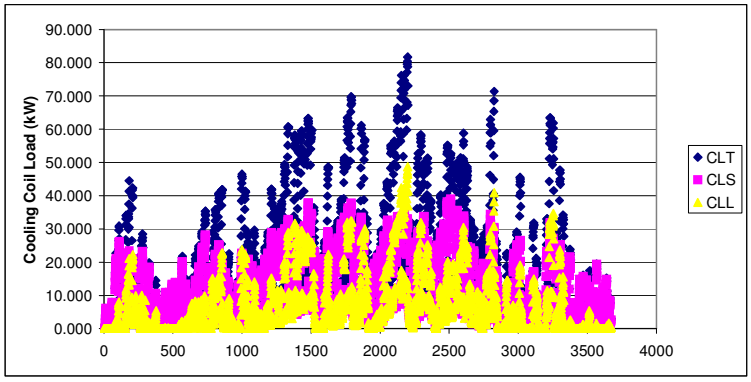
Cooling Coil Load (kW)
90.000
80.000
70.000
60.000
50.000
40.000
30.000
20.000
10.000
0.000
0
500
1000
1500
2000
2500
3000
3500
4000
CLT
CLS
CLL

Case CC220

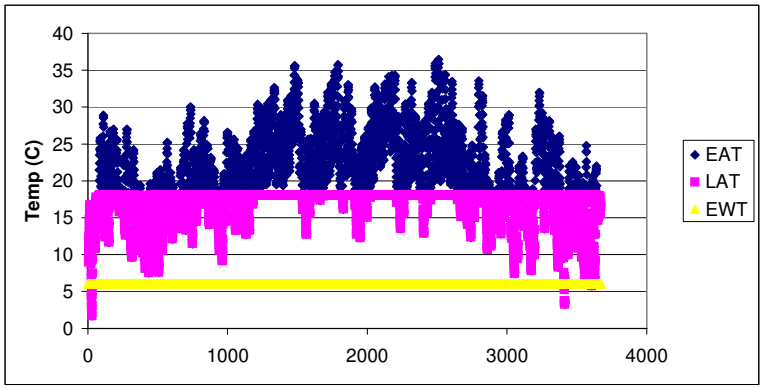
Temp (C)
40
35
30
25
20
15
10
5
0
0
1000
2000
3000
4000
EAT
LAT
EWT

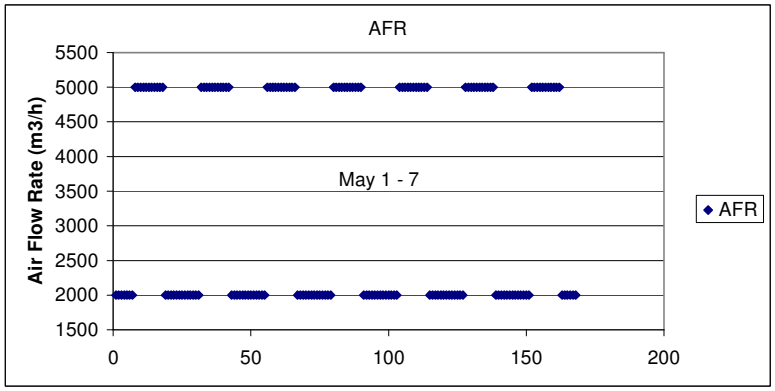
AFR
Air Flow Rate (m3/h)
5500
5000
4500
4000
3500
3000
2500
2000
1500
May 1 - 7
0
50
100
150
200
AFR

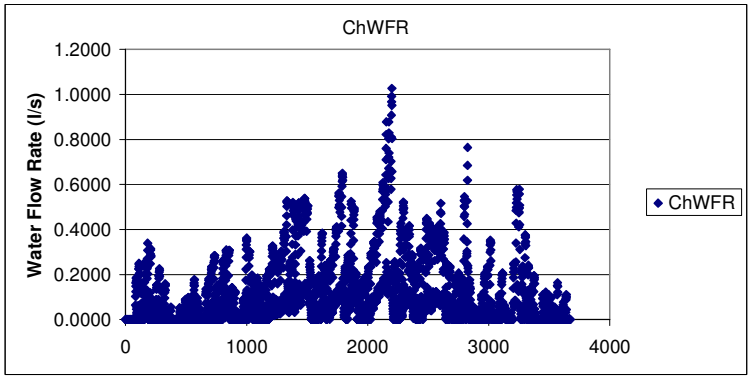
ChWFR
Water Flow Rate (l/s)
1.2000
1.0000
0.8000
0.6000
0.4000
0.2000
0.0000
0
1000
2000
3000
4000
ChWFR

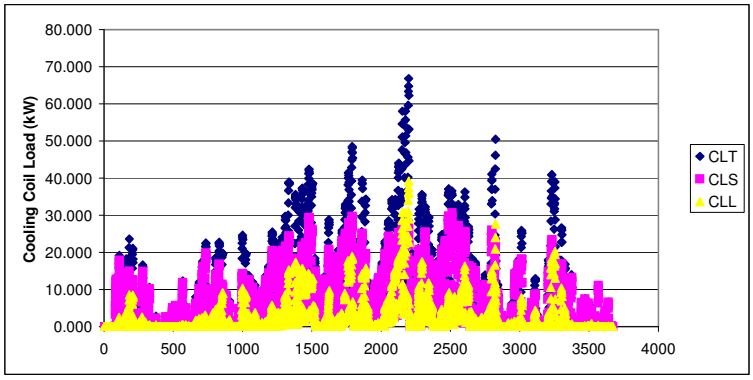

7.2.4 TUD – TRNSYS-TUD

Roots of the model

The TRNSYS-TUD cooling coil model is one of the TRNSYS ASHRAE Secondary Toolkit Components (Heat and Mass Transfer Components). These components are available for free from the Solar Energy Laboratory at the University of Wisconsin which is the original distributor of the TRNSYS program. The Solar Energy Laboratory also took care that the model was adapted strictly for use with the TRNSYS Program.

The model is a simple cooling and dehumidifying coil model that calculates the outlet liquid temperature, air dry bulb temperature and humidity ratio, and the total and sensible cooling capacity based for given inlet conditions based on nominal rated coil performance. For that reason it is not necessary to specify any detailed information neither about coil geometry nor about coil materials.

In the description of the model it is mentioned that "…the algorithm accounts for the heat and mass transfer associated with moisture condensation on the finned air-side surface of the coil in accordance with ASHRAE methods. It determines whether the finned surface is completely dry, completely wet, or partially wet and partially dry.

Simplifications in the algorithm involve the determination of overall heat transfer coefficients for the coil and the modeling of operation with a partially-wet fin surface. Overall heat transfer coefficients are determined from the performance of the coil at a single rating point and assumed to be constant at the other conditions. Part-wet coil performance calculations are not performed. If part-wet conditions are indicated, the coil is assumed to be either fully wet or fully dry, whichever gives the greatest total heat transfer rate. Each algorithm assumes water flow in a counter flow cross flow heat exchanger configuration and models the coil using equations for a counter flow heat exchanger. The model is most appropriate for coils with four or more rows." [1]

Changes to the model

Control

Originally the coil model did not include any temperature or flow control. That means leaving air temperature (and also humidity) was free floating depending on water and air side inlet conditions. In order to run cooling coil comparative test cases some kind of leaving air temperature control was added to the coil model at TUD. Finally three different control strategies were available:

1. No control:
   The leaving air and water side conditions are free floating.
2. Water flow control:
   The entering water temperature is known and water flow is controlled to maintain a given leaving air temperature set point.
3. Water temperature control:
   The entering water flow is known and coil entering water temperature is controlled to maintain a given leaving air temperature set point.

Both water flow and temperature controls are idealized control mechanisms, i.e. there is no control deviation while water flow and water temperature are within given limits:

$$0 \leq \text{Flow} \leq \text{Flow}_{max}$$
$$\text{Temp}_{min} \leq \text{Temp} \leq \text{Temp}_{max}$$

The 'No control'-option was used for the empirical test cases only.

Fluid properties

Physical properties of the cooling liquid may have an impact on coil performance. Originally the model was assuming pure water only. In order to run cooling coil validation tests the model was extended at TUD to also account for other cooling liquids than water. Actually the user has the choice between (1) pure water, (2) ethylene/glycol mixture, or (3) propylene/glycol mixture, respectively. When a glycol mixture is selected the percentage of glycol per mass has to be defined by the user as well. Physical properties of the glycol mixtures have been taken from the ASHRAE Handbook of Fundamentals [2].

Flow dependencies

The simple cooling coil model as found in the HVAC components library was assuming a constant overall heat transfer coefficient UA that was depending on the amount of condensation only but was independent from flow rates. As first sets of comparative validation test results have shown very big deviations between simulation results calculated with the original TRNSYS / ASHRAE model and those calculated by other participants it was decided to implement flow dependencies of the UA value. These flow dependencies have been defined and implemented as follows:

- Dry coil with no condensation

$$UA_{ext} = UA_{ext0}\left(\frac{Flow_{air}}{Flow_{air0}}\right)^{0.33}$$

$$UA_{int} = UA_{int0}\left(\frac{Flow_{water}}{Flow_{water0}}\right)^{0.67}$$

- Wet coil

  UA_{ext} = f(condensation) as defined in the origin

$$UA_{int} = UA_{int0}\left(\frac{Flow_{water}}{Flow_{water0}}\right)^{0.67}$$

The external UA_{ext} value refers to the air side of the coil whereas the cooling fluid side of the coil is covered by the UA_{int} value. The coil material by itself is not taken into account by a special UA value but is covered by the internal/external UA.

Known limitations of the model

The basic coil performance (UA_{ext}, UA_{int}) is estimated based on a single rating point only. In this way it is not possible to use several rating points – as defined in the test specifications based on experimental data – at the same time to calibrate the model. A similar problem occurs when different physical properties of the cooling fluid have to be used in either the rating point or in the simulation run.

[1] A Toolkit for Secondary HVAC System Energy Calculations. May 25,1992. Joint Center for Energy Management University of Colorado at Boulder

[2].ASHRAE Handbook of Fundamentals. 1996

7.2.5 ITG – Matlab/Simulink

Institut für Technische Gebäudeausrüstung Dresden
Forschung und Anwendung GmbH
Prof. Richter - Prof. Bolsius - Dr. Felsmann - Dr. Hartmann - Prof. Oschatz - Dr. Werdin

IEA SHC Task 34 / ECBCS Annex 43
Subtask D: Mechanical Equipment and Control Strategies

Cooling Coil - Modeler report

ITG - Institut für Technische Gebäudeausrüstung Dresden
Forschung und Anwendung GmbH
Bayreuther Str. 29
01187 Dresden
Germany

April 06, 2006

Report by Heiko Werdin

2 Model description

2.1 General

A cooling coil consists of tubes, fins, a collecting tube, and a distributing tube as shown in figure 2.1. It is assumed that air flows along the fins and an arbitrary fluid flows through the tubes. The current model includes water, ethylene glycol solution, and propylene glycol solution as selectable fluids.

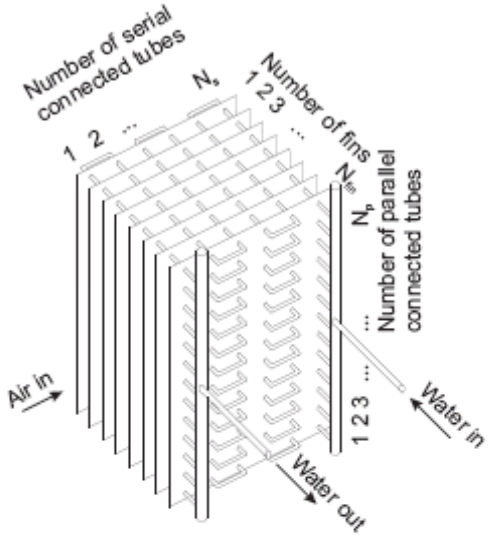

Figure 2.1: Sketch of a finned cooling coil

The cooling coil model discretises the real cooling coil in $N_s \cdot N_{fin}$ cells, where N_s is the number of serial connected tubes and N_{fin} is the number of fins on one tube, see figure 2.1.

Figure 2.2 shows a small cell of a finned cooling coil. It is assumed that the fin height H_{fin} is equal to the cell height H_{cell}. Moreover, the fin length L_{fin} is equal to the cell length L_{cell}.

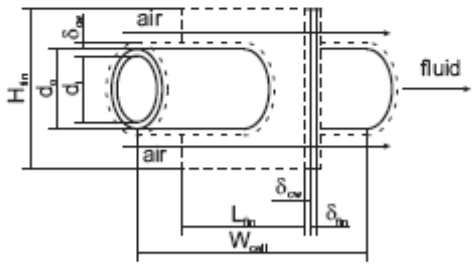

Figure 2.2: Sketch of a modeled cell as a part of a finned cooling coil

The model considers four parts of each cell in order to calculate the thermal and hygric behaviour of the cooling coil: the air-side zone, the boundary layer zone, the tube zone, and the fluid-side zone.

2.2 Fluid-side zone of a cell

The thermal behaviour of the fluid side of a cell is calculated according to

$$m_{fl} \cdot c_{p,fl} \cdot \frac{\partial \vartheta_{fl}}{\partial \tau} = \alpha_{fl} \cdot A_{fl} \cdot (\vartheta_w - \vartheta_{fl}) + \dot{m}_{fl} \cdot c_{p,fl} \cdot (\vartheta_{fl,in} - \vartheta_{fl}), \tag{2.1}$$

where:
- m_{fl} - mass of fluid in one cell in kg
- $c_{p,fl}$ - specific heat capacity of the fluid in J/(kgK)
- ϑ_{fl} - fluid temperature of the cell in °C
- τ - time in s
- α_{fl} - fluid-side heat transfer coefficient in W/(m²K)
- A_{fl} - fluid-side surface of the tube with heat transfer in one cell in m²
- ϑ_w - wall (tube) temperature of the cell in °C
- $\dot{m}_{fl}$ - fluid-side mass flow rate through the cell in kg/s
- $\vartheta_{fl,in}$ - fluid flow temperature into the cell in °C.

The fluid-side heat transfer coefficient α_{fl} is calculated with

$$\alpha_{fl} = \frac{Nu_{fl} \cdot \lambda_{fl}}{d_i}, \tag{2.2}$$

where:
- Nu_{fl} - Nusselt number of fluid-side zone in -
- λ_{fl} - thermal conductivity of the fluid in W/(mK).

The Nusselt number depends on laminar and turbulent flow, where a usage of a turbulator moves the transition to turbulent flow to lower Reynolds numbers.

$$Nu_{fl,lam} = \left(48.867 + \frac{2.567 \cdot Re_{fl} \cdot Pr_{fl} \cdot d_i}{W_{cell} \cdot N_{fin}}\right)^{0.333} \tag{2.3}$$

$$Nu_{fl,turb} = 0.0235 \cdot \left(Re_{fl}^{0.8} - 230\right) \cdot \left(1 + \frac{d_i}{W_{cell} \cdot N_{fin} \cdot N_s}\right)^{2/3} \cdot \left(1.8 \cdot Pr_{fl}^{0.3} - 0.8\right) \tag{2.4}$$

where:
- $Re_{fl} = \frac{v_{fl} \cdot d_i}{\nu_{fl}}$ - Reynolds number of fluid-side zone in -
- v_{fl} - velocity of the fluid in m/s
- ν_{fl} - kinematic viscosity of the fluid in m²/s
- Pr_{fl} - Prandtl number of the fluid in -
- W_{cell} - width of one cell in m
- N_{fin} - number of fins on one tube in -
- N_s - number of serial connected tubes in -

2.3 Tube zone of a cell

It is assumed that the thermal resistance of the tube wall is negligible and the wall is isothermal. So, the tube temperature can be calculated with the following partial differential equation

$$m_w \cdot c_{p,w} \cdot \frac{\partial \vartheta_w}{\partial \tau} = \alpha_{fl} \cdot A_{fl} \cdot (\vartheta_{fl} - \vartheta_w) + \frac{\lambda_{cw}}{\delta_{cw}} \cdot A_{air} \cdot (\vartheta_{bl} - \vartheta_w^*), \tag{2.5}$$

where: m_w - mass of wall (tube) in one cell in kg
$c_{p,w}$ - specific heat capacity of the wall (tube) in J/(kgK)
λ_{cw} - thermal conductivity of the condensed water in the boundary layer in W/(mK)
δ_{cw} - thickness of the boundary layer with condensed water in m
A_{air} - air-side surface of the tube and fin in one cell in m^2
ϑ_{bl} - surface temperature of the boundary layer in °C
ϑ^*_w - equivalent surface temperature of the wall (tube and fin) in °C.

The equivalent surface temperature of the wall combines tube temperature and fin temperature

$$\vartheta^*_w = \vartheta_{air} \cdot \frac{A_{fin}}{A_{air}} \cdot (1 - \eta_{fin}) + \vartheta_w \cdot \frac{A_{freetube} + \eta_{fin} \cdot A_{fin}}{A_{air}}, \tag{2.6}$$

where: A_{fin} - surface of a fin in m^2
η_{fin} - fin efficiency coefficient in -
$A_{freetube}$ - free surface of the tube in m^2 where $A_{freetube} = A_{air} - A_{fin}$.

2.4 Boundary layer zone

The boundary layer zone represents the condensed water around the tube and fin. It is assumed that the thickness of this zone on the tube is equal to the thickness on the fin as shown in figure 2.2. The thickness varies in dependency on the condensing and evaporating moisture mass flow. The maximum thickness of the boundary layer zone is fixed at a default value (e. g. 0.1 mm).

If the boundary layer reaches its maximum the waste condensing moisture drips down. It is assumed that the dripping water does not influence the tubes and fins situated below.

If the conditions turn completely the water of the boundary layer evaporates within the time. This process stops when the thickness of the boundary layer is zero. In that case, the surface temperature of the boundary layer is equal to the air-side temperature of the wall (tube) and the cell works in dry mode.

The temperature of the boundary layer zone is calculated in steady state as follows

$$\begin{aligned} &\alpha_{air} \cdot A_{air} \cdot (\vartheta_{air} - \vartheta_{bl}) + \dot{m}_{cw} \cdot (h_{ev} + c_{p,wv} \cdot \vartheta_{air} - c_{p,cw} \cdot \vartheta_{bl}) = \\ &\dot{m}_{ew} \cdot (h_{ev} + c_{p,wv} \cdot \vartheta_{bl} - c_{p,cw} \cdot \vartheta_{bl}) + \frac{\lambda_{cw}}{\delta_{cw}} \cdot A_{air} \cdot (\vartheta_{bl} - \vartheta^*_w), \end{aligned} \tag{2.7}$$

where: α_{air} - overall air-side heat transfer coefficient in W/(m^{2}K)
ϑ_{air} - air temperature in °C
$\dot{m}_{cw}$ - condensing moisture mass flow rate in kg/s
h_{ev} - enthalpy of evaporation in J/kg
$c_{p,wv}$ - specific heat capacity of water vapour in J/(kgK)
$c_{p,cw}$ - specific heat capacity of condensed water in J/(kgK)
$\dot{m}_{ew}$ - evaporating moisture mass flow rate in kg/s.

Equation (2.7) shows small differences between the condensing and evaporating moisture mass flow. It is assumed, that in case of evaporation the water of the boundary layer evaporates at the boundary layer temperature. The latent heat transfer is considered only. The

heating up process of the accrued water vapour from boundary layer temperature to air temperature (sensible heat transfer) is forced by the air side and is considered at the air-side zone.

Contrary to that, the heat transfer of condensing moisture mass flow consists of both sensible and latent parts in the boundary layer zone. The sensible cooling process can only be forced by the boundary layer. For that reason, it appears in equation (2.7).

The thickness of the boundary layer zone is determined by the condensing and evaporating moisture mass flow

$$\delta_{bl,n} = min\left[1E-4\,\mathrm{m}, max\left(0\,\mathrm{m}, \delta_{bl,n-1} + \frac{\int \dot{m}_{cw} d\tau}{\rho_{cw} \cdot A_{air}} - \frac{\int \dot{m}_{ew} d\tau}{\rho_{cw} \cdot A_{air}}\right)\right] \tag{2.8}$$

(2.9)

where: ρ_{cw} - density of the boundary layer water in kg/m^3

2.5 Air-side zone of a cell

The air-side zone of a cell is outside the boundary layer. It is influenced by air mass flow rate, flow temperature and humidity, sensible heat transfer to the boundary layer and evaporating moisture mass flow rate. It is assumed, that the air-side zone temperature and humidity are just like the leaving temperature and humidity and are calculated in steady state as follows

$$\begin{aligned} \alpha_{air} \cdot A_{air} \cdot (\vartheta_{air} - \vartheta_{bl}) =& \dot{m}_{da,in} \cdot (c_{p,da} \cdot \vartheta_{air,in} + x_{in} \cdot (h_{ev} + c_{p,wv} \cdot \vartheta_{air,in})) \\ & - \dot{m}_{da,in} \cdot (c_{p,da} \cdot \vartheta_{air} + x_{in} \cdot (h_{ev} + c_{p,wv} \cdot \vartheta_{air})) \\ & + \dot{m}_{ew} \cdot (c_{p,wv} \cdot \vartheta_{bl} - c_{p,wv} \cdot \vartheta_{air}), \end{aligned} \tag{2.10}$$

where:
- $\dot{m}_{da,in}$ - dry air mass flow rate into the cell in kg/s
- $c_{p,da}$ - specific heat capacity of dry air in J/(kgK)
- $\vartheta_{a,in}$ - entering air temperature in °C
- x_{in} - humidity ratio of entering air in kg/kg

The model of the air-side zone assumes that the whole air mass flow entering the cell reaches the temperature ϑ_{air}. After that, a moisture mass flow may cool down further and condense in case of condensing mode. The released energy is transferred to the boundary layer zone.

In opposite to that, in evaporating mode the evaporating moisture mass flow is mixed with the entering air. The leaving humidity ratio is calculated by

$$m_{da,cell} \cdot \frac{\partial x_{air}}{\partial \tau} = \dot{m}_{da,in} \cdot (x_{in} - x_{air}) + \dot{m}_{ew} - \dot{m}_{cw} \tag{2.11}$$

where: $m_{da,cell}$ - dry air mass in the cell in kg.

The air-side heat transfer coefficient α_{air} is determined by the Nusselt number for arbitrary bodies, see equation (2.2). The Nusselt number is a superposition of a laminar and turbulent Nusselt number along 1 tube

$$Nu_{air,1t} = 0.3 + \sqrt{Nu^2_{lam,air,1t} + Nu^2_{turb,air,1t}}, \tag{2.12}$$

$$Nu_{lam,air,1t} = 0.664 \cdot Re^{1/2}_{air} \cdot Pr^{1/3}_{air} \tag{2.13}$$

$$Nu_{turb,air,1t} = 0.037 \cdot \frac{Re^{0.8}_{air} \cdot Pr_{air}}{1 + 2.443 \cdot Re^{-0.1}_{air} \cdot \left(Pr^{2/3}_{air} - 1\right)} \tag{2.14}$$

(2.15)

where: $Nu_{lam,air,1t}$ laminar air-side Nusselt number along 1 tube
$Nu_{turb,air,1t}$ turbulent air-side Nusselt number along 1 tube.

and a geometrical factor f_{air} that depends on the number of serial connected tubes and the distances between the serial and parallel connected tubes as well as the outside diameter of the pipe and the geometry of the fins

$$Nu_{air} = \begin{cases} Nu_{air,1t} \cdot f_{air} & \text{if } N_s \geq 10 \\ Nu_{air,1t} \cdot \left[1 + (f_{air} - 1) \cdot \left(\frac{N_s - 1}{9}\right)^{0.25}\right] & \text{if } N_s < 10. \end{cases} \tag{2.16}$$

2.6 Condensing moisture mass flow

The condensing moisture mass flow results from the FICK's law and may simplified be written in the form

$$\dot{m}_{cw} = \beta \cdot A_{air} \cdot \left(\rho_{da,air} \cdot x_{air} - \rho_{da,bl} \cdot x_{s,bl}\right), \tag{2.17}$$

where:
- β - mass transfer coefficient of water vapour in air in m/s
- $\rho_{da,air}$ - density of dry air with air-side air temperature in kg/m^3
- $\rho_{da,bl}$ - density of dry air with boundary layer temperature in kg/m^3
- $x_{s,bl}$ - saturated humidity ratio of boundary layer temperature in kg/kg.

The condensing moisture mass flow has an enormous impact on the heat transfer of the air side and the boundary layer. That's why it is necessary to linearise the mass flow concerning the temperature.

Considering equation (2.11) in steady state, substitution of x_{air} in (2.17), and separation of $\dot{m}_{cw}$ to one side one yields

$$\dot{m}_{cw} = \frac{\beta \cdot A_{air} \cdot \dot{m}_{da,in}}{\beta \cdot A_{air} \cdot \rho_{da,air} + \dot{m}_{da,in}} \cdot \left(\rho_{da,air} \cdot x_{in} - \rho_{da,bl} \cdot x_{s,bl}\right). \tag{2.18}$$

The evaporating moisture mass flow rate is neglected because evaporation and condensation may not occur at the same time.

The entering humidity ratio represents an input that cannot be influenced. On the other hand, the saturated humidity ratio depends on the boundary layer temperature and can be linearised

$$x_{s,bl,n} = x_{s,bl,n-1} + \left.\frac{\partial x_{s,bl}}{\partial \vartheta_{bl}}\right|_{n-1} \cdot (\vartheta_{bl,n} - \vartheta_{bl,n-1}) \,, \tag{2.19}$$

where:
- n - current time in -
- $n-1$ - last time in -
- $\frac{\partial x_{s,bl}}{\partial \vartheta_{bl}}$ - first derivative of saturated curve with respect to temperature.

2.7 Evaporating moisture mass flow

The evaporating moisture mass flow may be treated in the same manner like the condensing moisture mass flow

$$\dot{m}_{ew} = \beta \cdot A_{air} \cdot (\rho_{da,bl} \cdot x_{s,bl} - \rho_{da,air} \cdot x_{air}) \,, \tag{2.20}$$

The evaporating moisture mass flow has an enormous impact on the heat transfer the boundary layer and a smaller one on the air-side zone. That's why it is necessary to linearise the mass flow concerning the temperature.

Considering equation (2.11) in steady state, substitution of x_{air} in (2.20), and separation of $\dot{m}_{ew}$ to one side one yields

$$\dot{m}_{ew} = \frac{\beta \cdot A_{air} \cdot \dot{m}_{da,in}}{\beta \cdot A_{air} \cdot \rho_{da,air} + \dot{m}_{da,in}} \cdot (\rho_{da,bl} \cdot x_{s,bl} - \rho_{da,air} \cdot x_{in}) \,. \tag{2.21}$$

The condensing moisture mass flow rate is neglected because evaporation and condensation may not occur at the same time.

The entering humidity ratio represents an input that cannot be influenced. On the other hand, the saturated humidity ratio depends on the boundary layer temperature and can be linearised according to equation (2.19).

PART II.
Heating Water System

Chapter 1 Introduction

This specification describes several comparative test cases for a hot water system which are dedicated to validate HVAC simulation software. It was developed within the International Energy Agency (IEA) programs: Solar Heating and Cooling (SHC) Task 34 and Energy Conservation in Building and Community Systems (ECBCS) Annex 43.

The tests are designed for testing the capability of building energy simulation programs to predict the performance of the mechanical equipment of buildings including their control systems.

Input data for simulation are provided in separate files as part of this specification.

Chapter 2 Overall test description

2.1 General

The tests are based on a hot water system as shown at Figure 2-1

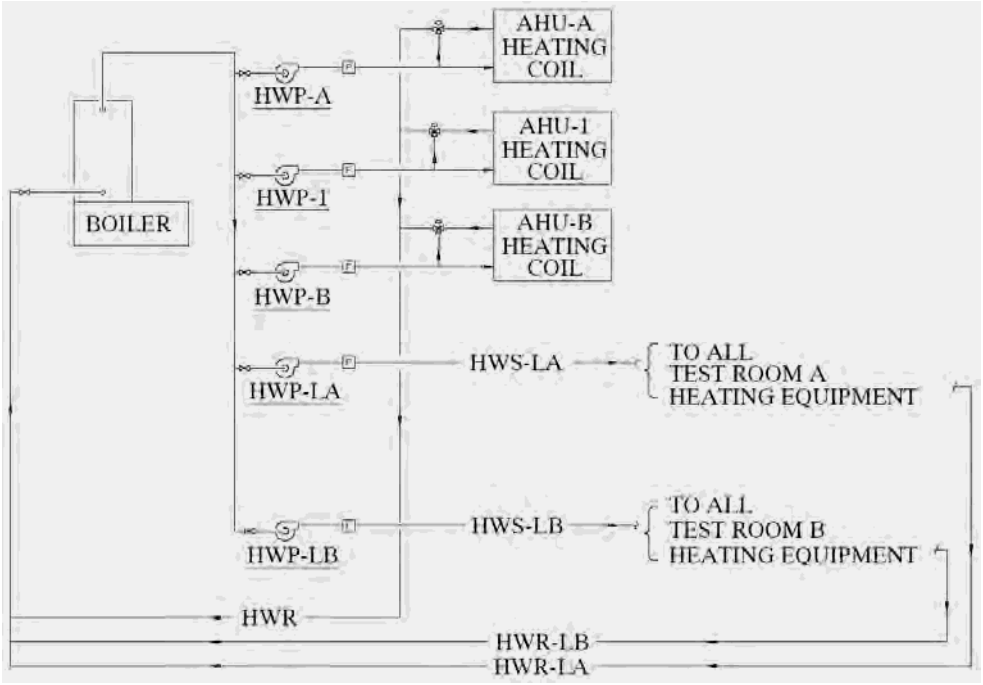

Figure 2-1 Simplified heating water piping schematic

The system consists of:

- A Gas fired condensing boiler
- Three heating coils located inside 3 different air-handling units
- Hydraulic network including circulating pumps and mixing valves

and is used to serve heating loads of an air conditioning system (AHU-Air Handling unit) as depicted in Figure 2-2.

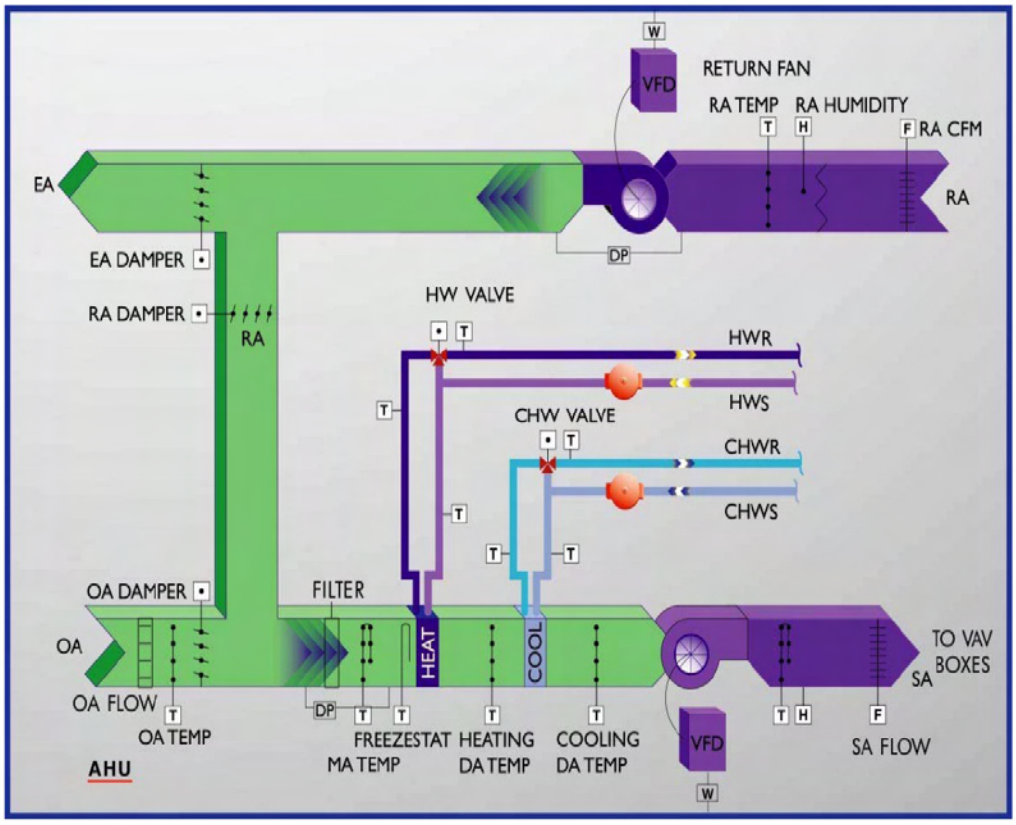

Figure 2-2 Schematic plot of the AHU system with measuring points

This system is installed at the Energy Resource Station located at Ankeny, Iowa (USA). Further details about the test facility are available at http://www.energy.iastate.edu/ers/. A lot of physical data and detailed information about the mechanical system required to setup a simulation model is available via the Iowa Energy Center FTP site. This site is a limited access, password protected site. Nevertheless the ERS staff would be able to provide detailed information to interested parties in response to any requests.

The idea behind this heating water system test case is as follows: For the validation of the simulation programs it should be possible to focus on the behaviour of the main components as well as have a look at the operation of the whole system. That is why the test case consists of three separate exercises as summarized in Table 2-1.

Table 2-1 Heating water system test case summary

# of exercise	Object of exercise	Comments
1	Condensing Boiler	- A comparative test - An empirical test
2	Heating coil	- A comparative test - An empirical test
3	Hydraulic network	No tests specifications provided but a description of the system

Some additional information about parameters and inputs required to run the simulations are given in the following chapters. There are also instructions on how to report the outputs of the simulation.

2.2 Physical properties of hot water

The heat transfer fluid for the heating water system is water with very low concentrations of chemical treatment additives to inhibit corrosion. An antifreeze solution is not used in the heating water circulation system.

2.3 Accuracy of data measurements

2.3.1 Heating Water temperature

Temperatures are measured using Resistance Temperature Detectors (RTD) with accuracy according to Industrial standard. The accuracy of the temperature sensors used for the heating water testing is the same as the Chilled Water Testing (see PART I of this report).

2.3.2 Heating water flow rate

The heating water flow rate was measured using electromagnetic flowmeters. The accuracy of the electromagnetic flow meter is +/- 0.5% of reading.

2.3.3 Measuring error compensation

Experimental data will be slightly corrected if necessary to get a nearly equalized energy balances (energy at air side = energy at water side). The corrections should be within the known error bands of sensors and will be documented for all input and output data used for validation of simulation models.

2.3.4 General

Modellers will be provided with both raw experimental data and corrected data that gives the opportunity to perform independent error compensation.
Further information on sensors and equipment can be get from the before mentioned ERS ftp site.

Chapter 3 Boiler

3.1 General

The gas fired hot water condensing boiler used for this validation task is designed for application in any closed loop hydraulic system. It relates the energy input directly to the fluctuating system load by an energy input modulation. When return water temperatures are low enough the boiler is capable to discharge flue gas condensate.
Some general information about the boiler can be taken from Table 3-1.

Table 3-1 Hot water boiler general data

Boiler	
Manufacturer	Aerco International
Boiler Unit Model	KC-1000-GWB
Boiler Type	Natural Gas Fired Hot Water
Fuel Consumption	28.32 m³/h @37.25 MJ/m³ 1,000 CFH gas @ 1,000 BTU/CF
Maximum Capacity	272,6 kW (930,000 BTU/hr)
Water Volume	87.1 l (23 gallons)
Control Range	10 … 104°C (50 … 220°F)
Water Flow Range	1.6 … 9.5 l/s (25 … 150 gpm)
ASME Working Pressure	1.04 MPa (150 psig)
Rated AFUE	92% (Efficiency varies with entering water temperature and firing rate)

A minimum water flow rate is required for proper and stable control operation whereas the maximum flow rate is to prevent erosion. Rated AFUE from the above-mentioned table is the Annual Fuel Utilization Efficiency and measures the amount of heat actually delivered to the heating system compared to the amount of fuel that must be supplied to the furnace. The AFUE refers only to the boiler's fuel efficiency, not its electricity usage.
From the outside views of the boiler given in Figure 3.1 the conditions of installation at the ERS can be seen. Air for combustion is drawn from outside (direct venting) as shown before. Figure 3-2 gives an inside view of the boiler to better understand functionality.
The description of the related items can be found in Table 3-2.

Figure 3-1 Outside views of the boiler

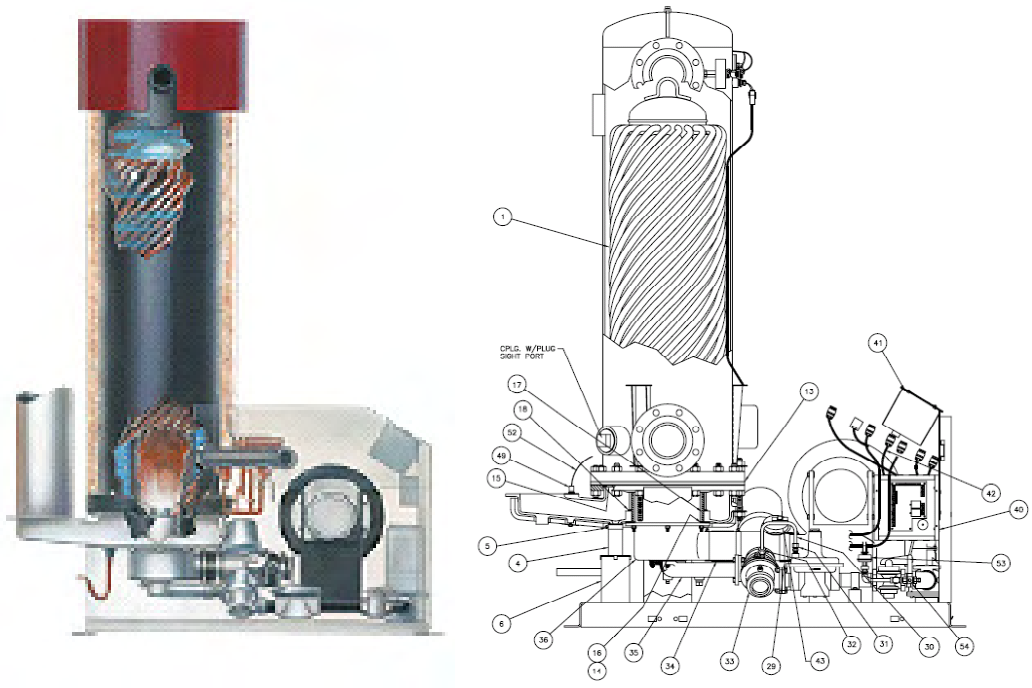

Figure 3-2 Inside view of the boiler (http://www.aerco.com)

Table 3-2 Description of boiler components

Item	Description
1	Heat exchanger assembly
6	Condensate cup assembly
17	Combustion chamber liner
23	Blower
29	Blower to air va, inlet house
33	Air / fuel valve
35	Gas inlet pipe
36	Burner assembly
41	Control box assembly

3.2 Burner

The boiler is equipped with a burner materially characterized by the information given at Table 3-3. With a modulation turn down ratio of 14:1 the capacity of the burner at the minimum firing rate is approximately 7% of full capacity.

Table 3-3 Burner general data

Burner	
Type	Nozzle Port Injection
Modulation Turn Down Ratio	14:1 Turndown
Capacity at Minimum Firing Rate	7% Capacity

3.3 Physical properties

3.3.1 Heating water system

The heat transfer fluid for the heating water system is water with very low concentrations of chemical treatment additives to inhibit corrosion. An antifreeze solution is not used in the heating water circulation system.

3.3.2 Natural gas

The properties of natural gas which have to be used for calculations are to be taken from Table 3-4.

Table 3-4 Properties of natural gas

Properties [Units/Conditions]	Value
Carbon content [mass %]	73.3
Hydrogen content [mass %]	23.9
Oxygen content [mass %]	0.4
Methane concentration [Volume %]	80 - 99
Ethane concentration [Volume %]	2.7 - 4.6
Nitrogen concentration [Volume %]	0.1 - 15
Carbon dioxide concentration [Volume %]	1 - 5
Sulphur concentration [ppm, mass]	<5

Methane number	69 - 99
Octane number	120 -130
Relative molar mass	17 - 20
Relative density [@15°C / 1 bar]	0.72 - 0.81
Stoichiometric air/fuel ratio [mass]	17.2
Lower heating/calorific value [MJ/kg]	38 - 50
Stoichiometric lower heating value [MJ/kg]	2.75
Flammability limits [lambda]	0.7 - 2.1

3.4 Performance data

The energy output of the boiler depends on return temperature and firing rate. By using efficiency curves depicted at Figure 3-3 the output of the boiler for a given energy input can be estimated.

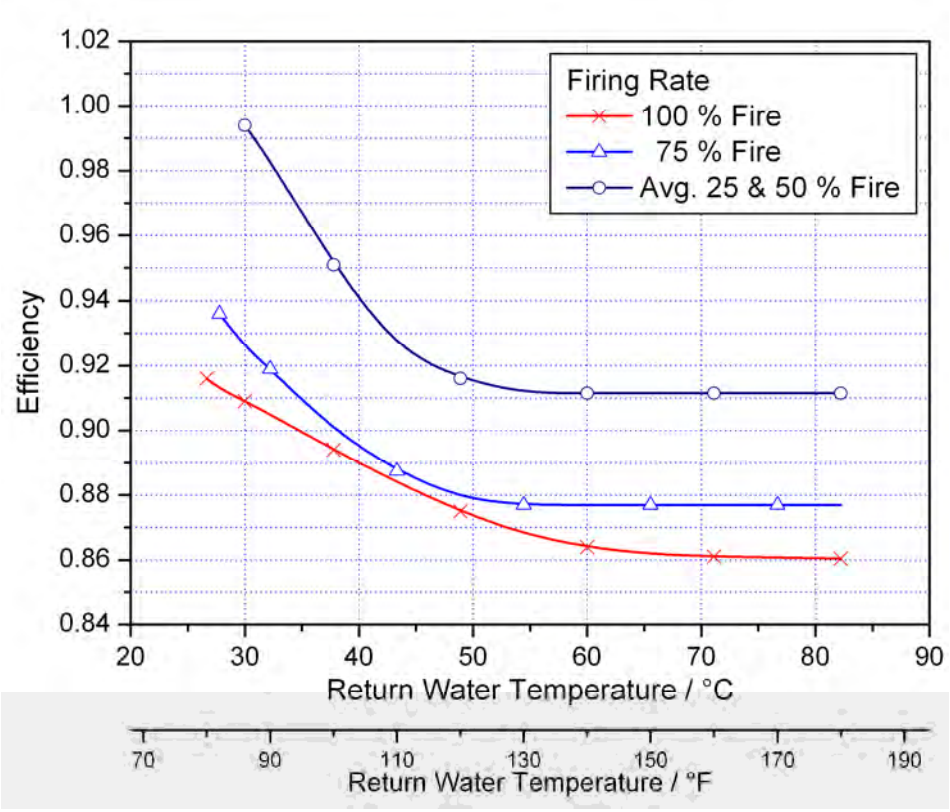

Figure 3-3 Efficiency Curves

3.5 Control

The electronics of the boiler offers selectable modes of operations. In the context of this validation task only control functions

- constant temperature internal set point and
- indoor/outdoor reset

will be covered. A state-of-the-art PID control system is employed to dynamically respond to changes throughout the heating plant operation. System temperatures can be controlled with virtually no overshoot, droop or short cycling. A header temperature of ±1.1°C (2°F) is assured during continual plant operation. All water sensors are internal to the boiler unit.

3.6 Electrical consumption

The total electrical consumption for the hydraulic boiler includes the combustion air fan (blower) as well as the control panel, air/fuel valve and safety shut off valve. There are three levels of electrical consumption:

1. Standby/Ready
   where the only electrical usage would be to power the control panels, lights, relays, etc
2. Prefire/Purge
   upon call for heating, the hydraulic boiler goes thru a transitional phase and performs pre-fire check diagnostics to prove pressure and temperature safeties are satisfied, initiates a purge mode where the electric forced draft combustion air fan activates and clears or purges the combustion chamber prior to igniting the new charge of natural gas. This short (one minute or less) transitional phase would have variations on the electrical power consumption as the control and valves are all active and the combustion air fan builds up power.
3. Firing
   while the hydraulic boiler is firing to satisfy the heating water load, the burner would modulate resulting in some minor fluctuations in electrical load. The combustion air fan operates continuously while the hydraulic boiler is firing - I believe the combustion air fan is constant speed/constant power, but I am not absolutely sure. A review of the electrical wattage data from the boiler should profile the above operating levels.

The combustion air fan has some variation in power. This is due to the modulation of the air/fuel valve. The air/fuel valve acts as a discharge damper on the combustion air fan to reduce the amount of combustion air flow while also modulating the gas flow to the burner. The combustion air fan speed is constant. As the firing rate of the boiler decreases, the volume of combustion air (and fuel) is reduced by the air/fuel valve. Consequently, the electrical power for the combustion air fan decreases. Table 3-5 contains total electric energy consumption recorded during a previous test with the boiler.

Table 3-5 Total electrical consumption for the hydraulic boiler

Status	Firing Rate	Power
Standby Mode	No call for heat, control panel only	27 W
Minimum Fire	10%	430 W
Mid Range Fire	64%	770 W
Full fire	100%	860 W

3.7 Boiler Comparative Test

3.7.1 Test configuration and overall goal

This comparative test focuses on the operation of the boiler system as described in the sections before. A schematic of the boiler system is depicted in Figure 3-4.

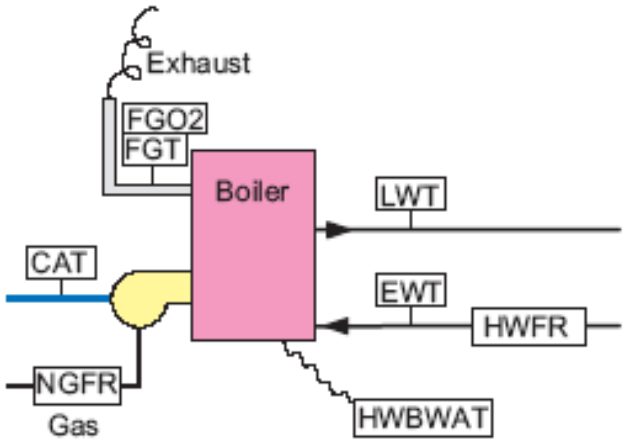

Figure 3-4 Scheme of the condensing boiler with measuring points

With regard to the boiler comparative test matrix (Table 3.6) two different strategies should be performed:

Supply water temperature set point depends on outside air temperature (cases HWB100-220). The dependency of supply water temperature set point on outside air temperature is according to Eq. (3.1). The return temperature entering the boiler is known and can be calculated using Eq. (3.2). Heating water flow rate is a constant.

$$T_{SP} = \max\left(\min\left(33^{\circ}C + \frac{18^{\circ}C - T_{OA}}{33\,K} \cdot 47\,K; 80^{\circ}C \right); 33^{\circ}C \right) \quad \textbf{(3.1)}$$

$$T_{R} = \max\left(\min\left(32^{\circ}C + \frac{18^{\circ}C - T_{OA}}{33\,K} \cdot 33\,K; 65^{\circ}C \right); 32^{\circ}C \right) \quad \textbf{(3.22)}$$

$$HWFR = 4.0\,l/s \quad \textbf{(3.3)}$$

Figure 3-5 shows heating water temperatures and heating water flow rate against outside air temperature.

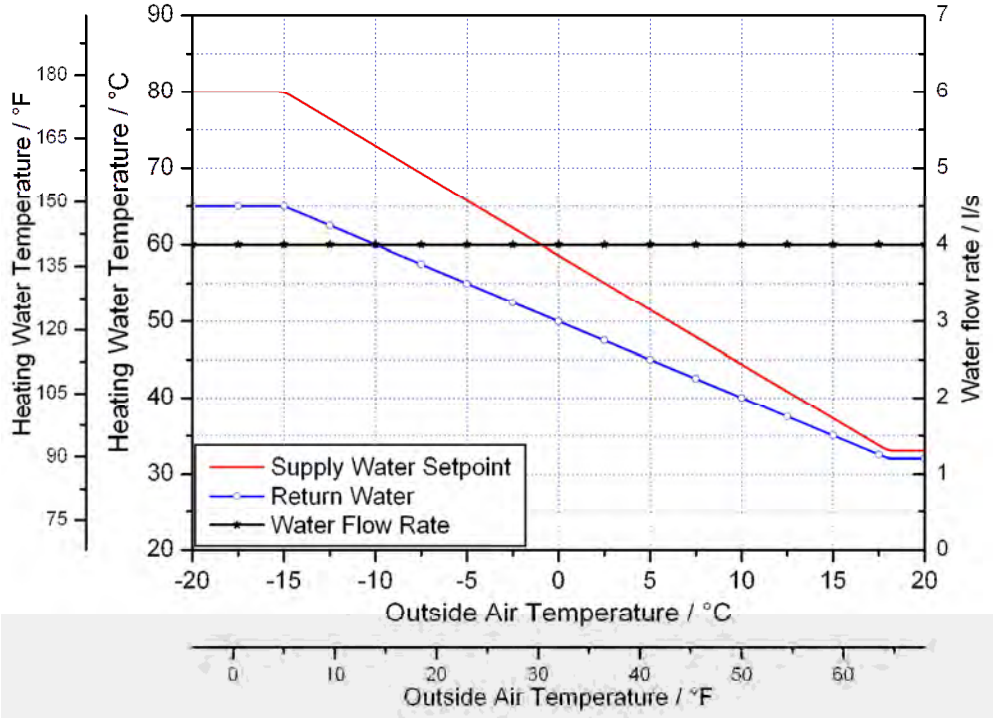

Figure 3-5 Supply water set point temperature, return water temperature and water flow rate for cases HWB 100-220

Supply water temperature set point is constant (cases HWB300-420) Supply water temperature set point is independent on outside air temperature fixed to a constant. The return temperature entering the boiler is known and can be calculated using Eq. (3.2). It is higher than return temperature used for cases HWB100-220 when supply water temperature set point depends on outside air temperature. Also heating water flow rate is changing. It can be calculated with Eq. (3.6).

$$T_{SP} = 80^{\circ}C \tag{3.4}$$

$$T_R = \max\left(\min\left(45^{\circ}C + \frac{18^{\circ}C - T_{OA}}{33\,K} \cdot 20\,K; 65^{\circ}C \right); 45^{\circ}C \right) \tag{3.5}$$

$$HWFR = 1.6\,l/s + \frac{18^{\circ}C - T_{OA}}{33\,K} \cdot 2.3\,l/s \tag{3.6}$$

Figure 3-6 shows heating water temperatures and heating water flow rate against outside air temperature.

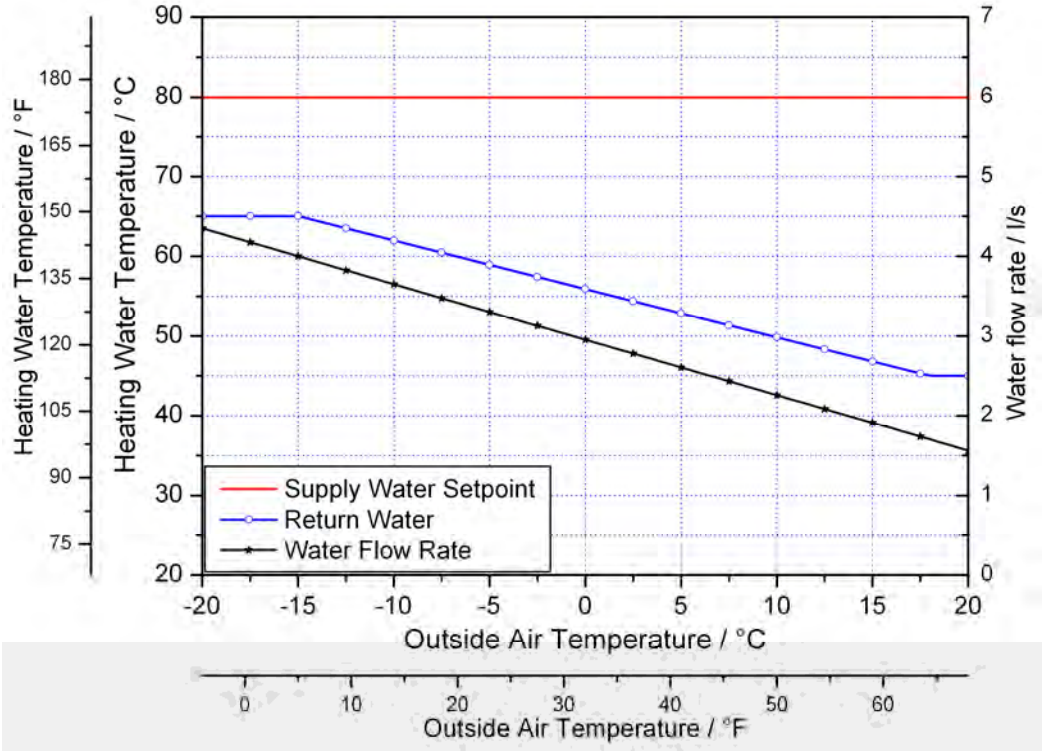

Figure 3-6 Supply water set point temperature, return water temperature and water flow rate for cases HWB 300-420

The temperature at the plant room is assumed to be 22°C.

3.7.2 Input Data

The outside air input conditions are taken from the Des Moines, Iowa TMY2 data set that is distributed as a part of this specification. Supply water temperature set point, return water temperature, and heating water flow rate are given by Eq. (3.1) to (3.6). Depending whether combustion air is taken from inside or outside a fixed room temperature of 25°C or outside air conditions have to be used respectively. The atmospheric pressure is set to 98.5 kPa.
The simulation time step should be chosen in a way that the full dynamic behaviour of the boiler model is preserved.
Table 3-6 gives an overview to all comparative tests.

Table 3-6 Boiler comparative test case matrix

Test Case	Configuration	Combust. Air	Condensing Boiler
HWB100	SPT=const HWFR=f(OA)	inside	Yes
HWB120			No
HWB200		outside	Yes
HWB220			No
HWB300	SPT=f(OA) HWFR=const	inside	Yes
HWB320			No
HWB400		outside	Yes
HWB420			no

3.7.3 Outputs

The following outputs are requested and should be submitted in a single file. Time step of the output data is 1 hour where values should be averaged.

Row	Shortcut	Description
1	Time	
2	OATEMP	Outside air temperature in °C
3	SPT	Supply temperature set point in °C
4	EWT	Boiler entering water temperature in °C
5	LWT	Boiler leaving water temperature in °C
6	HWFR	Heating water flow rate in l/s
7	HWBQLD	Boiler total thermal energy output in kW
8	HWBSTS	Boiler status in 0/1

9	HWBMod	Boiler Modulation in %
10	HWBeff	Boiler efficiency in %
11	NGFR	Natural gas flow rate in l/s
12	CAT	Combustion air temperature in °C
13	FGT	Flue gas temperature in °C
14	FG02	Flue Gas O2 Concentration in %
15	HWBWAT	Total electrical consumption of the boiler in W

3.8 Boiler Empirical Test

3.8.1 Test configuration and overall goal

The goal of this empirical test is to predict both heating loads as well as conditions of both air and water leaving the coil. Input data come from an experiment which was conducted at the ERS during February 21-28, 2006. Due to a system fault that occurred during the experiment data of February 26, are not available for further analysis. Simulation results will be compared to the measurements as well.

3.8.2 Data compensation

For boiler empirical test no data compensation was required. Thus no raw data are provided

3.8.3 Input Data

The following input data in a minute-by-minute time step for the 143 hr period February 21, 10 a. m. to February 28, 9:00 a.m. (excluding February 26th) are given in a single file HWBEmpInput1.txt:

Row	Shortcut	Description
1	Time	Month
2	Time	Day
3	Time	Hour
4	Time	Minute
5	SPT	Supply temperature set point in °C
6	EWT	Boiler entering water temperature in °C
7	HWFR	Heating water flow rate in l/s
8	CAT	Combustion air temperature in °C

3.8.4 Outputs

The following outputs also in minute-by-minute time steps are requested and should be submitted in a single file.

Row	Shortcut	Description
1	Time	
2	OATEMP	Outside air temperature in °C

3	SPT	Supply temperature set point in °C
4	EWT	Boiler entering water temperature in °C
5	LWT	Boiler leaving water temperature in °C
6	HWFR	Heating water flow rate in l/s
7	HWBQLD	Boiler total thermal energy output in kW
8	HWBSTS	Boiler status in 0/1
9	HWBMod	Boiler Modulation in %
10	HWBeff	Boiler efficiency in %
11	NGFR	Natural gas flow rate in m³/h
12	CAT	Combustion air temperature in °C
13	FGT	Flue gas temperature in °C
14	FG02	Flue Gas O2 Concentration in %
15	HWBWAT	Total electrical consumption of the boiler in W

Chapter 4 Heating Coil

4.1 Geometry

The high performance fin tube coil is an integral part of a central station air handling unit manufactured by Trane. It can be used for general purposes. The horizontal coil section operates as a full coil. It consists of a heating water single serpentine with 2 rows. Figure 4-1 shows an exterior view of the coil as well as directions of water and air flows.

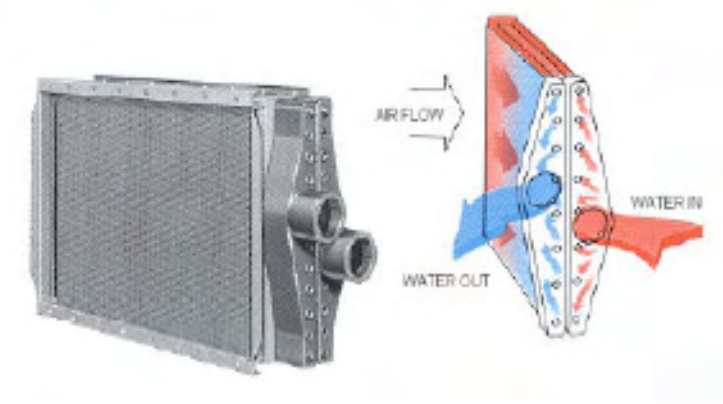

Figure 4-1 Standard water heating coil

Some general data about the coil can be taken from Table 4-1.
The given face area is the actual area. This may differ slightly from the nominal size due to rounding. The cast iron headers are brazed copper headers, extruded at tube-to-header joint for strength and low-resistance water flow.
Dimensions and sizes of the coil are given in Figure 4-2 with values C = 64.8 cm (25 1/2“), and D = 28.6 cm (11 1/4“). All dimensions are approximately.

4.2 Performance data

Information about the performance of the heating coil can be taken from the equipment submittal. However the submittal available for this heating coil only describes one operating state rated with ARI Standard 410[2]. From this single state again only limited knowledge about the full range of coil performance can be extracted. For this reason some experimental data are given additionally, that can be used to adjust the heating coil model.

[2] ARI Standard 410 for forced-circulation air-cooling and air-heating coils

Table 4-1 Heating coil general data

Heating Coil	
Manufacturer	Trane
Air Handling Unit Model	CLCH Size 06
Heating Coil Number	Trane Type "UW" coil
Heating Coil Type	Copper Tube / Aluminum Plate Fin
Heating Coil Header	Drainable Copper Header
Number of Passes / Rows	2 Rows / Standard Single Serpentine
Fin Spacing	384 Fins per meter (117 Fins per foot)
Finned Area	914 mm wide by 610 mm high (36 inches by 24 inches)
Coil Face Area	0.544 m² (30.3 ft²)
Tube Construction	Copper Tube – 1/2 " O.D.
Tube outside diameter	15.9 mm
Tube Wall Thickness	0.41 mm (0.016 inch)
Turbulators	none

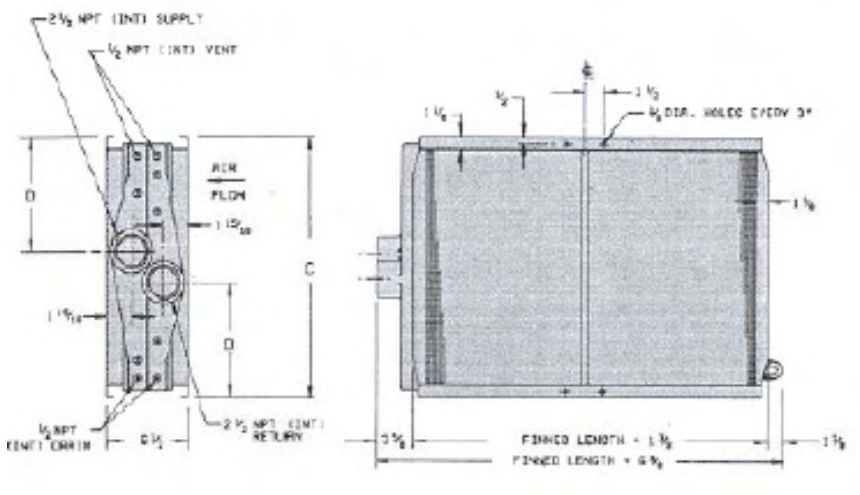

Figure 4-2 Heating coil dimension data

Figure 4-3 allows a look at the heating water coil header viewed from downstream of heating coil. Table 4-2 summarizes data from the manufacturer submittal.

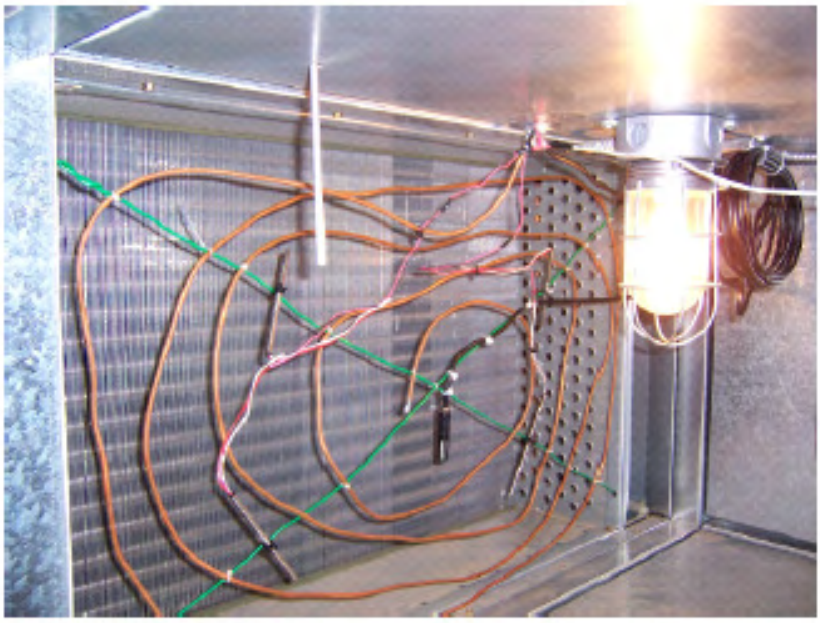

Figure 4-3 Photo of the heating coil taken from downstream side

Table 4-2 Heating coil performance data (Data marked with *) were calculated and are not part of the equipment submittal)

Heating Coil Performance		
Barometric pressure *)	kPa	101.3
Entering Air Temperature	°C Dry bulb	4.44
Entering Air Relative Humidity *)	%	50
Entering Air Moisture *)	kg/kg	0.00259
Entering Air Density *)	kg/m³	1.27
Leaving Air Temperature	°C Dry bulb	37.78
Leaving Air Moisture *)	kg/kg	0.0026
Leaving Air Density *)	kg/m³	1.13
Air Flow Rate at coil leaving air conditions *)	m³/h	5780

Air Pressure Drop	kPa	0.0498
Entering Liquid Temp.	°C	82.28
Leaving Liquid Temp.	°C	71.06
Liquid Flow	l/s	1.33
Liquid Pressure Drop	kPa	3.67
Total Heating Capacity	kW	61

The given coil rating is based on conditions as described in ARI-410. Values of entering temperatures as well as flow rates are within the ranges defined by the standard. The coil was provided with pure water. Performance data from Table 4-2 can thus be calculated as follows:

$$\begin{aligned}\dot{Q} &= \dot{m} c_p \Delta\vartheta \\ &= \dot{V} \rho c_p \Delta\vartheta \\ &= 1.33 \frac{l}{s} \cdot 974 \frac{kg}{m^3} \cdot 4.19 \frac{kJ}{kgK} \cdot \left(82.3^\circ C - 71.1^\circ C\right) \\ &= 61\,kW\end{aligned} \tag{4.1}$$

The air flow rate, which was originally not known from the manufacture's submittal, can be estimated from given temperatures and coil capacity. For that purpose the air density of coil entering air was calculated at an air relative humidity ratio of 50 %.
The air flow rate is then

$$\begin{aligned}SAFR &= \frac{\dot{Q}_{tot}}{\rho\, c_p \left(T_{in} - T_{out}\right)} \\ &= \frac{61\,kW}{1.133\,kg/m^3 \cdot 1.006\,kJ/kgK \cdot \left(37.78^\circ C - 4.44^\circ C\right)} \\ &= 5776\,m^3/h\end{aligned} \tag{4.2}$$

4.3 Heating Coil test logic

The validation of a heating coil model in the context of this IEA task should be done according to the overall test logic that is shortly described in this chapter.
There have been three tests created for cooling coil validation purposes:

- Comparative test (chapter 4.5),
- Empirical test I (chapter 4.6).

The tests should be run step-by-step beginning with the comparative test. The idea behind this consecutive process is to start with a simulation model that has been calibrated based on some general information about coil performance that was available from the manufacturer submittal and to end with a model calibrated based on detailed experimental data collected from coil operation in a real plant. From the manufacturer submittal only one single point of coil performance was known (see Table 4-2) that roughly represents a full load coil performance. No more information about part load performance is available for running the comparative tests. Thus the modeller has to run the comparative tests with their own standard model part load approach that can considerably differ between models. The additional calibration points provided to the modeller when running the empirical tests should allow calibrating the model with respect to both part load performance as well as real installation and operating conditions (i.e. physical properties of the chilled water) that differ from the performance conditions found in the manufacturer submittal.

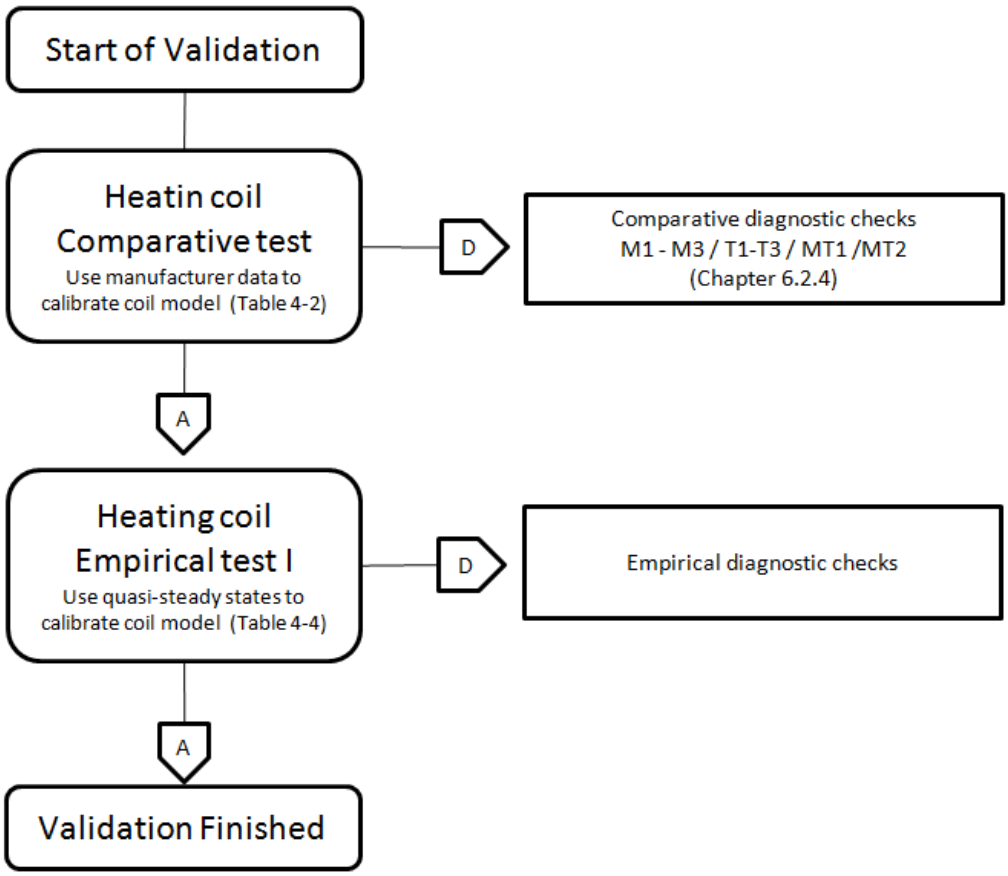

Abbreviations: A=Agree; D=Disagree

Figure 4-4 Heating coil overall test logic

The overall heating coil test logic is illustrated in Figure 4-4. It also refers to some diagnostic checks that can help to find the probable cause of errors, i.e. when the model predictions do not agree with results neither from other models nor from experimental data. Those diagnostic checks are described in Chapter 6.2.4.
Since there is no truth standard (as for instance an analytical solution would be) it is up to the modeller to decide whether their results are in agreement for a specific test case, or whether there is disagreement that requires further examination of their program or inputs.

4.4 Physical properties of hot water

The heat transfer fluid for the heating water system is water with very low concentrations of chemical treatment additives to inhibit corrosion. An antifreeze solution is not used in the heating water circulation system.

4.5 Heating Coil Comparative Test

4.5.1 Test configuration and overall goal

The goal of this comparative test is to predict both heating loads as well as operational conditions of water entering the coil required to maintain a given set point of discharge air temperature. The prediction horizon is limited to the months October - April. Outside air conditions are taken from a TMY2 data set.
There are in general two different configurations that can be used to control the performance of the coil:

1. Variable water flow rate with a constant water inlet temperature (m_{var})
   The performance of the heating coil is controlled by changing the mass flow rate through the coil. A schematic of the hydraulic circuit is depicted in Figure 4-5. The total water flow rate is the flow rate through the heating coil plus the flow rate in the by-pass line. The maximum water flow rate entering the coil is 1.33 l/s, which represents the nominal value, Table 4-2. This case also describes the built-in situation of the heating coil at the ERS and for this reason it could be used for an empirical validation of the heating coil model (see Chapter 4.5).

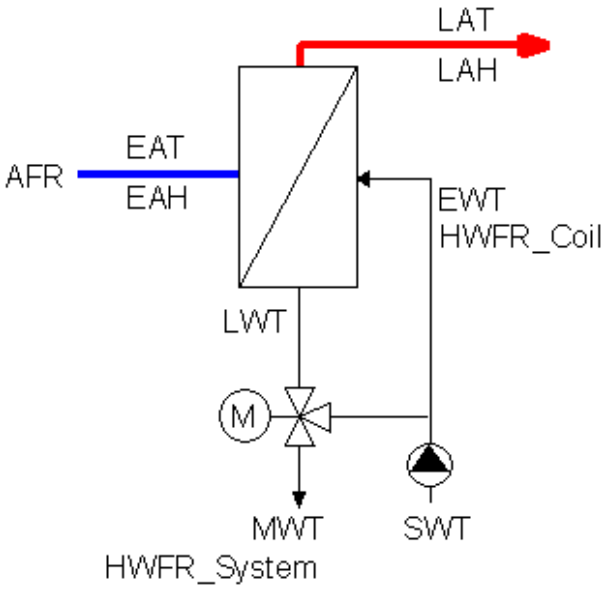

Figure 4-5 Heating coil with variable water flow rate

Constant water flow rate with a variable water inlet temperature (Tvar) The performance of the heating coil is controlled by changing the coil entering water temperature. A schematic of the hydraulic circuit is depicted in Figure 4-6. The coil entering water temperature results from the mixture of supply water temperature and return water temperature.

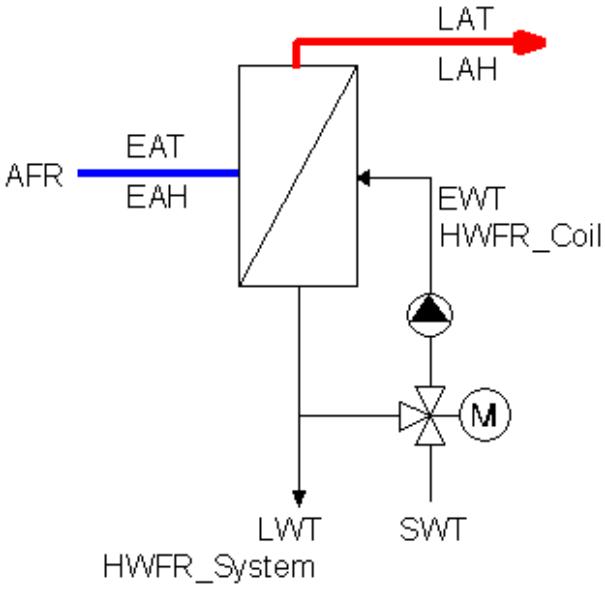

Figure 4-6 Heating coil with constant water flow rate

The constant water flow rate entering the coil is fixed at 1.33 l/s, which represents the nominal value, Table 4-2.

This comparative test does not take into consideration the action of the control valve and focuses on the operation of the heating coil only. If there is no heating load the hot water pump has to switch off.
For further Information on input data air side and water side please refer to chapter 4.4.2.

4.5.2 Input Data

The outside air side input conditions are taken from the Des Moines, Iowa TMY2 data set that is distributed as a part of this specification. The TMY2 weather is used for the comparative test only. It is average weather data for Des Moines, Iowa and does not represent any actual specific on-site weather data for the ERS.
It is assumed that there is 100% outside air with no re-circulated air through the coil. Furthermore two different systems have to be taken into consideration regarding the air flow rate:

1. Constant air volume (CAV)
   The air flow rate is constant all the time at 4500m³/h.
2. Quasi-Variable air volume (VAV)
   The air flow rate switches between 2000m³/h (6 p.m. to 7 a.m.) and 5000m³/h (7 a.m. to 6 p.m.); see Figure 4-7.

The time schedule given refers to the time of the day. A daylight saving effect was not taken into account. Air flow rate is defined at supply air conditions. As the impact of the supply fan on air side conditions is neglected supply air conditions (temperature, humidity) are identical to coil leaving air conditions.

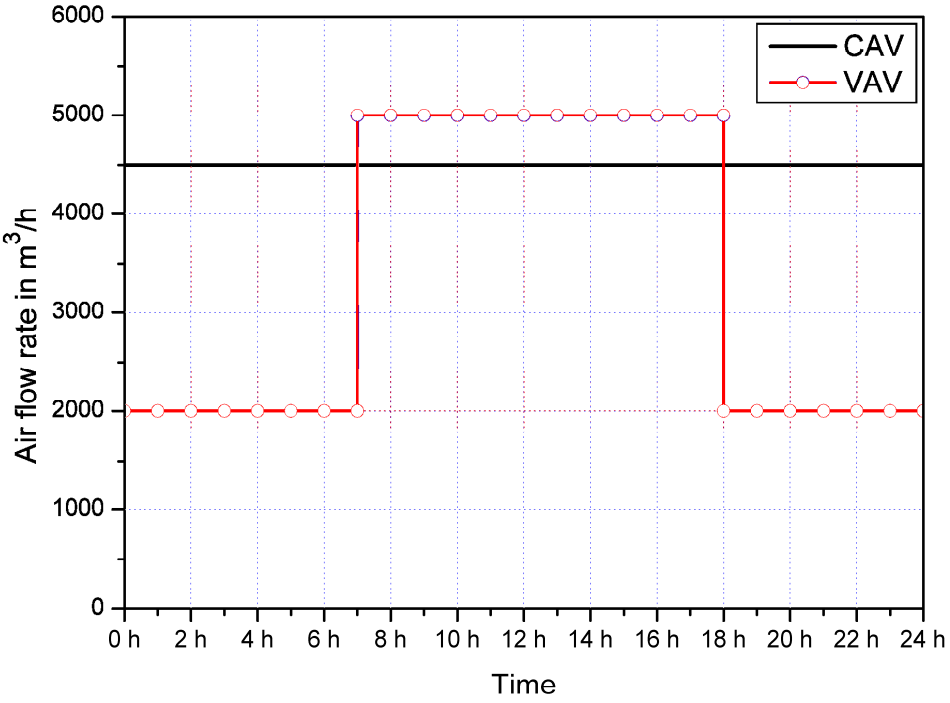

Figure 4-7 Air flow rate daily profiles

The discharge air set point temperature is fixed at also two different levels:

1. Low set point temperature
   The discharge air temperature is set to 13°C (55.4°F)
2. High set point temperature
   The discharge air temperature is set to 18°C (64.4°F)

Both set points do not vary and are thus to be held as a constant for the entire simulation period.

The heating water supply temperature (SWT) is constant at 70°C (158°F). Heating water supply temperature and entering water temperature are identical if the coil operates with a variable water flow rate.

The heating water does not contain any additives and can be assumed to be pure water.
The atmospheric pressure inside the coil is set to 98.5 kPa.

4.5.3 Outputs

The following outputs in hourly time steps for period October 1 to April 30 are requested and should be submitted in a single file.

Row	Shortcut	Description
1	Time	
2	EAT	Entering air temperature, dry bulb in °C
3	EArH	Entering air relative humidity in %
4	EAH	Entering air humidity in kg/kg
5	LAT	Discharge/Leaving air temperature, dry bulb in °C
6	LArH	Discharge/Leaving air relative humidity in %
7	LAH	Discharge/Leaving air humidity in kg/kg
8	AFR	Air flow rate in m³/h
9	EWT	Heating water coil entering temperature in °C
10	LWT	Heating water coil leaving temperature in °C
11	HWFR	Heating water flow rate through the coil in l/s
12	UA	Overall UA-Value of the coil in kW/K
13	HLT	Total heating load in kW
14	HLS	Sensible heating load in kW

The overall UA-Value of the coil has to be calculated from sensible cooling load and mean logarithmic temperature difference ΔT_m using Eq.(4.3).

$$UA = \frac{CLS}{\Delta T_m} \tag{4.3}$$

Mean logarithmic temperature difference ΔT_m is defined by Eq.(4.4)

$$\Delta T_m = \frac{(LWT - EAT) - (EWT - LAT)}{ln\frac{LWT - EAT}{EWT - LAT}} \tag{4.4}$$

Please refer to the right case number according to the test case matrix Table 4-3.

Table 4-3 Heating coil comparative test case matrix

Test Case	Config	Air Flow	DCA-ST
HX100	m_{var}	CAV	13
HX120			18
HX200		VAV	13
HX220			18
HX300	T_{var}	CAV	13
HX320			18
HX400		VAV	13
HX420			18

4.6 Heating Coil Empirical Test

4.6.1 Test configuration and overall goal

The goal of this empirical test is to predict both heating loads as well as conditions of both air and water leaving the coil. Input data come from an experiment which was conducted at the ERS during February 21-28, 2006. Due to a system fault that occurred during the experiment data of February 26, are not available for further analysis. Simulation results will be compared to the measurements as well.

In addition to the nominal performance data of Table 4-2 which are from the manufacturer submittal two quasi-steady state points given in Table 4-4 can be used to calibrate the heating coil model. The steady state points have been derived from experimental data.

For the empirical test of the heating coil the impact of the valve on the performance of the coil is eliminated and the hot water flow rate entering the coil $HWFR_{Coil}$ is given. Hot water flow rate through the coil has not been measured but was calculated based on the total flow rate from mass and energy balances at the three-way valve (Figure 4-5) by Eq.(4.3)

$$HWFR_{Coil} = HWFR_{System} \frac{MWT - EWT}{LWT - EWT} \quad \textbf{(4.5)}$$

Table 4-4 Quasi-steady state points based on experimental data for the empirical test (Data marked with *) have been calculated and are not part of the recorded experimental data)

Heating Coil Performance		#1	#2
Barometric pressure*)	kPa	99.0	97.7
Entering Air Temp.	°C	0.1	16.2
Leaving Air Temp.	°C	25.1	23.0
Leaving Air Moisture	kg/kg	0.00187	0.00389
Leaving Air Density*)	kg/m³	1.16	1.15
Air Flow Rate at coil leaving air conditions*)	m³/h	5470	5460
Entering Liquid Temp.	°C	69.3	69.9
Leaving Liquid Temp.	°C	50.9	37.4
Mixing Liquid Temp.	°C	62.2	67.9
Liquid Flow*)	l/s	0.59	0.09
Total Heating Capacity*)	kW	44.1	12.2

4.6.2 Data compensation

For heating coil empirical test only temperature of entering air had to be compensated according to Figure 4-8. Entering air is a mixture of approximately 90% outside air and 10% return air. There is no humidity data of entering air recorded but calculated based on moisture content and temperature of coil leaving air assuming that moisture content of air does not change when passing the heating coil.

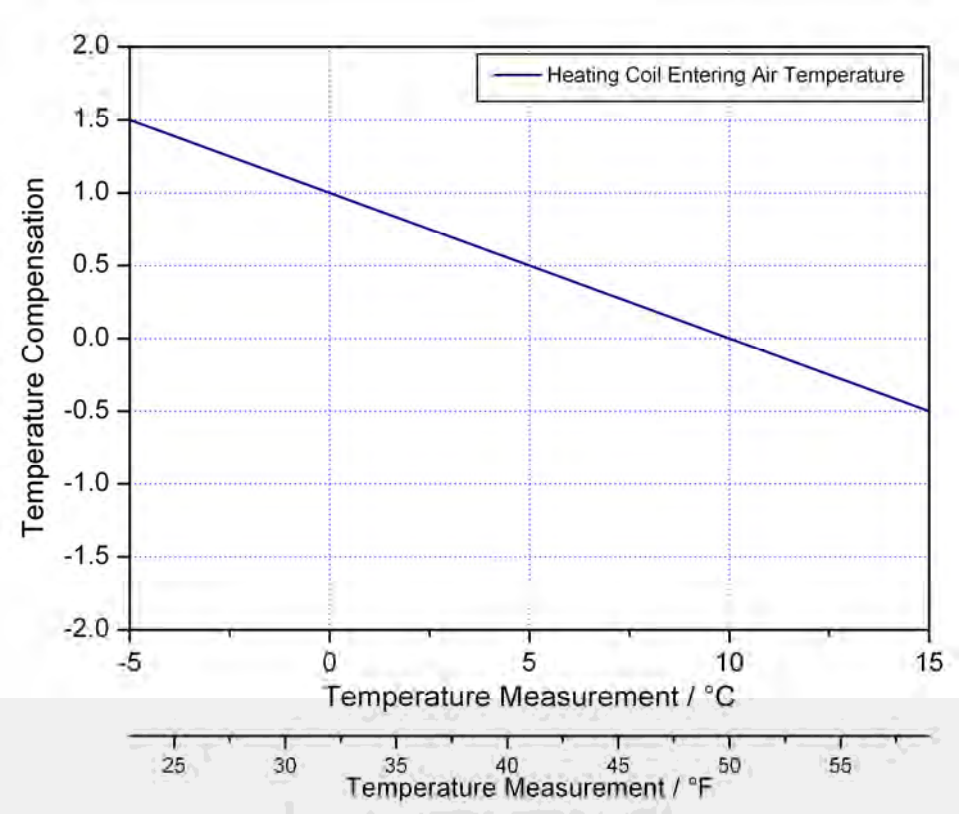

Figure 4-8 Heating coil empirical test - Compensation of temperature measurements

The file HCEmpInput1_raw.txt contains uncompensated raw experimental data where also leaving water temperature, mixed water temperature and hot water system flow rate are given instead of heating water flow rate through the coil.

4.6.3 Input Data

The test configuration corresponds to a coil with variable water flow as described in Figure 4-5. The water entering temperature is nearly constant at 69°C (156°F) as to be seen from Figure 4-9.

For this test the heat transfer fluid is pure water.

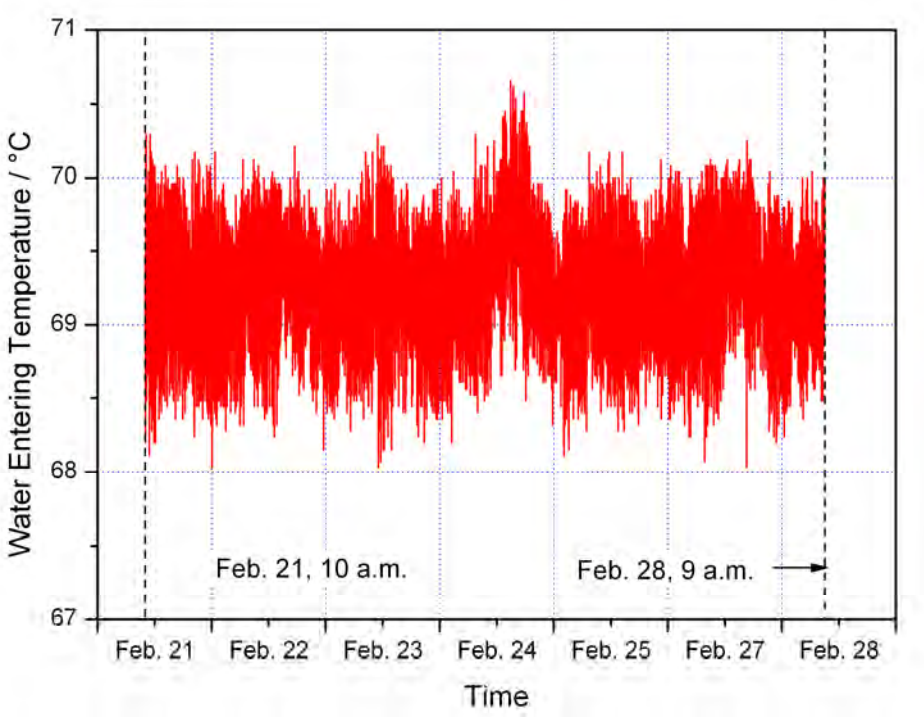

Figure 4-9 Water temperature entering the Heating coil

The following input data in a minute-by-minute time step for the 143 hr period February 21, 10 a. m. to February 28, 9:00 a.m. (excluding February 26th) are given in a single file HCEmpInput1.txt and should be used for validation purposes:

Row	Shortcut	Description
1	Time	Month
2	Time	Day
3	Time	Hour
4	Time	Minute
5	EAT	Coil Entering air temperature, dry bulb in °C
6	EArH	Coil Entering air relative humidity in %
7	AFR	Air flow rate in m³/h
8	AFR_T	Temperature of given air flow rate AFR
9	AFR_rH	Relative Humidity of given air flow rate AFR
10	EWT	Coil entering heating water temperature in °C
11	$HWFR_{Coil}$	Heating water flow rate through the coil in l/s
12	BARP	Barometric pressure in kPa

4.6.4 Outputs

The following outputs also in minute-by-minute time steps are requested and should be submitted in a single file.

Row	Shortcut	Description
1	Time	
2	EAT	Entering air temperature, dry bulb in °C
3	EArH	Entering air relative humidity in %
4	EAH	Entering air humidity in kg/kg
5	LAT	Discharge/Leaving air temperature, dry bulb in °C
6	LArH	Discharge/Leaving air relative humidity in %
7	LAH	Discharge/Leaving air humidity in kg/kg
8	AFR	Air flow rate in m³/h
9	EWT	Heating water coil entering temperature in °C
10	LWT	Heating water coil leaving temperature in °C
11	HWFR	Heating water flow rate through the coil in l/s
12	UA	Overall UA-Value of the coil in kW/K
13	HLT	Total heating load in kW
14	HLS	Total heating load in kW

Chapter 5 Hydraulic network, water circuit

5.1 General

In fact the hydraulic network investigated is only a small part of a more complex heating water system (see chapter 2). The view to only this network keeps the exercise manageable. Figure 5-1 shows a detailed 3D-drawing of the heating water system which is provided in the file 3d_piping_AHU_A_HWS.dwg.

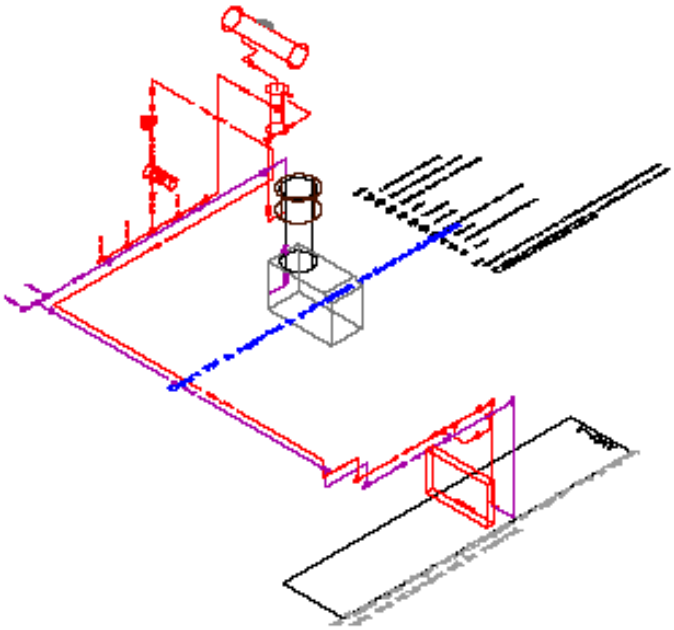

Figure 5-1 Hydronic3D

The modeling of the hydraulic system can either be done in a detailed way based on the information taken from the 3D-drawing or in a simplified way based on the scheme in Figure 2-1. Figure 5-2 shows the hydraulic connections and the mixing valve directly ahead the coil.

Figure 5-2 Hydraulic connections with mixing valves (heating and cooling coil)

5.2 Valve

The control valve is VG7842Nt+ three-way mixing valve manufactured by Johnson Controls. The k_V -value is 10m³/h with regard to a pressure drop of 100 kPa (the C_V –value is 11.6 gpm with regard to a pressure drop of 1 psi). Further technical information about the valve can be taken from Table 5-1. Figure 5-3 shows valve body and flow directions.

Table 5-1 Valve general data

Valve general data	
Product family	Cast Bronze
Body type	Three-Way Mixing
Flow characteristics	Linear
Nominal Size	DN25 (1in)
Kv (Cv)	10.0 m³/h (11.6 gpm)
Valve Stroke	13 mm (1/2 in)
Close off	1.255/1.469 MPa (182/213 psi)
Max. Operating Diff. Pressure	0.241 MPa (35 psig)
Leakage	0.01 % of Maximum Flow

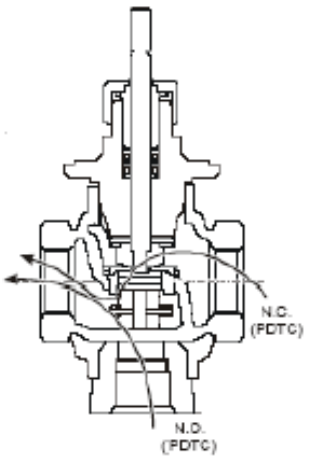

Figure 5-3 Valve body and flow directions

5.3 Pump

It is a Bell & Gossett 1 1/2 AA Series 60® maintenance-free in-line pump. Figure 5-4 shows an exterior view of the pump.

The performance of the pump can be either seen from the original equipment submittal in Figure 5-5 or from the extracted lines of total head and pump efficiency in Figure 5-6.

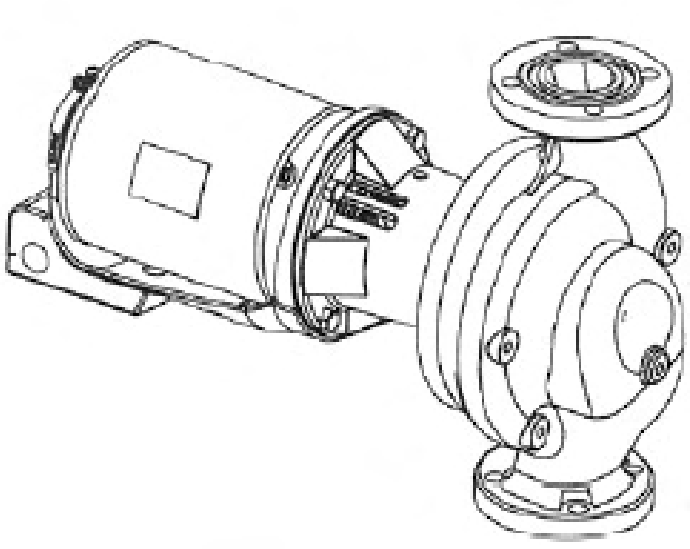

Figure 5-4 Hot water pump

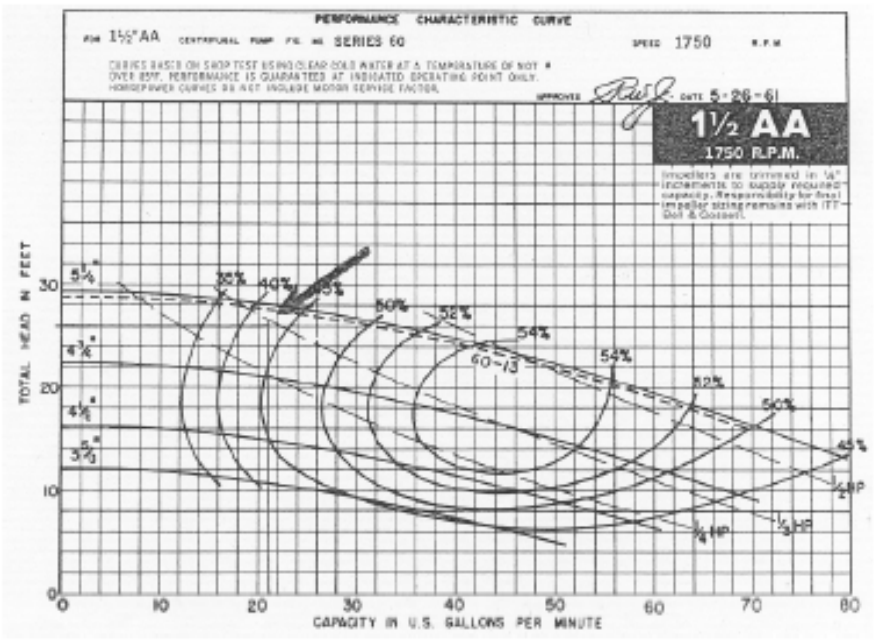

Figure 5-5 Pump performance curve

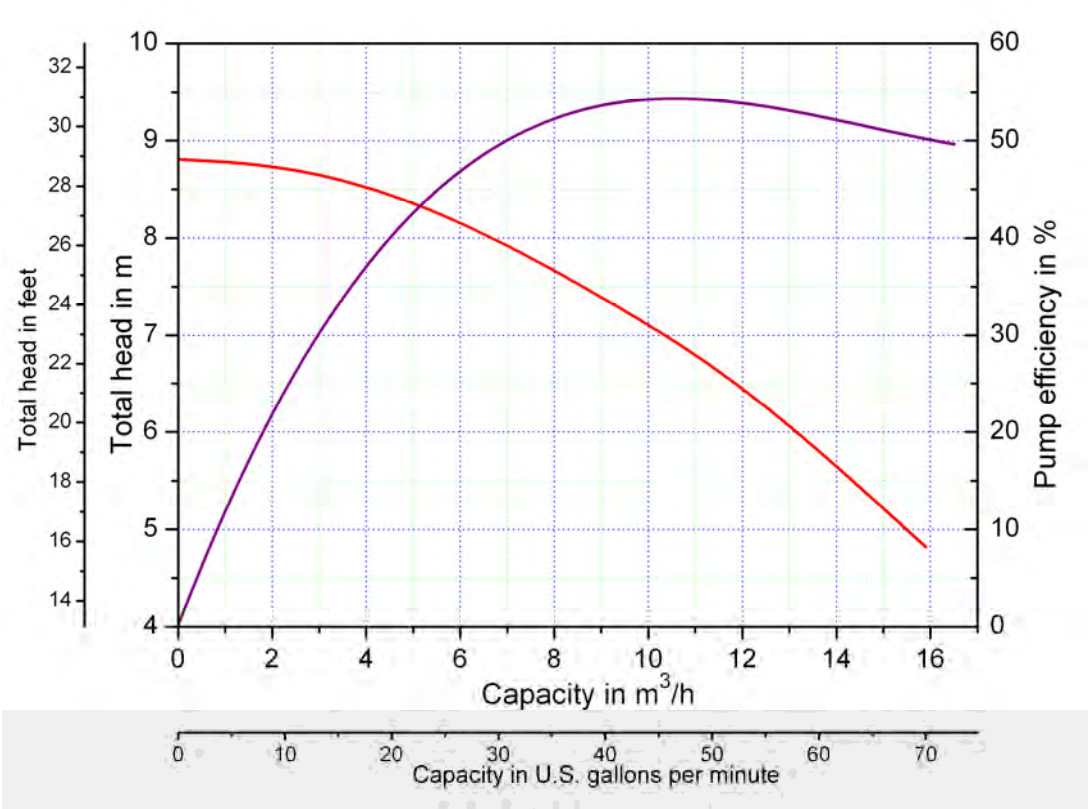

Figure 5-6 Heating water pump performance curve extract

5.4 Heating Coil

The high performance fin tube coil is part of a central station air handling unit manufactured by Trane. It can be used for general purposes. The horizontal coil section operates as a full coil. It consists of a chilled water single serpentine with 2 rows. Figure 4-1 shows an exterior view of a standard coil as well es directions of water and air flows.
Hydraulic performance data of the coil can be taken from Table 5-2. These data are valid only for a pure water fluid.

Table 5-2 Hydraulic performance data of the heating coil

Heating Coil Performance	
Fluid	Water
Flow Rate	1.33 l/s
Entering Fluid Temp.	4.44 °C
Leaving Fluid Temp.	37.78 °C
Pressure Drop	3.67 kPa

5.5 Boiler

In addition to the information given in chapter 3 Table 5-3 contains data that are related to the hydraulic performance of the boiler.

Table 5-3 Boiler data related to the hydraulic system

Boiler	
Water Volume	87.1 l (23 gallon)
Water Flow Range	1.6 … 9.5 l/s (25 … 150 gpm)
Rated Water Flow Rate	6.31 l/s (100gpm)
Water pressure drop @ rated flow rate	0.07m (0.23 ft)

5.6 Hydraulic System Empirical Test

5.6.1 Test configuration

The goal of this empirical test is to predict performance of a chilled water pump installed in a hydraulic network as depicted at Figure 5.1. The main impact on the operation of the pump is due to the changing valve lift. Input data come from an experiment which was conducted at the ERS during February 21-28, 2006. Due to a system fault that occurred during the experiment data of February 26, are not available for further analysis. Simulation results will be compared to the measurements as well. In addition the chilled water by-pass flow rate is requested for comparative analysis.

The heat transfer fluid for the heating water system is water with very low concentrations of chemical treatment additives to inhibit corrosion. An antifreeze solution is not used in the heating water circulation system.

5.6.2 Input data

There are only two input data: valve lift and heating water mixed temperature. These input data are provided in the file named HydrEmpInput1.txt.

Row	Shortcut	Description
1	Time	Month
2	Time	Day
3	Time	Hour
4	Time	Minute
5	HWT	Heating Water Temperature °C
6	HWCFDBK	Heating Water Mixing Valve Position % open.

The atmospheric pressure is assumed to be 98 kPa.

5.6.3 Data compensation

For the hydraulic empirical test no data compensation was required. Thus no raw data are provided

5.6.4 Outputs

The following outputs are requested and should be submitted in a separate file. The heating water by-pass flow rate will be used for comparative diagnosis only.

Row	Shortcut	Description
1	Time	
2	HWP	Pressure head of the pump in m
3	HWFR	Heating water flow rate in l/s
4	HWPWAT	Heating water pump power in W
5	HWFRB	Heating water by-pass flow rate in l/s

Chapter 6 Results

6.1 Boiler

6.1.1 Comparative Test

The comparative boiler test has been implemented by two programs only as specified in Table 6-1.

Table 6-1 List of participants of the comparative boiler test

Name of the program	Modeler
TRNSYS-TUD	Technical University Dresden, Germany
EES	Université de Liège, Belgium

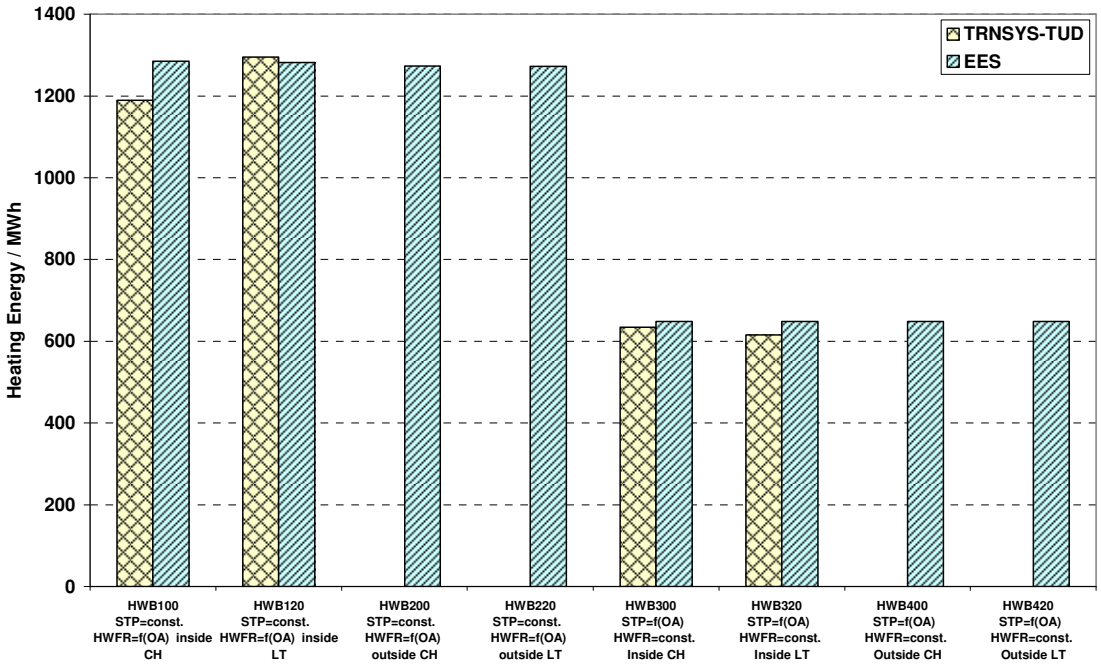

Figure 6-1 Boiler Comparative Test - Total Heating Energy

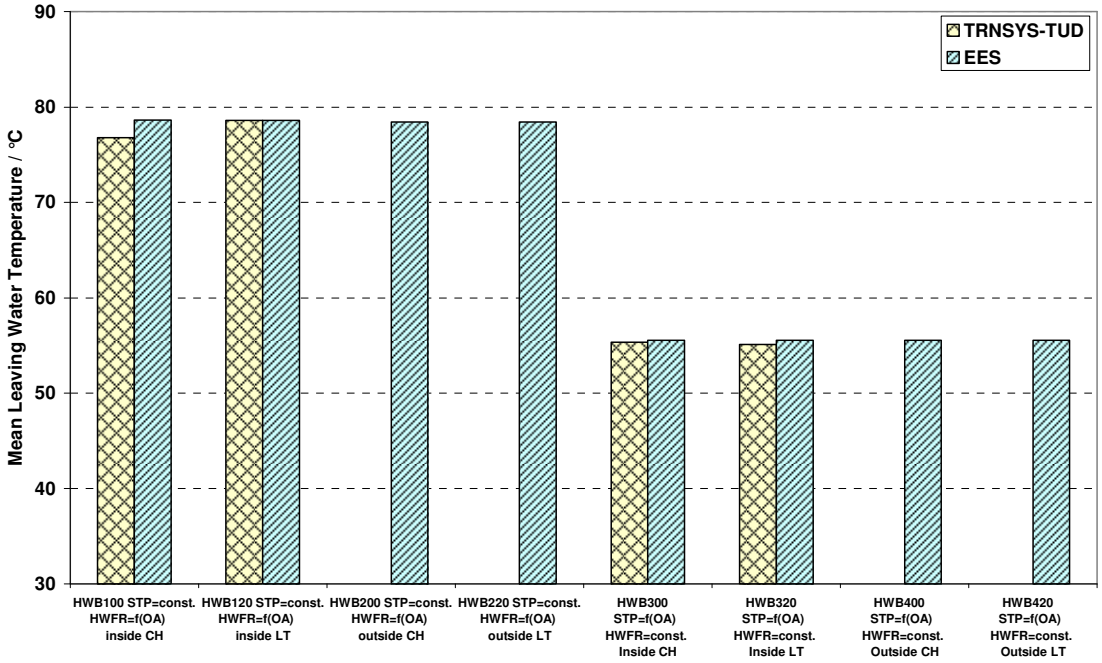

Figure 6-2 Boiler Comparative Test - Mean Leaving Water Temperature

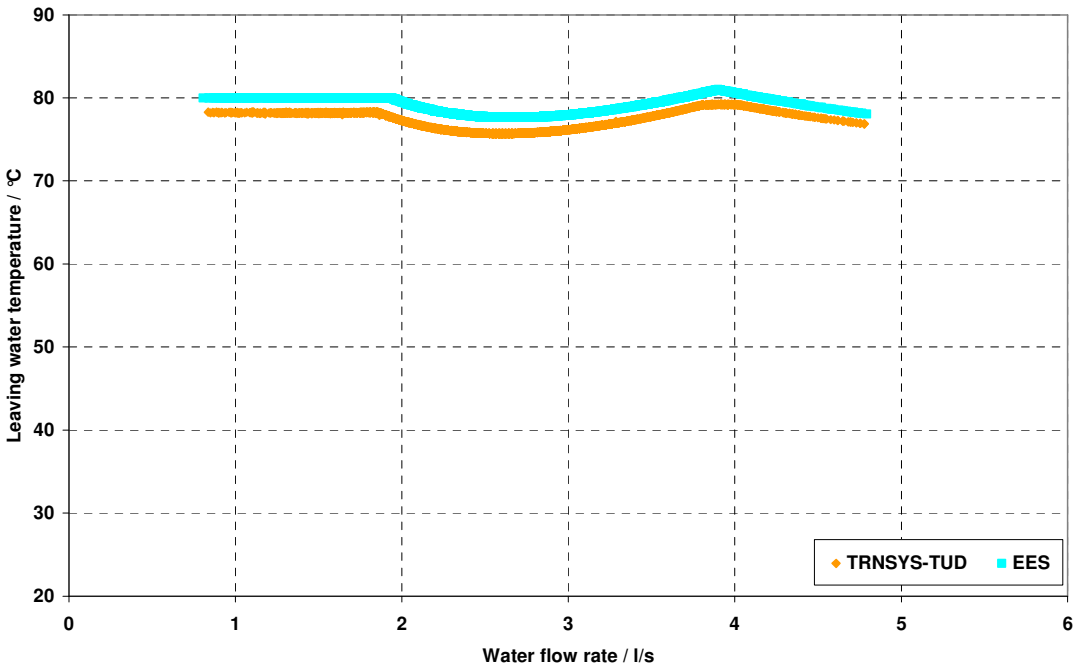

Figure 6-3 Boiler Comparative Test HWB100 - Leaving Water Temperature over water flow rate (diagnostic check B6)

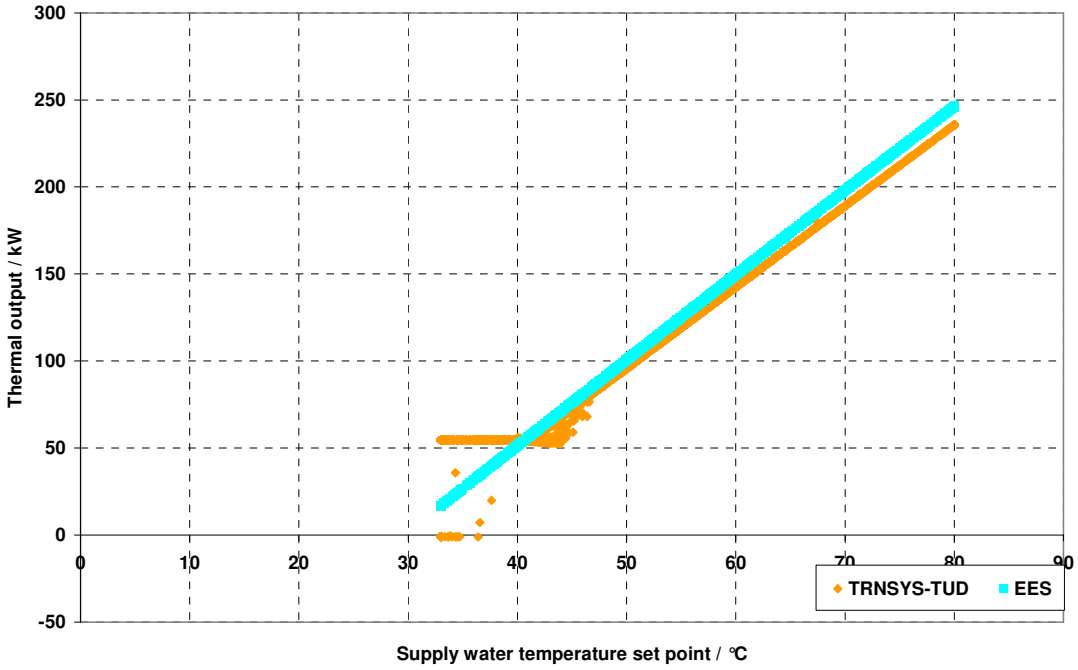

Figure 6-4 Boiler Comparative Test HWB300 – Thermal output over supply water temperature set point (diagnostic check B7)

6.1.2 Diagnosing Results

Boiler comparative test case does not represent truth standard. For that reason it is up to the modeller to decide whether a program successfully passes the test or not. Normally a program is qualified when its results are within the range of other validated programs and its results are in agreement for a specific test case. When simulation results do not agree with others the diagnostic logic flow diagram displayed in Figure 6-5 may help to detect the probable cause of such disagreement.

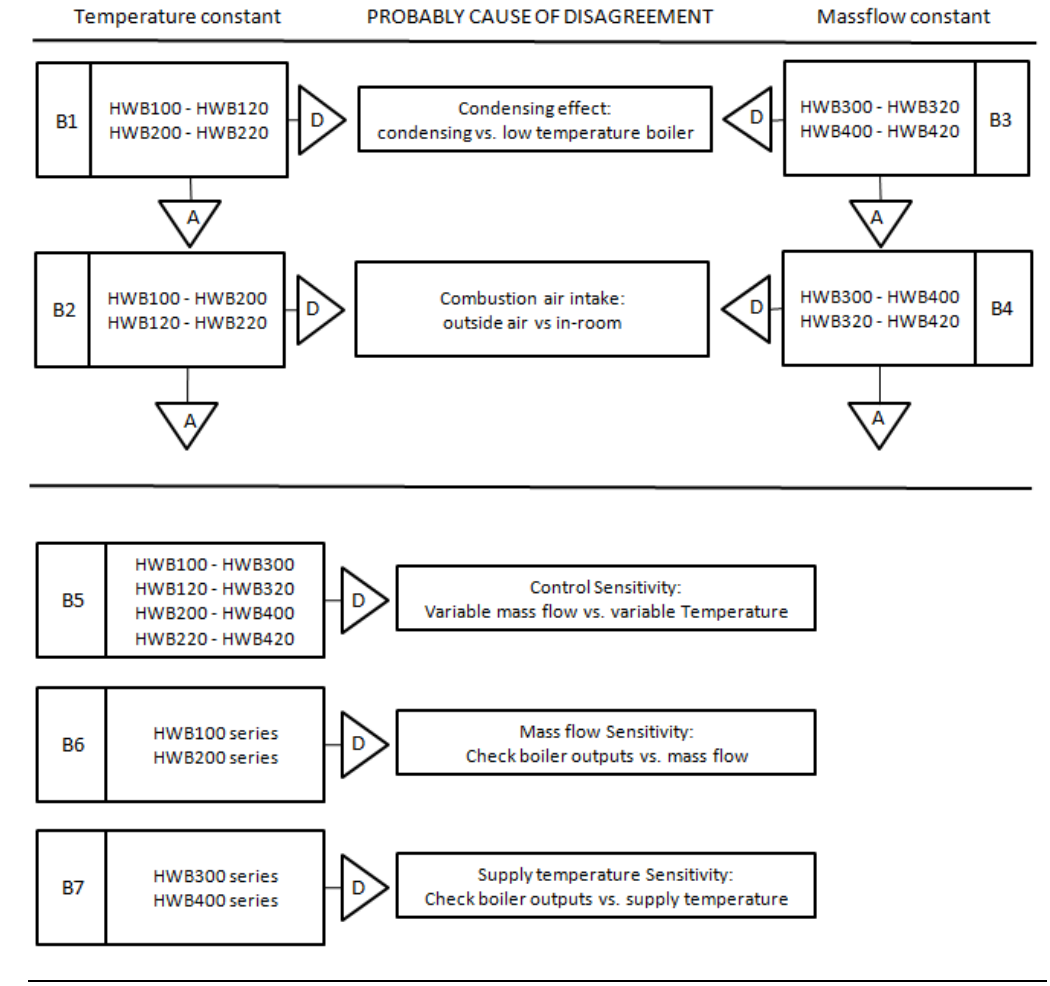

Figure 6-5 Hot water boiler comparative test cases diagnostic logic flow diagram B1-B7

Two examples for checks B6 and B7 are given in Figure 6-3 and Figure 6-4.

6.1.3 Empirical Test

The empirical boiler test has been run by two programs only specified in Table 6-2.

Table 6-2 List of participants of the empirical boiler test

Name of the program	Modeler
TRNSYS-TUD	Technical University Dresden, Germany
EES	Université de Liège, Belgium

The boiler has to keep leaving water temperature – it is the system supply water temperature - at a given level that is defined by the supply water temperature set point. For the empirical test this set point was set constant to 71.1°C (160 F). In fact supply water has a temperature of 69.5°C (157 F). Nevertheless models ware able to predict right boiler leaving temperature by taking into account both boiler control and internal heat transfer mechanisms. Figure 6-6 shows leaving water temperatures.

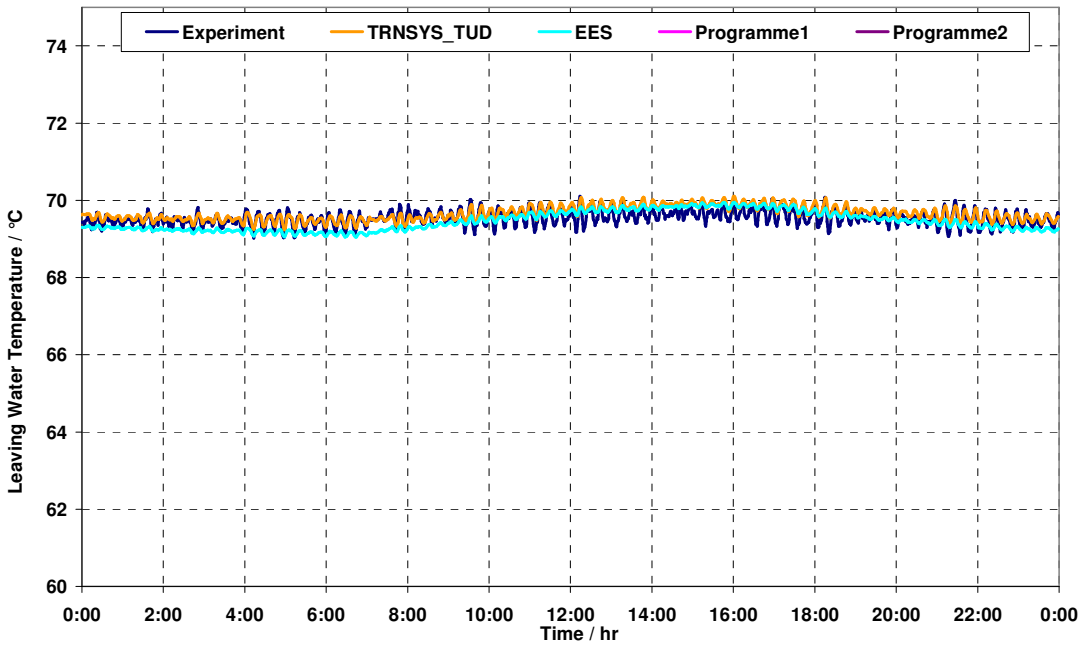

Figure 6-6 Boiler empirical test - Leaving water temperature

Since water flow rate and boiler entering temperature were given as inputs to the modeler the heating output of the boiler should be predicted correctly when also boiler leaving temperature is in accordance to the experiment. The averaged daily boiler heating load has a swing that varies the load between 80 and 130kW, see Figure 6-7. Simulation results deviate

approximately up to 5 kW from experimental data. Also boiler electric power is well predicted by the EES model. Some bigger deviations can be observed for natural gas flow predictions – here the difference is ±1m³ which is 7…10% of the recorded real site data. The flue gas temperature calculated by the EES model not only shows very big differences against the experiment it also is nearly constant whereas real data vary according to the load profile.

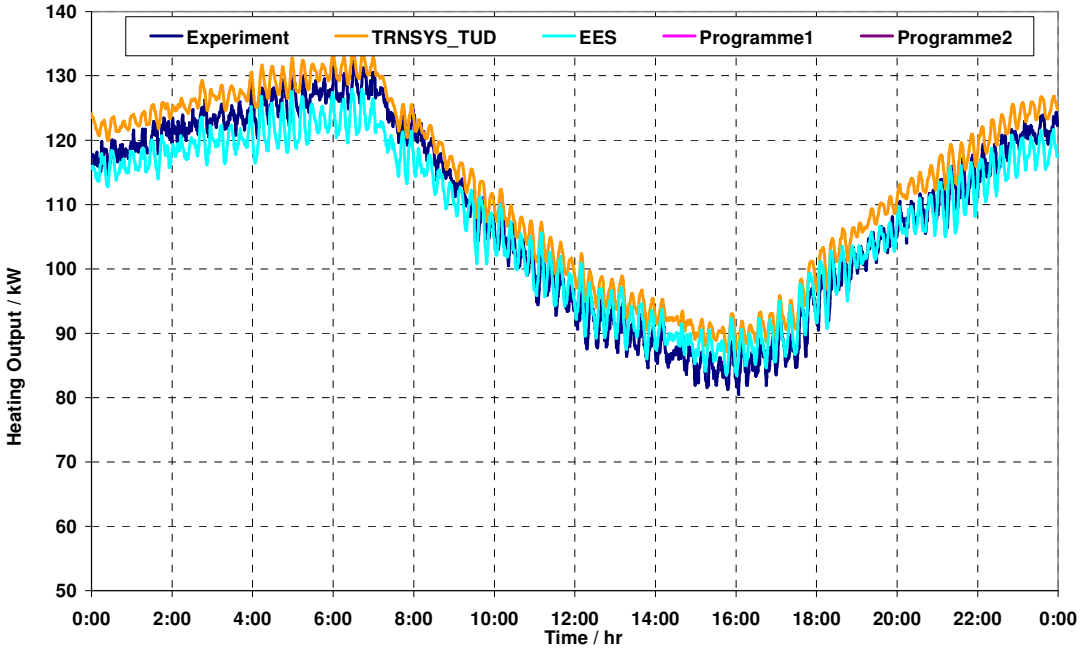

Figure 6-7 Boiler empirical test - heating output

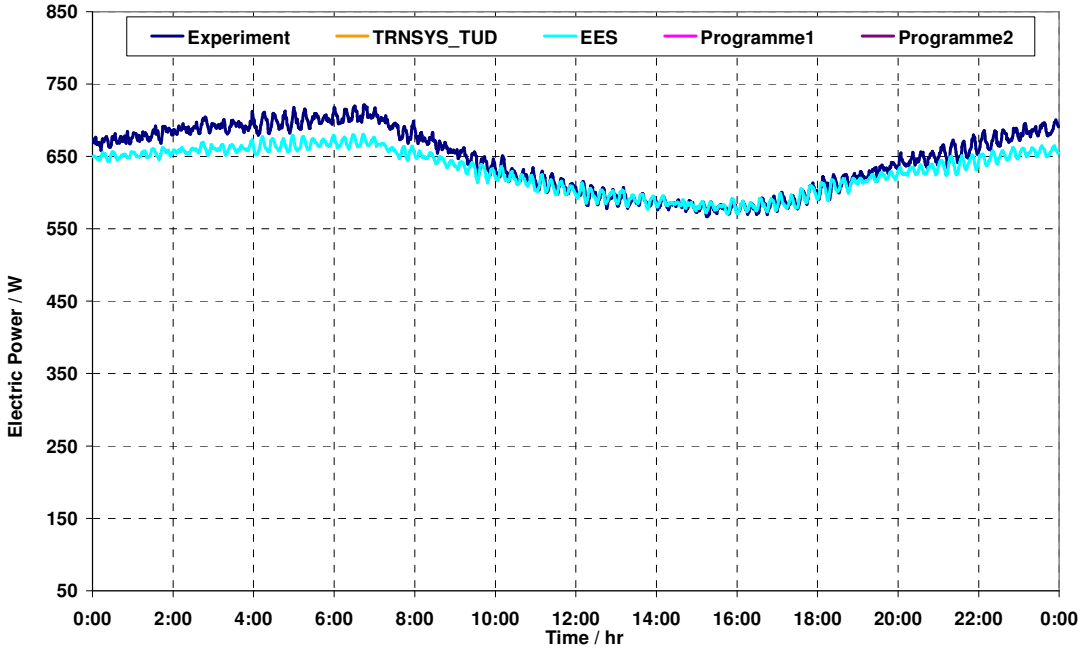

Figure 6-8 Boiler empirical test - boiler electric power

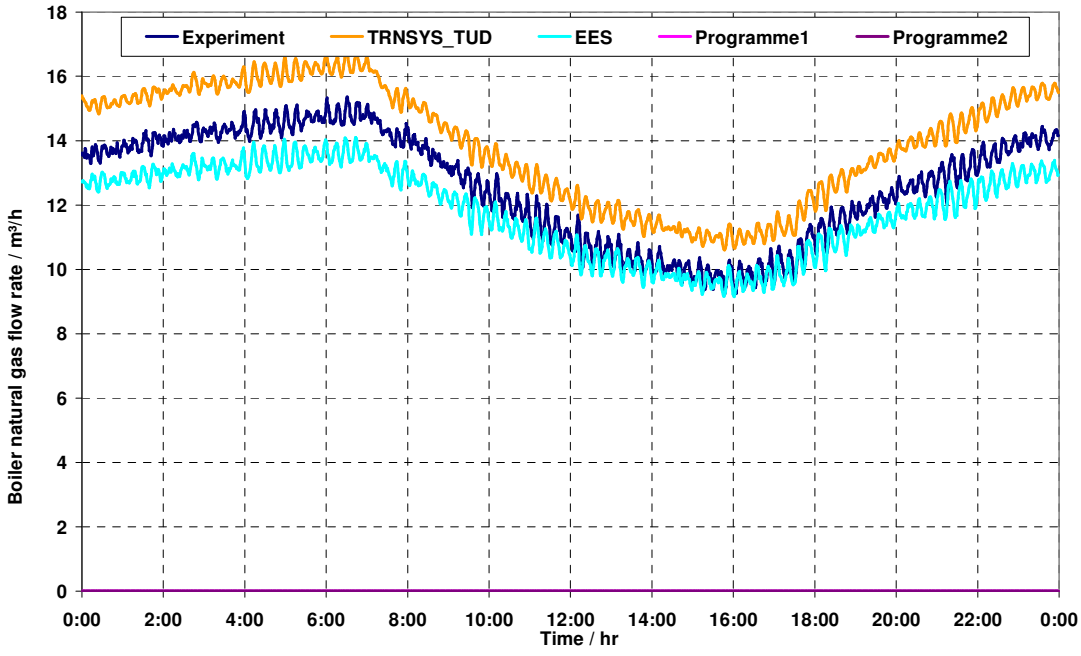

Figure 6-9 Boiler empirical test - Natural gas flow rate

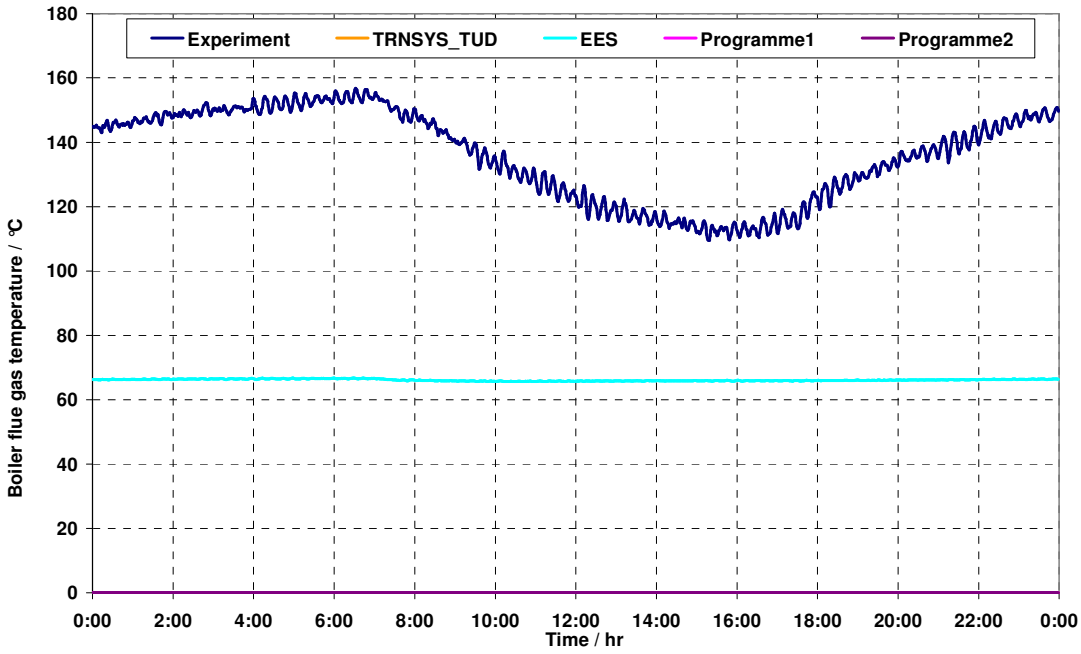

Figure 6-10 Boiler empirical test - Flue gas temperature

6.2 Heating Coil

6.2.1 A Short Description of Heating Coil Models

The modellers have been asked to give some detailed information on how their models work and on which general calculation approaches it is based on. Table 6-3 summarizes the answers submitted by the participants of this task. Two main findings can be described:

1. Most models get their characteristics from the performance data (Manufacturer point and/or additional points derived from measurements).But there are also two models that are based on geometry and material directly: Matlab/Simulink and EnergyPlus model. The Matlab/Simulink model uses similar approaches for both heating and cooling coil whereas EnergyPlus uses different approaches (see Table 6-22)
2. The EnergyPlus model is the only model that does not account for a variable heat transfer coefficient UA dependent from air/water flow rates.

Table 6-3 Summary of information about heating coil models submitted by the modelers

1. Program name and version number	**EES V7.888-3D**	**VA114 - version 2.25**	**EnergyPlus 2.2.0.023**	**TRNSYS-TUD**	**Matlab 6.5/Simulink**
2. Name of organization performed the simulations	Université de Liege, Belgium	Vabi Software bv	GARD Analytics, Inc.	TU-Dresden	iTG-Dresden
3. Name of person performed simulations and contact information	Vincent Lemort Laboratoire de Thermodynamique Campus Sart Tilman B49 B-4000 Liège Belgium Vincent.lemort@ulg.ac.be	A.Wijsman a.wijsman@vabi.nl	Michael Witte mjwitte@gard.com Bob Henninger rhenninger@gard.com	Clemens Felsmann Technical University of Dresden 01062 Dresden felsmann@itg-dresden.de	Heiko Werdin ITG Dresden Germany werdin@itg-dresden.de
4. Program status	Commercial	Commercial	U.S. Department of Energy Office of Building Technologies Washington DC	Research	Commercial
5. Time convention for weather data: first interval in the weather input lasts 00:00-01:00, climate is assumed constant over the sampling interval	Yes	Yes	Yes, if TimeStep is set = 1 hour. No, please specify: if TimeStep is set <1 hour the climate data is interpolated to determine the value at each time step	Yes, but it depends on the user how to handle weather data. It is possible to keep climate constant or to interpolate between to points.	No, climate is interpolated, weather data are assumed to be instantaneous values
6. The heat transfer between air and heating fluid is described by	three heat transfer coefficients: air to coil, coil metal, coil to heating fluid	three heat transfer coefficients: air to coil, coil metal, coil to heating fluid	one overall heat transfer coefficient	two heat transfer coefficients: air to coil and coil to heating fluid	three heat transfer coefficients: air to coil, coil metal, coil to heating fluid

	EES V7.888-3D	**VA114 - version 2.25**	**EnergyPlus 2.2.0.023**	**TRNSYS-TUD**	**Matlab 6.5/Simulink**
7. The heat transfer dependency on flow rate is taken into account	at the air side and the water side of the coil	at the air side and the water side of the coil	is not taken into account (so the UA is fixed)	at the air side and the water side of the coil	at the air side and the water side of the coil
8. Dependency on air flow rate is taken into account (laminar and turbulent region)	$\left(\frac{\text{Flow}_{air}}{\text{Flow}_{air0}}\right)^{0.6}$	$\left(\frac{\text{Flow}_{air}}{\text{Flow}_{air0}}\right)^{0.56}$	-	$\left(\frac{\text{Flow}_{air}}{\text{Flow}_{air0}}\right)^{0.33}$	U=f(NU,Re,Pr)
9. Dependency on heating fluid flow rate is taken into account (laminar and turbulent region)	$\left(\frac{\text{Flow}_{water}}{\text{Flow}_{water0}}\right)^{0.8}$	$\left(\frac{\text{Flow}_{water}}{\text{Flow}_{water0}}\right)^{0.8}$	-	$\left(\frac{\text{Flow}_{water}}{\text{Flow}_{water0}}\right)^{0.67}$	U=f(NU,Re,Pr)
10. Characteristics of heating coil model	derived from more measuring points	derived from the Manufacturer point only	derived from the user given dimensions of heating coil	derived from more measuring points	Mainly derived from the user given dimensions of heating coil and fine tuned based on manufacturer or measuring points
11. Dynamics of heating coil model	steady state model	steady state model	steady state model	steady state model	transient model

6.2.2 Comparative Test

The comparative heating coil tests have been run by five different programs as specified in Table 6-4.

Table 6-4 List of participants of the heating coil comparative test

Name of the program	Modeler
VA114	VABI Software BV, Delft, The Netherlands
Matlab/Simulink	ITG Dresden , Germany
TRNSYS-TUD	Technical University Dresden, Germany
EES	Université de Liege, Belgium
EnergyPlus	GARD Analytics, Inc., U.S.

The EnergyPlus model was able to provide simulation results for only the mass flow controlled heating coil.

Figure 6-11 shows a graph that summarizes the total amount of heating energy that is required during the validation period to maintain a given leaving air temperature set point under various conditions. It seems that this parameter is not very useful to detect possible disagreements between programs.

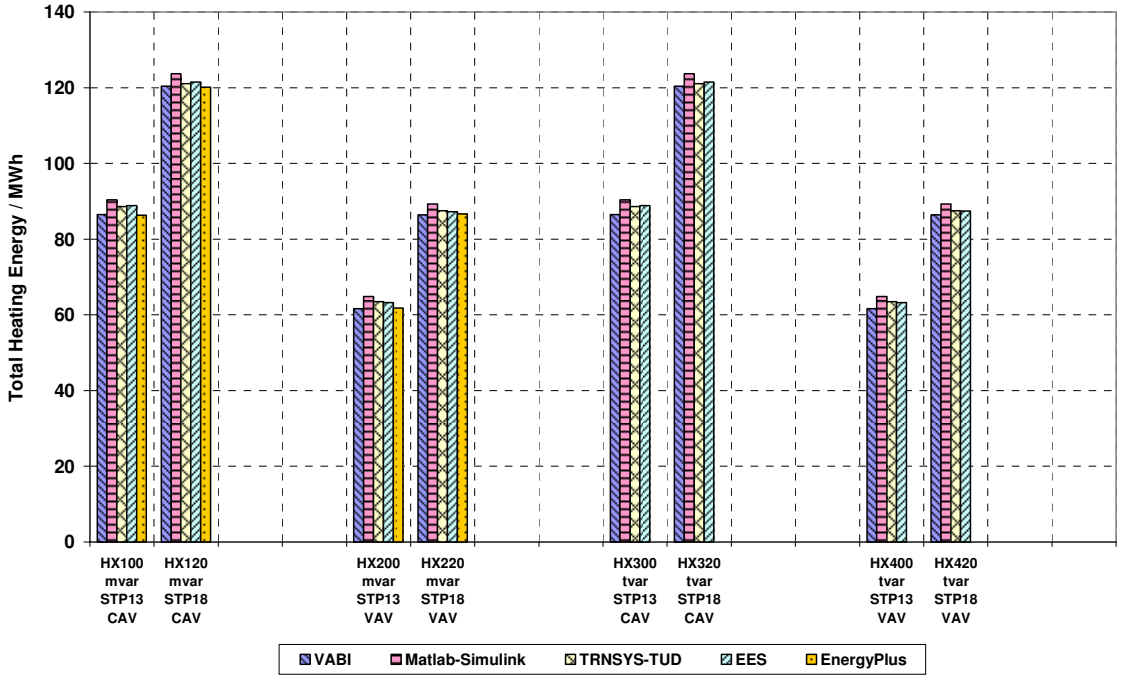

Figure 6-11 Heating Coil Comparative Test - Total Heating Energy

Also looking at some load profiles - Figure 6-12 and Figure 6-13 exemplary show two profiles for both a CAV and a VAV system - does not give any further information. Load profiles only show minor differences between programs.

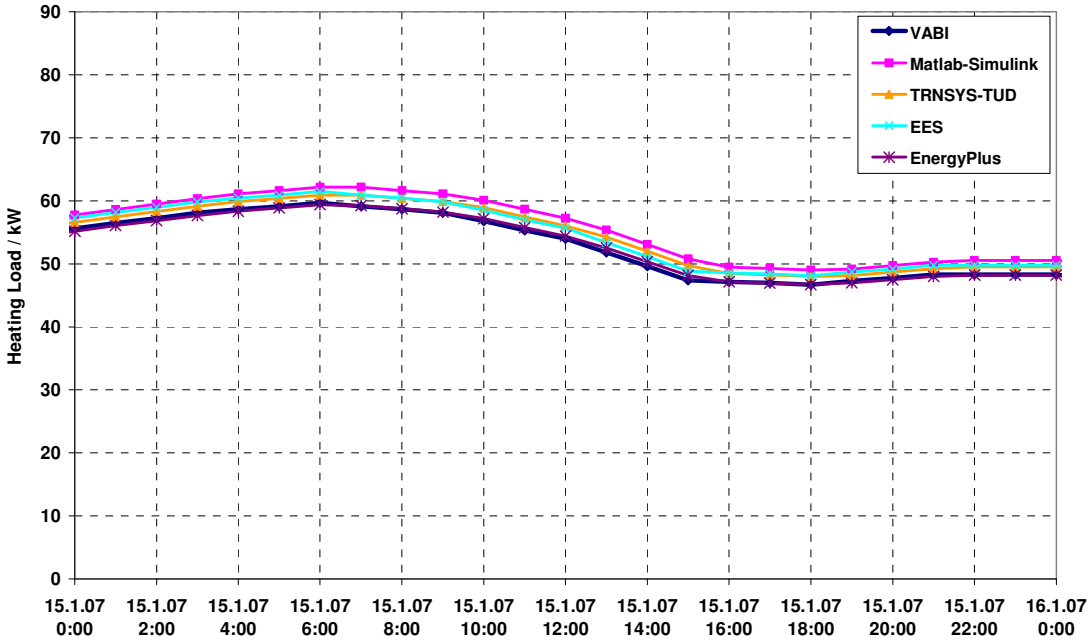

Figure 6-12 Heating Coil Comparative Test Case HX100 - Total Heating Load on January 15 (Coldest day)

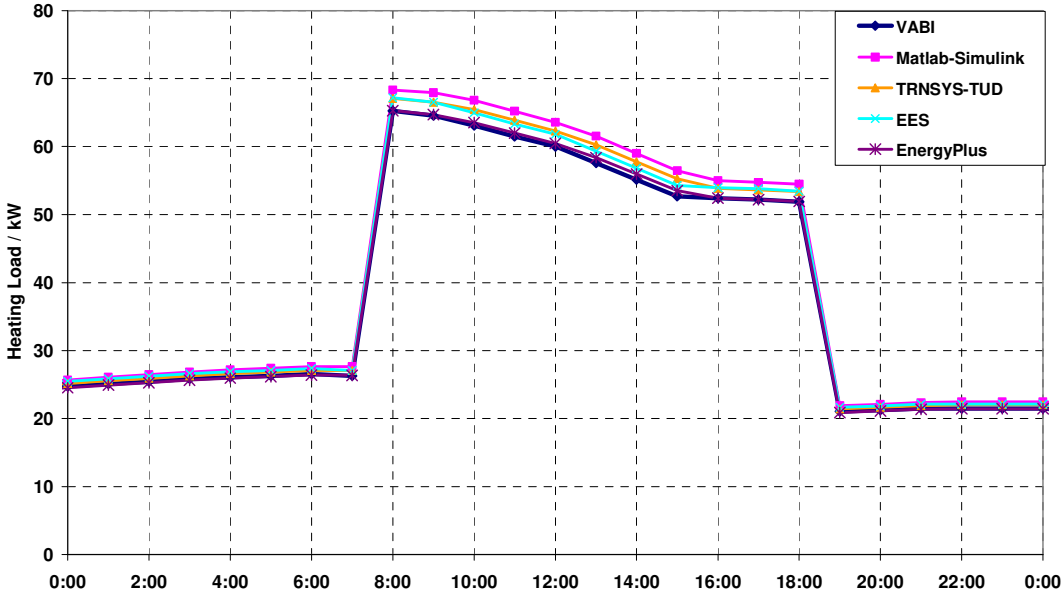

Figure 6-13 Heating Coil Comparative Test Case HX200 - Total Heating Load on January 15 (Coldest day)

Major differences between programs can be detected when looking at the control variables: hot water mass flow rate and coil entering water temperature.

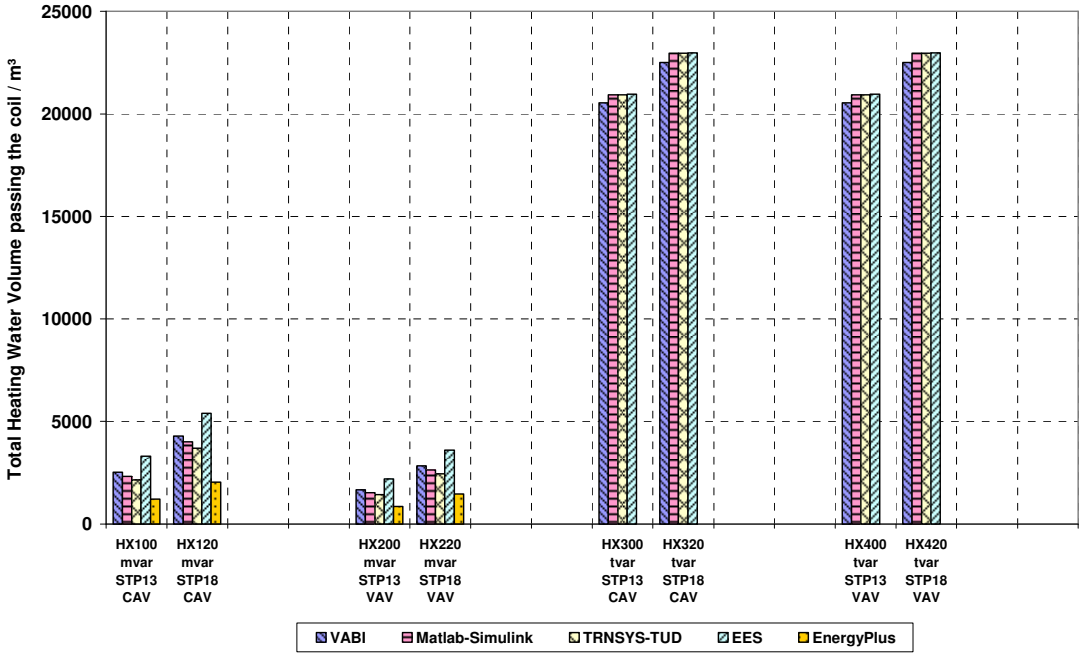

Figure 6-14 Heating Coil Comparative Test - Hot Water Volume circulated

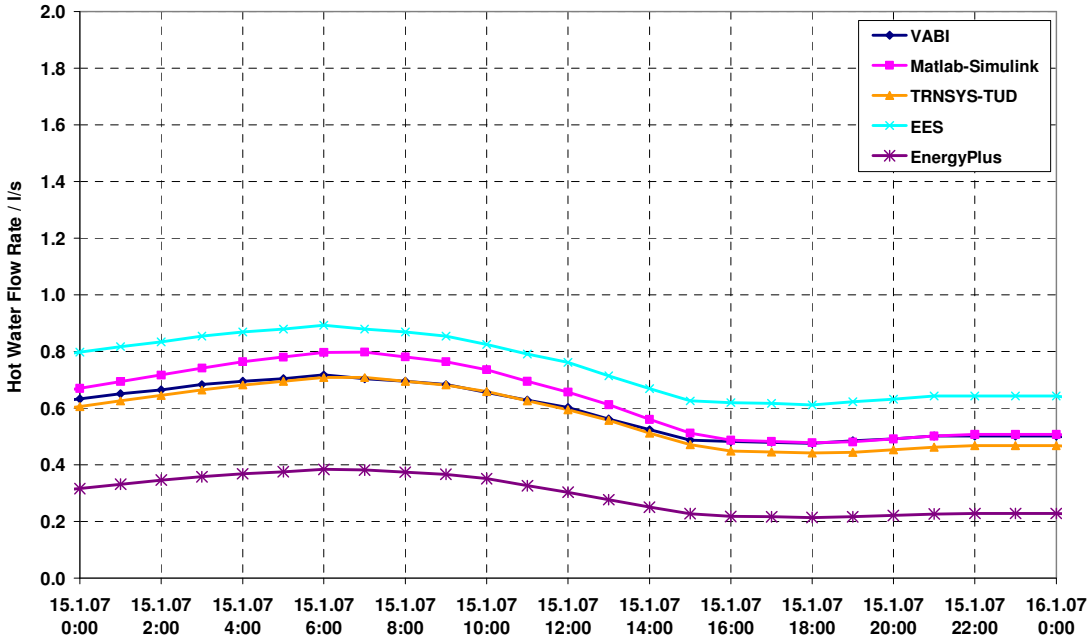

Figure 6-15 Heating Coil Comparative Test HX100 - Hot Water Flow Rate on January 15 (Coldest day)

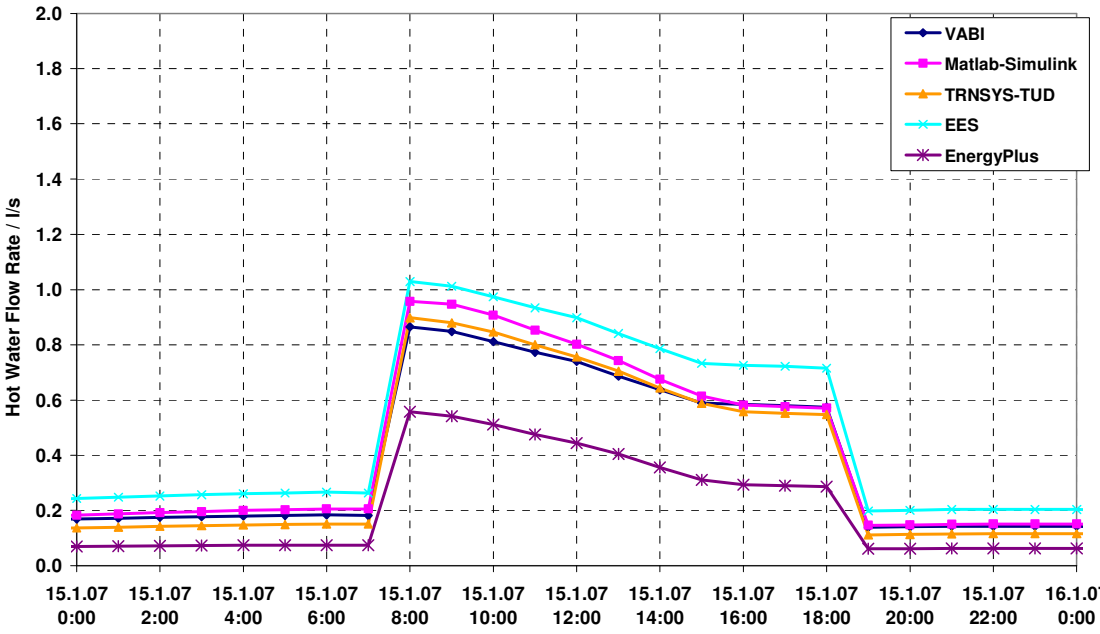

Figure 6-16 Heating Coil Comparative Test HX200 - Hot Water Flow Rate on January 15 (Coldest day)

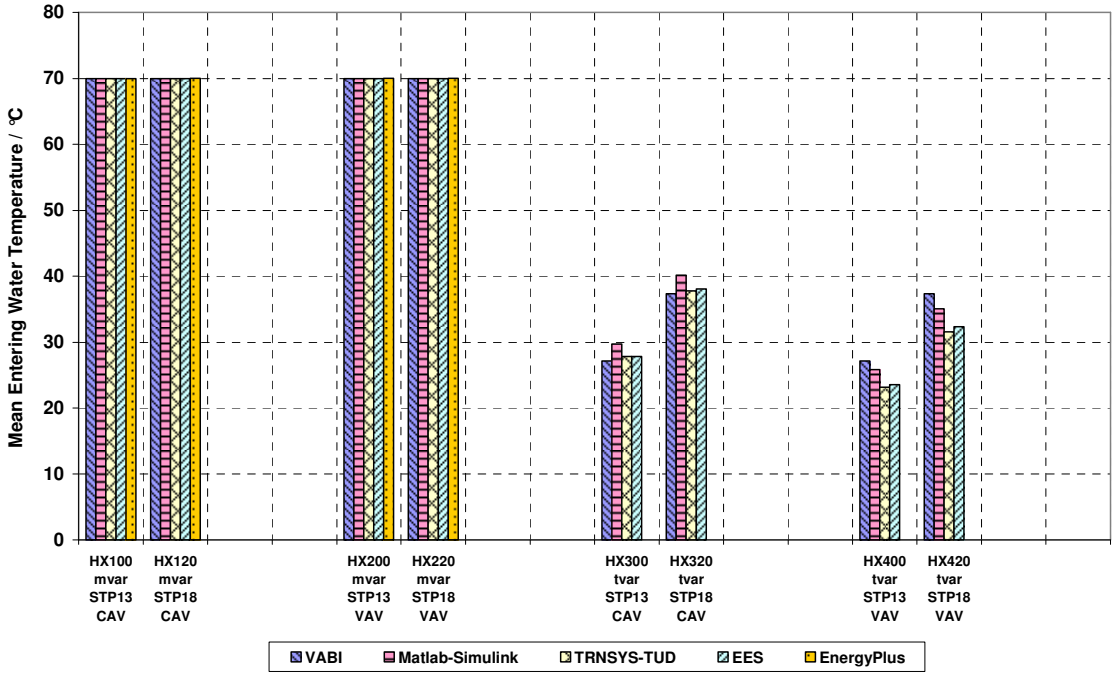

Figure 6-17 Heating Coil Comparative Test - Mean Entering Water Temperature

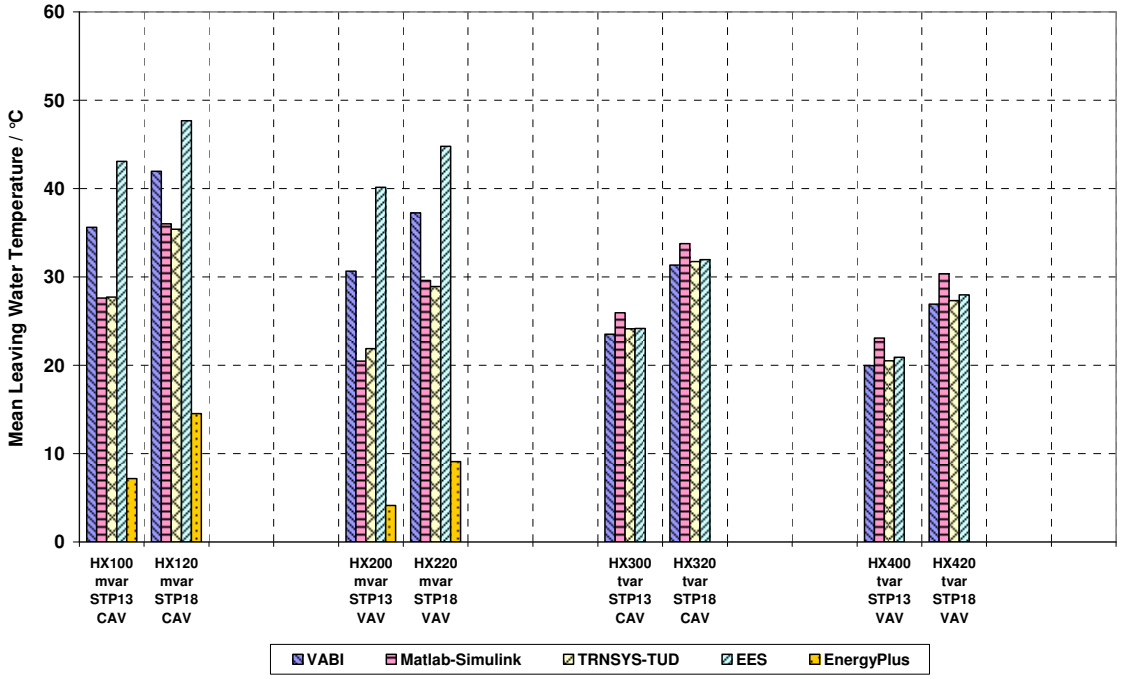

Figure 6-18 Heating Coil Comparative Test - Mean Leaving Water Temperatur

6.2.3 Empirical Test

The empirical heating coil test has been run by four different programs specified in Table 6-5.

Table 6-5 List of participants of the empirical heating coil comparative test

Name of the program	Modeler
VA114	VABI Software BV, Delft, The Netherlands
Matlab/Simulink	ITG Dresden , Germany
TRNSYS-TUD	Technical University Dresden, Germany
EES	Université de Liège, Belgium

Empirical validation based on real site measurements only makes sense if experimental data are reliable. Data used here have to be qualified by an agreement of air and water side energy balance at the heating coil. Figure 6-19 shows the averaged daily energy balance calculated from experimental data. The graph shows an almost perfect agreement that can be used for further validation purposes. Figure 6-20 contains a graph with the averaged daily heating load predictions from the different programs compared to the experimental data. As no program significantly disagrees with the experiment it seems to be a quite easy exercise to correctly

predict energy performance of a heating coil if calibration data are available. Also total amount of energy shown in Figure 6-21 does not disqualify one of the programs.

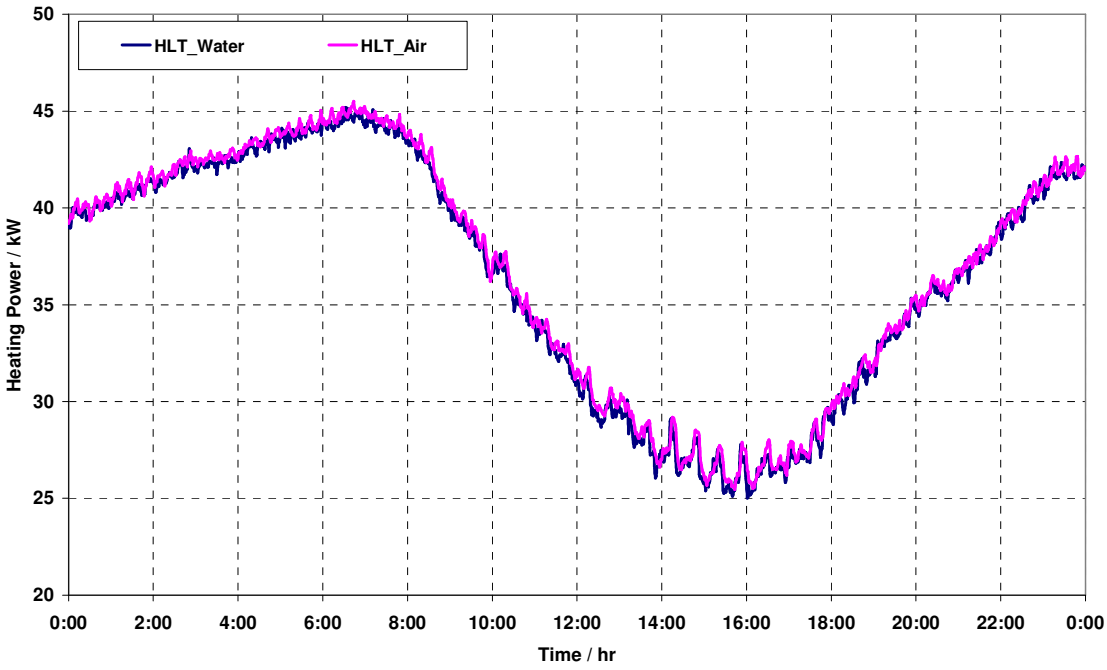

Figure 6-19 Heating Coil Empirical Test - Averaged Daily Energy Balance for the heating coil (Experiment)

In opposite to the heating load and energy predictions the leaving air and leaving water temperature predictions show some minor disagreements, see Figure 6-22 and Figure 6-23. But those disagreements are less than 1K. It is remarkable that leaving water temperature predictions are better for higher loads than for lower heating loads.

The UA-values provided from the models are quite similar but do not swing that much during the day although water flow rate through the coil varies within a range of 0.3 … 2.6 m³/h but air flow rate is constant at approximately 5100m³/h.

Some statistical data for this empirical test can be found in Table 6-6 (heating load), Table 6-7 (leaving water temperature), and Table 6-8 (leaving air temperature), respectively.

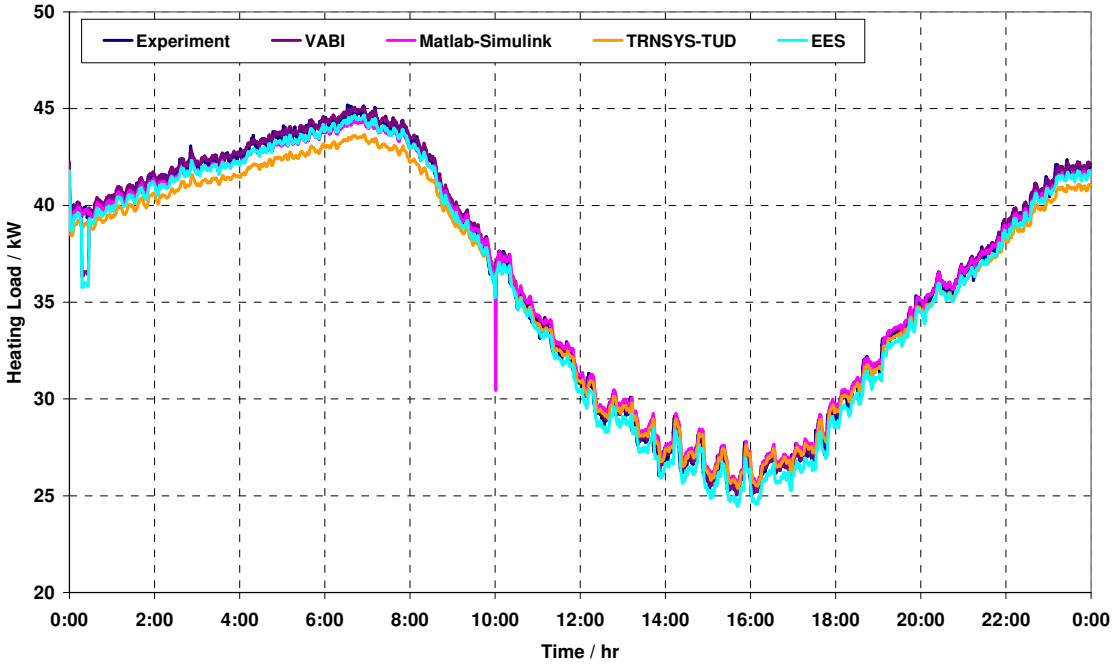

Figure 6-20 Heating Coil Empirical Test - Averaged Daily Heating Load

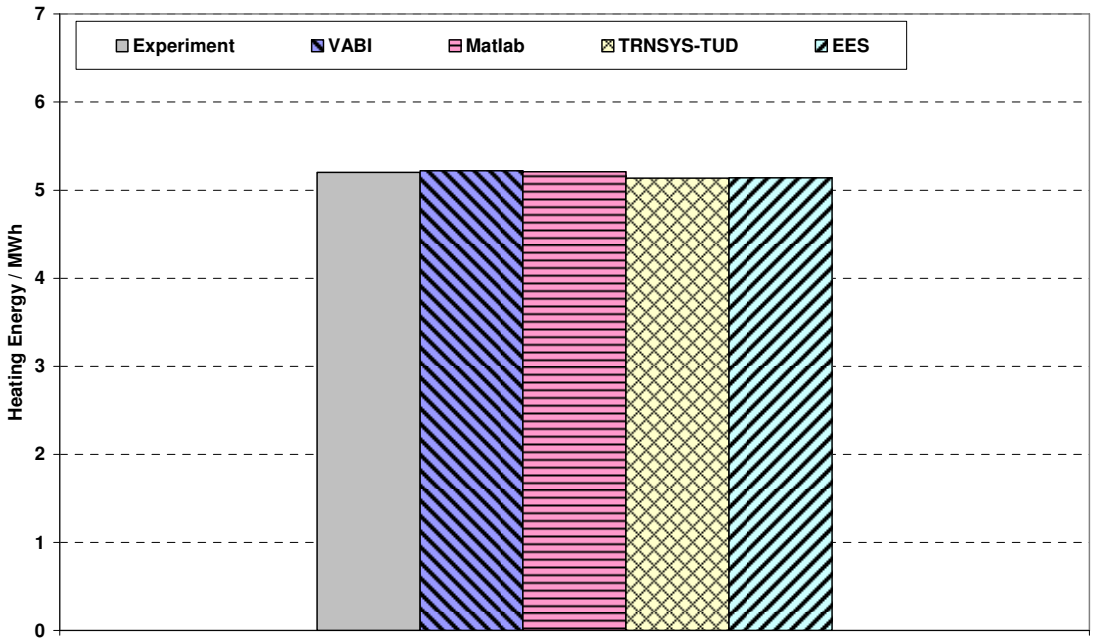

Figure 6-21 Heating Coil Empirical Test - Heating Energy

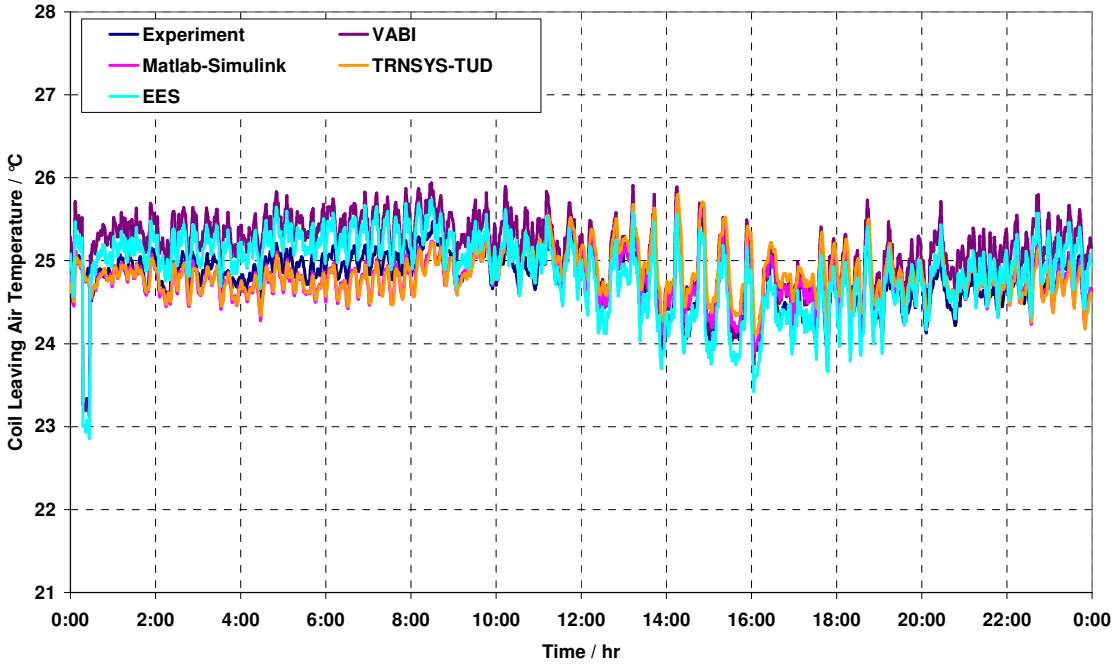

Figure 6-22 Heating Coil Empirical Test - Averaged Daily Coil Leaving Air Temperature

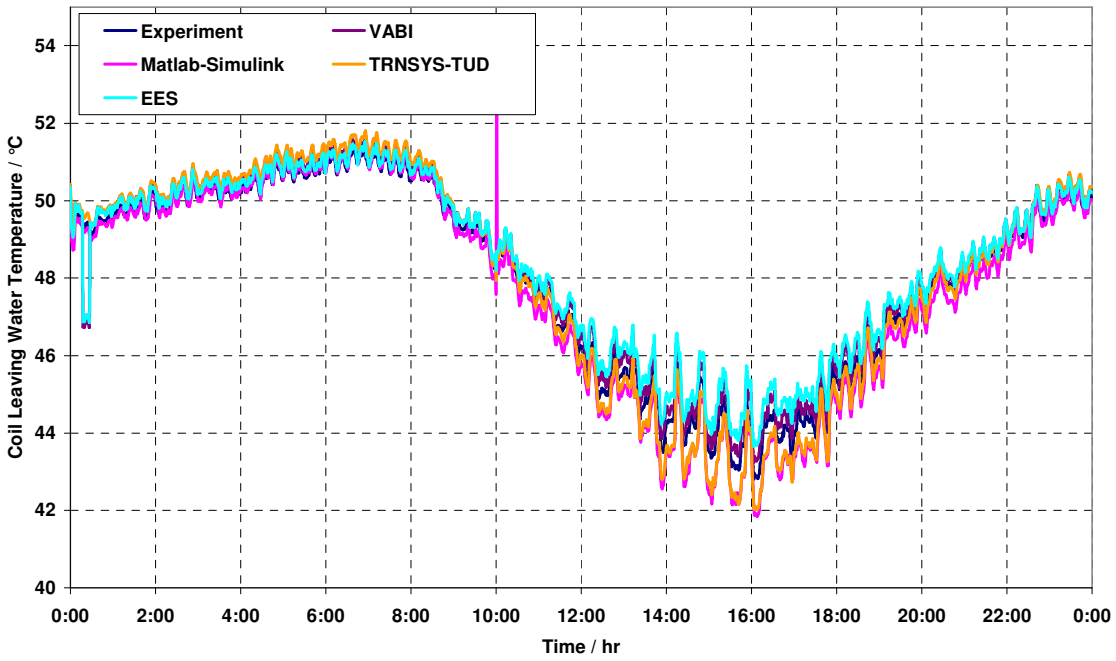

Figure 6-23 Heating Coil Empirical Test - Averaged Daily Coil Leaving Water Temperature

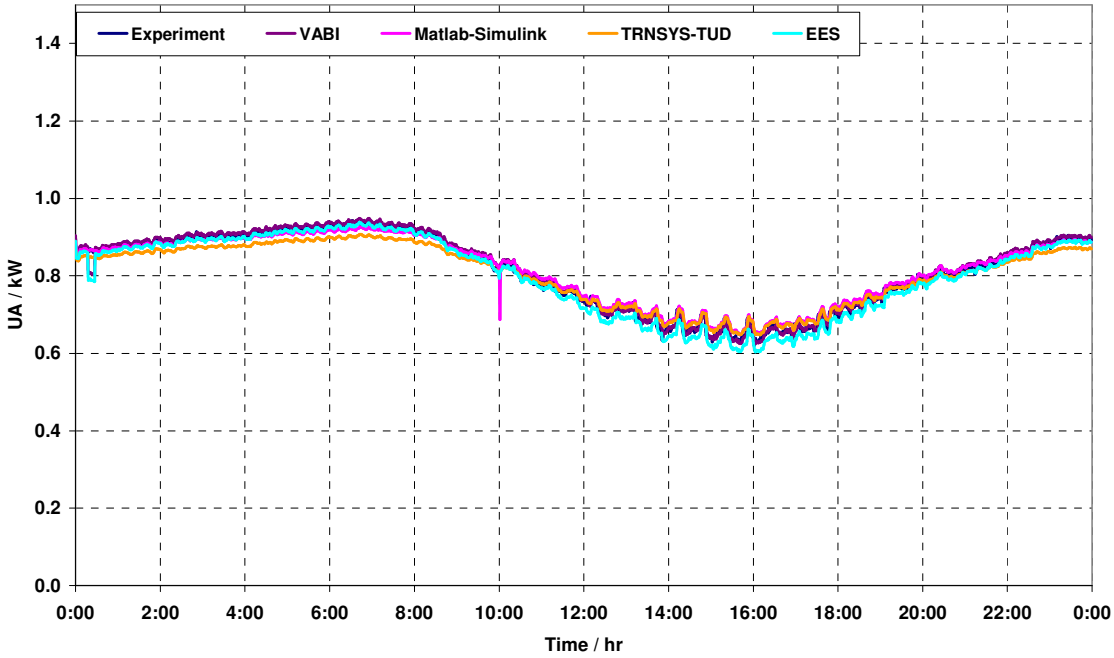

Figure 6-24 Heating Coil Empirical Tests – Overall Heat Transfer Coefficient UA

Table 6-6 Heating Coil empirical Test – Total Heating Load Statistics

HLT	Exp.	VABI	Simulink	TRNSYS-TUD	EES
$\overline{x}$	36.38	36.51	36.43	35.92	35.95
S	8.47	8.56	8.11	7.83	8.64
x_{min}	10.42	5.22	0.00	11.87	10.51
x_{max}	51.04	51.43	50.20	49.32	51.24
$\overline{D}$		0.13	0.05	-0.46	-0.43
$\overline{\lvert D \rvert}$		0.39	0.54	0.79	0.52
$\lvert D \rvert_{max}$		20.90	38.95	7.52	21.62
$\lvert D \rvert_{min}$		0.00	0.00	0.00	0.00
D_{rms}		0.83	0.81	0.97	0.94
$D_{95\%}$		0.90	1.27	1.78	1.18

Table 6-7 Heating Coil empirical Test – Leaving Air Temperature Statistics

LAT	Exp.	VABI	Simulink	TRNSYS-TUD	EES
$\overline{x}$	24.78	25.13	24.79	24.83	24.87
S	0.68	0.93	0.70	0.72	0.94
x_{min}	20.99	13.19	21.68	22.03	12.84
x_{max}	27.98	27.66	27.51	27.76	27.29
$\overline{D}$		0.35	0.01	0.05	0.09
$\overline{\lvert D \rvert}$		0.52	0.30	0.36	0.42
$\lvert D \rvert_{max}$		11.77	1.68	1.43	12.12
$\lvert D \rvert_{min}$		0.00	0.00	0.00	0.00
D_{rms}		0.71	0.37	0.45	0.64
$D_{95\%}$		1.00	0.69	0.88	0.86

Table 6-8 Heating Coil empirical Test – Leaving Water Temperature Statistics

LWT	Exp.	VABI	Simulink	TRNSYS-TUD	EES
$\overline{x}$	48.06	48.28	47.77	48.04	48.37
S	3.38	3.31	3.78	3.90	3.09
x_{min}	35.43	33.48	32.02	32.41	34.30
x_{max}	53.50	53.80	75.00	53.75	53.61
$\overline{D}$		0.22	-0.30	-0.02	0.30
$\overline{\lvert D \rvert}$		0.33	0.40	0.41	0.39
$\lvert D \rvert_{max}$		16.24	26.16	4.56	15.42
$\lvert D \rvert_{min}$		0.00	0.00	0.00	0.00
D_{rms}		0.71	0.65	0.60	0.78
$D_{95\%}$		0.93	1.05	0.83	1.40

6.2.4 Diagnosing Results

Comparative Test

Comparative test cases do not represent a truth standard but give the opportunity to compare simulation results to the outputs calculated with other models. Thus it is up to the modeller to decide whether to their results are in agreement for a specific test case, or whether there is disagreement that requires further examination of their program or inputs. If results are outside the range already defined by the outputs of other programs something seems to be wrong with the model. The following diagnostic flow diagram sketched in Figure 6-25 may help to locate the probable causes of disagreement between models.

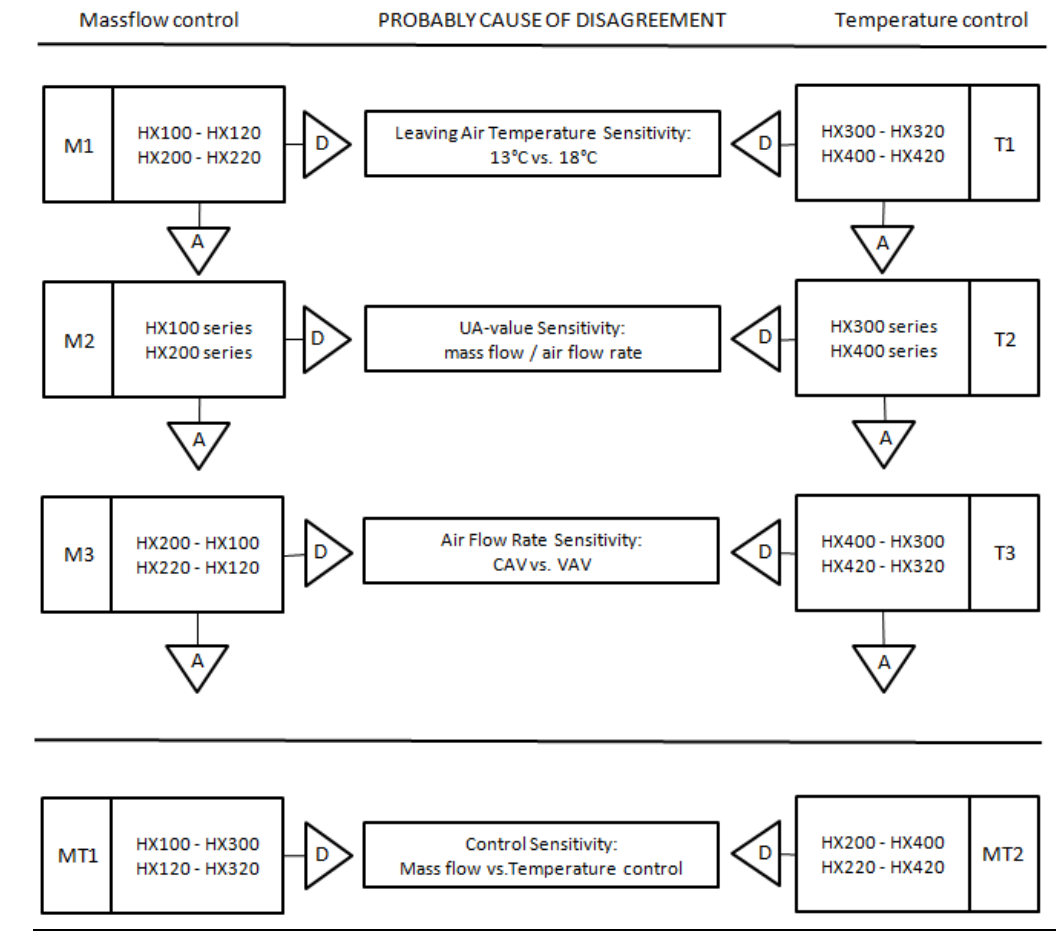

Abbreviations: A=Agree; D=Disagree

Figure 6-25 Heating coil comparative test cases diagnostic logic flow diagram M1-M3 / T1-T3 / MT1 & MT2

Three examples for diagnostic checks M1/T1 are shown in Figure 6-26, Figure 6-27, and Figure 6-28. The Figures illustrate that the impact of leaving air temperature set point on total

heating load is nearly the same for all programs but the impact on both the total water volume running through the coil as well as the mean leaving water temperature show some differences among programs. Sensitivity of heating load accounts for:

- Physical properties of fluids (density, heat capacity)
- Definition of air flow rate (air flow with entering conditions or with leaving conditions)
- Maximum heating load that can be transferred from the water to the air side of the coil.

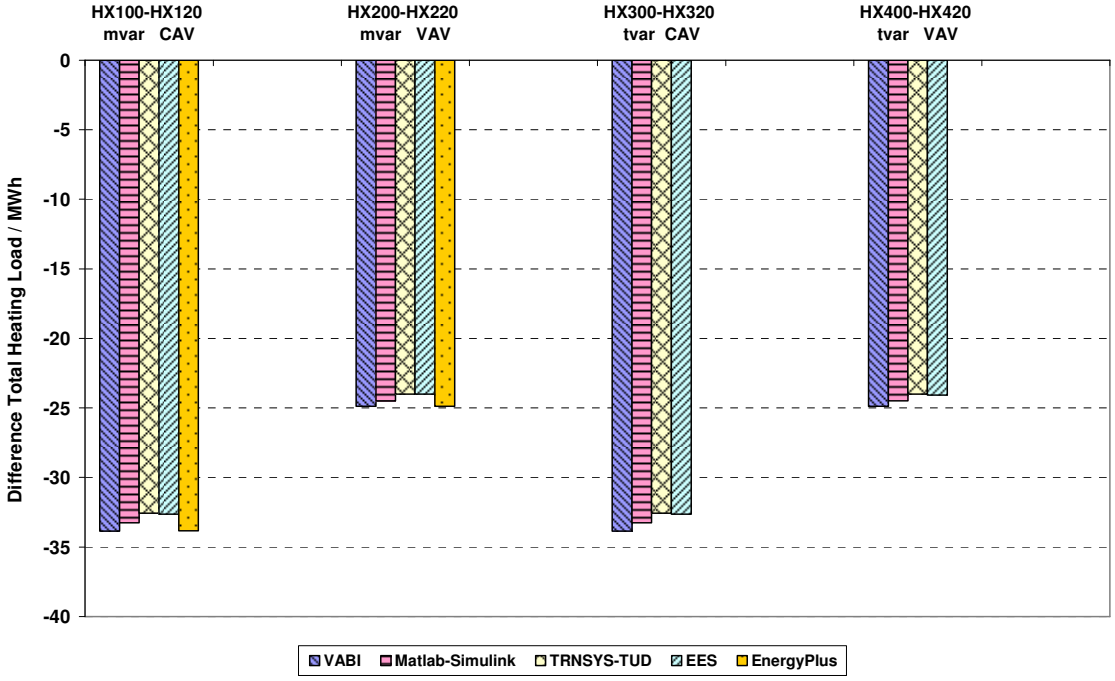

Figure 6-26 Heating coil comparative test: Sensitivity of total heating load against leaving air temperature set point; diagnostic check M1 /T1

Sensitivity of total water volume running through the coil and sensitivity of mean leaving water temperature are mainly driven by the heat transfer characteristic of the coil. This characteristic is described by the UA value. In case of constant mass flow rates, i.e. variable water temperature entering the coil (HX300-HX420) the water side has no additional impact on UA. Thus both water volume and temperature spread do not vary that much. I opposite to that the sensitivity is bigger for test cases HX100-HX220 with variable mass flow rate but constant water inlet temperature.

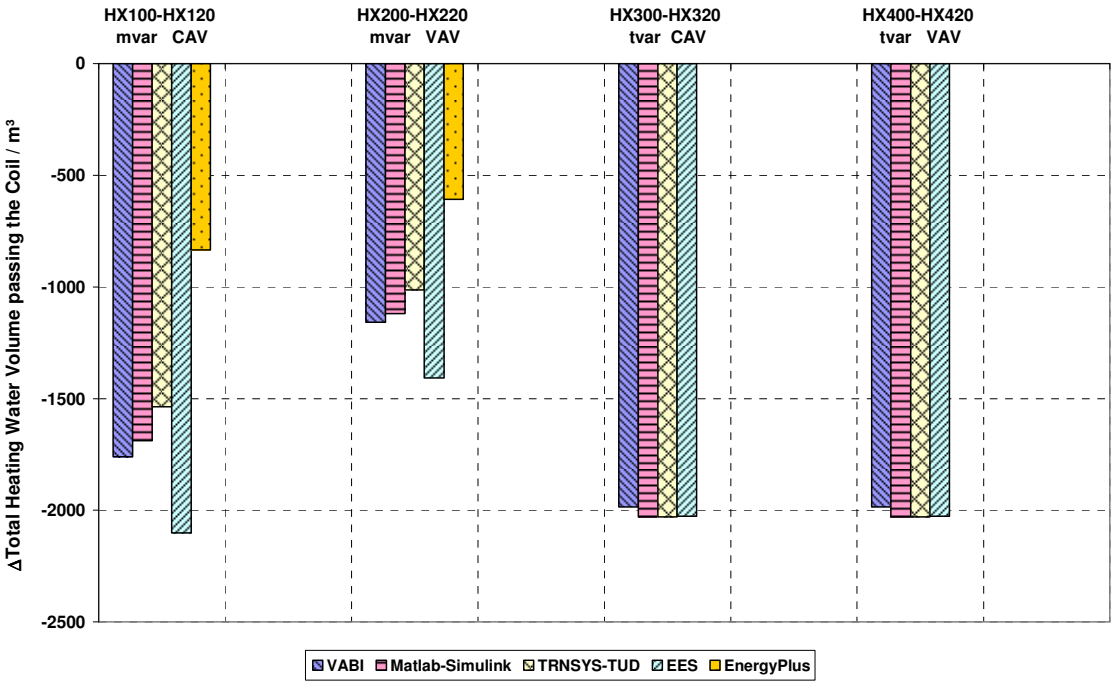

Figure 6-27 Heating coil comparative test: Sensitivity of heating water volume against leaving air temperature set point; diagnostic check M1 /T1

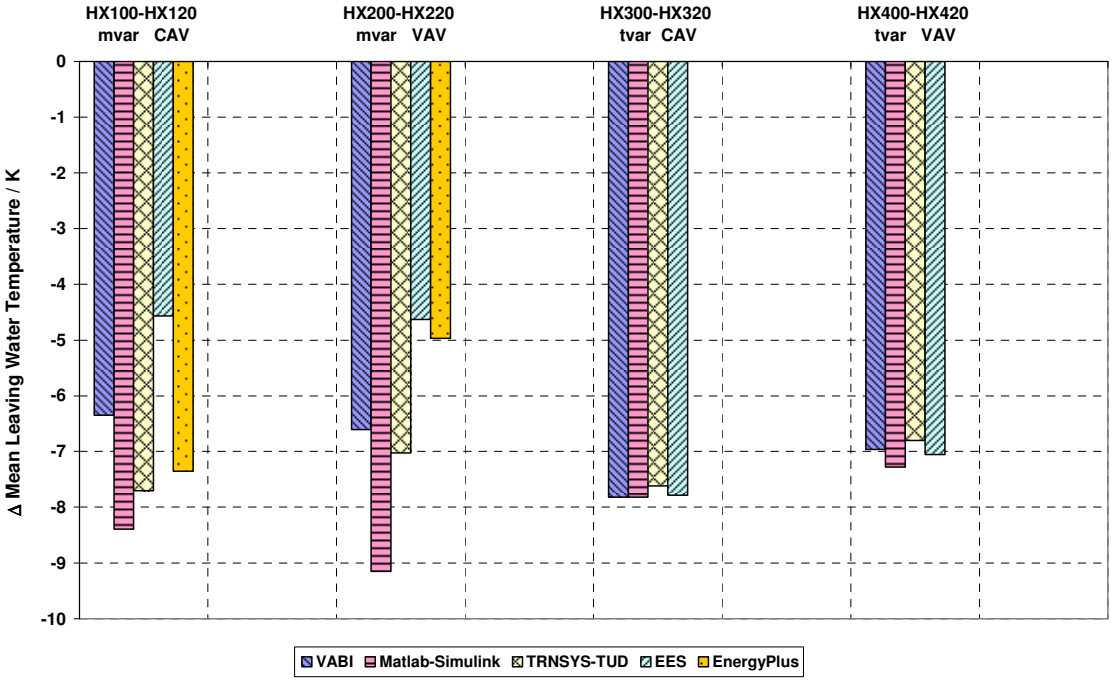

Figure 6-28 Heating coil comparative test: Sensitivity of mean leaving water temperature against leaving air temperature set point; diagnostic check M1 /T1

Since the UA-value of the heat exchanger mainly influences performance of the coil model it is important to primarily find an agreement on this issue. Diagnostic checks M2 and T2 refer to an UA value sensitivity check that analyzes UA dependencies on air and water flow rates. Figure 6-29 contains a graph that shows for the HX200 case the UA value of the heating coil in dependence on water flow rate through the coil. In this test case the air flow rate changes between two different levels. That is why two lines can be observed for each model. UA dependency on water flow rate is in general similar for all programs but for Energy Plus a completely different function can be observed. Although other UA dependencies on water flow rate seems to be similar small differences will have a big impact on heating coil performance, see Figure 6-15, Figure 6-16, and Figure 6-18, respectively. The Matlab/Simulink model distinguishes between laminar and turbulent water flow conditions. For that reason UA value is nearly constant for low water flows. Also the VABI model shows constant UA value but at much lower water flow rates. Figure 6-30 shows the results of the M2/T2 sensitivity check that also accounts for UA dependency on air flow rate.

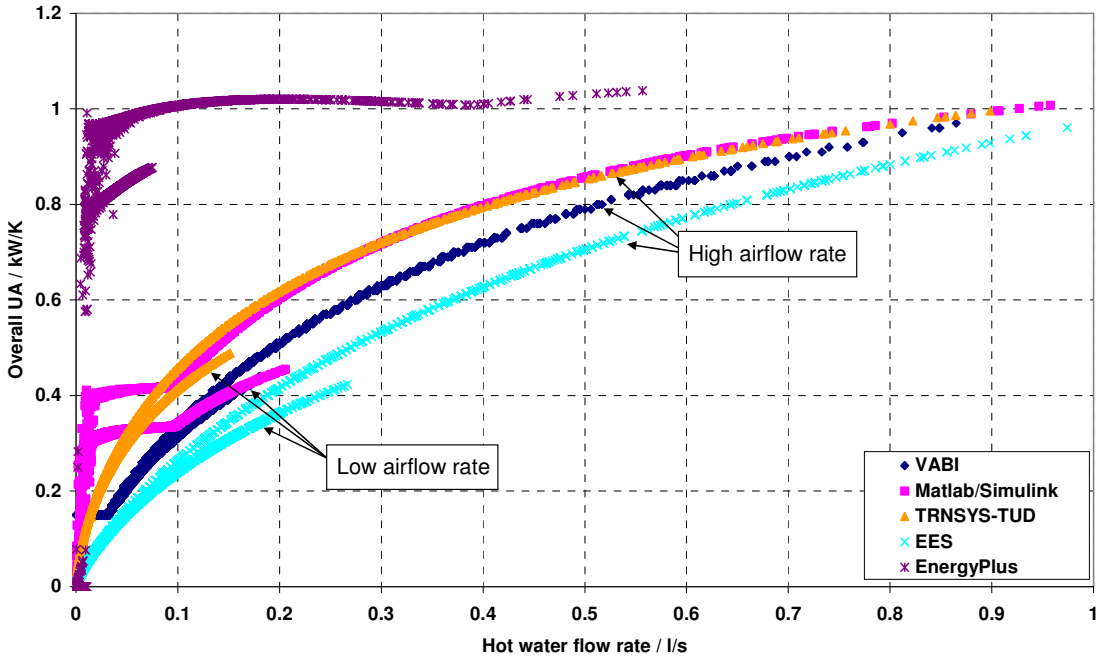

Figure 6-29 Heating coil comparative test HX200: UA-value sensitivity against water flow rate (air flow rate as parameter); diagnostic check M2 / T2

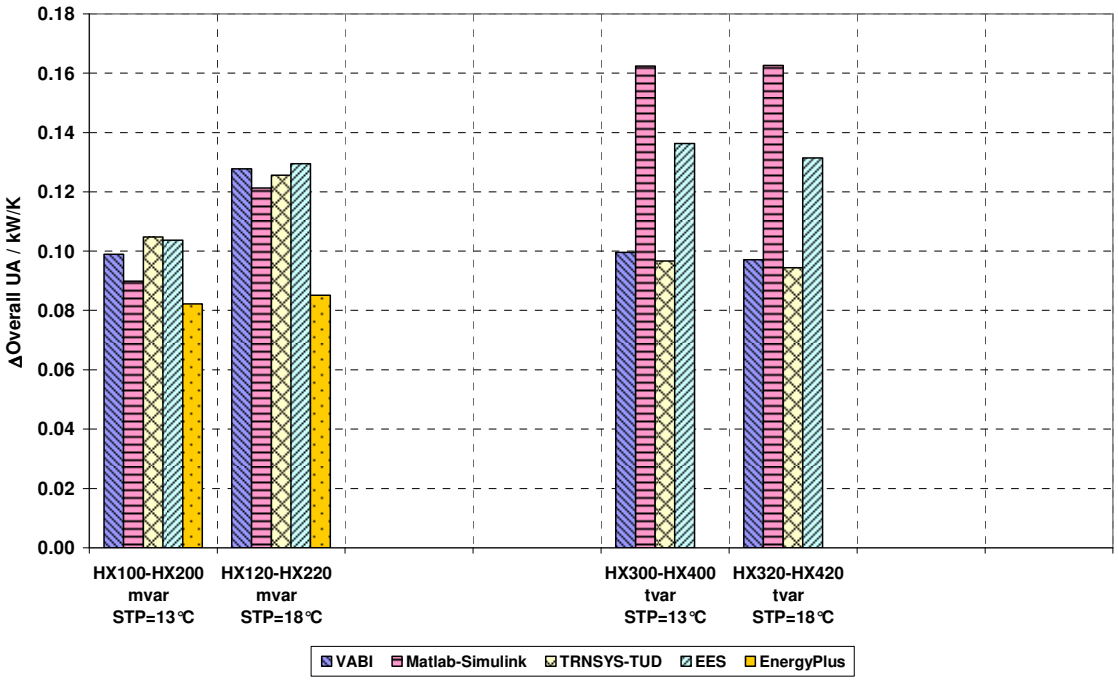

Figure 6-30 Heating coil comparative test: Mean UA-value sensitivity against air flow rate; diagnostic check M2 / T2

Some additional results from diagnostic checks M3/T3 are shown in Figure 6-31. The Figure shows the difference in the heating water volume that runs passes the coil when air flow rate scenario (CAV vs. VAV) is changed. If the coil is temperature controlled those differences should not indicate some disagreement because air flow is constant.

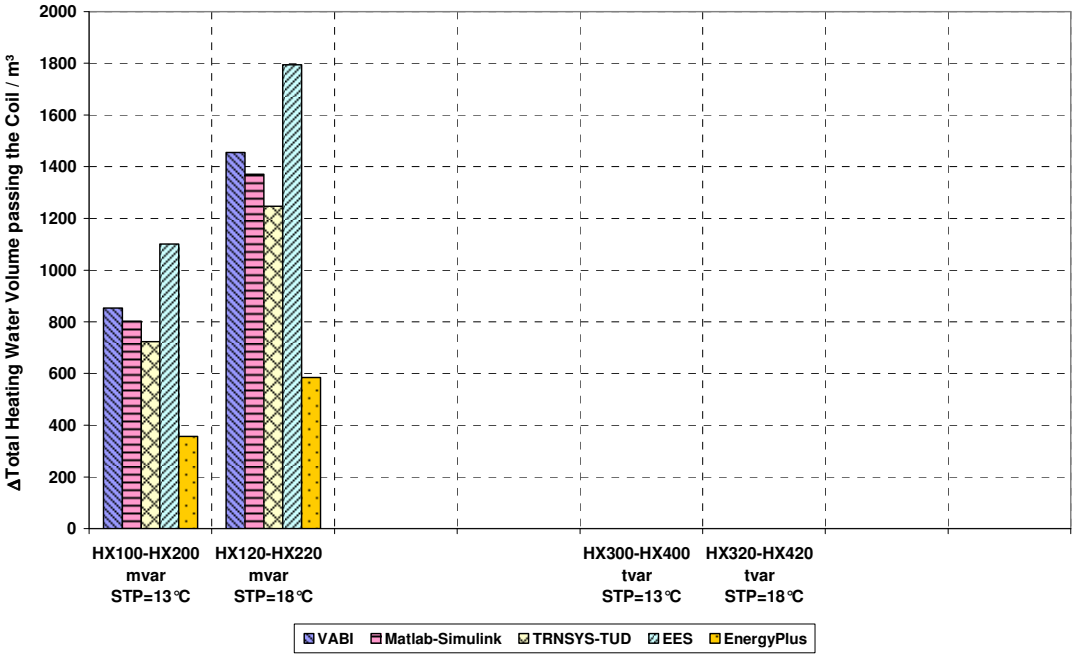

Figure 6-31 Heating coil comparative test: Sensitivity of heating water volume against air flow rate; diagnostic check M3 / T3

6.3 Hot Water Hydraulics

There are no results presented here because no runs have been performed by the participants of Subtask D.

Chapter 7 Modellers Reports

7.1 Boiler

7.1.1 ULG – EES

The modeller report from University of Liege is provided in a separate file. It is titled "Simulation of HVAC Components with the Help of an Equation Solver" written by Vincent Lemort, Andres Rodríguez and Jean Lebrun.

7.1.2 TUD – TRNSYS-TUD

The TRNSYS-TUD boiler model is originally based on the fuel oil boiler model developed during the IEA ECBCS Annex10 project. Later some changes have been made at TU Dresden to better fit the model to the TRNSYS-TUD code.
The model subdivides the thermal mass of the boiler (heat exchanger including water content) into three parts and also splits the total water flow rate through the boiler into a main flow and a bypass flow. The following picture may help to clarify the situation.

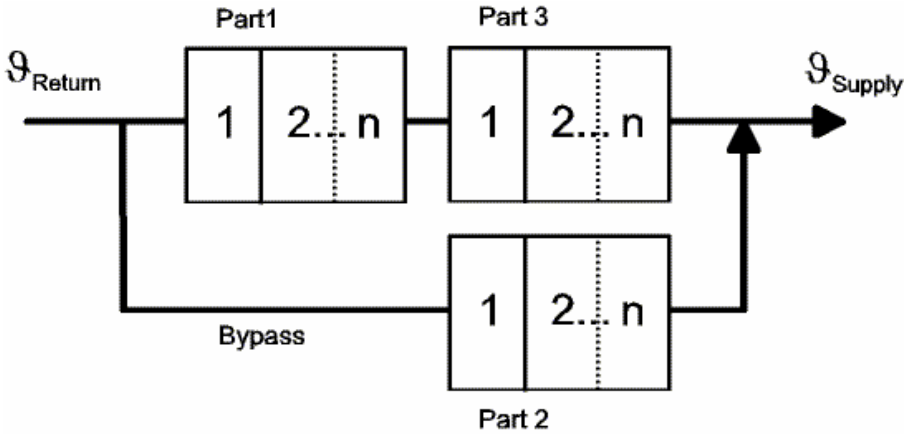

Figure: Modelling assumption used in the TRNSYS-TUD boiler model

Parts of the thermal mass are characterized as follows:

- Part 1: thermal mass in the main flow is heated when the burner is on
- Part 2: thermal mass in the main flow is not heated although the burner is on
- Part 3: thermal mass in the bypass flow is never heated

Each part of the thermal mass is again subdivided into several sections (the number n of the sections is variable). The energy balance for each of the sections can be written as:

Burner capacity – Heat losses = Heat flow (water) + heat storage

$$\dot{Q}_{Burner,s} - \dot{Q}_{Loss,s} = C_{Water,s} \cdot \left(\vartheta_{Out,s} - \vartheta_{Return,s}\right) + \frac{C_s}{\Delta t}\left(\vartheta_{out,s} - \vartheta_s\right)$$

The algorithm is calculating the outlet temperature of each of the sections which at the same time is the inlet temperature of the following section. The bypass mass flow rate is estimated based on the water content of the boiler and the portions of heated and unheated parts are estimated based on total boiler mass.

The efficiency of the boiler is calculated based on the current firing rate. Therefore the efficiency curves provided in the specification have been approximated and implemented into the TRNSYS input file.

The TRNSYS-TUD boiler model actually does not allow the output of flue gas temperature, and electric energy consumption of the boiler, respectively. In addition to that the model always refers to a boiler that is installed within a room. For that reason it was not possible to run comparative test cases that account for an outside air intake.
Some additional modelling effort is required to run the full test matrix.

7.2 Heating Coil

7.2.1 ULG – EES

The modeller report from University of Liege is provided in a separate file. It is titled "Simulation of HVAC Components with the Help of an Equation Solver" written by Vincent Lemort, Andres Rodríguez and Jean Lebrun.

7.2.2 VABI – VA114

IEA SHC Task 34 / ECBCS Annex 43
Subtask D: Mechanical Equipment and Control Strategies

Heating Coil - Modeler Report

VA114

VABI Software BV
P.O. Box 29
2600 AA Delft
The Netherlands

July 23, 2007 (third draft)

July 27, 2006 (second draft)
May 17, 2006 (first draft)

Report by A. Wijsman

Remark:
In the first draft of this report a description of the model and its assumptions are given. The IEA 43-Heating Coil – test cases [1] were carried out and reported [4].
In July 2006 the heating coil model was improved and the tests were done again. Information can be found in the second draft.
Now, July 2007, the heating coil was further improved. Comparisons within this IEA34/34-subtask led to accentuation of the definition of the air volume flow rate to be used for the tests. Beside the Manufacturer data point two extra points from empirical data came available to determine the coil characteristics. Re-runs were done. Information can be found in this third draft of the report.

Heating Coil – Modeler Report – VABI Software bv

Report by A. Wijsman and Szymon Szufa

1. Introduction

The Building simulation program VA114 is developed and distributed by VABI Software bv. The current version is 2.25.

The program calculates the Demand, the Supply, the Distribution and the Generation of heat and cold for a building with its energy supply system. Moreover the internal comfort temperature and overheating are calculated.

VA114 is a multi-zone program.

The time step applied in VA114 is 1 hour.

The heat and cold supply can happen by supply of conditioned air and by local devices.

The conditioning of the supply air can be in two steps:

- Pre-conditioning by a mixing valve, by heat recovery or by other
- Post-conditioning by heating coil, heating coil, humidifier, de-humidifier

The heating coil is fed by a warm water network. Air that passes this heating coil is heated.

The current program VA114 models a heating coil. In chapter 2 a description of the applied model is given.

The heating coil model was subjected to the IEA 43 – Heating Coil – tests [1]. In the first draft of this report [4] a description of the heating coil model and the results for the test cases are given:

- results of heating coil comparative tests
- results of heating coil empirical tests.

During the Iowa-meeting (April 2006) results for the Cooling Coil Tests showed reasonable discrepancies between the participating programs. The following questions raised:

- should flow dependency be taken into account?
- is one given data point (Manufacturer data) sufficient for characterization of the Cooling Coil model?

These questions are valid for the Heating Coil model too.

At VABI Software bv attention was paid to these questions:

- a literature study was done on the flow dependency of the heat transfer at the external (air) side and the one at the internal (water) side
- a method was developed to split the specific capacity of the coil in an external part and an internal part
- for this method an extra given data point of the coil is required.

The Heating Coil model was adapted and tested. In the second draft [5]of this report (July 2006) information is given.

Now, July 2007, the heating coil was further improved: distinguished are the external (air) side, the intermediate (metal) part and the internal (water) side. The method to determine these 3 individual parts has been adjusted.

Comparisons within this IEA34/34-subtask led to accentuation of the definition of the air volume flow rate to be used for the tests: to a volume flow rate belong air conditions (temperature and humidity)

Beside the Manufacturer data point two extra points from empirical data came available to determine the coil characteristics.

Re-runs for both comparative and empirical tests were done.

Background information and results of re-runs can be found in this third draft of the report.

2. Model description

In figure 1 a heating coil is shown schematically.

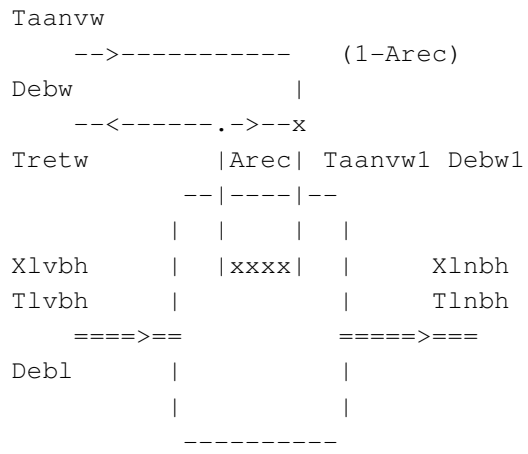

Figure 1: Heating Coil schematically

Explanation:

Water

Debw	= water mass flow in the warm water network
Taanvw	= water supply temperature of the warm water network
Tretw	= water return temperature of the warm water network
Debw1	= water mass flow over the heating coil
Taanvw1	= water temperature at entrance to the heating coil
Arec	= recirculation fraction
	= (Taanvw-Taanvw1)/(Taanvw-Tretw)

Air

Debl	= air mass flow through heating coil
Tlvbh	= air temperature at entrance of heating coil
Xlvbh	= air humidity at entrance of heating coil
Tlnbh	= air humidity at exit of heating coil
Xlnbh	= air humidity at exit of heating coil

Control of the unit happens by valve ‘x’:

- Arec = 0 ‘Maximum’ heating capacity
- Arec = 1 ‘Zero’ heating capacity

The water mass flow over the coil is constant, the supply temperature at the entrance of the coil is controlled by valve ‘x’.

Characteristics of heating coil

The model asks product information as input data: heating power at given water supply temperature, water return temperature, air temperature at the entrance, air temperature at the exit. In table 1 this information is shown.

From this input data follow the water mass flow and the air mass flow. With this information the specific capacity of the coil (W/K) is derived (see appendix A).

With this specific capacity the performance of the heating coil under any actual condition (water flow and supply temperature, air flow and supply temperature / humidity) can be determined.

Table 1: Input data for the heating coil (example)

```
-> 1. Verwarmbatterij
Vermogen (in W)- waterA/Rtemp.      - LuchtA/Rtemp.   -  deb.fract.
   QCEVWMX      TWBAT1A    TWBAT1R    TLBAT1A  TLBAT1R   DBFRW1
    61000.0       82.3       71.1       4.44    37.78    1.00
```

The model of the heating coil

The heating coil is modelled by subroutine 'Lbkvw', that calls Function 'Fqwwmax'.
The heat exchange in this model happens only sensible.

The specific capacity AFWW

In reality the specific capacity is built up out of 3 parts:

- the heat transfer between air flow and the heating coil external surface; the air flow rate influences this coefficient
- the heat transfer inside the heating coil
- the heat transfer between the heating coil internal surface and the heating fluid; the heating fluid flow rate influences this coefficient

The original VABI heating coil model assumes the specific capacity AFWW (in W/K) is constant, so independent of air flow rate and heating fluid flow rate. The specific capacity AFWW is treated as one parameter. No distinction is made between the 3 above mentioned parts.

In July 2006 the flow dependency was built in. It was assumed the specific capacity AFWW is split into two parts:

- an external AFWWEXT
- an internal AFWWINT

Now, July 2007, the model has been modified. It is assumed the specific capacity AFWW is split into three parts:

- an external AFWWEXT
- an intermediate AFMET
- an internal AFWWINT

The external AFWWEXT is between air flow and heating coil (including part of internal resistance); the intermediate AFWWMET is within the material of the heating coil; the internal AFWWINT is between heating coil (including part of internal resistance) and heating fluid.

The flow dependency is given by a correction factor 'f' for the two individual parts:

- at the external (air) side: $f_{air} = (flow_{air}/flow_{air,0})^{0.56}$
- at the internal (water) side: $f_{water} = (flow_{water}/flow_{water,0})^{0.80}$

So

- $AFWWEXT = f_{air} * AFWWEXT0$
- $AFWWINT = f_{water} * AFWWINT0$

And

$$AFWW = 1 / (1/AFWWEXT + 1/AFWWMET + 1/AFWWINT)$$

Remark: the AFWW has a lower limit, which is put on 10% of the AFWW0. That 10% is still an arbitrary value.

Important is to know the individual AFWWEXT0, AFWWMET and the AFWWINT0 for the given data point (Manufacturer data).

Definition:

- external AFWWEXT0 = 3,0 * A11*AFWW0
- internal AFWWINT0 = 3,0 * B11*AFWW0
- intermediate AFWWMET = 3,0 * C11*AFWW0

In series these three parts give the overall specific capacity AFWW0. This leads to the following relationship between A11, B11 and C11:

$$1,0/B11 = 3,0 - 1,0/A11 - 1,0/C11$$

with

$$1,0/3,0 \leq A11 < \text{infinitive}$$
$$1,0/(3,0-1,0/A11) \leq C11 < \text{infinitive}$$

From that one data point (Manufacturer data) nothing can be said about the individual parts. All 3 parts equally sized can be an assumption (so A11 = B11 = C11 = 1,0)

However in case two or more extra data points are available this is possible (see appendix B): A11 and C11 can be determined. Preferably the extra points must be far away from the first point (for instance at 20% of the air flow rate and/or at 20% of the water flow rate).

For the Heating Coil model three steps for the specific capacity AFWW are distinguished:

- step 1: AFWW is independent of the flows, so fixed
- step 2: AFWW is dependent on the flows, A11, B11 and C11 are assumed to be 1,0
- step 3: AFWW is dependent on the flows, A11, B11 and C11 are derived with the extra data points

The tests are carried out for those 3 modelling steps.

3. Modeling Assumptions

In general

- Comparative tests.
The heating coil model is tested insitu of the VA114 simulation program. Actual weather data from the Des Moines, Iowa TMY2-file is used to obtain the conditions of the air at the air inlet.

- Empirical tests
The heating coil model is tested outside the VA114 simulation program. Air flow rate, water flow rate, entering air temperature and entering water temperature are available from file HCEmpInput1.txt

Important are the heating fluid and atmospheric pressure:

- for what heating fluid and atmospheric pressure the manufacturer data is given
- type of heating fluid used during the tests and the actual atmospheric pressure.

The heating fluid for which the manufacturer data is given, is water. The tests are also done for water.

The atmospheric pressure for which the manufacturer data is given, is the atmospheric pressure at sea level (101,300 kPa); the atmospheric pressure during the tests is the atmospheric pressure at Des Moines (97,825 kPa – 294 m above sea level).

More specific

The specific capacity AFWW0 is derived from table 2a (see test procedure table 4.2.) and according to appendix A:

AFWW0 = 1109 W/K.
$Flow_{air,0}$ = 1,813 kg/s
$Flow_{water,0}$ = 1,299 kg/s

A second point is given in table 2b. According to appendix A:

AFWW = 930 W/K.
$Flow_{air}$ = 1,753 kg/s (97 %)
$Flow_{water}$ = 0,573 kg/s (44 %)

A third point is given in table 2c. According to appendix A:

AFWW = 375 W/K.
$Flow_{air}$ = 1,737 kg/s (96 %)
$Flow_{water}$ = 0,090 kg/s (7 %)

The heating fluid applied was water:

- specific mass SMW = 1000 kg/m^3
- specific heat SWW = 4180 J/kg.K

Table 2a: Input data for the heating coil – point #0
Data from table 4.2 – test specifications
Atmospheric pressure: 101.3 kPa

```
-> 1. Verwarmbatterij
Vermogen (in W)- waterA/Rtemp.      - LuchtA/Rtemp.   -  deb.fract.
   QCEVWMX      TWBAT1A    TWBAT1R    TLBAT1A  TLBAT1R   DBFRW1
    61000.0       82.3       71.1       4.44    37.78    1.00
```

Table 2b: Input data for the heating coil – point #1
Data from table 4.4 – test specifications
Atmospheric pressure: 99.0 kPa

```
-> 1. Verwarmbatterij
Vermogen (in W)- waterA/Rtemp.      - LuchtA/Rtemp.   -  deb.fract.
   QCEVWMX      TWBAT1A    TWBAT1R    TLBAT1A  TLBAT1R   DBFRW1
    44200.0       69.3       50.9       0.1      25.1     1.00
```

Table 2c: Input data for the heating coil – point #2
Data from table 4.4 – test specifications
Atmospheric pressure: 97.7 kPa

```
-> 1. Verwarmbatterij
Vermogen (in W)- waterA/Rtemp.      - LuchtA/Rtemp.   -  deb.fract.
   QCEVWMX      TWBAT1A    TWBAT1R    TLBAT1A  TLBAT1R   DBFRW1
    12200.0       69.9       37.4      16.0      23.0     1.00
```

4. Modeling Options and Conducted Tests

The tests involved:

- heating coil comparative tests
- heating coil empirical tests

Heating coil comparative tests

The heating coil model is tested insitu of the VA114 simulation program. Actual weather data is used to obtain the conditions of the air at the air inlet.

The tests involved the influence of:

- air volume flow rate over the heating coil
- type of heating fluid
- type of control at the "water" side
- air outlet temperature

Air volume flow rate over the heating coil
Two options: Constant air volume (CAV – constant all the time at 4500 m^3/h) and Quasi-Variable air volume (VAV – 2000 m^3/h from 6 p.m. to 7 a.m. and 5000 m^3/h for the other hours). Remark: the Air volume flow rate is defined at the conditions of the supply air/the air outlet

Type of heating fluid
Only one option: the tests were conducted for water as the heating fluid (IEA43ME= +11 or -11).

Type of control at the "water" side
Two options:

- the water inlet temperature is constant; the heating power is controlled by varying the water flow rate over the heating coil m_{var} (IEA43ME = positive value= +11)
- the water flow rate is constant; the heating power is controlled by varying the water inlet temperature T_{var} (IEA43ME = negative value = -11)

Air outlet temperature
Two options: the air outlet temperature has as set point 13 ^oC and 18 ^oC.

The conducted tests are numbered (HX100 etc.) and given in table 3.

Further information
Simulation period: 212 days – from October 1 till April 30.
Weather file: 14933.tm2 (Des Moines - Iowa)

Table3: Conducted tests

Testcase	Configuratie	Airflow	Fluid	DCA-ST	IEA43ME
				Degree C	
HX100	m_{var}	CAV	Water	13	11
HX120			Water	18	11
HX200	m_{var}	VAV	Water	13	11
HX220			Water	18	11
HX300	T_{var}	CAV	Water	13	-11
HX320			Water	18	-11
HX400	T_{var}	VAV	Water	13	-11
HX420			Water	18	-11

Heating coil empirical tests

The heating coil model is tested outside the VA114 simulation program. Air flow rate, water flow rate, entering air temperature, entering water temperature and atmospheric pressure are available from file HCEmpInput1.txt (period February 21, 10.00 h – February 28, 09.00 h; remark: February 26, 00.00 h – 24.00 h is skipped).

Remark: on that file are also the air temperature and the relative humidity at the position of the air flow meter.

A special subroutine was developed to read the data and to write the results to the results file.

5. Modeling Difficulties

Heating coil comparative tests

Air inlet temperature higher than the required set point
Heating of the air is only required in case the air inlet temperature is lower than the set point. In case the air inlet temperature is higher than the set point the air is not conditioned and leaves the heating coil with the same temperature. Also at the water side the water outlet temperature is the same as the water inlet temperature (70 ^{o}C)

Type of control at the "water" side
Standard the heating coil in VA114 has a constant water flow over the coil; heating power is controlled by varying the water inlet temperature (T_{var}).
For these IEA34/43 - tests the heating coil model was extended with the option "constant water inlet temperature"; heating power is controlled by varying the water flow over the coil (m_{var})

Required output simulation results
The required output is not standard coming from VA114. An adaption of the program was made to get the required output.

There are no other modeling difficulties.

Heating coil empirical tests

There are no other modelling difficulties.

General remark
Vabi Software BV thinks in this IEA-group special attention should be paid to uniform nomenclature for the input and output parameters. To be clear for future users of the tests.
At the moment the nomenclature is not uniform. This remark is valid for both the heating coil and the cooling coil tests.

6. Software errors discovered and/or Comparison between different versions of the same software.

No software errors were discovered until now.

7. Results

7.1 Results concerning given specifications heating coil

The specific capacity AFWW is derived from table 4.2. of the spec's [1] and according to appendix A:

Point #0 – Manufacturer data

Specific capacity AFWW	= 1109 W/K.
Air mass flow rate $Flow_{air}$	= 1,813 kg/s *)
Fluid mass flow rate $Flow_{water}$	= 1,299 kg/s

*) Belonging air volume flow rate = 5420 m3/h (at 20 ^{o}C and 101,3 kPa).

Point #1 – From empirical data

Specific capacity AFWW	= 930 W/K.
Air mass flow rate $Flow_{air}$	= 1,753 kg/s *)
Fluid mass flow rate $Flow_{water}$	= 0,573 kg/s

*) Belonging air volume flow rate = 5240 m3/h (at 20 ^{o}C and 101,3 kPa).

Point #2 – From empirical data

Specific capacity AFWW	= 375 W/K.
Air mass flow rate $Flow_{air}$	= 1,737 kg/s *)
Fluid mass flow rate $Flow_{water}$	= 0,090 kg/s

*) Belonging air volume flow rate = 5190 m3/h (at 20 ^{o}C and 101,3 kPa).

Remark: the range in fluid flow rates (0,09 – 1,30 kg/s) is very OK; the range in air flow rates (1,73 – 1,81 kg/s) is very bad!! This will influence the applicability of method to determine A11, B11 and C11 (see appendix B)

7.2 Results of the several tests

For the Heating Coil model three steps for the specific capacity AFWW are distinguished:

- step 1: AFWW is independent of the flows, so fixed
- step 2: AFWW is dependent on the flows; A11 = B11 = C11 = 1,0
- step 3: AFWW is dependent on the flows; A11, B11 and C11 are derived with the extra data points

The tests are carried out for those 3 modelling steps.

Heating coil comparative tests

Coil characteristics derived from data point #0 (Manufacturer data) are used for these calculations.

Remark: Step 3 is not possible with only one data point. Therefore data point #2 (Empirical data) was used as extra point (data point #2 has lowest water flow rate). This resulted in A11 = 0,82 and B11 = 1,28 (C11 = 1,0)

Results are available hourly and as total over the simulation period (October 1 till April 30).

The hourly results are available in file "Results hx-cases-hourly-i-20070719.xls"; the totals for the entire simulation period are given in table 4-i (see also file "Results hx-cases-totals-i-20070719.xls"). In this table the peak power is given too.

Remark: the index 'i' is indicating step1, step2 or step3

Comments to the totals
Step 1:

- The VAV-cases show a lower heating load than the CAV-cases. Two reasons: the lower '24-hour' average air flow rate (3375 m^3/h in stead of 4500 m^3/h) and the higher flow rate at day-time (at day-time the air inlet temperature is higher than at night time)
- Control at the "water" side by controlling the fluid flow (water inlet temperature is constant) gives the same heating load as by controlling the water inlet temperature. Reason: the supplied sensible heat is the same and the supplied latent heat is zero.
- Remark: maximum power is almost reached at January 15 at hour 8 (ambient temperature = -27,1 ^oC and Relative Humidity = 59,8 %) and is 73,35 kW (maximum power = 73,90 kW).

Step 2:

- Results are the same as for step 1, except for the cases HX220 and HX420. In those cases maximum capacity is demanded for.
- This is according to the expectations (see first draft of this report).

Step 3:

- Results are the same as for step 1 and 2, except for the cases HX220 and HX420. In those cases maximum capacity is demanded for.

Comments to the hourly results

At the air side the temperature is controlled at the required set point. All steps show the same result. At the water side the three steps show big differences.
For instance February 4 at 24.00 h (case HX100):

```
Step 1:  EWT = 70,00 °C; LWT =   4,68 °C; HWFR = 0,133 kg/s; HLT = 36,20 kW
Step 2:  EWT = 70,00 °C; LWT =  43,37 °C; HWFR = 0,325 kg/s; HLT = 36,20 kW
Step 3:  EWT = 70,00 °C; LWT =  39,82 °C; HWFR = 0,287 kg/s; HLT = 36,20 kW
```

Conclusions

The Heating Coil model has no influence on the annual heating load results except for the cases where the maximum capacity is asked for. However the Heating Coil Model has a big influence on what at the water side is happening.

Table 4-1: Total heating results for the several tests
Step 1 - AFWW is fixed

Testcase	Configuratie	Airflow	Fluid	DCA-ST	IEA43ME	Heating	Peak Heating
				Degree C		kWh	kW
HX100	m_{var}	CAV	Water	13	11	86484	59,712
HX120			Water	18	11	120351	67,030
HX200	m_{var}	VAV	Water	13	11	61579	65,216
HX220			Water	18	11	86457	73,348
HX300	T_{var}	CAV	Water	13	-11	86484	59,712
HX320			Water	18	-11	120351	67,030
HX400	T_{var}	VAV	Water	13	-11	61579	65,216
HX420			Water	18	-11	86457	73,348

Table 4-2: Total heating results for the several tests
Step 2 - AFWW is flow dependent – A11 = B11 = C11 = 1,0

Testcase	Configuratie	Airflow	Fluid	DCA-ST	IEA43ME	Heating	Peak Heating
				Degree C		kWh	kW
HX100	m_{var}	CAV	Water	13	11	86484	59,712
HX120			Water	18	11	120351	67,030
HX200	m_{var}	VAV	Water	13	11	61579	65,216
HX220			Water	18	11	86456	72,745
HX300	T_{var}	CAV	Water	13	-11	86484	59,712
HX320			Water	18	-11	120351	67,030
HX400	T_{var}	VAV	Water	13	-11	61579	65,216
HX420			Water	18	-11	86456	72,745

Table 4-3: Total heating results for the several tests
Step 3 - AFWW is flow dependent – A11, B11 and C11 determined from data points #0 and #2

Testcase	Configuratie	Airflow	Fluid	DCA-ST	IEA43ME	Heating	Peak Heating
				Degree C		kWh	kW
HX100	m_{var}	CAV	Water	13	11	86484	59,712
HX120			Water	18	11	120351	67,030
HX200	m_{var}	VAV	Water	13	11	61579	65,216
HX220			Water	18	11	86455	72509
HX300	T_{var}	CAV	Water	13	-11	86484	59,712
HX320			Water	18	-11	120351	67,030
HX400	T_{var}	VAV	Water	13	-11	61579	65,216
HX420			Water	18	-11	86455	72509

Heating coil empirical tests

Coil characteristics derived from data point #1 (Empirical data) are used for these calculations.

For step 3 data point #2 (Empirical data) was used as extra point. This resulted in A11 = 1,43 and B11 = 0,77 (C11 = 1,0)

Remark:
The here found A11, B11 and C11 differ considerably from those coefficients derived from data point #0 and #2. May be because the Manufacturer data (#0) is less trusty.

Tests are presented in the output file 'Results hx-exercise 2-emp-tot-20070719.xls' for all 3 steps.

In figure 2a – f the input data is given: air volume flow rate, fluid flow rate, entering air temperature, entering air relative humidity, entering air humidity and entering water temperature.

Air flow rate (~5000 m^3/h) and entering water temperature (~70 ^oC) are almost constant during this test.

In figure 3a – f the output data for the 3 steps is given: the heating load, the specific capacity AFWW, the leaving air temperature and leaving water temperature during a small period with low fluid flow rate and during a small period with high fluid flow rate.

The influence of the 3 steps are rather big!!!

More in detail:

At low fluid flow rates (time = 4400-4800 minutes; see figure 2b)

Step 1, fixed AFWW, gives with low fluid flow rates a too big heat transfer, which results in a higher air temperature at the outlet and a too low water temperature at the outlet.

Step 2, AFWW, split into 3 equal parts at design power, and dependent on flows, gives a result that seems to be one order better than step 1.

Step 3, AFWW, split into 3 parts based on extra data points, and dependent on flows, gives some more fine tuning with respect to step 2.

At high fluid flow rates (time = 5400-5800 minutes; see figure 2b)

The differences between the steps are much smaller.

Figure 2a: Empirical test input data: Air volume flow rate.

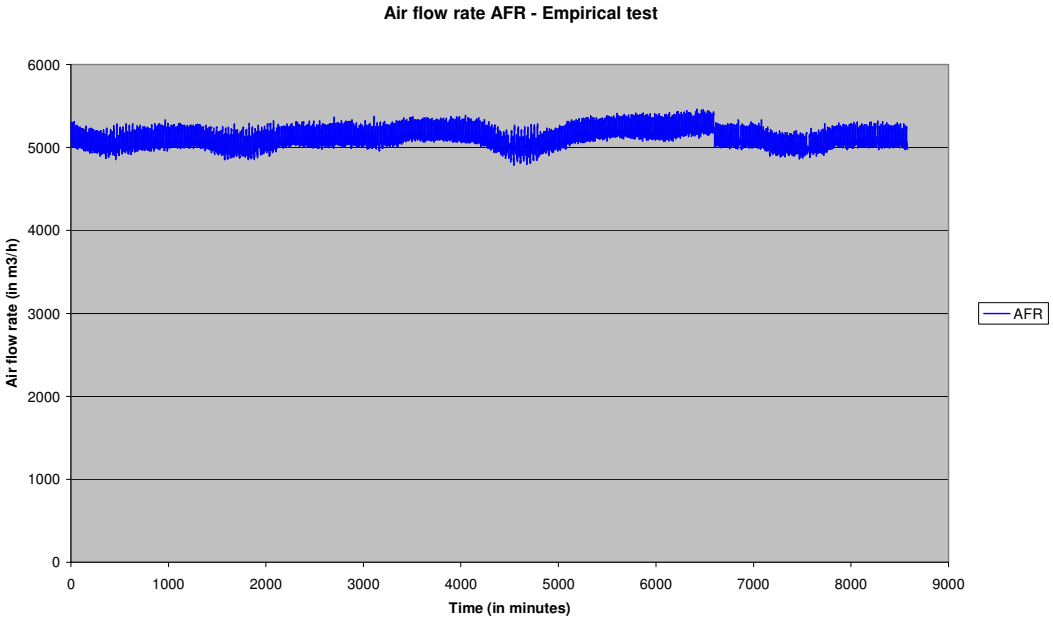

Figure 2b: Empirical test input data: Fluid volume flow rate.

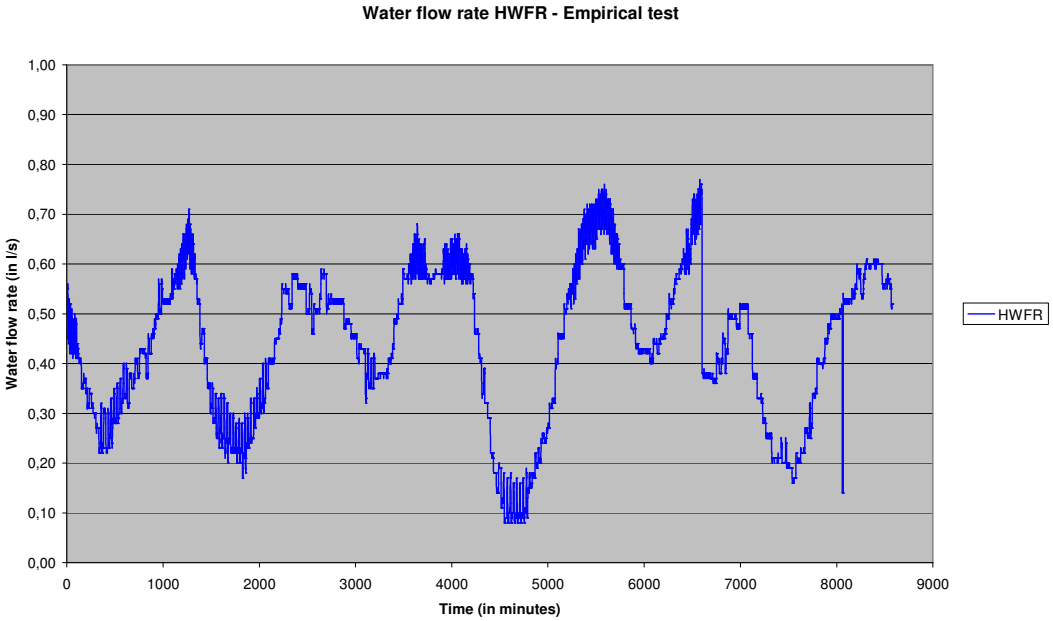

Figure 2c: Empirical test input data: Entering air temperature.

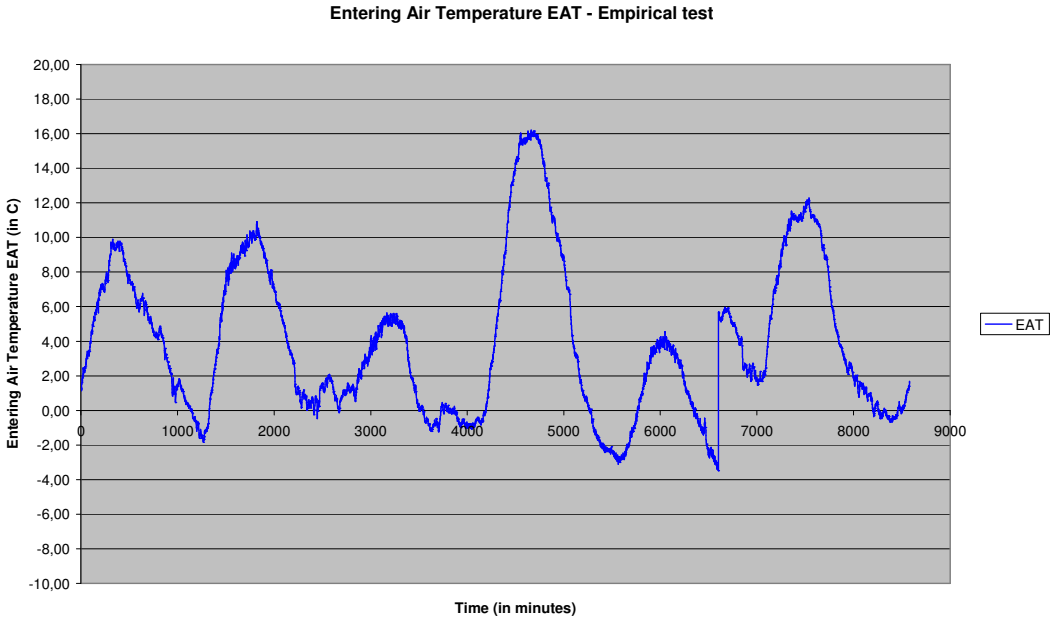

Figure 2d: Empirical test input data: Entering air relative humidity.

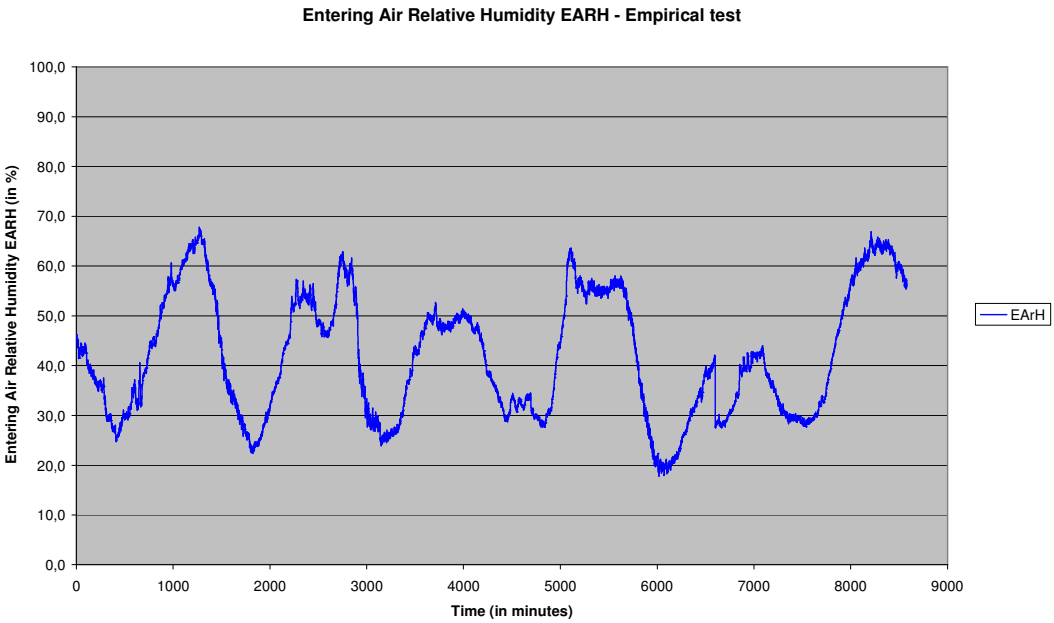

Figure 2e: Empirical test input data: Entering air humidity.

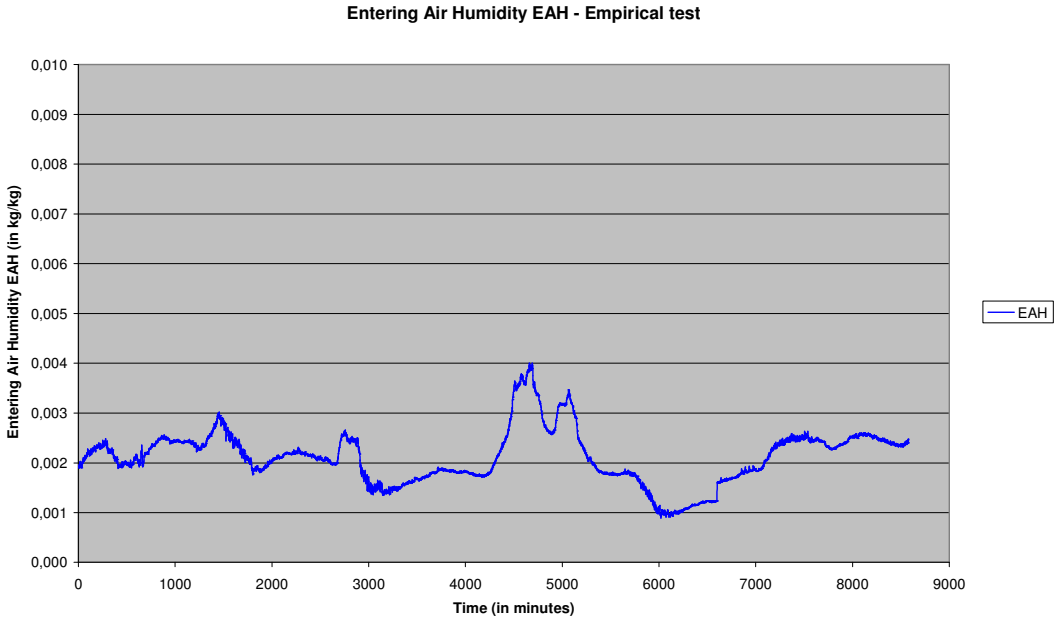

Figure 2f: Empirical test input data: Entering water temperature.

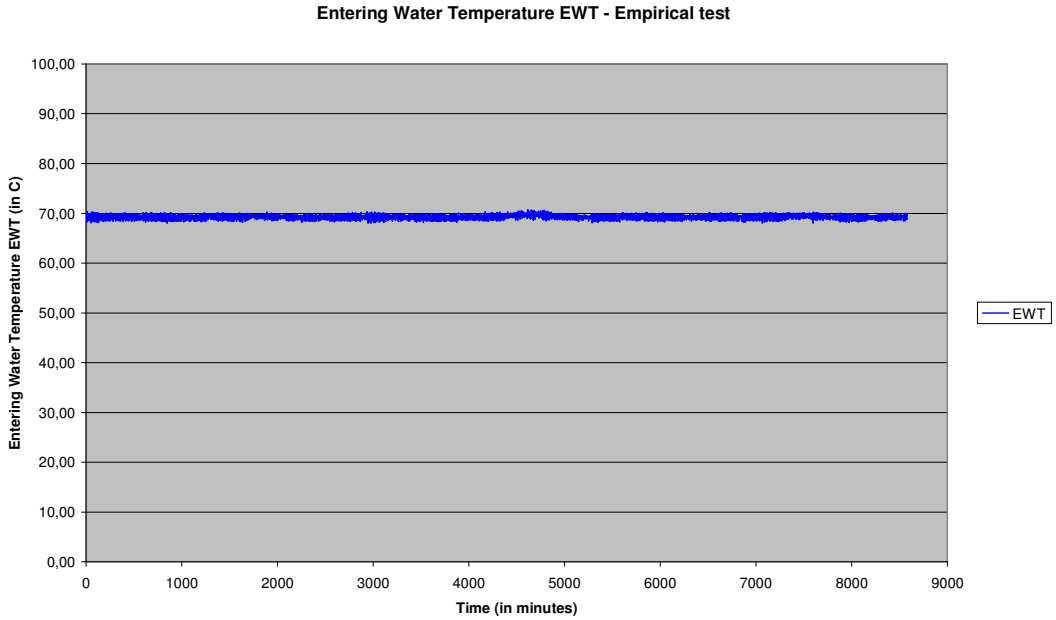

Figure 3a: Empirical test output data: Heating load.

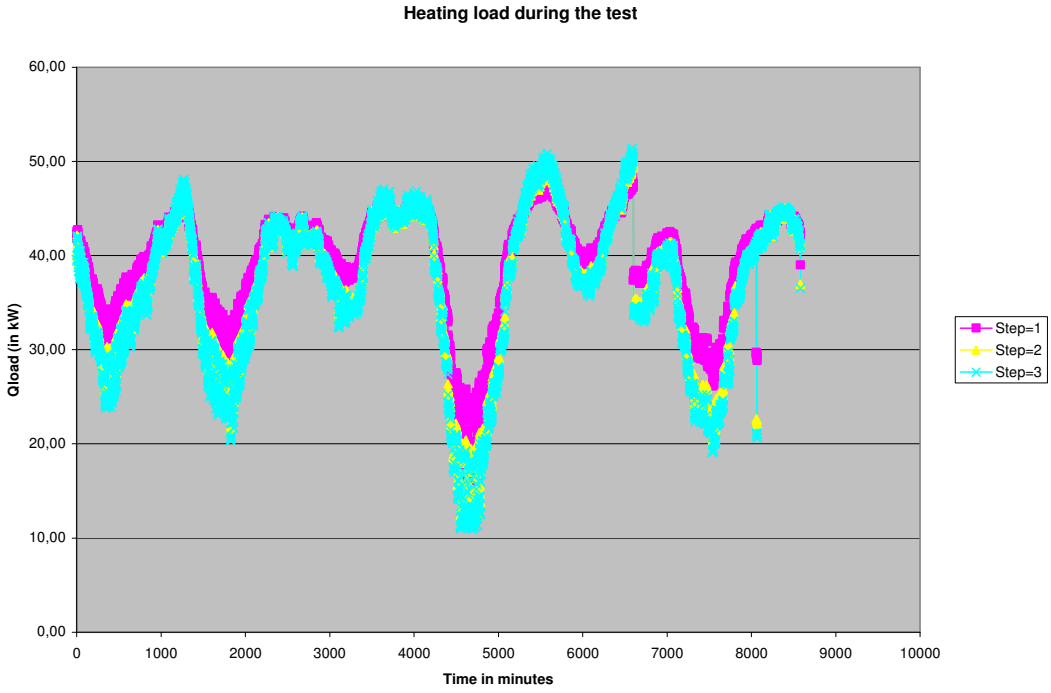

Figure 3b: Empirical test-output data: Specific Capacity

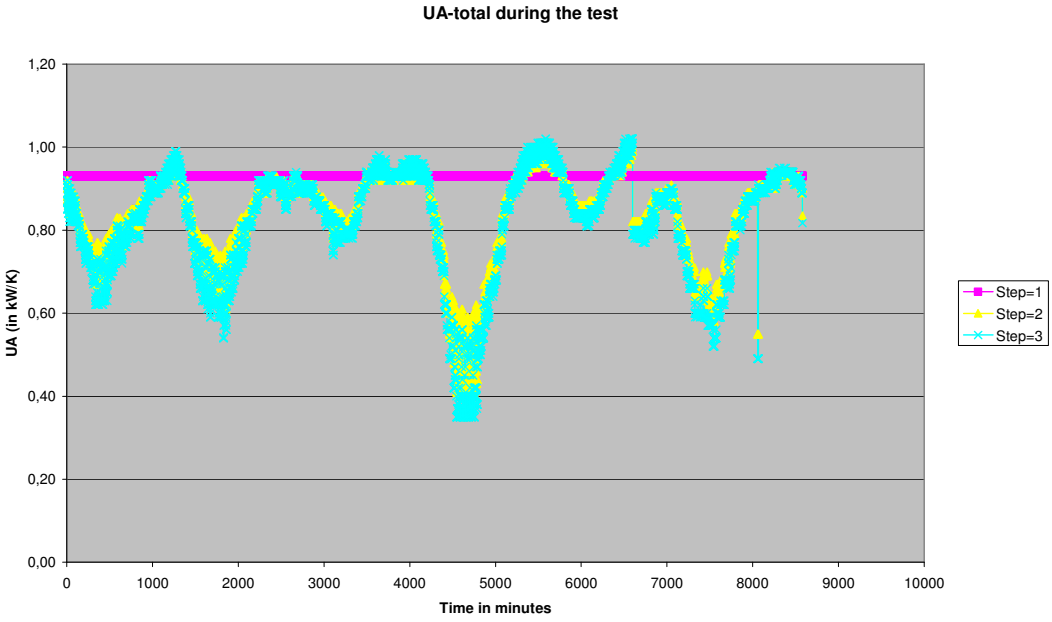

Figure 3c: Empirical test-output data: Leaving air temperature (low fluid flow rate)

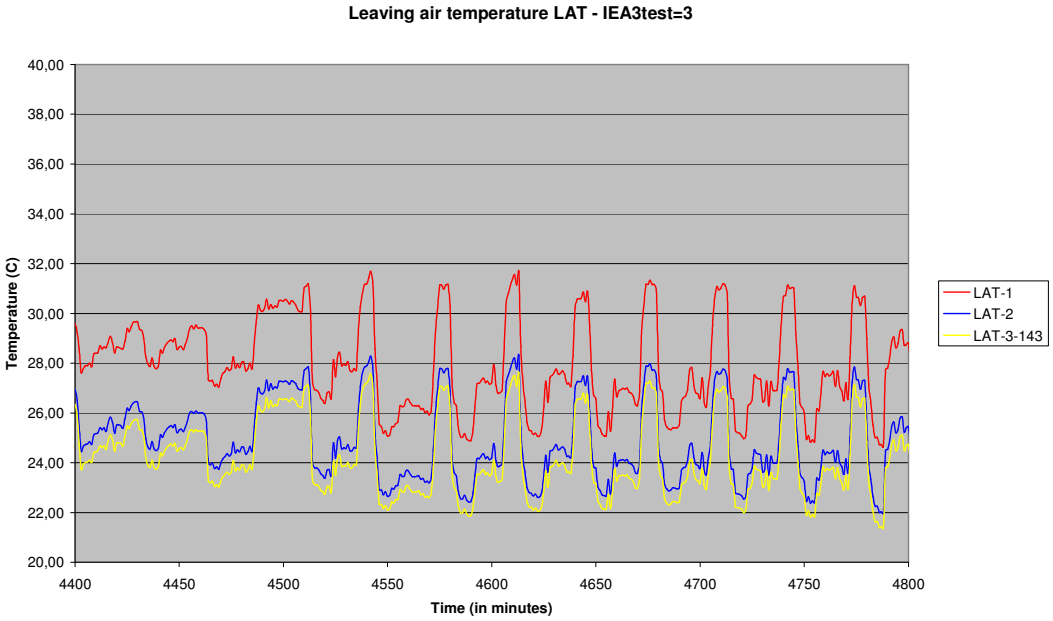

Figure 3d: Empirical test-output data: Leaving water temperature (low fluid flow rate)

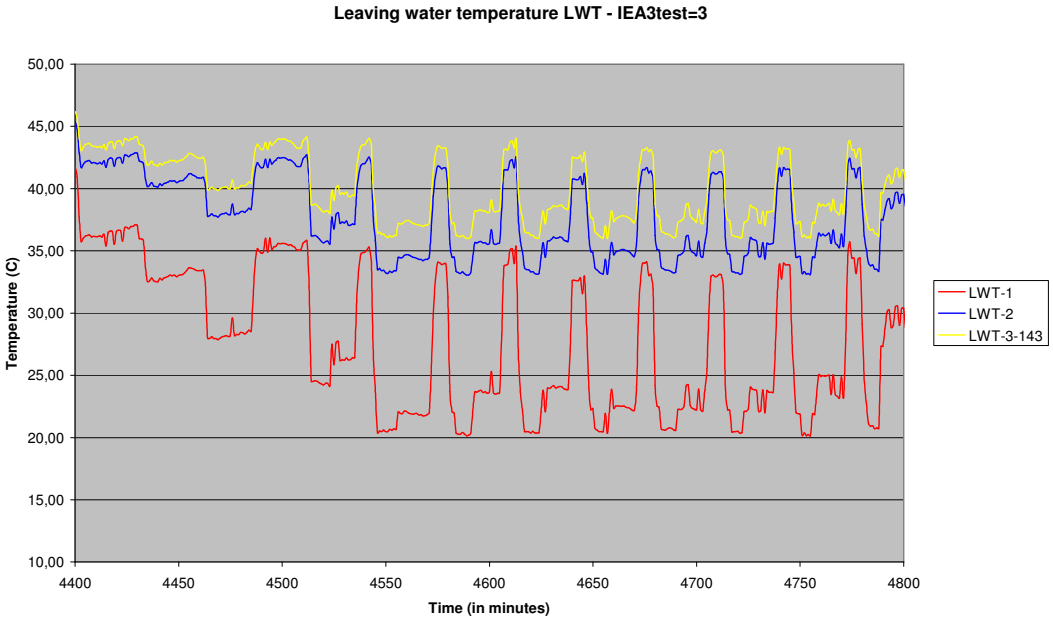

Figure 3e: Empirical test-output data: Leaving air temperature (high fluid flow rate)

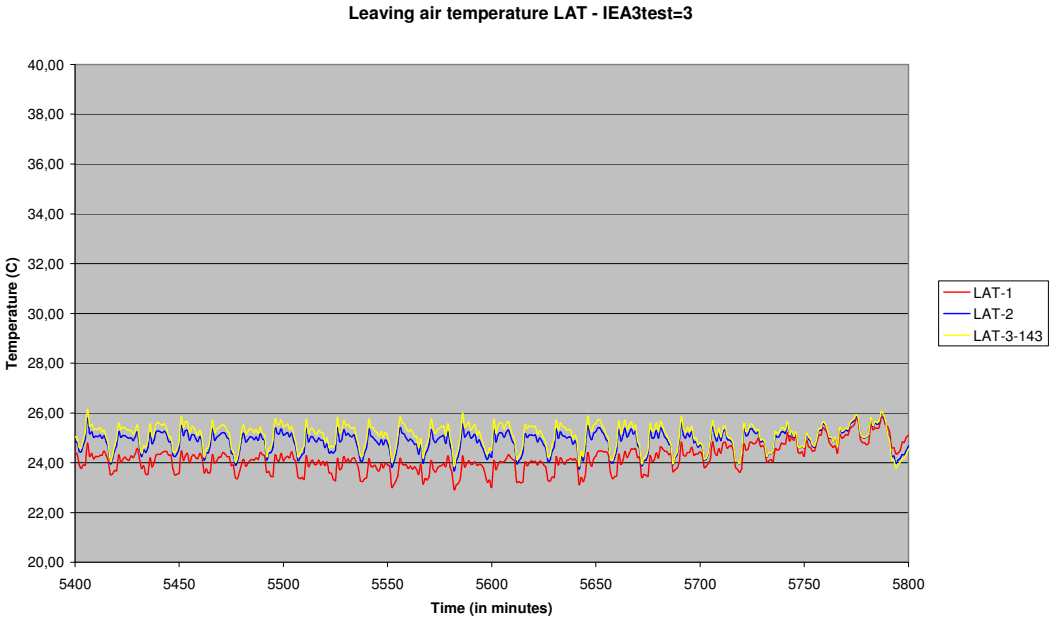

Figure 3f: Empirical test-output data: Leaving water temperature (high fluid flow rate)

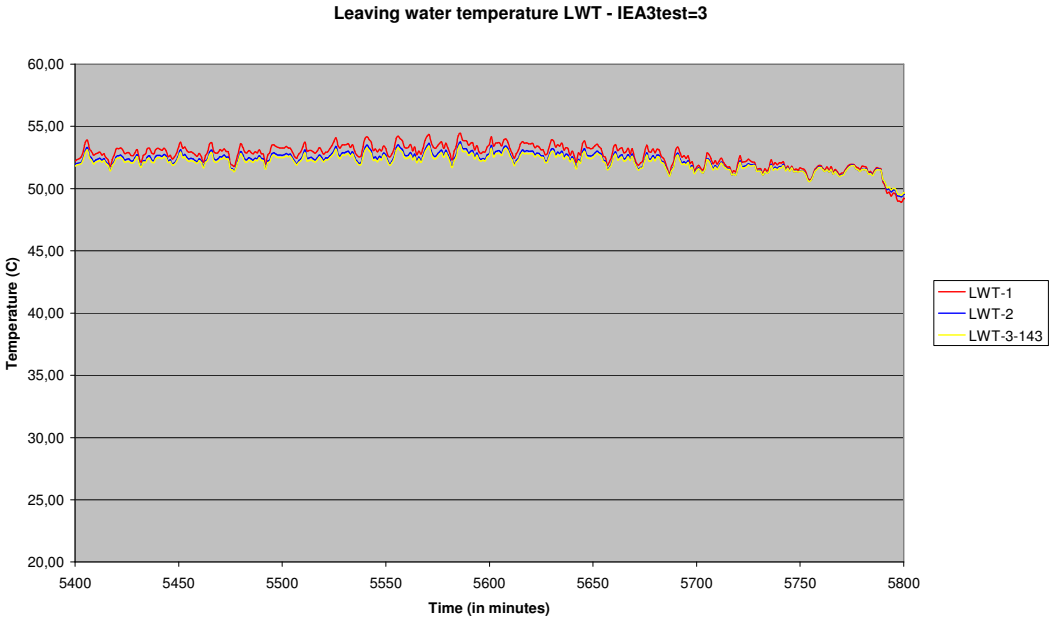

8. **Other** (optional)

No other tests were done

9. Conclusions and Recommendations

Test data and results of other participating heating coil models are available. A first comparison between models was made (see first draft of final report of this subtask) , which led to fine tuning of the test specs. Now a new comparison can be made, which will result in some smaller differences between the models.

Remark:
To determine the coil characteristics 3 data points (1 x Manufacturer and 2 x Emperical) were available. These points were not optimal:

- Is the Manufacturer point trusty?
- The air flow rate of all 3 data points was about the same (96-100%); it is required those flow rates are reasonably different (in range 20 – 100%)

Required are better data points: do only a few measurements but at defined flow rates (air – water is resp. 100%-100%, 20%-100%, 100%-20%, 20%-20%) instead of many measurements on undefined flow rates during a longer test period.

10. References

[1] Felsmann, C.
"Heating water system – a set of comparative and empirical test cases: exercise 2 – Heating Coil (chapter 4)", IEA: SHC Task 34 / ECBCS Annex 43, March 30, 2006.

[2] Felsmann, C.
"Chilled water system – a set of comparative test cases: exercise 2 – Heating Coil (chapter 4)", IEA: SHC Task 34 / ECBCS Annex 43, January 2, 2006.

[3] Wijsman, A.
"Cooling Coil – Modeler Report VA114 – draft 3", IEA: SHC Task 34 / ECBCS Annex 43, February 24, 2006.

[4] Wijsman, A.
"Heating Coil – Modeler Report VA114 – draft 1", IEA: SHC Task 34 / ECBCS Annex 43, May 17, 2006.

[5] Wijsman, A. and Szufa, S.
"Heating Coil – Modeler Report VA114 – draft 2", IEA: SHC Task 34 / ECBCS Annex 43, July 27, 2006.

Appendix A: Determination of the specific capacity of the heating coil

The specific capacity of the heating coil AFWW is the heat exchange per degree temperature difference (W/K) for the situation without condensation.

In figure A.1 the several parameters are defined.

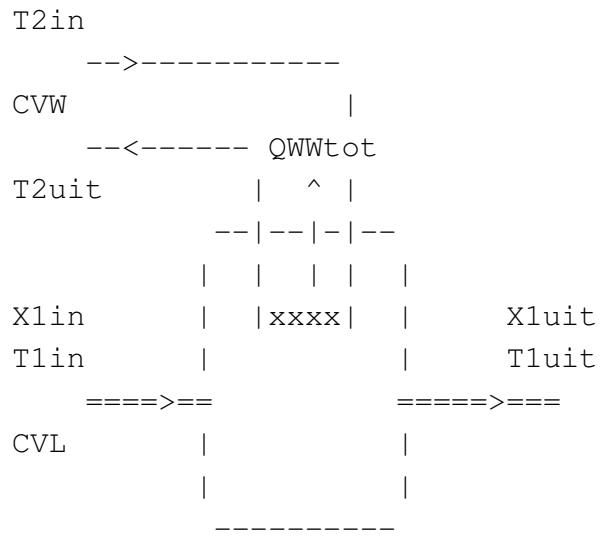

Figure A.1: Definition of the several parameters

In general the heat exchange is only dependent on the air temperature at the entrance.

From the input data are known:

- QWWtot
- T1in
- T1uit
- T2in
- T2uit

From this information the air flow rate, the water flow rate and the specific capacity AFWW can be derived (see next page)

Determination of air flow rate, water flow rate and specific capacity AFWW

```
Uitgewisseld vermogen water-lucht - QWW
- - - - - - - - - - - - - - - - - - - -

Luchtzijde
- - - - - -
Temperatuur -in                    - T1IN
Temperatuur -uit                   - T1UIT
Capaciteitsdebiet                  - CVL
CVL = -QWW/(T1IN-T1UIT)

Waterzijde
- - - - - -
Temperatuur -in                    - T2IN
Temperatuur -uit                   - T2UIT
Capaciteitsdebiet                  - CVW
CVW =  QWW/(T2IN-T2UIT)


Bepaling effectiviteit van de warmtewisselaar
Definitie:    QWW   = EFFWW * CVMIN * (T2IN-T1IN)

Kleinste capaciteitsstroom
CVMIN = MIN(CVL,CVW)

Effectiviteit
EFFWW = QWW / (CVMIN * (T2IN-T1IN))
EFFWW = MIN(EFFWW,0.9999)

Tegenstroom warmtewisselaar
IF (ABS(CVL-CVW).LE.0.00001) THEN
   Definitie: EFFWW = AFWW/(AFWW+CVMIN)
   AFWW  = CVMIN * EFFWW / (1.0-EFFWW)
ELSE
   Definitie: EFFWW = (EXP1 - 1.0) / (A1*EXP1 - B1)
              EXP1  = EXP(-ARG1)
              ARG1  = AFWW * (1.0/CVL-1.0/CVW)
   A1    = CVMIN/CVW
   B1    = CVMIN/CVL
   EXP1  = (1.0-EFFWW*B1)/(1.0-EFFWW*A1)
   ARG1  = -LOG(EXP1)
   AFWW  = ARG1 / (1.0/CVL-1.0/CVW)
ENDIF
```

Appendix B: Determination of A11, B11 and C11 from extra data points

At present time Manufacturer data is given for 1 point:

- Load Q
- Air inlet and air outlet temperature
- Water inlet and water out temperature

From this data follow air flow (FLOWair0) and water flow (FLOWwater0); also the overall UA-value of the coil can be derived (see appendix A).

At other air / water flow rates the overall UA-value will be different and that is dependent on the individual UA,air and UA,water:

$$UA = \frac{1}{1/UA,air + 1/UA,metal + 1/UA,water} \qquad (1)$$

UA,air and UA,water are both flow dependent:

$$UA,air = fair * UA,air0 \qquad (2a)$$

$$UA,water = fwater * UA,water0 \qquad (2b)$$

Factors fair and f water are correction factors for the flow dependency. Index '0' means at manufacturer flows.

Definition:

$$UA,air0 = 3.0 * A11 * UA0 \qquad (3a)$$

$$UA,water0 = 3.0 * B11 * UA0 \qquad (3b)$$

$$UA,metal = 3.0 * C11 * UA0 \qquad (3c)$$

So

$$1/B11 = 3.0 - 1/A11 - 1/C11 \qquad (3d)$$

Statement:

If data for a second and third point is available the ratio A11 and C11 (and B11) can be derived.

Ł Determination of A11 and B11 from 3 data points

Second data point:

For a second point the UA2, FLOWair2 and FLOWwater2 can be derived.

With equation (1)

$$UA2 = \frac{1}{1/UA,air2 + 1/UA,metal + 1/UA,water2} \quad (4)$$

With equations (2) in equation (4)

$$UA2 = \frac{1}{1/(fair2*UA,air0)+1/UA,metal+1/(fwater2*UA,water0)} \quad (5)$$

And equations (3) in equation (5)

$$UA2 = UA0 * \frac{3}{1/(fair2*A11) + 1/C11 + 1/(fwater2*B11)} \quad (6)$$

Define

$$frac2 = UA2/UA0 \quad (7)$$

From (6) and (7)

$$3/frac2 = 1/(fair2*A11) + 1/(fwater2*B11) + 1/C11 \quad (8)$$

Use equation (3d)

$$3/frac2 = (1/A11)/fair2+(3-1/A11-1/C11)/fwater2+1/C11 \quad (9)$$

or

$$3/frac2-3/fwater2 = 1/A11*(1/fair2-1/fwater2)+1/C11*(1-1/fwater2) \quad (10)$$

or

$$K2 = 1/A11*L2 + 1/C11*M2 \quad (11)$$

Two unknowns: A11 and C11

Third data point:

The same as for data point 2:

$$3/frac3-3/fwater3 = 1/A11*(1/fair3-1/fwater3)+1/C11*(1-1/fwater3) \quad (12)$$

or

$$K3 = 1/A11*L3 + 1/C11*M3 \quad (13)$$

Two equations and two unknowns

So there are two equations (11 and 13) and two unknowns (A11 and C11); so A11 and C11 can be derived.

$$A11 = (M3L2 - M2L3)/(M3K2-M2K3) \quad (14a)$$

and

$$C11 = (M2L3 - M3L2)/(L3K2-L2K3) \quad (14b)$$

Ł And the individual UA,air0 and UA,water0 and UA,metal are known.

Information about fair and fwater

From literature study it was found

$$fair = (FLOWair/FLOWair0)^{0.56} \quad (15a)$$

$$fwater = (FLOWwater/FLOWwater0)^{0.80} \quad (15b)$$

Both for turbulent flow. It was found in almost all cases the flow is turbulent.

Test of this method:

Take as second point Part,air = 20 % and Part,water = 20 % and the belonging load Q and the inlet and outlet temperature at both the water and the air side.

Determine UA2 and so frac2 (according to (7)). Determine fair2 and fwater2.

Take as third point Part,air = 50 % and Part,water = 50 % and the belonging load Q and the inlet and outlet temperature at both the water and the air side.

Determine UA3 and so frac3 (according to (7)). Determine fair3 and fwater3.

And so A11 and C11 become available.

Experience with this method:

With the 3 data points (#0 – Manufacturer data and #1, #2 - Empirical data) this method to determine A11, B11 and C11 was tested. The results were not so good. Probably caused by the fact the Manufacturer data is not so trusty. May be also the small range of the air flow rates causes this.

Below a simpler method, derived from this method, is given. That method supposes C11 is given.

Ł **Determination of A11 and B11 from 2 data points (C11 is given)**

The method is the same for the first two data points. It results in equation (11):

$$K2 = 1/A11*L2 + 1/C11*M2 \qquad (11)$$

Two equations with two unknowns.

It is now assumed the UA,metal is given, so C11 is known.

$$C11 = UA,metal/(3.0 * UA0) \qquad (16)$$

One unknown: A11

$$A11 = L2*C11/(K2*C11 - M2) \qquad (17)$$

Ł And the individual UA,air0 and UA,water0 and UA,metal are known.

Test of this simpler method:

Take as second point Part,air = 20 % and Part,water = 20 % and the belonging load Q and the inlet and outlet temperature at both the water and the air side.

Determine UA2 and so frac2 (according to (7)). Determine fair2 and fwater2.

And so A11 become available.

Experience with this method:

With the 2 data points (#1, #2 - Empirical data) this method to determine A11, B11 and C11 was tested. The results were reasonably good. For this simpler method the influence of C11 (from large to small) on the result (A11 and B11) was determined. For C11 > 10 the A11 = 0,60 and B11= 0,77; for smaller C11 it was found B11 is about independent (for this case?!) of C11 (B11 = 0,77). For some C11's (and belonging A11's) the tests were done. The influence was not so big. Therefore it was decided to take C11 = 1,0 and so A11 became 1,43

Remark: this method was tested too with data points #0 (Manufacturer data) and #2 (empirical data). The experience was the same, the resulting A11 (0,82) and B11 (1,28) were reasonably different!! Is it the Manufacturer datapoint??!!

7.2.3 Gard – EnergyPlus

IEA MECHANICAL EQUIPMENT COMPARATIVE HEATING COIL TEST REPORT CASES HX100, HX120, HX200, HX220 ENERGYPLUS VERSION 2.2.0.023

Prepared by
R. Henninger & M. Witte, GARD Analytics, Inc.

April 2008

1. Introduction

Software:	EnergyPlus Version 2.2.0.023
Authoring Organization:	U.S. Department of Energy Energy Efficiency and Renewable Energy Office of Building Technologies
Authoring Country:	USA

This report describes the modeling methodology and results for Round 2 of testing done for the IEA Heating Water System, Heating Coil Comparative Tests, Cases: HX100, HX120, HX200 and HX220 which were simulated using the EnergyPlus software. The specifications for the test suite are described in *Heating Water System – A Set of Comparative and Empirical Test Cases, IEA: SHC Task 34 / ECBCS Annex 43, Subtask D: Mechanical Equipment and Control Strategies* dated July 3, 2006 (referred to as the Heating Water System specification in this report). The other 12 cases that are part of the Heating Coil Comparative Test (Section 4.4 of the specification) could not be modeled by the EnergyPlus software due to the following limitation:

a) Varying water supply temperatures to heating coils with constant water flow rates cannot currently be modeled by EnergyPlus.

2. Modeling Assumptions

The following comments are provided in regards to user inputs that were used with EnergyPlus to model Cases HX100, HX120, HX200 and HX220 in the Heating Water System specification. Except where discussed below, all other requirements of the specification for these cases were met.

a) In order to generate the required heating coil load each hour of the simulation period as required by the Heating Water System specification, the EnergyPlus user must model the whole building including the building envelope, a thermal zone, HVAC system

including heating coil, and plant equipment including hot water boiler equipment. For this test situation, a one zone building was modeled with an adiabatic building shell, no windows and no internal loads.

b) Since Table 4.3 of the specification indicates that the air flow network is VAV for some cases, the HVAC system was modeled as a variable volume system using the SINGLE DUCT:VAV:NOREHEAT object in EnergyPlus with input parameters set as shown below:

```
SINGLE DUCT:VAV:NOREHEAT,
    ZONE ONE VAV Reheat,          !- Name of System
    COMPACT HVAC-ALWAYS 1,        !- System Availability schedule
    ZONE ONE Supply Inlet,        !- UNIT Air Outlet Node
    ZONE ONE Zone Equip Inlet,    !- UNIT Air Inlet Node
    1.25,                         !- Maximum air flow rate {m3/s}
    1.;                           !- Zone Minimum Air Flow Fraction
```

The VAV system as described in the specification is not a typical fully variable volume air flow system but is referred to in Section 4.4.2 of the specification as "Quasi-Variable Air Volume" since the air flow rate was either 2000 m3/h or 5000 m3/h depending on the time of day. The VAV system modeled in EnergyPlus was therefore forced to operate as a constant volume system by setting the zone minimum air flow fraction to 1.0. For Cases HX100 and HX120 the maximum air flow rate was set to 4500 m3/h (1.25 m3/s). For Cases HX200 and HX220 where supply air flow changed from 2000 m3/h (0.5555 m3/s) to 5000 m3/h (1.3889 m3/s) depending on time of day, two separate simulations were performed, one at the high flow rate and one at the low flow rate for the entire simulation period, and then the appropriate results were linked into the results spreadsheet. The supply fan heat added to the air stream was forced to be 0.0 by setting the fan delta pressure to 0.0. The VAV system supply air flow was set to 100% outdoor air as follows with the min and max flow rates set accordingly for each test case:

```
CONTROLLER:OUTSIDE AIR,
    SYSTEM-1 OA Controller,          !- Name
    NO ECONOMIZER,                   !- EconomizerChoice
    NO RETURN AIR TEMP LIMIT,        !- ReturnAirTempLimit
    NO RETURN AIR ENTHALPY LIMIT,    !- ReturnAirEnthalpyLimit
    NO LOCKOUT,                      !- Lockout
    PROPORTIONAL MINIMUM,            !- MinimumLimit
    SYSTEM-1 Mixed Air Outlet,       !- Control Node
    SYSTEM-1 Outside Air Inlet,      !- Actuated Node
    1.25,                            !- minimum outside air flow rate {m3/s}
    1.25,                            !- maximum outside air flow rate {m3/s}
    ,                                !- temperature limit {C}
    ,                                !- temperature lower limit {C}
    ,                                !- enthalpy limit {J/kg}
    SYSTEM-1 Relief Air Outlet,      !- Relief Air Outlet Node
    SYSTEM-1 Air Loop Inlet,         !- Return Air Node
```

```
    COMPACT SYSTEM-1 Outside Air Sched,  !- Min.Outside Air Schedule Name
    ;                                    !- Name of VENTILATION:
                                           MECHANICAL object
```

c) The heating coil was modeled using the COIL:WATER:SIMPLEHEATING object in EnergyPlus with input parameters set as shown below:

```
COIL:WATER:SimpleHeating,
    SYSTEM-1 Heating Coil,              !- Coil Name
    COMPACT HVAC-BOILER,                !- Available Schedule
    autosize,                           !- UA of the Coil {W/K}
    0.00133,                            !- Max Water Flow Rate of Coil {m3/s}
    SYSTEM-1 Heating Coil HW Inlet,     !- Coil_Water_Inlet_Node
    SYSTEM-1 Heating Coil HW Outlet,    !- Coil_Water_Outlet_Node
    SYSTEM-1 Supply Fan Outlet,         !- Coil_Air_Inlet_Node
    SYSTEM-1 Heating Coil Outlet,       !- Coil_Air_Outlet_Node
    UA and Design Water Flow Rate,      !- Coil Performance Input Method
    autosize,                           !- Nominal Capacity {W}
    82.2,                               !- Design Inlet Water Temperature {C}
    4.44,                               !- Design Inlet Air Temperature {C}
    71.22,                              !- Design Outlet Water Temperature {C}
    37.78;                              !- Design Outlet Air Temperature {C}
```

d) Number of timesteps per hour was set to 4 although results were reported on an hourly basis.

e) The 14933.tm2 weather file provided with the test suite was converted to EnergyPlus format (14933TM2.epw) using the EnergyPlus weather conversion program. As instructed in separate correspondence with Dr. Clemens Felsmann, author of the BESTEST Multi-Zone with Airflow specification, daylight savings time was ignored during the simulation.

3. Modeling Difficulties

Only four of the Heating Coil Comparative Test cases (HX100, HX120, HX200 and HX220) described in Section 4.4 of the specification were able to be modeled by EnergyPlus, and these were modeled with WATER as the heating. The other heating coil comparative cases could not be modeled by EnergyPlus due to one of the following reason:

a) They required the use a varying water supply temperature to the heating coils with the water flow rate remaining constant. EnergyPlus will allow different water supply temperatures but currently cannot control the supply temperature of the water entering the coil to meet the load.

Cases HX200 and HX220 both required that the supply air flow rate be fixed at two different values depending on the time of day: 2000 m3/h from 6 p.m. to 7 a.m. and 5000 m3/h from 7 a.m. to 6 p.m. This was modeled in EnergyPlus by two separate simulations, one at 2000 m3/h for the full simulation period and one at 5000 m3/h for the full simulation period. The results

summarized in the spreadsheet then linked to the proper hourly results from the two separate EnergyPlus runs. This does not introduce errors at the transitions because the heating coil input air stream was always 100% outdoor air and not affected by the zone conditions.

4. Results

As requested in Section 4.4.3 of the specification, the following hourly outputs over the seven month (October through April) simulation period are provide in an attached Excel spreadsheet named IEA Heating Coil Results-EnergyPlus-4-22-08-Ver220-023-NoLinks.xls.

1	Time	
2	EAT	Entering air temperature, dry bulb, C
3	EArH	Entering air relative humidity, %
4	EAH	Entering air humidity, kg/kg
5	LAT	Discharge/Leaving air temperature, dry bulb, C
6	LArH	Discharge/Leaving air relative humidity, %
7	LAH	Discharge/Leaving air humidity, kg/kg
8	AFR	Air flow rate, m3/h
9	EWT	Heating water coil entering temperature, C
10	LWT	Heating water coil leaving temperature, C
11	HWFR	Heating water flow rate through the coil, l/s
12	UA	Overall UA-Value of the coil, kW/K
13	HLT	Total heating load, kW
14	HLS	Sensible heating load, kW

Charts displaying some of the results from each of the four test cases are shown on the following pages. It should be noted that the target leaving air temperature for each case was maintained as required by the specification. A brief description of the controlling parameters for each test case is presented below.

Case HX100
Constant air flow = 4500 m3/h = 1.25 m3/s
100% outside air with conditions taken from 14933.tm2 weather file
Constant air discharge temperature from coil = 13C
Constant heating water supply temperature to heating coil = 70C
Variable heating water supply flow to heating coil
Maximum heating water supply flow rate = 1.33 l/s = 0.00133 m3/s

Case HX120
Constant air flow = 4500 m3/h = 1.25 m3/s
100% outside air with conditions taken from 14933.tm2 weather file
Constant air discharge temperature from coil = 18C
Constant heating water supply temperature to heating coil = 70C
Variable heating water supply flow to heating coil
Maximum heating water supply flow rate = 1.33 l/s = 0.00133 m3/s

Case HX200

Constant air flow = 2000 m3/h = 0.5555 m3/s from 6PM to 7AM
Constant air flow = 5000 m3/h = 1.3889 m3/s from 7AM to 6PM
100% outside air with conditions taken from 14933.tm2 weather file
Constant air discharge temperature from coil = 13C
Constant heating water supply temperature to heating coil = 70C
Variable heating water supply flow to heating coil
Maximum heating water supply flow rate = 1.33 l/s = 0.00133 m3/s

Case HX220

Constant air flow = 2000 m3/h = 0.5555 m3/s from 6PM to 7AM
Constant air flow = 5000 m3/h = 1.3889 m3/s from 7AM to 6PM
100% outside air with conditions taken from 14933.tm2 weather file
Constant air discharge temperature from coil = 18C
Constant heating water supply temperature to heating coil = 70C
Variable heating water supply flow to heating coil
Maximum heating water supply flow rate = 1.33 l/s = 0.00133 m3/s

Case HX100

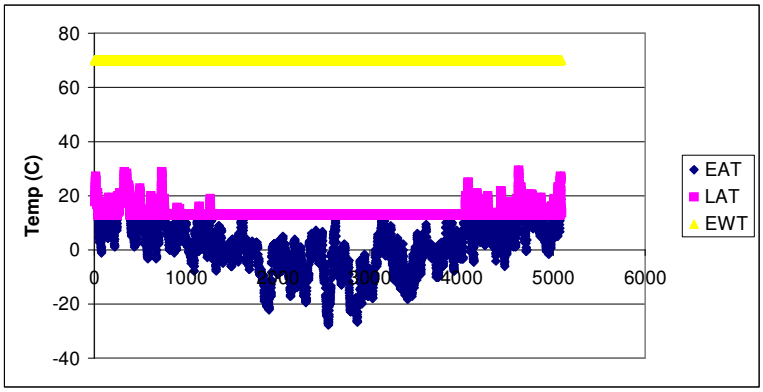
Temp (C)
80
60
40
20
0
-20
-40
0
1000
2000
3000
4000
5000
6000
EAT
LAT
EWT

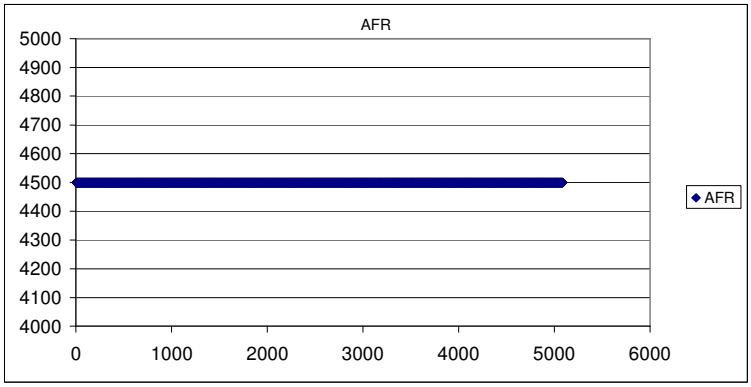
AFR
5000
4900
4800
4700
4600
4500
4400
4300
4200
4100
4000
0
1000
2000
3000
4000
5000
6000
AFR

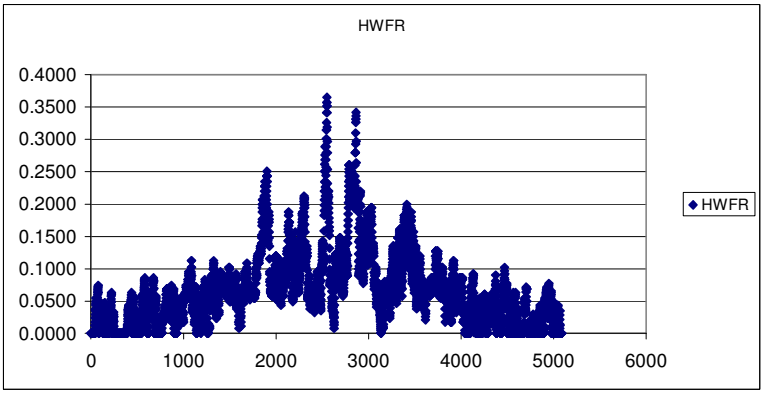
HWFR
0.4000
0.3500
0.3000
0.2500
0.2000
0.1500
0.1000
0.0500
0.0000
0
1000
2000
3000
4000
5000
6000
HWFR

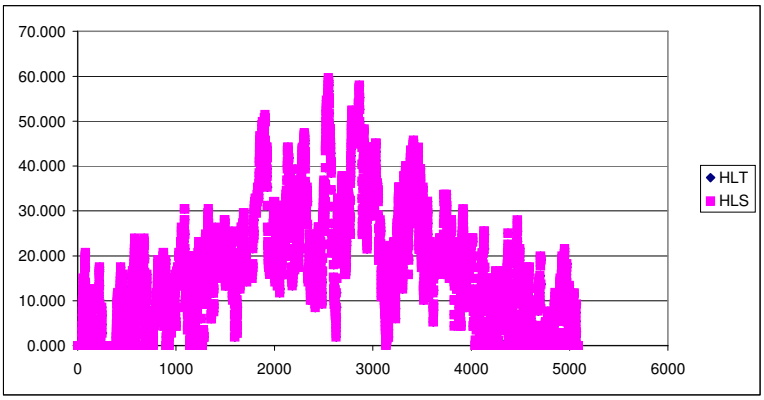
70.000
60.000
50.000
40.000
30.000
20.000
10.000
0.000
0
1000
2000
3000
4000
5000
6000
HLT
HLS

Case HX120

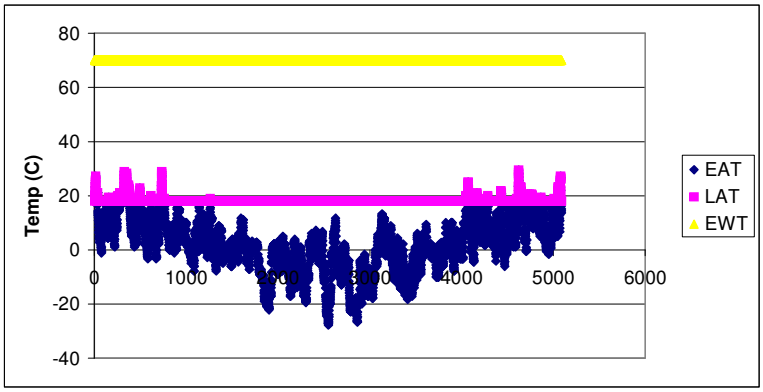
80
60
40
20
0
-20
-40
Temp (C)
0
1000
2000
3000
4000
5000
6000
EAT
LAT
EWT

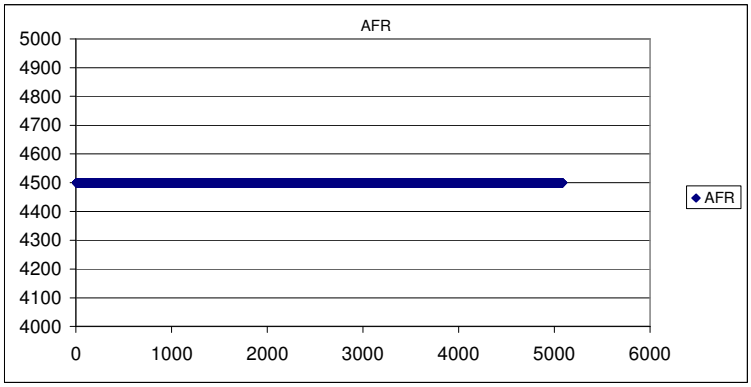
AFR
5000
4900
4800
4700
4600
4500
4400
4300
4200
4100
4000
0
1000
2000
3000
4000
5000
6000
AFR

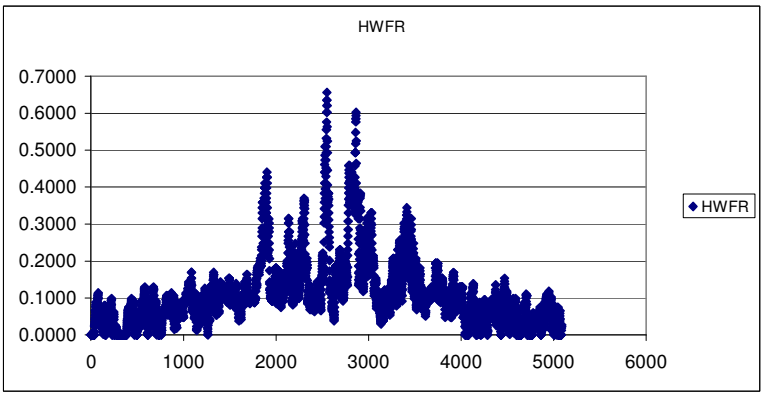
HWFR
0.7000
0.6000
0.5000
0.4000
0.3000
0.2000
0.1000
0.0000
0
1000
2000
3000
4000
5000
6000
HWFR

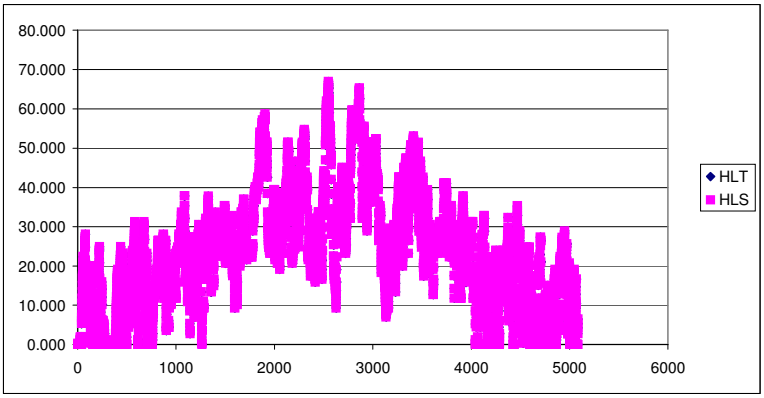
80.000
70.000
60.000
50.000
40.000
30.000
20.000
10.000
0.000
0
1000
2000
3000
4000
5000
6000
HLT
HLS

Case HX200

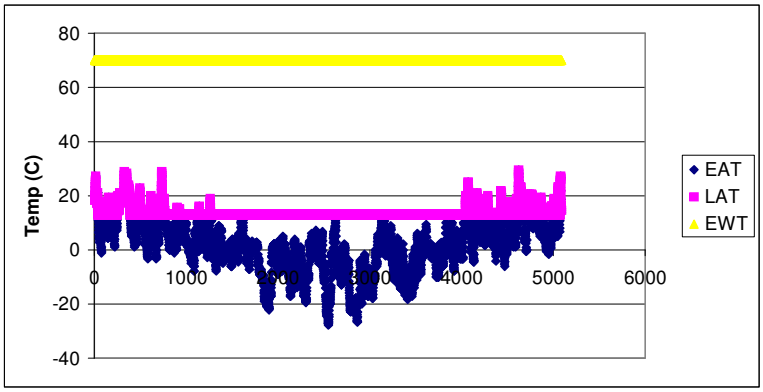
80
60
40
20
0
-20
-40
Temp (C)
0
1000
2000
3000
4000
5000
6000
EAT
LAT
EWT

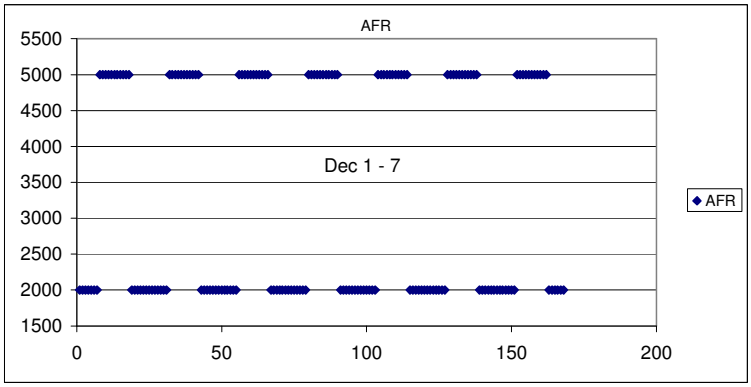
AFR
5500
5000
4500
4000
3500
3000
2500
2000
1500
Dec 1 - 7
0
50
100
150
200
AFR

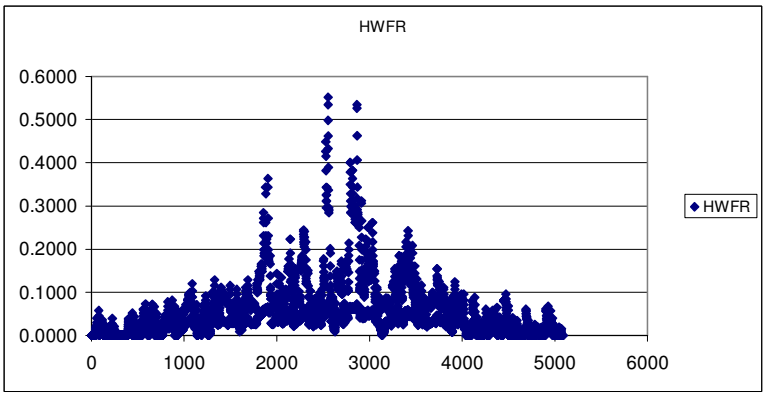
HWFR
0.6000
0.5000
0.4000
0.3000
0.2000
0.1000
0.0000
0
1000
2000
3000
4000
5000
6000
HWFR

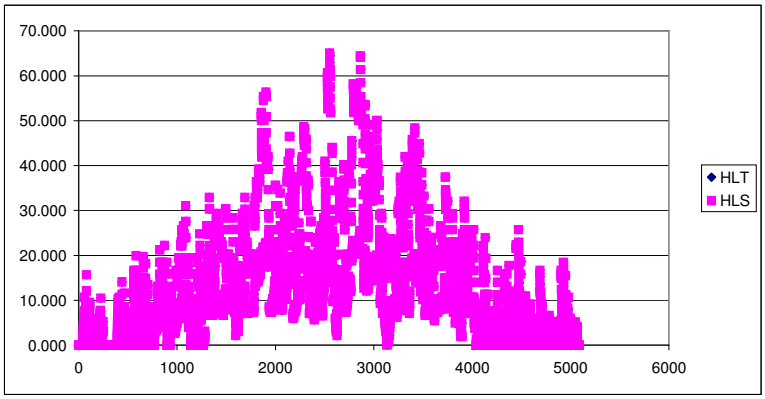
70.000
60.000
50.000
40.000
30.000
20.000
10.000
0.000
0
1000
2000
3000
4000
5000
6000
HLT
HLS

Case HX220

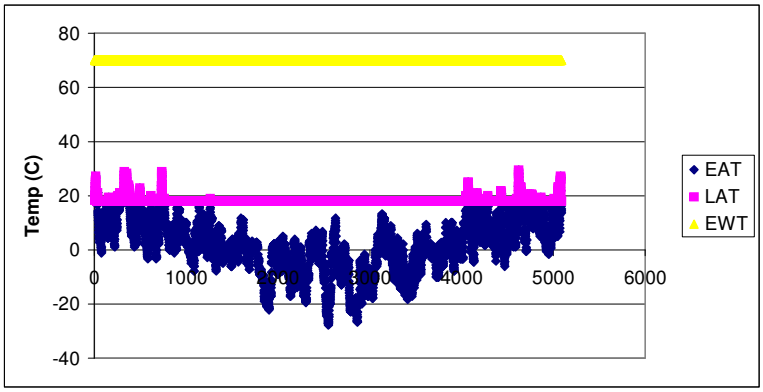
80
60
40
20
0
-20
-40
Temp (C)
0
1000
2000
3000
4000
5000
6000
EAT
LAT
EWT

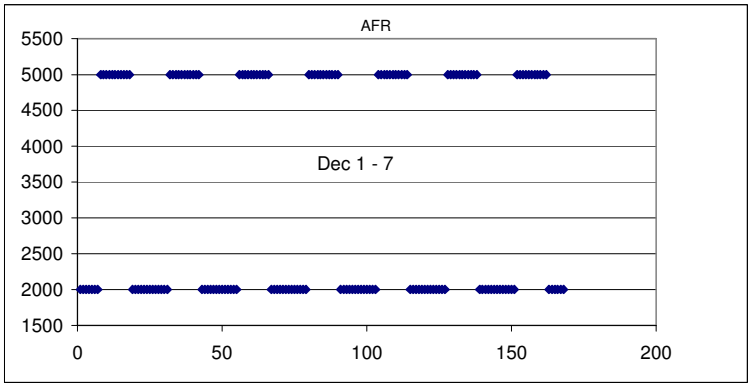
AFR
5500
5000
4500
4000
3500
3000
2500
2000
1500
Dec 1 - 7
0
50
100
150
200

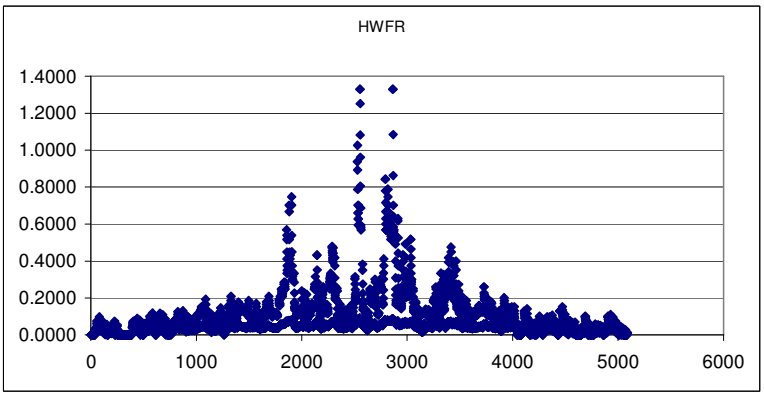
HWFR
1.4000
1.2000
1.0000
0.8000
0.6000
0.4000
0.2000
0.0000
0
1000
2000
3000
4000
5000
6000

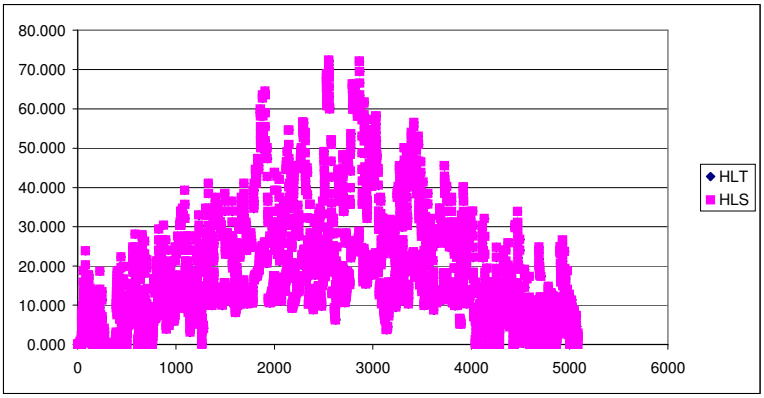
80.000
70.000
60.000
50.000
40.000
30.000
20.000
10.000
0.000
0
1000
2000
3000
4000
5000
6000
HLT
HLS

7.2.4 TUD – TRNSYS-TUD

Roots of the model

The TRNSYS-TUD heating coil model is very similar to the cooling coil model described in the modeller report (PART I, Chapter PART I.7.2.47.2.4) provided in this report. It is one of the TRNSYS ASHRAE Secondary Toolkit Components (Heat and Mass Transfer Components). These components are available for free from the Solar Energy Laboratory at the University of Wisconsin which is the original distributor of the TRNSYS program. The Solar Energy Laboratory also took care that the model was adapted strictly for use with the TRNSYS Program.

The model originally was a simple cooling and dehumidifying coil model that calculates the outlet liquid temperature, air dry bulb temperature and humidity ratio, and the total and sensible cooling capacity based for given inlet conditions based on nominal rated coil performance. For that reason it is not necessary to specify any detailed information neither about coil geometry nor about coil materials.

The heating coil model operates in dry regime only.

Changes to the model

Control

Originally the coil model did not include any temperature or flow control. That means leaving air temperature (and also humidity) was free floating depending on water and air side inlet conditions. In order to run heating coil comparative test cases some kind of leaving air temperature control was added to the coil model at TUD. Finally three different control strategies were available:

4. No control:
   The leaving air and water side conditions are free floating.
5. Water flow control:
   The entering water temperature is known and water flow is controlled to maintain a given leaving air temperature set point.
6. Water temperature control:
   The entering water flow is known and coil entering water temperature is controlled to maintain a given leaving air temperature set point.

Both water flow and temperature controls are idealized control mechanisms, i.e. there is no control deviation while water flow and water temperature are within given limits:

$$0 \leq \text{Flow} \leq \text{Flow}_{max}$$
$$\text{Temp}_{min} \leq \text{Temp} \leq \text{Temp}_{max}$$

Compared to the cooling model an inverse control strategy had to be taken into account: When leaving air temperature is too high do not increase (as for the cooling coil) but decrease entering water temperature and/or water flow through the coil. The 'No control'-option was used for the empirical test cases only.

Fluid properties

Physical properties of the heating liquid may have an impact on coil performance. Originally the model was assuming pure water only. In order to run cooling coil validation tests the model was extended at TUD to also account for other cooling liquids than water. Actually the user has the choice between (1) pure water, (2) ethylene/glycol mixture, or (3) propylene/glycol mixture, respectively. When a glycol mixture is selected the percentage of glycol per mass has to be defined by the user as well. Physical properties of the glycol mixtures have been taken from the ASHRAE Handbook of Fundamentals [2].
Since the portion of glycol in the heating fluid can be neglected the coil model was running with pure water.

Flow dependencies

The simple coil model as found in the HVAC components library was assuming a constant overall heat transfer coefficient UA when the coil is dry. As first sets of comparative validation test results have shown very big deviations between simulation results calculated with the original TRNSYS / ASHRAE model and those calculated by other participants it was decided to implement flow dependencies of the UA value. These flow dependencies have been defined and implemented as follows:

$$UA_{ext} = UA_{ext0}\left(\frac{Flow_{air}}{Flow_{air0}}\right)^{0.33}$$

$$UA_{int} = UA_{int0}\left(\frac{Flow_{water}}{Flow_{water0}}\right)^{0.67}$$

The external UA_{ext} value refers to the air side of the coil whereas the heating fluid side of the coil is covered by the UA_{int} value. The coil material by itself is not taken into account by a special UA value but is covered by the internal/external UA.
UA_{ext} and UA_{int} are estimated from the total UA_{tot} simply assuming a ration of

$$UA_{ext} / UA_{int} = 70\% / 30\%$$

Known limitations of the model

The basic coil performance (UA_{ext}, UA_{int}) is estimated based on a single rating point only. In this way it is not possible to use several rating points – as defined in the test specifications based on experimental data – at the same time to calibrate the model. A similar problem occurs when different physical properties of the heating fluid have to be used in either the rating point or in the simulation run.

[1] A Toolkit for Secondary HVAC System Energy Calculations. May 25,1992. Joint Center for Energy Management University of Colorado at Boulder

[2].ASHRAE Handbook of Fundamentals. 1996

7.2.5 ITG – Matlab/Simulink

There is no extra modeller report available for the heating coil model. Nevertheless it was mentioned by the modeller that the heating coil model is based on the same approach as the cooling coil model. A description of the cooling coil model can be found in Chapter 7.2.5 (Part I of this final report).

Discussion and Conclusions

Improvements to the Test Specification as a Result of the Field Trials

A number of improvements and revisions to the test specifications were made during the field trials based on comments by the IEA SHC Task 34 / ECBCS Annex 43 participants. Typically the following issues had been pointed out:

- Overall test logic.
  Some discussions have been needed to agree on the overall test logic. It wasn't difficult to agree on the subdivision of chilled and hot water tests according to the components of both systems (boiler, chiller, coils) but took a while to find a specific logic related to certain components. This was caused by the original intention to only provide the modeller with information submitted from the manufacturer. Unfortunately these data can not be used for empirical validation since there are some deviations in the performance of components. That is why additional quasi steady-state performance data for the coils have been provided that will allow the modellers to calibrate their models according to the built-in situation. Normally those data will not be available for simulation.
- Missing information
  Information that is needed to setup a simulation model has been taken from manufacturer's submittals if available. On modeller's request some additional information has been extracted from the empirical data. As an example the control strategy as well as electric power of the chiller (Figure 3-8 to Figure 3-10) have been approximated based on measured data.
- Unit conversion
  Technical data sheets submitted by the manufacturer predominantly are written in IP units. The pretension was to write a test specification that prefers SI units instead but also provides additional IP unit information as well. A wrong unit conversion could have a significant impact on the performance of the models. It was helpful to get the feedback of the experts to avoid unit conversion errors.

What we have learned

The participants of the project IEA Task34/Annex43 Subtask D have been asked what they have learned during their work on the different validation tests and if any bugs have been detected in their simulation software that requires some corrections and improvements in the source code. The answers of the modellers are summarized in this section.

ULG / EES:

University of Liege has implemented all of the validation tests and also has submitted a comprehensive modeller report which gives a full insight on how their EES models work. What the modellers have learned is as follows:

- The chiller empirical tests could be passed without numerical instabilities detected in the program.

  The compressor performance tables should always be given as part of the chiller performance data. This exercise showed that they allow a pretty good identification of the compressor model parameters. This was confirmed by the analysis of the experimental data (where the compressor was "dissociated" from the heat exchangers by imposing the saturation pressures as input of the compressor model). Moreover, the condensing power could also have been given in these compressor performance tables. Based on this additional information, the heat exchange coefficients introduced in the modelling could have been better identified. Analysis of the experimental results showed that it was necessary to account for the fan control in the model (in order to represent the air flow rate decrease when entering air temperature decreases). The proposed fan control model seems realistic. However, it could certainly be improved if more information on the fan control was made available. Moreover, the identification of the condenser parameters would have been easier if the air flow rate was given in the (full load and part load) performance tables.
- In the cooling coil comparative tests the simultaneous calculation of the dry and the wet regimes sometimes lead to numerical instabilities (because of the imposed set point on the leaving air temperature). More exactly, the numerical code may not converge when describing the wet regime while the coil is actually working in dry regime. The two regimes have finally been described separately. For the points where the wet regime didn't converge, the dry regime was selected.
- In the cooling coil empirical tests no numerical problems have been encountered. Nevertheless it appears that the nominal point given by the manufacturer doesn't constitute enough information for identifying the parameters of the model. The parameters of the model have been retuned using fourteen additional quasi-steady state points extracted from experimental data. In order to have a good agreement between the measurements and the predictions by the model, an additional resistance had to be added to the metal resistance to account for fouling of the refrigerant pipes.
- The condensing boiler model has been improved to avoid any numerical instability. The available manufacturer data appeared not to constitute enough information for identifying the parameters of the model. Actually, some important information, such as the fuel data is missing. It has been demonstrated

that even with excessively high heat exchanger efficiencies, the overall boiler efficiency given by the manufacturer is not reached under the conditions of the empirical test. Therefore, another parameter identification using the available experimental data from the empirical test was conducted. Predictions by the model, with its new identified parameters, are now very close to the experimental data. Unfortunately, these data correspond to a boiler working only in dry regime. Consequently, this exercise didn't make possible the empirical validation of the condensing boiler model (more exactly, its ability to describe the condensation regime).

- The heating coil comparative tests have been passed without numerical instabilities that have been encountered.
- The heating coil empirical test has shown that as for the cooling coil, with only one performances point, the three thermal resistances in the model can be identified provided the ratio between the air- and water-side resistances as well as the ratio between the metal and the air-side resistances is guessed. The initial identification of the parameters based only on the manufacturer point seemed to overestimate the water-side convective resistance. The metal resistance was probably underestimated. This assumption was partially verified with the identification of the parameters based on three performance points (the nominal manufacturer performance points and two quasi-steady state points extracted from experimental data). These three points allowed the identification of the water-side resistance and the combined metal and air-side resistance. However, since the three points are characterized by air mass flow rates close to each other, the identification of the air-side resistance was not possible. Empirical simulation shows that the model is able to correctly predict the heating capacity and the overall heat transfer coefficient.

VABI / VA114:

In VA114 no real bugs were found during the tests, but the work led to several improvements on the modelling of the heating coil and the cooling coil:

- The atmospheric pressure and the applied heat transfer fluid are asked as extra to the Manufacturer data of the coils (input data of the program). Until now atmospheric pressure at sea level and water as heat transfer fluid were assumed.
- The specific heat transfer capacity of the coil (UA-value) is divided into 3 parts (water - coil construction, internal of the coil construction, coil construction – air). The heat transfer rates at the water and at the air side depend on flow rates. Until now the specific heat exchange capacity was divided into 2 parts and independent of flow rate.
- The coil control at the water side is possible in two ways: temperature controlled (control of the water inlet temperature of the coil) and mass flow controlled

(control of the water flow rate through the coil). Until now it was only temperature controlled.

Other important items are:

- The definition the 'air flow rate' in the system. What means "an air supply volume flow rate of 1000 m3/h"? In VA114 this means "1000 m3/h of dry air at 20 °C and at local atmospheric pressure".
- The Manufacturer data is not always consistent: heat flow rate at the water side is not always the same as the heat flow rate at the air side.
- The Manufacturer data is given for one operating point only. It was learned that this is not sufficient to describe the cooling coil and heating coil in detail. Different Methods were proposed and studied to determine the characteristics of the coil from more operation points.
- The original VA114 modelling of the coils was sufficient accurate to determine the required heat exchange between water and air to obtain the required air supply conditions. However it was too simple to determine the belonging water flow rate and water outlet temperature. The improved modelling of the coils can handle that much better.

So the tests and work were very helpful to improve our software tool.

GARD Analytics / EnergyPlus

The EnergyPlus modellers did not uncover any bugs in the EnergyPlus software when running the Mechanical Equipment Heating and Cooling Tests. The tests did point out some limitations of EnergyPlus however due to the fact that the modellers could not model some of the tests as requested.

- For the heating coil comparative tests EnergyPlus could not model cases HX300, HX320, HX400 or HX420 because they required the use of a varying water supply temperature to the heating coils with the water flow rate remaining constant. EnergyPlus will allow different heating water supply temperatures but currently cannot control the supply temperature of the water entering the heating coil to meet the load.
- For the cooling coil comparative tests EnergyPlus could not model glycol solutions as a chilled water fluid. Only water can currently be modelled as a chilled water fluid.
- For the cooling coil comparative tests EnergyPlus could not model cases CC300, CC320, CC340, CC360, CC400, CC420, CC440 or CC460 because they required the use of a varying water supply temperature to the heating coils with the water flow rate remaining constant. EnergyPlus will allow different

cooling water supply temperatures but currently cannot control the supply temperature of the water entering the cooling coil to meet the load.

TU Dresden / TRNSYS-TUD

Technical University of Dresden was mainly responsible to design and setup the tests. Experiments have been prepared in co-operation with the ERS. Technical University of Dresden also had to provide modellers with a readable and sufficient specification that enables the modellers to run the simulations. Beside this also some of the validation test have been run at TUD using both components developed at TUD and components public available. Experiences gained during the project are:

- Different simulation models used by different participants ask for different information to set up the models. Some of this information is hardly to get because knowledge about configuration and/or performance of components are too detailed (from the manufacturer's point of view) or not well documented (in an existing system).
- Data submitted from the manufacturer including performance curves can not be directly assigned to an existing system. Performance data under laboratory conditions may differ from those under real world conditions. For that reason new sets of calibration point have been extracted from the experimental data (see PART I: Table 4-4, Table 4-6, and PART II: Table 4-4, respectively).
- There is a different understanding among people on which information should be provided to the modeller for validation purposes. Normally only data available from the manufacturer submittal can be used for the parameterization of simulation model. For this empirical validation work, experimental data was used to calibrate simulation inputs (set up the models). Such data have been provided to the modellers otherwise there is no chance to consider for the differences between laboratory (manufacturer data are based on) and real world conditions (experimental data used for validation are based on).
- From both heating and cooling coil test it was found that models with a heat transfer coefficient UA that is independent from the coil flow rates are not able to predict coil performance correctly when either flow rates are changing (i.e. when the air flow rate is variable or the coil is controlled by changing liquid mass flow) or nominal rating point is at different flow rates than under test conditions.
- For the coil validation tests it is quite easy to predict sensible heating and/or cooling loads since they are based on simple energy balances. It is much more difficult to predict latent cooling load due to dehumidification and/or condition of the liquid fluid leaving the coil. This might have a big impact on the assessment of control quality. Such uncertainties also should be taken into account when an overall simulation approach is used to predict the performance

of the whole system: Chiller performance would depend significantly on the chilled water parameters leaving the cooling coil and also boiler performance would depend on hot water parameters leaving the heating coil.

- The ERS test facility offers excellent opportunities to run experiments that can be used for the empirical validation of computational models representing the mechanical equipment in an HVAC system. Also dynamic effects can be easily observed due to the minute wise time step data are collected.
- Coil models seem to be very common. A lot of different coil models are available either commercial or public. They are quite easily to use and easily to calibrate. In opposite to that chiller models or models of a boiler are more complex and need more experiences on how to use them in the right way according to a given test description. May be that is the reason that 5 participants have run the coil tests but only two parties were participating the chiller and boiler tests, respectively.
- It would have been nice to have any more diagnostic power especially in the comparative test cases which would mean:
  - Artificial entering conditions (no real climate data or data from TRY)
  - Recording of step responses
  - Parameter variation.
- It would have been nice to have more validation on control mechanisms especially on valve control.
- Simulation models are not always able to predict all the values that have been measured during the experiment.

ITG Dresden / Matlab/Simulink

ITG Dresden has provided results for the cooling/heating coil tests only. They found that the measurements made a contribution to tune some model parameters. These calibrations were not possible with the manufacturer's data only. The test series were chosen partially well. ITG missed some step responses with the goal to detect typical dynamic behaviour. Perhaps some tests to determine the accurate threshold of condensation on constant boundary conditions would have been helpful to improve more detailed models, because there are very often some tuneable parameters that have to be adapted to certain circumstances.

Recommendation for future work

Based on the lessons learned in this joint IEA SHC-Task34 / ECBCS-Annex43 some recommendation for future work in the field of validation of mechanical equipment and HVAC system models can be derived.

At first the design of comparative test cases should be done particular with regard to strong diagnostic power of the test. This means:

- Nearly the full area of operation from low part load to peak load should be covered by the test conditions.
- The impact of certain design parameters on the performance of the HVAC system model should be analysed.
- The impact of variable inputs on the performance of the mechanical equipment should be analysed using standardised tests for controllers, i.e. step response.

Dynamic effects should be taken into account if they are relevant for the performance of the components. For that reason the tests should focus on a limited time-frame rather than a (half-) annual time period of simulation.

The design of empirical test cases depends on the opportunities given in the test facility. In a laboratory or in a test facility that offers conditions similar to a lab also artificial boundary conditions can be created that allow to operate the equipment apart from real world conditions but better covering the potential area of operation. This was done during this project in the Cooling coil empirical test II. Empirical tests should be performed in addition to comparative tests to show differences between theory and real world. It is obvious that a high effort must be undertaken to collect reliable experimental data suitable for empirical validation purposes.

A third aspect is related to a whole system approach that does not only target on the validation of certain components (i.e. chiller, coil, boiler) but also accounts for the simultaneous operation of the whole system. Doing this the interaction of components can be checked. Inaccurate predictions propagate from one component to the next and will be intensified or compensated.